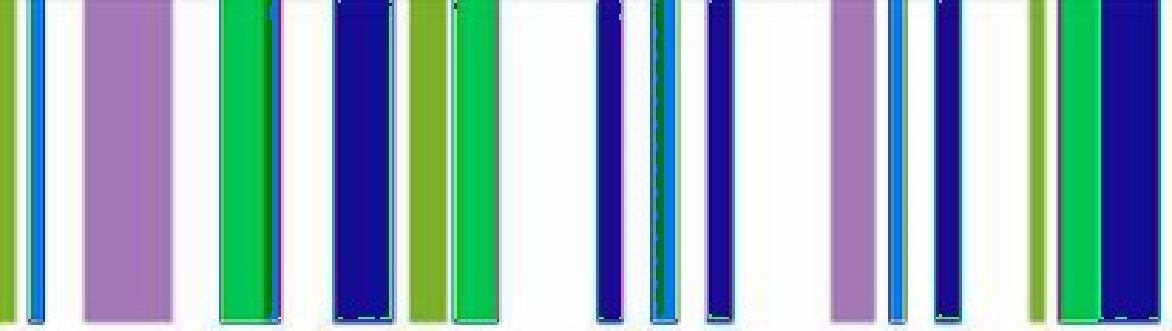

NATO Science for Pea
Chemistry

Technologic
in Sensing ar
Chemical,
Radiological,
and Ecologi

Technological Innovations in Sensing and Detection of Chemical, Biological, Radiological, Nuclear Threats and Ecological Terrorism

NATO Science for Peace and Security Series

This Series presents the results of scientific meetings supported under the NATO Programme: Science for Peace and Security (SPS).

The NATO SPS Programme supports meetings in the following Key Priority areas: (1) Defence Against Terrorism; (2) Countering other Threats to Security and (3) NATO, Partner and Mediterranean Dialogue Country Priorities. The types of meeting supported are generally “Advanced Study Institutes” and “Advanced Research Workshops”. The NATO SPS Series collects together the results of these meetings. The meetings are co-organized by scientists from NATO countries and scientists from NATO’s “Partner” or “Mediterranean Dialogue” countries. The observations and recommendations made at the meetings, as well as the contents of the volumes in the Series, reflect those of participants and contributors only; they should not necessarily be regarded as reflecting NATO views or policy.

Advanced Study Institutes (ASI) are high-level tutorial courses to convey the latest developments in a subject to an advanced-level audience

Advanced Research Workshops (ARW) are expert meetings where an intense but informal exchange of views at the frontiers of a subject aims at identifying directions for future action

Following a transformation of the programme in 2006 the Series has been re-named and re-organised. Recent volumes on topics not related to security, which result from meetings supported under the programme earlier, may be found in the NATO Science Series.

The Series is published by IOS Press, Amsterdam, and Springer, Dordrecht, in conjunction with the NATO Emerging Security Challenges Division.

Sub-Series

A.	Chemistry and Biology	Springer
B.	Physics and Biophysics	Springer
C.	Environmental Security	Springer
D.	Information and Communication Security	IOS Press
E.	Human and Societal Dynamics	IOS Press

http://www.nato.int/science
http://www.springer.com
http://www.iospress.nl

Series A: Chemistry and Biology

Technological Innovations in Sensing and Detection of Chemical, Biological, Radiological, Nuclear Threats and Ecological Terrorism

edited by

Ashok Vaseashta
Institute for Advanced Sciences Convergence and Int'l Clean Water Institute
Norwich University Applied Research Institutes
Herndon, VA USA

VTT/AVC U.S. Department of State
Washington DC USA

and

Eric Braman and Philip Susmann
Norwich University Applied Research Institutes
Northfield, VT, USA

Published in Cooperation with NATO Emerging Security Challenges Division

Proceedings of the NATO Advanced Study Institute on Technological Innovations in Detection and Sensing of Chemical, Biological, Radiological, Nuclear - (CBRN) Threats and Ecological Terrorism
Chisinau, Moldova
June 6-17, 2010

Library of Congress Control Number: 2011940795

ISBN 978-94-007-2490-7 (PB)
ISBN 978-94-007-2487-7 (HB)
ISBN 978-94-007-2488-4 (e-book)
DOI 10.1007/978-94-007-2488-4

Published by Springer,
P.O. Box 17, 3300 AA Dordrecht, The Netherlands

www.springer.com

Printed on acid-free paper

All Rights Reserved
© Springer Science+Business Media B.V. 2012
No part of this work may be reproduced, stored in a retrieval system, or transmitted in any form, or by any means, electronic, mechanical, photocopying, microfilming, recording or otherwise, without written permission from the Publisher, with the exception of any material supplied specifically for the purpose of being entered and executed on a computer system, for exclusive use by the purchaser of the work.

Preface

The primary objective of the NATO Advanced Study Institute (ASI) titled "Technological Innovations in Detection and Sensing of Chemical-Biological-Radiological-Nuclear-High yield explosive (CBRNE) Threats and Ecological Terrorism" was to present, exchange, and promote a contemporary and comprehensive overview of how nanostructured materials, devices, and systems can be used to combat CBRNE threats and ecological terrorism.

The geopolitical landscape of the twenty-first century offers more complex, dynamic, and unpredictable global challenges than those encountered in the previous century. Despite the unparalleled level of military/technological dominance that the United States and NATO Allies; the evolving asymmetric, kinetic, and unconventional threats from non-aligned terrorist groups continue to evolve and escalate. Adversaries and terrorist groups have demonstrated a strong will and interest to wage unconventional war against Western targets despite their limited technological capabilities and lack of sophistication in conducting such operations. In fact, the unsophisticated conformations of CBRNE threats pose more technical challenges in both point and stand-off detection. The rapid advances in both science and technology coupled with universal internet access have inspired both non-state and state-sponsored actors to new levels of creativity in the development of novel and non-traditional threat agents. It is apparent that asymmetric threats have changed the traditional nature of the battlefield. Accompanying the evolution of asymmetric threats is the relative ease of their transport and engagement; thus broadening the potential battlefield and virtually eliminating the generally accepted premise of homeland as a safe haven from catastrophic, man-made disasters. Finally, the terrorist toolkit includes direct attacks against persons, economic infrastructure, and the environment in pursuit of their own personal and political agendas. Furthermore, drinking water distribution systems are vulnerable to intentional and/or inadvertent contamination. Such contamination can be accomplished with classic and non-traditional chemical agents, toxic industrial chemicals (TICs), and/or toxic industrial materials (TIMs). Conventional methods employed to sense/detect such contaminants use commercial-off the shelf (COTS) systems and broad-spectrum analytical instruments with interpretive algorithms to detect and characterize toxic contaminants. The current

threat environment requires detection of complex contaminant signatures in addition to recycled pharmaceuticals present in water supplies. Hence it is critical to seek revolutionary solution pathways to such challenges, such as using advanced sciences convergence (ASC) involving inter/Trans disciplinary fields.

It is well known that materials approaching nanoscale dimensions exhibit characteristics with numerous unique and previously unexploited applications. Advances in synthesis and characterization methods allow the means to study, understand, control, and even manipulate the transitional characteristics between isolated atoms and molecules and bulk materials. Technological advances arise from the potential of nanoscale materials to exhibit properties that are attributable to their small size, physical characteristics, and chemical composition. Recently, functional and architectural innovations in nanoscale materials have initiated applications in chemical and biological sensing; environmental pollution sensing, monitoring, mitigation and remediation; nano-biotechnology; plamonics; and in-vivo analysis of cellular processes. A nanotechnology-based sensor platform enables direct electrical detection of chemical and biological agents in a label-free, highly multiplexed format over a broad dynamic range. Advances made over the last few years provide new opportunities for scientific and technological developments in nanostructures and nanosystems with new architectures and improved functionality. The field is very active and rapidly developing, and covers a wide range of disciplines. The advancement of molecular biology and its application in environmental microbiology has represented significant advancement in the ability to rapidly detect waterborne microbial pathogens. Molecular methods, coupled with high-throughput parallel process may provide a greater range of microorganism detection. The advances in of new technologies, viz. biosensors, biochips, lab-on-chip, e-tongue, plasmonics, etc. have brought in new and promising approaches. The ASI focus was also to summarize recent methodologies in sensing/detecting contaminants flow in water distribution system with the objectives that appropriate remediation strategies are exercised before its entry in residential/commercial/industrial distribution. Furthermore, decentralized sensing plays a crucial role from an international security standpoint.

The ASI aimed to address several important and relevant issues related to enhancing security using advanced technological solutions. Several invited lectures, focused seminar sessions, and student presentations addressed a range of issues such as technological advances in chemical-biological sensors using nanomaterials; advanced sciences convergences for international defense and security, and water-based contaminants sensing/detection and mitigation.

The ASI was attended by participants from 23 countries thus exemplifying the international vision of NATO Peace for Security endeavours. The ASI provided an international forum for the exploration of many key scientific and technological advancements employing nanostructured and advanced materials. Despite of initial organizational issues, the NATO ASI was well organized and received by the participants. To maximize global participation, the organizing committee focused on a promotional strategy that yielded a wide range of NATO and partner countries representation and most importantly, a wide range of participation from multiple scientific disciplines.

Lectures covering the basic principles and state-of-the-art applications of nanostructured and advanced materials for chemical-biological sensors were conducted by 17 experts recognized for advances in nanotechnology. Focused seminar sessions, poster sessions, and interactive feedback sessions stimulated extended interactions between participants and subject matter experts. As a venue for collaborative learning, the interactive lectures and sessions drew enthusiastic response and sharing of information and ideas from all participants.

The ASI was held at the Hotel Villa Verde in Chisinau, the capitol and largest municipality in the Republic of Moldova. The facility supported formal and informal settings for structured and spontaneous learning and sharing of ideas. The meeting lasted 11 days, with a day free to visit local historical sites. The downtown shops, restaurants, and pubs provided a much-needed break after lectures and in-depth discussions at the ASI. The unique balance of technical and social interactions materialized in alliances between participants, which have been evidenced by continued correspondence in the months following the ASI. The co-directors interpret the ongoing interaction and positive feedback from participants as an affirmation of a successful ASI.

Such a constructive ASI is the outcome of efforts by participants, lecturers, presenters, and co-directors in addition to a host of caring individuals who supported their work. Much appreciation is extended to Hotel Villa Verde management who ensured gracious hospitality to all participants. We would like to acknowledge tireless logistics support from Marina Turcan, Camellia Popescu, Doğa Kavaz and Tamer Çırak.

We offer our gratitude to Dr. Walter Kaffenberger, the director of the NATO Scientific Affairs Division and Ms. Allison Trapp for unwavering encouragement, generosity, and support of the ASI. Ms. Annelies Kersbergen with the NATO Publishing Unit of the Springer Academic Publishers has provided us with much appreciated expertise in publishing our proceedings. NSF provided travel support for some of the participants and is acknowledged immensely for generous support. Thanks are due to the Vaseashta Foundation for several travel and poster awards to support scientific community. The co-directors are confident that ASI participants will continue research collaborations that began in Chisinau in the advancement of nanotechnology and advanced sciences convergence that enhance security for all mankind.

Directors
Herndon, VA and Washington, DC USA — Ashok Vaseashta
Chisinau, MOLDOVA — Nicolae Enaki

Organizational Support
Reshef Tenne, Anatolie Sidorenko, Brian Nordmann, and Emir Denkbas

Contents

Part I
General and Invited Key Lectures

Chapter 1
Technological Innovations to Counter CBRNE Threat Vectors and Ecotage

Countering CBRNE Threats and Ecotage

Ashok Vaseashta*

Abstract The ubiquitous presence of sensors for enhanced situational awareness necessitates an innovative, articulate, and focused review of their design, architecture, functionality, and interoperability. A comprehensive overview of the latest and state-of-the art technological innovations in point and stand-off sensing/detection platforms with the objective of countering threats arising from chemical-biological-nuclear-high yield explosives (CBRNE) is the focus of this investigation. Ongoing research efforts and future research directions based on advanced approaches, including nanomaterials to develop materials, devices, and systems for potential use in sensing and detection of such threat vectors are articulated. The concept of advanced sciences convergences is introduced to examine the feasibility of potentially new and innovative research directions for persistent surveillance of CBRNE agents and infectious diseases. The intentional release of such agents in the environment constitutes ecological sabotage. Advanced sensing/detection platforms for CBRNE are used to detect threats to the environment. Issues associated with the use of nanomaterials regarding societal implications and dual-use concerns are addressed by studying fate and transport and the development of guidelines for a risk-assessment model. A roadmap of the future of nanomaterials, in terms of complexity, a nexus of disciplines, and its emerging potential to provide advanced, futuristic, and a paradigm-shifting platform is presented.

*Contents of this manuscript are the sole responsibility of the author and may not reflect the views/policy of the U.S. Department of State or the U.S. Government.

A. Vaseashta (✉)
Institute for Advanced Sciences Convergence, and Int'l Clean Water Institute, Norwich University Applied Research Institutes, 13873 Park Center Rd. Suite 500, Herndon, VA, USA

AVC/VTT, U.S. Department of State, 2201 C Street, N.W, Washington, DC, USA
e-mail: prof.vaseashta@nanoknowledge.info

A. Vaseashta et al. (eds.), *Technological Innovations in Sensing and Detection of Chemical, Biological, Radiological, Nuclear Threats and Ecological Terrorism*, NATO Science for Peace and Security Series A: Chemistry and Biology,
DOI 10.1007/978-94-007-2488-4_1, © Springer Science+Business Media B.V. 2012

Keywords CBRNE sensors • Ecotage • Water • Satellite • ASC • Biomimetic

1.1 Introduction

The challenge of the geopolitical landscape of the twenty-first century poses more complex, dynamic, and unpredictable challenges than those faced by our nation in the previous 100 years. Securing critical infrastructures and life-sustaining ecosystems are significant, omnipresent, and dynamic challenges for the scientific and defense communities. Tactically, the unsophisticated nature of chemical, biological, radiological, nuclear, and environmental (CBRNE) threats poses significantly greater technical challenges in both point and stand-off detection. Despite the unparalleled level of the technological dominance of the U.S. military; the evolving asymmetric, kinetic, unconventional, and unsophisticated nature of threat from non-aligned terrorist groups and adversaries continues to grow. This threat is growing due to increased globalization and mobility within society, the explosion in chemical and biotech expertise and the relative ease with which chemical weapons can be prepared at off-sites, and the means by which pathogens can be covertly engineered, transported and released or dispersed. Furthermore, drinking water distribution systems are vulnerable to intentional and/or inadvertent contamination with classic and non-traditional chemical agents, toxic industrial chemicals (TICs), and/or toxic industrial materials (TIMs), in addition to recycled pharmaceuticals. Conventional methods employed to sense/detect such contaminants use commercial-off the shelf (COTS) systems and broad-spectrum analytical instruments with interpretive algorithms. Beyond terrorism and warfare, industrial accidents such as the Deepwater Horizon oil spill and catastrophic natural events such as hurricanes, earthquakes and tsunamis have contributed to massive environmental contamination and will benefit from sensing/detection systems used for defense and security applications. Consequently, preparedness and mitigation of CBRNE threats from such routes is a priority for governments and the greater international community.

1.2 Threat Vectors – Emerging, Persistent, Dual-Use, and Avant-Garde

Beyond uncontrollable and inevitable acts of nature; CBRNE threats pose heightened concerns for government and defense sectors. A substantial segment of the scientific community believes that the probability of a terrorist event taking place in the foreseeable future is finite. The obligation of any Defense organization is to protect the masses in a climate of terrorism characterized by “having nothing to lose” and motivated by radical ideology. Consequently, it is imperative that the scientific community, in conjunction with defense organizations, develop plans with an understanding of the science and technology (S&T) required to detect, predict,

deter, and interdict these threats using interdisciplinary approaches, instruments, and techniques. Understanding the characteristics of CBRNE threats and early detection may prevent or minimize a potentially catastrophic occurrence. The focus of this paper is to examine CBRNE threats and means by which nano and advanced technologies can prevent and mitigate damages from CBRNE threats. The scientific study of nanoscale materials and systems is a promising field and offers potential solutions. Methodologies such as Advanced Science Convergence (ASC) are discussed as a framework for S&T intelligence (S&TI) to provide enabling and disruptive technologies for CBRNE mitigation and potential solution pathways to better prevent technology surprise.

1.2.1 Emerging Threats

Most potential threats have been classified by a severity of hazard (SH) ranking based on toxicity, flammability, or reactivity. Notwithstanding many conventional and well characterized TICs/TIMs, there are many other emerging, persistent, dual-use, and unconventional threat vectors that must be identified and mitigated using advanced technology platforms.

Genetically modified organisms (GMO) refers to an organism whose genetic material has been altered using genetic engineering, such as recombinant DNA or DNA molecules from different sources, giving it modified genes with many applications in pharmaceutical, experimental medicine, agriculture, transgenic microbes for performance enhancement and treating medical conditions, and transgenic animals for phenotypic and experimental research. Despite its many uses, research on GMO coupled with recent advances in nucleic acid synthesis, lack of in-situ detection of a novel gene, transcription promoter to trigger gene expression, and lack of reference materials and standards have caused concerns, especially in agro-terrorism. Synthetic biology, likewise, is modifying the DNA of an organism to change the information content, such as selecting desired mutations, inducing mutagenesis, altering genes or regulatory elements, cloning, designing biological components and systems that otherwise do not exist naturally. Synthetic biology provides the tools to "redesign" the genomes of existing microbes to increase their efficacy or provide new functionalities. The successful "redesign" of the bacterium Mycoplasma genitalium, which has the smallest known bacterial genome, yet possesses all of the bio-chemical machinery needed to metabolize, grow, and reproduce, has been readily available in open literature and on the Internet. The goal of this "minimum genome project" is to build a basic microbial platform to which new genes can be added, thereby creating organisms with desired characteristics and functionalities. Likewise, "synthetic genomics" refers to the set of technologies that make it possible to construct any specified gene (or full genome) from synthesis to a custom designed base pair series, e.g. short strands of synthetic DNA called "oligonucleotides" which are produced chemically and are generally between 50 and 100 base-pairs in length. There are reports of research teams assembling the live infectious poliovirus from

customized commercial oligonucleotides, using a map of the viral genome available on the Internet; others have used synthetic oligonucleotides to construct ϕX174 – a bacteriophage (containing 5,386 DNA base-pairs) in only 2 weeks, and a synthesized so-called Spanish influenza virus which was responsible for the 1918–1919 flu pandemic that killed between 50 and 100 million people worldwide. Synthetic biology is subject to potential misuse, in terms of enhanced virulence, resistance to control agents, altering host defense, and increasing environmental stability and/or spread. Similar to GMO, limited detection methods exist for emerging synthetic biological threats requiring countermeasures using advanced technology platforms.

Dual-use is a term often used in the political and diplomatic context to state that a technology can be used for both peaceful and military ambitions. Although used primarily in context of nuclear proliferation, the use of GMO and synthetic biology as bioweapons poses a major concern. Use of functionalized nanomaterials has been identified as a potential dual-use concern and is currently been investigated by the author.

1.2.2 Persistent Threats

Water is fundamental to sustaining life. Despite of its essential nature, drinking water distribution systems are vulnerable to intentional and/or inadvertent contamination. Such contamination can be accomplished with classic and non-traditional chemicals. The current threat environment requires detection of complex contaminant signatures in addition to recycled pharmaceuticals present in water supplies. A growth in human population and associated increased demands on water poses a significant challenge in maintaining adequate yet acceptable water quality in various sectors. The demand for clean water extends beyond residential and municipal needs. High volumes of high purity water are critical for most industries and laboratories, e.g., environmental remediation, hydrocarbon processing, catalysis and chemical processing, food and beverage, mining and hydrometallurgy, pharmaceuticals, power generation and semi-conductors. For many years, most developed countries have had easy access to high-quality, fresh water that was relatively easy to obtain, treat and transport. However, global water shortage problems are becoming more widespread with population growth, drought, and industrial expansion. There are increasing concerns about the availability of usable water, and many communities and industries alike are faced with dramatic reductions in traditional fresh water supplies and deteriorating water quality in the form of contaminated wells, runoffs, and other ground supplies. Global water scarcities increase the urgency for the preservation of fresh water resources and increased water reclamation efforts (i.e., wastewater treatment, remediation, water reuse, and desalinization); management of global water resources is critical to creating sustainable water supplies for residential, agricultural, and industrial purposes, energy conservation, and improved quality of life. It is critical to observe the association between the basic need for clean drinking water and water resources, and national security concerns and policy. There are numerous national threats emanating from the growing crisis of global freshwater

scarcity. Many of the earth's freshwater ecosystems are being critically depleted and used unsustainably to support growing residential and industrial demands; thereby increasing ecological destabilization, and creating a greater regional divide thus directly impacting current political, economical and social landscapes.

Yet another security challenge is securing nuclear materials, controlling contraband and preventing proliferation. Nuclear security consists of complementary programs involving international legal and regulatory structure, intelligence and law enforcement agencies, border and customs forces, point and stand-off radiation detectors, personal protection equipment, preparedness for emergency and disaster, and consequence management teams. There are several policies and governmental initiatives on national and international fronts that seek to control use and transport of nuclear materials; however, this paper will explore nano-enabled scientific and technological means for sensing and mitigating accidental or intentional radiation and nuclear incidents.

Catastrophic weather events, climate change, industrial, warfare, and terrorism have damaging effects to the environment that can be detected and mitigated through nanotechnology sensing and remediation. Another source of environmental damage is eco-terrorism defined by the Federal Bureau of Investigation (FBI) as "the use or threatened use of violence of a criminal nature against people or property by an environmentally oriented, subnational group for environmental-political reasons, or aimed at an audience beyond the target, often of a symbolic nature". Ecological sabotage (ecotage) is often seen as indistinguishable from ecoterrorism. In the present context, ecological terrorism and ecotage are used in context of intentional contamination of the environment (air, water, and even soil) in order to cause harm to the population, infrastructure, and/or denial-of-service.

1.3 Nanotechnology in Support of Countermeasures

The application of nanoscale materials and system shows great promise in combating CBRNE threats. Nanoscale materials exhibit unique properties that are attributable to their small size such as surface structure, physical characteristics, and chemical composition. Because nanomaterials have geometrical dimensions comparable to the smallest engineered entity, and the largest molecules of the living systems, and fundamental physical quantities, they offer uniqueness due to enhanced surface activity and with appropriate functionalization. Furthermore, advances in material synthesis, device fabrication and characterization techniques have provided the means to study, understand, control, or even manipulate the transitional characteristics between isolated atoms and molecules, and bulk materials, providing additional sensing/detection capabilities. Typically, reduced dimensional systems are characterized, in which one or more dimensions are reduced (in nanometers) such that material begins to display quantifiable novel characteristics. The onset of deviation from bulk to reduced dimensions has resulted in many unique electrical, optical, and mechanical characteristics [1–4]. For solids, typically reduced dimensions amount to reduction of the coordination number; hence the electrons have less opportunity to hop from site to

site; thus reducing kinetic energy of electrons. A higher Coulomb interaction at a site enhances electron correlation and Mott-transition. Furthermore, the symmetries of the system are lowered and the appearance of new boundary conditions leads to surface and interface states. A change of the quantization conditions alters the Eigenvalue spectrum and transport properties of the solid. A high surface area/volume ratio in nanoscale materials alters mechanical and other physical properties and hence surface stresses existing in nanomaterials have a different bonding configuration. The difference between surface and bulk properties become enhanced as the surface area/volume ratio increases with decreasing structural dimension resulting in better sensing/detection capability. Studies to calculate surface elastic constants using MD simulations, the curvature effect using the Cauchy-Born rule, and electronic effects via effective nuclei-nuclei interaction using DFT calculations provide better understanding of surface and interface effects in nanoscale dimensions. Size and surface collectively control interactions of nanoscale materials due to existence of large boundaries in its surroundings and thus interplay of physico-chemical interactions. The surface free-energy is size-dependent and hence increases almost inversely with the decreasing feature sizes of the material. The collective response of a nanomaterial-medium system that is attributable to reduced dimensions is vital to developing a scientific model that predicts its response as a sensor.

A nanotechnology based sensor platform enables direct electrical detection of biological and chemical agents in a label-free, highly multiplexed format over a broad dynamic range [5]. For instance, nanoscale resonators [6] have allowed various research groups to detect mass of molecules by detecting change in resonance frequency with mass [7]. Surface effect may play a role in resonant frequency shift if the thickness of the biomolecular layer becomes comparable to the resonator's thickness; although, the surface stress effect may affect the resonant frequency shift. We have employed plasmonics using the surface plasmon resonance (SPR) on the optical response [8] as a function of biological molecule interactions resulting from adsorbate-substrate bonding. Many other platforms based on flexoelectricity [9], electrochemical sensing [10, 11], biomimetic [12], catalysis [13], carbon-filled polymers [2], and cantilever [14] based platforms have been studied. A full potential and complexity of tasks to be performed by such platform can be extrapolated by ASC and some of the foresight tools, as discussed in a later section. Figure 1.1a shows a list dimensional capabilities and Fig. 1.1b, a roadmap for nanomaterials based on current achievements, drivers, and foresight tools.

1.4 Advanced Sciences Convergence

Advanced Sciences Convergence refers to the early monitoring and identification of emerging scientific advances across multiple disciplines that create revolutionary, integrated and cross-cutting technologies to break through existing solution paradigms. The process of ASC is to understand how different disciplines, focusing on discrete problems and applications, can coalesce into an integrated system to

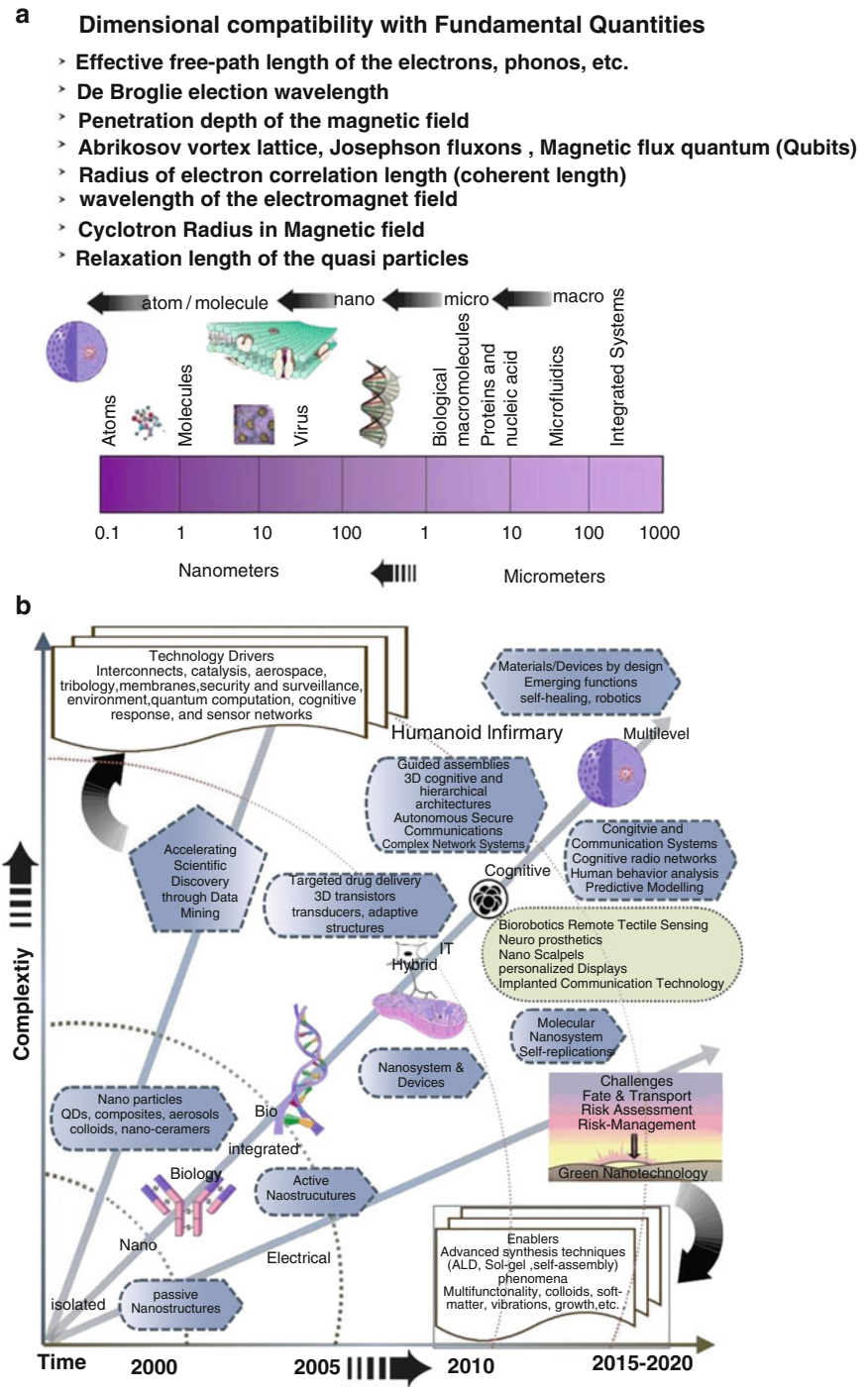

Fig. 1.1 (**a**) Dimensional compatibility [3], (**b**) Roadmap of nanomaterials [2, 3]

solve a seemingly intractable problem. It requires understanding of far-reaching end goal that is not yet defined, but can be described in terms of desired actions or qualities of the eventual system. Multiple approaches, some of which may be high risk research, can be pursued simultaneously to create components of the system. A patchwork of emerging scientific advances is constructed through a strategic planning process to create a fully integrated system.

The first step in this high-level analysis is to identify the specific requirements and design a strategic approach based on the intersection of global cutting edge scientific advances with the most critical operational requirements identified in collaboration with the user community. The convergence process requires monitoring domestic and international developments in multiple disciplines. These data mining operations are focused in areas identified through the strategic planning process as having a high potential for meeting some desired characteristic of the solution system. Constant cross pollination among multiple disciplines is required to identify emerging patterns within the larger scientific community. The ASC process requires the sharing of findings to determine if theoretical constructs can be applied to a different discipline. These operations are the basis for team brainstorming, expert elicitations, and creating concept maps of potential solution paths. The data mining operations and analysis require both human data mining expertise and human domain expertise, and consist of a number of supporting tasks.

These events present an opportunity to understand the community in which the science is being conducted, as well as to meet the leaders within the specific field and permits the team to network within a field, gaining an understanding of the direction in which the discipline is evolving. The overall process starts with strategic planning to describe the solution system supported by data mining and investigation of emerging science. Brainstorming and cross pollination assist the ASC process by identifying potential emerging additions to the solution system. Due care and diligence is required to verify the viability of a research entity and feasibility of the scientific effort. It is an ongoing iterative process which includes greater understanding of the science, research entity, eventual technology, and system integration. Advances are supported by tapping into multiple databases to develop not only individual science but also the nature of the integrated solution system. Using ASC, three tools were developed viz. Technology Foresight and Roadmapping (TechFARM™), Automated Data Mining, Analysis, and Surveillance (ADAMS™), and New and Emerging S&T Trends Surveillance (NESTTS™). Details of these tools are described elsewhere [15], suffice it to mention that tools, in conjunction of future oriented S&T analysis, also termed as future trends analysis (FTA) approaches and strategy, as shown in Fig. 1.2a, b provide focus and direction.

1.5 Nanotechnology Based Sensors for CBRNE Threats

The past decade has seen the development of various nanoscale materials with new architectures and improved functionalities for applications in chemical and biological sensors [1], environmental pollution sensing [2], monitoring [2, 16, 17], mitigation

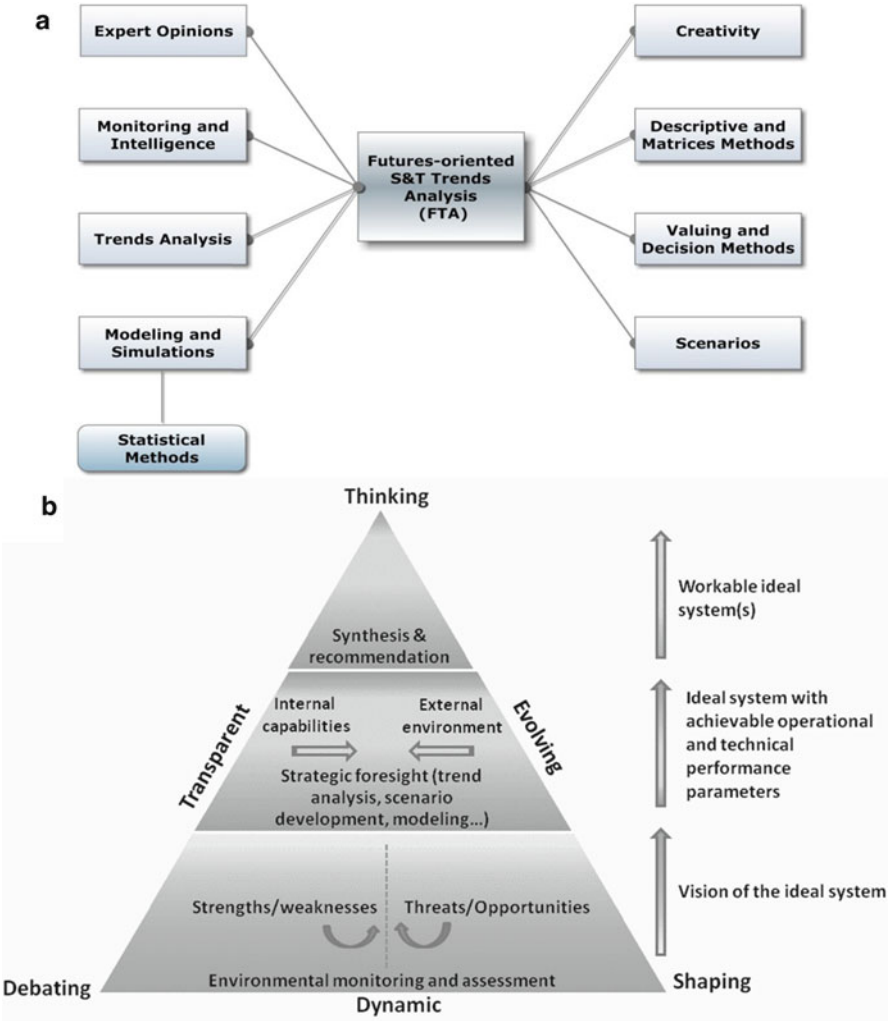

Fig. 1.2 (*a*) Approaches and strategy used in future trends

and remediation [18], next-generation energy generation and storage devices [2], nano-biotechnology, nanophotonics [2], and *in-vivo* analysis of cellular processes and futuristic platforms in health and clinical medicine [14, 19]. Chemical, biological, and explosive agents display certain characteristic features and phenomenology which may be interrogated by remote and sampled detection, discrimination, and identification techniques and systems. Several commonly employed technologies include Mass Spectrometry [20], Ion Mobility Spectrometry [21], Surface Acoustic Waves [22], Fourier Transform Infrared Spectrometry [23], Differential Absorption LIDAR [24], Laser-Induced Fluorescence [25], Surface Plasmon Resonance (SPR) [8, 16], Immunoassay [26], Polymerase Chain Reaction (PCR) [27],

Laser-Induced Breakdown Spectroscopy [28] and LIDAR Backscatter systems [29]. For chem.-bio sensing, nucleic acids offer analytical chemists a powerful tool for recognition and monitoring of many important compounds. Recent advances in molecular biology are used to study the effects of proteins and drugs on gene expression, viz. gel mobility shift, filter binding, DNA foot-printing and fluorescence-based assays [30]. Most of these methods; however, are indirect and require various labeling strategies. Electrochemical DNA biosensors play an important role for clinical, pharmaceutical, environmental and forensic applications, because they provide rapid, simple and low-cost point-of-care detection of specific nucleic acid sequences [2, 8].

In recent years, there has been a growing interest towards design of electrochemical DNA biosensors that exploit interactions between surface-confined DNA and target drugs/biological molecules for rapid screening. Binding of small molecules to DNA primarily occurs in three modes: electrostatic interactions with the negative-charged nucleic sugar-phosphate structure, binding interactions with two grooves of DNA double helix, and intercalation between the stacked base pairs of native DNA. Most electrochemical sensors use different chemistries; and employ interactions between the target, the recognition layer and an electrode. We followed numerous approaches to electrochemical detection including direct electrochemistry of DNA and devices based on DNA-mediated charge transport chemistry. In direct electrochemical DNA sensors, the analysis is based on a guanine signal where a base-pairing interaction recruits a target molecule to the sensor, allowing monitoring of drug/biological molecule-DNA interactions, which are related to the differences in the electrochemical signals of DNA binding molecules for DNA barcoding. It is vital to develop sensing strategies to maintain critical dynamics of target capture to generate a sufficient recognition signal. Standard electrochemical techniques, such as differential pulse voltammetry (DPV), potentiometric stripping analysis (PSA), square-wave voltammetry (SWV), etc. are used as genosensors. Since genosensors are compatible with existing micro and nanofabrication technologies, they enable design of low-cost, devices that offer potential for detection and diagnosis of inherited diseases and potential for detecting pathogenic bacteria, tumors, genetic disease, and forensics via credit card-sized sensor arrays.

In the realm of biological threats, we conducted a study of functionalized self-assembled monolayer (SAM) as organized layer of amphiphilic molecules as biosensors that use biological molecules – usually enzymes, antibodies, or nucleic acids, to recognize simple molecules of interest via hydrogen bonding, charge-charge interactions, and other biochemical interactions to provide molecular information. Recent work on affinity biosensors to deliver real-time information about the antibodies to antigens, cell receptors to their glands, and DNA and RNA to nucleic acid with a complimentary sequence provide several applications.

In an effort to detect gas and vapors, response of a nanomaterials based gas sensor is studied based on reactions replacement of atoms at the sensing surface of these materials which relies on a change of the resistance of the oxide. Depending on the free electron density in the space charge layer, the depletion region is increased. Since electric properties are influenced by the depletion layer, variation

in electrical conductivity indicates sensor response. Similarly, moisture can influence the resistance or conductivity of oxide materials via two pathways: first, the adsorption of monolayer/s of water molecules at the surface; and second, the process of formation of a parallel resistance path by capillary condensation of water via adsorption of the water molecules as protons and hydroxyl groups within pores. The sensitivity and response of nanomaterials of metal-oxide sensors is highly dependent on the roughness of the substrate, which is caused by the increasing surface area and porosity of the film surface modifications in the film surface morphology. The sensitivity (and selectivity) of a sensor can be improved by parameters such as decreasing the crystallite size, the valence control, and using noble metal catalysts.

Carbon Nanotubes (CNTs) are conducting, can act as electrodes, generate electro-chemiluminescence (ECL) in aqueous solutions, and can be derivatized with a functional group that allows immobilization of biomolecules. CNTs have high surface/volume ratios for adsorption, and have surface/weight ratios ~300 m^2/g. The uniform chemical functionalization of CNTs is a key to the formation of biosensors. Oxidation of nanotubes with HNO_3-H_2SO_4 leads to high concentrations of carboxylic, carbonyl, and hydroxyl groups on a surface and removal of the tip to expose the tube interior. Carboxyl groups can readily be derivatized by a variety of reactions allowing linking of biomolecules such as proteins, enzymes, DNA, or even metal nanoparticles. The covalent modification of nanotubes facilitates the creation of well-defined probes, which are sensitive to specific intermolecular interactions of many chemical and biological systems. Integration of the transducer and probe enables quick, accurate, and reversible measurement of target analytes without reagents. NT-based electronic devices using sequence-specific attachment with molecular-recognition features of DNA have been studied.

Covalent modification of single wall CNTs (SWNTs) offers mapping of functional groups at a molecular resolution. Furthermore, chemical processes to link catalysts, such as transition-metal complexes, to the ends of CNTs are useful in creating or modifying the structures at a molecular scale, creating interconnections for electronic devices, and even developing new classes of materials. Covalent functionalization of the sidewalls of SWNTs provides stability and best accessibility; but at the expense of damaging the sidewalls; thereby diminishing the mechanical and electronic properties. However, non-covalent routes to CNTs functionalization offer ease of synthesis and minimum disruption of the tubular structure. During interaction with the polymer coatings, the electrical properties of the nanotubes are altered, enabling detection of the molecules leading to a very sensitive sensing mechanism. In addition to nanotubes, novel materials such as porous silicon [31] and porous carbon [32], with porosities of comparable dimensions to those of the biomolecules have been used for biosensor applications. The mesoporous carbon matrix is used for stable immobilization of the biological molecule, and C60 serves as an electron mediator. Both C60 and NTs are good electron mediators when used with a mesoporous carbon matrix or modified metal electrodes. CNT-based transducers, however, show a significant advantage over porous silicon due to defect free structures, and also because the NTs promote homogenous electron transfer reactions.

Investigations using SAM based SPR and Atomic Force Microscopy (AFM) techniques detect several pathogens. The SPR detection technique is rapid, real-time, and requires no labeling, and involves immobilizing antibodies by a coupling matrix on the surface of a thin film of precious metal, such as nanoparticles of gold deposited on the reflecting surface of an optically transparent wave-guide. The precise angle at which SPR occurs depends on several factors. A main response is the refractive index of the metal film, to which target molecules are immobilized using specific capture molecules or receptors along the surface, that cause a change in the SPR angle. This can be monitored in real-time by detecting changes in the intensity of the reflected light, producing a sensorgram. The rates of change of the SPR signal can be analyzed to yield apparent rate constants for the association and dissociation phases of the reaction. When the antigens interact with antibodies, the refractive index of the medium surrounding the sensor changes thus producing a shift in the angle of resonance proportional to the change in the concentration of antigens bound to the surface.

Sensor platforms, viz.: (a): chemo-mechanical micro-cantilever array to provide a quantitative and label-free platform for high-throughput multiplexed biomolecular analysis for detection of various biomolecules based on binding, (b): microarrays chips fabricated using technique matrix assisted pulsed laser evaporation (MAPLE) and laser induced forward transfer (LIFT) for deposition of biopolymers and a variety of biomolecules to detect dangerous gases, aerosols and micro-organisms, and (c): aligned-CNT probes for biomolecular recognition based on charge transport at the CNT transducer with the accuracy down to molecular level for quantitative and selective detection of a range of metabolites including cholesterol, ascorbic acid and uric acid, have been studied. Several other concepts being considered are resonance based [6] shock-wave generators that only could detonate military explosives but will also detect biological and chemical weapons. The shock wave can be used for targeted delivery of drugs, chemotherapy, and cure cells without affecting the whole body. Likewise, nanothermite – a composite of fuel and an oxidizer, which in turn generate combustion waves that can hit velocities ranging from mach 4–7, can safely be used for killing cancer cells. Using electrospinning, we have investigated nanofibers prepared from high performance polymer composites embedded with metal oxides, glasses coated with rare earth metals, and biocompatible compounds for sensing, and even controlling electrical, optical, and chemical and biological response (Fig. 1.3).

Satellites play a major role in communication, navigation, climatology, surveillance, and environmental monitoring, and support many applications. Nanophotonics and micro/nano electromechanical systems (MEMS/NEMS) hold the potential to revolutionize the field of satellite design for environmental pollution monitoring. We have conducted experiments with nanoscale metal-oxides sensors to detect pollution [17]. The sensors were connected to a personal digital assistant (PDA) with GPS and wireless communication capability and web-server. Using data from this prototype device, we have superimposed data from satellite to cross-reference the pollution coordinates.

A variety of nanomaterials have been studied for their abilities to detect and mitigate pollutants in air, water, and soil. We have investigated various ways in which nanomaterials can successfully be used to reduce/isolate atmospheric pollution,

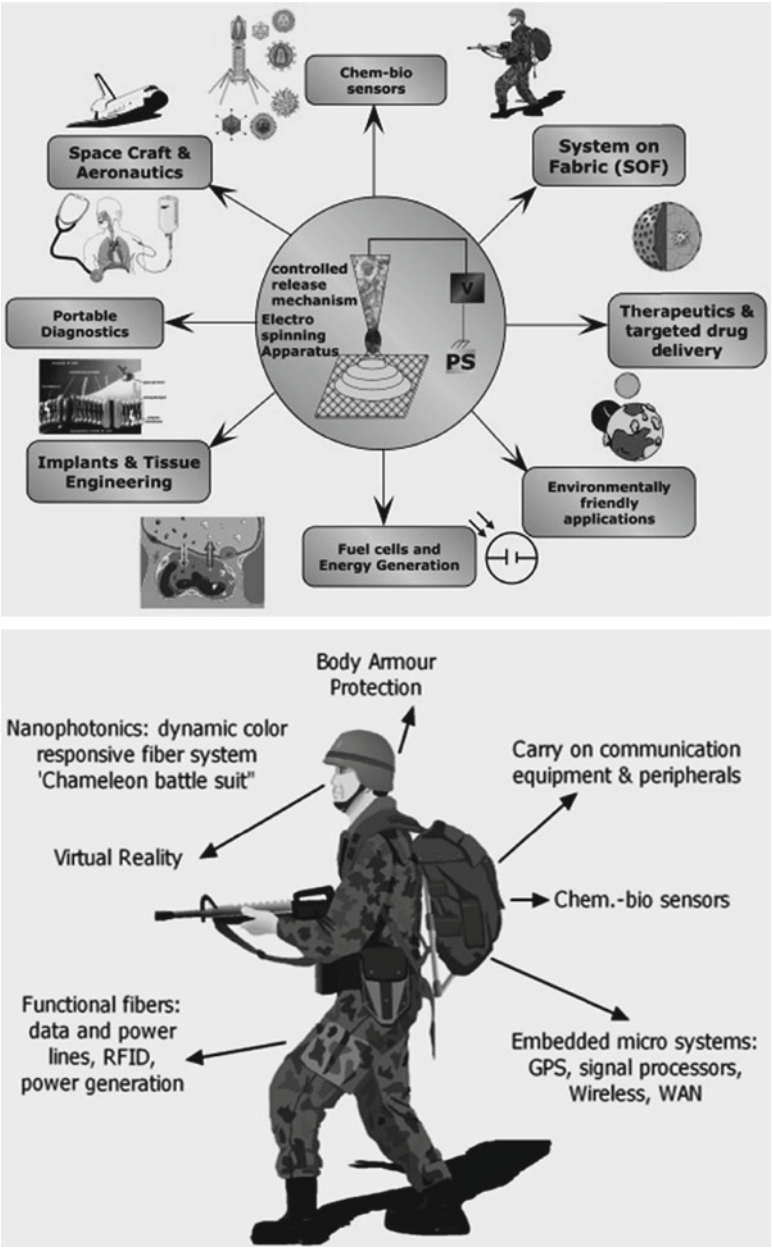

Fig. 1.3 Use of electrospinning for chem.-bio sensors, health and medicine [8]

such as use of CNT filled in a polymer composite matrix to create a static discharge to remove PM from incoming air, and chemical protective clothing, and breathing filtration masks. Employing immobilized TiO_2 films, produced by sol-gel process, we explored removal of indoor odors under weak UV illumination. At 10 ppmv,

weak UV light of 1 μW/cm^2 was sufficient to decompose such compounds in the presence of TiO_2 photocatalysts. In an experiment, 150 μl of an E. coli suspension, containing 30,000× cells was placed under weak UV (1 mW/cm^2) illuminated TiO_2-coated glass plate showing antibacterial effect [14].

The eradication of waterborne diseases is an overwhelming challenge. However, the devastating effects of infectious microorganisms may be minimized and controlled through efficient methods of monitoring and detection. Direct pathogen identification and isolation is difficult if not impossible. Indirect "indicator organism" based inferences have been used for decades as indicators of contaminated water. Traditional and standard bacterial detection methods for identifying waterborne pathogens are often not suitable for routine monitoring due to their high cost, inadequate sensitivity, or lengthy processing time. Moreover, all conventional methods require a priori knowledge of the pathogen. There is a growing global public health concern about the emergence and reemergence of waterborne microbial pathogens that occur through a complex interaction of social, economic, and ecological factors. Currently, indicators for water quality do not take into account new and emerging microbes. Astoundingly, only ~1% of microorganisms have actually been characterized; the spectrum of new disease is expanding, antimicrobial resistance is increasing, and waterborne diseases once believed to have been done away with are reemerging. Clearly, more effective methodologies are needed for monitoring and detection.

The advancement of molecular biology and its application in environmental microbiology will significantly advance rapid detection of waterborne microbial pathogens. Molecular biology-based alternative methods have improved the speed of detection from multiple days, as required for cell culture methods, down to a few hours. For example, real-time PCR allows for rapid (4–6 h) and specific detection of target genome and also yields quantitative estimation of the concentration of the microorganism in the water environment. Hand-held nucleic acid analyzers, miniaturized real-time thermal cycler, have been developed for real-time PCR detection of waterborne pathogens, such as *Cryptosporidium parvum* and *E. coli O157:H7*, with the cell culture-PCR to detect waterborne pathogens. The methods are relatively specific and will not detect all pathogens. However, molecular methods, coupled with high-throughput parallel process may detect microorganisms over a greater range.

1.5.1 Point and Stand-Off Detection/Sensor Platforms

In addition to advance and nanotechnology, we used the ASC approach along with TechFARM™, ADAMS™ and NESTTS™ to study chemical and biological sensors/detectors to equip war fighters with capabilities that are mostly transparent in operation; fully capable in the event of a chemical-biological attack; detect multiple agents in real-time with high specificity, selectivity, and sensitivity; transmit data to central location for situational awareness; and have the capability to re-generate

themselves. The overall goal is to develop an integrated system consisting of many sub-systems (some already developed) to sense/detect multiple chem-bio agents simultaneously. There are several challenges that must be overcome to bring such a system to reality: systems integration between nano/micro/macro; the possibility of synthetic biomolecules for which complex algorithms must be employed to decipher a complex environment; and dosage level issues, below which chemical agents do not produce noticeable effects. The two most important metrics for the sensing and transduction systems are time to detect concentration to enable appropriate response and response consistent with the species detected.

Given the complex environment described above, the challenges at subsystem levels occur to evaluate overall effectiveness and efficacy of the sensor systems. Nanotechnology based sensor platforms enable multiple sensing mechanisms to be incorporated on a platform – typically in a lab-on-chip (LOC) format. In addition to common sensing functions, the sensor and transduction system must demonstrate capabilities in the following areas: logistics, response to interference, response to unknown agents, low power consumption, weight/size, reagentless/low-reagent consumption, cross-validated response, secure signal transmission capability. Achieving such an autonomous system will require some additional advances in both nano and biotechnologies, particularly in the areas of energy storage and smart or self-healing materials to produce rugged, reliable, and effective response in the field. Critical technical challenges arise from the integration of self-healing materials and systems/platform integration.

1.5.1.1 Point Detection Platforms

Most of the platforms discussed in Sect. 1.5 require analysis based on sampling, hence are point contact. The analysis is accurate, real-time (in most cases), and conform to sensor metrics of specificity, selectivity, and sensitivity. However, due to the extreme nature of some chemical-biological agents, it is not always feasible to have either a direct or close contact with such environments. In such cases, stand-off detection systems are necessary.

1.5.1.2 Stand-Off Detection/Sensing Platforms

Ideally, a set of methodologies adopted to detect CBRNE agents and contamination should be amenable to both field and laboratory analysis, and provide fast, reliable, and real-time detection and differentiation of chemical, biological (e.g., bacteria, virus, pathogens), VOC, TIC/TIM, pharmaceuticals, and other contaminants at a distance. Generally, optical properties of nanomaterials are considered for stand-off detection/sensing applications when combined with biotechnology and quantum mechanics. Several other approaches include use of nanoparticles, more specifically, quantum dots for catalysis or carriers to enable transduction. A few examples are surface-enhanced Raman spectroscopy (SERS) and localized surface plasmon

resonance. Yet another application is in metamaterials or negative refractive index materials for potential applications in satellite imaging elements. Potential challenges arise in that the source of illumination must have sufficient light intensity with minimum power consumption. Further, intensity based measurements are susceptible to intensity-based noise in signals and require appropriate signal extraction software. Yet another stand-off detection methodology is generation of THz regime electromagnetic waves using carbon nanotubes (CNTs) that identify signatures in reflected/scattered beam of potential chemical-biological agents. Significant challenges still remain in the generation of high frequency using CNTs and also producing CNTs of same chirality. In almost all cases, signal transduction is one of the areas where revolutionary advances could be generated by leveraging NBIC convergence. Technologies that exploit the unique optical, electrical, and mechanical properties of nanomaterials, and find ways to efficiently couple those nanomaterials to sensing elements will be critical. Integration of the following functionalities of stand-off detection will further enhance their utility: multiplex, parallel processing sensors/actuators interface, battle space suits interface, war fighters status, alerts, and warnings, biotechnologies integration: antidote, prophylaxis, HPE administration, bioinformatics – multi-source fusion, machine learning and recognition: adaptive and self-reflective systems.

1.5.2 Bio-Inspired Systems, Biomimickry, and Opto/Bio-Cloaking

Nature offers a diverse wealth of responsive and multifunctional surfaces, whose properties are unmatched by current artificial materials. As we observe nature closely, many characteristics such as hydrophobic nature of lotus leaf, adhesive force of gecko, camouflage by animals, mechanical strength of spider web, etc., combined with better understanding of the characteristics of advanced and nanomaterials; it is feasible that nanomaterials may present some characteristics allowing us to mimic nature by the synergistic effect of materials formation and further complemented with surface functionalization. By the synergistic effect of laser induced texturing surface functionalization schemes, 3D structures exhibiting controlled dual-scale roughness which mimics the hydrophobic nature of the Lotus leaf, and also depending on the functional entities attached to the structures pH-, Photo-, Electro-, and Chemo-responsiveness can be obtained for microfluidic applications. By creating biomimetic siderophore analogues, Shanzer et al. [12] studied effects of iron-sequestering siderophores to extract scarce iron (III) and hence microorganisms from their environment, that involved arranging the hydroxamic acid moieties arranged along a linear chain, such as ferrioxamine B on three identical side arms in a tripodal arrangement such as ferrichrome, or more complex arrangements such as coprogen. The biomimetic siderophore analogues can also be designed for a particular bacterium to distinguish between related uptake systems of different microorganisms. Also, by employing "drop-on-demand" multiscale biotechnical engineering, three dimensional cell

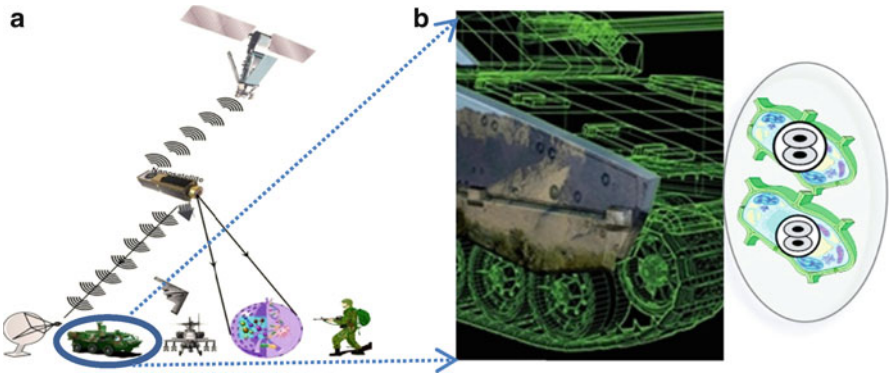

Fig. 1.4 (**a**) Optical cloaking and (**b**) Biomimickry – artist's rendition

structures of organotypic cell in conjunction with nanomaterials to replenish or replace certain protein compounds are likely to mimic cells the in-vivo environment allowing study of extracellular matrix (ECM), intercellular and cell-to-matrix interactions, and soluble factors and mechanical forces including microfluidic perfusion.

Furthermore, by integration of proteins with synthetic membrane materials, such as ABA triblock copolymer membranes (PMOXA-PDMS-PMOXA) of varied thicknesses as platform materials for Langmuir film-based functionalization with the OmpF pore protein from *E-coli* on the air/water interface, provides basis for bio-cloaking films for mimicry of cellular membrane surfaces toward the enhancement of implant biocompatibility. The field is relatively new and many other studies are in progress to see if biomimicking/bio-cloaking can enhance sensing/detection of chemical-biological agents, toward a wide spectrum of applications in nanoscale medicine, including high-throughput drug testing, energy conversion for powering medical devices, and defense application, as shown in Fig. 1.4a, b.

1.5.2.1 Persistent Surveillance of Emerging Diseases Patterns

The Term "Biosurveillance" is commonly referred to as the process of data gathering with appropriate analysis and interpretation of biosphere data that might relate to disease activity and threats to human or animal health – whether infectious, toxic, metabolic, or otherwise, and regardless of intentional or natural origin – in order to achieve early warning of health threats, early detection of health events, and overall situational awareness of disease activity. Because of international trade, travel, and migration patterns, pathogens can spread contagious diseases fairly rapidly. Hence, early warning and persistent surveillance to monitor any new infections or diseases, unintentional or otherwise, to map emerging patterns is a key security imperative to containment and remediation with minimum loss. Persistent surveillance requires increased CB (Cat.A-C) RN, Zoonotic and infectious disease detection/diagnostic

capabilities in fielded systems large pathogen collection and reference materials library, and the ability to integrate existing biosurveillance tools and data fusion capability to include medical and environmental information. Nanomaterials based sensors/detectors in conjunction with bioinformatics and other "omics" provide full-spectrum capability to ensure sustained public health and medical readiness to prepare against bioterrorism and infectious disease outbreaks.

1.6 Nanomaterials and Societal Concerns

Reduced dimensional aspect attributes that provide novel sensing characteristics are also believed to be responsible for bioadverse response pathways for toxicity of nanomaterials. Consequently, nanoparticle toxicity is studied in context of its ability to induce tissue damage through the generation of oxygen radicals, electron-hole pairs, and oxidant stress by abiotic and cellular responses resulting in pro-inflammatory, mitochondrial injury and pro-apoptotic cellular effects in the lung, cardiovascular system and brain [34]. It is further believed that nanoparticles absorb cellular proteins which could induce protein folding and thiol cross-linking; leading to neuro-toxicity and reduced enzymatic activity. Nanoparticles which are cationic in nature are also believed to induce toxicity via acidifying endosomes that lead to cellular toxicity and apoptosis in epithelial lung through endosomal rupture through proton sponge mechanism (PSM), mitochondrial targeting, and cytosolic deposition. Nanomaterials composed of redox-active elements are particularly reactive and can possibly provoke potentially damaging chemical transformations. Furthermore, even chemically benign nanoparticles may become activated by light absorption. It is thus essential to investigate the long-term consequences of NPs upon crossing blood-brain-barrier (BBB) and its distribution in cortex and hippocampus over time to ensure their safety (nanosafety) using a set of tools termed as Nanopathology, such as x-ray fluorescence microscopy (XFM) for distribution, magnetic resonance imaging (MRI) to measure metal concentrations in cerebrospinal fluid, etc. One approach to determining the safe application of nanomaterials in biology is to obtain a deep mechanistic understanding of the interactions between nanomaterials and living systems (bio-nano-interactions).

Our previous studies have shown that due to the formation of high-temperature combustion processes during detonation, combustion, and explosion of weapon systems, nano-sized airborne pollution is created and released in the immediate environment that is likely to contaminate humans, animals and surroundings depending upon air-currents and other atmospheric conditions. Likewise in some parts of Europe and China, unfiltered burning and recycling of e-waste is creating release of metal nanoparticles along with obnoxious hydrocarbons, and volatile organic compounds (VOCs). Nanopathology – a novel diagnostic tool through which we can show the presence of micro- and nano-sized inorganic particles in pathological tissues of unknown aethiology, thus demonstrating the exposure and the dispersion of the environmental pollution in the human body. Experiments were also conducted

using Field Emission Gun Environmental Scanning Electron Microscope and Energy Dispersive Spectroscopy. Earlier results of this preliminary investigation warrant further investigations of the role of nanoparticles in the human health. We also are looking into extension of our studies for disease surveillance of possible dual-use of nanoparticles in case of domestic/international terrorism and war activities, in addition to investigating sites with high emission of carcinogenic nanoparticles. Our investigation in conjunction with high-spectral imaging will serve as a tool for disease surveillance by means of identification of new biomarkers of pathology and tracking, and in the future for new forms of customized medicine for nanodetoxification. The study of fate and transport of nanomaterials via a matrix of parameters such as exposure routes, chemical composition, distribution, metabolism, and agglomeration and excretion rate provide a comprehensive overview of interaction pathways. An ontological modality is used to identify its relationship to other items in the lexicon; viz. to enable information retrieval from various sources, databases, and via expert elicitation. Other contributing factors range from biodegradation and bioaccumulation, thermodynamic properties, interfaces, and free energy of nanoparticles as a function of particle size, composition, and phase and crystallinity influence particle dissolution in a biological environment. The accumulation, dispersion, and functional surface groups play an important role in cytotoxicity and in evaluating pathways of cellular uptake, subcellular localization, and targeting of subcellular organelles. Hence, fundamental understanding of a nanomaterial-surrounding medium is vital to sustaining technological advances of nanoscale materials as catalyst for new scientific and technological avenues.

1.7 Conclusion, Discussion, and Path Forward

More in-depth study of nanotechnology will help understand how to bridge length and time scales from atoms and molecules to complex structure and devices, and promises revolutionary abilities to sense and respond effectively to CBRNE threats. Nanomaterials are enabling technologies for situational awareness, C4ISR, and "infospheres" comprised of data from sensors, actuators, communications interfaces, alerts and warnings; and antidotes and prophylaxis. Nanotechnologies-based systems have demonstrated sensitivity, selectivity, and specificity towards chemical-biological materials and may also be prepared to attract specific molecular configurations. The challenge lies in identification of synthetic biomolecules. From the convergence standpoint, nanotechnologies play an integral and vital part in hardware implementation. Sensors interfaced with biotechnology domains play a significant role and may even overlap with cognitive sciences domain. Sensors/actuators systems consisting of additional components, such as nanoantennas will demonstrate massive connectivity. To achieve "ideal" sensor platforms, many questions remain at the material level. In view of ever increasing complexity and unpredictable nature of threat vectors, it is crucial to utilize advanced technologies in conjunction with ASC, as countermeasures.

References

1. Vaseashta A, Dimova-Malinovska D, Marshall J (2005) Nanostructured and advanced materials. Springer, Dordrecht
2. Vaseashta A, Mihailescu I (2007) Functionalized nanoscale materials, devices, and systems. Springer, Dordrecht
3. Magarshak Y, Sergey K, Vaseashta A (2009) Silicon versus carbon. Springer, Dordrecht
4. Vaseashta A (2012) The potential utility of ASC – analytic methods to depict, assess, and forecast trends in neuroscience and neurotechnologic development(s), and use(s). In Giordano J (ed.) Advances in Neurotechnology: premises, potential and problems. (Vol. 1, Advances in neurotechnology: ethical, legal and social issues series, Giordano J, Series Editor). CRC Press, Boca Raton, 2012.
5. Erdem A (2008) Electrochemical sensor technology based on nanomaterials for biomolecular recognition. In: Vaseashta A, Mihailscu IN (eds) Functionalized nanoscale materials, devices, and systems. Springer, Dordrecht
6. Pokropivny V, Pokropivny P, Vaseashta A (2005) Ideal nano-emitters and panel nano-devices based on 2D crystals of superconducting nanotubes. In: Vaseashta A et al (eds) Nanostructured and advanced materials. Springer, Dordrecht, pp 367–370
7. Denkbas E et al (2012) Nanoplatforms for detection, remediation, and protection against chem-bio-warfare. In: Vaseashta A, Braman E, Susman P (eds) Technological innovations in sensing and detection of chemical, biological, radiological, nuclear threats and ecological terrorism. Springer, Dordrecht
8. Vaseashta A, Stamatin I (2007) Electrospun polymers for controlled release of drugs, vaccine delivery, and system-on-fibers. J Optoelectron Adv Mater 9(6):1506–1613
9. Petrov A (2012) Disposable membrane sensors for biohazardous substances. In: Vaseashta A et al (eds) Technological innovations in sensing and detection of chemical, biological, radiological, nuclear threats and ecological terrorism. Springer, Dordrecht
10. Erdem A (2012) Nanomaterials based sensor development towards electrochemical sensing of biointeractions. In: Vaseashta A et al (eds) Technological innovations in sensing and detection of chemical, biological, radiological, nuclear threats and ecological terrorism. Springer, Dordrecht
11. Wang J (2003) Nanoparticle-based electrochemical DNA detection. Anal Chem Acta 500:247
12. Shanzer A, Felder CE, Barda Y (2009) Natural and biomimetic hydroxamic acid based siderophores. In: Patai's chemistry of functional groups. Wiley, Hoboken
13. Guidotti M et al (2011) Nano-structured solids and heterogeneous catalysts: powerful tools for the reduction of CBRN threats. In: Vaseashta A et al (eds) Technological innovations in sensing and detection of chemical, biological, radiological, nuclear threats and ecological terrorism. Springer, Dordrecht
14. Vaseashta A, Riesfeld R, Mihailescu I (2008) Green nanotechnologies for responsible manufacturing. In: MRS 2008 Spring Proceedings, vol 1106/1106-PP03-06, Published online by Cambridge University Press
15. Vaseashta A et al (2011) NBIC, GRAIN, BANG, and TechFARM– ASC for Surveillance of Emerging S&T Trends, Proc. of the 4th Int'l Seville Conf. on Future Oriented Technology Analysis, May 2011
16. Vaseashta A, Erdem A, Stamatin I (2006) Nanobiomaterials for controlled release of drugs & vaccine delivery. MRS 2006 Spring Proceedings, Vol 920, Jan 2006, pp 0920-S06-06 doi: 10.1557/PROC-0920-S06-06, Published online by Cambridge University Press 01 Feb 2011
17. Pumakaranchana O, Phonekeo V, Vaseashta A (2008) Semiconducting gas sensors, remote sensing technique and internet GIS for air pollution monitoring in residential and industrial areas. In: Vaseashta A, Mihailescu I (eds) Functionalized nanoscale materials, devices and systems. Springer, Dordrecht
18. Vaseashta A et al (2007) Nanostructures in environmental pollution detection, monitoring, and remediation. Sci Technol Adv Mater 8:47–59

19. Tripathi RD et al (2007) Arsenic hazards: strategies for tolerance and remediation by plants. Trends Biotechnol 25(4):158–165
20. Hagan N et al (2011) MALDI mass spectrometry for rapid detection and characterization of biological threats. ACS Symp Ser 1065:211–224. doi: 10.1021/bk-2011-1065.ch012. ISBN13: 9780841226128, eISBN: 9780841226135, Publication Date (Web): June 6, 2011. Copyright © 2011 American Chemical Society
21. Krebs MD, Zapata AM, Nazarov EG, Miller RA, Costa IS, Sonenshein AL, Davis CE (2005) Detection of biological and chemical agents using differential mobility spectrometry (DMS) technology. IEEE Sens J 5(4):696–703
22. Khuri-Yakub BT et al (2007) The Capacitive Micromachined Ultrasonic Transducer (CMUT) as a chem/bio sensor. IEEE Ultrasonics Symposium, New York, pp 472–475
23. Swim CR (2004) Sources for standoff chem-bio detection, Unclassified Report. U.S. Army edgewood chemical biological center, Aberdeen Proving Ground
24. Saito Y et al (2001) Possibility of hard-target lidar detection of a biogenic volatile organic compound, ν-pinene gas, over forest areas. Appl Opt 40(21):3572–3574
25. Killinger D (2003) Optics in chemical and biological weapons detection. Defense section of Optics Report, on-line Journal: www.opticsreport.com. 19 Aug 2003
26. Wild D (2005) The immunoassay handbook. Elsevier, Kidlington
27. Erdem A, Karadeniz H, Caliskan A, Vaseashta A (2008) Electrochemical DNA sensor technology for monitoring of drug–DNA interactions. NANO: Brief Rep Rev 3(4):229–232
28. Barbini R, Colao F, Fantoni R, Lazic V, Palucci A, Capitelli F, van der Steen HJL (2000) Laser induced breakdown spectroscopy for semi-quantitative elemental analysis in soils and marine sediments. In: Proceedings of EARSeL-SIG-Workshop LIDAR, Dresden/FRG, 1, 16–17 June 2000
29. Tamer F et al (2008) Lidar backscatter signal recovery from phototransistor systematic effect by deconvolution. Appl Opt 47(29):5281–5295
30. Eccleston JF et al (2005) Fluorescence-based assays. Prog Med Chem 43:19–48
31. Schmedake T, Cunin F, Link J, Sailor M (2002) Standoff detection of chemicals using porous silicon "Smart Dust" particles. Adv Mater 14:1270
32. Lee J, Kim J, Hyeon T (2006) Recent progress in the synthesis of porous carbon materials. Adv Mater 18(16):2073–2094
33. Vaseashta A (2008) In: Linkov I et al (eds) Risk, uncertainty and decision analysis for nanomaterials: environmental risks and benefits and emerging consumer products. Springer, Dordrecht
34. Kikkeri R et al (2007) Toward iron sensors: bioinspired tripods based on fluorescent phenol-oxazoline coordination sites. Inorg Chem 46(7):2485–2497

Chapter 2
Emerging Technologies: Biosecurity and Consequence Management Implications

Biosecurity and Consequence Management

Dana Perkins and Brian Nordmann

Abstract The natural outbreaks of disease and pandemics are transnational threats that create international challenges when detection and containment are not timely due to scarce human and material resources. Whether the cause of those outbreaks is natural or intentional in origin, the main goal of consequence management operations is to save lives. The consequence management process is a continuum of inter-connected phases such as planning, preparation, response, and recovery. The rapid advances of life sciences and the emergence of dual-use technologies such as synthetic biology and nanotechnology pose additional challenges in terms of planning for the unknown potential threats whether they may be synthetic microorganisms with unpredictable dissemination patterns or nanoscale-manipulated biological agents evading current detection capabilities. The US National Strategy for Countering Biological Threats is emphasizing prevention while continuing to support the national preparedness goals and response/recovery capabilities. The recent policies, guidelines, and recommendations on overhauling the biological risk management in the United States are a proactive stance to a rapidly changing global environment. They include optimization of the current oversight frameworks and active engagement of the industry and academia in order to reduce the risk that individuals with ill intent may exploit the commercial application of nucleic acid synthesis technology to access genetic material derived from or by encoding Biological Select Agents or Toxins. We are also actively seeking to increase our knowledge of health effects of various types of nanomaterials, and how to assess, control, and prevent harmful exposure, taking into consideration the numerous gaps

D. Perkins (✉)
US Department of Health and Human Services, Office of the Assistant Secretary for Preparedness and Response, Washington, DC, USA
e-mail: dana.perkins@hhs.gov

B. Nordmann
U.S. Department of State, 2201 C. St. NW, Washington, DC, USA

A. Vaseashta et al. (eds.), *Technological Innovations in Sensing and Detection of Chemical, Biological, Radiological, Nuclear Threats and Ecological Terrorism*, NATO Science for Peace and Security Series A: Chemistry and Biology,
DOI 10.1007/978-94-007-2488-4_2, © Springer Science+Business Media B.V. 2012

that currently exist with regard to the distinct behavior of nanoparticles compared to the same chemical or material at "macro-scale". Fundamentally, a biological incident, whether it is of natural, accidental, or deliberate origin, constitutes a public health problem and the United States is engaged with the international community to enhance our collective capability to address emerging health security threats.

Keywords Synthetic biology • Nanotechnology • Biosecurity

2.1 Harnessing the Power of the Microbe

The field of "life sciences" research includes numerous integrated and related areas of scientific inquiry which deal with understanding life at the level of ecosystems, organisms, biological systems, organs, cells, and molecules. The last 50 years were marked by significant achievements in this field; in particular microbiology, agricultural science, botany, animal science, bioinformatics, genomics, proteomics, synthetic biology, environmental science, public health, pharmacodynamics, modeling, statistics, and all applications of the biological sciences disciplines and methodologies. Arguably the most significant enabler of this progress was the inter-disciplinary collaboration among life- and non life-scientists and the blurring of border lines delineating particular fields of expertise. A microbiologist, for instance, may now call herself (or himself) a "geneticist", "environmental scientist", "bioinformatician", "pharmacologist", or a plethora of other names, based on the various applications of microbiology. She (he) could no longer be faithfully represented by a Louis Pasteur-like figure but by the "Hive Mind" of scientific enterprise empowered by technology and catalyzed by the Wiki-style collective intelligence. Like the fictional Borg in the *Star Trek* universe, scientists are continuously adapting and assimilating the current body of knowledge in pursuit of higher achievements.

In architecture, Antoni Gaudi (1852–1926) transcended the Modernist-style by "borrowing" elements from nature and striving to integrate materials, processes and poetry in his work, creating the most audacious and innovative organic concepts in his architectural masterpieces. From basic science to industrial application, we are now seeing biology-inspired technologies revolutionizing the areas of food, environment, energy, and health.

The field of "biomimicry" brings together biologists, engineers, and designers in an attempt to solve some of the world's grand challenges. For example, harnessing the viruses' ability to target specific tissues and deliver their genetic payload, they are now used as "carriers" of gene therapeutics [1], and bacteria are studied for powering fuel cells [2] or cleaning up the environment of pollutants. In 1994, a "DNA computer" was used to solve a mathematical problem, called the directed Hamilton Path problem (aka " the traveling salesman" problem, finding the shortest route between a number of cities, going through each city only once) [3].

Undergraduate students in The International Genetically Engineered Machine (iGEM) Competition [4] were able to solve even more complex Hamilton Path

challenges by manipulating the DNA of the *Escherichia coli* bacteria [4]. Already scientists are talking about "biochips" replacing the traditional silicon-based microprocessors and taking computing to new levels where the Moore's Law leaves off. Judging from the sophistication and innovative thinking of the iGEM projects, they foreshadow life sciences future.

The biotech revolution was supported by the discovery and advancement of high-throughput genome sequencing tools and resources spurred by the initiation (and 2003 completion) of the human genome undertaken by the International Human Genome Sequencing Consortium (i.e. the "Human Genome Project") [5]. Humans and microbes, we all have the genetic potential for adapting to particular environmental circumstances via traditional (structural gene changes) or epigenetic mechanisms (changes in gene expression without altering the genetic information). A human being is intimately connected with the microbiome and the understanding of our co-existence with the complex microbial community and how it affects our genotype-phenotype connection has the potential of significant achievements in personalized medicine applications.

The traditional way of doing biology, by observation and by dissection, is now being complemented by an engineering approach, modifying and building biological systems from standardized parts. The field of synthetic biology and its convergence with nanotechnologies could lead to well-characterized biologically inspired systems with predictable properties and functions. As Drew Endy put it, "Engineers hate complexity. I hate emergent properties. I like simplicity. I don't want the plane I take tomorrow to have some emergent properties while it is flying" [6]. We are thus moving beyond the passive reading of genetic code into writing and editing it… The assembly of artificial biological systems (both self-replicating and non-self-replicating) that perform desired functions in a predictable manner is now a reality. For example, infectious poliovirus was produced by chemical synthesis [7], the 1918 influenza virus was "resurrected" by reverse genetic engineering [8], and the bacterium Mycoplasma mycoides was "jumpstarted" to life with a man-made genome of about 850 genes [9].

New tools and the convergence of molecular biology, chemistry, applied physics, and nanoengineering in life sciences enable scientists "to boldly go where no man has gone before": manipulation of living systems at the molecular level. For example, quantum dots (QDs) are now used for individual molecule labeling and real-time visualization of biological processes [10, 11] and single-molecule, real-time DNA synthesis could be visualized by using the zeromode waveguide (ZMW) nanofabricated hole [12]. The DNA can serve as a scaffold for complex nano-scale machinery. These DNA origami scaffolds are packed with man-made synthetic sequences that could be used to position DNA-binding molecules or nano-circuits such as in plasmonic devices. The DNA origami are envisioned to enable the creation of artificial ribosome producing custom enzymes, matrices for supporting artificial organs, or a DNA origami network designed to support a neuronal network connected to electrical circuitry [13].

Nano-biotechnology is no longer confined to the research laboratory but has found its way into pioneering the frontiers of life sciences applications by using

nanofabricated materials and devices to study and engage with biological systems at subcellular and molecular levels. These rapid advances of science and the tremendous insight they confer into life processes as well as the uncertainty of predicting scientific discovery, also spurred ethical concerns about tinkering with life and its creation. Such ethical concerns are beyond the scope of this paper but the authors personally subscribe to the thinking of Antoni Gaudi who once said *"The creation continues incessantly through the media of man. But man does not create… he discovers"*.

2.1.1 Quo Vadis, Biotech?

Harnessing the power of the microbes and the human ability to "think big" at nano-level, could potentially change at the fundamental level how we power the economy, provide food resources, sustain the environment, and improve the health of people, animals, and plants. Creating "green" microbial factories for chemicals, complex recombinant proteins, or fuels, is a strong impetus for the field of synthetic biology, in particular for the creation of novel microorganisms using synthetic DNA made from off-the-shelf chemicals. Environmental challenges could be tackled by using engineered or synthetic bacteria to absorb heavy metals, detect contaminants with biosensors, produce fuels using sunlight and carbon dioxide, and converting industry waste to carbon dioxide or water. The microbes could power sensors in harsh or remote settings or self-sustaining robots that "eat" organic waste to generate their own power.

Similarly, nanotechnology applications in medicine are only limited by our imagination and may include enhanced prosthetics, nano-structured implants/scaffolds for tissue regeneration, *in vivo* nano-sensors or nano-sized "physician" assistance (delivering treatments at the site of diseased tissue or cell), nano-enhanced physical and cognitive performance, and exploiting the quantum effects to create "smart" nano-materials, bionics, biomimetics, neuromorphic engineering, and brain-machine interface systems.

2.2 The Dual Use Dilemma

Whether by design or as an inadvertent consequence, life sciences results could have a deleterious effect on the health of people, animals, plants, and the environment. The ability of microbes to adapt to environmental conditions and the lack of predictability when bacteria designed for remediation are transferred to natural environments emphasize the importance of standardization principles emphasized by synthetic biology but also constitute an example of inadvertent harmful consequences (e.g. catastrophic ecological collapse) which may arise from well-intended research.

For the military, biotechnologies can provide opportunities for new types of battlefield sensors, improving military medicine and enhancing human performance, microbial manufacturing of vaccines and nutrients, use of novel portable power sources, bio-based decontamination technologies and textiles, and biomimicry-inspired forms of camouflage and concealment.

Unfortunately, the same "Hive Mind" of collective intelligence may be misused for nefarious purposes and could enable the creation of asymmetric advantages and the ability to render existing threat mitigation capabilities irrelevant. For example, genetic sequences for assembling novel biological agents to be used as weapons, could be purchased from gene foundries, chimeric agents can be created by genetic engineering or synthetic means, and tinkering with microbial metabolic pathways could lead to the production of novel chemicals which are not regulated by domestic measures or international agreements. On the battlefield, swarms of miniature bio-powered robots with stealth technology (employed as IEDs) could prove challenging for the future warrior as they may be difficult to defeat or detect. Nanotechnology-based future scenarios involve the next generation of explosives or neuro-cognitive warfare with significant potential impact on optempo and force protection.

Biology is no longer confined to the research laboratories but taken as a hobby by enthusiasts and practiced in garages, kitchens, and living rooms. So the next biological weapon could be produced not by a State-sponsored program but by an individual tinkering in his own garage.

The availability of technologies and materials coupled with the rapid pace of scientific developments and the convergence of previously distinct scientific fields, constitute a challenge to the traditional institutional and regulatory frameworks addressing the dual use dilemma.

2.2.1 Governance Options for Dual Use Research of Concern

Although the misuse of dual use research is likely a low-probability event, potential consequences of misuse are high. Based on recommendations of the National Science Advisory Board for Biosecurity (NSABB),[1] the U.S. Government is working on developing guidelines for the oversight of life sciences research with dual use potential. The draft Guidelines on Oversight of Life Sciences Research with Dual Use Potential are envisioned to set forth standards for oversight and articulate specific responsibilities, but they incorporate maximal flexibility as to how those

[1]The NSABB is a Federal advisory committee providing advice to the Secretary of Health and Human Services, the Director of the National Institutes of Health, and the heads of all Federal entities that conduct, support or have an interest in life sciences research. The purpose of the NSABB is to provide, as requested, advice, guidance, and leadership regarding biosecurity oversight of dual use research, defined as biological research with legitimate scientific purpose that may be misused to pose a biologic threat to public health and/or national security. Additional information on the NSABB can be found at www.biosecurityboard.gov

standards and responsibilities are met at the local level.[2] The Guidelines also emphasize that the default position should be the responsible conduct and communication of dual use research, and that in only the rarest of instances, if ever, would it be appropriate to not conduct or not communicate research because of dual use concerns. Therefore, the expectation is that oversight of life sciences research with dual use potential will not significantly impede the conduct and pace of the science, and that when dual use risks are identified, they can be responsibly managed.

Current efforts of governance of dual use research of concern are focused on scientists operating within a university or institutional setting. As such, other communities or individuals such as those practicing experiments at home as a hobby or established scientists not considering themselves "life scientists" or lacking appropriate training of biological risk management, may not be reached. Thus, raising awareness within the society as a whole about the possible biological risks and the need for the responsible conduct of research and increased vigilance will be critical.

President Obama recently articulated his vision to prevent the proliferation of biological weapons and bioterrorism, in the National Strategy for Countering Biological Threats[3] The Strategy has a clear, over-arching goal toward which all of us could significantly contribute to: PROTECT against the misuse of the life sciences:

- Promote global health security: Activities that should be taken to increase the availability of and access to knowledge and products of the life sciences that can help reduce impacts of outbreaks of infectious disease whether of natural, accidental, or deliberate origin.
- Reinforce norms of safe and responsible conduct: Activities that should be taken to reinforce a culture of responsibility, awareness, and vigilance among all who utilize and benefit from the life sciences to ensure that they are not diverted to harmful purposes.
- Obtain timely and accurate insight on current and emerging risks: Activities that serve to improve threat identification, notification, and assessment capabilities as well as our understanding as to the global progress and presence of the life sciences to help identify and understand new and emerging challenges and inform appropriate actions to manage the evolving risk.
- Take reasonable steps to reduce the potential for exploitation: Activities that are targeted to identify, sensitize, support, or otherwise safeguard knowledge and capabilities in the life sciences and related communities that could be vulnerable to accidents or misuse.
- Expand our capability to prevent, attribute, and apprehend: Activities that are intended to further hone the Nation's ability to identify and stop those with ill intent to reduce the risk of single, multiple, or sequential attacks.

[2] National Science Advisory Board for Biosecurity, *Proposed Framework for the Oversight of Dual Use Life Sciences Research: Strategies for Minimizing the Potential Misuse of Research Information* (Washington, DC: June 2007), oba.od.nih.gov/biosecurity/biosecurity_documents.html

[3] *National Strategy for Countering Biological Threats* available at: http://www.whitehouse.gov/sites/default/files/National_Strategy_for_Countering_BioThreats.pdf

- Communicate effectively with all stakeholders: Activities that should be conducted to ensure the Federal Government is advancing cogent, coherent, and coordinated messages.
- Transform the international dialogue on biological threats: Activities targeted to promote a robust and sustained discussion among all nations as to the evolving biological threat and identify mutually agreed steps to counter it.

2.2.2 *E Pluribus Unum: State Parties to the Biological Weapons Convention and the Unity of Biosecurity Mission*

The Biological Weapons Convention (BWC), formally known as the Convention on the Prohibition of the Development, Production and Stockpiling of Bacteriological (Biological) and Toxin Weapons and on Their Destruction (aka the Biological and Toxin Weapons Convention), was the first multilateral disarmament treaty that banned the production and use of an entire category of weapons. It was opened for signature on April 10, 1972, and entered into force on March 26, 1975.

The BWC Member States hold Review Conferences every 5 years (1980, 1986, 1991, 1996, 2001, 2006 – next one in 2011). Between these review conferences States Parties have pursued various activities and initiatives to strengthen the effectiveness and improve the implementation of the Convention. For example, the 6th Review Conference created the 2007–2010 intersessional process which consists of 4 sets of annual meetings prior to the 7th review Conference (each set includes a 1 week Meeting of Experts, followed by a 1 week Meeting of States Parties); established the Implementation Support Unit (ISU); established an action plan for universalization and improving national implementation; improved the CBM information exchange process; worked on enhancing provision of assistance; and built a network of national points of contact.

While disagreements on various issues still exist within the BWC forum, bioterrorism prevention, improvement of laboratory biosafety/biosecurity and fostering a culture of responsibility in the life sciences with respect to dual use biological science and technology as well as building public health capacity to respond to man-made or natural incidents or hazards were topics of common interest among BWC Member States in the 2007–2010 inter-sessional process.

2.2.3 *NATO Science for Peace and (Bio) Security Programme*

NATO *Science for Peace and Security Programme* (SPS) aims to contribute to security, stability and solidarity among nations, by applying the best technical expertise to problem solving. At a time when biological threats are reaching an unprecedented level on the global "concern scale" and they require a customized political, scientific, and operational approach, this program could have a significant impact on

countering biological threats by transcending into a "*Science for Peace and (BIO) Security Programme*". The areas of focus are already generally defined in the current SPS programme e.g. *Defence against terrorist threats* (*Study of human factors in defence against terrorism*) and *Countering other threats to security* (*Human and societal dynamics*; *Biotechnology/bioscience* not related to CBRN events).

The NATO group of experts that worked on revising the NATO's new strategic concept called on the Alliance *"to become more versatile to face new dangers from sources that are geographically and technologically diverse"*. This is an obvious call for technical solutions and situational awareness of the relevant scientific advancements. The revision of NATO's Strategic Concept is an opportunity to define NATO's role in combating bioterrorism, not only in offering assistance post-event but also in positioning itself as a network for support and assistance in national preparedness planning, civil-military integration in emergency response, and empowering civil society to get involved in national security policy development, public education, promoting a culture of security awareness, and strengthening communities' resilience to bioterrorism. By shifting its focus to prevention instead of response and by addressing non-state threats in synergy with other relevant organizations and stakeholders, NATO could strengthen the array of mutually enforcing elements that comprise the global web of bioterrorism deterrence.

The distinctive challenges of countering biological threats could not be effectively tackled without in-house scientific expertise and mobilization of the NATO "Hive Mind" of scientific intelligence. As John F. Kennedy once said: "*The problems with this world cannot possibly be solved by skeptics or cynics whose horizons are limited by the obvious realities. We need people who can dream of things that never were.*"

Disclaimer The views, opinions, findings, and conclusions expressed in this paper are those of the authors and do not necessarily represent the views of the Department of Health and Human Services or its components, or the official policy or position of the Department of State, or the U.S. Government.

References

1. Perkins D (2005) Virus signaling and apoptosis in the central nervous system. Front Biosci 10:2804–2819
2. Chaudhuri SK, Lovley DR (2003) Electricity generation by direct oxidation of glucose in mediatorless microbial fuel cell. Nat Biotechnol 21:1229–1232
3. Adleman L (1994) Molecular computation of solutions to combinatorial problem. Science 266:1021–1024
4. iGEM website: http://2010.igem.org/Main_Page. Accessed 7 Aug 2010
5. International Sequencing Consortium website: http://www.intlgenome.org. Accessed 7 Aug 2010
6. Soft Machines website: http://www.softmachines.org/wordpress/?p=389. Accessed 7 Aug 2010
7. Cello J et al (2002) Chemical synthesis of poliovirus cDNA: generation of infectious virus in the absence of natural template. Science 297:1016–1018
8. Tumpey TM et al (2005) Characterization of the reconstructed 1918 Spanish influenza pandemic virus. Science 310(5745):77–80

9. Gibson DG, Glass GI et al (2010) Creation of a bacterial cell controlled by a chemically synthesized genome. Science 329(5987):52–56
10. Bruchez M Jr, Moronne M, Gin P, Weiss S, Alivisatos AP (1998) Semiconductor nanocrystals as fluorescent biological labels. Science 281(5385):2013–2016
11. Chan WCW, Nie S (1998) Quantum dot bioconjugates for ultrasensitive nonisotopic detection. Science 281(5385):2016–2018
12. Eid J, Fehr A, Gray J, Luong K, Lyle J, Otto G, Peluso P, Rank D, Baybayan P, Bettman B et al (2009) Real-time DNA sequencing from single polymerase molecules. Science 323:133–138
13. Sanderson K (2010) What to make with DNA origami. Nature 464:158–159

Chapter 3
Bio-Inspired Computing, Information Swarms, and the Problem of Data Fusion

Bio-Inspired Computing

Brian Nordmann*

Abstract The problem of information overload becomes a huge challenge, particularly when attempting to understanding how to introduce more and more disparate data streams into a data system. Little has been done on how to make those data streams understandable and usable by an analyst. A new paradigm is constructed here, unconstrained by the limits of the current desktop computer, to develop new ways of processing and analyzing data based on the behavior of cellular scale organisms. The additional issue of analytic "groupthink" or "information swarms" is also addressed, with potential solutions to the problem of "paralysis by analysis."

Keywords Bioinspiration • Biomimicry • Bioderivation • Computation • Information swarms

3.1 Introduction

Information is the new coin of the realm. The amount of information available on all subjects has markedly increased. A study by the University of California- San Diego found that, on average, Americans hear, see, or read 34 gigabytes of information a day – about 100,000 pages of information a day. That number has increased by about 5% annually since 1980 [1]. The analyst trying to make sense of this data onslaught is fighting a losing battle. The answer thus far has been one of brute force: the rate increase in available information does not yet equal the rate of computer

*This paper is the sole responsibility of the author and may not reflect the views of the U.S. Department of State or the U.S. Government.

B. Nordmann (✉)
U.S. Department of State, 2201 C St, NW, Washington, DC 20520, USA
e-mail: nordmabr@state.gov

A. Vaseashta et al. (eds.), *Technological Innovations in Sensing and Detection of Chemical, Biological, Radiological, Nuclear Threats and Ecological Terrorism*, NATO Science for Peace and Security Series A: Chemistry and Biology,
DOI 10.1007/978-94-007-2488-4_3, © Springer Science+Business Media B.V. 2012

speed as calculated by Moore's Law [2], therefore, to the computer hardware specialist, there is no problem necessitating a solution. The ability of an analyst to make sense of all this information is critical for national security. Information is needed to be accurate, reliable, and timely. Data needs to be usable. Data is no longer managed as a single piece of information. The interrelationship of one piece of data with other data has new importance.

Today, metadata has taken precedence. Metadata can be defined as all the information associated with a single piece of information. Consider the sentence "The quick, brown fox jumped over the sad, lazy dog" as a collected observation. A fox was observed; brown in color and quick. Presumably it was timed to determine its quickness. What exactly was its speed? There was also a dog – lazy but of unidentified color. It was observed long enough for the observer to know it was lazy; the length of observation should be noted. Why no color? Where did the jumping occur? Where was the observer in relation to the event? What were the meteorological conditions? The answer to each one of those questions could be considered a piece of metadata, which could be stored and tracked on a computer to support future analysis. They call that storage "memory" but it's a far cry from what we mean when we refer to human memory.

The human eye sees the fox jumping over the dog as a single event. It is entirely possible that the human ear hears the sound of the interchange between the fox and dog before the animals are in sight. The brain may need to determine that it is a dog and a fox, and not a fox and a log or two foxes, but some activity is noted immediately. It is also conceivable that the activity triggers a back memory in the human brain – a "Proustian Memory" [3] – that has little immediately recognizable relevance to the observed action but, on retrospect, may be directly applicable.

This paper begins with a very simple premise and hypothesis: computers are unsupportive of human endeavor and ingenuity. As such, the concept of the personal computer must be recreated from scratch to help address the wide variety of issues that face us today.

The average person has not one or two, but more likely dozens of computers in the house and office today. Computers literally control our lives – from the automated alarm clock in the bedroom, the timed coffee pot in the kitchen, to the fuel injected or gas-electric hybrid vehicle in the driveway. With such a wide variety of microprocessors to choose from, how can I pick one and say it is stifling human creativity?

We will begin this study with an explanation of three related, but different, terms: bioinspiration, biomimicry, and bioderivation.

- Bioinspiration is the development of a synthetic system that performs the same function of that of a living organism, even if the scheme is quite different from that employed by the organism.
- Biomimicry is the adaptation of a mechanistic principle of a living organism to replicate that action in a synthetic material.
- Bioderivation uses an existing biomaterial in concert with an artificial material to create a hybrid [4].

3.2 Bioinspiration on a Human Scale

This paper focuses on bio-inspiration. Simply, because at its simplest definition, a computer takes an input and expresses an output. At its most complex, a computer takes an input and expresses an output – nothing more, nothing less! A single cell organism does the same thing: it takes an input and responds with an output. But a single cell organism, despite lacking a brain or central nervous system does something else: it learns. Failure to learn would likely result in a condition dangerous or deadly to the survival of the organism.

Let us momentarily evolve beyond the single-cell organism to a much larger organism, a human being. The average human relies on five different senses (or "inputs"): sight, hearing, taste, smell, and touch. The loss of any of these senses may complicate life, but likely will not threaten the existence of the person. In many cases, the other senses will compensate for the loss of one sense by increasing the capability of the other senses. The computer, of course, has no such luxury of redundancy.

Worse, computer designers – both hardware and software designers – do not seem to recognize or appreciate the differences between the machine on the desk and the machine in the head. They are not building computers on a human scale or to support human ingenuity.

Consider, for example, the computer mouse – the handheld device for moving the cursor along the screen. This should facilitate and stimulate the brain, but it actually hinders the ability to think. A typical desktop computer mouse pad working surface is 19 × 23 cm (for a laptop computer it is much smaller, about 3 × 4 cm). That is your entire space devoted to working.

Now, consider how a person thinks when they are trying to solve a problem. They walk back and forth, gesture wildly with their hands, perhaps talk out loud even if there is no one else in the room. That is a human-scale workspace, far larger than 19 × 23 cm. Cram that workspace down to a mouse pad and you don't focus inspiration, you stifle it. There are innovations that are trying to eliminate the mouse pad – huge multi-touch screens for two or three analysts to work at a time – but they are still far too expensive for a traditional office or laboratory space.

But it's not simply a question of gesticulating madly defining either deep thinking or an insane rant. It has been demonstrated in studies of the learning disabled that multi-sensual learning (visuomotor or sensorimotor behaviors) increases the ability to learn:

The human brain, which has evolved over millions of years of evolutionary development, is adaptable and has developed in response to the complex cognitive needs of the human being. The brain's ability to function effectively, however, is dependent on lower neural structure. Since the child's brain still has the quality of plasticity or adaptability, the assumption is that the brain of a child with motor defects can be reorganized through activities designed to enhance sensory integration and thereby normalize behavior [5].

Since that was written 30 years ago, it has been shown that mental agility in older humans can also be enhanced by increased visuomotor activity. Why, then, must it be presumed that multi-sensorial activity is unimportant to people in the prime of their working and thinking lives?

3.3 Information Swarms

What is an information swarm? It is the phenomenon of intelligence analysts [6] to all converge on the same answer, not because it is necessarily the "right" answer, but because it is the most readily-accessible or most "obvious" answer. The analysts swarm to the answer like bees to a flower. It is quick, it is defensible, and, more times than not, it is wrong.

There is an element of simplification that is, in part, a necessity when trying to understand the world around us. Herbert Simon calls it "bounded" or limited rationality [7, 8]. The mind cannot cope with the complexity of the world it faces. Consequently, we construct a simplified model of reality to use everyday. Our behavior is bounded by the limits of that mental model. When information enters the model which we have not previously prepared to accept, we have incongruity, or dissonance, which must be resolved [9].

A number of theories in "consistency" or "cross pressure" have been developed since Fritz Heider originally approached the topic in the mid-1940s [10]. The general conclusion of all these theories is the same: when there is conflicting or dissonant information, the general response is to either fit the information into the analyst's *weltanschauung*, or reject the information [11]. This has been confirmed in a number of studies; even scientists, often thought to be dispassionate recorders of phenomena, face the same problem: scientists are biased toward confirming their own beliefs [12]. Philip E. Tetlock, for example, identifies three different psychological perspectives (skeptics, complexifiers, and fundamentalists) and concludes that, while each has components of validity, none are fully useful in predicting activity in international politics [13, 14]. More important in a critique of the analytical process is the tendency to continue to hold to beliefs even after they have been proved wrong [15]! This tendency is fatal to the notion of intelligence being the fulcrum in any policy-making decision regarding national security.

That intelligence failures occur should not be surprising; that the Intelligence Community (IC) has sometimes been proved correct may be more of the surprise [16]. Intelligence failure – essentially a "mistaken view of the external world" can be the result of several factors: a subordination of intelligence to policy; unavailability of information when and where needed; received opinion (conventional wisdom); and mirror-imaging are often identified as root causes of intelligence failure [17]. Intelligence is a profession of cognition [18]. It is, therefore, critical to recognize and respond to the problem of cognitive dysfunction.

But what if the observed phenomenon does not contradict the analyst's belief structure? What happens when all the reference groups (religion, peers, family, teachers, society, etc.) agree? The result is a non-conscious ideology; a set of beliefs and attitudes

which is accepted implicitly but remains outside the awareness of the analyst because "alternative conceptions of the world remain unimagined [19]." This is the fate of the "information swarm." As the IC continues to pursue the concept of "alternative analyses" it's critical to remind the analysts and the policy-makers that the alternatives are only as good as the imaginations that developed them. The possibility of imagining an alternative outside of an analyst's experience is unlikely, if not impossible.

But, while some in the leadership of the IC recognize the problems of cognition and belief patterns, few seem to realize the fundamental institutional barriers to correcting the problem. If the IC truly wants "alternative analysis", it needs alternative thinkers. This may involve recruiting new analysts who do not fit the mold of traditional IC analysts and may not have the ability to "pass" the traditional security background check to work in the IC. It may, in fact, be necessary to develop an "alternate universe" CIA, working away from the traditional CIA headquarters and away from the traditional analytic thinking [20]. Just as Apple Computers and Atari in Silicon Valley reinvented the traditional office in the 1970s and 1980s, the CIA may need to reinvent its processes.

And the computer systems that support the IC will need to be reinvented. Computationally, it requires computers that can "identify" outlier data. Consider again the human computer, walking down the street of a familiar city. The senses are bombarded with data inputs. Yet, the brain ignores everything except what is needed to travel down the street. But, if something unusual or potentially dangerous on the perception periphery is identified by one of the senses, the brain is able to adjust, analyze, and respond. It has responded to outlier data.

Analytic thought is, for all intents and purposes, taking in a series of data inputs and extracting an output – an analytic conclusion. This is the gist of what occurs when an intelligence analyst takes intelligence data – no matter the sources – and produces an intelligence assessment or a prediction of the future. Here, too, is a need for responding and analyzing outlier data.

Desirably, a computer should be a multi-sensor receptor, much like any single cell organism. A single cell organism "understands" and responds to its environment, despite not having a central nervous system or "eyes" or "ears" [21]. Research in adapting these capabilities to sensors is a potentially productive field. One such effort is adapting a reconfigurable computing tissue – a homogeneous two-dimensional tissue "skin" tissue with the entire sensor being operated by an artificial genome [22]. Calcium ion channels, signaling both internally and externally to the cell, are another potentially configurable sensor [23].

3.3.1 Cognitive Dissonance and the Intelligence Analyst

> The greatest derangement of the mind is to believe in something because one wishes it to be so. Louis Pasteur [24].

Cognitive dissonance is the conflict between a person's beliefs and a decision the person has made [25]. Cognitive dissonance was first expressed by Professor Leon Festinger, then Professor of Psychology at Stanford University in his 1957 study,

A Theory of Cognitive Dissonance. Festinger's hypothesis, simply put, is: "The existence of dissonance, being psychologically uncomfortable, will motivate the person to try to reduce the dissonance and achieve consonance; When dissonance is present, in addition to trying to reduce it, the person will actively avoid situations and information which would likely increase the dissonance."[26].

As Festinger pointed out, dissonance – inconsistency – could be replaced by any number of other "notions" (hunger, frustration, and disequilibrium) and still be a valid theory. Festinger defined cognition as "any knowledge, opinion, or belief about the environment, about oneself, or about one's behavior." In short, everything an intelligence analyst must consider in assessing a problem. The application of this theory to the problem of intelligence analysis is then immediately apparent.

Richards J. Heuer tested the theory while working at the Defense Advanced Research Projects Agency (DARPA).

He concluded:

- The analyst who thinks back about how good his past judgments have been will normally overestimate their accuracy;
- The intelligence consumer who thinks about how much he learned from our reports will normally underestimate their true value to him;
- The overseer of intelligence production who conducts a postmortem of an intelligence failure to evaluate what we should have concluded from the information that was available will normally judge that events were more readily foreseeable than was in fact the case[27].

3.3.2 The Problem of Data Fusion

It is necessary to understand the challenges of intelligence analysis in order to understand how exponentially increasing the available data to the analysts impedes, not improves, analysis. A surprise attack, such as the Japanese attack on Pearl Harbor or the World Trade Center attacks of 9/11, is considered an intelligence failure. Are such failures avoidable? More importantly, were such attacks truly the result of failures in the intelligence process? In general, there are two schools of thought regarding the impact of intelligence analysis. The schools are the "Orthodox School," which argues that "the inherent pathologies and obstacles in the work of intelligence make every attempt of surprise attack an almost certain success," and the "Revisionist School," which argues that "the roots of surprise attacks lie in avoidable failures of certain intelligence people."[28]; but there is a flaw in the opening assumption of both schools of thought: both assume the "failures" to be the fault of the intelligence analytic process.

There is a long-standing debate within the Intelligence Community as to the definition of "intelligence analysis." The debate centers on whether analysis is a structured methodology or intuition – science versus art [29]. Intuition, in fact, has been redefined as "unstructured methodology," perhaps as a sop to those who are concerned about the appearance of the art versus science debate having such a critical role in national security.

In 1949, a scant 2 years after the establishment of what is now known as the Intelligence Community via the National Security Act of 1947, Sherman Kent authored what is now considered "the most influential book ever written on U.S. intelligence analysis [27]," Strategic Intelligence for American World Policy [30]. Kent attempted to define strategic intelligence as: knowledge (what is known), organization (who knows it), and activity (the work of the intelligence organization). It is, to a large extent, the template used by organizations within the Intelligence Community to this day. It was not, however, without its detractors. Willmoore Kendall, for example, wrote a review of the book in World Politics [29] which challenged most of Kent's arguments and conclusions [31]. Kendall argued that Kent had "not worked out in his own mind what an ideal set of intelligence arrangements … would be like, and thus has no standard against which to measure the magnitude of the shortcomings he exposes." Kendall believed Kent had a misguided view of the function of intelligence (as primarily a wartime activity) and challenged Kent's belief that the analytic process was empirically-based, as opposed to Kendall's predilection for it being a theoretical research process [32].

Kent's basic concern was the relationship of the intelligence analyst to the policymaker, a relationship he rightly characterized as "one of the utmost delicacy." Kent identified the professional challenge of serving two masters: analytic integrity and policy clients [7]. Obviously, listing two such issues as different masters creates a sort of "Hobson's choice" [33], with no good alternative options. In reality, there needs be no choice between the two alternatives; one should be able to maintain analytic integrity and still support the needs of the policymaker. Kent, however, believed strongly that there was a great chasm between policymaker and intelligence analyst.

Kent believed the analytic process was undermined by either of two alternatives: when the analyst is too removed from the policymaker and, conversely, when the analyst is too close to the policymaker. Kent concluded that being too removed from the policymaker was the greater problem of the two. This, however, Kent found to be an organizational impediment, not the fault of the analyst. Kendall, on the other hand, is even more pessimistic than Kent in this regard. He asks rhetorically "Does it not follow that, as regards the great decisions about foreign policy, it is highly probable that our undertakings will fail and our statesmen plan in ignorance?"[34]. But, again, this presents an arrogance that is misplaced. It assumes that the policymaker is ignorant absent the intelligence analyst's input. There is little in the literature to suggest such a situation. The classic case of so-called intelligence failure, Pearl Harbor, was not the result of ignorance by the policymaker, but rather was because the policymaker deemed other factors had greater importance than the resultant "failure" [35].

Kent stated in the forward to Strategic Intelligence that many of the ideas in the book were not his but rather the ideas of George S. Pettee, a professor at Amherst College and the author of an earlier book, The Future of American Secret Intelligence. Pettee, like Kent, had one basic understanding of the role of intelligence:

> The simple fact remains that the United States cannot have a national policy comparable to its commitments unless it has the means to form such a policy and to base it upon the best possible knowledge of the facts and circumstances [36].

The analytical "process" is not as organized or process-oriented as one might expect or hope. Richards J. Heuer, in his classic study, Psychology of Intelligence Analysis, identifies four principles of perception that are interrelated and confounding to the analytic thought process

- We tend to perceive what we expect to perceive;
- Mind-sets tend to be quick to form but resistant to change;
- New information is assimilated to existing images;
- Limited exposure to blurred or ambiguous stimuli interferes with accurate perception even after more or better information becomes available [37].

Here the Intelligence Community faces a conundrum. One way to counter having a hide-bound analytical staff unwilling to move from its world-view is to bring in "new blood" with no preset motivations or beliefs. But a young staff has the significant drawback of not having the necessary historical, cultural, and language skills to fully analyze and understand intelligence on a day-to-day basis. And, in light of some of the objections during the Iraq WMD debate, might a novice analyst not be more susceptible to having a conclusion be "pre-cooked" by a superior than a hardened veteran?

The then-current Deputy Director of National Intelligence for Analysis, Thomas Fingar, has no less sanguine a view of the immediate future of intelligence analysis in the Community. Speaking before the Council on Foreign Relations, he said it bluntly: "To improve analysis, we need better analysts."

Part of that problem is the lack of experts in analytic positions. Fingar describes the problem as being like the letter "J" – a small group of senior experts, already past (or near) the age for retirement; a dearth of mid-career analysts; and a long leg of new hires. Fingar states that about 55% of all analysts in the IC joined after 9/11. Another senior level official in the DNI described it as "40% are within 5 years of being hired and another 40% are within 5 years of retirement." It is hard, if not impossible, to maintain currency with that sort of turnover. That fact, coupled with a 25% reduction in staff as a result of the so-called Cold War "peace dividend" destined the IC to a tumultuous managerial nightmare from the 1990s until today.

Other critics of the IC are equally pessimistic. Bowman Miller, a professor at the National Defense Intelligence College, echoed Fingar's charge, arguing that "filling intelligence gaps and avoiding "intelligence failures" (policy decisions, somehow never account for failures) demand more than adding analytic manpower and creating new tools; first and foremost, they require more expertise. More analysts are needed to couple analytic depth with conceptual breadth, while recognizing and trying to mitigate the perennial problems of cognitive bias and "group-think" pressures to conform."

How, then, can it be expected for an analyst – whether an intelligence analyst sitting in a cubicle in the basement of CIA headquarters, or a seasoned "politico" sitting in a walnut-paneled office at the State Department – to be able to carve a path through all these biases and barriers to (for lack of a better phrase) "free thought"? The analyst must find the balance between the tyranny of "experts" and the tyranny

of the lowest common denominator. Secondly, the analyst must find the balance between ignorance of the facts and hardening of the cognitive synapses. And all of *THIS* presumes that the collectors of data have managed to collect information of value to the question at hand and successfully saved the data in a form and location that is retrievable by the analyst.

3.4 Conclusion

The ability to ingest data and make a reliable assessment from that information is dependent upon a number of factors. For reliable, consistent data it is important for sensors to adapt to incoming data streams. This will be essential both for survival as well as for data integrity. The ability of the analyst to understand and assess the incoming data free of any internal or external biases is also critical. It may, in fact, be a more important factor than the analyst's level of expertise or subject knowledge. But one over-riding issue is that tools designed to help the analyst must not actively impede the analytic process. Computers should be designed with a philosophy of freeing thought, not stifling or controlling thought. Designing computers on a bio-inspired template would be a good first step.

References

1. Read K (2010) May I have my attention, please? AARP – the Magazine, (July/August), pp 32–33
2. Bohn RE, Short JE (2009) How much information? 2009 Report on American Consumers. Global Information Industry Center, UC, San Diego
3. Proust M (1927) Remembrance of things past. Grasset and Gallimard, Paris
4. National Research Council (2008) Inspired by biology. The National Academies Press, Washington, DC, p 2
5. Lerner J (1981) Learning disabilities. Houghton Miffl in, Boston
6. Simon HA (1976) Administrative behavior. The Free Press, New York
7. Heuer RJ Jr (1999) Psychology of intelligence analysis. Center for the Study of Intelligence, Washington, DC
8. Sperlich P (1971) Conflict and harmony in human affairs: a study of cross-pressures and political behavior. Rand McNally & Company, Chicago
9. Bem DJ (1970) Beliefs, attitudes, and human affairs. Brooks/Cole Publishing Company, Belmont, p 25
10. Armstrong JS (1985) Long-range forecasting – from crystal ball to computer. Wiley, New York, p 433
11. Tetlock PE (1992) Good judgment in international politics: three psychological perspectives. Polit Psychol 13(3):517–539
12. Festinger L (1957) A theory of cognitive dissonance. Row, Peterson, and Company, Evanston, pp 71–72
13. Janis IL (1983) Groupthink: psychological studies of policy decisions and fiascoes. Houghton Mifflin Company, Boston

14. Shulsky AN, Schmitt GJ (2002) Silent warfare – understanding the world of intelligence. Brassey's, Inc., Dulles, pp 61–67
15. MacEachin DJ (2005) Analysis and estimates – professional practices in intelligence production. In: Sims JE, Gerber B (eds) Transforming U.S. intelligence. Georgetown University Press, Washington, p 117
16. Bem SL, Bem DJ (1970) Case study of a nonconscious ideology: Training the woman to know her place. In: Beliefs, attitudes, and human affairs. Belmont, Brooks/Cole Publishing Company, Belmont
17. Godlewski RJ (2008) Cultivating creativity within intelligence analysis. Am Intell J 25(2):85–87
18. Bray D (2009) Wetware – a computer in every living cell. Yale Press, New Haven
19. Teuscher C, Mange D, Stauffer A, Tempest G (2001) Bio-inspired computing tissues: towards machines that evolve, grow, and learn. IPCAT 2001, April 24, 2001
20. Bruni LE (2008) Cellular semiotics and signal transduction. In: Barbieri M (ed) Introduction to biosemiotics – the new biological synthesis. Springer, Dordrecht, pp 365–407
21. Clark RM (2004) Intelligence analysis – a target-centric approach. CQ Press, Inc., Washington, p 1
22. Dixon N (1976) On the psychology of military incompetence. Jonathan Cape, London, 164
23. Festinger L (1957) A theory of cognitive dissonance. Row, Peterson, and Company, Evanston, p 3
24. Heuer RJ Jr (1978) Cognitive biases: problems in hindsight analysis. In: Westerfield HB (ed) Inside CIA's private world – declassified articles from the agency's internal journal, 1955–1992. Yale University Press, New Haven, pp 333–334
25. Honig OA (2007) A new direction for theory-building in intelligence studies. Int J Intell Count Intell 20(4):699–716
26. Marrin S (2007) Intelligence analysis: structured methods or intuition? Am Intell J 25(1):7–16
27. Davis J (1992) The Kent-Kendall debate of 1949. Stud Intell 36(5):91–103
28. Kent S (1949) Strategic intelligence for American world policy. Princeton University Press, Princeton
29. Kendall W (1949) Review: the function of intelligence. World Polit 1(4):542–552
30. Davis J (Undated) Sherman Kent's final thoughts on analyst-policymaker relations. Sherman Kent Center, Washington, DC, p 12
31. Wohlstetter R (1962) Pearl Harbor – warning and decision. Stanford University Press, Stanford
32. Pettee GS (1946) The future of American secret intelligence. Infantry Journal Press, Washington, p 117
33. Steele RD (2002) The new craft of intelligence – personal, public, & political. OSS International Press, Oakton, p 13
34. Diamond J (2004) Compiling an intelligence estimate. USA Today, Washington
35. Fingar T (2008) Remarks and Q&A by the Deputy Director of National Intelligence for Analysis & Chairman of the National Intelligence Council. The Council on Foreign Relations, New York, p 14
36. Tenet G (2007) At the center of the storm – my years at the CIA. Harpers Collins Publishers, New York, p 14
37. Miller BH (2008) Improving all-source intelligence analysis: elevate knowledge in the equation. Int J Intell Count Intell 21(2):337–354

Chapter 4
Nanoparticles: A New Form of Terrorism?

Nano-eco-terrorism

A.M. Gatti and S. Montanari

Abstract Nanotechnologies offer numerous, very promising possibilities to solve old problems due to the matter properties at nanolevel. The opportunities presented are far-reaching, novel and unprecedented. But the enthusiasm for this revolution is tarnished by some concerns about the safety of nanoparticles for human and environment health. Their ability to negotiate the physiological barriers has already been demonstrated. The present study shows that unintentional, not engineered, nanopollution is already present in the environment, particularly because of the use of high-temperature combustion processes (internal-combustion engines, incinerators, high-technology weapons' explosion, etc.) and that presence contaminates humans, animals and environment. The paper takes into considerations public worldwide-known events where unintentional important release of nanoparticles occurred and discusses the effects that they induced in humans and animals. Biological samples affected by lymphoma, leukemia, and cancer of soft tissues of soldiers who served during the Gulf War and Balkan War and of people exposed to the 9/11 pollution are considered and specific analyses have been carried out in those pathological samples by means of Field Emission Gun Environmental Scanning Electron Microscopy coupled with an Energy Dispersive Spectroscopy. These pieces of evidence induce to consider the role of nanoparticles and their impact on the human health with attention, also for their possible terroristic use.

Keywords Nanoparticles • Nanopathology • Nanotoxicit • Ecoterrorism

A.M. Gatti (✉)
Laboratory of Biomaterials, Department of Specialist Surgeries, University of Modena and Reggio Emilia, via Campi 21A, Modena, Italy
e-mail: antonietta.gatti@unimore.it

S. Montanari
Nanodiagnostics srl, Via E.Fermi, San Vito Modena, Italy

A. Vaseashta et al. (eds.), *Technological Innovations in Sensing and Detection of Chemical, Biological, Radiological, Nuclear Threats and Ecological Terrorism*, NATO Science for Peace and Security Series A: Chemistry and Biology,
DOI 10.1007/978-94-007-2488-4_4, © Springer Science+Business Media B.V. 2012

4.1 Introduction

Nanoparticles have shown to possess very interesting characteristics that, suitably applied, are already widely used industrially. The impulse given to this new type of research and their immediate applications to develop products meant for large, common use leave no time to evaluate the ethical implications implicit in a wide use of products not fully evaluated, for instance, from a toxicological point of view. The absence of regulations for nanoscaled materials allows manufactures to market products without carrying out specific tests specially related to the full life-cycle of the product or informing the consumers of the nanocontent listing it in the product's label. This situation implies that, if there are side effects due to the use of those products, they are not observed as possibly connected with the nanoproduct's use and prospective epidemiological studies will not reach any conclusion, since a homogenous exposure of these consumers is not known or considered.

In this situation of uncertainty, while waiting for specific rules and standards, it should be mandatory to develop researches anticipating this need. The research we carried out started from three simple facts:

1. engineered and non-engineered nanoparticles are already present in the environment, released by nanotechnological activities and by uncontrolled (in terms of release) high-temperature combustive processes like those occurring in car engines, power plants, incinerators, explosions, etc.;
2. man and animals are already in contact with those particles;
3. nanosized particles can negotiate the physiological barriers because of their tiny size, reaching the deepest districts of the organism.

Thanks the European project Nanopathology, (FP5-QOL-2002-147; www.nanopathology.it) [1] we developed a novel diagnostic tool through which we can show the presence of micro- and nanosized inorganic particles in biological tissues, most of which we found to be affected by pathologies of unknown etiology.

The diagnosis makes use of a novel type of ultramicroscopic investigation to check possible exposures to inorganic micro- and nanoparticles humans and animals underwent. The analyses carried out were meant to identify those foreign bodies remained trapped in biological tissues.

After having examined more than 1,300 biological samples, mostly pathological ones, we can give a definite answer: inorganic micro- and nanoparticles, be they inhaled (with contaminated air) and/or ingested (with contaminated food), can be found virtually in any organ [2]. Once inhaled, they can reach the pulmonary alveoli and move to the blood within a few tens of seconds. A similar phenomenon occurs to ingested particles [3, 4].

In the subjects affected by hypercoagulative diathesis, those particles can trigger the formation of blood thrombi reaching the lung circulation (pulmonary thromboembolism), if the phenomenon occurs in the veins, or virtually any organ, if the reactions occurs in the arteries, causing stroke or myocardial infarction [5]. But most particles reach any district of the organism where they are trapped and seen as foreign bodies.

Interestingly, under particular conditions those particles can enter the cell nuclei without killing them but potentially interacting with the DNA and can trigger cancerogenic reactions [6, 7]. In our experience, no biological mechanism exists capable of eliminating those invaders and the obvious reaction induced is the one typical of foreign bodies.

After evaluating possible sites where an important release and the following high concentration of non-engineered nanoparticles occurred and where important effects were clearly detectable, we identified, among others, two sites where such nanocontaminants were released and studied the effects. The first is related to the terroristic attack of 9/11 and the second considers the events of the 1st and 2nd Gulf war and the Balkan wars.

Analytical investigations on the environmental pollution generated after the attack of two aircraft in New York and the following collapse of the buildings hit along with a number of biological analyses on sanity and rescue workers and firefighters, as well as the war pollution discovered in Iraq and the observation of pathological tissues of veterans allowed us to express some concerns about the impact of micro- and nanopollutants on humans and animals.

4.2 9/11: The Domino Side Effects of a Terroristic Attack

The attack to the World Trade Center by two airplanes caused two explosions in the upper part of the Towers. The red-yellow flames developed indicated that the temperature was very high, most probably in excess of 2,000°C. The combustion caused the immediate sublimation and aerosolization of the two airplanes and everything present at least in the upper part of the towers: glass, ceramic materials, plastic, wood, computers, metals, etc. The high temperature created nanoscaled particulate matter and a black dust cloud mainly due to the aircraft pulverization that developed and moved from Down Manhattan toward other urban areas. The real extent of that nanoscaled fall-out is unknown, but there can be no doubt that it interested a wide area. So, people living at a comparatively long distance from the site of the disaster inhaled that ultrafine matter. A very short time later, the mechanical collapse of the Twin Towers generated a white dust cloud, different from the first one not only in color but in size of the particles – as they were mostly micrometric – and in chemical composition, since much of them came from the structure of the buildings. That dust, heavier and coarser than the former, invaded the ground and the aerial spaces around the skyscrapers.

In a short communication we sent to the Herald Tribune for the first anniversary of the event, we predicted that “more mourning will occur as a consequence of the pollution generated both by the combustion in the upper part and by the mechanical crush of the buildings”, but we also expressed a doubt about the immediate recognition by medical doctors of a link between the inhalation of that dust and the diseases that started to make their appearance in New York. The creation after 1 year of a

Health Registry by the Council of Downtown Manhattan in order to give an answer to the requests of explanations made by citizens was the best evidence that a suspicion of a link existed.

It is not clear how many people actually fell ill after 9/11, since the Registry considers only the sanity and rescue workers and the firefighters (about 70,000 units). People who worked in the vicinity of the Twin Towers but lived outside the Manhattan area were not included. As a guess, a possible number of the people who fell ill after 9/11 might range from 200,000 to 300,000.

What is actually happening is an unexpected (how really unexpected?) domino effect impacting on many aspects of society, not least economy. But what is most important is that the number of victims is bound to increase within the next few years, since many pathologies take a relatively long time to grow manifest, and asbestos mesothelioma (asbestos fibers are nanoparticles) can serve as an example. The symptoms are many and multifarious: from asthma to allergies, from atypical pneumonia to pleurisy, many idiopathic diseases, and different forms of cancer, chronic fatigue, neurological diseases, autoimmune symptoms and diabetes. But the list should be much longer.

Specific studies on Post Traumatic Syndrome in children and also in neurodevelopmental symptoms due to mother's exposure during pregnancy to polybrominated diphenyl ethers (PBDEs) present in the fire retardants used by firefighters showed an increased ratio if compared with the situation before 9/11, and so did malformations and miscarriages.

People who were physically present during the collapse and/or worked there developed some neurological symptoms not clearly understandable if not hypothesizing an uptake of metallic nanoparticles that reached the brain. Also the birth of malformed babies could be related to the mother's exposure to the 9/11 pollution. Personal studies carried out in other polluted areas revealed that fetal malformations can be correlated with mothers' exposure to environmental submicronic toxic particulate matter. In fact, inside the fetal internal organs submicronic toxic particles were found that were present in the environmental industrial pollution where the mother lived [8].

We had the opportunity to analyze the dust of the Tower collapse that was collected from objects that were unburied from the ruins and from 2 firefighters' fatigue dresses and helmets, put in cellophane bags by their owners without any cleaning after having been engaged 3 months at Ground Zero.

The dust showed to be composed of particulate matter with a size ranging from tens of microns down to tens of nanometers and the particle composition had a surprise in store. In fact we found Iron compounds containing also Antimony, Sulfur and Chromium, Cerium and Lead compounds, other made of Silver or Gold containing also Sodium, Aluminum, Silicon, Chlorine, Potassium, Calcium, Iron Zinc, Nickel, and Copper. Such compounds had been never found before since they come from uncontrolled, casual combustion.

Rescue and sanitary workers, firefighters, volunteers and common people kept inhaling this dust for months as did the dogs employed at Ground Zero that eventually died of lung cancer. Since men and animals ate on the spot, it is possible and

very likely that that dust was also ingested besides being inhaled. The tiny size of this particulate matter made the particles more insidious since, small as they are, they can easily negotiate every physiological barrier and, as mentioned above, have the possibility to be transferred into all the internal organs. And the finer they are, the more easily they can reach any anatomical district, the deeper the reaction and, as a matter of conjecture, the more difficult their removal is, if a possibility of being effectively removed actually exists.

In New York we worked with a scientific Foundation called FASE which had approved a detoxification treatment proposed by the Council of Downtown Manhattan on Ground Zero workers affected by different illnesses. In the course of that undertaking we observed a possible mechanism of elimination of that kind of dust. The method of detoxification applied scheduled a 3-week cycle of daily saunas with light gymnastic exercises and a pharmacological treatment mainly based on vitamins. In order to verify the ground of this hypothesis and the bounty of the results, we collected and analyzed the sweat of 12 subjects after a sauna. Those patients were affected by chronic chronic-fatigue, severe asthma and severe dermatitis. Drops of sweat mostly from the chest skin were collected in sterile vials. Starting 48 h before the sauna, the workers were requested to clean the breast skin only with water and not to use soap, deodorants, perfumes, creams, etc. 20 ml of the sweat collected were spread on a cellulose filter, dehydrated and observed under Field Emission Gun Environmental Scanning Electron Microscope coupled with an Energy Dispersive Spectroscopy to check the chemical composition of sweat and debris, if any.

Among crystals of Sodium chloride, an obvious finding, we identified particles smaller than 1 μm and with different compositions. Particles of Iron, Antimony or Lead-Antimony, Lead-Chromium, Zinc or Barium sulfate, Titanium-Barium, Bismuth-Chlorine, Silver and also Gold compounds. Figure 4.1 shows a particle (one of many) detected in the sweat of a firefighter. We do not know if he inhaled or ingested it at Ground Zero during his 3-month stint there, but it is singular that some chemical compositions found in the dust collected at Ground Zero are peculiarly similar to that found in the sweat years later.

What we cannot know is how much of the dust contained in the organism is gotten rid of that way, as we have no idea of the quantity actually present in the subject.

None of these alloys (from the technical point of view the vast majority of those particles are alloys) is present in any handbook of metallurgy or of materials, since they come from an uncontrolled, occasional combustion. Compounds like Barium sulfate, for instance, can come from the mechanical crush of the Towers and may belong to their building materials. Their appearance on the skin surface after 4 years from inhalation or ingestion and as a result of sauna cycles might mean that they were stored in a fatty tissue and released by drastic heat cycles through the skin pores. The partial recovery of the patient we observed could mean that the partial elimination of these foreign bodies was sufficient to improve their health. The internal presence of the dust in all organs and tissues trigger the defense mechanisms, but they are not successful since they cannot destroy physically the toxic particles.

After having checked many other more or less similar cases without any occasional relation with the one of Manhattan, once again these pieces of evidence

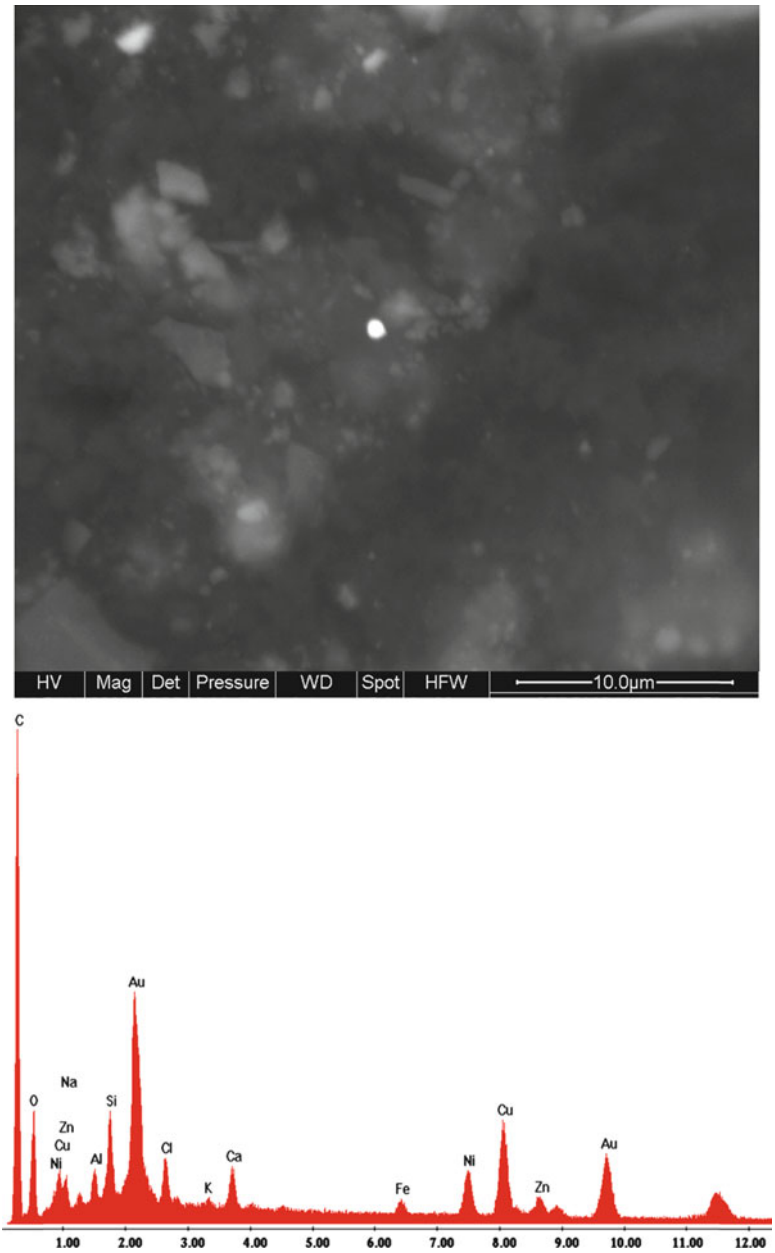

Fig. 4.1 Submicronic spherical particle composed of Carbon, Oxygen, Gold, Sodium, Aluminum, Silicon, Chlorine, Potassium, Calcium, Iron, Nickel, Chromium, Zinc

testify that inhaled or ingested nanosized dust can induce adverse health effects. In most instances it does not cause instantaneous toxic reactions, but delayed symptoms of diseases can occur whose etiology is erroneously diagnosed or not diagnosed at all.

Medicines have no real effect against this kind of internal pollution. Economy can be negatively influenced by the working days lost, by the costs of drugs and hospitalization, and by the cost of remediation (when possible) carried out on the environment. The domino effect of such a type of terroristic attack is self-evident.

4.3 The Exposure Scenario Created by the Twenty-First Century Wars: The Gulf and Balkan War Syndrome

The explosion of high-technology weapons against a target or of a large quantity of ammunition accumulated to be destroyed creates airborne micro- and nano-particles. Bombs based on depleted Uranium (DU), Tungsten, or pyrophoric metal generate a very high temperature, generally in excess of 3,000°C degrees, e.g. 3,036–3,063°C for Uranium [9] and about 5,000°C for Tungsten. Both temperatures are high enough to have the target aerosolize along with everything located within the volume. The explosion produces an airborne pollution with a new chemistry, due to an uncontrolled combustion. The elemental composition of the bomb combines in accidental, albeit physically and chemically possible, ways, forming new materials that are not mentioned elsewhere. Behaving many ways like gases, those particulate pollutants, spherical and hollow, are released in the surrounding atmosphere and fall after a while on soil, water, vegetables, etc.

The particulate matter pollutes battlefield and soldiers, civilians, NGO members, animals, and whoever happens to be present in the area. We performed investigations on some hundred soldiers' pathological tissues after exposures in the Gulf (2001) and in the Balkans war [1]. The weapon-produced nano-pollution was detected and its chemistry verified. No debris containing DU was ever detected in those subjects (it was in other circumstances), but only an ample variety of heavy metals, which is easily understandable, because the quantity of Uranium involved in an explosion is negligible.

As described, micro- and nanoparticles can reach virtually any anatomical district. So, among many other organs and tissues, nanoparticles were identified in the pathological specimens of brains affected by neuroglioblastoma and in the seminal fluid of soldiers affected by non-Hodgkin's lymphoma or gonad cancer.

It is only natural that this uncontrolled, and, as a matter of fact, uncontrollable pollution can be inhaled also by the civilians that live in the area, but, since those particles can float in the lower atmosphere for a long time and can be carried by the wind a long way from the place where they were generated, also people living relatively far from that area can be contaminated, though, as a rule of thumb, the farther from the origin, the lesser concentrated the particles are. In any case, it must be noticed that a predominant wind can carry the dust in one particular direction, thus

leaving a comparatively close-to-the-source area relatively clean. Also animals can inhale that dust and ingest it by feeding on the polluted grass. People and animals involved in a war may so share a common lot.

Dust has always been produced by the explosion of ammunition, but what makes the difference now in comparison with the past is that the concentration of nanoparticles is far higher because of the unprecedented temperatures involved, and also small animals like insects can be damaged by this phenomenon. It is a fact that, after bombing Afghanistan in 2004, most of the local bees disappeared, a phenomenon we observed in other comparable circumstances.

Side effects of the new wars are under everyone's eyes: young soldiers clinically certified as healthy, return from a 6–8-month mission and start to grow ill [10]. After a while the health problem involving veterans from the Balkans, Iraq or Afghanistan could no longer be hushed and it was amply discussed by journalists worldwide, unfortunately not always expert enough to be able to present it in correct terms.

The consequences of that contamination are not confined to the primary victims alone who, in any case, can grow sterile, but, in some instances, involve also their families or partners. Burning-semen disease is a condition actually affecting their sexual partners and the birth or the miscarriage of malformed babies is a misfortune to the whole family. But few demonstrations of the responsibility of that fine and ultrafine dust were presented because of the difficulty to assess the effective exposure the soldiers underwent. They are not equipped with sensors capable of detecting and quantifying nanopollution, and, in addition to that, those who analyse the pathological tissues do not have the cultural background to be able to appreciate the problem nor the instruments to verify the presence of non-biocompatible, non-biodegradable, sometimes inherently chemically toxic, pollution in the pathological samples they observe.

Can the war micro- and nanopollution be the cause of the Palestinian men's sterility that Arafat denounced in one of his last interviews before he died? The continuous bombing may produce in some subjects a neurological stress that makes them choose not to procreate, but what is certain and independent of psychology is that an environmental pollution like the one described persists for years. The new-technology weapons of Israel (Depleted or Enriched Uranium, Phosphorus, etc.) can contaminate the Gaza Strip territory in an irreversible way (most particles we detected are not degradable through natural processes), but they themselves, the Israeli, can be acutely contaminated in particular during their infantry raids. Nanoparticles are really democratic: they attack the "enemy" but also, and impartially, they do attack those who generated them.

4.4 Conclusion

A devious fact is the delay elapsing between the exposure and the onset of the pathologies, pathologies whose course can be slowed down by the use of palliative drugs, for example anti-inflammatory, but not stopped. The new pollution

contaminates the environment, inducing alterations in the flora and the fauna, but nobody can predict the entity and quality of the effects and how long this pollution can last in the territory. In fact the end of a war in terms of fighting and bombing does not coincide automatically with the disappearance of that contamination and the end of its effects. Silently, Nature reacts to those insults with mechanisms that are still largely unknown because the Planet has never had a chance to measure itself against such an assault and we have no experience. *The truth is that we are playing with Nature without knowing the rules of the game.* What we cannot afford to ignore is that nanosized pollution can interact directly with the living organisms and with vital parts of the cell like the DNA, the code to our existence [7].

References

1. Gatti A, Montanari S (2008) Nanopathology: the health impact of nanoparticles. Pan Stanford Publishing Pte Ltd, Singapore
2. Nemmar A, Hoet PH, Vanquickenborne B, Dinsdale D, Thomeer M, Hoylaerts MF, Vanbilloen H, Mortelmans L, Nemery B (2002) Passage of inhaled particles into the blood circulation in humans. Circulation 105(4):411–414
3. Ballestri M, Baraldi A, Gatti AM, Furci L, Bagni A, Loria P, Rapanà R, Carulli N, Albertazzi A (2001) Liver and kidney foreign bodies granulomatosis in a patient with maloocclusion, bruxism, and worn dental prostheses. Gastroenterology 121:1234–1238
4. Gatti AM (2004) Biocompatibility of micro- and nano-particles in the colon (part II). Biomaterials 25(3):385–392
5. Gatti A, Montanari S, Gambarelli A, Capitani F, Salvatori R (2005) In-vivo short- and long-term evaluation of the interaction material-blood. J Mater Sci Mater Med 16:1213–1219
6. Hansen T, Clermont G, Alves A, Eloy R, Brochhausen C, Boutrand JP, Gatti A, Kirkpatrick J (2006) Biological tolerance of different materials in bulk and nanoparticulate form in a rat model: sarcoma development by nanoparticles. J R Soc Interface 3:767–775
7. Gatti A, Quaglino D, Sighinolfi GL (2009, Spring) A morphological approach to monitor the nanoparticle-cell interaction. Int J Imaging 2(S09):2–21
8. Gatti A, Bosco P, Rivasi F, Bianca S, Ettore G, Gaetti L, Montanari S, Bartoloni G, Gazzolo D (2011) Heavy metals nanoparticles in fetal kidney and liver tissues. Front Biosci 1(E3):221–226
9. Technical Report (Annual) of the Air Force Armament Laboratory (1978) Armament Development and Test Center, Eglin Air Force Base, Florida (USA), Project no. 06CD0101 (from Oct 1977 to Oct 1978)
10. Gatti A, Montanari S (2008) Nanopollution: the invisible fog of future wars. The Futurist 42(3):32–34

Chapter 5
Nano Sensing Devices – Future Directions

Challenges and Opportunities

Nora Savage, Ph.D.

Abstract Nanotechnology offers tremendous opportunities for developing sensing and monitoring devices that are small and inexpensive with rapid response time of multiple analyte detection. In addition, there is the potential for these sensors to have "smart" or active capabilities embedded in them. These devices can help meet critical challenges identified in the environmental, occupational, biological and national security areas.

Keywords Sensors • Environment • Smart devices

5.1 Introduction

Nanotechnology offers the monitoring and sensing sciences a world of novel, miniature, and "smart" devices. In a world that is becoming increasingly global, in both commercial production as well as manufacturing and distribution, robust, sensitive, accurate, and adaptive sensing devices are in high demand. From regulatory agencies to corporations to private citizens, there is a huge market for integrative sensing devices. Applications include personal and national security sensing, ecological monitoring of biological, chemical, and radiological materials, biomedical assessing, and product quality monitoring and control. This article examines the current challenges for environmental monitoring and detection that can enable holistic ecological assessments using nanotechnology.

N. Savage, Ph.D. (✉)
ORD, NCER, U.S. EPA, Mail Code 8722p, 1200 Pennsylvania Avenue, N.W.
Washington, DC, USA
e-mail: savage.nora@epa.gov

A. Vaseashta et al. (eds.), *Technological Innovations in Sensing and Detection of Chemical, Biological, Radiological, Nuclear Threats and Ecological Terrorism*,
NATO Science for Peace and Security Series A: Chemistry and Biology,
DOI 10.1007/978-94-007-2488-4_5, © Springer Science+Business Media B.V. 2012

5.2 Ecological Assessment

Challenges in the ecological assessment area include limitations in detection capacities, multi-analyte detection needs, integration of miniaturized components, devices which go beyond detection and monitoring to perform or trigger actions, and analysis in complex real-world mixtures. Nanotechnology, alone or in combination with bio-, info- and cognitive technologies offers one path forward towards meeting these challenges.

In the environmental nanotechnology area there are monitoring and sensing needs which can be classified in two categories. The first is in the area of developing monitoring and sensing devices that are miniature and inexpensive, capable of rapid detection of multiple analytes, accurate, robust, and precise in complex mixtures. In addition, such devices should be "smart" or able to perform an action subsequent to detection. Nanotechnology has fantastic potential to meet these needs and to provide devices which can enable a more holistic assessment of our air, soil, and water environments. Support for development of these sensors can be achieved through research grants, small business awards and collaborative industrial-academic-government partnerships.

The second category of need for environmental sensors in the nanotechnology area is the detection and quantification of engineered nanomaterials as distinguished from no other incidental or natural nanomaterials. This need is especially critical for regulatory and public health agencies. For example, fullerenes have been detected in automotive exhaust (incidental) and are also engineered for specific products, including drug delivery vehicles and composite materials. Omowunmi Sadik has explored not only using engineered nanomaterials to detect conventional pollutants, but also developing innovative sensing techniques for identification and quantification of engineered nanomaterials in environmental media [1].

Precise and accurate miniature sensors are needed for environmental remediation, quality control, and environmental assessment of air, soil and water prior to, during and following remediation. While low-power mobile sensors that can respond to various chemical, biological, radiological, and energetic compounds have been developed by researchers, the capacity to sense and perform in complex environmental mixtures still presents a challenge. Interferences with non-target or confounding compounds which can produce false negative or false positive results and the capacity for sensing equipment to become fouled currently hamper sensing and detection capabilities. Certain natural environments that are harsh present additional challenges due to extreme temperatures, pressures, salinity, pH, or other factors. Research and development to address these challenges are key to enabling appropriate risk assessment and management policies and environmental protection.

Engineered nanomaterials, as one class of emerging compounds, present a unique challenge to the sensing and monitoring research community. As novel compounds are developed and commercialized, the need to develop devices for new analytes increases. New devices should be adaptable such that as novel compounds enter our environment, detection and monitoring capabilities keep pace. Conversely,

in sensing and monitoring existing analytes, there is a need to ensure that toxic compounds which are present but not anticipated in a specific environment, are nonetheless detected and quantified.

The incorporation of "smart" technology, i.e. the ability to perform some specified action depending upon the nature, concentration and location of the analyte(s) and to trigger subsequent action as well as self-repair (in the event of failure or trauma) will enhance this capability. Such devices can enable warnings to operation and maintenance personnel as well as to the general public, in the event of potential exposure to toxic compounds. Such alerts would also meet national security needs in the event of terrorist activities.

Anticipated capabilities would include the ability to detect minute concentrations of a variety of compounds simultaneously, to record the collected data, to transmit the data to a central facility in a user-friendly format, to provide warnings for dangerous levels of toxic compounds, to isolate targeted compounds in order to minimize environmental and human impacts, and to treat or remove potentially harmful compounds. Accordingly, the technology would allow for the detection of minute concentrations of multiple compounds simultaneously and for the implementation of rapid responses to safeguard public health and the environment.

The work of Wan Shih at Drexel University involves the use of highly piezoelectric microcantilever arrays for in-situ, rapid, and simultaneous multiple pathogen quantification in aquatic environments [2]. Additionally, the work of Joseph Wang [3] and associates involves the remote sensing of compounds using DNA recognition in the development of electrochemical sensing devices.

Finally and perhaps most importantly, currently there is very limited ability to identify an unknown compound without capturing, separating, and subjecting collected samples to a battery of complex and time-consuming laboratory testing. Sensors that can provide the quantification and identification of multiple compound in a complex environmental or medical media, in real-time and using a robust, mobile device are a critical need. Nanotechnology provides an opportunity for reductions in size and energy requirements, magnification of power and enhancement of sophistication that could vastly expand the capacity and use of sensors while revolutionizing the collection and manipulation of data and information provided.

Sample collection is a key aspect of sensor systems, and if performed accurately or poorly, can result not only in erroneous data but also in subsequent inappropriate and inadequate assessments. However a sufficient sample amount must be collected to provide a reliable signal and quantification. Nanotechnology offers a tremendous opportunities to meet these requirements and address these limitations.

Another challenge in the detection and quantification of biological organisms is the requirement not only to detect the presence of the organism, but to ascertain the viability. The detection of the DNA of a specific biological pathogen that is not viable could result in the unnecessary expenditure of resources. However, a sensing device that can rapidly and accurately detect viable biological agents is a critical need for national security and public health protection.

As novel sensor devices are developed, made smaller and more efficient, and become increasingly multi-functional, there will be an attendant need to ensure that

there is minimal or no pollutant burden associated with the manufacture, use, and end-of-life of these devices. Towards that end, sensors should be equipped with recyclable and, to the extent possible, biodegradable parts. As nanotechnology moves beyond the passive incorporation of engineered nanomaterials towards more active structures and materials, awareness of the potential for environmental litter will increase in significance. The development and deployment of sensor devices which can be ubiquitously placed in various environmental settings and either degrade into useful constituents (i.e. food source for indigenous microbial populations, nutrient source for plants, etc.) will enable the collection of important data on the environment for holistic assessment while minimizing or eliminating adverse impacts. This will be especially crucial for miniature sensors that are deployed to detect hazardous compounds and are not expected to be retrieved from the environmental setting.

Another requirement for these devices is that they are both robust and operationally easy to deploy and use. In addition, the capture data that can be easily manipulated and accessed is critical. Often the more complex the sensing device, are, the less sturdy and robust it is. Minor forces and small accidents can render these either inoperable or malfunctioning. In addition, the difficulty inherent in the use and maintenance can result in erroneous data collection. The resultant poor data quality and quantity will lead to inaccurate environmental assessment and, consequently, he failure to identify critical ecological and occupational compounds and pathogens.

5.3 Summary and Future Recommendations

Overall, nanotechnology offers a wide variety of solutions and opportunities to meet current and future challenges for sensing and monitoring technologies. Examples include reduced material and energy usage, minimization of sample preparation, reduction in sample collection, real-time analysis, active and adaptive capabilities, accurate and precise multi-analyte detection, and environmentally-benign design. These capabilities will enable the rapid, holistic assessment and management of the natural environment, occupational environments, and the enhanced protection of national security.

References

1. Sadik OA (2009) JEM spotlight: applications of advanced nanomaterials for environmental monitoring. Foreword. J Environ Monit 11:25–26
2. Yi JW, Shih WY, Mutharasan R, Shih W (2003) In situ cell detection using piezoelectric lead zirconate titanate-stainless steel cantilevers. J Appl Phys 93(1):619
3. Wang J (2005) Nanomaterial-based amplified transduction of biomolecular interactions. Small 1:1036–1043; Barcoded Nanomaterials 2:1069

Chapter 6
Metallic Films with Fullerene-Like WS_2 (MoS_2) Nanoparticles: Self-Lubricating Coatings with Potential Applications

Fullerene-Like Nanoparticles

O. Eidelman, H. Friedman, and R. Tenne

Abstract Metallic films impregnated with fullerene-like-WS_2 (MoS_2) nanoparticles were fabricated on stainless steel and Ti-Ni substrates using galvanic and electroless deposition. The coatings were obtained from aqueous suspensions containing the metallic salts as well as the dispersed nanoparticles. Tribological tests showed that the films have low friction and wear. Such coatings could be useful for numerous civilian and defense-related applications.

Keywords Fullerene-like nanoparticles • Inorganic nanotubes • Coatings • Tribology

6.1 Introduction

In recent years, the emergence of nanotechnology has led to the development of a new group of nanocomposite materials: electrodeposited composite coatings containing a variety of nanoparticles in the metal matrix [1]. Among these are the fullerene-like (IF) nanoparticles (NP) of WS_2 and MoS_2, which were first reported more than a decade ago [2]. Figure 6.1 shows the transmission electron microscope (TEM) micrograph of a fullerene-like (IF) MoS_2 nanoparticles (a); a group of IF-WS_2 nanoparticles (b) and a magnified image of one such nanoparticle (c). The closed-cage; multiwall and hollow structure of these nanoparticles are clearly delineated. These nanoparticles, when added to lubricating fluids were found to exhibit superior solid lubrication behavior. More recently, several reports were published in which IF-WS_2 (IF-MoS_2) nanoparticles were incorporated into metallic films [3, 4]

O. Eidelman • H. Friedman • R. Tenne (✉)
Department of Materials and Interfaces, Weizmann Institute, Rehovot, Israel
e-mail: reshef.tenne@weizmann.ac.il

A. Vaseashta et al. (eds.), *Technological Innovations in Sensing and Detection of Chemical, Biological, Radiological, Nuclear Threats and Ecological Terrorism*, NATO Science for Peace and Security Series A: Chemistry and Biology,
DOI 10.1007/978-94-007-2488-4_6, © Springer Science+Business Media B.V. 2012

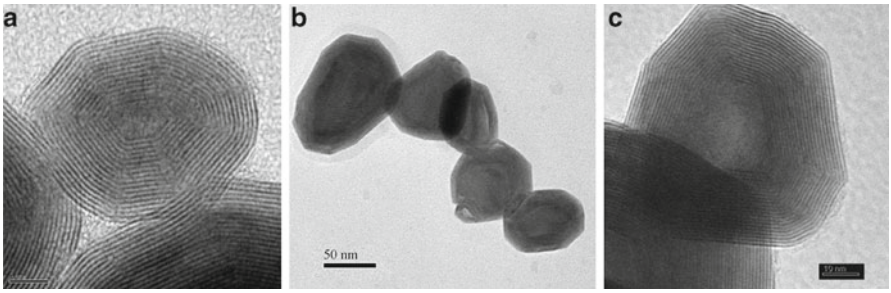

Fig. 6.1 TEM micrograph of a group of IF-MoS_2 nanoparticle (**a**); IF-WS_2 nanoparticles (**b**) and magnified image of one such NP (**c**) (with 10 nm scale bar)

endowing them a self-lubricating character. These coatings were produced from electrolytes containing metals, such as nickel and cobalt. In the past decades, chromium coatings were produced from solutions based on chromic acid (CrO_3) which are known to be highly toxic and oxidative and have a slow deposition rate. These coatings are characterized by their high hardness values (ca. 1,000 kg mm^{-1}- VHN). Electroplating from hexavalent chromium ion solutions faces a possible ban as a result of the serious health and environmental risks involved [5]. Progress in the development of Cr (III) baths for electrodeposition has been slow, largely due to the complex nature of the chemistry and electrochemistry of Cr (III) species in aqueous solutions. Further attempts were made in recent years to produce coatings of metal alloys, such as Co-W, Ni-W, Fe–Cr, Cr–Ni, Fe–Cr–Ni and Cr–Co. These new compositions, which were shown to exhibit relatively high hardness (<800 VHN), were fabricated in order to replace the hexavalent chromium (Cr(VI)) electroplating process [5–7]. A limited amount of work has been carried out to date in the field of chromium composite coatings [8]. Survilienė et al. [9] have shown that the presence of a low quantity of Co(II) ions in the Cr(III) bath enhanced the appearance of the deposits and provided superior corrosion resistance (and possibly an improvement in hardness, too).

In general, acceptable alternatives to chromium are usually said to require comparable hardness, about 1,000 kg/mm (VHN), as well as exhibit acceptable sliding or abrasive wear resistance. The Hall-Petch law, as applied to nanostructured materials, can be used to provide some guidelines in the selection of suitable candidates based on hardness. The law states that the toughness or yield strength of a material is inversely proportional to the average grain size. Of greater interest is the more generalized relationship between grain size and properties that states that as the grain size of the material decreases into the nanocrystalline range (<100 nm), hardness and wear resistance usually increases and the coefficient of friction decreases. As an example, the Vickers hardness of bulk conventional nickel increases from about 140–300 VHN for a grain size of a 100 nm to about 650 VHN for a grain size of 10 nm [10].

The aim of the present study is to show the significance of metal coatings impregnated with IF nanoparticles, which are endowed with self-lubrication character. In

particular, hard chromium-rich coatings impregnated with IF-WS_2 (IF-MoS_2) nanoparticles produced by electroplating process from trivalent chromium electrolyte, are discussed.

6.2 Experimental Details

6.2.1 Electroplating of Cr-Co-Zn-(IF-WS_2)

To facilitate the deposition of the nanoparticles their surface was first sensitized in $SnCl_2$/HCl solution and consecutively activated in $PdCl_2$/HCl solution. The Cr-Co-Zn film deposition took place in an aqueous solution under argon gas bubbling conditions. The solution reagents were based on the composition of a solution prepared by Hamid et al. [8]. The solution preparation followed a strict regimen which appeared to be crucial for the successful Cr/IF deposition. It was found that the inclusion of tiny amounts of cobalt (and zinc) ions in the bath promoted the deposition of the chromium film. After the preparation, the solution is left to age, and after several days the surfactant CTAB (cetyl trimethyl amino bromide) is added. This procedure is followed by a second 2 weeks aging period. Galvanostatic electrodeposition was carried out at a current density ≈ 70 mA/cm^2.

6.2.2 Tribological Measurements

The friction coefficient and wear of the substrate with the metallic coatings were measured with and without IF-WS_2 nanoparticles. The dry friction tests were performed using a ball-on-flat set-up at room temperature. A hardened stainless steel ball with a diameter of 2 mm was slid against a flat sample (the coated stainless steel). The load used in the present experiments was 0.5 N (virgin contact pressure, $P = 1$ GPa). The reciprocating sliding velocity of the steel ball was 0.08 mm s^{-1} during 90 cycles. The length of the wear track was 1.5 mm. Both friction coefficient and wear were measured during the friction tests. The flat samples and steel ball were rinsed in hexane and acetone using an ultrasonic bath and then dried before and after the test.

6.3 Results

Figure 6.2 shows SEM micrographs of the chromium rich coating containing the IF-WS_2 nanoparticles at low (a) and high (b) magnifications. The deposited film seems to be somewhat smoother than the substrate but with larger peak to valley distance value. The edge of the coating was inspected at an oblique angle in this

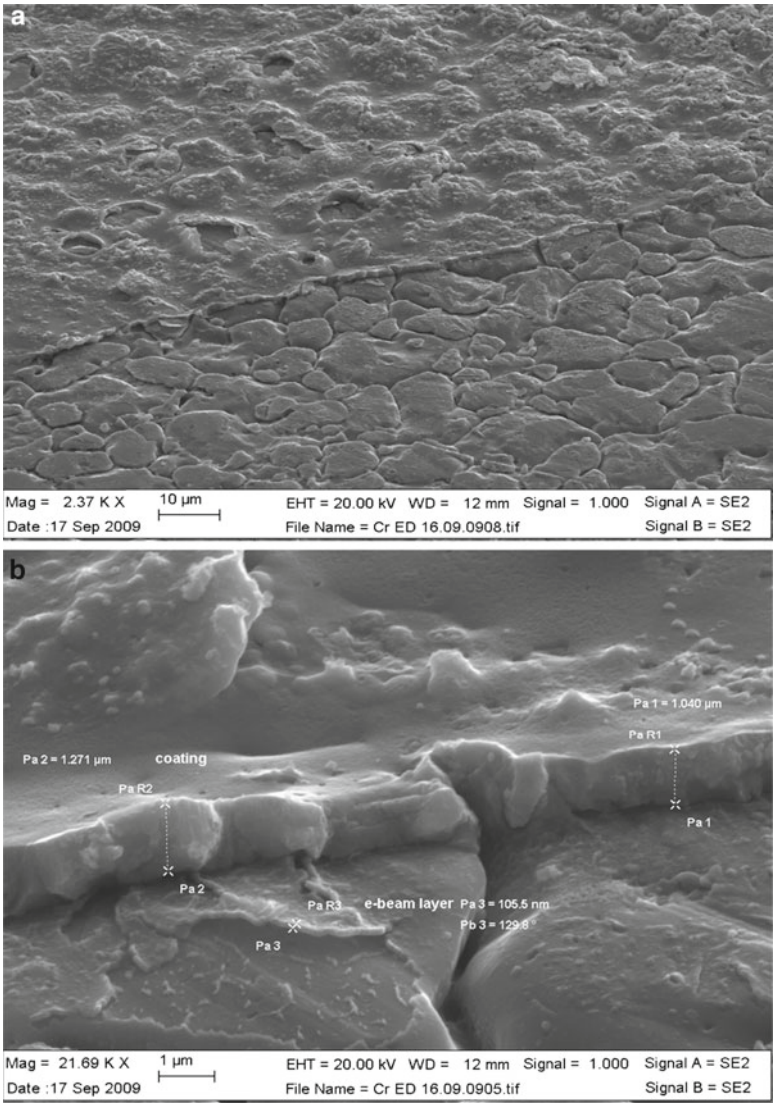

Fig. 6.2 SEM micrographs showing the pure Cr-rich films deposited onto stainless steel substrate in low (**a**) and high (**b**) magnifications

case, which allows determining the film-thickness. The typical coating thickness is found to be somewhat larger than 1 µm. The film looks quite uniform and continuous and well adhering to the underlying substrate. The Faradeic efficiency of a typical deposition process was close to 50%, which suggests that substantial amount of the current went to the reduction of hydrogen.

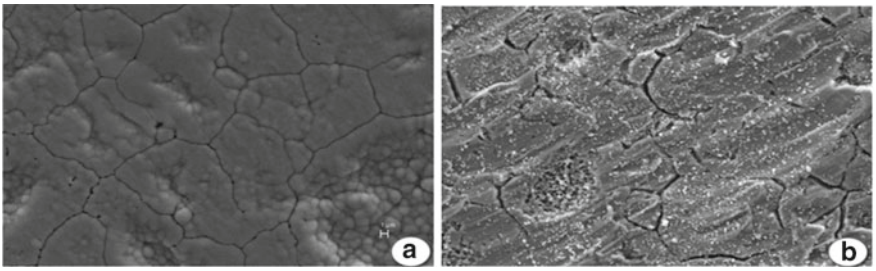

Fig. 6.3 SEM top-view of electrodeposited films: (**a**) Cr and (**b**) Cr+IF-WS_2 coatings before annealing

Figure 6.3a, b show SEM micrographs (top-view) of the surface morphology obtained by electrodeposition of the pure chromium rich (Cr) film and Cr+IF-WS_2 film, respectively. The electrodeposited Cr film is composed of highly dense Cr nodules about 1 μm in diameter each. Nonetheless the film appears quite smooth and uniform. Cracking, which is typical for chromium films, is probably the result of stress relaxation due to lattice mismatch with respect to the underlying substrate. It was observed that the IF nanoparticles were quite uniformly distributed on the film surface. Nonetheless, the nanoparticles seem to be accumulated in the pitted areas (see arrow in Fig. 6.3b) and in cracks, suggesting some nonuniformity at the film surface. This nonuniformity can be of electrical and/or chemical nature. Furthermore, the nanoparticles seem to be properly dispersed in the film forming small agglomerates or as individual nanoparticles. Annealing of the film was carried out in argon atmosphere. After annealing at 490°C, the morphology of the sample surface looks quite similar to the non-annealed one (Fig. 6.3b).

EDS analysis of the agglomerates and the surface underneath indicates that the IF concentration is not uniformly distributed along the film depth, with the majority of the nanoparticles close to its surface. The addition of Co^{2+} to the plating bath improved the chromium coating quality. It also had a favorable effect on the amount and uniformity of the dispersed IF nanoparticles in the metal matrix. Guglielmi [11] proposed a successive two-step adsorption mechanism for the incorporation of inert particles during the co-deposition process. In the first step, a loose adsorption of the particles occurs, while in the second step, strong adsorption to the underlying metal surface is affected. The second step is thought to be the rate determining step in the co-deposition of nanoparticles, which was assumed to be electric-field assisted. It may be furthermore assumed that Co^{2+} and Zn^{2+} are adsorbed onto the nanoparticles surface. This effect combined with the use of the cationic surfactant CTAB induces a positive charge on the nanoparticle surface. Thus the nanoparticles are attracted to the negatively charged cathode, leading to a more pronounced particle adsorption. This assumption is further supported by the fact that an anionic surfactant (SDS) was also tested but to no avail. Almost no deposition of IF-WS_2 nanoparticles to the Cr surface was observed in this case. It is thought that these two effects increased

Table 6.1 Nanoindentation analysis of the Cr+IF films on SS substrate (values in brackets are standard deviation)

	Unannealed		Annealed (within wear crack)		Annealed (outside wear crack)	
	E	H	E	H	E	H
Gpa VHN (Kg/mm^2)	182 (16)	32 (0.4) 294	183 (53)	3.2 (0.6) 294	174 (78)	3.2 (1.7) 294

the amount of IF nanoparticles co-deposited to the metal surface. These observations also suggest that the nanoparticles-surface was *a priory* negatively charged, which was also confirmed through pH measurements. It was found that the pH of a 5% water/IF suspension was somewhat acidic (pH 5–6), suggesting that OH^- ions were adsorbed onto the IF nanoparticles surface.

EDS analysis with 10 kV bias showed that, notwithstanding the large oxygen and carbon content, the Cr was the majority phase (70 at.%) of the electrodeposited coating while the Zn and Co make together about 10 at.% with the remaining contributed by oxygen and carbon. The W to S ratio is found to be 1:1.7 in the electrodeposited film, which is in accordance with previous studies [2, 12]. The W/Cr ratio was found to be about 1/30 confirming that IF-WS_2 nanoparticles made some 3–4% of the film content. At higher bias (20 kV), the W/Cr ratio decreases suggesting a strong gradient of the IF nanoparticles concentration, which are preferably present at the surface of the film or at a near surface region.

6.3.1 Nanoindentation Analysis

Modulus (GPa) and hardness (GPa) measurements were performed by nanoindentation analysis. The hardness values are also reported as the equivalent VHN obtained using the multiplicative factor of 92.65. The results of this analysis are shown in Table 6.1.

This analysis shows that, irrespective of the annealing process, the hardness of the film is well below the expected values of ca. 1,000 VHN. These values are lower than those of a pure SS substrate (ca. 500 VHN) and are reminiscent of the film thickness (about 1 μm) and the seeding layer of the NP, which is rather soft.

6.3.2 Tribological Analysis

In previous studies [2, 12], nickel and cobalt films containing ca. 5% of IF-WS_2 nanoparticles were shown to exhibit strong a self-lubricating effect. Tribological tests showed that these films exhibited friction coefficients below 0.1 under

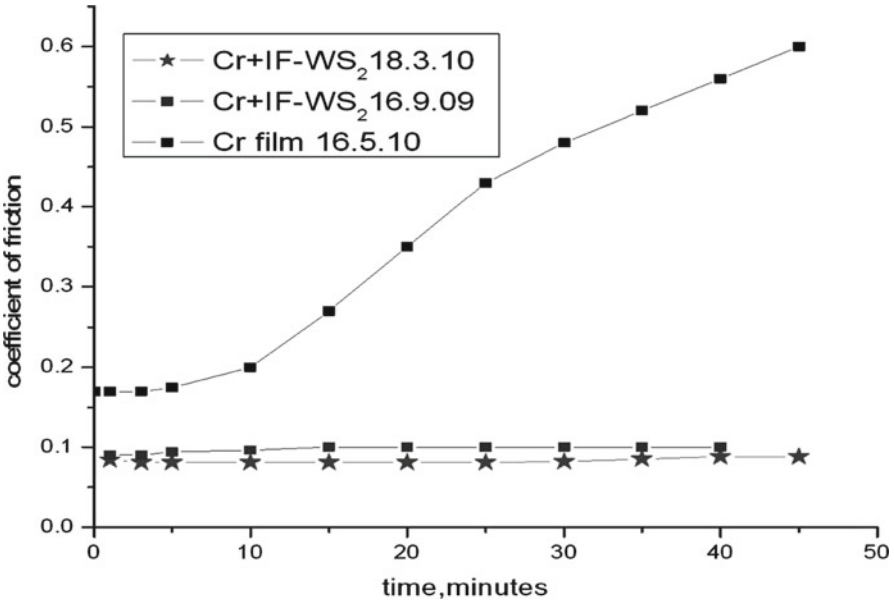

Fig. 6.4 Time dependence of the friction coefficient for the and the Cr+IF and Cr films obtained by electroplating

ca. 1 GPa load and very small wear for as long as the test has lasted. The time evolution of the friction coefficient of Cr and Cr+IF films measured with a ball against the metal surfaces is presented in Fig. 6.4. Furthermore, the friction coefficient of the SS substrate reported before [2] exhibits a large increase within the first 5 min (0.12–0.55). The friction coefficient of the chromium coated film increases gradually from 0.17 to 0.62 after 30 min, the latter value typical for the SS substrate. This suggests that the pure chromium film can not withstand the harsh tribological conditions and is oxidized and consumed during the tribological test. Contrarily, the friction coefficient of the Cr+IF film remains at a constant and low value (0.08) during the entire duration of the test (30 min). These values are comparable with those obtained from Co films impregnated with IF nanoparticles [2]. However, the IF concentration in Co film was appreciably higher (>5%) than in the present case. The friction coefficient of the softer Ni–P films is somewhat smaller (ca. 0.06–0.07) [12]. Nonetheless, the IF impregnation in the chromium rich coating provides satisfactory tribological behavior which is uncommon for such hard coatings. As for the wear values, the diameter of the scar on the ball was measured to be 105, 84 and 50 μm for the substrate with (e-beam deposited) Cr film; electrodeposited Cr film and electrodeposited Cr film impregnated with IF nanoparticles, respectively. These large differences are also a reflection of the self-lubricating nature of the Cr+IF film.

6.4 Discussion

In the case of the IF nanoparticles impregnated into metal [2, 12] or polymer films [13], the nanoparticles are gradually released by the wear and are therefore initially confined to the relevant tribological interface. This release is possibly accompanied by damage and exfoliation of the nanoparticles. At the same time, the nanoparticles can slide-roll and serve also as spacers between the two interfaces. The previous studies [2, 12] indicate also that the impregnated IF nanoparticles slow down the severe tribochemical oxidation of the metal surface. Typically, brittle oxides lead to higher friction and wear. The protection of the surface against oxidation can also lead to a reduced local temperature at the interface. Furthermore, the WS_2 nanoparticles, which are released from the metal coating during the test, play a chemical role as a sacrificial reducing agent, thereby preventing the rapid surface oxidation of the film during the tribological tests.

Cobalt-chromium alloys are used extensively in the medical technology for such applications as stents, heart valves, pacemakers, etc. Their biocompatibility has been studied [14]. The present work shows that cobalt-chromium films containing IF nanoparticles can be prepared on stainless steel and other metallic substrates. These films exhibit strong self-lubricating effect even in the absence of any liquids, like body fluids.

In conclusion, a method for fabricating chromium-rich coatings from Cr(III) solutions with impregnated IF nanoparticles is described in the present work. This coating is found to be quite hard and at the same time exhibit low friction coefficient and wear. Such films can find variety of medical, aerospace and defense-related applications.

Acknowledgment We are grateful to Dr. Rosentsveig for the synthesis of the IF-WS_2 nanoparticles and to Prof. L. Rapoport, to Dr. S.R. Cohen for the nanoindentation measurements and Dr. A. Moshkovith for the tribological tests. Prof. Tenne is the Drake family chair of Nanotechnology and director of the Helen and Martin Kimmel Center for Nanoscale Science.

References

1. Low CTJ, Wills RGA, Walsh FC (2006) Electrodeposition of composite coatings containing nanoparticles in a metal deposit. Surf Coat Technol 201:371–383; Bicelli LP, Bozzini B, Mele C, D'Urzo L (2008) A review of nanostructural aspects of metal electrodeposition. Int J Electrochem Sci 3:356–408
2. Friedman H, Eidelman O, Feldman Y, Moshkovith A, Perfiliev V, Rapoport L, Cohen H, Yoffe A, Tenne R (2007) Fabrication of self-lubricating cobalt coatings on metal surfaces. Nanotechnology 18:115703
3. Chen WX, Xu ZD, Tenne R, Rosenstveig R, Chen WL, Gan HY, Tu JP (2002) Wear and friction of Ni–P electroless composite coating including inorganic fullerene-like WS_2 nanoparticles. Adv Eng Mater 4:686–690
4. Samorodnitzky-Naveh GR, Redlich M, Rapoport L, Feldman Y, Tenne R (2009) Inorganic fullerene-like tungsten disulfide nanocoating for friction reduction of nickel-titanium alloys. Nanomedicine 4:943–950

5. Li B, Lin A, Gan F (2006) Preparation and characterization of Cr–P coatings by electrodeposition from trivalent chromium electrolytes using malonic acid as complex. Surf Coat Technol 201:2578–2586
6. Dasarathy H, Riley C, Coble HD (1994) Electrodeposition of cobalt-chromium alloy from trivalent chromium solutions. J Electrochem Soc 141:1773–1779
7. Capel H, Shipway PH, Harris SJ (2003) Sliding wear behavior of electrodeposited cobalt–tungsten and cobalt–tungsten–iron alloys. Wear 255:917–923; Weston DP, Shipway PH, Harris SJ, Cheng MK (2009) Friction and sliding wear behavior of electrodeposited cobalt and cobalt-tungsten alloy coatings for replacement of electrodeposited chromium. Wear 267:934–943
8. Hamid ZA, Ghayad IM, Ibrahim KM (2005) Electrodeposition and characterization of chromium–tungsten carbide composite coatings from a trivalent chromium bath. Surf Interface Anal 37:573–579
9. Survilienė S, Jasulaitienė V, Češūnienė A, Lisowska-Oleksiak A (2008) The use of XPS for study of the surface layers of Cr–Co alloy electrodeposited from Cr(III) formate-urea baths. Solid State Ion 179:222–227
10. Brooman EW (2004) Wear behavior of environmentally acceptable alternatives to chromium coatings- nickel-based candidates. Met Finish 102:75–82; Brooman EW (2004) Wear behavior of environmentally acceptable alternatives to chromium coatings: cobalt-based and other coatings. Met Finish 102:42
11. Guglielmi N (1972) Kinetics of deposition of inert particles from electrolyte baths. J Electrochem Soc 119:1008–1009
12. Redlich M, Gorodnev A, Feldmean Y, Kaplan-Ashiri I, Tenne R, Fleischer N, Genut M, Feuerstein N (2008) Friction reduction and wear resistance of electro-codeposited Ni + IF-WS_2 coating for improved orthodontic stainless steel wires. J Mater Res 23:2909–2915; Redlich M, Katz A, Rapoport L, Wagner HD, Feldman Y, Tenne R (2008) Improved orthodontic stainless steel wires coated with inorganic fullerene-like nanoparticles of WS_2 impregnated in electroless nickel–phosphorous film. Dent Mater 24:1640–1646
13. Svahn F, Csillag S (2011) Formation of low-friction particle/polymer composite tribofilms by tribopolymerization. Tribol Lett 41:387–393
14. Williams DF (2008) On the mechanisms of biocompatibility. Biomaterials 29:2941–2953

Chapter 7
Disposable Membrane Sensors for Biohazardous Substances

Disposable Membrane Sensors

Alexander G. Petrov

Abstract The concept of bilayer lipid membrane sensing is elaborated. Disposable bilayer lipid membrane sensors permit both stochastic and deterministic sensing regimes. Technology for membrane sensor preparation is described in details. Stochastic membrane sensing using ion channels is described. Detection of cyanobacterial toxins in waters by means of a stochastic sensing (ion channel induction) reveals a signature for a particular toxin type. This signature is especially well revealed by using the method of current-voltage surfaces, which establishes a bridge between stochastic and deterministic sensing by applying a time-averaging procedure. Flexoelectricity of membranes provides another way of deterministic sensing, of a stimulus-response type. The flexoelectric response is modulated by adsorption of the analyte over the membrane surface. Detection of environmental pollution of waters by heavy metal ions (Cd^{++} and Hg^{++}) is thereby rendered possible. This approach is confronted with a stochastic sensing of the same metal ions by alteration of the channel open/closed probability and average channel current of two familiar channels, gramicidin and alamethicin.

Keywords Lipid membranes • Ion channels • Flexoelectricity

7.1 Introduction

Bilayer lipid membranes are self-assembled aggregates of amphiphilic lipid molecules in water. Amphiphilic (biphilic) molecules consist of two distinct parts: a polar, often ionic, head and a nonpolar, often hydrocarbon, tail. These two parts

A.G. Petrov (✉)
Soft Matter Division, Institute of Solid State Physics, Bulgarian Academy of Sciences,
72, Tzarigradsko chaussee, 1784 Sofia, Bulgaria
e-mail: director@issp.bas.bg

A. Vaseashta et al. (eds.), *Technological Innovations in Sensing and Detection of Chemical, Biological, Radiological, Nuclear Threats and Ecological Terrorism*,
NATO Science for Peace and Security Series A: Chemistry and Biology,
DOI 10.1007/978-94-007-2488-4_7, © Springer Science+Business Media B.V. 2012

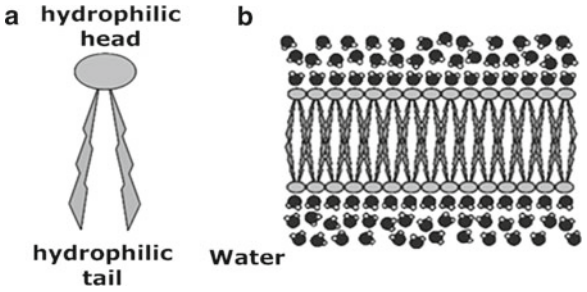

Fig. 7.1 Scheme of (**a**) lipid molecule and (**b**) lipid bilayer formed in water

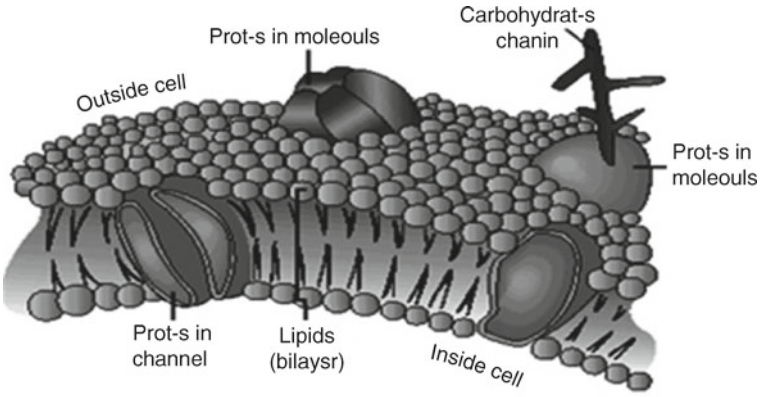

Fig. 7.2 Cell membrane – proteins are embedded inside the lipid bilayer

are named hydrophilic and hydrophobic respectively. Amphiphilic molecules in water solutions tend to self-assemble, forming above a certain concentration 3D lyotropic liquid crystals, named also lyotropic mesophases. For this process lyotropic mesogens with high enough molecular weight and well expressed molecular asymmetry are necessary. A very common group of lyotropic mesogens comprises soaps and detergents. Another group of lyotropic mesogens is provided by lipid molecules. On Fig. 7.1 one can see a single, 2D lipid bilayer that is a prototype for a biological membrane.

Biomembranes are built up by lipid molecules according to the general principles of lyotropic liquid crystals [1]. Celebrated "fluid lipid – globular protein mosaic model" [2, 3] implies that lipids are organized in a liquid crystalline bilayer in which integral proteins are embedded (Fig. 7.2). Membranes with high protein concentration, where lipids do not form a continuous bilayer but rather patch the spaces between proteins, while proteins themselves are arranged in a double tiered pattern, are also well known (cf. "structure-function unitization model of biomembranes") [4]. In both cases, though, the principles of liquid crystal physics [5] (viz., long range translational disorder vs. long range orientational order of constituent flexible lipid chains or rod-like protein molecules) are valid.

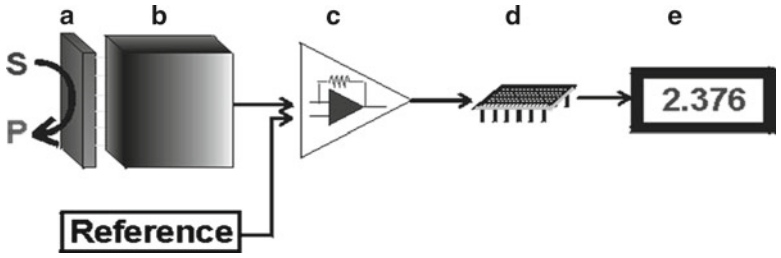

Fig. 7.3 Design principles of biosensors: (**a**) Biocatalyst – converts analyte into product. (**b**) Transducer – detects the occurrence of reaction and converts it into an electrical signal. (**c**) Amplifier – amplifies usually tiny signal to a useable level. (**d**) Microprocessor – signal is digitised and stored for further processing, e.g. integration, derivatisation, etc. (**e**) Display – usually for analyte concentration. In membrane sensors (**a**) and (**b**) are usually integrated

Biological lipid membranes separate the interior of a cell from the outside world. Sub-cellular compartments are also separated by lipid membranes. The amphiphatic nature of the lipids assembles these molecules in such a way that a large hydrophobic barrier is created. The hydrophobic barrier prevents the flow of charged molecules across the membrane. However, to allow for a facilitated passage of ions or molecules from one side of the compartment to the other; the lipid membrane is spanned by particular proteins adapted perfectly to the hydrophobic lipid environment. Some examples of membrane proteins are: ATPases, G-protein coupled receptors, light harvesting membrane proteins, and ion channels (Fig. 7.3).

Biological membranes offer by far the most selective and specific sensors in vivo. Containing many diverse peptides in lipid environment, they ensure on molecular level the specific features required for sensing [6]. Applying a biomimetic approach we may hope to match the membrane excellent selectivity and specificity in vitro.

Ion channels are essential for many cellular functions, including electrical excitability, synaptic transmission, hormone release, intracellular Ca^{2+} signaling, salt/water balance, fluid secretion, cell volume regulation. In a broad sense, ion channels can be classified as voltage-gated, ligand-gated, intracellular messenger- gated, or constitutively active [7]. Ion channels, in addition being gated by their primary activator (or inhibitor), are also substantially modulated by phosphorylation, dephosphorylation, accessory proteins, ion concentrations, pH, interactions with scaffolding and/or cytoskeletal proteins, and other "secondary" effectors. Thus, cellular regulation of ion channel activity can be extremely complex [8] (Fig. 7.4).

Many investigations on the potential use of ion channels in biosensor devices have been carried out for the last two decades. With the availability of the patch-clamp technique, the presence of ion channels has been established in all sorts of biomembranes [9]. A patch clamp method was originally developed for the investigation of single ion channels. To this aim, small patches of native membranes were sealed at the tips of glass micropipettes. The patch clamp method is well described in the literature. With the development of the tip-dip technique formation of model

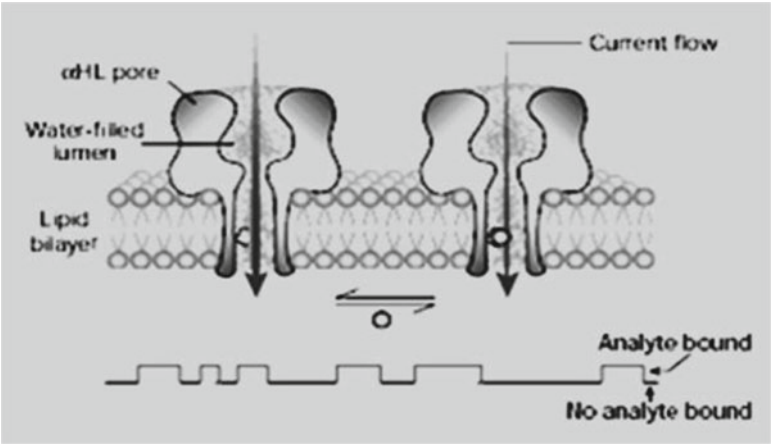

Fig. 7.4 A single engineered pore, placed in a planar lipid bilayer. Under applied potential, a current flows through the pore carried by ions in salt solutions bathing both sides of the bilayer. The pore contains a binding site for an analyte represented by the green ball in the fig [11]. Each time the analyte binds to the pore the current is modulated as illustrated in the trace

phospholipid membranes on patch clamp pipettes from lipid monolayers also became possible. Thus, the method became available for reconstituted channel studies as well.

Deterministic sensors operate on the basis of some physical law. In practice, a totally deterministic relationship is unlikely due to unpredictable factors. Where the influence of several unknown factors is sizable, exact prediction is not possible, but it may be possible to predict to within a known confidence interval – or to predict the probability that a particular value will be observed at a particular time. This is called a stochastic (or probabilistic) process.

Stochastic sensors have been the subject of considerable recent interest as a result of their ability for reconfigurable, rapid, multi-analyte detection as well as their potential for sequencing DNA. These sensors are created by placing a nanometre-sized pore in an insulating membrane and measuring the ionic transport through the pore in the presence of the molecules of interest. The magnitude, duration, and rates of occurrence of the resultant current blockades allow rapid determination of analyte concentration as well as discrimination between similar molecular species [10].

Stochastic sensing has several advantages over conventional sensing including high sensitivity, a rapid and continuous response, and wide dynamic range [11, 12]. The scheme of action of a stochastic sensor, based on a single pore placed in a planar lipid bilayer is given on Fig. 7.4.

A membrane has a number of mechanical degrees of freedom: area stretching, thickness compression, shear deformation, chain tilting, and, notably, curvature deformation. The last one, curvature, is just a liquid crystal degree of freedom since membrane curvature is equivalent to a splay of lipid chains (under the condition that chains remain parallel to the local normal in each point of the curved bilayer).

Flexoelectricity is a fundamental property of biomolecular layers relating their mechanical and electrical degrees of freedom. It is closely related to mechanosensitivity, electromotility and mechanotransduction, basic properties of living systems (see our general reviews [13, 14]). Understanding the mechanism of mechanosensitivity would open the way for construction of artificial bioelectronic mechanosensors [15–17].

7.2 Lipid Bilayer Membranes Containing Ion Channels

In our experiments, lipid bilayers (membranes) were self-assembled at the tips of glass patch pipettes using the method of Coronado and Latorre [18] from lipid monolayers formed by spreading the membrane-forming solution onto the surface of electrolyte solutions contained in Petri dishes (see Fig. 7.5). This technique is named tip-dip patch clamp and it was used in all our experiments with model membranes.

Membranes were tested both with voltage ramps from −100 to +100 mV and with current recording at constant voltage. The data were analyzed using current-voltage surfaces software [19].

7.2.1 Interaction of Lipid Bilayers Containing Channel-Forming Peptides with Cadmium and Mercury Ions

Let us consider lipid/peptide model membranes with multimeric ion channels formed by aggregation of peptide monomers. Depending on the biphilic asymmetry and shape asymmetry [20–22] two limiting types of peptide aggregates could be expected (Fig. 7.6): cylindrical and semi-toroidal. The former are likely to be formed by roughly cylindric peptides with hydrophilic groups located on one side of the cylinder only (e.g. alamethicin, δ-toxin etc.) (Fig. 7.6a). The latter are to be expected

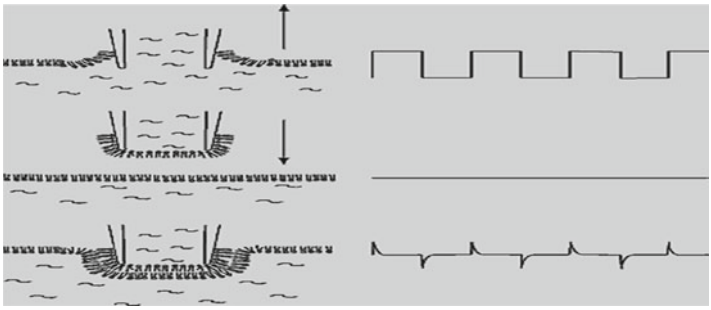

Fig. 7.5 Scheme of lipid bilayer formation at the tip of patch pipette on *left* and corresponding current recordings on *right*

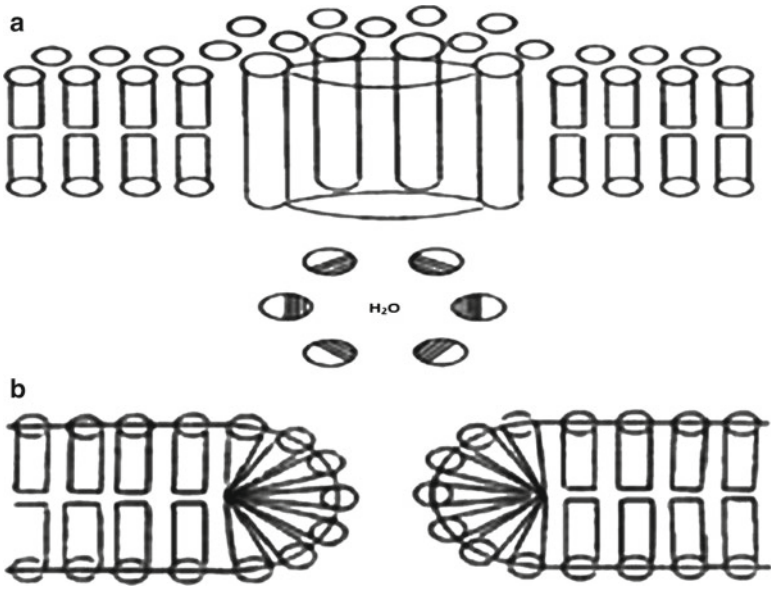

Fig. 7.6 Two types of aggregation of defect-forming molecules (peptides) in lipid bilayers. (**a**) channel; an aggregate of cylindrical molecules featuring transverse biphilic asymmetry (hydrophilic portions hatched in surface view illustrated below); (**b**) pore; an aggregate of wedge-shaped molecules featuring longitudinal biphilic asymmetry

for edge-shaped peptides with hydrophilic groups located on the thicker end of the wedge (Fig. 7.6b). We will designate the first type as a channel and the second type as a pore. Intermediate types of aggregates are also possible.

Heavy metals (Hg, Cd etc.) are known human toxicants, with the nervous system as a major target [23]. What is not clear is how some of these metals act on the nervous system. They have many potential targets, with membrane-bound signaling proteins, such as ion channels, being particularly vulnerable. Heavy metals may also act on the lipid components of the membranes of nerve cells, thereby, adversely influencing the excitable properties of these cells.

In the present investigation two channel-forming peptides were used: gramicidin (Gram) [24] and alamethicin (Alm) [25]. Lipid membranes were self-assembled at the tips of patch pipettes using the tip-dip patch clamp method of Coronado and Latorre [18]. Aqueous solutions of $HgCl_2$ and $CdCl_2$ were added to the Petri dish to final concentrations in the micromolar range.

7.2.1.1 Hg^{2+} and Cd^{2+} with Gramicidin D Ion Channels

Gramicidin is a heterogeneous mixture of six antibiotic compounds, gramicidins A, B and C, making up 80%, 6%, and 14% respectively all of which are

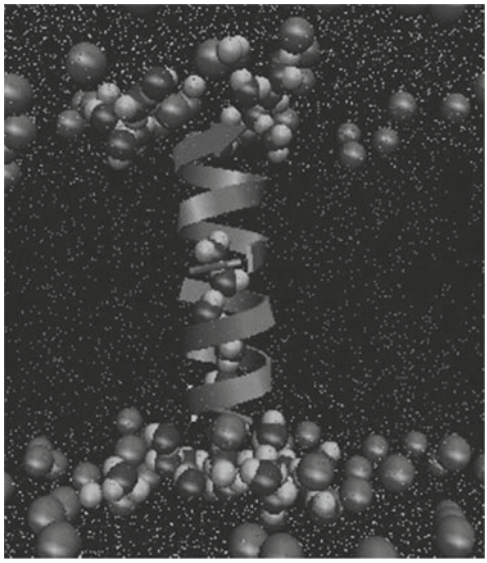

Fig. 7.7 Molecular model of Gram

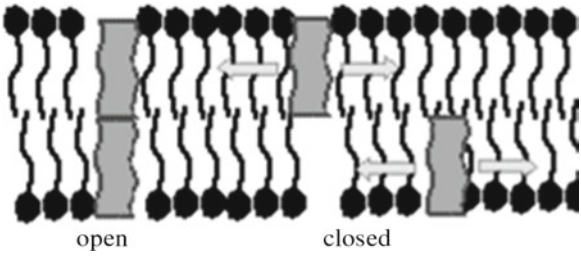

Fig. 7.8 Scheme of Gram ion channel

obtained from the soil bacterial species Bacillus brevis and called collectively gramicidin D. Gramicidin D are linear peptides; that is chains made up of 15 amino acids [4]. The chain assembles inside of the hydrophobic interior of the cellular lipid bilayer to form a β-helix. The helix itself is not long enough to span the membrane but it dimerizes to form the elongated channel needed to span the whole membrane.

The first example of a single-molecule experiment on an identified functional biomolecule was conducted over 30 years ago: the observation of current flow through a single ion-conducting channel formed by the peptide antibiotic gramicidin in a planar lipid bilayer [26] (Figs. 7.7 and 7.8).

The effects of the heavy metals ions Cd^{2+} and Hg^{2+} on channels formed by gramicidin D in lipid bilayers have been investigated [24]. Cadmium and mercury

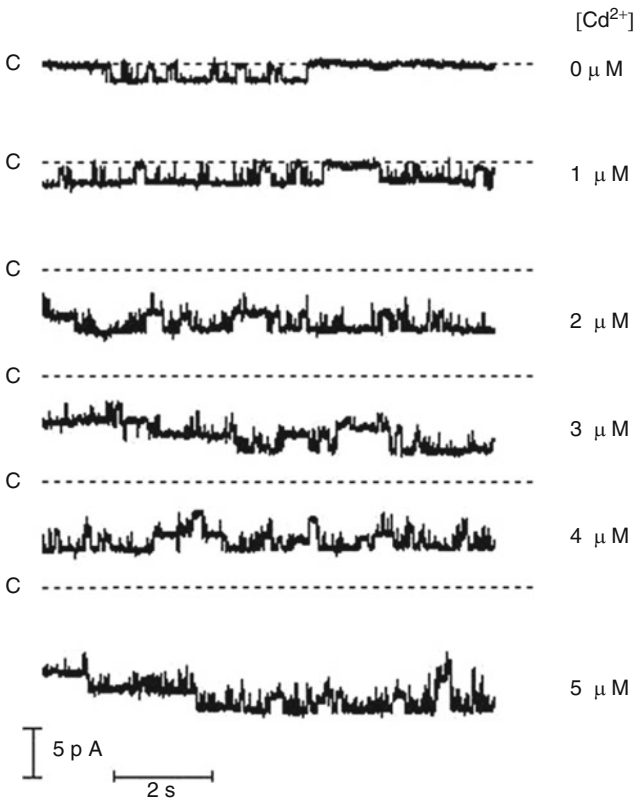

Fig. 7.9 Records of Gram channel currents with added Cd^{2+} in the range 0–5 μM (bath 100 mM KCl, pH 7.0; −80 mV holding potential). Closed current level is denoted by C

increase the open probability of gramicidin D channels. The conductance of these peptide channels is influenced by the heavy metals in a non-monotonic concentration-dependent manner. In the absence of the heavy metal salt, channel openings were alternated with relatively long closings. Cd caused a marked increase in open channel probability, resulting in simultaneous openings of channels – Figs. 7.9 and 7.10.

Figure 7.11 shows current traces representing the effect of Hg^{2+} on openings and closings of Gram channels. An abrupt increase of total current at 3 μM is also typical for the rest of investigated membranes (Fig. 7.12). This may be due to a leak current of $HgCl^{+}$ ions through the lipid bilayer. The halogen salts of Hg are known to readily penetrate pure lipid bilayers as halogenated ions Hg Hal^{+} [27]. This is due to the stepwise dissociation of these salts, where the dissociation constant of the first step to halogenated ion is much larger than the second one to complete dissociation.

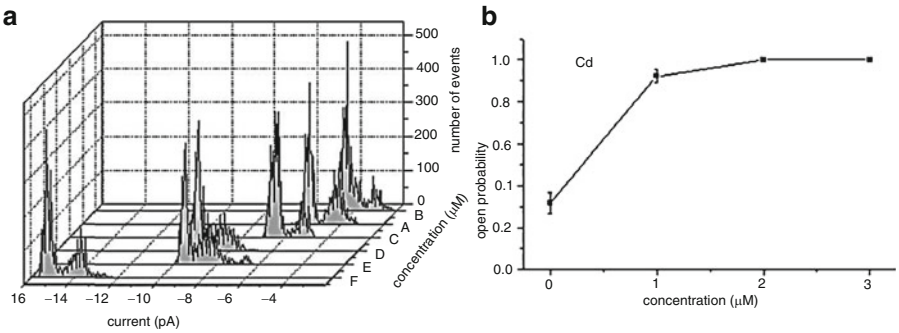

Fig. 7.10 Concentration-dependent cadmium ion effects on gramicidin channels in Soybean lecithin membrane ($CdSO_4$ stock solution added to bath in the indicated final concentrations). (**a**) Current histograms of channel records, (**b**). Gram channel open probability vs. Cd concentration. Data are averaged area ratios from the Gaussian fit of current histograms of 5 independent membranes

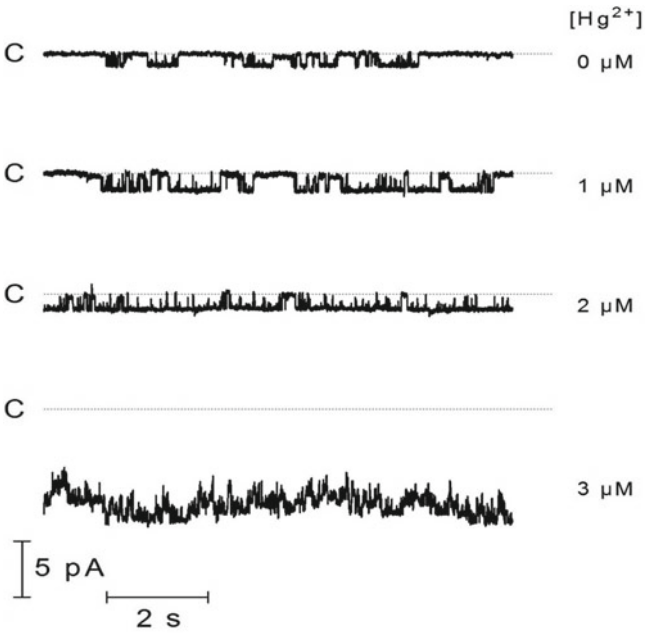

Fig. 7.11 Records of Gram single channel currents with added Hg^{2+} in the range 0–3 μM (bath 100 mM KCl, pH 7.0; −80 mV holding potential). Closed current level is denoted by C

7.2.1.2 Hg^{2+} and Cd^{2+} with Alamethicin Ion Channels

Alamethicin (Alm) is a peptide antibiotic produced by trichoderma viride. It contains the non-proteinogenic amino acid 1-amino isobutyric acid (Aib), which strongly induces helical peptide structures (Fig. 7.13). The peptide sequence

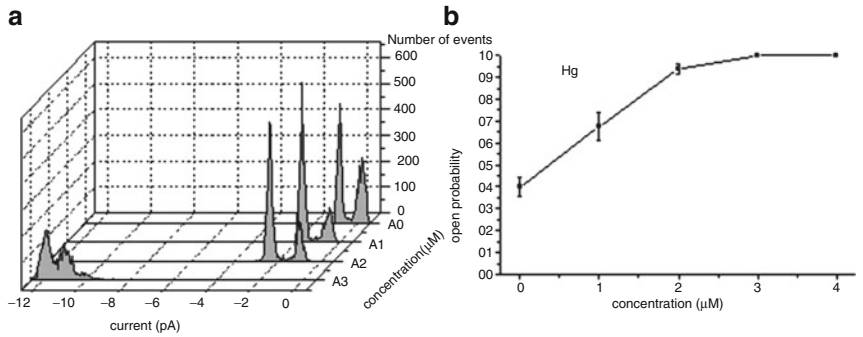

Fig. 7.12 Concentration-dependent mercury ion effects on gramicidin single channel in Soy lecithin membrane ($HgCl_2$ stock solution added to bath in the indicated final concentrations): (**a**) Current histograms of channel records (**b**) Gram channel open probability vs. $HgCl_2$ concentration. Data are averaged area ratios from the Gaussian fit of current histograms of 5 independent membranes

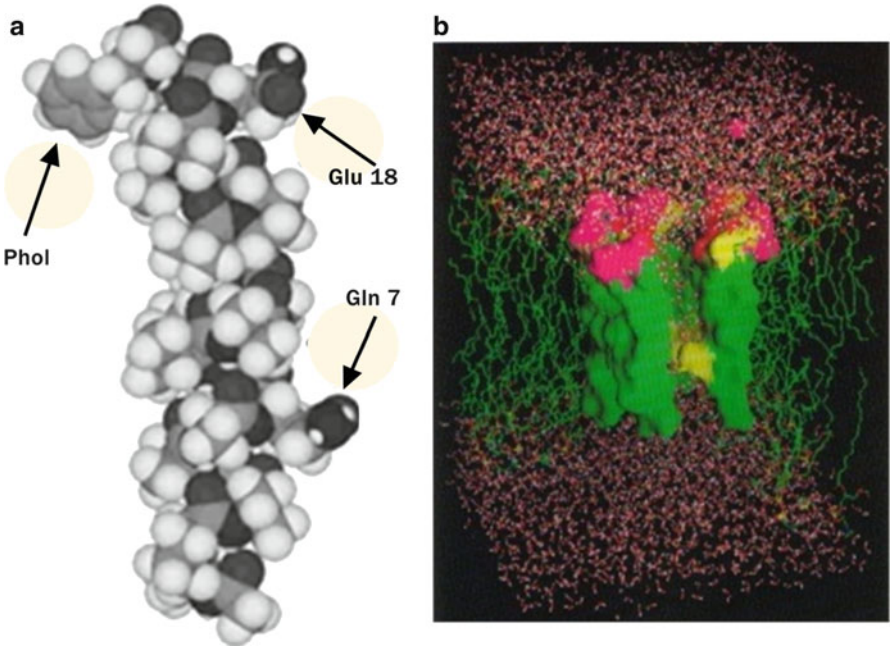

Fig. 7.13 Alamethicin: (**a**) Crystal structure according to Fox and Richards, (**b**) Model of alamethicin ion channel

is: Ac-Aib-Pro-Aib-Ala-Aib-Ala-Gln-Aib-Val-Aib-Gly-Leu-Aib-Pro-Val-Aib-Aib-Glu-Gln-Phl (Ac = acetyl, Phl = phenylalaninol). In cell membranes Alm forms voltage dependent ion channels by aggregation of several molecules into a "bundle" or "barrel" structure which traverses the lipid bilayer. Single Alm channel recordings show multiple conductance levels (see Fig. 7.14).

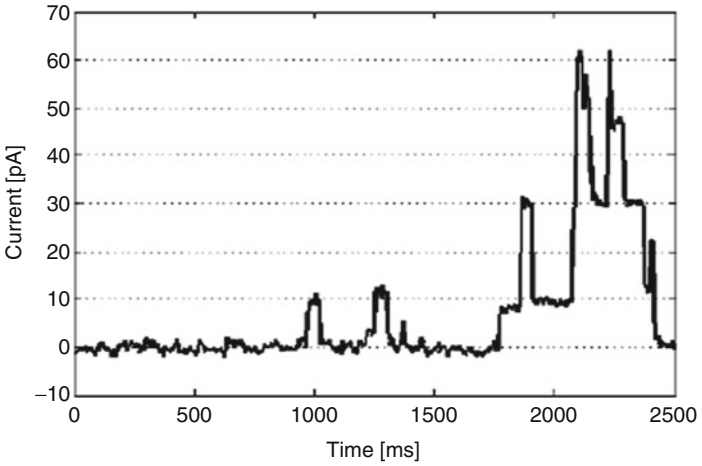

Fig. 7.14 Current recording of a single Alamethicin channel in a patch membrane of soy lecithin, 0.5 M NaCl, pH7, 80 mV

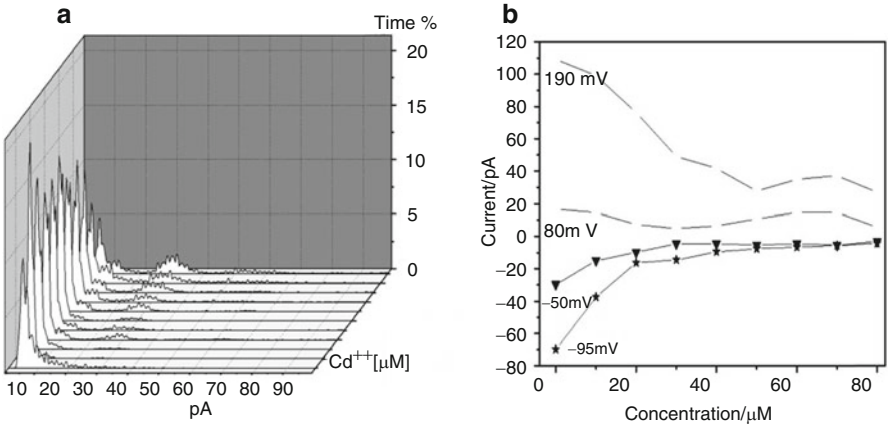

Fig. 7.15 Effects of cadmium ions on alamethicin channels in Soy lecithin membrane ($CdCl_2$ stock solution added to bath in the indicated final concentrations): (**a**) Current histograms of channel records, (**b**) Time-averaged current for 4 individual membranes at the indicated holding potentials

From our experiments [25], it is evident that Cd^{2+} inhibits Alm channel activity. The monotonic character of this inhibition is evident in Fig. 7.15a, which shows Ala channel histograms for concentrations ranging from 0 to 80 μM. The effect of Cd^{2+} concentration on the order of p_o of the second Ala conductance level is shown in Fig. 7.15b for 4 independent membrane preparations at various holding potentials. Apart from the curve at 190 mV all other curves demonstrate a monotonic inhibition of open probability.

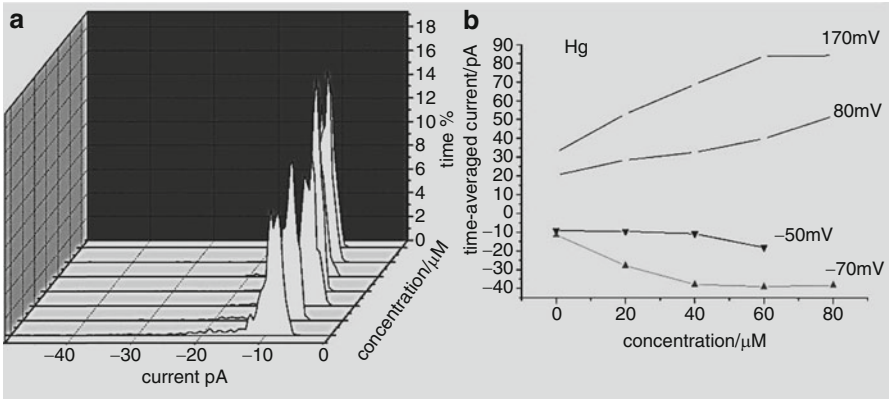

Fig. 7.16 Effects of Hg ions on Alm channels ($HgCl_2$ stock solution added to bath in the indicated final concentrations): (**a**) Current histograms of channel records at holding potential −70 mV. (**b**) Time-averaged current for 4 individual membranes at the indicated holding potentials (concentration range 0–80 μM; bath 500 mM NaCl, pH 7)

Our finding of Cd-induced inactivation of Alm could favorably be compared with the Ca-induced inactivation of the same channel found earlier [28, 29].

Hg^{2+} caused a monotonic increase in the open probability of Alm channels (Fig. 7.16). Channel current histograms of a membrane at several $HgCl_2$ concentrations are given on Fig. 7.16a, while Fig. 7.16b presents the second Alm conducting level opening probability of 4 independent membrane preparations at various holding potentials as a function of $HgCl_2$ concentration. It is well-known that Ala ion channels display conductance asymmetry when Alm is added to the bath only: channels appear only at negative membrane potentials [30, 31] (Fig. 7.17a). Figure 7.17 shows another Hg effect on Alm channel opening: symmetrisation of the I-V curve (Fig. 7.17b); i.e. channel openings appear at positive pipette potentials.

Present investigation is aimed to model Cd^{2+} and Hg^{2+} effects on the two components of a native membrane: the lipid matrix and the ion channels. This would then provide a clue for their neurobiological effect on native ion channels in neural and muscle membranes. It is known that the behavior of Gram and Alm channels depends heavily on the membrane environment in which they are formed. Membrane fluidity affects the Gramicidin-A dimer dissociation rate so that in more fluid membranes the channel lifetime is reduced [32, 33]. A similar observation was made for Alm where transition rates between different conducting states were found dependent on the membrane fluidity.

Our results demonstrate that ion channels are influenced in a specific way: is activated by both ions, while Alm in activated by mercury, but deactivated by cadmium. Control experiments (not shown) evidence that SL lipid membranes without channels are also sensitive to these heavy metal ions at some critical concentrations (around 5 and 50 μM), and tend to develop metastable lipid pores that could lead to increased leak current and, eventually, electric breakdown [34]. The results of this investigation suggest that the different effects of Cd^{2+} and Hg^{2+} could be used to discriminate between these two ions.

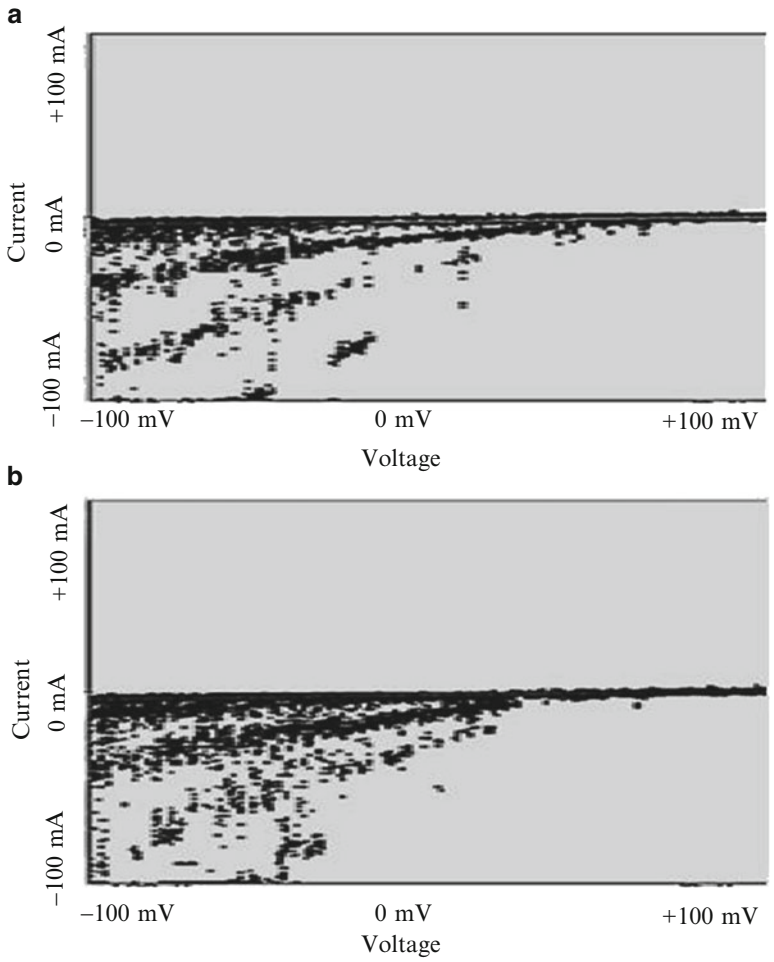

Fig. 7.17 I-V surfaces for alamethicin channels. Symmetrisation of the I-V curve: (**a**). Alm channels' I-V surfaces in a patch clamped membrane after adding Alm to the bath. (**b**) I-V surfaces of the same membrane after $HgCl_2$ addition to bath

7.2.2 Membrane Sensing of Cyanotoxins

Microcystins and nodularins are the most widespread cyanotoxins. They can be found in cyanobacterial blooms ranging from freshwater bodies to oceans. They can be very toxic for plants and animals including humans. The presence of cyanobacterial toxins in drinking water supplies poses a serious problem to water treatment facilities, since not all technical procedures are able to effectively remove these toxins to below acceptable levels.

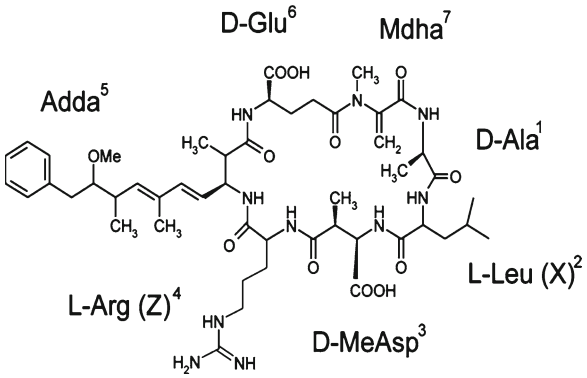

Fig. 7.18 Molecular structure of microcystin

7.2.2.1 Microcystin-LR

Microcystins are a group of cyclic heptapeptide (7 amino acids) hepatotoxins (liver toxins), containing special β-amino acid ADDA (*(all-S,all-E)*-3-Amino-9-methoxy-2,6,8-trimethyl-10-phenyldeca-4,6-diene acid) (Fig. 7.18). There have been approximately 60 different microcystins identified to date. The most common and potently toxic is Microcystin-LR (MC-LR).

The cycle contains hydrophilic aminoacids and serves as a polar head, while the residue of the nontypical aminoacif ADDA is hydrophobic and serves as nonpolar tail. The overall molecular structure thus features a wedge-like steric asymmetry that is a prerequisite for self-assembling in multimers having the structure of an inverted toroidal pore of the structure shown on Fig. 7.6b.

Lipid bilayers of diphytanoyl lecithin (DPhL) in which a cyanobacterial toxin, Microcystin-LR (MC-LR) was incorporated from the ambient solutions, were found to be a convenient model for toxin sensing [35]. These model membrane were formed on the tips of glass micropipettes were investigated using path-clamp methodology. Emplacement of MC-LR from the bathing solution was enhanced by transmembrane voltage. MC-LR pores could be recorded over a wide voltage range, their opening probability being first increased and then reduced at high membrane potential. The pores exhibited several open pore conductance levels. Presumably, these pores feature the structure displayed on Fig. 7.6b. Ion gradient experiments established that MC-LR pores are cation selective, but discriminate only weakly between K^+ and Na^+.

The toxin containing membranes are subjected to slow voltage ramps and the current responses are patch-clamp amplified, recorded and processed by a current-voltage software to provide an averaged picture of all conductance states of a toxin-induced pore (Fig. 7.20b).

7.2.2.2 Nodularin

Nodularin (NODLN) is a cyclic pentapeptide hepatotoxin (Fig. 7.19). It contains two aminoacids less in his cycle. Interestingly, both NODLN and MCYST contain the unusual aminoacid ADDA:

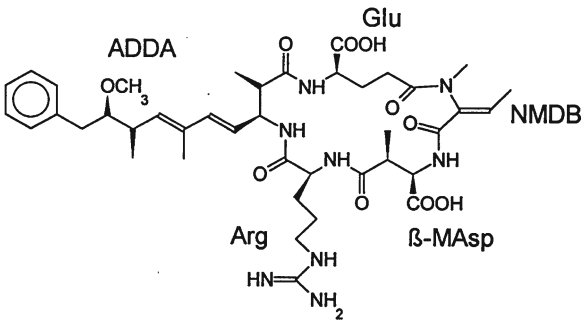

Fig. 7.19 Molecular structure of nodularin

Lipid bilayers of Diphytanoil lecithin (DPhL), in which NODLN was incorporated from the bathing solution, were also investigated [36]. It was found that NODLN also induces conductive pores in membranes. These pores also exhibit many open conductance states. They are also of the type displayed on Fig. 7.6b. However, since the NODLN is a pentapeptide, while MCYST is a heptapeptide, the steric asymmetry of the two molecules differ (compare Fig. 7.18 Fig. 7.19).

Consequently, the number of toxin monomers necessary to complete an inverted pore (cf. Fig. 7.6b) is different (higher for NODLN), and the conductances of the various open states (obtainable by recruiting a few more monomers) should be different, too. Correspondingly, the current-voltage surfaces look quite different, thus providing a signature of a particular toxin type. The results described above suggest that a lipid membrane containing multimers of pore-forming toxin molecules provides a convenient way to detect the toxins and to discriminate between them.

7.3 Flexoelectricity

Flexoelectricity is a phenomenon of curvature-induced electric polarization of liquid crystal membrane, in which the molecules of the membrane are uniaxially oriented. Flexoelectricity is a liquid crystal analogue of piezoelectricity. Instead of a translational mechanical degree of freedom of a membrane in the case of piezoelectricity (i.e., area stretching, thickness compression, etc.), flexoelectricity involves an orientational degree of freedom, the membrane curvature. Flexoelectricity stands for a reciprocal relationship between electric and mechanical degree of freedom of a membrane, i.e., curvature-induced membrane polarization (direct flexoeffect) or voltage-induced membrane curvature (converse flexoeffect). The theory of this phenomenon was considered in several papers of ours [1, 37–40]. Many native membranes (e.g. mitochondria, chloroplasts, erythrocytes, pseudopodia, muscle membrane etc.) are known to exhibit changes of curvature. This implies that flexoelectricity is a fundamental biological phenomenon and may be a mechanism for coupling the mechanical and electrical degrees of freedom of a biological membrane (Fig. 7.21) [41]. Flexoelectricity enables membrane structures to function like soft micro- and nano-machines, sensors and actuators, thus providing important input to molecular electronics applications.

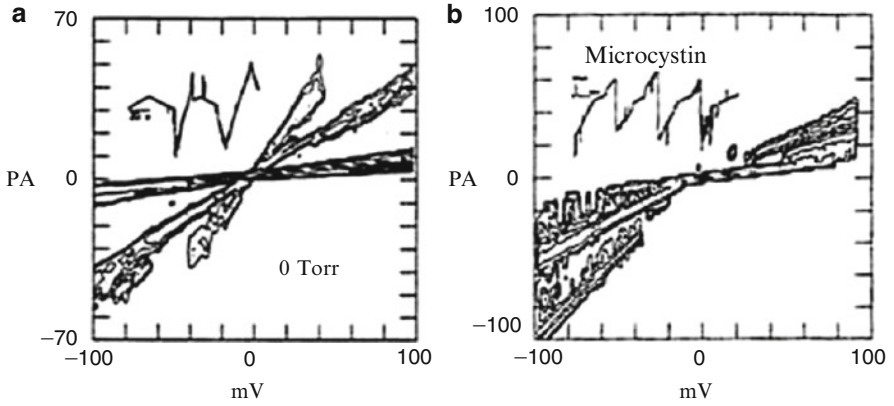

Fig. 7.20 Current-voltage surfaces: (**a**) of NODLN containing bilayer: (**b**) of Microcystin-LR containing bilayer. Insets: individual current ramps before processing. These currents were obtained as responses to slow voltage ramps (−100–100 mV) with a triangular (**a**) or sawtooth (**b**) shape. The corresponding (I-V) pairs were binned is pixels over the I-V plane, and isoprobability lines were drawn by the dedicated software through the pixels with the same probability of the I-V pairs, illustrating the cross-sections of the probability surface projected over the I-V plane

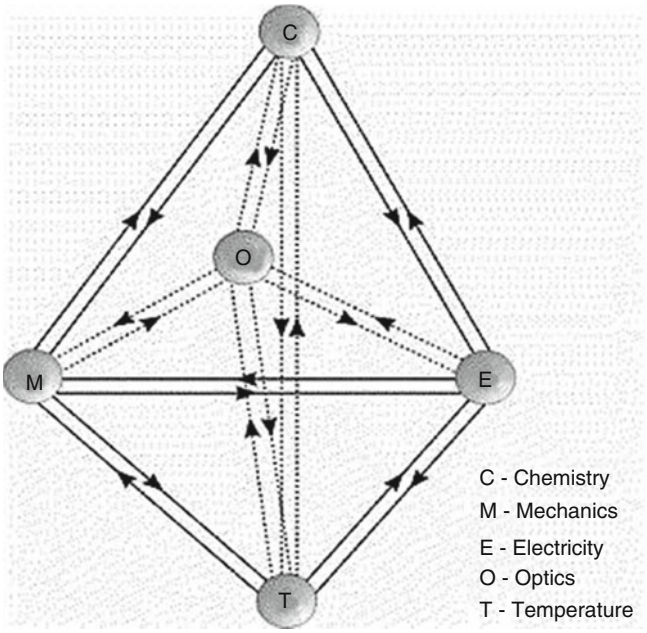

Fig. 7.21 Possible mechanisms of energy interconversion in flexible, electro-, photo-, chemi- and thermo-active membranes. Effects involving 2 degrees of freedom of the membrane system can be marked by two letters (e.g., ME and EM, the direct and converse flexoeffect) and those involving 3 degrees of freedom by three letters (e.g., OME, opto-mechano-electric effect, viz. photo flexoelectric effect)

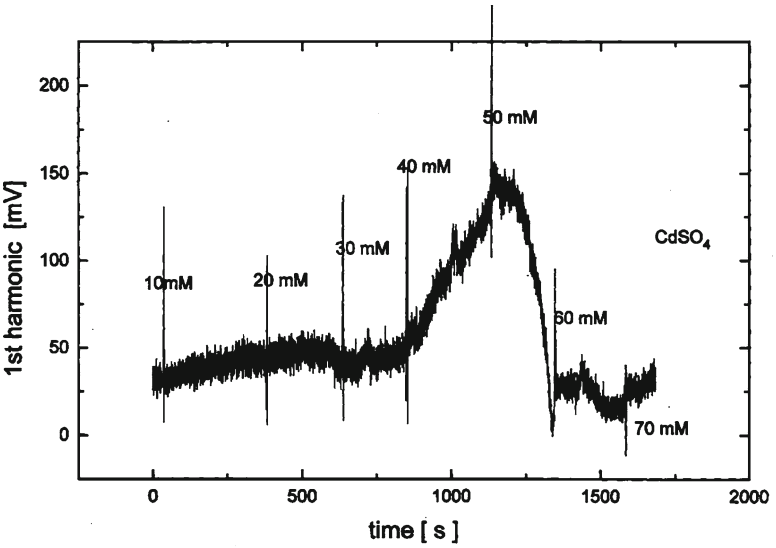

Fig. 7.22 Time dependence of the 1st harmonic of the flexoelectric current of Membranes treated with Cd^{2+} at 410 Hz

7.3.1 Flexoelectricity of Lipid Bilayers Treated with Cd^{2+} and Hg^{2+}

In this investigation [16], the use of patches of membranes as flexoelectric sensors detecting the presence of heavy metal ions in aqueous solutions was reported. The idea of using the flexoelectric properties of artificial membranes to sense chemical species is based on the concept that the flexoelectric response of an oscillating membrane is strongly dependent on the adsorption of charged or dipolar species at the membrane surface [42].

Soy Lecithin membranes was prepared using patch-clamp technique. An oscillating pressure for inducing membranes curvature oscillation was provided by a piezo-sounder.

In this investigation was found that Cd^{2+} initially enhanced the flexoelectric response but at higher concentrations the response was reduced in amplitude (Figs. 7.22 and 7.23):

Flexoelectric response of membranes treated with Hg^{2+} decreased monotonically with Hg^{2+} increasing concentrations and trends to saturate above 5 mm (Fig. 7.24):

The opposite effects at low concentrations of Cd^{2+} and Hg^{2+} on the flexoelectric response could be used to discriminate between their salts.

In conclusion, possible application of flexoelectric membranes as sensors for ion and dipolar species follows from the great sensitivity of flexoresponse to such adsorbed molecules. First prototypes of such sensors using black lipid membranes [16] or patch-clamped bilayers [43] have already been demonstrated.

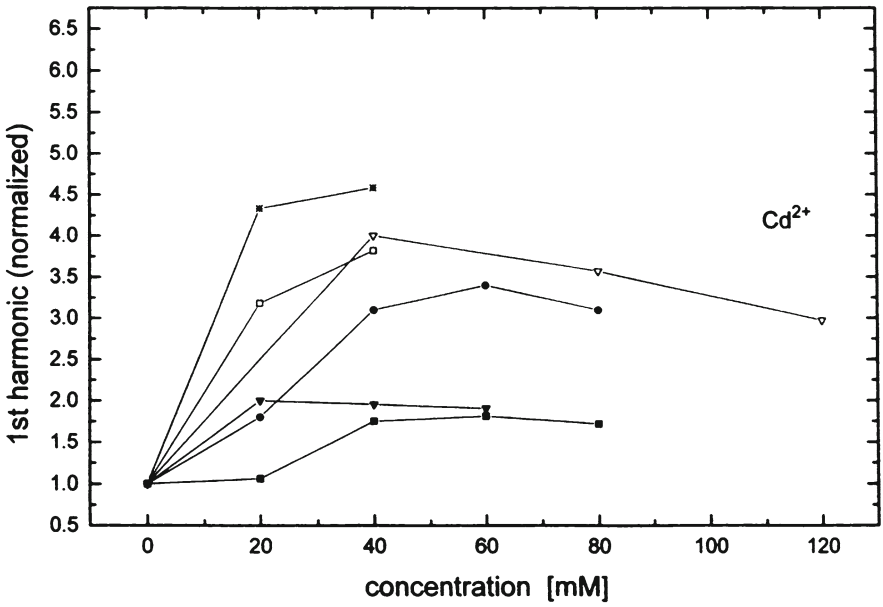

Fig. 7.23 Normalized 1st harmonic of flexoelectric current of several membranes treated with Cd^{2+} vs. the concentration of Cd^{2+}, 410 Hz

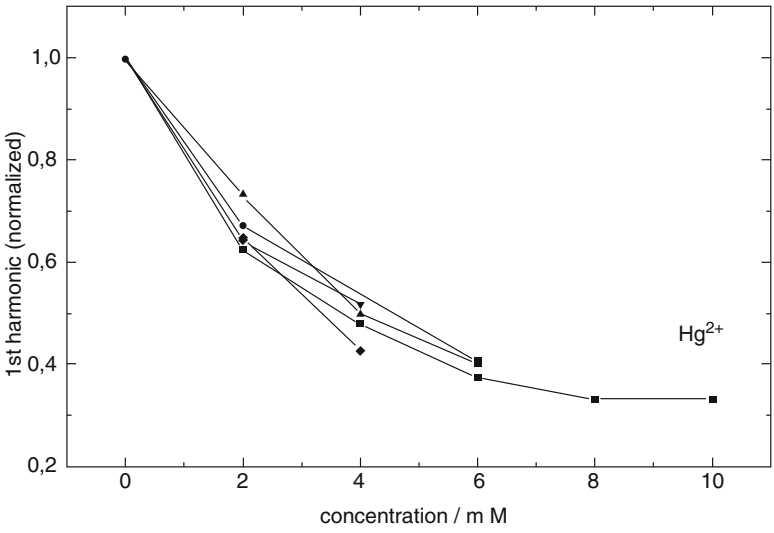

Fig. 7.24 Normalized 1st harmonic of flexoelectric current of several membranes versus the concentration of Hg^{2+}, 410 Hz

7.4 Conclusion

A specific feature of the membrane sensors described in this review is their disposable character. That means the sensor is prepared before the measurement, used to detect the species, and then discarded. The life time of lipid bilayers is normally limited to one laboratory day. A longer term membrane sensor could still be prepared, if needed, by stabilizing lipid bilayers by some chemical means: cross linking of polymerizable lipids, polyamines [44] etc. Individual acts of pore sensing are stochastic, while time averaged values of pore currents are deterministic. Deterministic is also the flexoelectric sensing using lipid membranes. Pursuing the biomimetic approach we could match the excellent membrane selectivity and sensitivity *in vitro*.

References

1. Brown GH, Wolken JJ (1979) Liquid crystals and biological structures. Academic, New York/San Francisco/London
2. Singer SJ, Nicolson GL (1972) The fluid mosaic model of the structure of cell membranes. Science 175:720–731
3. Singer SJ (1992) The structure and function of membranes - a personal memoir. J Membr Biol 129:3–12
4. Burkhart BM (1999) Gramicidin D conformation, dynamics and membrane ion transport. Biopolymers 51:129
5. Petrov AG (1999) The lyotropic state of matter: molecular physics and living matter physics. Gordon & Breach Science Publishers, London/New York
6. Gennis RB (1989) Biomembranes: molecular structure and function. Springer, New York/Berlin/Heidelberg, pp 323–369, Ch. 9
7. Hille B (ed) (2001) Ion channels of excitable membranes, 3rd edn. Sinauer, Sunderland
8. Lyford LK, Rosenberg RL (2003) In: Tien HT, Ottova-Leitmannova A (eds) Planar lipid bilayers (BLMs) and their applications. Elsevier Science B.V, Amsterdam/Boston, Ch.13
9. Kelly MI, Woodbury DJ (2003) In: Tien HT, Ottova-Leitmannova A (eds) Planar lipid bilayers (BLMs) and their applications 2003. Elsevier Science B.V, Amsterdam/Boston, Ch.25
10. Schmidt J (2005) Stochastic sensors. J Mater Chem 15:831–840
11. Bayley H (2000) Stochastic sensing with protein pores. Adv Mater 12:139–142
12. Bayley H, Cremer PS (2001) Stochastic sensors inspired by biology. Nature 413:226–230
13. Petrov AG (2002) Flexoelectricity of model and living membranes. Biochim Biophys Acta 1561:1–25
14. Petrov AG (2006) Electricity and mechanics of biomembrane systems: flexoelectricity in living membranes. Anal Chim Acta 568:70–83
15. Naydenova S, Hristova K, Todorov A, Petrov AG (1989) On the use of black lipid membranes as pressure sensors. In: 2nd international conference "molecular electronics and biocomputers", Russian Academy of Sciences, Moscow 1989, Russian Academy of Sciences, Abstracts pp 91–92
16. Zheliaskova A, Naydenova S, Marinov Y, Mellor IR, Usherwood PNR, Petrov AG (2001) Detection of heavy metal ions ($Cd2^{+}$ and Hg^{2+}) by their influence on flexoelectricity of patch clamped membranes. C R Acad Bulg Sci 54(12):53–56
17. Petrov AG, Usherwood PNR (1994) Mechanosensitivity of cell membranes: ion channels, lipid matrix and cytoskeleton. Eur Biophys J 23:1–19
18. Coronado R, Latorre R (1983) Phospholipid bilayers made from monolayers on patch-clamp pipettes. Biophys J 43:231–236
19. Sansom MSP, Mellor IR (1990) Analysis of the gating of single ion channels using current-voltage surfaces. J Theor Biol 114:213–223

20. Derzhanski A, Petrov AG (1982) Multipole model of the molecular asymmetry in thermotropic and lyotropic liquid crystals. Volume and surface effects. Mol Cryst Liq Cryst 89:339
21. Petrov AG, Derzhanski A (1987) Generalized asymmetry of thermotropic and lyotropic mesogens. Mol Cryst Liq Cryst 151:303
22. Petrov AG (1988) "Generalized lipid asymmetry and instability phenomena in membranes", Ninth school biophysics membrane transport. School Proceedings. Agricultural Academy, Wroclaw vol 2. Agricultural Academy, Wroclaw, pp 67–86
23. Carpenter DO (1994) The public-health significance of metal neurotoxicity. Cell Mol Neurobiol 14:591–597
24. Naydenova S, Mellor IR, Petrov AG (2003) Effect of heavy metal ions on lipid bilayers containing gramicidin channels. C R Acad Bulg Sci 56(3):63–68
25. Naydenova S, Zheliaskova A, Ugrinov R, Marinov Y, Petrov AG (2003) Ion channel-containing lipid membranes interacting with heavy metal ions. J Mater Sci Mater Electron 14:815–816
26. Hladky SB, Haydon DA (1970) Discreteness of conductance change in biomolecular lipid membranesin the presence of certain antibiotics. Nature 225:451–453
27. Nekrassov BV (1962) Kurs obshchej khimii. GNTIHL, Moscow
28. Halland JE, Cahalan MD (1982) Calcium-induced inactivation of alamethicin in asymmetric lipid bilayers. J Gen Physiol 79:387–409
29. Cahalan MD, Hall JE (1982) Alamethicin channels incorporated into frog node of Ranvier-calcium-induced inactivation and membrane-surface charges. J Gen Physiol 79:411–436
30. Vodyanoy I, Hall JE, Balasubramanian TM (1983) Alamethicin-induced current-voltage curve asymmetry in lipid bilayers. Biophys J 42:71–82
31. Cafiso DS (1994) Alamethicin: a peptide model for voltage gating and protein -membrane interaction. Annu Rev Biophys Biomol Struct 23:141–165
32. Lundbaek JA, Andersen OS (1994) Lysophospholipids modulate channel function by altering the mechanical-properties of lipid bilayers. J Gen Physiol 104:645–673
33. Lundbaek JA, Birn P, Girshman J, Hansen AJ, Andersen OS (1996) Membrane, stiffness and channel function. Biochemistry 35:3825–3830
34. Melikov KC, Frolov VA, Shcherbakov A, Samsonov AV, Chizmadzhev YA, Chernomordik LV (2001) Voltage-induced nonconductive pre-pores and metastable single pores in unmodified planar lipid bilayer. Biophys J 80:1829–1836
35. Petrov AG, Ramsey RL, Codd GA, Usherwood PNR (1991) Modeling mechano-sensitivity in membranes: effects of lateral tension on ionic pores in a microcystin toxin_containing membrane. Eur Biophys J 20:17–29
36. Usherwood PNR (1995) Pores formed in lipid bilayers and in native membranes by nodularin, a cyanobacterial toxin. Eur Biophys J 24:69–76
37. Petrov AG (1991) Flexoelectricity of membranes and electric double layers. In: Jennings BR, Stoylov SP (eds) Colloid and molecular electrooptics. Institute of Physics Publ, Bristol/ Philadelphia, pp 171–176
38. Petrov AG, Spassova M, Fendler JH (1996) Nanoparticles in solids and solutions. In: Fendler J, Dekany I (eds) Proceedings of the NATO advanced research workshop, Kluwer Academic Publs., Netherlands, pp 175–183
39. Petrov AG, Sachs F (2002) Flexoelectricity and elasticity of asymmetric biomembranes. Phys Rev E 65:021905–021910
40. Petrov AG, Miller BA, Hristova K, Usherwood PNR (1993) Flexoelectric effects in model and native membranes containing ion channels. Eur Biophys J 22:289–300
41. Petrov AG, Naydenova S, Marinov Y, Ivanov G, Todorova L, Angelov T, Dencheva M (2002) Biomolecular layers: advances and perspectives. In: Jubilee proceedings of institute of solid state physics. Bulgarian Academy of Sciences, Sofia, pp 96–112
42. Petrov AG, Sokolov VS (1986) Curvature_electric effect in black lipid membranes. Eur Biophys J 13:139
43. Sun K (1997) Toward molecular mechanoelectric sensors: flexoelectric sensitivity of lipid bilayers to structure, location, and orientation of bound amphiphilic ions. J Phys Chem 101:6327–6330
44. Zheliaskova A, Naydenova S, Petrov AG (2000) Interaction of phospholipid bilayers with polyamines of different length. Eur Biophys J 29:153–157

Chapter 8
Nano-Structured Solids and Heterogeneous Catalysts: Powerful Tools for the Reduction of CBRN Threats

Heterogeneous Catalysts Against CBRN Threats

M. Guidotti, A. Rossodivita, and M.C. Ranghieri

Abstract In the field of non-conventional CBRN weapons, the recent rapid development of nanotechnology and catalysis over nanosized solids provides innovative tools for the detection, protection and decontamination against these threats. By improving the efficiency of the countermeasures and by minimizing the negative effects of a deliberate use of CBRN agents, the practical application of the new technologies will readily represent a step forward in lowering the vulnerability of the civilian populations and in preventing the use of mass destruction weapons by terrorist groups or by 'rogue states' supporting terrorists' activity. In such scenario, some relevant examples of nanosystems applied to the defense from non-conventional warfare agents will be here presented and commented. The key role of nanotechnology and heterogeneous catalysis for a multidisciplinary approach in counteracting CBRN threats will be highlighted too.

Keywords Nanotechnology • Heterogeneous catalysis • Mesoporous materials • Non-conventional warfare agents • Decontamination • CBRN agent abatement

M. Guidotti (✉)
CNR-Istituto di Scienze e Tecnologie Molecolari, via Venezian 21, Milan, Italy

1st Field Unit, E.I.-S.M.O.M. Military Corps, Milan, Italy
e-mail: m.guidotti@istm.cnr.it

A. Rossodivita
Dipartimento di Cardiologia, Ospedale S. Raffaele e Fondazione Scientifica, via Olgettina 40, Milan, Italy

M.C. Ranghieri
1st Field Unit, E.I.-S.M.O.M. Military Corps, Milan, Italy

A. Vaseashta et al. (eds.), *Technological Innovations in Sensing and Detection of Chemical, Biological, Radiological, Nuclear Threats and Ecological Terrorism*, NATO Science for Peace and Security Series A: Chemistry and Biology,
DOI 10.1007/978-94-007-2488-4_8, © Springer Science+Business Media B.V. 2012

8.1 Introduction

'Armis bella non venenis geri' – Wars are fought with weapons, not with poisons.
A condemnation by Roman jurists of well poisoning – (1st century A.D.)

Throughout the history of humankind, any new scientific discovery of technological advance has shown the risk of a 'dual' use for peaceful purposes or for warfare. In the field of non-conventional chemical/biological/radiological/nuclear (CBRN) weapons, the recent exponential development of nanoscience and nanotechnology is leading not only to the development of new and unpredictable threats [1–4], but also to the development of innovative and efficient tools for the detection, monitoring and abatement of CBRN agents [5, 6].

During the twentieth century, the rapid set-up of effective countermeasures, minimizing or eliminating the negative effects of a deliberate use of chemical or biological weapons, reduced the vulnerability of fighters in warfare scenarios and contributed to reduce (or even eradicate) the extended use of C and B agents in every conflict. In fact, thanks to the development of protection devices, such as activated-carbon gas masks, polymer-based protecting suits or decontaminating solutions or powders, the effects of a tactical use of C or B weapons in battlefield have been minimized and the high development level reached by protection capabilities acted as a real deterrent (at least for Western countries) during WWII and later [7].

Nevertheless, at the beginning of twenty-first century, the new global equilibria and the ever-increasing threat of terrorism prompted the governments worldwide and the research organizations at national level to pay particular attention to novel methods of protection against non-conventional weapon attacks. In this aim, nanoscience, nanotechnology and biotechnology are the emerging disciplines that can give rise to unprecedented methods, tools and equipment to counteract efficiently and effectively CBRN threats [8]. So, the higher the level of development of defense techniques, the lower will be the risk of mass destruction weapons in a warfare or terrorist scenario and the lower will be the vulnerability of populations, military personnel and emergency first responders.

8.2 Catalytic Nanosystems Against CBRN Agents

Nanosystems are chemical objects whose dimensions are included in the range between 1 and 100 nm. They show peculiar chemical and physical properties thanks to quantum effects and to the presence of wide surfaces and interphasal domains [9]. Among them, nanoparticles possess very high surface to volume ratios. Their atoms have a higher average energy than atoms in larger structures, because most of them are exposed (in edge and corner positions) and are therefore characterized by a very high dispersion and large amounts of available coordination sites.

This particular mix of characteristics is ideal for heterogeneous catalysis. The exposed active sites of a solid catalyst must interact efficiently with substrate

molecules and must promote their transformation. For this reason, most heterogeneous catalysts are based on nanoparticles: namely, inorganic oxide nanoparticles (where metal atoms are in high-oxidation state in combination with oxygen) and/or metal nanoparticles (with metal sites in low-oxidation state).

Nanosystems with catalytic properties can thus play a relevant role in preventing or minimizing the negative effects of chemical, biological and, to a lesser extent, radiological agents. Nanosized catalytic systems (*nanocatalysts*) can find application not only in the detection [10], but also in the protection, decontamination and abatement steps during the defense action against a hazardous agent. Especially in the removal and destruction of CBR(N) agents, nanocatalysts have shown (and still are showing) the most promising applications.

8.3 Selected Examples

8.3.1 Nanosystems for Individual Protection and Decontamination

In last years, the attention of both scientific open and patent literature moved from traditional chemical decontamination (requiring huge amounts of solvents and oxidizing or caustic reagents) to the catalytic decontamination, based on heterogeneous (solid-liquid or solid-vapor) catalysts, which are able to convert highly toxic species into non-toxic secondary products under ambient conditions, thanks to the use of low amounts of added reactants (or not at all).

In terms of advantages, abatement processes based on heterogeneous catalysis typically imply simpler chemical steps, lower energy requirements and a better use of the reactants with respect to conventional stoichiometric (non-catalytic) techniques. Furthermore, in the case of nanocatalysts all these features are enhanced, as the concentration of highly active catalytic sites, per unit of mass, is higher than in traditional non-nanosized systems. This also means improved conditions in terms of safety, environmental and economical sustainability as well as lower costs for the disposal of the detoxified by-products.

The focus is thus moving from a *passive adsorption* (removal) towards a *self-cleaning adsorption* (*in situ* abatement) of the hazardous agent. Practically, conventional decontamination methods based on chemical or physical techniques, such as dissolution, removal, degradation (oxidation or alkaline hydrolysis) and combustion are being replaced by the use of reactive sorbent materials, as oxidation promoters or photocatalysts activated by sunlight.

For instance, nanostructured metal oxides (typically oxides from Zn, Ti, Fe, Mn, Mg, Al, Zr or Cu) have very high specific surface areas and a large amount of defective crystalline edges, corners and sites that are much more reactive than their bulk counterpart. They are able to decompose nerve and vesicant chemical agents (or simulants of these compounds) into non-toxic by-products. Nanowires and

nanofibers are particularly suitable for these purposes as they can be easily incorporated in textiles and clothes.

In particular, ZnO-TiO_2 nanofibers (ZnO from 40 to 60 mol% in TiO_2), obtained by electrospinning technology with polyvinylpyrrolidone as a binder, with diameters between 60 and 600 nm, are able to decompose paraoxon (a nerve agent simulant) or 2-chloroethyl ethyl sulfide (CEES; a mustard agent simulant) in acetone solution at room temperature, without any further addition of reactants [11]. Under these conditions, up to 90% and 70% of the initial amount of paraoxon and CEES are detoxified in 50 and 10 min, respectively. The catalytically active sites on the surface of zinc titanate fibers, in fact, promote the spontaneous slow hydrolysis of the agent and enhance the oxidation of sulfides to sulfoxides and sulfones (less toxic or non-toxic compounds), in the case of sulfur mustards.

Typically, no additional water is necessary to carry out the hydrolysis, as the natural ambient moisture or the water molecules physisorbed onto or intercalated within the oxidic fibers are sufficient to transform the hazardous chemical agent into a non-toxic by-product [12]. In such nanocatalysts, a key role is played by the large amount of homogeneously dispersed and accessible Lewis acid sites, constituted by the metal site (Ti(IV), Zn(II), Mn(IV), etc.), available at accessible positions (Scheme 8.1). The surface hydroxyls, formed by the interaction of water with the metal centers, act as nucleophiles and lead to the hydrolytic degradation of the phosphorous- or sulfur-containing aggressive agent.

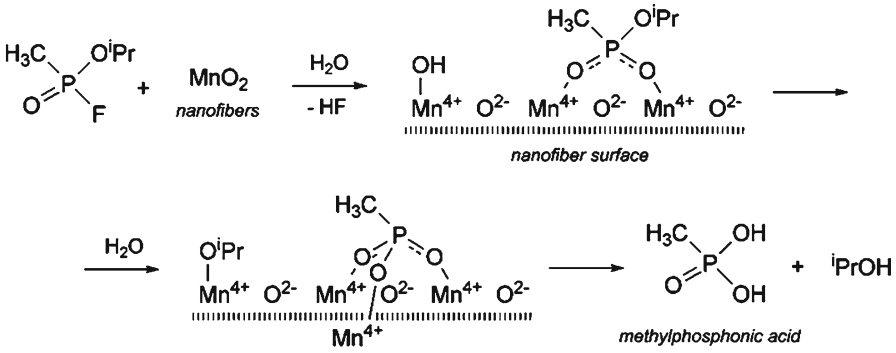

Scheme 8.1 Hydrolytic degradation of a nerve agent (sarin) over manganese dioxide nanofibers in the presence of water

Such effect, in fact, is far less effective over non-nanosized bulk materials. By comparing the performance of nanocrystalline zinc oxide with conventional bulk zinc oxide in the solventless detoxification of nerve agents, it appears that the half-life of sarin is *ca*. 60 times lower over nano-ZnO than over bulk ZnO (*i.e*. 0.16 h *vs*. 6.81 h, respectively) [13].

This kind of nanofibers can constitute the active sorption layer in a composite textile and finds application in the production of new classes of individual permeable

protection suits, as a replacement for the widely-used active carbon. Lighter suits can therefore be produced, as the active adsorption layer does not reach saturation, and a simpler disposal of the used equipment is possible, as the aggressive agent is no longer present in/on the protection device, but it is degraded in non-toxic (or poorly toxic) secondary products.

Such spontaneous hydrolysis and oxidation processes can also be further promoted when nanocatalysts act as photocatalysts as well. In such applications, TiO_2 nanoparticles or nanowires are the materials of choice. The ability of nanodispersed titanium oxide (anatase) to collect high-energy solar light (the violet and UV range of solar radiation) and generate powerful free-radical oxidant species (in particular, highly-reactive singlet oxygen from dioxygen in air) is exploited in the abatement of environmental pollutants as well as of hazardous chemical or biological agents [14–16]. As a relevant example, TiO_2 can be obtained in macroscopically long nanowires and assembled into free-standing membranes [17]. Such 'nanowire papers' are mechanically (rather) resistant, chemically inert up to 700°C and can be sterilized by calcination or high-energy UV light. Additionally, they have an adjustable pore size which lets atmospheric O_2 in, but blocks macromolecules, toxins, viruses and bacteria out. These features are suitable for the manufacture of self-cleaning filter systems for the detoxification of breathable air from C and B agents, hence avoiding (or reducing) rapid accumulation of pollutants in the filters.

TiO_2-based systems have already found application, for instance, in active protecting body creams, joining shielding and decontaminating actions [18]. The formulation of such creams include mixtures of perfluorinated polyethers and polytetrafluoroethylenes (with barrier properties) together with 3% of pyrogenic TiO_2, featuring particle diameter of *ca.* 30 nm (the active component in abatement). When applied to bare skin, the cream proved to be highly effective against nerve agents vapors (mainly G agents, with, for example, 99% abatement of soman in vapor phase).

Analogously, some nanosized decontamination powders are commercially available and they mix the hydrolytic action of MgO nanoparticles (*ca.* 10–20 nm in diameter) with the photocatalytic activity of TiO_2 [19]. As main advantages, such binary system does not need additional oxidants, as it relies on the free-radical activation of molecular oxygen, and it is effective in the rapid decomposition of nerve agents (99.9% abatement of VX in 10 min) as well as of airborne bacterial spores (such as anthrax), even at room temperature. Once again, the peculiar chemical combination of MgO and TiO_2 nanoparticles implies very high local concentration, in close proximity, of Lewis acid (Mg^{2+} atoms in the lattice of MgO nanocrystals), Lewis basic (O^{2-} atoms in MgO) and oxidant catalytic sites (the *in situ* formed oxygen radicals over TiO_2), with an exponential increase of the catalyst's activity with respect to non-nanosized materials.

More recently, nanostructured composite materials, based on hybrid inorganic-organic compounds, have also shown promising features, in terms of activity and abatement performance, and can find several 'smart' applications in the field of self-decontaminating devices. A relevant example of multi-functional material is a new class of electrospun nanofibrous polymers based on a dimethylacrylamide-methacrylate

copolymer backbone, supporting both chemical and biological decontamination [20]. Polyurethanes containing the redox enzymes glucose oxidase and horseradish peroxidase exert a remarkable bactericidal activity against gram positive and gram negative bacteria, converting halide ions from the local environment into active halogens. Simultaneously, *N*-alkyl-4-pyridinium aldoxime (4-PAM) halide-acrylate copolymers offer nucleophilic activity for the detoxification of C agents and act as internal sources of halide ions. In the best tests, the composite nanofibers have shown complete kill of *Escherichia coli* (>6 log units) within 1 h at 37°C and 85% abatement diisopropylfluorophosphate (a nerve agent analog) in 30 min.

8.3.2 Nanosystems for Extensive Decontamination and Abatement

Nanostructured porous materials are generally considered as valid solid supports for catalysts to be used in the abatement and destruction of wide amounts of toxic compounds and, in particular, of large stockpiles of chemical warfare agents. The abatement techniques based on heterogeneous catalysts are valid alternatives to conventional procedures involving incineration and thermal destruction. Mesoporous silica materials (such as MCM-41, HMS or SBA-15 silica [21]) possess a very high specific surface area (around 1,000 $m^2\ g^{-1}$, or even more) and a highly accessible porous network at nanometric level. They are thus comparable to widely-used active carbon, in terms of adsorption properties and capacity. However, they are chemically more defined, more easily functionalized and regenerable than the latter. Redox catalytic species (typically V, Ti, Mn, Mo, etc.) can be deposited and dispersed into the internal channels and pores of these solids, thus creating a redox-active heterogeneous catalyst.

For instance, in vanadium-doped nanostructured mesoporous silica a large number of evenly dispersed, highly accessible V(V) catalytically active sites are present and can be employed in the selective oxidation (and detoxification) of sulfur-mustard simulants (CEES) in the presence of liquid oxidants, such as hydrogen peroxide or organic hydroperoxides (alkylhydroperoxides) [22]. Over these catalysts, the deadly organic sulfides are selectively converted into non-toxic sulfoxides, whereas, by conventional thermal abatement techniques remarkable and hazardous amounts of sulfones and carbon monoxide are also produced as by-products. Clearly, since stoichiometric quantities of liquid oxidant are required, together with the solid catalyst, such nanostructured materials are not suitable for individual protection or decontamination equipment. Nevertheless, they offer good selectivity to the desired non-noxious compounds and can be satisfactorily recovered and recycled for further use [23].

Analogously, high specific surface area nanostructured materials with functional sites are finding extensive application in the abatement of heavy metals and also of metal radionuclides, hence in the remediation of chemical and/or radiological contamination [24]. Thanks to the deposition of chelating ligands with a high

chemical affinity towards the heavy metal ions or the radionuclides within the mesopores, it is possible to remove efficiently and selectively the contaminating species from a liquid effluent (*e.g.* industrial wastes, polluted drinkable water or radiologically contaminated liquids). The internal channels of the nanostructured porous material are, in fact, fully covered by organic linkers bearing chemical functional groups that are specifically designed for the removal of toxic metals (typically, organic moieties with –SH functional groups are ideal for binding heavy metals) or for the strong retention of actinide ions (nitrogen-containing heterocyclic moieties are suitable for the chelation and removal of Np(V), U(VI), Pu(IV), etc.; Scheme 8.2). These materials can be recovered and reused, after a regeneration cycle in the presence of concentrated HCl aqueous solutions (as they were ion-exchange resins). Therefore, if one compares the material-lifetime and the cost of these functionalized nanostructured materials with the ones of conventional widely-used ion-exchange resins or activated carbon powders, it appears that, even if the specific cost of the material is far higher for the nanostructured material (*ca.* 150 USD kg^{-1} *vs.* 50 USD kg^{-1} and 2 USD kg^{-1}, for ion-exchange resins and activated carbon, respectively), the depolluting efficiency of the former is some orders of magnitude higher than for the latter two materials (in terms of grams of pollutant species per kilogram of adsorbent material) and therefore the global cost assessment (total cost of the process per gram of pollutant removed) can be largely favorable towards the use of innovative nanostructured adsorbents (*e.g.* a total cost of *ca.* 2000 USD *vs.* 261,000 USD per kilogram of Hg removed has been estimated for the decontamination of an aqueous solution of 0.2 mg L^{-1} over a functionalized nanostructured material and a conventional activated carbon, respectively) [25].

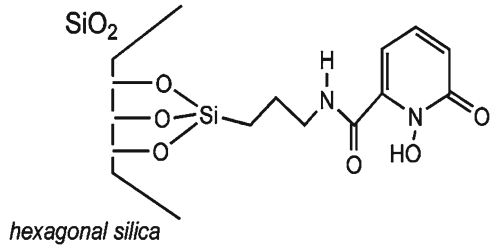

Scheme 8.2 Organic linker, containing 1,2-hydroxypyridinone for the chelation of actinide ions, anchored onto the internal surface of a hexagonal nanostructured silica material

8.4 Conclusions

Any progress in the state-of-the-art about CBRN agent destruction will also result in strengthening the global preparedness and response to non-conventional threats. By improving the efficiency of the countermeasures and by minimizing the negative effects of a deliberate use of CBRN agents, the practical application of the new technologies will readily represent a step forward in lowering the vulnerability of

the civilian populations and in preventing the use of mass destruction weapons by terrorist groups or by "rogue states" supporting terrorists' activity.

Nanosciences, nanotechnology and heterogeneous catalysis can play a relevant role in developing new individual protection systems, improving decontamination capabilities and providing more efficient and sustainable CBRN abatement methods. Nevertheless, as in industrial chemistry increasing attention is paid towards *green chemistry*, new protection and decontamination processes and techniques must be both economically and environmentally sustainable. In this aim, only a multidisciplinary effort from experts from different research areas (materials science, chemistry, biology, physics, engineering, etc.) and active in different environments (academia, industry and military) can lead to concrete results that can be exploited and applied in a short-term time period.

Acknowledgements The authors gratefully acknowledge Prof. A. K. Vaseashta, for the kind invitation to the NATO Advanced Study Institute held in Chisinau (Moldova). M.G. also thanks the Italian Ministry of Education, University and Research for financial support through the Project "ItalNanoNet" (Rete Nazionale di Ricerca sulle Nanoscienze; prot. no. RBPR05JH2P).

References

1. Gatti AM, Rivasi F (2002) Biocompatibility of micro- and nanoparticles. Part I: in liver and kidney. Biomaterials 23(11):2381
2. Gatti AM, Montanari S (2008) Nanopathology: the health impact of nanoparticles. Pan Stanford, Singapore
3. Barnard AS (2006) Nanohazards: knowledge is our first defence. Nat Mater 25:245
4. Kostarelos K (2008) The long and short of carbon nanotube toxicity. Nat Biotechnol 26(7):774
5. Guidotti M, Ranghieri M, Rossodivita (2010) Nanosystems and CBRN threats: a resource worth exploiting, a potential worth controlling. In: Trufanov A, Rossodivita A, Guidotti M (eds) Pandemics and bioterrorism – transdisciplinary information sharing for decision-making against biological threats, vol 62, NATO science for peace and security series – E: human and societal dynamics. IOS-Press, Amsterdam, pp 117–126
6. Reynolds JG, Hart BR (2004) Nanomaterials and their application to defense and homeland security. JOM 56(1):36
7. Bismuth C, Borron SW, Baud FJ, Barriot P (2004) Chemical weapons: documented use and compounds on the horizon. Toxicol Lett 149:11
8. Altmann J, Gubrud M (2004) Anticipating military nanotechnology. IEEE Technol Soc Mag 23:33
9. Psaro R, Guidotti M, Sgobba M (2008) Nanosystems. In: Bertini I (ed) Inorganic and bio-inorganic chemistry, vol II, Encyclopedia of life support systems (EOLSS). EOLSS Publishers Co. Ltd, Oxford, pp 256–307. ISBN 978-1-84826-665-0
10. Woolard DL, Trew RJ, Polla DL, Stroscio MA, Varshney U, Jensen J, Jensen JO, Lugli PO, Aono M (2008) Nanosensors for defense and security. IEEE Sens 8(5–6):641–646
11. Ramaseshan R, Ramakrishna S (2007) Zinc titanate nanofibers for the detoxification of chemical warfare simulants. J Am Ceram Soc 90(6):1836
12. Mahato TH, Prasad GK, Singh B, Batra K, Ganesan K (2010) Mesoporous manganese oxide nanobelts for decontamination of sarin, sulphur mustard and 2-(chloroethyl)ethylsulphide. Microporous Mesoporous Mater 132:15

13. Mahato TH, Prasad GK, Singh B, Acharya J, Srivastava AR, Vijayaraghavan R (2009) Nanocrystalline zinc oxide for the decontamination of sarin. J Hazard Mater 165:928
14. Panayotov DA, Morris JR (2009) Thermal decomposition of a chemical warfare agent simulant (DMMP) on TiO_2: adsorbate reactions with lattice oxygen as studied by infrared spectroscopy. J Phys Chem C 113:15684
15. Grandcolas M, Louvet A, Keller N, Keller V (2009) Layer-by-layer deposited titanate-based nanotubes for solar photocatalytic removal of chemical warfare agents from textiles. Angew Chem Int Ed 48:161
16. Mattsson A, Lejon C, Stengl V, Bakardjieva S, Oplustil F, Andersson PO, Osterlund L (2009) Photodegradation of DMMP and CEES on zirconium doped titania nanoparticles. Appl Catal B Environ 92:401
17. University of Arkansas Daily Headlines (2006). Nanowire-paper offers strength, flexibility, from August 22, 2006. http://nanotechwire.com/news.asp?nid=3385. Accessed 20 Oct 2011
18. Hobson ST, Braue EH, Lehnert EK, Klabunde KJ, Koper OP, Decker S (2001) Active topical skin protectants using reactive nanoparticles. US Patent US6403653 to US Department of the Army
19. FAST-ACT® NanoScale website. http://www.fast-act.com. Accessed 20 Oct 2011
20. Amitai G, Murata H, Andersen JD, Koepsel RR, Russell AJ (2010) Decontamination of chemical and biological warfare agents with a single multi-functional material. Biomaterials 31:4417
21. Corma A (1997) From microporous to mesoporous molecular sieve materials and their use in catalysis. Chem Rev 97:2373
22. Ringenbach CR, Livingston SR, Kumar D, Landry CC (2005) Vanadium-doped acid-prepared mesoporous silica: synthesis, characterization, and catalytic studies on the oxidation of a mustard gas analogue. Chem Mater 17:5580
23. Livingston SR, Kumar D, Landry CC (2008) Oxidation of 2-chloroethyl ethyl sulfide using V-APMS. J Mol Catal A 283:52
24. SAMMS Technical Summary Pacific northwest national laboratory. http://samms.pnl.gov/samms.pdf. Accessed 20 Oct 2011
25. Yantasee W, Fryxell GE, Lin Y, Wu H, Raymond KN, Xu J (2005) Nanostructured electrochemical sensors based on functionalized nanoporous silica for voltammetric analysis of lead, mercury, and copper. J Nanosci Nanotechnol 5:1537

Part II
Policy/Political/Regional

Chapter 9
Nuclear Terrorism – Dimensions, Options, and Perspectives in Moldova

Nuclear Terrorism – Perspectives in Moldova

Ashok Vaseashta, P. Susmann, Eric W. Braman, and Nicolae A. Enaki

Abstract Securing nuclear materials, controlling contraband and preventing proliferation is an international priority to resolve using technology, diplomacy, strategic alliances, and if necessary, targeted military exercises. Nuclear security consists of complementary programs involving international legal and regulatory structure, intelligence and law enforcement agencies, border and customs forces, point and stand-off radiation detectors, personal protection equipment, preparedness for emergency and disaster, and consequence management teams. The strategic goal of UNSCR 1540 and the GICNT is to prevent nuclear materials from finding their way into the hands of our adversaries. This multi-jurisdictional and multi-agency effort demands tremendous coordination, technology assessment, policy development and guidance from several sectors. The overall goal envisions creating a secured environment that controls and protects nuclear materials while maintaining the free flow of commerce and individual liberty on international basis. Integral to such efforts are technologies to sense/detect nuclear material, provide advance information of nuclear smuggling routes, and other advanced means to control nuclear contraband and prevent proliferation. We provide an overview of GICNT and several initiatives supporting such efforts. An overview is provided of technological advances in support of point and stand-off detection and receiving advance information of nuclear material movement from perspectives of the Republic of Moldova.

A. Vaseashta (✉) • P. Susmann • E.W. Braman
Institute for Advanced Sciences Convergence NUARI, 13873 Park Center Road, Street 500, Herndon, VA, USA
e-mail: avaseash@norwich.edu

N.A. Enaki
Institute of Applied Physics of Academy of Sciences of Moldova, Chisinau, Republic of Moldova

A. Vaseashta et al. (eds.), *Technological Innovations in Sensing and Detection of Chemical, Biological, Radiological, Nuclear Threats and Ecological Terrorism*, NATO Science for Peace and Security Series A: Chemistry and Biology,
DOI 10.1007/978-94-007-2488-4_9, © Springer Science+Business Media B.V. 2012

Keywords Nuclear • Terrorism • Policy • Moldova

9.1 Introduction

Winston Churchill once stated that we have a shared transatlantic responsibility to "faithfully serve great causes." The U.S. Government, NATO, and EU have ranked developing effective partnerships to meet the global challenge of weapons of mass destruction (WMD) terrorism amongst the highest priorities since it poses a grave threat to international peace and security. The U.S. strategic approach hinges on six objectives outlined in the National Strategy, viz. determine terrorists' intentions, capabilities, and plans to develop or acquire WMD; deny terrorists access to the materials, expertise, and other enabling capabilities required to develop WMD; deter terrorists from employing WMD; detect and disrupt terrorists' attempted movement of WMD-related materials, weapons, and personnel; prevent and respond to a WMD-related terrorist attack; and define the nature and sources of terrorist-employed WMD devices. There are four generally accepted categories of WMD that terrorists may seek to acquire and use in attack scenarios: nuclear, radiological, biological, and chemical.

The first threat lies in nuclear weaponry. Scientific and technical information regarding the assembly of nuclear weapons – some of which is now available on the Internet and in unsecured medical facilities, has increased the risk that a terrorist organization in possession of sufficient fissile material could develop. Terrorists work with a variety of facilitators to develop nuclear capabilities. These facilitators include black market proliferators or transnational criminal networks that seek to profit from the sale of unsecured nuclear material, a delivery device, or technical knowledge gathered from nuclear experts involved in a national nuclear program. Some terrorists seek to acquire radiological materials for use in a radiological dispersal device (RDD) or "dirty bomb". Most radiological materials lack sufficient strength to present a public health risk, but public panic and the economic disruption caused by a RDD would be significant.

At a historic meeting during 30–31 October 2006, representatives from 13 governments convened in Rabat, Morocco and reached agreement on a "Statement of Principles", as well as a Terms of Reference (TOR) for implementation and assessment of the Global Initiative to combat Nuclear Terrorism (GICNT). Within a three short years, the GICNT garnered support from 76 partner nations with the International Atomic Energy Agency (IAEA), European Union (EU), and International Criminal Police Organization (INTERPOL) as official observers. The objectives of the GICNT were to gather experience and expertise from the nonproliferation, counter proliferation, and counterterrorism disciplines, to;

- Put together collective capabilities and resources to strengthen the overall global architecture to combat nuclear terrorism.

- Offer the opportunity for nations to share information and expertise in a legally non-binding environment.

Several follow-up meetings after the Rabat summit focused on developing partnership capacity to combat nuclear terrorism on a systematic basis consistent with national legal authorities and obligations under relevant international legal frameworks, notably the Convention for the Suppression of Acts of Nuclear Terrorism, the Convention on the Physical Protection of Nuclear Material (and its 2005 Amendment), United Nations Security Council Resolutions (UNSCR) 1373 and 1540. The states concerned with this threat to international peace and security were asked to commit to implementing the following eight principles on a voluntary basis:

- Develop, if necessary, and improve accounting, control and physical protection systems for nuclear and other radioactive materials and substances;
- Enhance security of civilian nuclear facilities;
- Improve the ability to detect nuclear and other radioactive materials and substances in order to prevent illicit trafficking in such materials and substances, to include cooperation in the research and development of national detection capabilities that would be interoperable;
- Improve capabilities of participants to search for, confiscate, and establish safe control over unlawfully held nuclear or other radioactive materials and substances or devices using them.
- Prevent the provision of safe haven to terrorists and financial or economic resources to terrorists seeking to acquire or use nuclear and other radioactive materials and substances;
- Ensure adequate respective national legal and regulatory frameworks sufficient to provide for the implementation of appropriate criminal and, if applicable, civil liability for terrorists and those who facilitate acts of nuclear terrorism;
- Improve capabilities of participants for response, mitigation, and investigation, in cases of terrorist attacks involving the use of nuclear and other radioactive materials and substances, including the development of technical means to identify nuclear and other radioactive materials and substances that are, or may be, involved in the incident; and
- Promote information sharing pertaining to the suppression of acts of nuclear terrorism and their facilitation, taking appropriate measures consistent with their national law and international obligations to protect the confidentiality of any information which they exchange in confidence.

To date, the GI partners, comprising of 82 nations, have conducted over 30 Global Initiative workshops, conferences, and exercises aimed to build capacity to prevent, detect, and respond to acts of nuclear terrorism. Notwithstanding such efforts, several gaps in the following three critical areas remain, viz.:

- Strengthening detection and forensics
- Denying safe haven and financing to terrorists
- Deterring terrorist intentions to acquire and use nuclear devices

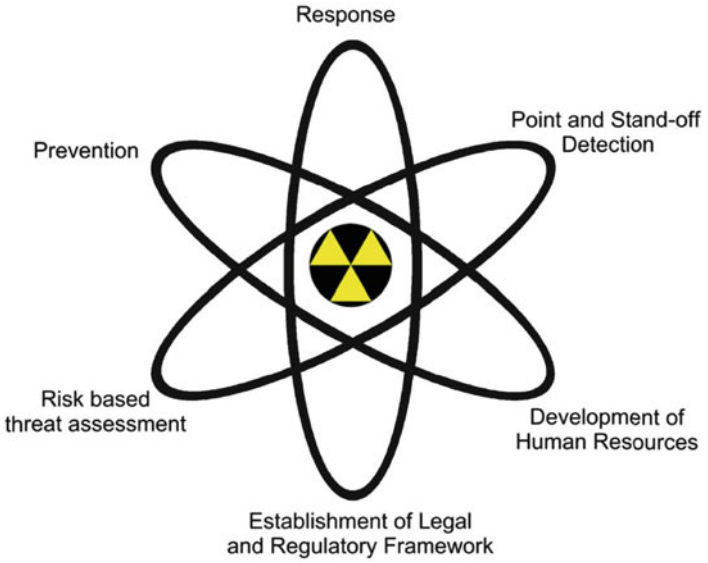

Fig. 9.1 Objectives of nuclear security

The overall objectives of nuclear security are thus risk based assessment, establishment of legal and regulatory framework, development of human resources, technological advancement for detection, prevention and strategic response, as summarized by Fig. 9.1 below.

These approaches support existing initiatives, viz.: Proliferation Security Initiative (PSI), the Export Control and Related Border Security (EXBS) Program, the Nuclear Smuggling Outreach Initiative (NSOI), Second Line of Defense (SLD) Program, Secure Freight Initiative (SFI), Container Security Initiative (CSI), International Counter-proliferation Program (ICP), Cooperative Threat Reduction (CTR) Programs, and Joint Intelligence Preparation of the Operational Environment (JIPOE). Furthermore, various agencies in the U.S. and the E.U have initiated projects with former Soviet Union (FSU) countries to provide incentives to use the nuclear technology to support the GICNT initiatives. Several initiatives and broad agency announcements (BAA) by the Defense Advanced Research Projects Agency (DARPA) and Intelligence Advanced Research Projects Activity (IARPA); such as "Tools for Recognizing Unconscious Signals of Trustworthiness" (TRUST) Programs support such missions.

The outcome is a global system that protects and controls nuclear materials so that they can be safely processed, stored, utilized, and transported by authorized individuals. GICNT guides the formation of national policies and programs, sets budget and resource priorities, and provides a means to focus and coordinate different departments and agencies within the national government and within a federalist system among all levels of government. Despite its tremendous potential, the

GICNT presents significant programmatic and resource challenges due to highly complex and interdependent modern economies. The challenge for those responsible for securing such materials is to manage and secure resources from terrorists. From a nuclear security stand-point, further challenges are in detection/sensing, determining trafficking pathways, and technological means to prevent unauthorized transfer, transaction, and transportation of such materials, as indicated GICNT principles 3, 6, 7 and 8. We address these issues using advanced electronic materials, quantum-based encryption to provide security, Web based algorithms, and cognitive sciences based methodology. The technologies exist in Moldova, and its close proximity to Black sea region provides unique advantage in addressing these issues from a regional perspective. Effort to strengthen the Black-sea security programs will also help to strengthen efforts keep nuclear materials more secure internationally.

9.2 Challenges and Opportunities

The Republic of Moldova, although not a member of GICNT, offers a unique perspective to counter threat of nuclear terrorism. The geographic location of Republic of Moldova, with its strong and rich background in Nuclear Physics, Quantum Computing, and Modeling and Simulation offers various technological options in support of point and stand-off detection, forensics, identifying and locating illicit traffic routes using social network approach, and enhancing security by way of secure communication and deciphering chatter by adversaries.

9.2.1 Moldova and Its Proximity in Black Sea Region

Republic of Moldova is a country located in south Eastern Europe, sandwiched between Romania and Ukraine. Historically being influenced by the Byzantine Empire, Moldova kept its Latin language origin and Christian-orthodox traditions. The regional environment is effective in fostering and stimulating the development of strong links between NATO, EAPC Partner and Mediterranean Dialogue countries. Due to its geographical location, the country is a politically strategic point for international focus. In a recent meeting with the NATO Assistant Secretary General for Public Diplomacy, Pres. Voronin discussed issues of cooperation in the field of regional security and combating illegal migration. He backed the proposal for creation of a NATO information center in Chişinău, in view of many issues relating to regional stability. Similar initiatives by the U.S. Department of State to help stabilize the Republic of Moldova and regions in its proximity are underway and are discussed later.

An additional challenge posed by a separatist regime which controls a narrow strip of land in eastern Moldova known as “Transnistria”, as shown in Fig. 9.2, also known as Trans-Dniester or Transdniestria – a breakaway territory located mostly in

Fig. 9.2 Black sea region, Moldova, and Transnistria

a strip between the Dniester River and the eastern Moldovan border to Ukraine. Since its declaration of independence in 1990 and subsequent War of Transnistria in 1992, it is governed de facto by the unrecognized Pridnestrovian Moldavian Republic (PMR, also known as "Pridnestrovie"). As part of 1992 War of Transnistria agreement, a three-party (Russia, Moldova, Transnistria) Joint Control Commission supervises the security arrangements in the demilitarized zone, comprising 20 localities on both sides of the river. In a NATO-resolution from 18 November 2008, Russia was urged to withdraw its military presence from the Transdniestrian region of Moldova.

In the autumn of 2006 the Transnistria leadership agreed to let an OSCE inspectorate examine approximately 20,000 ammunitions and military equipment due to concerns that Transnistria may traffic arms or nuclear material. The separatist-controlled Transnistria region of Moldova remains a potential area for terrorist activity; although the OSCE has reported that no evidence exists to support claims of terrorist activities. Moldova participated in a number of theoretical and practical antiterrorism assistance training events, seminars, exchanges, and conferences organized by the U.S. Embassy. Trafficking in persons (TIP) programs improved law enforcement personnel/officers' ability to identify and prosecute traffickers, while protecting victims of trafficking through the implementation of better laws and assistance for their social and economic integration. In FY 2009, the United States increased support for the re-integration of the breakaway region of Transnistria through increased economic growth and civic-participation programs in that region. In FY 2009, USG assistance expanded across the Dniester River to include Transnistrian stakeholders. This expansion included providing support to establish a legal clinic in Transnistria to provide legal services, grants to non-governmental

organizations (NGOs) in three communities in Transnistria to support the region's first ever community-led improvement projects, and training in journalism and business to five media outlets. Some additional missions and treaties are pending declassification but support from GICNT and GTSN will provide much needed stability and control to this regional conflict.

9.3 Technologies to Counter Threats of Nuclear Terrorism

A substantial segment of the scientific community believes that the probability of a terrorist event to take place in foreseeable future is finite. The obligation of a civilized society is to protect the masses in a climate of terrorism – characterized by "having nothing to lose" and motivated by radical ideology. Recruitment by terrorists within civilized society has grown from finding a "needle in a haystack" to "hay in a haystack". Consequently, it is imperative that the scientific community develop plans with an understanding of technological tools available to us to detect, predict, deter, and interdict these threats.

Advances in sciences and technology, computer sciences, genomics, neuroscience, materials science, nanotechnology and other disciplines have transformed the technology landscape, and promise to revolutionize life from synergetic convergence of disciplines. The interdisciplinary scientific community must address knowledge-driven transformations across scientific fields to develop materials, devices, and systems to overcome the aforementioned challenges. The latest technological innovations result from potential of nanoscale materials to exhibit unique properties that are attributable to their small size such as enhanced and surface area and physical characteristics [1]. Advances in material synthesis, device fabrication and characterization techniques have further provided the means to study, understand, control, or even manipulate the transitional characteristics between isolated atoms and molecules, and bulk materials. The potential and risk for inadvertent or deliberate introduction of contaminants in the environment, food and agricultural products, due to global threats of terrorism make decentralized sensing an important research area. A nanotechnology based sensor platform enables direct electrical detection in a label-free, highly multiplexed format over a broad dynamic range. Recently, various nanoscale materials with new architectures and improved functionality have been developed with applications in chemical and biological sensors [2], environmental pollution sensing [2], monitoring [3], mitigation and remediation [4], next-generation energy generation and storage devices, nano-biotechnology, nanophotonics, in-vivo analysis of cellular processes and futuristic platforms in health and clinical medicine [2]. Substantial segment of the scientific community is confident that nanoscience and nanotechnology will revolutionize research and its applications to provide unprecedented means to forewarn and/or protection against the potential and risk for inadvertent or deliberate contamination.

9.3.1 Point and Stand-Off Detection

Real-time radiation detectors have become an essential component of emergency personnel who are tasked to respond to accidents, emergency incidents and/or terrorist attacks, which could involve radioactive material. Additional reasons include lost sources, nuclear industrial accidents, and the possibility of nuclear weapons being used in a war. To meet this ever increasing demand, considerable research into new sensors/detectors is underway, including efforts to enhance the sensor performance through the material response, sensor networks, and manufacturing technologies. A thorough understanding of physical properties of the materials exposed to radiation sources is vital for an effective design of dosimeters. Generally, detection of radiation is based on the fact that both the electrical and the optical properties of the materials undergo changes upon exposure to ionizing radiation. Interaction between energetic radiation and semiconductors results in loss of energy which is ultimately converted to form electron-hole pairs. Energy levels produced by irradiation have recombination centers, which can reduce the carrier lifetimes by several orders of magnitude. Properties of metal oxide materials are directly or indirectly connected to the presence of defects, oxygen vacancies. Oxygen vacancies are known as color centers, or F centers. It is believed that ionizing radiation causes structural defects, leading to a change in their density upon exposure to γ-rays. The formation of color centers has been associated with an increase in electrical conductivity, in which free electrons are produced as a result of band-to-band transitions and trapping of these electrons in oxygen ion vacancies. It is generally accepted that two distinct processes are responsible for the formation of color centers, following bombardment with ionizing radiation. The primary mechanism results in defect formation, while the secondary one gives rise to the stabilization of the centers. The model for color center kinetics assumes that the level of the radiation damage should be dose rate dependent. As color centers are created under irradiation, they also annihilate even under room temperature. During irradiation, both annihilation and creation coexist. The color center density will reach equilibrium at a level, depending on the applied dose rate. The band structure and the existence of an energy gap are believed to be dependent upon the arrangement of nearest atomic neighbors and the existence of local or short-range order. Radiation may increase the bond angle distortion so that the optical absorption edge shifted to the lower energies. The values of the optical band gap for as-deposited and γ-irradiated specimens were estimated using the Mott and Davis model for the indirect allowed transition. The change in conductivity caused by the formation of new energy levels under the action of radiation is difficult to estimate, since neither the energy nor the number of new levels is accurately known. The ionizing energy of new levels is high and the low-lying levels may carry out the donor as well as the acceptor impurity effects, owing to this compensating effect. In the initial stage of irradiation, the resistance increases in any material containing donors or acceptors of low ionizing energy. If the irradiation is continued after the compensation of the impurities present in the original crystal, the formation of acceptor levels is permanent. The deep lying energy levels produced

by irradiation are very effective recombination centers, which can reduce the carrier lifetimes by several orders of magnitude.

Some the technological drivers for point (contact) and stand-off (from distance) detection are universal detection of radiological sources, sensitivity, cost, resolution, robustness, accuracy, connectivity, ease of use, portability, and automation. To design such a system, an optimum approach will be to design multiple sensors, multiple sample matrix, intelligent data analysis with sampling control, transceiver with network capability, integrated single chip design and with an on-chip power source. This has resulted in the development of a handheld prototype device that may be used for interfacing resistive based sensor arrays for real-time radiation monitoring. The system boosts a modular nose head design allowing different arrays to be connected quickly. This allows the device to be configured for a specific task, if required. The system can interface to an array with several sensors, whose analog signals are multiplexed en-route to the ADC. The PDA is capable of storing the data for further analysis and has built-in software to display the acquired data in real time. The PDA has the capability to run pattern recognition algorithms to execute classification of radiation types and doses. Even hybrid sensor arrays could be interfaced to the system allowing for a dual functioning device, encompassing gas/chemical and radiation detection functionality. For example, half the array could make up gas sensors for the detection of the explosives, and the other half could make up radiation sensors, allowing the overall system to be used for security and military applications. Thin film devices are recommended for low-dose applications and thick film devices for higher dose applications. The properties of thick film devices were restored after annealing. This suggests that these films can be reused on a repeatable basis. Generally, the sensitivity of the devices varies greatly with the composition of the materials used. A networked configuration of these prototype devices is shown in Fig. 9.3, and can be configured to a specific radiation dose based on sensor film thickness and device structure [5].

9.3.2 Intelligence Based Methodologies

Effective risk analysis involves identifying, assessing, and mitigating risk to a satisfactory level. Risk analysis is a process of evaluating critical assets and systems, threats, vulnerabilities, and controls for mitigating threats. Outcomes of risk assessment form a strategic plan for managing risks. Three pillars of risk analysis are to assess, manage, and communicate. Assessment is the process of identifying risk. Managing is the process of mitigating risks in an optimal manner. Communication ensures that policy and decision makers and the general public understand outcomes of risk assessment and risk management. High quality decisions are characterized by the following elements:

- Appropriate framing of decisions
- Analysis of creative alternatives

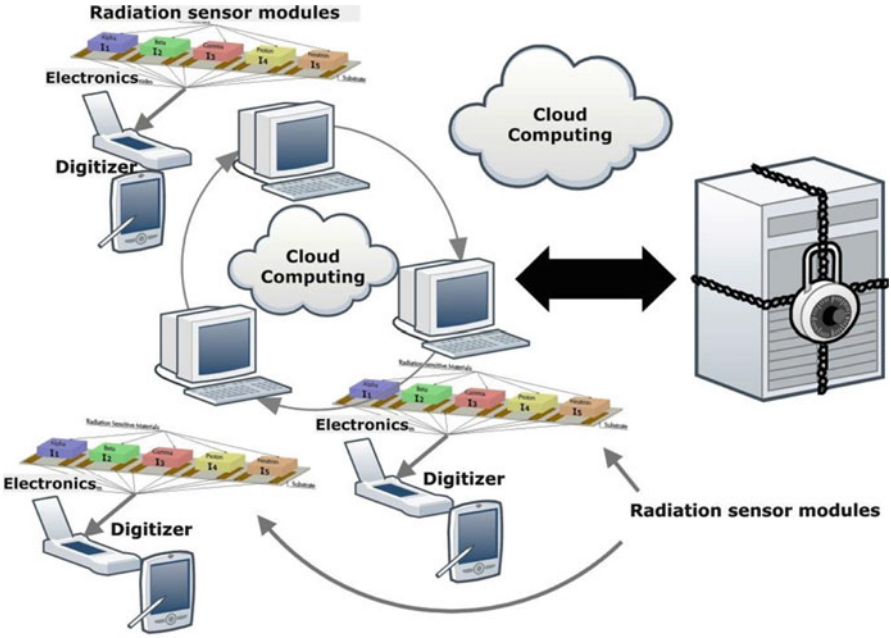

Fig. 9.3 Radiation sensor with multiple sensors

- Accurate information and sound models
- Clear preferences for future status
- Sound logic
- Commitment to process and outcomes.

Policy and decision makers are increasingly relying on expert-opinion elicitation techniques for forecasting advances, reliability, and risks related to science and technology [6]. Structured expert-opinion elicitation techniques effectively support complex decision-making in the face of risk and uncertainty [7].

We have introduced the concept of using a structured expert-opinion elicitation technique, a computerized Delphi technique to assess risk and making predictions based on input by expert panels. A typical forecasting process includes (a) unreliable information including incomplete, inaccurate, unrepresentative historical data about threats, vulnerabilities, and occurrences leads to poor quality risk analysis decisions; (b) unreliable forecasting including bad estimates of probabilities and excluding outlier events impacts the quality of risk analysis decisions; (c) host of cognitive biases including representativeness, availability, anchoring and adjusting, optimistic biases, risk biases, and a false sense of control may negatively affect risk analysis processes; and (d) finally, dysfunctional group dynamics arising from strong personalities, organizational hierarchies, and miscommunications impede the risk analysis process and resulting decisions. The Delphi Technique, as shown

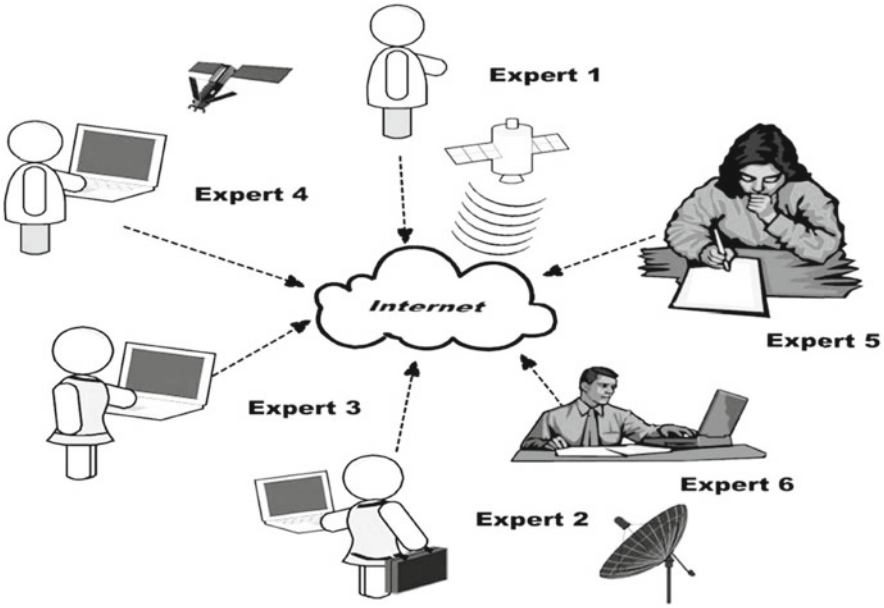

Fig. 9.4 Conceptualization of expert elicitation using Delphi

in Fig. 9.4, however, is a structured interactive group communications technique effective for reaching consensus about judgments, forecasts, or decisions from expert panels [8]. The Delphi process occurs as follows:

- Facilitator distributes survey to the expert panel.
- Survey is answered anonymously and independently by expert panel.
- Facilitator summarizes and distributes results and rationale.
- Expert panel anonymously and independently reviews summarized results and rationale. Panelists may revise individual responses, optional.

The process of eliciting, summarizing, and distributing anonymous and independent responses continues until consensus, stable responses, or a given number of rounds is met. The Delphi Technique benefits decision making and forecasting processes involving expert panelists in many ways. First, the Delphi technique supports expert panels ranging from a few participants to a few thousand participants. Second, the Delphi technique effectively overcomes constraints in time, geographic location, cost, or anonymity needs. Third, the Delphi technique proves effective when actuarial, technical, or economic data is unavailable thus mandating expert judgment. Fourth, the Delphi technique has proven effective in the exploration and forecasting of novel, complex, or uncertain problems or events. Finally, the technique overcomes social barriers related to diversity, hierarchy, personality, or hardened conflicts. Because the Delphi technique has proven merit in forecasting trends and

risks for many scientists, researchers, policy, and decision makers; the authors propose a future investigation involving a Delphi Study for assessing other security risks.

In addition to conducting a feasibility analysis of employing the Delphi methodology, additional approaches to provide intelligence information are – Textual Data Mining (TDM) – a process by which large quantities of unstructured textual records are efficiently queried to retrieve relevant information on a topic of interest. The TDM process includes software tools that allow a research analyst to display a taxonomy that clusters the records by topical similarity and allows the analyst to visualize patterns in the database that would not otherwise be apparent.

The software tools also have a robust search capability that allows the analyst to quickly and efficiently search databases for additional information including information on prolific research authors and activities working in the technology area of interest. Likewise, use of Web 2.0/3.0 to develop solutions is employed in support of national security and intelligence gathering information on routes of illicit trafficking of nuclear materials. Social network based applications such as Second Life virtual environment, Moodle Learning systems, and SLoodle (second life object oriented distance learning environment) have already shown great success. It is anticipated that use of Web 2.0/3.0 will accelerate the process of identifying leading edge advances in different disciplines relevant to defense applications. To enhance security of communication, we intend employing quantum encryption [9]. Using TRUST of IARPA, we are pursuing additional technologies for information gathering. The overreaching goal of this project is to significantly advance the IC's capabilities to assess who can be trusted under certain conditions and in contexts relevant to the IC, potentially even in the presence of stress and/or deception. The program seeks to conduct research that will bring together sensing and validated protocols to develop tools for assessing trustworthiness by using one's own ("Self") signals to assess another's ("Other") trustworthiness under certain conditions and in specific contexts, which can be measured in scientifically-credible experimental protocols.

9.3.3 Advanced Sciences Convergence

The process of ASC is to understand how different disciplines, focusing on discrete problems and applications, can be coalesced into a system to solve an intractable problem. It requires understanding of a far-reaching end goal that is not yet defined but can be described in terms of desired actions or qualities. In the U.S., Nanotechnology, Biotechnology, Information Technology and Cognitive Sciences (NBIC) convergence was defined as a new transformational concept resulting from seminal publication by the National Science Foundation (NSF), Department of Commerce and World Technology Evaluation Center (WTEC), Inc., in June 2002, followed by the JASON Defense Advisory Panel report in November 2002. These documents provided the necessary foundation for a new appreciation of the next phase of the development of the individual NBIC disciplines. A 2002 NSF report

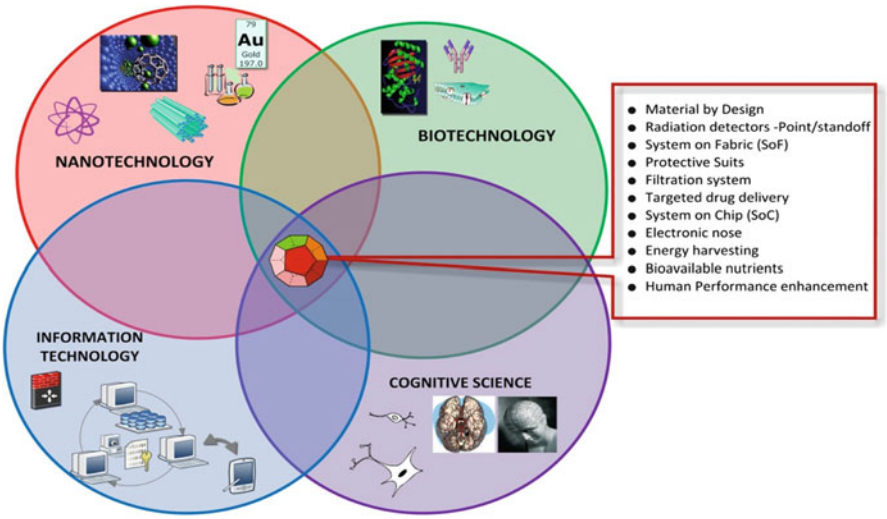

Fig. 9.5 NBIC convergence and possible applications

proposed a new "Renaissance" in technology built on the nanoscale using four principles; material unity, interfacing technologies, understanding complexity and optimizing integration to augment human performance. The main idea behind the NBIC concept is that in the future the lines between novel materials (hardware), biological systems, and information processing and exchange in the form of computers and cognition will disappear resulting in integrated systems that incorporate sensing, analysis, and awareness at the nanoscale. The opportunities for commercial and military applications are enormous, as noted by reports within the U.S. and around the world. A July 2003 copy of the "Issues in Defense Science and Technology" from Defense Research and Development Canada (DRDC) was titled: "Convergence of Technologies for Innovative Disruption", which described potential capabilities resulting from synergy between NBIC disciplines are summarized below and in Fig. 9.5.

- Expanded human cognition and communication enabled by brain implants, new drugs, rapid learning and direct brain-machine interfaces.
- Improved human health and physical capabilities enabled by nano-biosensors to monitor and repair bodily functions, and systems that enhance human sensors.
- Responsive and collaborating autonomous intelligent systems to support decision-making and nano robots for surveillance.

A similar interest was expressed by the European Commission (EC) High Level Expert Group (HLEG) in Converging Technologies (CTs) reports published in 2004. One of the reports entitled "Converging Technologies-Shaping the Future of European Societies", addresses NBIC advances in the U.S. and their potential

impact to the economic future of the European Union. Asian countries are also contributing to NBIC advances with individuals from Japan, India, and China as the main contributors.

9.4 Summary and Way Forward

This report provides a brief overview of ongoing activities employing the latest state-of-the art activities to sense/detect presence of nuclear materials in close proximity and using remote, hand-held, portable and networked devices. Additional tools such as Delphi, Web 2.0/3.0, and TDM are used to provide advance information of nuclear material trafficking routes. Advanced cognitive tools are developed which can be used by law enforcement and peace keeping mission officers to interview and be able to detect confidence level of the response. Security of communication is enhanced using quantum encryption. Collectively, all these tools will provide a sense of security supporting GICNT principles in Black Sea region, with Republic of Moldova as a key player.

References

1. Web sources: http://www.state.gov and http://www.iarpa.gov
2. Vaseashta A, Mihailescu IN (2008) Functionalized nanoscale materials. Springer, Dordrecht/ The Netherlands
3. Vaseashta A, Vaclavikova M, Vaseashta S, Gallios G, Roy P, Pummakarnchana O (2007) Nanostructures in environmental pollution detection, monitoring, and remediation. Sci Technol Adv Mater 8:47–59
4. Vaseashta A, Stamatin I (2007) Electrospun polymers for controlled release of drugs, vaccine delivery, and system-on-fibers. JOAM 9(6):1506–1613
5. Korostynska O, Arshak K, Arshak A, Vaseashta A CBRNE and ecological terrorism detection in Vaseashta A Springer, Dordrecht, The Netherlands (in press)
6. Ayyub B (2001) Elicitation of expert opinions for uncertainty and risks. CRC Press, Boca Raton
7. Rowe G, Wright G (2001) Expert opinions in forecasting: the role of the Delphi technique. In: Armstrong JS (ed) Principles of forecasting: a handbook for researchers and practitioners. Kluwer Acad Publishers, Norwell, pp 125–144
8. Linstone H Turoff M (2002) (eds) The Delphi method techniques and applications, NJIT: URL: http://is.njit.edu/pubs/delphibook
9. Enaki N, Turcan M, Vaseashta A (2008) Two photon multi mode laser model based on experimental observations. J Optoelectron Adv Mater 10(11):3016

Chapter 10
Integrative Convergence in Neuroscience: Trajectories, Problems, and the Need for a Progressive Neurobioethics

Convergence in Neuroscience – The Need for Neurobioethics

J. Giordano

Abstract The advanced integrative scientific convergence (AISC) model represents a viable approach to neuroscience. Beyond simple multi-disciplinarity, the AISC model unifies constituent scientific and technological fields to foster innovation, invention and new ways of addressing seemingly intractable questions. In this way, AISC can yield novel methods and foster new trajectories of knowledge and discovery, and yield new epistemologies. As stand-alone disciplines, each and all of the constituent fields generate practical and ethical issues, and their convergence may establish a unique set of both potential benefits and problems. To effectively attend to these contingencies requires pragmatic assessment of the actual capabilities and limits of neurofocal AISC, and an openness to what new knowledge and scientific/technological achievements may be produced, and how such outcomes can affect humanity, the human condition, society and the global environment. It is proposed that a progressive neurobioethics may be needed to establish both a meta-ethical framework upon which to structure ethical decisions, and a system and method of ethics that is inclusive, convergent and innovative, and in thus aligned with and meaningful to use of an AISC model in neuroscience.

Keywords Neuroscience • Genetics • Cyberscience • Convergence • Neuroethics

J. Giordano (✉)
Center for Neurotechnology Studies, Potomac Institute for Policy Studies, Arlington, VA, USA

Oxford Centre for Neuroethics, University of Oxford, Oxford, UK
e-mail: jgiordano@potomacinstitute.org

A. Vaseashta et al. (eds.), *Technological Innovations in Sensing and Detection of Chemical, Biological, Radiological, Nuclear Threats and Ecological Terrorism*, NATO Science for Peace and Security Series A: Chemistry and Biology,
DOI 10.1007/978-94-007-2488-4_10, © Springer Science+Business Media B.V. 2012

10.1 Progress in Neuroscience: From Multi-disciplinarity to Integrative Convergence

As a titular field, neuroscience was "formed" by a unification of multiple disciplines devoted to studying nervous systems. Historically, the neuroscience has employed anatomical, chemical, and physiological approaches to develop "tools-to-theory heuristics" that have been instrumental to formulating an evermore detailed understanding of the brain. Of course, the conjoinment of approaches and disciplines is certainly not new to science, and it could rightly be claimed that such "technique and technology sharing" has been, and canonically remains *de rigueur* in much of scientific practice [1], and reflects the multi-disciplinarity, and technical variety of neuroscience [2]. But it is important to note that over the past 25 years, the pace and breadth of advancement(s) in the constituent fields subsumed under the rubric of neuroscience has dramatically increased, and thus, when purposively employed together to meet intellectual challenge(s) and/or technical impediments, the capabilities and advancements achievable through such inter-theoretical and –technical cooperation have become synergistic. This process, termed advanced integrative scientific convergence (AISC), is not merely a technical sharing, but instead represents a synthetic mind-set that explicitly seeks to foster innovative use of knowledge-, skill-, and tool-sets toward (1) elucidating the nature and potential mechanism of scientific questions and problems, (2) de-limiting existing approaches to question/problem resolution; and (3) develop novel means of addressing and solving such issues. I posit that in this way, AISC enables (a) concomitant "tools-to-theory" and "theory-to-tools" heuristics, and (b) translation of both heuristics and tools to praxis. Indeed, the AISC model is being increasingly employed within neuroscience to engage and direct genetic, nano-scale and computational (i.e. – cyber) methods and advancements in the creation of new neurotechnologies, and uses that affect – and have potential to change – numerous dimensions of the human condition.

10.1.1 Convergence: De-Limiting yet Problematic

The use of the AISC model in neuroscience offers promise for novel uses of existing techniques and technologies, as well as employment of new approaches in the prevention, treatment and rehabilitation and/or management of previously intractable neurological diseases and injury. This is vital, given that many current treatments are constrained by factors including (1) a lack of specificity of techniques (e.g. transcranial and/or direct magnetic stimulation), (2) size restrictions and cumbersome configurations of micro- and macroscale devices, and (3) difficulties of matching certain types of neurologic data (e.g.- from neuroimaging, neurogenetic studies) to databases that are large enough to enable statistically relevant, and meaningful comparative and/or normative inferences [3]. Current and planned uses of AISC approaches in neuroscience are aimed at overcoming these (and perhaps other) constraints.

Toward such ends key future steps would entail the convergent formulation and use of nanoscale, genetic, and computational methods.

These developments are rapidly advancing and exciting. It is reasonable to assume that (1) assessment of neurological structure and function, and (2) manipulation of neural activity has become, and will continue to be increasingly valued and publically accepted, as these means improve and are made evermore commercially available. A variety of influences, including public need and desire, political initiatives, and the market will drive and ensure this valuation, and establish the call and impetus for further development and/or sustained use [4].

The "Technological Imperative" generates a broad "if we have it; use it" maxim [5], and in many ways, there is appreciable merit to at least considering such use, and AISC approaches to, and in neuroscience have gained momentum. Indeed, the concept of an "advanced integrative convergent" approach in the neurosciences is something of a *fait accompli*, and so I argue that questioning *if* this paradigm will be employed would be of little value. Instead, I offer that inquiries about what the AISC approach will yield, and how its outcomes and products may change the values and conduct of science and society are, however, meaningful, given the power of convergent science to affect the speed and breadth of innovation and discovery. Somewhat more appropriate questions, then, are: (1) how AISC approaches can be employed in neuroscience; (2) what practical and ethical issues, concerns, and problems might arise as a consequence, and (3) what systems of risk analysis and mitigation might be required to meet these challenges, and guide the employment of neuroscience and neurotechnology [6].

Important to addressing these questions is a depiction of the relative capabilities, limitations and ethical problems of the constituent disciplines of nanotechnology, genetics, and cybertechnology that are subsumed within an AISC model of neuroscience. In the past, the activities, outcomes and products of these fields have been relatively maintained within "silos" of research and use (see Fig. 10.1) [7, 8].

However, following the Human Genome Project, there was an increasing call, and impetus to de-silo these fields (as well as others) in order to promote more consilient agendas of research and its translation into clinical care and social practices. In neuroscience, this was evidenced by the congressionally declared Decade of the Brain (1990–2000) which, while failing to achieve so-called "big science" status, *did* effectively establish inter-disciplinary programs of neuroscience, fractured some of the academic and research silos, and tended to cultivate a more collaborative *Zeitgeist* within the neuroscientific community [9].

However, this can be viewed as a double-edged sword –although academic and research silos can create restrictions upon true collaboration(s) and cooperation, they can also confer some protection (of funding, and against informational spillover effects into the public realm). Once silos are dissolved, limitations can become diminished or removed, but so too may be the ability to recognize and apprehend the relative limits upon the pace and extent of scientific discovery, and the use of its knowledge and products. As a result we may encounter effects, burdens, and harms that were as yet unknown, and/or unforeseen, and thus there is significant risk that the pace, breadth and depth of scientific and technological capability may outstrip

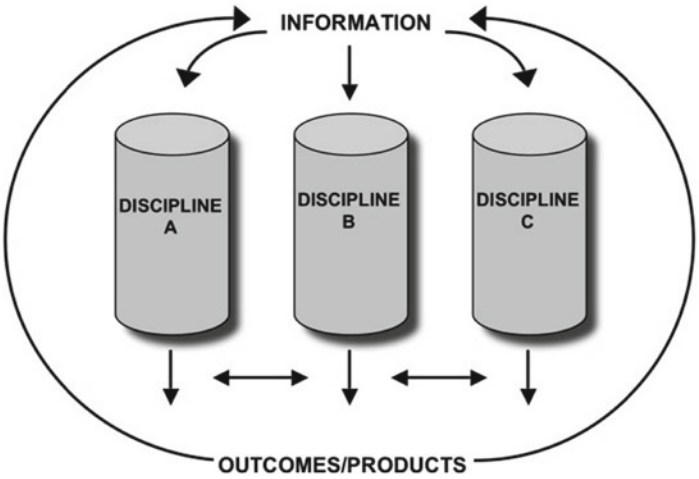

Fig. 10.1 Diagrammatic representations of siloed configuration of scientific activity and outcomes

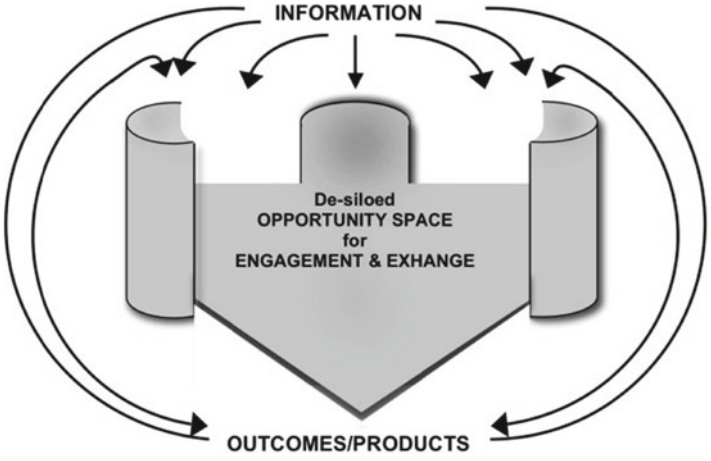

Fig. 10.2 Diagrammatic representation of de-siloed configuration of scientific activity and outcomes

that of the ethical deliberations that could most genuinely evaluate and regulate the social impact of such innovation (see Fig. 10.2). I posit that while an AISC model of neuroscience is a current reality and important to progress, its real value is dependent upon an equally advanced, integrative system of ethics that can effectively analyze and balance positive and negative trajectories of progress, increase viable benefits and militate against harm(s). Obviously, this would require evaluation of

both the ethical issues germane to the constituent AISC disciplines and those generated by the ASIC model of neuroscience itself.

10.2 Constituent Disciplines in the AISC Model of Neuroscience: Practical and Ethical Issues

Addressing each discipline in turn allows for an overview of the capabilities, as well as the practical and ethical issues and burdens that these fields confer –as stand-alone pursuits, and when conjoined in an AISC model of neuroscience. To re-iterate, both the promise and potential problems of these fields can become cumulative – if not actually synergistic – when de-siloed within the AISC model. I posit that elucidation of these possible benefits and risks is important to, and establishes a basis for, the formulation of a system of ethical analyses that can inform guidelines and policy, and navigate and steer AISC-based neuroscience and neurotechnology research and use.

10.2.1 Nanoscience

Nanoscience has enabled assembly of very small scale materials and devices that (1) allow *in vivo* sub-cellular manipulation of biological systems, (2) can serve as platforms for access to, and articulation of substrates at the sub-nano (i.e.- pico and femto) and supra-nano (e.g.- micro and milli) scalar levels; (3) may further an understanding of quantum-mechanical interactions possible at the sub-nanoscale, and (4) allow passage of nanoscale materials into the central neural compartment (via blood-brain and/or blood-CSF barrier access) for the subsequent assemblage of high nanoscale and/or supra-nanoscale molecules (e.g.- drugs), devices and network systems capable of modifying neural structure and function. This would potentiate heretofore unachievable capability to introduce various ligands and structural components to the brain, and therefore allow unparalleled (a) access, (b) site specific targeting of various brain loci and networks; (c) use of highly specific biosensor and biotransmitter systems, and (d) control of neural function, from the cellular to network-system levels [10–12]. These applications are summarized in Table 10.1.

Those nanotechnologies that are used to access and manipulate neurological systems (viz. – "neuro-nanotechnology"; e.g.- nano-neuropharmacological ligand platforms; use of nanomicelles and/or quantum dots; etc.), and/or nanoscientific applications to neurotechnologies that enable intervention at the nanoscale (viz- nano-neurotechnology; e.g.- nano-neuropharmacology/ pharmaceutics; nanoscale neuro-robotics, nanoscalar neuroprostheses, etc.) when taken together, evoke far-reaching implications that can – and likely will – impact bioengineering, medicine, and society, and that generate a host of technical, ethical, legal and socio-cultural issues. As presented in Table 10.2,

Table 10.1 Benefits of nanoscience

In vivo sub-cellular access/manipulation
a. CNS access
b. Specific targeting
Sub/supra-nanoscalar articulation
a. In vivo intracellular biosensors/biotransmitters
b. Networks and scaffolds
Engagement of mechanical-quantum interface

Table 10.2 Issues/problems of nanoscience

Variable, inchoate constructs of "good" use
Harms by commission/omission (e.g., "grey goo" scenarios)
Impact upon autonomy (e.g., nano-neurobots)
Inequitable distribution/use

these include, but are not limited to both "first –order" ethical concerns regarding (1) the ways that nanoscalar neurotechnologies might be employed to effect various socially-defined, but inchoate constructs of "good", (2) risks of harm (by commission and/or omission) incurred through the use or misuse of this still nascent biotechnology, (3) impact of using these technologies in ways that affect individuals' autonomy, and (4) the distribution of any good afforded by nano-neurotechnological advancement(s). As well, we are likely to incur "second-order" ethical questions and issues regarding (1) what such technology "means" relative to conceptualizations and constructs of autopoietic devices (i.e. – "synthetic life" scenarios), (2) notions of the human being and humanity, and (3) the viability and/or in viability of extant philosophical and ethical approaches/systems to apprehend and accommodate new realities afforded by nanoscalar access and manipulation of the brain, body and life [12–14].

10.2.2 Genetics

Given the inherent diversity of individuals' neural development and expression, it is clear that neuroscience would be oriented toward a personalized approach to the treatment of neurological and psychiatric disorders, and genetics has been viewed as a potentially important resource to achieve this goal [15]. Elucidation of the neural genome has allowed a more thorough examination of those genes that putatively establish and control development and activity of the central and peripheral nervous systems. To some degree, this has enabled identification of genes that are involved (to varying extent) in phenotypic expression of the "normal" (i.e. – non-pathologic) structure and function of nerve, spinal cord and brain. As well, genetic 'markers' of certain neuropathological conditions have been identified, as have the presence of genetic factors that could establish predisposition to such pathologies [16]. Yet, simple elucidation

Table 10.3 Benefits of genetics

Identification of genes involved in disease/dysfunction
Pharmacogenetic specificity
Prediction of genetically-based effects
Use of genes as targets or biomarkers for other viable therapeutic targets
Genetic stem cell modification
Genoplasty (auto- and xenochimeroplasty)

does not necessarily confer therapeutic benefit (vide infra), hence genetic markers are being considered as possible targets for therapeutic – or preventive – intervention, either directly (via gene-inhibition) or indirectly (via transcriptional or post-transcriptional approaches). Moreover, genetic manipulation of homotypic, as well as xenotypic *ex vivo,* and/or *in vitro* cell cultures or lines establishes viable means for neural stem cell-, and transplantation-based therapeutics (see Table 10.3).

However, the applicability of genetic analyses and interventions are limited by a number of factors: First, genetic patterns do not linearly express phenotype(s), and thus, single genes rarely code for single effects (but more commonly produce a multiplicity of phenotypic expressions), and multiple genes are often responsible for a particular (phenotypic) effect. This makes direct genotype-to-phenotype predictions difficult, particularly for those conditions that appear to involve multi-factorial inheritance, and heterogeneous patho-etiologies and substrates (as is common in a number of neurologic and neuropsychiatric spectrum disorders) [17–19] If and when genetic information is a valid indicant of phenotypic expression, questions are then whether such assessment (1) is correlative, predictive, or diagnostic, and (2) can be used to implement some form of (preventive or therapeutic) intervention [20]. These may be regarded as "practical" or "technical" questions (viz.- in the first case, referring to the realistic validity of genetic typing to infer pathologic trajectories; and in the second, if techniques/technologies are available to mitigate the progression or effect(s) of genetically-induced disorders). Yet, these issues also prompt ethico-legal questions about ontological "values" placed upon and/or inferred from genetics, in general, and neurogenetics more specifically; how neurogenetic data might be used, misused or abused (in medical, economic and/or social contexts);[21] economic, occupational and/or social stigmatization of identified neurogenotypes for various conditions or states [22], and whether to provide neurogenetic information, predictions and diagnoses to patients (as well as their families, insurance providers, employers, etc.) if prevention and/or treatment is not available (refer to Table 10.4) [23–25].

10.2.3 Computational (Cyber) Science

I opine that computational science has been one of the singularly most important contributions to – and subsequently in – brain research. The prototypical "tools-to-theory" heuristics that have become a working standard of neuroscience were based upon

Table 10.4 Issues/problems of genetics

Ambiguity of genotype –› phenotype prediction
Ontological effects
Stigmatization
Predictive vs. therapeutic capabilities
Distribution of genetically-engineered products
Uncertainty of genetically-engineered products

Table 10.5 Benefits of cyberscience

Rapid, robust information • Acquisition • Storage • Analysis • Use
Multi-scalar integrative information use/sharing
Vast network capacity
Tool-to-theory heuristic

John von Neumann's computational concept(s) of mind, as derived from McCulloch and Pitts' earlier work in logical calculus [26–28]. The "tools-to-theory" heuristic has been important to the development of dynamical systems' network models of brain ~ mind function, as reflective of both (1) information gained from computationally-based neuroimaging data, and (2) functional analysis of engineered non-linear neural(–like) networks. The use of computational capability has deepened the level of statistical analyses that can be applied to any/all neuroscientific data, and it could be argued that advances in computational image translation, and computer-based statistical parametric modeling/analyses provided means with which to actualize neuroimaging as a legitimate experimental and clinical technique [29]. Furthermore, the basic heuristics have been expanded into a "tools-to-theory-to-tools" paradigm that engages computational technology to establish conceptual and technical bases important to neuro-robotics, neuro-prosthesis/orthotics, and perhaps autopoietic machines (Refer to Table 10.5) [30, 31].

Computational technology is a powerful mechanism and medium through which to facilitate (if not enable) the capability of extant neurotechnology, and the integration with other advanced scientific disciplines and technologies within an AISC model.

Genetics (in general, and more specifically neurogenetics), and neuroimaging tend to be limited by a lack of available data with which to make (1) intra-subject, temporal comparisons (e.g.- using amassed time-point and/or lifespan data); (2) small group and cohort inter-subject single- and multiple-timepoint comparisons; (3) single subject and cohort-to-population comparisons; and (4) population-to-cohort and/or -subject normative inferences. As depicted in Figs. 10.3 and 10.4, current iterations of computational technology and cybersystems: (1) maximize storage and retrieval through parallel processing; (2) are scalable and customizable;

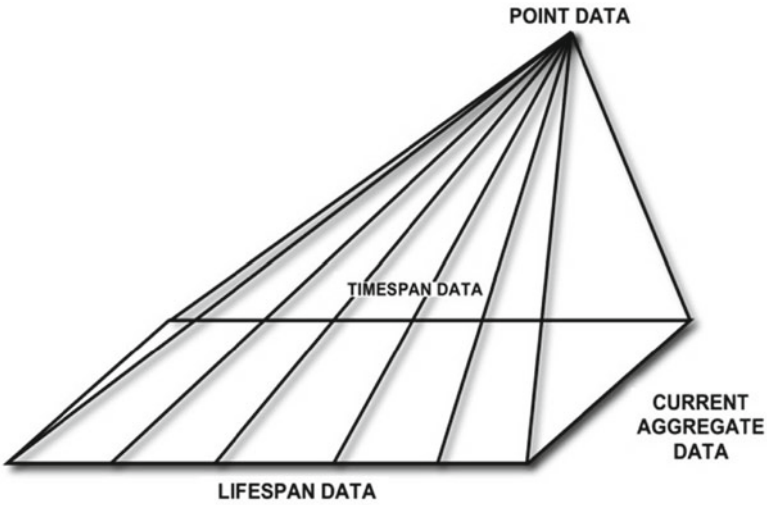

Fig. 10.3 Diagrammatic representation of computational approaches to intra-subject data analysis

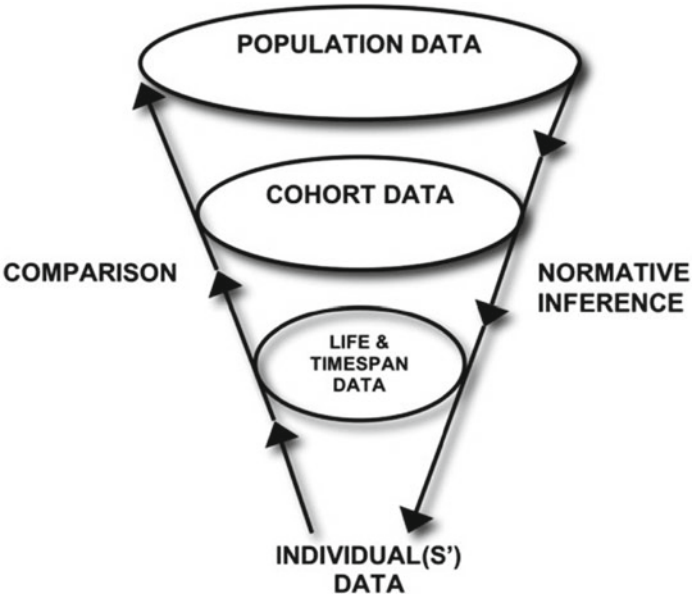

Fig. 10.4 Diagrammatic representation of computational approaches to inter-subject, cohort and population analysis

and (3) can bridge extant gaps in comparative, analytic, predictive methods (Fig. 10.3) and normative capability (Fig. 10.4) of genetics and neuroimaging. This de-limits the validity, reliability and utility of these approaches through the development and employment of variable scale databanks that utilize cloud computing and

Table 10.6 Issues/problems of cyberscience

Accessibility
Security issues
Misuse/alteration of information
Runaway effects (e.g., "Terminator scenarios")
Reliance effects (e.g., "total crash" fears)

storage mechanisms to allow for rapid, real-time data acquisition, analysis and use. In addition, the "cybersphere" creates a nexus for the dissemination, exchange and acquisition/engagement of information from science and technology, and as such is a medium and forum for (iteratively advancing) scientific convergence, integration and socio-cultural influence [32, 33].

As with any form of science and technology, issues arise that can affect the utility and value of cybersystems. Although a complete review of the strength and limitations of cybertechnology is beyond the scope of this chapter, herein are presented those (principal) practical and ethical problems that are most relevant to the neurofocal engagement of an AISC model. As summarized in Table 10.6, these can be (1) classified as issues of (a) inappropriate access, (b) inapt use/misuse, (c) data modification, and (d) "downstream" effects (e.g.- individual and group socio-economic and legal manifestations of accessed, misused or manipulated datasets), and (2) bracketed to reveal underlying tensions between (a) accessibility and sanctuary; (b) privacy and protection, and (c) libertarian sentiments and calls for control [34].

10.3 Analysis of Benefits and Risks

The scope and force of the epistemic and technological wave created by AISC is such that progress occurs as an inherent tendency of the paradigm and process. Obviously, the speed, slope and valence of possible trajectories that any such advancement(s) might assume are variable, and dependent upon some calculus of (1) the capabilities and limitations of each of the constituent disciplines of AISC, (2) the viable proximate, intermediate and (conceptually) long-term outcomes and effects of employing AISC; (3) relative benefits, burdens, risks and harms that could be incurred through the use of specific AISC techniques and technologies, and (4) potential effect(s) upon, and influence(s) of external (e.g.- socio-cultural, economic and/or political) forces upon the conduct, tenor and utilization of AISC outcomes and products. Thus, any realistic appraisal of the *quo vadis* question of the AISC model requires (1) pragmatic evaluation of the capabilities of each and all of the constituent disciplines, and (2) grounding to the particular questions and/or problems of the point of focus (in this case, neuroscience).

The potential benefit and problems fostered by AISC are such that realistic assessment of the aforementioned factors is mandatory before deciding to employ this approach. The initiative – or threshold – inquiry must establish how using AISC

might affect specific knowns and unknowns of the focal field, and if and what new issues, questions, and risks will be generated. This prudential question establishes a foundation upon which to realistically assimilate and appropriately frame scientific capability and information (e.g. – epistemological and technical gap identification, analysis and compensation); generate models to plot possible and probable outcomes; analyze viable alternatives; establish preference(s) for future status; and commit to prudent, responsible enactment of the AISC process, and iterative evaluation of any/all of its outcomes.

As detailed throughout this volume, and summarized in this chapter, each and all of the constituent disciplines operational within the AISC model manifest certain risk. As Vaseashta has noted, AISC occurs in, targets, and in some ways may incur "…a climate of uncertainty and change" [35]. I believe that this well-defines the intellectual and practical space in which cutting-edge science and technology are articulated. In this light, I have argued against the use of a simple precautionary principle to govern the pace and direction of scientific effort [36]. That is because I feel that the intrinsic "character" of frontier science is shaped by change, and any benefit(s) that could be incurred by the use of frontier scientific and/or technological applications are (rather naturally) viewed as proximate, while risks, burdens, and harms tend to arise after a period of time. I have opined that a more realistic – and useful – stance is one of preparedness, in which benefits, threats, and vulnerabilities are identified and assessed, and integrative models and methods of science and ethics are employed to target, mitigate and/or counterbalance these risks and maximize durable good(s).

10.4 The Need – and Role – for a Progressive, Integrative *Neurobioethics*

To be sure, the landscape of scientific and technological capability is, and will be continuously changing, and the ethico-legal and social architectonics of this landscape will be equally – or perhaps increasingly – shifting, as well. How then can we appropriate the ethical deliberation necessary to (1) apprehend the changing realities of scientific capability and effect(s); (2) identify which extant moral theories and systems may and/or may not be viable in ethical analyses and guidance; and (3) develop some combination of effective benefit: risk analysis, and preparedness? [37]

Any such ethical analysis would need to utilize the methods of ethics, at very least to establish an algorithm or framework with which to employ those ethical systems and tools that are best suited to the issues at hand. As shown in Fig. 10.5, this multistep process begins with assessment of the facts, agents and circumstances comprising the ethical issue. But facts must be current, and the contexts and constructs of agents and circumstances must be pragmatically evaluated.

Thus, ethics relies upon science – particularly if ethical decisions are to be made that affect the conduct of science and/or its use in society. In this way, I concur with Eric Racine that the scientific focus and inter-disciplinarity of bioethics is important [38], and this is certainly true of any ethical approach to, or analysis of AISC, given

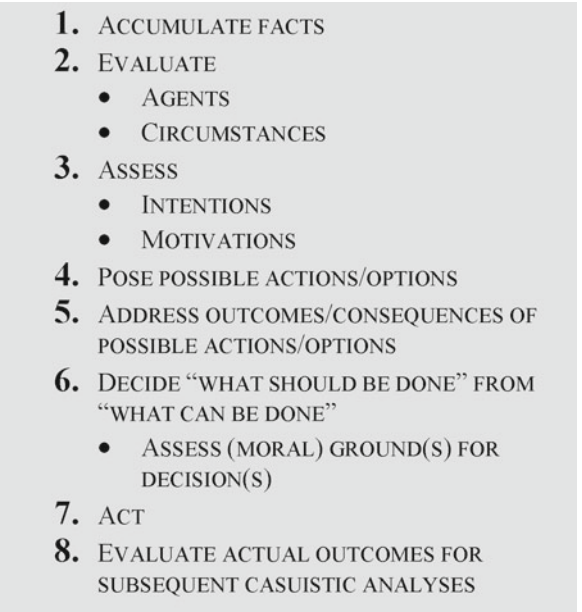

Fig. 10.5 Depiction of steps in ethical analysis and decision-making

its constituent biosciences. At this level, what Edmund Pellegrino refers to as "hyphenated ethics" come into play (e.g.- genethics, nano-ethics; cyber-ethics, etc.), as these explicitly deal with the exigencies fostered by research in, and application of the respective sciences (E.D. Pellegrino: Personal communication, 16 September 2010). To some extent, neuroethics sits in this domain, as one of its "traditions" entails assessment and guidance of ethical issues that arise in and from neuroscience and its uses in medicine and society [39]. But I have argued that neuroethics may also serve as a form of contemporary meta-ethics, given that its other tradition studies the putative neural bases of moral cognition and action. In this tradition, neuroethics – perhaps better termed "neuromorality" – is about the ways that moral decisions are intuited, processed and made. Taken together, neuroethics in its two traditions must account for the bio-psychosocial relevance of knowledge, actions and the ways that science and technology can change the world and the human organism [40, 41].

I argue that neuroethics, or more accurately *neuro-bioethics,* may offer something profound and practical to the AISC paradigm: First, neuroethics-as-neuromorality provides a naturalistic framework for ethical analysis that is well-aligned with the missional orientation and tasks of AISC; namely, to approach existing, novel and/or seemingly intractable problems using innovative methods based upon an understanding of neural operations in decision-making. In other words, neurobioethics, like AISC is both a mirror and lens to view problem-solving, innovation and decision-making. Second, neurobioethics engages the deliberations of those ethical sub-specialties that deal with the peculiar issues generated by constituent disciplines of the AISC model (e.g. – genetics, nanoscience, cyberscience, etc.). Third, in so

doing it too becomes an integrative convergent process, de-siloing neuroethics (genethics, nanoethics, and cyberethics, etc.) and in this way fosters pluralism and innovation. Fourth, this approach establishes the intersection of the knowns and unknowns of these constituent sciences (and their potential social effects) as the basis from which to predicate any/all ethical analysis and guidance; and fifth, it allows a relative flexibility in the focus and scope of approach. In other words, like AISC, it enables an interchanging "tip of the spear" to reflect specific avenues and points of inquiry, interest and application.

Neuro-bioethics explicitly focuses upon how change, uncertainty and progress *in neuroscience* are affected by – and affect – progress in genetics, nanoscience and cyberscience; not as only as stand-alone entities or a simple concatenation of scientific methods, tools and techniques, but rather as a true convergence that conflates ideas, process and technologies in a purposive way. I opine that other ethical disciplines could (or maybe should) adopt a similar approach, so as to (1) incorporate this inter-disciplinarity (e.g.- geno-bioethics; nano-bioethics), (2) be inclusive of the most current neuroscientific and neuroethical knowledge (about the brain ~ mind, moral cognition, decision-making, etc.), and (3) assimilate this knowledge with information gained through the working processes of AISC.

In counter, it could be posed that this is something of a *reductio ad absurdam*, and that in reality, this actually describes ethics at-large. While I balk at – and have argued against – refutations of the utility and benefit of specialized domains of (bio) ethics, I do not wholly disagree with the concept of an inclusive ethical paradigm. But if ethics-at-large is to be applied to, and useful for, assessment and guidance of AISC, then any ethical approaches utilized must be pluralist, cosmopolitan and grounded to the natural realities of both what the human is, and how our biological condition and socio-technological drives have, can and likely will affect what we will become [42].

Neil Levy has suggested that to some extent, neuroethics may provide a "…new way of doing ethics" [43], I concur, or at very least, pose that neurobioethics could contribute a valuable lesson and/or some structure and method toward this end.

10.5 The Importance of Informed Policy

However, to effectively do so, and to meaningfully contribute to any form of guidance and enactment of AISC, such ethical systems cannot be merely speculative. Rather, this ethical process must be dynamic, and accurately assess and reflect (1) the most current capabilities, directions and trends in science and technology; (2) the views and values of professionals involved in these enterprises, and (3) the various social realms that will be affected by – and influence – scientific research and its potential uses. In other words, in order to assume a stance of preparedness, responsibility and prudence in guidance and action, it must be an ethics of expertise and experience. I hold that such expertise is axiomatic to any assumption of prudence, which by definition, dictates practical wisdom [44]. The practicality of this

wisdom obtains and entails insights of multiple experts from a range of (scientific and humanities') disciplines, as well as the public [45].

Indubitably, science and technology will advance, and there is a need to both be prepared for the contingencies of such advancement, and accept responsibility for the directions and valence that such developments might assume. If the AISC model is to work, then the technical rectitude and ethical soundness of any/all innovations and accomplishment(s) must be addressed, regarded and viewed as salient ends (i.e. – the *telos*) of the process. It is naïve to think that science, or ethics alone can effect these ends, as neither science nor ethics exist in a social vacuum or amidst social stasis. The articulation of both science and ethics require infra- and extra-structural support that is fostered and garnered by funding and administration. These are aspects of policy, and to most effectively serve science and society, any such policy must be well-informed. This speaks yet again to my call for de-siloing. If this information is to reach and affect policy-makers, scientists and ethicists must (1) first engage active discourse and dialectic toward defining the parameters and benefits of achieving the AISC model in practice; (2) collaboratively communicate with media, the public, and representatives of those agencies influential to policy formulation, and (3) proactively engage grassroots efforts toward a "books-to-bench-to-boardroom" approach that can compel and shape ethically sound policy to sustain AISC.

10.6 Conclusions

The AISC model represents a viable approach to neuroscience. Beyond simple multi-disciplinarity, the AISC model conjoins constituent scientific and technological fields to foster innovation, invention and new ways of addressing seemingly intractable questions. In this way, AISC can yield novel methods, generate new trajectories of knowledge and discovery, and lead to the development of new epistemologies. As stand-alone disciplines, each and all of the constituent fields generate practical and ethical issues, and their convergence may establish a unique set of potential benefits and problems. To effectively attend to these contingencies requires (1) pragmatic assessment of the actual capabilities and limits of neurofocal AISC, (2) an openness to what new knowledge and scientific/technological achievements may be produced, and (3) recognition of how such outcomes can affect humanity, the human condition, society and the global environment. A progressive neurobioethics may establish both a meta-ethical framework upon which to intuit and structure ethical decisions, and a system and method of ethics that is inclusive, convergent and innovative, and therefore could be aligned with, and important to the AISC paradigm.

Acknowledgements This work was supported, in part by funding from NATO, grants from the Office of Naval Research and the Nour Foundation; the IGERT Program of the University of New Mexico, the William H. and Ruth Crane Schaefer Endowment, and ongoing subsidies provided by

the Center for Neurotechnology Studies of the Potomac Institute for Policy Studies, USA. Thanks to Prof. A. Vaseashta PhD for continued collaboration in studies of integrative scientific convergence, and to Sherry Loveless for editorial assistance and graphic artistry.

References

1. Simonton DK (2004) Creativity in science: chance, logic, genius, and zeitgeist. Cambridge University Press, Cambridge
2. Valenstein ES (2005) The war of the soups and sparks. Columbia University Press, New York
3. Giordano J (2011) Stud Ethics Law Technol 5(1):1–9
4. Giordano J, Boswell MV, Benedikter R (2010) J Ethics Biol Eng Med 1(2):135–142
5. Lenk H (1963) Technokratie als Ideologie. Kohlhammer, Stuttgart
6. Giordano J, DuRousseau D (2011) J Cog Technol 15(2):5–10
7. Cole S (1983) J Sociol 84:958–977
8. Brannigan A, Wanner RA (1983) Can J Sociol 8:135–151
9. Giordano J, Olds J (2010) Am J Bioeth Neurosci 1(4):12–14
10. Drexler KE (1998) Nanosystems: molecular machinery, manufacturing and computation. Wiley, Baltimore
11. Gabriel G, Gomez R, Bongard M, Benito N, Fernandez E, Villa R (2009) Biosens Bioelectron 4:1942–1948
12. Giordano J, Akhouri R, McBride DK (2009) J Long Term Eff Med Implants 5(9):45–54
13. Grunwald A (2005) Sci Eng Ethics 11(2):187–201
14. Hester RE, Harrison RM (2007) Nanotechnology: consequences for human health and the environment, vol 24, Issues in environmental science and technology. Royal Society of Chemistry Publishing, London
15. FitzGerald K, Wurzman R (2010) In: Giordano J, Gordijn B (eds) Scientific and philosophical perspectives in neuroethics. Cambridge University Press, Cambridge
16. Williams RB, Marchuk DA, Gadde KM et al (2003) Neuropsychopharmacology 28:533–541
17. Harper PS, Clarke A (1990) Lancet 335:1205–1206
18. Plomin R, McGuffin P (2003) Annu Rev Psychol 54:205–228
19. Giordano J, Wurzman R (2008) Depress Mind Body 4(1):2–5
20. Walters LR (1986) Nature 320:225–227
21. Kitcher P (1996) The lives to come: the genetic revolution and human possibilities. Simon and Schuster, New York
22. Annas G (1993) JAMA 270:2346–2350
23. Parens E (2004) Hastings Cent Rep 34(suppl1):S1–36
24. Burris S, Gostin LO (2004) In: Burley J, Harris J (eds) A companion to genethics. Blackwell, London
25. Wolf S (1995) J Med Ethics 23:345–349
26. von Neumann J (1958) The computer and the brain. Yale University Press, New Haven
27. McCulloch WS, Pitts W (1943) Bull Math Biophys 5:115–133
28. Gigerenzer G, Goldstein DG (1996) Creat Res J 9(2/3):131–144
29. Culham JC (2006) In: Cabeza R, Kingstone A (eds) Handbook of functional neuroimaging of cognition. Cambridge University Press, Cambridge
30. Birbaumer N, Cohen LG (2007) J Physiol 579:621–636
31. Hinterberger T, Widmann G, Lal TN et al (2008) Epilepsy Behav 13:300–306
32. Rosenthal A et al (2010) J Biomed Inform 43(2):342–353
33. Smith K et al (2004) NeuroImage 22(4):1646–1656
34. Hassan U et al (2008) NeuroImage 39(2):693–706
35. Vaseashta A (2012) Technological innovations in sensing and detection of chemical, biological, radiological, nuclear threats and ecological terrorism. Springer, Dordrecht

36. Giordano J (2010) Synesis 1(1):2–4
37. Giordano J (2011) Hum Prospect 1(1):2–6
38. Racine E (2010) Pragmatic neuroethics. MIT Press, Cambridge
39. Roskies A (2002) Neuron 35:21–23
40. Giordano J (2010) In: Giordano J, Gordijn B (eds) Scientific and philosophical perspectives in neuroethics. Cambridge University Press, Cambridge
41. Giordano J (2011) AJOB Neurosci 3(2):9–13
42. Benedikter R, Giordano J, FitzGerald K (2010) J Futures 42(10):1102–1109
43. Levy N (2001) AJOB Neurosci 3(2):1–7
44. Aristotle (1966) Nicomachean ethics (trans: Ross D). Oxford University Press, London
45. Giordano J (2009) Pain: mind, meaning and medicine. PPM Press, Glen Falls

Chapter 11
Nanomaterials in Environmental Contamination, Their Nanotoxicological Peculiarities

Nanomaterials in Environmental Contamination

G. Kharlamova and N. Kirillova

Abstract Eco-nanothreat arises from a lack of knowledge about new states of matter (spheroidal molecules of carbon, nanostructures, nanoparticles and nanophases). Newly discovered nanomaterials are likely to have different behavior and properties than their predecessors. New approaches for creating nanotechnologies are developed by using nanomaterials. Nanotechnology is considered as a panacea for resolving global problems that may affect the duration and quality of life. However, progress in technology historically leads to positive and negative consequences, thus the same can be expected from nanotechnology. Several un-researched threats may arise from uncontrolled development of nanotechnology. Some scientists foresee nanotechnological and nanodemocratic threats connected to possible undesirable self-replication of different nanosystems, and uncontrolled application of cheap ubiquitous personal nanosensors for permanent surveillance of individuals. In addition, little research is aimed to study how nanomaterials may attribute to environmental contamination. Finally, the influence of nanoparticles and nanostructures on the human organism may also be threatening in certain circumstances.

Keywords Nanomaterials • Nanoobject • Nanoparticle • Nanostructure • Environment • Contamination • Eco-nanothreats • Nanotoxicological peculiarities

G. Kharlamova (✉) • N. Kirillova
Kiev National Taras Shevchenko University, 64 Volodymyrska Street,
03001 Kiev, Ukraine
e-mail: akharlamova@ukr.net

A. Vaseashta et al. (eds.), *Technological Innovations in Sensing and Detection of Chemical, Biological, Radiological, Nuclear Threats and Ecological Terrorism*,
NATO Science for Peace and Security Series A: Chemistry and Biology,
DOI 10.1007/978-94-007-2488-4_11, © Springer Science+Business Media B.V. 2012

11.1 Introduction

Nano particles and devices have the potential to solve many problems for humanity but may also pose harm if not properly controlled. Nanoparticles are not poison, but because they can transfer into living organism, they may also pose a threat to normal, healthy functioning. At the end of the last century, several important discoveries in nano science were made. First, unique electronic microscopes of nanodimensional levels were created that allowed a new state of a matter (nanosized objects) to be detected. Second, under manipulation at atomic (atoms), molecular (molecules) and nanosized levels, we can now obtain essentially new and programmed substances, to create nanorobots that include optical and electronic nanodimensional devices. Thus, a completely new principle of creation has arisen in nanotechnology. (It is noted that modern bulk-technologies manipulate by macroobjects). The epoch of nanominiaturization such as nanochemistry, nanotechnology, nanomedicine and so on has begun. By the depth of influence on modernity, nanotechnologies are comparable to the discovery of radioactivity or computer revolution.

Unfortunately, there is little research devoted to the influence of nanomaterials on public health. Even experts on synthesis of nanoobjects and investigation of their properties know little about problems arising from the ecological character of these new carriers of new properties. The study of influence of these new, untraditional for macrosystems properties, on the environment and, first of all, on human health is imperative. However, in order to understand eco-nanothreats arising from nanoworld objects, research must determine basic sources of how eco-nanothreats arise, and their chemical and nanotoxicological features.

11.2 Classification of Nanomaterials and Nanoobjects – New State of Matter

The opening of a new state of substance (new type of a matter) such as spheroidical molecules of carbon with a hollow core, nanodimensional anisotropic structures and isotropic particles have changed all our representations about composition and structure of our world and became the epoch-making beginning in the knowledge of unknown world – the nanoworld. It is well known that substances can demonstrate new, unique properties depending on the size and morphology of nanoobject. The ability to study materials at the nano level is epoch arising to a new formation of a science and new approach for creation. Accordingly, the terminology of nanoscience is being formulated as research continues. Accordingly, this research specifies the following concepts and terminology within the realm of nanoscience.

First, it is expedient to consider that the science about objects of nanoworld is nanology (instead of nanoscience) and experts in area of nanology are nanologists (instead of nanoscientists) [1]. The main sections of nanology, undoubtedly, are nanochemistry and nanotechnology as bases of creation of nanolook on an atom-molecular

nature of the environmental nanoworld. Nanochemistry is a science about synthesis, structure and properties of this new type of substance (nanochemical objects), and nanotechnology is a science of a creative manipulation at an atom-molecular level and nano-miniaturization of technological processes [2].

Second, according to the nomenclature IUPAC nanoparticle is accepted to consider as the aggregate of atoms by the size less 100 nm and containing amount of atoms less than 10^6, but being a part of a volumetric material. As we see, in this definition there are too many discrepancies. If a nanoparticle is the aggregate of atoms, then what, in such case, is the aggregate? If the aggregate, as it is accepted to consider, is spontaneous (electrostatic) congestion of separate particles, it can not be a part of a material (part of macroscopic phase), in which composition, crystalline structure and chemical bonds are strictly individual. On the other hand, spheroidal molecules of fullerene and single-walled carbon nanotube also frequently are named nanoparticles. However, a molecule cannot be a part, it is always strictly individual. As such, carbon nanotubes should be considered as a nanomaterial or nanostructure, but not a nanoparticle.

It is necessary also to note that not all nanoparticles are nanochemical objects (or can be a subject of nanochemistry). The term nanoparticle informs only about the 0D-size (<100 nm) particle of macroscopic phase (macrophase), but not about the change of its functional (physico-chemical) features. Therefore, nanoparticles that show nanosized effects (crystalline structure and the properties essentially depend on their size), should be called nanoreactors [3]. We believe that the term nanoreactor is not quite suitable for new carriers of properties or new states of the given chemical substance. Nanoparticles, which are on one hand, a nanodimensional part of macrophase, and on the another hand have essentially other physic-chemical and electronic properties, may be termed nanophases [1]. So, a nanoparticle of gold by the sizes 3–5 nm, having icosahedral structure [4] may be named nanophase instead of nanoreactor [3] gold. The temperature of nanophase melting of gold is essential (more than on 400K) and changes depending on amount of atoms [4]. The transition from macrophase to nanophase is a new and unique example of transition of amount in quality.

Basically, current objects of nanochemistry (or nanochemical objects) can be classified according to their size, morphology and nature of chemical bonds on:

- spheroidical molecules with hollow core: fullerenes, single-walled nanotubes;
- zero-dimensional (isotropic) particles, in particular, metals and oxides;
- one-dimensional (anisotropic) structures: multi-walled nanotubes, wires, rods, belts, nails;
- two-sized structures: graphene;
- zero-dimensional spheres: onions, toroids;
- nanomaterials.

On Figs 11.1 and 11.2, we demonstrate nanostructures of various substances [5–10]. Some morphologies of carbon, silicon carbide and boron nitride are extremely unusual and permit more detailed discussion of the mechanisms of the growth of nanostructures of different substances [1, 2].

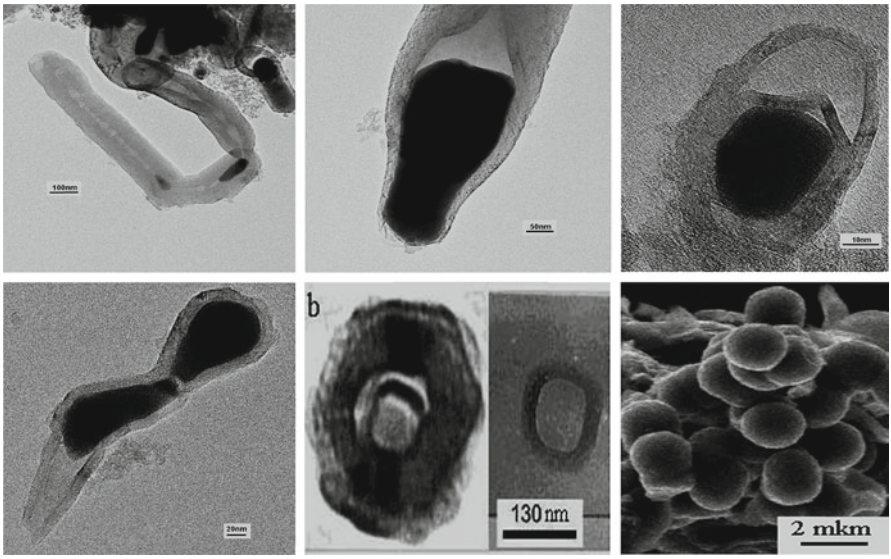

Fig. 11.1 TEM images of unusual morphologies of multi-walled carbon nanotubes with metallic nanoparicles inside, toroids and onions [5, 6]

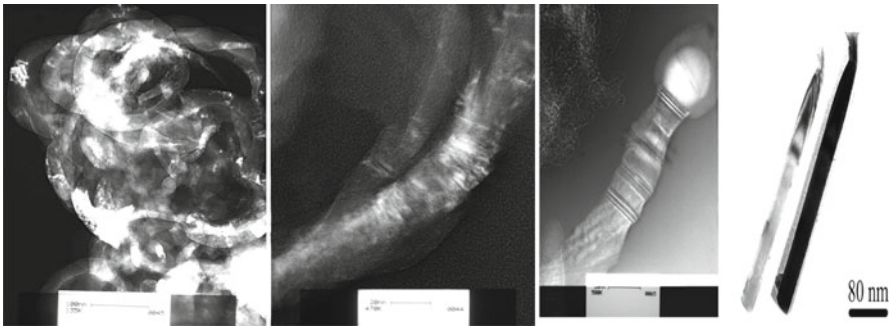

Fig. 11.2 Nanothreads of boron nitride and silicon carbide [7, 8]

It is important to note that nanomaterials may be classified on:

- nanostructured materials that units of building are nano-sized (0D, 1D and 2D) objects (nano-structures, nano-particles);
- mainly powdery materials containing nano-sized objects (nano-structures, nano-particles as ingredients);
- isolated nanostructures as the components of building of more complex systems.

So, nanomaterials make up nanoobjects. Thus scientists are obligated to develop novel unique classifications of toxicity and impacts on human health and properties for nanoobjects. The old standards can not simply be applied to the nanoworld and nanothreats, nor can the older methods of investigation.

11.3 Chemical Peculiarities of Nanoobjects

The study of physic-chemical and electronic properties of the isolated objects of nanochemistry (nanotube, nanorod, onion or nanophase) is complicated because there are no methodologies or appropriate devices for working with nanodimentional objects. Nonetheless large scale industrial manufacture of substances in nanodimension states already occurs. In particular, the amount of synthesized carbon nanotubes exceeds 100 Tons/year [11]. Worldwide manufacture of TiO_2 nanoparticles composes almost two millions Tons/year within sunscreen and cosmetic creams, antiseptics, tooth paste, shampoo, textiles, clothes, food packing, dyes, and plastics. Thus, nanoparticles are distributed within the air, water, foodstuff, clothes, and creams. This underscores the need to understand chemical features nanochemistry objects to foresee possible aggressive and harmful impact as environmental pollutants. Basic chemical features of nanoobjects as new carriers of properties follow [2]:

- nanosmall size comparable with the size of some molecules;
- molecules can be in solid state;
- high curvature of surfaces;
- unusual morphology: tubes, tapes, rods, onions, toroids, sphere (Figs. 11.1 and 11.2);
- a number of free valences on surface and huge free energy: an extremely high reactivity compared to radicals;
- difficulty of detection and subsequent removal of nanomaterials from the environment by means of traditional methods of filtration;
- nontoxic nanoparticles can interact to different components of living organism;
- nanoparticles in organism can be catalysts that form toxic substances;
- spheroidal molecules are extremely strong electrons acceptors as strong carcinogenic substances;
- properties of nanophase [1] and nanostructures depend on their size and shape; carbon nanostructures especially partially destroyed onions and multi-walled nanotubes (Fig. 11.3) can be capacious containers for synthesized carcinogenic substances and can exert double influence on health of the people.

So, we establish that the molecules of various substances are located on a surface of carbon structures (Fig. 11.3) obtained at pyrolysis of hydrocarbons [12]. In particular, from prepared benzene (toluene) extracts, thread-like colored crystals grow (Fig. 11.3). Preliminary research has shown [13, 14] that these transparent macrothreads consist of more thin microthreads and contain practically only carbon (Fig. 11.4). It is possible that the transparent threads contain hydrogen also.

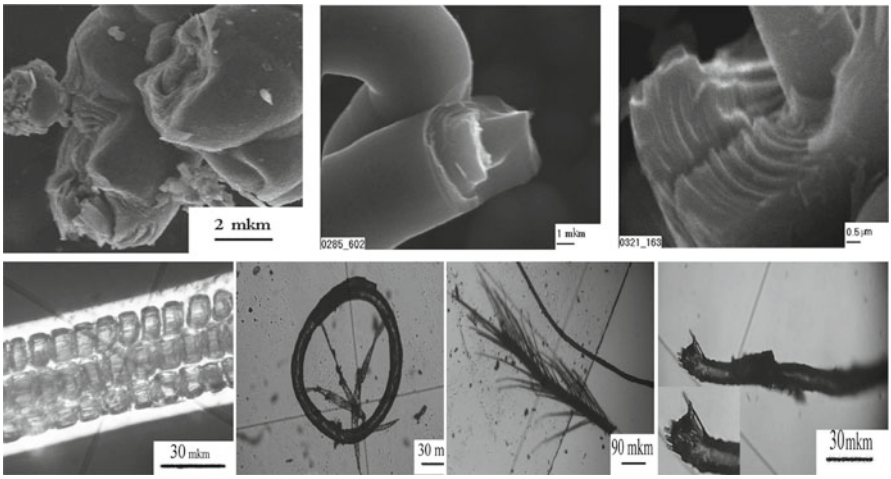

Fig. 11.3 Partially destroyed carbon structures (*up*) and transparent colored carbon threads (*below*)

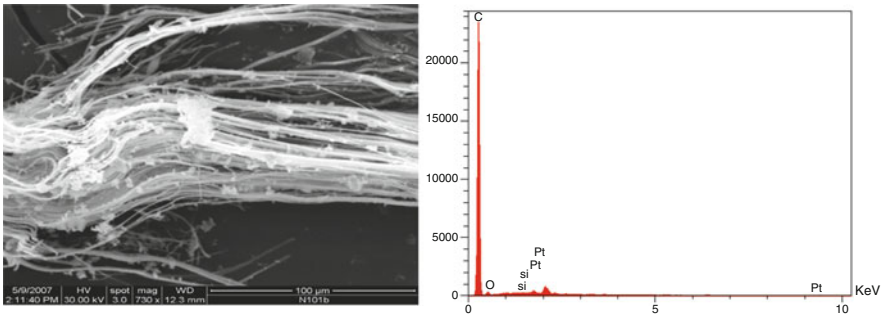

Fig. 11.4 SEM image and XDA spectrum of transparent thread of carbon

11.4 Basic Nanotoxicological Features of Nanoobjects

Uncontrollable distribution of new substances presents unpredictable threats for human organisms. Environmental contamination from products of exhaust gases (predominantly by carbon nanoparticles and lead) leads to the increased mortality rates of 20%. But the emission of carbon nanoparticles in the atmosphere from different anthropogenic sources (machines, aeroengines, power-stations, melting, plasma, welding, and heat treatment of polymers) increases constantly each year. Furthermore, nanoparticles of various substances are distributed everywhere. They are found in many products, although labels don't typically list presence of nanoparticles. Nanoparticles of titanium and zinc oxides (TiO_2 and ZnO) have been used

in cosmetics, particularly in sunscreens. Nanoparticles of selenium, silver, zinc oxide, titanium dioxide and other inorganic substances can get into food from packaging.

Their small size allows penetration into human organisms by all accessible routes:

- through respiratory system (adsorbing on a large surface of lungs, some of them soak in blood);
- through gastrointestinal tract;
- through skin pores (particularly through damaged skin).

Nanoobjects in the digestive tract are capable of transforming from micro- to nanophase, continuously changing toxicological properties and, hence, physiological effects. Extremely chemically active nanoobjects easily overcome biological barriers in living organisms. The experiments on animals and fish indicate that from the circulatory system they can get directly into brain. So, from 1,000 of nanoparticles of iridium (or gold), one particle may enter the brain while ten nanoparticles enter the liver.

It is important to emphasize that toxic properties of nanoparticles of metals and oxides are mainly connected to active forms of oxygen generated by these nanophases. Nanoparticles of zinc (of more than 22 nm in size) cause induction of active forms of oxygen in cells, anemia (decrease in the concentration of hemoglobin in blood) and disorders of cardiovascular system [15].

The study of influence of nanoparticles of gold on an embryo shows that particles of the size 0,8 nm, then 1,5 nm are the most toxic [16]. Nanoparticles of silver the size 5–50 nm have strong antibacterial activity and toxicity in the livers of rats [17, 18]. The mechanism of development of toxicity is connected with oxidative stress and increased permeability of a membrane [18]. Aluminum nanoparticles promote overgrowth of organism's tissue causing formation and duplication of cells [19].

Fractional introduction suspension of iron nanoparticles (doses 1,000, 2,000 and 5,000 mg/kg) result to development of inflammatory processes on a mucous stomach and intestines (of mice, birds and fish), and also change during formation, development and maturing of blood cells [20].

Inhalation impact on rats nanoparticles of iron oxide (by size 22 or 280 nm) in doses 0,8 and 20 mg/kg cause an induction of the active forms of oxygen in cells and infringement of system of curtailing of blood [20]. Nanoparticles of iron oxides can cause also metallic (zinc) fever [21, 22].

Extremely active nanoobjects of usually inert substances can interact with human organism forming different and, perhaps toxic substances. Nanoparticles (by size 20 or 250 nm) titanium dioxide (TiO_2) inhaled by rats may accumulate in fabrics [23] and damage DNK lymph cell and cells of a brain. TiO_2 and ZnO nanoparticles catalyze photooxidation. Toxicity of TiO_2 develops from continuous generation by nanoparticles of the active forms of oxygen that may lead to occurrence of oxidative stress [14, 24–29]. The amount of the active forms of oxygen depends not only on the size of nanoparticles, but also from structure TiO_2 either crystalline or amorphous [30].

Carbon nanotubes show toxicity depending on their entrance into animal organisms. Rats and mice that inhale carbon nanotubes experience inflammation, accumulation of fiber in pulmonary fabric, and increased weight of the lungs are observed [16, 28]. Carbon nanotubes are capable of penetrating a membrane, and can accumulate inside cells and reduce dimensions. Single-walled nanotubes at concentration 25, 50, 100 and 150 mg/ml inhibit the proliferation of embryonic cells of a human kidney [30, 31]. Single-walled carbon nanotubes activate the growth of neoplasms in kidneys [31] and various carbon nanostructures are capable of inducing active oxygen with unpaired electron (radical) that can inflict damage to cellular structures at certain concentrations [31]. Carbon nanotubes distributed on fabrics can enter the digestive systems, and some organs show reduced viability. Single-walled and multi walled carbon nanotubes differ by a degree of toxicity and their ability to induce oxidative stress [17, 30].

Intravenous injection of fullerenes (or its water soluble forms) in doses of 15 and 25 mg/kg in rats resulted in the death of 2 of 20 rats within 5 min. Fullerenes that were almost completely connected to fibers of plasma, decreased liver activity and induced oxidative damage of its cells [31, 32].

Unusual nanotoxicological features of nanoobjects and nanomaterials may cause the synthesis of new physiologically active substances. These new obtained substances can change the biological barriers of the host organism. In such cases mutation of the host organism is inevitable.

11.5 Conclusions

New practically uninvestigated nanoobjects (spatial molecules, nanostructures, nanoparticle nanophases and nanomaterials) of various common substances (carbon, silver, gold, iron, TiO_2 and ZnO) are distributed everywhere (air, water, foodstuff, cosmetics and packing). They can and enter very easy into living organism. Because of their nano dimensions, they can easily enter living organisms; and because of their extremely high reactivity, they can inter-react and destroy different human organs.

References

1. Kharlamov AI, Kirillova NV (2009) Fullerenes and hydrides of fullerenes as products transformation (polycondensation) of molecules of aromatic hydrocarbons. Rep Acad Sci Ukraine 5:110–118, Russian
2. Kharlamov AI, Kirillova NV, Skripnichenko AV, Gubareni NI, Fomenko VV (2010) Nanochemical peculiarities of nanostructures, nanophases and nanoparticles. Rep Acad Sci Ukraine 4:100–108, Russian
3. Buchachenko AL (2003) Nanochemistry is a direct route to high technologies of new century. Uspechi Chem 72(5):419–437, Russian

4. Pul Ch, Ouens F (2005) *Nanotechnologies*, Series: The world of materials and technologies. Texnosfera, Moscow, p 336 (Russian)
5. Kharlamov AI, Ushkalov LN, Kirillova NV, Fomenko VV, Gubareny NI, Skripnichenko AV (2006) Synthesis of onion nanostructures of carbon at pyrolysys of aromatic hydrocarbons. Rep Acad Sci Ukraine 3:97–103, Russian
6. Kharlamov AI, Loythenko SV, Kaverina SV, Fomenko VV (2004) Toroidal nanostructures of carbon. Single-walled 4-, 5- and 6-hedrons and nanorings. Rep Acad Sci Ukraine 1:95–100, Russian
7. Kharlamov AI, Kirillova NV, Karachevtseva LA, Kharlamova GO, Kharlamova GO (2003) Low-temperature reactions between vaporizing silicon and carbon. Theor Exp Chem 39(6):374–379
8. Kharlamov AI, Kirillova NV (2002) Gas-phase reactions of formation of silicon carbide nanofilaments from silicon and carbon powders. Theor Exp Chem 38(1):59–63
9. Kharlamov AI, Kirillova NV, Loytchenko SV et al (2002) Synthesis of elongated nanostructures of silicon carbide from powdery silicon and carbon. Rep Acad Sci Ukraine 10:98–105
10. Kharlamov AI, Kirillova NV, Kaverina SV (2003) Hollow and thread-like nanostructures of boron carbide. Theor Exp Chem 39(3):141–146
11. Endo M (2008) Carbon nanotubes: growth, structural control and safety for applications, CarboCat-111. International symposium on carbon for catalysis. Conference Proceedings, Berlin, 9–12 Nov 2008, p 5
12. Kharlamova G, Kirillova G, Kharlamov N, Skripnichenko A (2008) Novel transparent molecular crystals of carbon. In: Vaseashta A, Mihailescu I (eds) Functionalized nanoscale materials, devices, and systems. Springer, Dordrecht, pp 373–379
13. Kharlamov A, Kirillova N, Fomenko V (2007). In: Mehmetli E, Koumanova B (ed) The fate of persistent organic pollutants in the environment. Springer Science+Business Media B.V., Dordrecht, pp 425–441
14. Kharlamov AI, Kirillova NV, Zytheva ZA (2007) New state of carbon: transparent thread-like anisotropic crystals. Rep Acad Sci Ukraine 5:101–106
15. Wang B (2006) Acute toxicity of nano- and micro-scale zinc powder in healthy adult mice. Toxicol Lett 161:115–123
16. Glushkova AV, Rodilov AS, Rembovskii VR (2007) In: Rachmanin YA (ed) Methodological problems of study and appraisal bio- and nanotechnologies (nanowave, particle, structure, processes, bioobjects) in human ecology and hygiene of environment. Materials of plenum of scientific counsel on man, pp 20–27 (Moscow)
17. Lewinski N, Colvin V, Drezek R (2008) Cytotoxicity of nanoparticles. Small J 4(1):26–49
18. Allsopp M, Walters A, Santino D (2007) Nanotechnologies and nanomaterials in electrical and electronic goods: a review of uses and health concerns. Greenpeace Res Lab, December, 22 p
19. Chen L (2008) Manufactured aluminum oxide nanoparticles decrease expression of tight junction proteins in brain vasculature. Neuroimmune Pharmacolo 3:286–295
20. Kovalenko LV, Folmanis GE (2006) Biological active nanopowders of iron. Science, Moscow, 124
21. Alt V, Bechert Th, Steinrücke P, Wagener M, Seidel P, Dingeldein E, Domann E, Schnettler R (2004) An in vitro assessment of the antibacterial properties and cytotoxicity of nanoparticulate silver bone cement. Biomaterials 25(18):4383–4391
22. Oberdörster G, Oberdörster E, Oberdörster J (2005) Nanotoxicology: An emerging discipline from studies of ultrafine particles. Environ Health Perspect 113:823–839
23. Hoet P, Bruske-Holfeld I, Salata O (2004) Nanoparticles – known and unknown health risks. J Nanobiotechnol 2:12
24. Ostiguy C, Lapointe G, Ménard L, Cloutier Y, Trottier M, Boutin M, Antoun M, Normand C (2006) Health effects of nanoparticles. IRSST Report R-469, August 2006, Montréal. 57 pages
25. Kang SJ (2008) Titanium dioxide nanoparticles trigger p53-mediated damage response in peripheral blood lymphocytes. Environ Mol Mutagens 49(5):399–405

26. Long TC, Tajuba J, Sama P, Saleh N, Swartz C, Parker J, Hester S, Lowry GV, Veronesi B (2007) Nanosize titanium dioxide stimulates reactive oxygen species in brain microglia and damages neurons in vitro. Environ Health Perspect 115(11):1631–1637
27. Zhu MT, Feng WY, Wang B, Wang TCh, Gu YQ, Wang M, Wang Y, Ouyang H, Zhao YL, Chai ZF (2008) Comparative study of pulmonary responses to nano- and submicron-sized ferric oxide in rats. Toxicology 247:102–111
28. Lu N (2008) Nano titanium dioxide photocatalytic protein tyrosine nitration: a potential hazard of TiO_2 on skin. Biochem Biophys Res Commun 370(4):675–680
29. Heinlaan M, Ivask A, Blinov I, Dubourguier HCh, Kahru A (2008) Toxicity of nanosized and bulk ZnO, CuO and TiO_2 to bacteria Vibrio fischeri and crustaceans. Chemosphere 71:1308–1316
30. Jiang J, Oberdrster G, Elder A, Gelein R, Mercer P, Biswas P (2008) Does nanoparticle activity depend upon size and crystal phase?. Nanotoxicology 2(1):33–42
31. Donaldson K, Aitken R, Tran L, Stone V, Duffin R, Forrest G, Alexander A (2006) Carbon nanotubes: review of their properties in relation to pulmonary toxicology and workplace safety. Toxicolo Sci 92(1):5–22
32. Zhua S (2006) Toxicity of an engineered nanoparticle (fullerene, C60) in two aquatic species, Daphnia and fathead minnow. Mar Environ Res 62:5–9

Chapter 12
The Transnistria Equation

Transnistria

Ashok Vaseashta and S. Enaki

Abstract Transnistria is a breakaway republic situated on the left bank of the river Nistru. We discuss issues dealing with a factual description of the conflict apparition, evolution and present-day situation.

Keywords Separatist republic • Human rights • Soviet Army

12.1 General Overview

Transnistria is a breakaway republic situated on the left bank of the river Nistru (also known as Trans-Dniestr or Prednistrovia), with an area of about 3,362.33 km^2 and population of about 555,500 people. Russia is the only country that has legally recognized the self-declared independence of Transnistria. The European Community (including the Moldovan authorities) officially calls Transnistria an Autonomous Territorial Unit. It is the leading territorial issues facing Moldovan Authorities since then 1992 war between Moldova and Transnistria. According to New York Times " Transnistria is a narrow swath of territory that legally is part of

A. Vaseashta (✉)
Institute for Advanced Sciences Convergence and Int'l Clean Water Institute, Norwich University Applied Research Institutes, 13873 Park Ctr. Rd. Ste. 500, Herndon, VA 20171, USA
e-mail: avaseash@norwich.edu

S. Enaki
Academy of Economic Sciences, Chisinau, Republic of Moldova

A. Vaseashta et al. (eds.), *Technological Innovations in Sensing and Detection of Chemical, Biological, Radiological, Nuclear Threats and Ecological Terrorism*, NATO Science for Peace and Security Series A: Chemistry and Biology,
DOI 10.1007/978-94-007-2488-4_12, © Springer Science+Business Media B.V. 2012

Moldova, a poor country bordering Romania, that since the early 1990s, with the support of Moscow, a nationalist, pro-Russian separatist movement in Transnistria has been trying to break away from Moldova [1]."

It is safe to call the Moldovan Transnistria equal in gravity to the Georgian Ossetia. The Transnistrian region has been publicly criticized due to its human right violations, uncontrolled borders, and various power pressures applied by the self-proclaimed government and president, Igor Smirnov. To this day, negotiations regarding Transnistrian conflict have made little progress and warrant international intervention [2, 3].

12.2 Historical Perspectives

In ancient times, the area where Transnistria is now located has been inhabited by Indo-European tribes for millennia, being a borderland between the ancient states of Dacia and Scythia. Migrating from the North, Slavs were present on the shores of the Nistru River from the second half of the sixth century. In fact, even the Romanian population situated on the territory in which the Republic of Moldova is located now is referred to, in some historical sources, as "Russo-Vlahs" a term that has been attributed to the population in this region due to the interaction with the Slav tribes which invaded the territory sporadically in the ancient times.

During the middle Ages, Transnistria's regions and cities were cited in documents dated from the fifteenth century, as well as documents dating in the seventeenth to eighteenth centuries, each territory belonging either to the Moldavian Region or to the present-day Ucraine. Yet the region of Transnistria has been referred to as a whole only after the Russo-Turkish war, due to the fact that in 1792, the region became part of the Russian Empire. In that year, the general Alexander Suvorov founded modern Tiraspol as a Russian border fortress. Until the Russian Revolution of 1917, the current Transnistria was divided between the imperial guberniyas of Podolia, Kherson, and Bessarabia. Most of the territory which now is Transnistria was part of the larger New Russia region; hence it saw a strong colonization process, with a multitude of ethnicities being settled.

Transnistria became an autonomous political entity in 1924 with the proclamation of the Moldavian ASSR, which included today's Transnistria (4,000 km^2) as well as an adjacent area (9,000 km^2) around the city of Balta in modern-day Ukraine, but nothing from Bessarabia, which at the time was part of Romania. In fact, the republic was formed in response to the unification of Romania, wherein the Moldavian ASSR was created in response to the Soviet Union's desire to eventually incorporate Bessarabia (the present-day Republic of Moldova). Later on, the Moldavian SSR was organized by a decision of the Supreme Soviet of the USSR in 1940 comprising a part of Bessarabia (taken from Romania on 28 June, after the Molotov-Ribbentrop pact and a Soviet ultimatum addressed to the Romanian King Carol II), and a part of the Moldavian ASSR which is roughly equivalent to present-day Transnistria.

In the 1980s, Mikhail Gorbachev's policies of perestroika and glasnost in the Soviet Union allowed political liberalization at a regional level. This led to the creation of various informal movements in the Moldavian SSR, and the resurgence of pro-Romanian nationalism among ethnic Moldovans. The most prominent of these movements was the Popular Front of Moldova. Since the spring of 1988, PFM demanded from the Soviet authorities to declare Moldovan the only state language, to return to the use of the Latin alphabet and to recognize the shared ethnic identity of Moldovans and Romanians. The first two demands were endorsed by the Supreme Soviet of the Moldavian SSR in 1989 in addition to the declaration of a shared Moldova-Romanian linguistic identity. The Popular Front won the first free parliamentary elections in the Moldavian SSR in the spring of 1990, and its agenda started slowly to be implemented.

On 2 September 1990, the Pridnestrovian Moldavian Soviet Socialist Republic was proclaimed as a Soviet republic by an ad hoc assembly, the Second Congress of the People's Representatives of Transnistria. In the interest of preserving a unified Moldavian SSR within the USSR and in preventing the situation escalating further into violence, the then Soviet President Mikhail Gorbachev declared the Transnistria proclamation to be lacking legal basis and annulled it by presidential decree on 22 December 1990. Nevertheless, no significant action was taken against Transnistria and the new authorities were slowly able to establish control of the region.

The War of Transnistria followed armed clashes on a limited scale which broke out between Transnistrian separatists and Moldova as early as November 1990 at Dub sari. Volunteers, including Cossacks, came from Russia and Ukraine to help the separatist side. In mid-April 1992, Moldova created its own Defense Ministry with the former 14th Soviet Army's military equipment to be retained by Moldova. Starting from 2 March 1992, there was concerted and increasing military action between Moldova and Transnistria. The former Soviet 14th Guards Army entered the conflict in its final stage, opening fire against Moldovan forces. Since then, Moldova has exercised no effective control or influence on Transnistrian authorities. A 21 July 1992 ceasefire agreement holds to this day.

12.3 Population

Due to its agitated history and intense colonization, Transnistria remains to this day a region with a rather diverse population. In 2004, Transnistrian authorities organized a separate census from the 2004 Moldovan Census. In total, in the areas controlled by the breakaway authorities of Tiraspol, there are 555,347 people, including 177,635 Moldovans (31.99%), 168,678 Russians (30.37%), 160,069 Ukrainians (28.82%), 13,858 Bulgarians (2.50%), and also Gagauzians, Gypsies (Roma), Jews, Poles and others.

Of these, 439,243 live in Transnistria itself, and 116,104 live in localities controlled by the authorities from Tiraspol, but formally belonging to other districts of Moldova (the city of Bender (Tighina), the communes of Proteagailovca,

Gîsca, Chițcani, Cremenciug, and village of *Roghi* of commune Molovata Nouă). Moldovans (Romanians) are the most numerous ethnic group, representing an overall majority in the two sub-districts in the central Transnistria (Dubăsari sub-district, and Grigoriopol sub-district).

The ethnic composition of the region has not been stable in recent history, with the most notable change being the decreasing share of Moldovan and Jewish population segments and increase of the Russian population.

12.4 Human Rights

The human rights record of Transnistria has been criticized by several governments and international organizations. The 2007 Freedom in the World report, published by the US-based Freedom House, described Transnistria as a "non-free" territory, having an equally bad situation in both political rights and civil liberties.

Also, on July 13 2007, a report was presented by Marios Matsakis to the European Parliament, entitled "Human Rights Violation in Transnistria", which condemns the "strict and frequent" violation of human rights by the Transnistrian separatist authorities. It stated that "a quick resolution of the conflict between Moldova and Transnistria is necessary to be insured" and seriously condemned the repressions, harassment and persecution of citizens and NGOs which work in Transnistria, cases committed by the Transnistrian totalitarian system. The presentation required a quick resolution of the "frozen conflict" from the region. He underlined that the territorial integrity of Moldova must not be doubted and the governing system from Tiraspol is "illegal and non-recognized". However the voted resolution has no juridical power, even though it asks the European Union to become a full participant at the resolution of the Transnistrian conflict [4].

The human right violations affect every area in the Transnistrian society. According to OSCE, the media climate in Transnistria is restrictive and the authorities continue a long-standing campaign to silence independent opposition voices and groups. Alternative viewpoints were stifled by widespread censorship. Transnistrian local authorities insist that public education for ethnic Moldovans in their mother tongue be done using the Soviet-originated Moldovan Cyrillic, and have restricted the usage of the Latin script for the Moldovan language to only six schools. Four schools of the six, that taught the Moldovan language using Latin script, were closed by the authorities, who claimed the schools refused to apply for official accreditation. The schools were later reopened amid pressure from the European Union, but as private institutions [5].

The Bureau of Democracy, Human Rights, and Labor within the US Department, presented a brief description of the Human Right situation in the Republic of Moldova. The Sections cited several grave violations of the human rights such as Arbitrary or Unlawful Deprivation of Life, Disappearance, Torture and Other Cruel, Inhuman, or Degrading Treatment or Punishment, Prison and Detention Center Conditions, Arbitrary Arrest or Detention, which cited several violations made by the separatist authorities of the Transnistrian self-proclaimed republic [6].

One of the most high profile cases involved Ilie Ilaşcu, who was convicted in 1993 of killing two Transnistrian officials. He was initially sentenced to death by Transnistria's Supreme Court. This was repealed to a life prison sentence. Three other associates were sentenced to 12–15 years' imprisonment and confiscation of their property. Ilaşcu was released in 2001, following a decision of the European Court of Human Rights, while the other three were released in 2004 and 2007 when they finished serving their sentences. In the case of "Ilaşcu and Others v. Moldova and Russia" (2004), the European Court of Human Rights (ECHR) found their detention arbitrary and did not recognize the sentence. It also demanded that Moldova and Russia release the other Ilie Ilaşcu Group members, Andrei Ivanțoc and Tudor Petrov-Popa, at that time still imprisoned in Transnistria.

12.5 Proposed Approach and Path Forward. Novelty of Approach

According to New York Times, when Chancellor Angela Merkel had dinner in June 2010 outside Berlin with President Medvedev of Russia, she surprised her guest by making a highly unusual proposal. If Russia is interested in cooperating with Europe, especially on security issues, then it should contribute by helping to resolve the long-running conflict in Transnistria, said Mrs. Merkel, whose country has some of the closest political and economic ties with Russia. Also the New York Times states that until Mrs. Merkel broached the issue with Russia, Europe had all but forgotten about this frozen conflict, even though it is on Europe's doorstep. Brussels left it largely up to the 56-member Organization for Security and Cooperation in Europe (OSCE) to try to mediate, but to little avail.

There is, for once, cautious optimism among some OSCE. officials. "Chancellor Merkel's initiative, by focusing high-level attention on the Transnistria conflict, can help achieve the first serious negotiations in years," said an OSCE official familiar with the process who spoke on condition of anonymity. "Negotiations will be hard on all sides, and a constructive spirit, willingness to compromise and persistence will be needed to reach a lasting settlement," the official added.

This path would definitely ease the further negotiations with the Russian and Transnistrian Authorities leading to a more democratic Transnistria. The major issue with Transnistria is its uncontrolled border that may become a flagella of terrorism and human and weapons traffic. Several other approaches of the Transnistrian conflict were proposed, of which the most notorious one is known as the Kozak Memorandum.

The Kozak Memorandum, officially Russian Draft Memorandum on the Basic Principles of the State Structure of a United State in Moldova, was a 2003 proposal aimed at a final settlement of relations between Moldova and Transnistria. It was seen as an extension of the 1997 Moscow Memorandum but was ultimately rejected by Moldovan president Vladimir Voronin. The plan, presented in mid-November 2003 by Russia, was a detailed proposal for a united asymmetric federal Moldavian state. According to the memorandum Russian troops (no more than 2,000 strong,

without heavy armaments) would remain in Transnistria for the transitional period but not later than 2020. The memorandum caused various public demonstrations in Moldova, and after its rejection an official visit of the Russian president Vladimir Putin was canceled [7].

Another approach was made by the Romanian historian and savant Neagu Djuvara. In an interview for the Romanian Paper "Adevarul" (translation "The Truth"), the historian treats the delicate subject and proposes an adherence of the Transnistrian territory to Ukraine, given the fact that the majority of the population is Russian speaking population, but with the permission of the Moldovan-Romanian population to access freely the Moldovan territory and special border legislation that would permit such actions. The adherence of Romania to the European Union and therefore the formation of the Republic of Moldova as a frontier state and as a potential European Union candidate make the Transnistria issue a highlight of the political agenda of Moldova. Given the politic tensions within the Republic of Moldova, the Transnistrian conflict cannot be solved unless the European Union and the NATO forces take an active involvement within the issues present to date. Only joint efforts and harmonious politic and social actions would lead to a peaceful and rapid reintegration of the Transnistrian territory within the Republic of Moldova. An increase of soft pressure would be desirable, but with cautions as to avoid another South Ossetia situation, given the politic resemblance of these two regions.

References

1. Dempsey J (2010) Letter – Challenging Russia to fix a frozen feud. New York Times
2. Herd GP, Moroney JP (2003) Security dynamics in the former soviet bloc. Routledge, New York
3. Zielonka V (2001) Democratic consolidation in Eastern Europe. Oxford University Press, Oxford/New York
4. Radulescu G (2010) Letter - We will be minorities in our country. Adevarul, Neagu Djuvara
5. Boonstra J (2007) Democratisation programme. FRIDE, Moldova, transnistria and European democracy Policies
6. Bureau of Democracy, Human Rights, and Labor (2007) Moldova
7. Brinza G (2006) The region – will transnistria become a new Russian enclave? http://www.seeurope.net/files2/pdf/rgn0906/19_Transnistria.pdf

Part III
Sensors/Detectors

Chapter 13
Real Time Detection of Foodborne Pathogens

Applications in Food Quality Monitoring and Biosecurity

V. Velusamy, K. Arshak, O. Korostynka, Ashok Vaseashta, and C. Adley

Abstract Contamination of foods by harmful bacteria by natural events or malicious intent poses a serious threat to public health and safety. This review introduces current technologies in detecting pathogens in food and foodborne illnesses. Causes of foodborne diseases and trends impacting foodborne diseases such as globalization and changes in micro-organisms, human populations, lifestyles, and climates are addressed. In addition, a review of the limitations in detecting pathogens with conventional technologies is presented. Finally, a review of nanostructured and nanomaterials based sensing technologies by pathogen, detection limits, and advantages is described.

Keywords Pathogens • Biodiversity • Food quality • Monitoring

13.1 Introduction

The presence of microorganisms especially in food is a natural and unavoidable occurrence. Meat, dairy, and poultry products are important reservoirs for many of the foodborne pathogens, including *salmonella, campylobacter, listeria, Bacillus cereus and Escherichia coli O157:h7*. Infectious doses of these pathogens as low as ~10 bacterial cells, increase the vulnerability of the elderly, infants, and people

V. Velusamy • K. Arshak (✉) • O. Korostynka • C. Adley
University of Limerick, Limerick, Ireland
e-mail: khalil.arshak@ul.ie

A. Vaseashta
Institute for Advanced Sciences Convergence, NUARI, 13873 Park Center Road. Suite 500, Herndon, VA, USA

A. Vaseashta et al. (eds.), *Technological Innovations in Sensing and Detection of Chemical, Biological, Radiological, Nuclear Threats and Ecological Terrorism*, NATO Science for Peace and Security Series A: Chemistry and Biology,
DOI 10.1007/978-94-007-2488-4_13, © Springer Science+Business Media B.V. 2012

with immunological deficiencies or organ transplants. In recent years, there has been greater recognition of the importance of *Biosecurity* in relation to protection of the environment. Biosecurity is a set of preventive measures designed to reduce the risk of transmission of infectious diseases, quarantined pests, invasive alien species, living modified organisms [1]. The need for biosecurity in food and agriculture has intensified with economic globalization, rapid improvements in communications, transport and trade, technological progress, and increased awareness of biodiversity and the environment. So far a major constraint in pathogen monitoring for food safety and biosecurity is the speed of detection. Rapid response to potential threats and cautious awareness to prevent tactics of bioterrorism are vital for public safety and international security. In recent years, numerous research efforts are being made for fast, accurate, and even ultrasensitive biosensors for real-time detection of pathogenic microorganisms. Currently, developing such tools for instant pathogen recognition has been considered as one of the top issues on emerging bio threats prevention.

13.2 Foodborne Diseases

Despite advances in hygiene, consumer knowledge, food treatment and processing, foodborne diseases caused by pathogenic microorganisms or microbial toxins still represent a significant threat to public health worldwide. The World Health Organization (WHO) defines foodborne illnesses as diseases, usually either infectious or toxic in nature, caused by agents that enter the body through the ingestion of food. Though the global incidence of foodborne disease is difficult to estimate, it has been reported that in 2009, diarrhea has caused 1.1 million deaths in people aged 5 and over and 1.5 million deaths in children under the age of 5, and a significant proportion of these results from consumption of food and water mainly food of animal origin with microbial pathogens and toxins. Also, in 2005 alone 1.8 million people died from diarrhoeal diseases and a great proportion of these cases can be attributed to consumption of contaminated of food and drinking water [2]. In industrialized countries, the percentage of the population suffering from foodborne diseases each year has been reported to be up to 30%. For, example, the Centers for Disease Control and Prevention estimated that around 76 million cases of foodborne diseases, resulting in 325,000 hospitalizations and 5,000 deaths occur each year in the USA [3].

13.2.1 Causes of Foodborne Disease

Although chemical contaminants, biological contaminants and natural toxins or anti-nutritional factors are the causes for foodborne diseases, most of the cases are thought to be of microbial origin [4]. Microorganisms cause foodborne illness by one of the two mechanisms, namely infection and intoxication:

13.2.1.1 Infection

When viable organisms (bacteria, viruses or parasites) are present in food and enter the body, *where* their growth and metabolism produce the disease response. For example bacteria causing infection include *Campylobacter*, *Salmonella*, *Listeria monocytogenes*, and *Escherichia coli* O157:H7.

13.2.1.2 Intoxication

When the presence and (usually) growth of an organism in the food because of incorrect storage are accompanied by the accumulation of a toxin that is ingested with the food and causes illness. For example, organisms causing intoxication include the bacteria *Bacillus cereus*, *Clostridium botulinum* and *Staphylococcus aureus*, algae and mycotoxins (mould toxins).

13.2.2 Emerging Fodborne Pathogens

Some foodborne diseases are well recognized, but are considered emerging because they have recently become more common. Emerging Foodborne Pathogens are those causing illnesses that have only *recently appeared* or been recognised in a population or that are well recognised but are *rapidly increasing* in incidence or geographic range.Though there are various food borne pathogens that have been identified for food borne illness, *Campylobacter*, *Salmonella*, *Listeria monocytogenes*, and *Escherichia coli* O157:H7 have been generally found to be responsible for majority of food borne outbreaks [5, 6]. For example, in Ireland, *Camplyobacter* is the most important cause of sporadic cases of foodborne illness. According to a recent EU study it has been reported that nearly all chicken produced in Ireland is contaminated with a *campylobacter*. The level of incidence in Ireland was 98% nearly one-third higher than the European average, according to the European Food Safety Agency. It is now the number-one cause of food poisoning in Ireland, with 1,758 cases in 2008 and provisional data showing 1,823 reported cases in 2009 [7]. Also, most of the earlier and recent food products recalls are also due to these pathogens [8].

13.2.3 Emerging Foodborne Diseases Major Trends

New foodborne disease threats occur for a number of reasons. The new challenges arise from the globalization of trade in food, changes in lifestyles and eating patterns, international travel, environmental pollution and climate change, deliberate contamination, natural and manmade disasters, nonhuman use of antimicrobial agents and food from new technologies:

13.2.3.1 The Globalization of the Food Supply

A large outbreak of cyclosporiasis occurred in North America during 1996–1997, which linked to contaminated raspberries imported from South America [9].

13.2.3.2 The Inadvertent Introduction of Pathogens into New Geographic Areas

Vibrio cholerae was introduced into waters off the coast of southern United States when a cargo ship discharged contaminated ballast water in 1991. It is likely that a similar mechanism led to the introduction of cholera for the first time this century into South America in 1991 [9].

13.2.3.3 Tourists, Refugees, and Immigrants Exposed to Unfamiliar Foodborne Hazards While Abroad

International travellers may become infected by foodborne pathogens that are uncommon in their countries. It is estimated that about 90% of all cases of salmonellosis in Sweden are imported [9]. The possible increased risk of botulism among migrant workers, who may import home-produced foods that are not transported under refrigerated conditions, is now becoming an important issue in many European countries and especially in Ireland. In 2006, for first time foodborne botulism was reported in Ireland. A person had consumed a homemade pork pie which he had brought back to Ireland following a trip to his country, but which had been improperly stored in his luggage during transit. Type A and B botulism toxins were identified in the food samples [10].

13.2.3.4 Changes in Micro-Organisms

Changes in microbial populations can lead to the evolution of new pathogens, development of new virulent strains in old pathogens, development of antibiotic resistance that might make a disease more difficult to treat, or to changes in the ability to survive in adverse environmental conditions.

13.2.3.5 Change in the Human Population

The population of highly vulnerable persons is expanding world-wide because of ageing, malnutrition, HIV infections and other underlying medical conditions. People with a weakened immune system also become infected with foodborne pathogens at lower doses which may not produce an adverse reaction in healthier persons. Seriously ill persons, suffering, for example, from cancer or AIDS, are

more likely to succumb to infections with *Salmonella, Campylobacter, Listeria, Cryptosporidium*, and other foodborne pathogens. In developing countries reduced immunity due to poor nutritional status render people, particularly infants, children and particularly for the elderly, more susceptible to foodborne infections.

13.2.3.6 Changes in Lifestyle

Greater numbers of people go out and eat meals prepared in restaurants, canteens, fast food outlets, and by street food vendors. In many countries, the boom in food service establishments is not matched by effective food safety education and control. Unhygienic preparation of food provides ample opportunities for contamination, growth, or survival of foodborne pathogens.

13.2.3.7 Climate Change

Weather also have an effect on the risk of foodborne diseases [11]. Climate change could cause changes in the incidence of infectious disease in Artic regions as well. Higher ambient temperatures in the Artic may result in an increase in some temperature sensitive foodborne disease such as gastroenteritis, paralytic shellfish poisoning and botulism [12]. An investigation relating environmental temperature and Salmonella infections with ten European populations indicated that in most countries the infections were peak in the late summer months, after the peak in temperatures [13].

There are many methodical programs like good agricultural practices [14, 15], good manufacturing practices [15, 16] hazard analysis and critical control point (HACCP) [17, 18] and the food code indicating approaches [19], which can significantly reduce the pathogenic micro-organisms in food. But still, the role of pathogen detection technology is vital, which is the key to the prevention and identification of problems related to health and safety.

13.3 Pathogen Detection from Conventional to Analytical Techniques

One of the major difficulties in detecting foodborne pathogens is that, they are mostly present in very low numbers (<100 Colony Forming Unit (CFU)/g) in the middle of millions of other bacteria. Therefore, there are more chances for these micro-organisms to get lost during detection. Rapid, selective and sensitive detection technologies for pathogenic bacteria are significant in disease control, environmental monitoring and food safety. Conventional methods for the detection and identification of microbial pathogenic agents mainly rely on specific microbiological and biochemical identification. Conventional methods can be classified into three types and are depicted in Fig. 13.1.

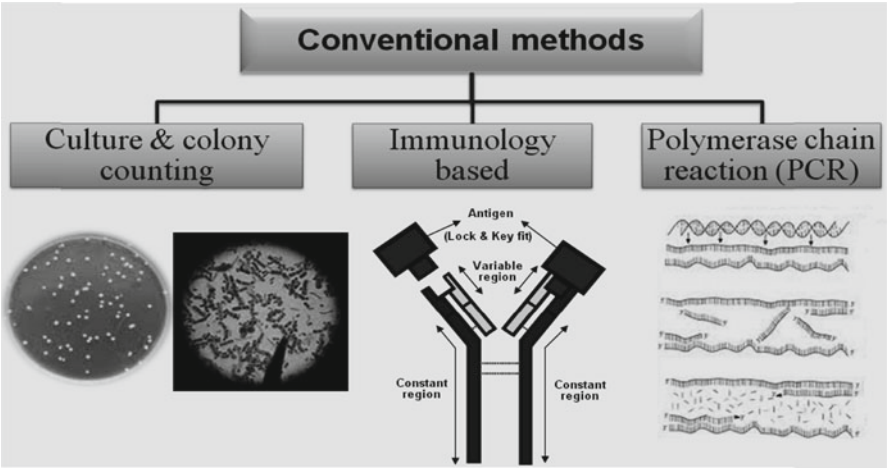

Fig. 13.1 Conventional methods for the identification and detection of microbial pathogens

- The *culture and colony counting method* [20, 21], involves counting of bacteria.
- The *immunology-based method* [22–24], involves antigen–antibody interactions.
- The third *polymerase chain reaction (PCR) method* [21, 25, 26], which involves DNA analysis.

Despite these approaches being powerful and error-proof, most of them are laborious, complex and time consuming and expensive. Although both qualitative and quantitative information of the tested micro-organisms can be obtained, they are greatly restricted by assay time, also initial enrichment is needed in order to detect pathogens which typically occur in low numbers in food.

13.3.1 Detection of Pathogens Using Analytical Methods

In recent years, there has been much research activity in the area of biosensor development for detecting pathogenic micro-organisms. A biosensor is an analytical device, which converts a biological response into an electrical signal. The transducer plays an important role in the detection process of a biosensor. Wide varieties of transduction methods have been developed in the past decade for the detection of foodborne pathogens. Although there are new types of transducers constantly being developed for use in biosensors, the transduction methods such as optical, electrochemical and mass based are the most popular and common methods. A comprehensive review for the detection of foodborne pathogens in the perspectives of biosensors have been reported [27].

Among the other transducing techniques, electrochemical detection is more beneficial due to its rapid performance, cost effectiveness, simple procedures and

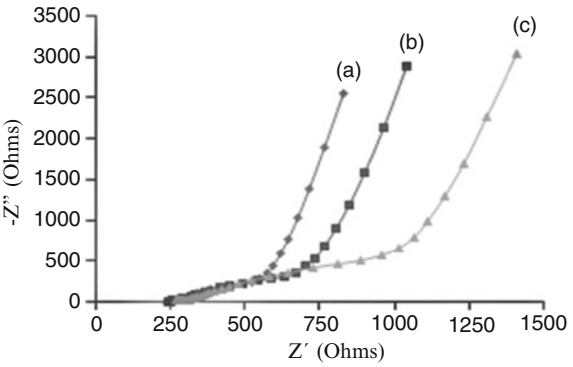

Fig. 13.2 Nyquist plot of (**a**) the PPy film, (**b**) PPy/ss-DNA capture immobilized surface, (**c**) after the hybridization with complementary target DNA [31]

moreover, suitable for in situ analysis [27–30]. For example, the impedimetric detection of label-free DNA specific to the foodborne pathogen *Bacillus cereus* has been reported [31] using polypyrrole (PPy) as an immobilization matrix and the corresponding Nyquist plot is shown in Fig. 13.2. The paper reported that the hybridization event was clearly distinguishable from complementary and non-complementary sequences using impedance spectroscopy and the total duration for impedimetric detection was less than 5 min.

Biosensors offer several advantages over existing techniques which includes limited hands-on time, high-throughput screening, improved detectability, real-time analysis and label-free detection methods and devices.

13.3.2 New Trends in the Rapid and Sensitive Detection of Pathogens

Within the growing and increasingly complex area of nanotechnology, its integration with biosensors holds great promise for addressing the analytical needs of detection systems. In this context, great attention has been paid in recent years to nanostructured materials of different chemical composition, produced as nanoparticles, nanowires, nanorods and nanotubes. These nanostructures have raised great expectations with respect to rapid and sensitive detection and they are the mostly used matrices for the design of nanobiosensors. Zelada-Guillen et al. [32] demonstrated aptamer-based Single wall carbon nanotube potentiometric sensors which are highly selective and can be successfully used to detect living microorganisms. The assay was in close to real time, making the detection of pathogens as easy as measuring the pH value. The paper reported that a highly accurate linear response can be obtained with good reproducibility and without any kind of pretreatment, starting at ultralow concentrations of bacteria and a dynamic range of four logarithmic units (0.2–10^3 CFU/mL). Some of the real time detection techniques based on nanostructures and nanomaterials are given in Table 13.1.

Table 13.1 Real time detection techniques based on nanostructures and nanomaterials

Transduction and type of nanostructure/materials used	Pathogen	Limit of detection	Advantages	Ref
Electrochemical detection using silver-enhanced Au NP(s)	E. coli and Bacillus subtilis cells	–	Cost-effective and suitable for real-time analysis	[33]
Surface-enhanced Raman scattering (SERS) using Au nanosphere and Au nanorod particles	–	10^1–10^5 CFU/mL	Accumulation time-60-s. Suitable for real-time analysis	[34]
Direct-charge transfer (DCT) based on Polyaniline nanowires	Bacillus cereus	10^1–10^2 CFU/mL	Suitable device for rapid field-based diagnosis	[35]
Colorimetric detection using antibody-conjugated oval-shaped Au NP(s)	Salmonella	10^4 CFU/mL	Potential for rapid, on-site pathogen detection	[36]
Two-photon luminescence microscopy (TPL) using Au nanorods	Bacillus subtilis spores		Suitable device for rapid field-based diagnosis	[37]
Potentiometric detection using single-walled carbon (SWCNT) nanotubes	Bacteria	(0.2–10^3) CFU/mL	Simple positive/ negative tests can be carried out in real zero-tolerance conditions and without cross reactions	[32]

13.4 Conclusion

Food biosecurity has become a high-priority area in food safety, in parallel with other bio-terrorism and agro-terrorism issues. If biosecurity measures are not followed, we spend more time and more money in trying to solve the disease when it does appear. Though conventional pathogen detection methods are sensitive, they lag behind the analytical methods by detection time. However, the analytical techniques like optical and electrochemical detection have some disadvantages as well, considering sensitivity and cost. Therefore, new rapid methods are considered necessary for better performance. Although many techniques to enhance the response of biosensors by modifying the sensors with different functional materials have been developed, further research and development is essential before biosensors become a real and reliable choice to detect pathogens directly in the food and in the mixed food matrices.

References

1. FAO (2003) Biosecurity in food and agriculture. Rome http://www.fao.org/DOCREP/MEETING/006/Y8453E.HTM
2. WHO (2007) Food safety and food-borne illness. Fact Sheet No. 237 (Reviewed March 2007), World Health Organization, Geneva
3. CDC (2005) Foodborne illness: frequently asked questions. Centers for disease control and prevention, Atlanta
4. WHO (EU) (2004) Food and health in Europe: a new basis for action. European series: No. 96 World Health Organization (Europe), WHO Regional Publications, Copenhagen
5. Alocilja EC, Radke SM (2003) Market analysis of biosensors for food safety. Biosensors Bioelectron 18(5–6):841–846
6. Chemburu S, Wilkins E, Abdel-Hamid I (2005) Detection of pathogenic bacteria in food samples using highly-dispersed carbon particles. Biosensors Bioelectron 21(3):491–499
7. Gleeson C (2010) Health warning as 98pc of all chicken has dangerous bug. In: The Irish independent, Dublin. Available from http://www.independent.ie/health/latest-news/health-warning-as-98pc-of-all-chicken-has-dangerous-bug-2102860.html. Accessed 18 March 2010
8. Belson K, Fahim K (2007) After extensive beef recall, topps goes out of business. The New York Times, [Newspaper] New York, Available from http://www.nytimes.com/2007/10/06/us/06topps.html?pagewanted=all. Issue: 6 October 2007
9. WHO (2002) Foodborne diseases: emerging. Fact Sheet No:124 (Revised January 2002), WHO World Health Organization, Geneva
10. FSAI (2006) Annual report, 2006 Food Safety Authority of Ireland, Dublin
11. Frumkin H, Hess J, Luber G, Malilay J, McGeehin M (2008) Climate change: the public health response. Am J Public Health 983(3):435–445
12. Parkinson AJ, Butler JC (2005) Potential impacts of climate change on infectious diseases in the Arctic. Int J Circumpolar Health 64(5):478–486
13. Kovats RS, Edwards SJ, Hajat S, Armstrong BG, Ebi KL, Menne B (2004) The effect of temperature on food poisoning: a time-series analysis of salmonellosis in ten European countries. Epidemiol Infect 132(3):443–453
14. Kay D, Crowther J, Fewtrell L, Francis CA, Hopkins M, Kay C, McDonald AT, Stapleton CM, Watkins J, Wilkinson J, Wyer MD (2008) Quantification and control of microbial pollution from agriculture: a new policy challenge?. Environ Sci Policy 11(2):171–184
15. Umali-Deininger D, Sur M (2007) Food safety in a globalizing world: opportunities and challenges for India. Agric Econ 37:135–147
16. Mucchetti G, Bonvini B, Francolino S, Neviani E, Carminati D (2008) Effect of washing with a high pressure water spray on removal of Listeria innocua from Gorgonzola cheese rind. Food Control 19(5):521–525
17. Taylor E (2007) A new method of HACCP for the catering and food service industry. Food Control 19(2):126–134
18. Jin SS, Zhou J, Ye J (2008) Adoption of HACCP system in the Chinese food industry: a comparative analysis. Food Control 19(8):823–828
19. Piatek DR, Ramaen DLJ (2001) Method for controlling the freshness of food products liable to pass an expiry date, uses a barcode reader device that reads in a conservation code when a product is opened and determines a new expiry date which is displayed. Patent Number: FR2809519-A1
20. Sanders SQ, Boothe DH, Frank JF, Arnold JW (2007) Culture and detection of Campylobacter jejuni within mixed microbial populations of biofilms on stainless steel. J Food Prot 70(6):1379–1385
21. Lofstrom C, Knutsson R, Axelsson CE, Radstrom P (2004) Rapid and specific detection of Salmonella spp. in animal feed samples by PCR after culture enrichment. Appl Environ Microbiol 70(1):69–75

22. Jechorek RP, Johnson RL (2008) Evaluation of the VIDAS (R) staph enterotoxin II (SET 2) immunoassay method for the detection of Staphylococcal enterotoxins in selected foods: collaborative study. J AOAC Int 91(1):164–173
23. Sunwoo HH, Wang WW, Sim JS (2006) Detection of Escherichia coli O157:H7 using chicken immunoglobulin Y. Immunol Lett 106(2):191–193
24. Schneid AD, Rodrigues KL, Chemello D, Tondo EC, Ayub MAZ, Aleixo JAG (2006) Evaluation of an indirect ELISA for the detection of Salmonella in chicken meat. Braz J Microbiol 37(3):350–355
25. Murphy NM, McLauchlin J, Ohai C, Grant KA (2007) Construction and evaluation of a microbiological positive process internal control for PCR-based examination of food samples for Listeria monocytogenes and Salmonella enterica. Int J Food Microbiol 120(1–2):110–119
26. Shearer AEH, Strapp CM, Joerger RD (2001) Evaluation of a polymerase chain reaction-based system for detection of Salmonella enteritidis, Escherichia coli O157: H7, Listeria spp., and Listeria monocytogenes on fresh fruits and vegetables. J Food Prot 64(6):788–795
27. Velusamy V, Arshak K, Korostynska O, Oliwa K, Adley C (2010) An overview of foodborne pathogen detection: in the perspective of biosensors. Biotechnol Adv 28(2):232–254
28. Huang Q, Liu HY, Fang B (2009) Development of electrochemical DNA biosensors. Prog Chem 21(5):1052–1059
29. Wei D, Bailey MJA, Andrew P, Ryhaenen T (2009) Electrochemical biosensors at the nanoscale. Lab on a Chip 9(15):2123–2131
30. Pedrero M, Campuzano S, Pingarron JM (2009) Electroanalytical sensors and devices for multiplexed detection of foodborne pathogen microorganisms. Sensors 9(7):5503–5520
31. Velusamy V, Arshak K, Yang C, Yu L, Korostynska O, Oliwa-Stasiak K, Adley C (2010) Label-free detection of Bacillus cereus DNA hybridization using electrochemical impedance spectroscopy for food quality monitoring application. In: Fifth IEEE Sensors Applications Symposium (SAS), Limerick, Ireland: IEEE, pp 135–138
32. Zelada-Guillen GA, Riu J, Duzgun A, Rius FX (2009) Immediate detection of living bacteria at ultralow concentrations using a carbon nanotube based potentiometric aptasensor. Angew Chem-Int Edit 48(40):7334–7337
33. Yeung SW, Lee TMH, Cai H, Hsing IM (2006) A DNA biochip for on-the-spot multiplexed pathogen identification. Nucleic Acids Res 34(18):7
34. Temur E, Boyaci IH, Tamer U, Unsal H, Aydogan N (2010) A highly sensitive detection platform based on surface-enhanced Raman scattering for Escherichia coli enumeration. Anal Bioanal Chem 397(4):1595–1604
35. Pal S, Alocilja EC, Downes FP (2007) Nanowire labeled direct-charge transfer biosensor for detecting Bacillus species. Biosens Bioelectron 22(9–10):2329–2336
36. Wang SG, Singh AK, Senapati D, Neely A, Yu HT, Ray PC (2010) Rapid colorimetric identification and targeted photothermal lysis of salmonella bacteria by using bioconjugated oval-shaped gold nanoparticles. Chem-Eur J 16(19):5600–5606
37. He W, Henne WA, Wei QS, Zhao Y, Doorneweerd DD, Cheng JX, Low PS, Wei A (2008) Two-photon luminescence imaging of bacillus spores using peptide-functionalized gold nanorods. Nano Res 1(6):450–456

Chapter 14
Nanosized and Nanostructured II-VI Semiconductors: Chemical Sensor Applications

Nanosized and Nanostructured II-VI Chemical Sensors

Diana Nesheva

Abstract Principles of chemical sensing are considered and examples from the literature of chemical sensors including II-VI semiconductor nanomaterials are given. A new method for improving the discrimination of semiconductor thin-film gas sensors is introduced, which uses the amplitude and phase of the photocurrent response to a modulated light source. Preparation of nanocrystalline CdS and CdSe thin films of various thicknesses (30–200 nm) by physical vapour deposition is described. Data from room temperature studies of the effect of exposure to a set of vapours (water, ethanol, ammonia, acetone) on the film resistance and quartz-crystal microbalance frequency are presented.

Keywords Chemical sensing • II-VI nanosized and nanostructured semiconductors • Electrical resistance • Photoluminescence • Photoconductivity • Thermal evaporation

14.1 Introduction

Chemical sensing is fundamental to the economic development, national security, and quality of life. Therefore chemical sensors for both gases and liquid phase gain an increasing importance for the control of chemical processes, environmental issues, for medical and safety purposes.

The use of semiconductors in chemical sensor applications is well-established [1] because a number of properties of a semiconductor material can be changed by

D. Nesheva (✉)
Institute of Solid State Physics, Bulgarian Academy of Sciences,
72 Tzarigradsko Chaussee Blvd, 1784 Sofia, Bulgaria
e-mail: nesheva@issp.bas.bg

A. Vaseashta et al. (eds.), *Technological Innovations in Sensing and Detection of Chemical, Biological, Radiological, Nuclear Threats and Ecological Terrorism*,
NATO Science for Peace and Security Series A: Chemistry and Biology,
DOI 10.1007/978-94-007-2488-4_14, © Springer Science+Business Media B.V. 2012

adsorbing chemicals. The chemical sensing is associated with surface phenomena rather than with bulk ones and therefore sensors using thin film technology are normally developed. Because of the huge surface-to-volume ratio of nanosized materials and the high porosity of nanoparticle layers and assemblies a high sensitivity and short response time are expected [2] for sensor using such materials. The first results on nanoparticle assembly sensors are very promising, but there still exist problems with the reproducibility and mass production of such sensors. On the other hand, gas sensors in the form of ultra thin or nanostructured films are highly sensitive and reliable with a low performance/price ratio and therefore the active work on such sensors is going on. In this paper, a brief overview on recent progress in chemical sensing applications of II/VI nanomaterials is described.

14.2 Chemical Sensors

14.2.1 Principles of Chemical Sensing, Sensor Sensitivity and Selectivity

Semiconductor chemical sensors operate on the basis of adsorbate induced changes mainly in the film resistance, photoconductivity, optical absorption and fluorescence. The direct measurement of the changes in the electrical and optical properties is quite convenient.

The dark conductivity is governed by a combination of charge carrier density, and the carrier mobility. Adsorption may change both the carrier concentration (by doping, by altering the concentration of electronic defects or, in the case of polar molecules, by surface band-bending through the electrostatic effect) and the mobility by the alteration of the potential barrier height between crystalline grains. When film or particle size is reduced to nanometers, energy band bending is no longer restricted to the surface region but extends into the bulk of the grains. Thus, the properties of the whole film or the grain may change dramatically due to solid-gas interactions. The presence of adsorbates also influences the photoconductive and photoluminescence (PL) properties of films such as CdS, CdSe and ZnO by creating defects affecting the radiative and non-radiative recombination in the films [3].

To be effective, a chemical sensing technology must provide sufficient sensitivity, selectivity and stability. Robustness and portability are also highly desirable characteristics. Nanotechnology offers a high sensitivity since the high integrated interface of ensembles of quasi one- or zero-dimensional semiconductors allows a large density of molecules to get adsorbed.

Frequently, different gases produce similar changes in conductivity, and further measurements, e.g. of the response time or activation energy, are required to distinguish between them. A way to achieve a better selectivity is the method proposed in [4]. It is based on measurement of the amplitude and phase of the photocurrent response to a modulated light source and these data are used to obtain the energy

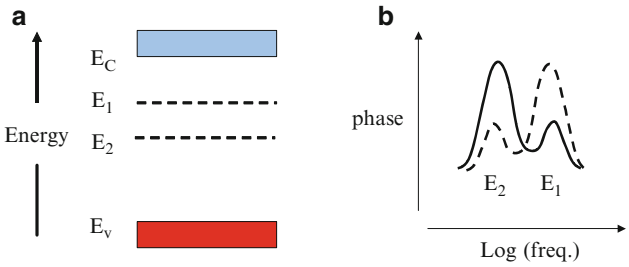

Fig. 14.1 (**a**) Energy band diagram with two idealised localised states at energies E1 and E2, associated with electronic defects. (**b**) Density of states if no adsorbate is present (*solid line*) and when a certain gas is present (*dashed line*). The character of the defect is modified as a consequence of the adsorption process

distribution and capture properties of the localized density of states as well as the changes induced by the adsorbate. Figure 14.1 illustrates schematically the basis of the proposed gas sensing application.

14.2.2 Examples of Chemical Sensors Using II-VI Nanomaterials

The properties of interest for chemical sensing with II-VI nanomaterials include strong resistance change or high quantum yields in combination with broad absorption spectra, narrow size tunable PL, and exceptional resistance to both photobleaching and chemical degradation. In order to achieve high sensitivity and selectivity a chemical tailoring of the outer surface of the semiconductor nanoparticles is applied to control their solubility and stability [2, 5, 6]. Further coating of the nanoparticle surface with suitable ligands (called functionalization) has a strong effect on its luminescent response to specific chemical species. Recent advances in the application of II-VI semiconductor nanocrystals as chemical and biochemical sensors are reviewed in [2, 5–7]. Below, for of lack of space, only a few examples will be given to illustrate the applicability of these materials in chemical sensing.

The selectivity of CdS nanoparticles has been successfully altered [8] to respond either to Zn^{2+} or Cu^{2+} ions, simply by changing their capping layer. While polyphosphate-capped CdS quantum dots responded to almost all mono and divalent metal cations (showing no ion selectivity), thioglycerol-capped CdS nanocrystals were sensitive only to Cu^{2+} and Fe^{3+}.

CdSe semiconductor quantum dots (QDs) were synthesized with surface modifying groups to enhance their response towards the detection of aromatic hydrocarbons [9]. Reversible PL enhancement and quenching upon QD/PMMA film exposure to toluene and xylene vapors were observed. Unmodified films had detection limits for xylenes and toluene of 250 and 500 ppm, while detection limits of 15 ppm xylenes and 50 ppm toluene were achieved with the modified films.

It has been reported [10] that multiple ZnO nanorods are sensitive to H_2 at 112°C or O_3 at room temperature while normally ZnO is sensitive at 300°C. It has also been demonstrated [11] that ZnO nanorods showed dramatic changes in conductance upon exposure to polar liquids. The ZnO nanowires displayed [12] high sensitivity to ammonia in the range of 40–1,000 ppm with a response time of 5 s at any concentration (40–1,000 ppm).

14.3 Chemical Sensor Behavior of II-VI Nanostructured Layers Prepared by Thermal Evaporation in Vacuum

Single layers of CdS (30–200 nm) were deposited at room substrate temperature and substrates fixed above the heated crucible containing CdS powder. Layers from CdSe (10–100 nm) were prepared on both fixed and rotating substrates; the latter spent 1/10 of the turn time above the crucible [13]. Atomic force microscopy measurements have revealed that the grain size decreases with decreasing layer thickness (Fig. 14.2).

The effect is strongest in the CdSe layers deposited on rotating substrates; the nanocrystal size in the 50 nm layers estimated from Raman scattering experiments was ~8 nm [14].

Room temperature investigations of the effect of exposure to a set of vapours (water, ethanol, ammonia or acetone vapour in air) on the changes in the CdS layer resistance have detected a quite strong response of all CdS layers to water and ammonia vapours (Table 14.1). At 300 K CdSe layers were rather insensitive with the exception of the '50 nm' layers on rotating substrates which have shown a very good sensitivity to all vapours (Table 14.1). The last observation has been ascribed to a much greater integral interface area between the small nanocrystals and indicated that the deposition of CdSe layers on rotating substrates is quite promising for gas-sensor applications.

The large interface area of nanostructured materials can be also very useful for designing of quartz-crystal microbalance (QCM) sensors for direct mass detection

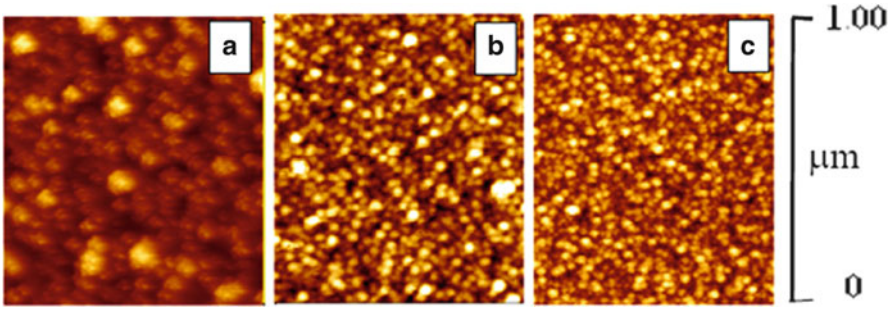

Fig. 14.2 AFM surface topographic images of three CdSe layers deposited on fixed Corning 7059 glass substrates maintained at 300 K. The film thickness was: (**a**) 100 nm, (**b**) 50 nm, (**c**) 30 nm

Table 14.1 Changes of the resistance of CdS and CdSe thin films upon exposire to vapours of ethanol, water, ammonia and acetone in air (R_{vac} and R_{exp} denote the film resistance in vacuum and upon exposure, respectively)

Layer thickness (nm)	AFM apparent nanocrystal size(nm)	Resistance change, R_{vac}/R_{exp}			
		Ethanol	Water	Ammonia	Acetone
CdS on fixed substrates					
50	~250	1.45	1×10^{6}	7×10^{4}	1.7
100	~500	2×10^{2}	1×10^{6}	3×10^{2}	2
CdSe on rotating substrates					
50	~20	4×10^{3}	2×10^{3}	9×10^{2}	1×10^{3}
100	~50	25	30	25	21

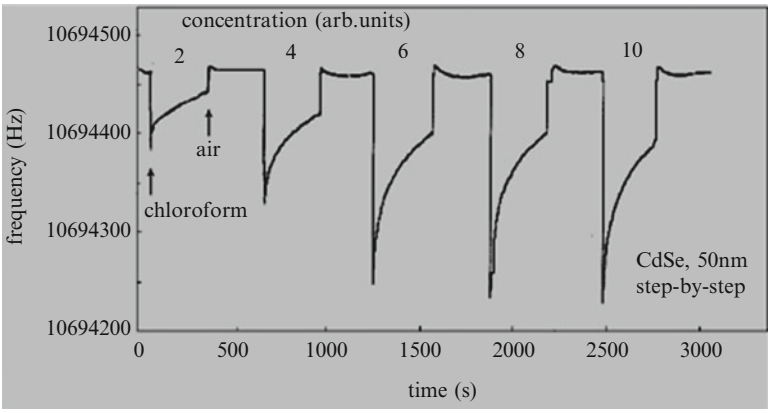

Fig. 14.3 Changes of the resonance frequency of a piezoresonator with two 50 nm CdSe films deposited on its both sides upon exposure to chloroform vapour in air with various concentrations

in nanograms. In such sensor the detector is a piezoresonator having a linear relationship between the resonance frequency and the adsorbed mass and the receptor is a sorption layer. We cared out room temperature experiments to study the sensitivity to chloroform of QCM structures with two 50 nm CdSe films deposited on the both sides of rotating quartz crystals. The obtained results have indicated a quite fast response and short recovery time (Fig. 14.3).

Experiments are in progress on the chemical sensing properties of the CdS, CdSe thin films, as well as of ZnSe and $Zn_xCd_{1-x}Se$ films of various thicknesses prepared by thermal evaporation in vacuum.

14.4 Conclusions

The above short review of results from chemical sensing experiments illustrates that: (i) nanosized and nanostructured II-VI semiconductors are promising materials for preparation of a variety of very sensitive and selective chemical sensors and

(ii) the standard thermal vacuum evaporation technique can be successfully applied for preparation of nanostructured thin films with good prospective for chemical sensing at room temperature.

Acknowledgements This work has been partially supported by the NSF of Bulgaria under grant D002-123/2008. The author is very grateful to Prof. R. Capan for the QCM measurements on the CdSe thin films performed in the Balikesir University.

References

1. Sberveglieri G (ed) (1992) Gas sensors. Kluwer, Dordrecht
2. Patra MK, Manzoor K, Manoth M, Negi SC, Vadera SR, Kumar N (2008) Nanotechnology applications for chemical and biological sensors. Defence Sci J 58:636–649
3. Patel M, Pu CJJ, Sharpe LR (1995) The effects of adsorption of gaseous ambients on the photoluminescence intensity of a powdered CdS:Te phosphor. Langmuir 11:2003–2011
4. Reynolds S, Aneva Z, Levi Z, Nesheva D, Main C, Smirnov V (2007) Potential gas sensor applications of semiconductor thin films based on changes in photoresponse. J Optoel Adv Mater 9:209–212
5. Sapsford KE, Pons Th, Medintz IL, Mattoussi H (2006) Biosensing with luminescent semiconductor quantum dots. Sensors 6:925–953
6. Jorge P, Martins MA, Trindade T, Santos JL, Farahi F (2007) Optical fiber sensing using quantum dots. Sensors 7:3489–3534
7. Huang XJ, Choi YK (2007) Chemical sensors based on nanostructured materials. Sensor Actuator B 122:659–671
8. Chen Y, Rosenzweig Z (2002) Luminescent CdS quantum dots as selective ion probes. Anal Chem 74(19):5132–5138
9. Vassiltsova OV, Zhao Zh, Petrukhina MA, Carpenter MA (2007) Surface-functionalized CdSe quantum dots for the detection of hydrocarbons. Sensor Actuator B 123:522–529
10. Kang BS, Heo YW, Tien LC, Norton DP, Ren F, Gila BP, Pearton SJ (2005) Hydrogen and ozone gas sensing using multiple ZnO nanorods. Appl Phys A 80:1029–1032
11. Kang BS, Ren F, Heo YW, Tien LC, Norton DP, Pearton SJ (2005) pH measurements with single ZnO nanorods integrated with a microchannel. Appl Phys Lett 86:112105–112107
12. Wang XH, Zhang J, Zhu ZQ (2006) Ammonia sensing characteristics of ZnO nanowires studied by quartz crystal microbalance. Appl Surf Sci 252:2404–2411
13. Nesheva D, Fizgerald AG, Aneva Z, Main C, Petrova A, Reynolds S (2008) Preparation of nanocrystalline CdSe single layers by thermal evaporation in vacuum. Nanosci Nanotech 8:107–110
14. Nesheva D, Aneva Z, Reynolds S, Main C, Fizgerald AG (2006) Preparation of micro- and nanocrystalline CdSe and CdS thin films suitable for sensor applications. J Optoel Adv Mater 8:2120–2125

Chapter 15
Nanomaterials Based Sensor Development Towards Electrochemical Sensing of Biointeractions

Electrochemical Sensors Based on Nanomaterials for Biointeractions

Arzum Erdem

Abstract Electrochemical sensor platforms can offer great promise for exploring a difference in biointeraction process occurred in solution and also at surface. Various nanomaterials; such as nanoparticles, nanowires, carbon nanotubes etc. have recently been under attention to be aimed for development of novel electrochemical sensors for screening of the interactions between the compounds and biomolecules; drugs, toxins, proteins, and nucleic acids; DNA, or PNA.

Keywords Electrochemical biosensor • Nanomaterial • Biointeractions

15.1 Introduction

Many important technological advances have been progressed for the development of sensors to monitor interactions and recognition events of biomolecules in solution and at the solid substrates. The growth of highly developed biosensors could affect significantly the areas of genomics, diagnostics, drug discovery and environmental monitoring [1–4].

Recent advances in sensor technology based on nucleic acid have led to the development of various biosensors for gene sequence analysis and numerous ligand binding studies [2–4]. The nanoscale sensors based on nanoparticles, nanowires,

A. Erdem (✉)
Faculty of Pharmacy, Analytical Chemistry Department, Ege University,
Bornova 35100, Izmir, Turkey
e-mail: arzum.erdem@ege.edu.tr

A. Vaseashta et al. (eds.), *Technological Innovations in Sensing and Detection of Chemical, Biological, Radiological, Nuclear Threats and Ecological Terrorism*,
NATO Science for Peace and Security Series A: Chemistry and Biology,
DOI 10.1007/978-94-007-2488-4_15, © Springer Science+Business Media B.V. 2012

nanotubes and other nanomaterials have recently received considerable attention [1, 4–11]. Electrochemical biosensors coupling the inherent specificity of nucleic acid recognition reactions with the high sensitivity of physical transducers by the advantages of various nanomaterials, hold great promise for sequence-specific detection for clinical, environmental, forensic investigations and other applications in security, since these nanomaterial based sensors can bring some important advantages; more sensitivity and selectivity by resulting in a greatly simplified protocol.

An overview is reported here about the progress on nanomaterials based electrochemical sensor technology for the interactions between the compounds/biomolecules (drugs, toxins, proteins etc.) and nucleic acids.

15.2 Nanomaterial Based Electrochemical Sensor Technology for Monitoring of Biointeractions

Electrochemical sensors based on numerous nanomaterials and different transducers have been recently developed in response to clinical demands as giving promising results in aspect of chip-based technology for gene sequence analysis and ligand binding studies [1, 4–22].

A variety of sensor technologies can provide a unique platform in order to immobilize biomolecular receptors by using the following immobilization techniques: adsorption, crosslinking or entrapment, complexation, covalent attachment, and other related methods on nanomaterials [16, 23, 24].

A disposable electrochemical DNA sensor developed using carboxylated single walled carbon nanotubes (SWCNTs) was introduced by Erdem et al. [11] for monitoring of biomolecular interactions, especially yielding a very attractive approach for the sensitive detection of interaction between an anticancer drug, daunorubicin (DNR) and nucleic acids by intercalation process. The voltammetric results were found in a good agreement with the ones of electrochemical impedance spectroscopy (EIS) that was also used to characterize the successful construction of carbon nanotubes modification onto the surface of disposable graphite electrodes (PGEs). After the surface confined interaction between 5 μM DNR and 50 μg/mL DNA, the detection limit was calculated as 278 nM and 184 nM, respectively by using DNA modified PGE, and DNA modified CNT-PGE. The biomolecular binding of anticancer drug dacarbazine (DCBN) in the presence of titanium dioxide nanoparticles was investigated electrochemically based on the signal enhancement [25]. DNA immobilized multiwalled carbon nanotubes (MWCNTs) based sensor was developed for the electrochemical monitoring of berberine's interaction with dsDNA in cancer cells [26] and the oxidation signals of a redox marker, cobalt phenanthroline complex, $Co(phen)_3^{3+}$, and guanine was consequently measured by screen printed carbon electrodes (SPEs).

Another example could be given about 4-nonylphenol (4-NP) that was reported to affect the health of wildlife and humans through altering endocrine function. A novel electrochemical sensor for sensitive and fast monitoring of 4-NP was developed

by titanium oxide (TiO2) nanoparticles and gold nanoparticles (AuNPs) for the enhancement of electron conduction and sensitivity [27].

Aptamers represent nucleic acid based receptor molecules which can be considered as a highly versatile sensing element for the development of aptamer-based sensors [28–32]. Among these, the specific and sensitive detection of aptamer-protein interactions and the development of different assay formats in combination with the electrochemical sensor technology are of growing interest [32–39]. For instance, Wei et al. [39] developed an aptamer-based electrochemical sensor for amperometric detection of Botulinum neurotoxin (i.e., among the most well known toxics list addressing biosafety concerns). This electrochemical aptasensor presented the analysis scheme resulting within 24 h with a lower limit of detection (LOD) of 40 pg/ml, which is much shorter than the current record as 4 days.

The electrochemical nanobiosensors have also a key importance especially for food analysis due to its resulting with sensitive, selective, quick and inexpensive analysis. Deng et al. [40] presented a facile and efficient route to prepare silk derived carbon mat modified with Au@Pt urchilike nanoparticles (Au@Pt NPs) for electrochemical monitoring Escherichia coli (E. coli). It was found that the Au@Pt NPs modified S-derived carbon fiber was sensitive to detect the E. coli activities with a low detection limit.

Prabhakar et al. [41] reported a nucleic acid electrochemical sensor using conducting polymer gold nanostructures for screening of pathogen-specific DNA and PNA (peptide nucleic acid) probes related to *Mycobacterium tuberculosis* at the surface of polyaniline (PANI)–Au electrode. The lower detection limits were found for PNA–PANI/Au electrode as 0.125×10^{-18} min, and for DNA–PANI/Au electrode as 2.5×10^{-18} min within 30 s of hybridisation time. The authors reported also that the sensor development of nanocomposites and functionalised conducting polymers could be possible in order to detect other pathogens, including *Salmonella typhimurium* and *Nesseria gonorrhea.*

15.3 Future Directions

A variety of nanomaterials and nanofabrication technologies have recently been under attention to be aimed for development of novel sensor platforms. The overview was reported herein about the progress on nanomaterials based electrochemical sensor technology for the interactions between the compounds/biomolecules (drugs, toxins, proteins etc.) and nucleic acids; DNA, or PNA. If at all possible, nanomaterial based electrochemical sensors may be integrated with the chip technology by using easy sample handling, and quick and inexpensive analysis for spesific biointeractions, especially immediate detection of biological, or chemical warfare agents, and viral or bacterial pathogens.

Acknowledgements A.E would like to express her gratitude to the Turkish Academy of Sciences (TUBA) as the associate member of TUBA for their support.

References

1. Wang J (2005) Nanomaterial-based electrochemical biosensors. Analyst 130:421–426
2. Palecek E, Fojta M (2001) Detecting DNA hybridization and damage. Anal Chem 73:74 A–83 A
3. Dean PM, Zanders ED, Bailey DS (2001) Industrial-scale, genomics-based drug design and discovery. Trends Biotechnol 19:288–292
4. Erdem A (2007) Nanomaterial-based electrochemical DNA sensing strategies. Talanta 74:318–325
5. Salem AK, Chao J, Leong KW, Searson PC (2004) Receptor-mediated self-assembly of multi-component magnetic nanowires. Adv Mater 16:268–271
6. Erdem A, Papakonstantinou P, Murphy H (2006) Direct DNA hybridization at disposable graphite electrodes modified with carbon nanotubes. Anal Chem 78:6656–6659
7. Karadeniz H, Erdem A, Caliskan A, Pereira CM, Pereira EM, Ribeiro JA (2007) Electrochemical sensing of silver tags labelled DNA immobilized onto disposable graphite electrodes. Electrochem Commun 9:2167–2173
8. Hahm J, Lieber CM (2004) Direct ultrasensitive electrical detection of DNA and DNA sequence variations using nanowire nanosensors. Nano Lett 4:51–54
9. Patolsky F, Lieber CM (2004) Nanowire nanosensors. Mater Today 8:20–28
10. McFarland AD, Van Duyne RP (2003) Single silver nanoparticles as real-time optical sensors with zeptomole sensitivity. Nano Lett 3:1057–1062
11. Erdem A, Karadeniz H, Caliskan A (2009) Single-walled carbon nanotubes modified graphite electrodes for electrochemical monitoring of nucleic acids and biomolecular interactions. Electroanal 21:464–471
12. Kuhr WG (2000) Electrochemical DNA analysis comes of age. Nat Biotechnol 18:1042–1043
13. Koehne JE, Chen H, Cassell AM, Ye Q, Han J, Meyyapan M, Li J (2004) Miniaturized multiplex label-free electronic chip for rapid nucleic acid analysis based on carbon nanotube nanoelectrode arrays. Clin Chem 50:1886–1893
14. Wang J (2005) Carbon-nanotube based electrochemical biosensors: a review. Electroanal 17:7–14
15. Mathur S, Erdem A, Cavelius C, Barth S, Altmayer J (2009) Amplified electrochemical DNA-sensing of nanostructured metal oxide films deposited on disposable graphite electrodes functionalized by chemical vapor deposition. Sensor Actuat B:Chem 136:432–437
16. Zhang S, Wright G, Yang Y (2000) Materials and techniques for electrochemical biosensor design and construction. Biosens Bioelectron 15:273–282
17. Caliskan A, Erdem A, Karadeniz H (2009) Direct DNA hybridization on the single-walled carbon nanotubes modified sensors detected by voltammetry and electrochemical impedance spectroscopy. Electroanal 21:2116–2124
18. Besteman K, Lee JO, Wiertz FG, Heering HA, Dekker C (2003) Enzymecoated carbon nanotubes as single-molecule biosensors. Nano Lett 3:727–730
19. Karadeniz H, Erdem A, Caliskan A (2008) Electrochemical monitoring of DNA hybridization by multiwalled carbon nanotube based screen printed electrodes. Electroanal 20:1932–1938
20. Muti M, Kuralay F, Erdem A, Abaci S, Yumak T, Sinağ A (2010) Tin oxide nanoparticles-polymer modified single-use sensors for electrochemical monitoring of label-free DNA hybridization. Talanta 82:1680–1686
21. Yapasan E, Caliskan A, Karadeniz H, Erdem A (2010) Electrochemical investigation of biomolecular interactions between platinum derivatives and DNA by carbon nanotubes modified sensors. Mat Sci Eng B:Solid 169:169–173
22. Erdem A, Papakonstantinou P, Murphy H, Mcmullan M, Karadeniz H (2010) Streptavidin modified carbon nanotube based graphite electrode for label-free sequence specific DNA detection. Electroanal 22:611–617
23. Pividori MI, Merkoci A, Alegret S (2000) Electrochemical genosensor design: immobilisation of oligonucleotides onto transducer surfaces and detection methods. Biosens Bioelectron 15:291–303

24. Erdem A (2007) Genosensor technology for electrochemical sensing of nucleic acids by using different transducers. In: Alegret S, Merkoci A (eds) Electrochemical sensor analysis (ECSA)-comprehensive analytical chemistry book, vol 49. Elsevier, Amsterdam, pp 403–411
25. Song M, Zhang R, Wang X (2006) Nano-titanium dioxide enhanced biosensing of the interaction of dacarbazine with DNA and DNA bases. Mater Lett 60:2143–2147
26. Ovádeková R, Jantová S, Letasiová S, Stepánek I, Labuda J (2006) Nanostructured electrochemical DNA biosensors for detection of the effect of berberine on DNA from cancer cells. Anal Bioanal Chem 386:2055–2062
27. Huang J, Zhang X, Liu S, Lin Q, He X, Xing X, Lian W, Tang D (2010) Development of molecularly imprinted electrochemical sensor with titanium oxide and gold nanomaterials enhanced technique for determination of 4-nonylphenol. Sensor Actuat B:Chem 152:292–298
28. Gronewold TMA, Glass S, Quandt E, Famulok M (2005) Monitoring complex formation in the blood-coagulation cascade using aptamer-coated SAW sensors. Biosens Bioelectron 20:2044–2052
29. Jiang Y, Fang X, Bai C (2004) Signaling aptamer/protein binding by a molecular light switch complex. Anal Chem 76:5230–5235
30. Bini A, Tombelli S, Centi S, Macsini M (2007) Analytical performances of aptamer-based sensing for thrombin detection. Anal Chem 79:3016–3019
31. Wang J, Li G, Jan MR (2004) Ultrasensitive electrical biosensing of proteins and DNA: carbon-nanotube derived amplification of the recognition and transduction events. J Am Chem Soc 126:3010–3011
32. Jacob AH, Wang J, Kawde AN, Xiang Y (2006) Quantum-dot/aptamer-based ultrasensitive multi-analyte electrochemical biosensor. J Am Chem Soc 128:2228–2229
33. Erdem A, Karadeniz H, Mayer G, Famulok M, Caliskan A (2009) Electrochemical sensing of aptamer-protein interactions using a magnetic particle assay and single-use sensor technology. Electroanal 21:1278–1284
34. Tombelli S, Minunni M, Macsini M (2007) Aptamers-based assays for diagnostics, environmental and food analysis. Biomol Eng 24:191–200
35. Kawde AN, Rodriguez MC, Lee TMH, Wang J (2005) Label-free bioelectronic detection of aptamer–protein interactions. Electrochem Commun 7:537–540
36. Bang GS, Cho S, Kim BG (2005) A novel electrochemical detection method for aptamer biosensors. Biosens Bioelectron 21:863–870
37. Song S, Wang L, Li J, Fan C, Zhao J (2008) Aptamer-based biosensors. Trend Anal Chem 27:108–117
38. Centi S, Tombelli S, Minunni M, Macsini M (2007) Aptamer-based detection of plasma proteins by an electrochemical assay coupled to magnetic beads. Anal Chem 79:1466–1473
39. Wei F, Ho C-M (2009) Aptamer-based electrochemical biosensor for Botulinum neurotoxin. Anal Bioanal Chem 393:1943–1948
40. Deng L, Guo S, Zhou M, Ling L, Chang L, Shaojun D (2010) A silk derived carbon fiber mat modified with Au@Pt urchilike nanoparticles: a new platform as electrochemical microbial biosensor. Biosens Bioelectron 25:2189–2193
41. Prabhakar N, Arora K, Singh H, Malhotra BD (2008) Polyaniline based nucleic acid sensor. J Phys Chem B 112:4808–4816

Chapter 16
Emission of Weak Electrons Towards Sensing Nanoobjects

Weak Electrons to Sense Nanoobjects

Y. Dekhtyar

Abstract To characterize nanoobjects, a non-contact technique is preferable. Low energy electron has a mean free path on in a solid that is on order of nanoscale. Emission of these electrons from a solid is considered to characterize nanoobjects for sensing applications. This paper considers applications and limitations of weak electron emission for chemical and radiation sensors.

Keywords Weak electrons emission • Nanoobjects • Characterization • Sensors

16.1 Introduction

When an object is measured, its properties become available from interaction between the measuring instrument and an entity under test. The features of the latter are altered as a result and uncertainty remains about the object. The "uncertainty" is high for nanoobjects that may be "perturbed" and significantly influenced by the measurement procedure. Therefore "soft", non-contact characterization of such nanoobjects is of great importance.

The properties of the solid nanoobject are derived by the valence electrons, and their emission is used to characterize its entity and possible applications. The external energy for emitting the electron should be very low to avoid disturbing the object under test. The minimal energy that is necessary to supply to the electron cannot be less than the electron work function φ. In this case, the escaped electron has kinetic energy, close to zero. Capabilities of the pre-threshold emission of weak electrons to characterize nanoobjects for specific applications are reviewed.

Y. Dekhtyar (✉)
Biomedical Engineering and nanotechnologies Institute, Riga Technical University,
Kalku 1, 1658 Riga, LV, Latvia
e-mail: dekhtyar@latnet.lv

A. Vaseashta et al. (eds.), *Technological Innovations in Sensing and Detection of Chemical, Biological, Radiological, Nuclear Threats and Ecological Terrorism*,
NATO Science for Peace and Security Series A: Chemistry and Biology,
DOI 10.1007/978-94-007-2488-4_16, © Springer Science+Business Media B.V. 2012

16.2 Limitations of Weak Electrons Emission to Characterize Nanoobjects

16.2.1 Geometrical Limitation

As a prior condition, a mean free path (L) of the emitting electrons must not exceed size of the nanoobject. In this case, the energy (E) to escape the electron is limited with L, as shown in Fig. 16.1 [1] demonstrating dependence of L on E. Because typical values of the electron work function (φ) are placed in a range 1–5 eV [2], the corresponding magnitudes of L range from 10 to 100 nm. This means that the electron emission based measurements could be employed for the nanoobjects sized to this range.

16.2.2 Maximal Sensitivity Limitation

The nanoobject under examination must be excited with electrons having energy close to φ, such that there is none to minimum change in structure. For emission to occur photon excitation is needed and resulting emission current (I) is generally described as Eq. 16.1. [3]:

$$I = A(h\nu - \varphi)^m, \tag{16.1}$$

A – Coefficient of proportionality,
$h\nu$ – Energy of the photon ($h\nu > \varphi$),
m – Index.

As noted in [4], $m > 1$ in the majority of electron transitions resulted by the photons. This means that the emission current "works" as the amplifiers of φ.

On the other hand, the value of φ depends on the design of the emitting layer energy bands, electron affinity and surface charge [3]. The latter could both decrease and increase φ. For instance, in a case of insulators or wide gap semiconductors, the negative charge absorbed by the slowly surface states generally increases φ. However narrow gap semiconductors (Si, Ge, etc.) are characterized with the Fermi level pinning at the surface energy gap midst [5]. Because the Fermi energies of a bulk and the

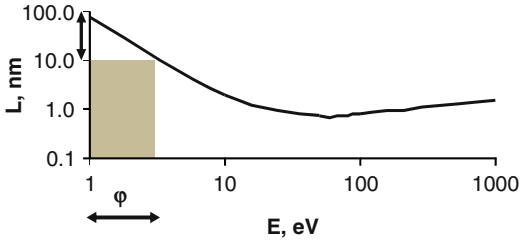

Fig. 16.1 A magnitude of L in a solid material in dependence on E [1]

surface must be equal, the valence and conductivity bands are bent with the values of φ decreasing and increasing for the p- and n-types semiconductors correspondingly. As a result, the surface layer is saturated with electrons (p-semiconductor) or holes (n-semiconductor). These charge carries absorbed by the slow surface states to influence the surface charge: the surface of the p-semiconductor is charged negatively, the φ value increasing. The opposite surface charge is typical for the n-semiconductor.

16.2.3 Limitation of Quantum Mechanics

When the electron leaves the atom it acquires location uncertainty Δx because of the Heisenberg uncertainty principle. To ensure that the emitted electron escapes from the nanoobject, its size should be larger than Δx:

$$\Delta x \geq \frac{h}{4\pi \Delta p} \tag{16.2}$$

H – Planck constant, $h = 4.14 \times 10^{-15}$ eV sec;
Δp – Uncertainty of the atom's momentum *p*.

Assuming that the atom had the zero momentum before interaction with the photon, the "contact" between these two particles could increment *p* until the photon momentum value ($h\nu/c$, c – speed of the light). Therefore

$$\Delta p = \frac{h\nu}{c}$$

Typically $\varphi \cong 5$ eV for the solid matter [2]. Because the magnitudes of the photon energy should be in accordance with the condition $h\nu \geq \varphi$, one could calculate that $\Delta x = 0.2$ nm. However in some cases, φ could be rather small and corresponding Δx significantly increases.

Summarizing, the pre-threshold emission mode could be effectively applied to characterize solid nanoobjects when they are sized in a range from 10 to 100 nm; and the electron transitions induced by the photons give the value of the index $m > 1$ (disordered materials, indirect band-band as well as local state-band transitions in crystals as noted in [4]).

16.3 Weak Electrons Emission Targeted for Nanoobjects Applications

16.3.1 Surface Charge and Attachment of Bio Objects

Following the general adhesion theory [6], attaching the particle to the substrate is controlled by attracting and repulsing forces. The first force has typically a van der Waals origin; however the second one is electrostatic. Therefore engineering of the

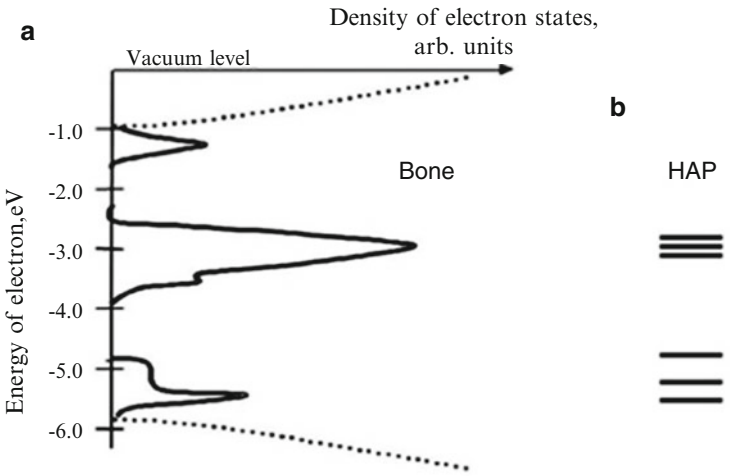

Fig. 16.2 (**a**): Electron states in bone [4] and (**b**): HAP [5]

substrate surface charge could be employed to influence attaching of the particle. The electron work function increment is the direct index of the surface charge alteration.

16.3.1.1 Cells Creating Bone

A human bone consists of the hydroxyapatite (HAP) polycrystalline/amorphous matrix assembled from nanoparticles and organic matter where HAP is filled in [7]. The bone passes remodeling cycles during the organism life [7, 8]. This process has three main steps [8]. The cells called osteoclasts are attached by the bone and provide its local resorption. Next, the cells called osteoblast are attached to the cavity formed by the osteoclasts to develop a new bone unit. After that, the bone unit is not influenced by the osteoclast/osteoblast cells during several years period. Disturbing of cells attachment to the bone leads to skeletal diseases, such as osteoporosis [7]. Osteoporosis affects 75 million people in developed countries [9]. Thus, "right" attachment of the cells to the bone is of paramount importance.

Because electron states of the bone [4] and HAP ($Ca_5(PO_4)_3OH$)) [10] ceramics assembled from nanoparticles are alike (Fig. 16.2) one can assume that the bone surface charge can be controlled due to engineering of the HAP properties. Particularly, the surface charge of HAP could be altered due to shifting of the proton (H^+) coupled to oxygen to the symmetrical position under the high pressure at the hydrogen atmosphere [11]. Such the procedure increased φ that was estimated for the condition $I = 0$ from the regularity $I = f(h\nu)$. Moreover the number of the osteoblasts attached to HAP correlated with its φ (Fig. 16.3) [11].

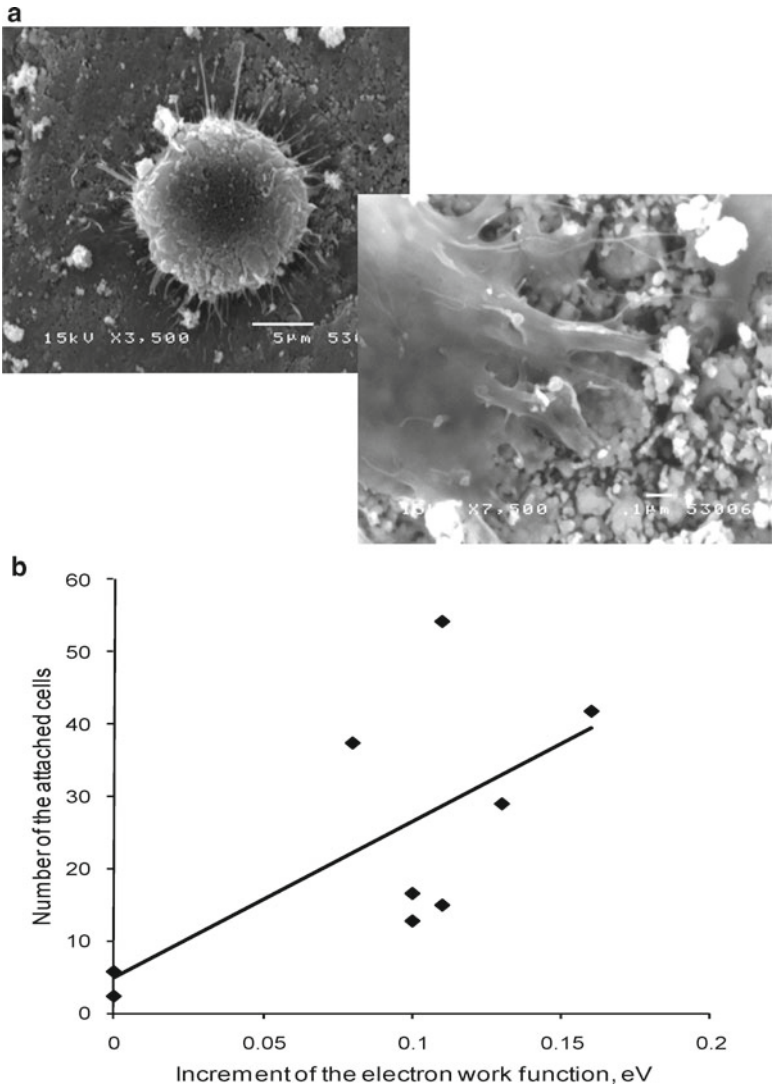

Fig. 16.3 Osteoblast attached to HAP (**a**); the number of the attached osteoblasts depended on the HAP electron work function increment that directly relate to the surface negative charge [11]

16.3.1.2 Nanolorry for Virus Like Particles

Virus like particles (VLP) are organic molecular structures that have organization similar to the viruses. However VLP does not have DNA or RNA inside. When the pharmacy is filled in the VLP they are in use as the drug delivery system addressing the specific biocells. To reach treatment of the human diseases, VLP having the drug inside are injected into the organism. To enhance treatment, VLP local concentration in the vicinity of the cell should be high.

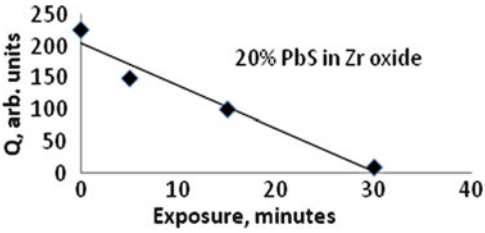

Fig. 16.4 Influence of the radiation exposure on the electron emission from PbS nanodots imbedded in Zr oxide glass [13]

There are two ways to provide this. The concentration of the injected VLP is high. In this case toxic effects could appear. The other approach delivers high concentration of VLP directly to the cell, the average concentration in the organism being not high. For this, the number of VLP could be pinned to a single nanoparticle that becomes a carrier (nanolorry). To minimally disturb the VLP surface structure that is responsible for cell recognition, a weak communication to couple VLP and the nanolorry is preferable. A physical attachment is the most suitable for this in contrast with the chemical one.

Because VLP has a surface charge, the nanolorry was selected to have the opposite electrical charge at the surface to attach VLP [12]. Nanoparticles prepared from Silicon (Si) having the different conductivity type were employed as the nanolorry. The specific VLP that were characterized with the greatest density of the positive surface charge were successfully attached just to the p-type Si, that surface had the highest negative charge in contrast with the n-type of Si and lowest φ [2].

16.3.2 Electron Emission for Sensing

16.3.2.1 Radiation Sensor

When the radiation dose absorbed by the object is measured, both directly traveling in and scattered particles of radiation are detected. Scattering depends particularly on the boundary of the radiated entity. Such the processes are of the great importance in a case of the micro- and nano-objects (microorganisms, macromolecule, etc.). In these cases, the absorbed dose could be detected by the best way, when the detector is sized to the measured item.

The PbS nanodots imbedded into the Zr oxide glass were demonstrated as the possible detectors providing the signal by the emission of weak photoelectrons [13]. The specific maximum responsible for the emission from PbS dots was identified at the $dI/dhv = f(hv)$ spectrum. The square (Q) of the maximum related to the exposure of the electromagnetic radiation (ultraviolet) (Fig. 16.4).

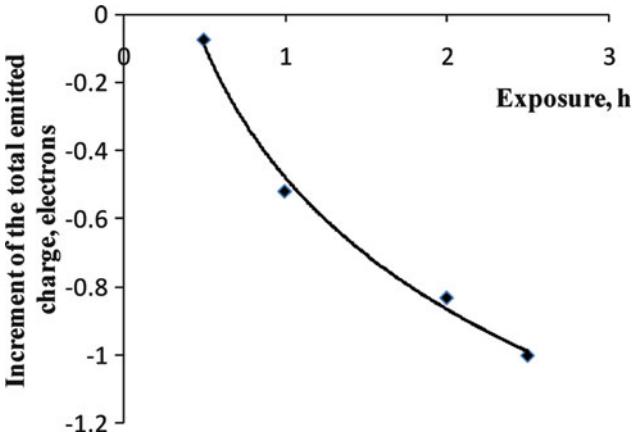

Fig. 16.5 Correlation of the emitted charge increment with Si substrate exposure in the benzole fog

16.3.2.2 Chemical Sensor

Desorption of chemical molecules previously adhered to the semiconductor surface alter its density of the electron states.

If the photoelectron emission current is measured simultaneously, its magnitude follows desorption. Therefore the total emitted charge of electrons compared with the emission from the surface that does not have adhered molecules identifies the number of the desorbed entities.

Figure 16.5 demonstrates correlation of the emitted charge increment (difference between the emitted charge from the surface adhering of the molecules and native (clean) one) on exposure of the Si substrate in the benzole fog. A sensitivity of such the approach was evaluated as 10^{-5} gram/cm^2 (of the substrate surface).

16.4 Conclusion

Emission of the weak electrons could be in use to characterize nanoobjects having a size in a range 10–100 nm. The quantum mechanics limitation gives the size uncertainty around 0.2 nm, when the pre-threshold mode of emission is employed. At the same mode the surface charge measurements are amplified with the electron emission current. Characterization of the substrate surface charge engineered to attach the micro-, nano-particles is available from measurements of the electron emission current detected at the pre-threshold mode. Sensors of radiation for nano-dosimetry and adhered to the substrate chemical molecules could be reached on the base of the pre-threshold emission of weak electrons. The sensitivity of the chemical sensor, particularity to the benzole molecules could be achieved as 10^{-5} gram/cm^2 (of the substrate surface).

Acknowledgements The author is deeply indebted to Mrs Kristina Perovicha for her permission to use the measurement results.

References

1. Ibach H (1977) Electron spectroscopy for surface analysis. Springer-Verlag, New York, p 315
2. Fomenko VS (1981) Emission properties of materials. Naukova Dumka, Kiev, p 338, in Russian
3. Dobrecov LN, Gomoyunova MV (1966) Emission electronics. Nauka, Moscow, p 564, In Russian
4. Dekhtyar Yu (2008) Photo- dual and exoelectron spectroscopy to characterize nanostructures. In: Vaseashta A, Mihailescu IN (eds) Functionalized nanoscale materials, devices, and systems for chem.-bio Sensors, Photonics, and energy generation and storage, Springer, Dordrecht, The Netherlands, pp 169–183
5. Nesterenko BA, Snitko OB (1983) Physical properties of atomic clean surface of semiconductors. Naukova Dumka, Kiev, p 264
6. Derjaguin BV, Landau LD (1941) Theory of the stability of strongly charged lyophobic sols and of the adhesion of strongly charged particles in solutions of electrolytes. Acta Physica Chimica 14:633–642
7. Dempster DW (1996) Bone remodeling. In: Riggs BL, Melton LJ (eds) Osteoporosis. Etiology, diagnosis and management, Lippincott-Raven Publisher, New York, pp 85–108
8. Hill PA, Orth M (1998) Bone remodeling. Br J Orthod 25:101–107
9. International Osteoporsis Foundation (2009). http://www.iofbonehealth.org/facts-and-statistics.html#factsheet-category-14 Accessed 20 Aug
10. Rosenman G, Aronov D, Oster L, Haddad J, Mezinskis G, Pavlovska I, Chaikina M, Karlov A (2007) J Lumin 122–123:936–938
11. Dekhtyar Yu, Polyaka N, Sammons R (2008) Electrically charged hydrohyapatite enhances immobilization and proliferation of osteoblasts. Proc IFMBE 20:357–360
12. Dekhtyar Yu, Kachanovska A, Mezhinskis G, Patmalnieks A, Pumpens P, Renhofa R (2008) Functionalized nanoscale materials, devices, and systems for chem.-bio sensors, photonics, and energy generation and storage. In: Vaseashta A, Mihailescu IN (eds). Functionalized nanoscale materials, devices, and systems for chem.-bio sensors, photonics, and energy generation and storage, Springer, Dordrecht, The Netherlands, pp 347–350
13. Dekhtyar Yu, Polyaka N, Reisfeld R, Romanova R, Saraidarov R, Sudnikovics A (2008) Proceeding of the 6th International conference on medical physics “Medical physics in the Baltic States”, Kaunas, Lithuania, pp 27–31

Chapter 17
Modeling of a New Type of an Optoelectronic Biosensor for the Monitoring of the Environment and the Food Products

Optoelectronic Biosensor for Monitoring Environment

S. Khudaverdyan, O. Petrosyan, J. Dokholyan, D. Khudaverdyan, and S. Tsaturyan

Abstract A new optical biosensor has been developed for detecting and quantifying aflatoxins that are commonly found in a variety of agricultural products. In the biosensor we use a high-tech semiconductor material – silicon for the efficient high-accuracy registration of narrow spectral bands or specific wavelengths. On its base, we develop a structure with two oppositely directed potential barriers. The total current conditioned by these barriers depends both on the external voltage and on the wavelength of the absorbed radiation. It is possible to modify these parameters and obtain high-accuracy data on mycotoxic contaminants in food and provender in natural conditions.

Keywords Photodetector • Biosensor • Spectral characteristics • Photogeneration

17.1 Introduction

Today mycotoxins are considered to be the most important risk factors in dietology. They have much higher chronic effect than the effect of the toxins of plants, pesticides and food supplements [1]. In agriculture calorimetric and luminescent sensors are applied for identification of mycotoxins. The method is based on the ability of mycotoxins for natural fluorescence [1, 2]. In fact, there is an urgent need for the use of fast-acting highly sensitivity methods of the identification of mycotoxins since it is very important for public health and economic profitability [3–5]. We solve the problem by means of a new principle of selective registration of optical radiation

S. Khudaverdyan (✉) • O. Petrosyan • J. Dokholyan • D. Khudaverdyan • S. Tsaturyan
State Engineering University of Armenia, 105 Teryan Str, Yerevan, Armenia
e-mail: khsuren@seua.am

A. Vaseashta et al. (eds.), *Technological Innovations in Sensing and Detection of Chemical, Biological, Radiological, Nuclear Threats and Ecological Terrorism*, NATO Science for Peace and Security Series A: Chemistry and Biology,
DOI 10.1007/978-94-007-2488-4_17, © Springer Science+Business Media B.V. 2012

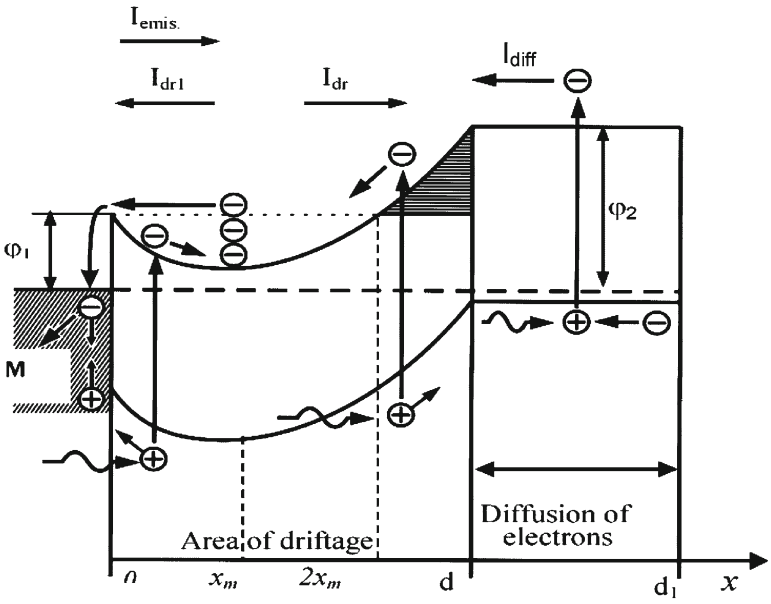

Fig. 17.1 Structure of the photodetector and the potential distribution for electrons in π – base

which allows us to detect mycotoxins not only by their fluorescence, but also by their ability to absorb certain wavelengths. The work covers the field of optoelectronics which is based on silicon technology. The silicon technology has considerably changed and has rapidly grown within the last 5 years. According to the Road Map of Communication Technology of Massachusetts Institute of Technology (MIT), silicon is considered one of the top ten best technologies [6].

17.2 Research Method

The work [7] reports a solid-state two-barrier structure with spectrophotometric properties in the UV and visible radiation regions. In the structure the interference of the oppositely-directed potential barriers is changed by external voltage, and low-intensity radiation does not influence the regularities of such change.

The structure of the sensor is presented in Fig. 17.1. It consists of the Schottky barrier (the contact metal – *n* – *Si*) and *n-p* junction [7]. Depletion regions of junctions cover the whole base of the structure with thickness *d*. The contact point x_m of these regions has potential energy φ_m and can be shifted by external voltage from zero to *d*. The depths of depletion regions change one at the expense of another. This involves the corresponding change of values of drift and diffusion photocurrents I_{dr1} and $I_{dr2} + I_{diff}$ created by junctions (Fig. 17.1).

The base thickness is d ≤ 1 μm (in Fig. 17.1). It is considerably less than the diffusion length of holes in the *n*-type base. Therefore, in the n-type base we observe not the recombination of photo generated electrons, but the electron emission through the low barrier φ_1 due to their storage in the potential well. The following equation presents:

$$qn_f v_T e^{-\frac{\varphi_1-\varphi_m}{kT}} = qF_0\left(1-e^{-\alpha d_1}\right) \tag{17.1}$$

I_{dI} does not make contribution into the external photocurrent since the holes of the depletion region of the surface barrier enter the metal and recombinate with a part of emitted electrons. Therefore, at the absorption of the integrated flux of radiation, the photocurrent is created by the minority carriers which photo generate in the depletion region of *n-p* junction by,

$$I_{dr} = qF_0 S\left(e^{-\alpha x_m} - e^{-\alpha d}\right)$$

and in the diffusion region by

$$I_{diff} = SqF_0 \frac{\alpha L_n}{1+\alpha L_n} e^{-\alpha d}$$

The resultant expression for the photocurrent is

$$\sum_{i,j} I_{Ph.i,j} = \sum_{i,j} I_{dri,j} + \sum_{i,j} I_{diff\ i,j} = Sq \sum_i \sum_j F_0(\lambda_i)\left(e^{-\alpha_i x_{mj}} - \frac{e^{-\alpha_i d}}{1+\alpha_i\ w}\right) \tag{17.2}$$

where α is the absorption coefficient of electromagnetic radiation, F_0 - the total flux of incoming photons per unit area, q – electron charge, v_i – thermal velocity of electrons, $F_0\left(1-e^{-\alpha d}\right)$ - the number of photo generated electronic-hole pairs in the base and in the diffusion region for quantum yield $\beta = 1$ at the absence of reflection from surface, d_1 – active region of the photodetector.

$i = 1,2,3, \ldots$ changes in integral flux with the change of wavelength of radiation, and $j = 1,2,3, \ldots$ changes with the change of bias voltage; $F(\lambda_i)$ is total flux of incoming photons with wavelength λ_i. The width of p-region w is smaller than the diffusion length of electrons in p-region L_n. For this reason the value L_n was replaced by w.

With the increase of the applied voltage (+ on Schottky barrier) the minimum of potential energy of electrons is shifted to the left, and more short waves take part in the photocurrent generation.

To give the exact description of the change of the position x_m, φ_m and the photocurrent value subject to parameters of radiation absorbed in structure, we studied the system of equations connecting the structural parameters with the radiation parameters and the external voltage. As a result, we got the following analytical expressions:

$$\begin{cases} 2\dfrac{\varphi_1-\varphi_m}{kT}+2\dfrac{n_f}{N_d}\left[e^{-(\varphi_1-\varphi_m)/kT}-1\right]=\left[\left(\dfrac{\varphi_2-\varphi_1+qV}{kT}\right)\cdot\dfrac{L_s}{d-2x_m}-\dfrac{d-2x_m}{L_s}\right]^2 \\ \displaystyle\int_0^{(\varphi_1-\varphi_m)/kT}\frac{dy}{\left[y+(n_f/N_d)\left(e^{-y}-1\right)\right]^{1/2}}=\frac{\sqrt{2}x_m}{L_s} \qquad y=\frac{\varphi-\varphi_m}{kT} \\ J_f=qn_fV_Te^{-\left(\frac{\varphi_1-\varphi_m}{kT}\right)}=qF_0\left(1-e^{-\alpha d_1}\right) \end{cases} \tag{17.3}$$

where φ_m is the minimum of potential energy of free electrons in the base, $n_f e^{-\frac{\varphi_1-\varphi_m}{kT}}$ – the number of photo generated electrons with potential energy φ_1. It should be noted that photo carriers are absent in the section $2x_m < x \le d$ where $\varphi_2 \ge \varphi \ge \varphi_1$ due to the emission through low barrier φ_1.

17.3 Research Results and Discussion

We carried out the modeling of the process of the detection of mycotoxins in foodstuffs and provender for toxins with the following parameters:

We considered the ultimate allowance for Aflatoxin B [8] in ready food (up to 5 mkg/kg) and in food raw materials (up to 10 mkg/kg) approved by the developed countries. The number of molecules for 1 g of substance will be: Aflatoxin B*1* – $9.6 \cdot 10^{12}$ molecules, Aflatoxin *M1* – $9.2 \cdot 10^{12}$molecules, Sterigmatocystin – $9.2 \cdot 10^{12}$ molecules.

The curves of spectral absorption of toxins are received by means of the system of equations (17.3) and the equation for photocurrent (17.2), where the unknown quantities are x_m, $\varphi_m$and n_f which are dependent on V, F_0 and α. Figure 17.2 shows the dependence of integral photocurrent on the change of the position of x_m, corresponding to the absorption depth $1/\alpha$.The values of wavelengths corresponding to $1/\alpha$ are presented along X-axis. When calculating $F_0(\lambda_i)$ we take the number of incident quanta per unit area equal to the number of molecules of toxins. The figure shows that the absorption depths of wavelengths for different toxins are spatially separated.

Considering the law of absorption $F(\lambda_i)=F_0(\lambda_i)e^{-\alpha_i x_{m_j}}$ we calculated the absorption depth and threshold shift Δx_m of the minimum of potential energy x_m for corresponding waves (Table 17.1). The difference of the absorption depths of waves for different toxins is rather big. Therefore, it is possible to capture alternately the contribution of separate wavelengths in the output photocurrent by the threshold shift x_m. In the threshold value Δx_m we considered the threshold of sensitivity of the photodetector equal to 10^{-14} Wt $\cdot$Hz$^{-1/2}$ [9]. The sensitivity according to the voltage (x_m) reaches a rather big value and can be easily measured. The results are presented in Table 17.2.

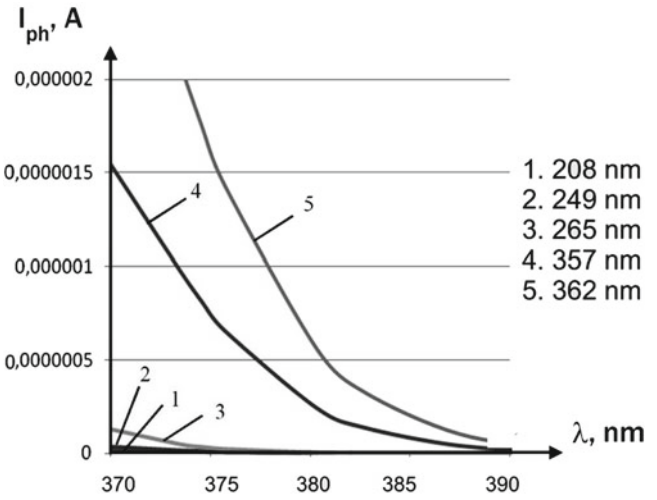

Fig. 17.2 Curves of spectral absorption of toxins

Table 17.1 Experimental toxins and parameters

	Molecular weight	Absorption in UV region (wavelength – nm)
Aflatoxin B*1*	312	265, 362
Aflatoxin *M1*	328	265, 357
Sterigmatocystin	324	208, 249

Table 17.2 Toxin absorption depths, threshold shifts, and sensitivities

	Absorption depth, nm	Threshold shift $\Delta x_{m,nop.}$, nm	Sensitivity x_m according to voltage, mB/nm
Aflatoxin B*1*	130,6–271,6 Δ=141	3,34–6,94 Δ=3,6	1.42,9.56
Aflatoxin *M1*	130,39–253,71 Δ=123,32	3,308–6,436 Δ=3,128	1.42,9.45
Sterigmatocystin	153,05–148,68 a Δ=4,37	3,92–3,81 Δ=0,11	0.56,0.91

17.4 Conclusion

In the described two-barrier structures at longitudinal illumination it is possible to change the integral photocurrent at the expense of separate waves by changing the external voltage. The spectral resolution of such structures at threshold values of photocurrent change makes ~1 nm. For the detection of toxins in food and provender the required spectral resolution is from 0.11 nm for Sterigmatocystins up to 3.6 nm for Aflatoxin B1 which is feasible within the described methods.

References

1. Haughey SA, Baxter GA, Jones CEN, O'Kennedy R, Stapleto S (2007) The detection of aflatoxins by optical biosensor analysis. XXV International congress of mycotoxins and phycotoxins, 25–27 May, Istanbul. Wageningen Academic Publishers, Wageningen, The Netherlands, p 430
2. Ngundi MM, Shriver-Lake LC, Moore MH, Lassman ME, Ligler FS, Taitt CR (2005) Array biosensor for detection of ochratoxin A in cereals and beverages. Anal Chem 77:148–154
3. Patel PD (2002) (Bio)sensors for measurement of analytes implicated in food safety. Trends Anal Chem 21:96–115
4. Zheng MZ, Richard JL, Binder J (2006) A review of rapid methods for the analysis of mycotoxins. Mycopathol 161:261–273
5. Schneider E, Curtui V, Seidler C, Dietrich R, Usleber E, Maertlbauer E (2004) Rapid methods for deoxynivalenol and other trichothecenes. Toxicol Lett 153:113–121
6. UK Silicon Photonics (2008) EPSRC Reference:EP/F001894/1
7. Khudaverdyan S, Dokholyan J, Arustamyan V, Khudaverdyan A, Clinciu D (2009) On the mechanism of spectral selective sensitivity of photonic biosensors. Nucl Instrum Meth A 610:314–316, ELSEVIER
8. European Commission. Food and Agriculture Organization EC/FAO (2004) Memorandum of anderstanding, concerning the establishment of strategic partnership between the food and agriculture organization of the United Nations and the commission of the European Communities in the field of development and humanitarian affairs
9. Khudaverdyan A (2009) About shot noise and speed of two barrier structures with thin base. Bull SEUA Ser Model Opt Contr 12(1):88–92

Chapter 18
Fast, Contactless Monitoring of the Chemical Composition of Raw Materials

Contactless Monitoring of Chemical Composition

O. Ivanov, Zh. Stoyanov, B. Stoyanov, M. Nadoliisky, and Ashok Vaseashta

Abstract A technique to monitor chemical composition of materials during manufacturing of ceramic products, in particular – of bricks, is investigated. The technique of monitoring is likely to offset environmental pollution and save energy. For this purpose, we use the Surface photo charge effect, which is generated for each solid body interacting with electromagnetic field. The measurement is express and can be performed in-situ in production conditions. The experimental work has shown that different samples of the investigated materials with different compositions produce different signals specific to each sample. For the same material, the signal varies with the change in chemical composition. More specifically, it is shown that for the material from which the bricks are fired, the signal is a function of the percentage of coal sludge. The results indicate that the characterization technique as a viable technique for control of incoming raw materials.

Keywords Bricks • Ceramic products • Monitoring the chemical composition • Field-matter interaction

O. Ivanov (✉) • Zh. Stoyanov
Georgi Nadjakov Institute of Solid State Physics, Bulgarian Academy of Sciences,
72, Tzarigradsko Chaussee, Blvd., 1784 Sofia, Bulgaria
e-mail: ogi@phys.bas.bg

B. Stoyanov • M. Nadoliisky
University of Architecture, Civil Engineering and Geodesy, Sofia, Bulgaria

A. Vaseashta
Institute for Advanced Sciences Convergence, International Clean Water Institute,
Herndon, VA, USA

A. Vaseashta et al. (eds.), *Technological Innovations in Sensing and Detection of Chemical, Biological, Radiological, Nuclear Threats and Ecological Terrorism*,
NATO Science for Peace and Security Series A: Chemistry and Biology,
DOI 10.1007/978-94-007-2488-4_18, © Springer Science+Business Media B.V. 2012

18.1 Introduction

Many industries require constant monitoring of the chemical composition of the raw materials during production process. This is necessitated by the technological requirements for maintaining a high quality final product. The safety of the factory is another priority that can be met by the constant control of what goes in. We have developed a technique that is likely to implement such in-situ monitoring and control. This report examines the possibility of monitoring chemical composition during the manufacture of ceramics and bricks in particular. The production process is energy intensive due to its huge energy consumption. In order to reduce energy consumption of the product combustible waste materials such as coal slurries are added to the raw material. The coal slurries ignite and burn when blanks are inserted in the furnace. Thus, figuratively speaking, bricks are self-baked. This way a serious environmental problem is solved too, because there are large quantities of coal sludge requiring special measures in order to be disposed of. A constant monitoring of the quantities of combustible additives is necessary; otherwise the quality of the bricks deteriorates.

Different methods exist for the control of the chemical composition of such materials, for example: X-ray diffraction (DRX) and Mass Spectrometry (MS) have been used in for physico-chemical characterization of bricks [1]. Laser-induced breakdown spectroscopy (LIBS) is an interesting method for the study of powdered samples, in particular – the production materials for bricks and tiles [2]. In addition Fourier-transformation Raman spectroscopy (FT-Raman spectroscopy) and X-ray fluorescence spectrometry (XRF) are applied for quality control of clays [3]. Finally, by X-ray electron probe, the soil mineral component is examined [4]. But these and similar methods have disadvantages. They are too slow, complicated or expensive and generally not suitable for use in production conditions to provide continuous monitoring.

Our research has shown that for this purpose an effect with the working title of Surface photo charge effect (SPCE) can be used. It is generated by any solid body interacting with electromagnetic fields. The measurement is express and can be performed on-line in production conditions. The equipment is not expensive. Surface photo charge effect is very attractive for various practical applications. The SPCE is based on the fact that, on irradiation with an electromagnetic field all the investigated solids generate an alternating potential difference, the frequency of which is equal to the frequency of the incident electromagnetic wave. The voltage is measured contactless between the irradiated sample and a second solid whose potential is assumed to be zero. In a real experiment, the measurement is between the studied solid and the common earth terminal of the system. In contrast to other similar effects, the SPCE is present in every solid and each solid generates a specific signal. An important feature of the SPCE is its significant dependence on the specific properties of the irradiated samples. This fact reveals opportunities for a rapid and contactless analysis, not only of solids, but also of liquids and gases [5].

18.2 Results and Discussions

As was mentioned above one of the features of SPCE, which is discussed in this article, is that each solid generates a specific signal. The amplitude of this signal depends on the chemical composition of the solid. This, naturally, renders an elucidation that we could quickly and without any physical contact, monitor the composition of a variety of samples [5]. Quality control is carried out by checking whether a set of samples which are of interest to us, always generate the same signal.

A schematic diagram of the experimental set-up we used in our research can be found in [6]. For our study we used samples of clay, coal and coal slurries and mixtures of clay and coal slurries. All the samples were the same weight – 150 g. We analyzed them in ground form. They were placed in special holders ensuring that the upper surface of the sample has the same composition as the composition of the entire volume. For this purpose the holders enabled easy mixing of samples and release of the material volume to the surface.

To make sure that it is possible to work with the materials of interest to us, we initially examined wide spectra of samples of coal, coal sludge, clay and a mixture of clay and coal sludges. Table 18.1 shows the results of a study of a series of such samples. The results are in relative units.

The aim of our work is to verify that the signal generated by SPCE changes as a function of the chemical composition of samples. In this respect – we present the results of a study of the generated signal as a function of the percentage of sludge. On Fig. 18.1 is presented in graphic form how the electrical signal changes as a function of the quantity of sludge.

The data presented in Table 18.1 clearly shows that each material generates a specific signal. This result meets our expectations and opens the possibility for this kind of research. Interestingly, in sample N 4, which is a mixture of clay and sludge, there is a significant increase of the signal compared to signals generated by the two components separately. Another intriguing aspect is that the signal tends to increase when the percentage of carbon contained in the sample is decreased. A similar trend is continued in the results of Fig. 18.1. It should also be noted that samples with N 4, Table 18.1, which represent a mixture of clay and sludge generated a relatively heterogeneous signals in amplitude compared to other types of samples. They were taken at the same time from a brick production factory and should have had the same percentage between the two components. This probably

Table 18.1 Comparison of series of samples of interest on this work's topic

No.	Compound	Measured signal [Arb. Units]
1	Coal	0.55
2	Sludge with high concentration of coal	2.64
3	Sludge with lower concentration of coal	2.82
4	Clay with sludge	3.72
5	Clay	2.8

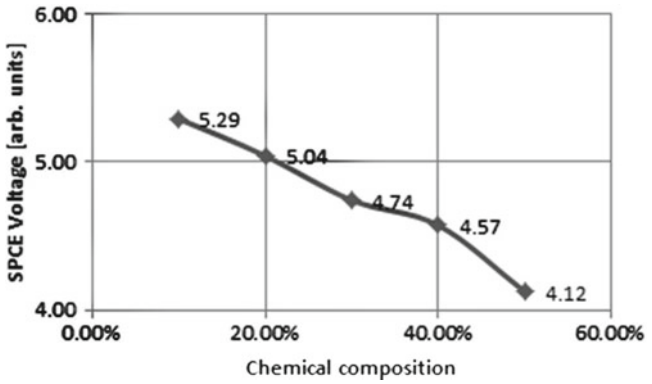

Fig. 18.1 Changes in the measurement signal as a function of the added quantity coal sludge

means that the mixture of clay and sludge in the devices of the plant is not sufficiently homogeneous.

The most important information, in terms of the theme of this work, is incorporated into the results given in Fig. 18.1. They show that the measured signal from the Surface photo charge effect is proportional to the amount of coal slurries added to the clay. Thus a positive answer is given to the fundamental issue raised in our study. Namely, it is possible through the proposed method to control the percentage of this additive.

It should be noted that different batches of clay and sludge have lots of different possible variations in chemical composition. It is therefore necessary for the entry of new inputs to determine whether there is a need for a new calibration. Also, in addition to controlling the chemical composition of the mixture of coal and sludge, such a system could be applied to them separately. Then an adequate response to changes in one of two components could be provided. There are also possible random deviations within one batch of raw materials. These deviations can be sifted through accumulation of a sufficient number of measurements.

The proposed method to control the chemical composition of incoming raw materials is relatively simple compared to other methods used for this purpose. Some of which were mentioned. It could be carried out in production conditions, including continuous measurements for automatic adjustments of the composition. In this case a small part of the final mixture must pass through the sensor and then be returned to the mainstream. The methods existing until now do not offer the possibility of continuous monitoring. The cost of our system is expected to be low. It does not contain expensive or difficult to maintain elements.

Such a system could be used in various industries for the control of incoming raw materials. This will affect positively the quality of the manufactured products. Beyond improving the technological conditions of work such a system also provides a high degree of security against terrorist attacks to which incoming raw materials are highly vulnerable. Their properties can be strongly modified by intruders who want to sabotage the production process. On the other hand there are practically no methods easily applicable for continuous quality control of incoming raw

materials. This work aims to fill this gap. In the future we plan to develop a system for liquid and solid samples. Such devices could work together with other control methods and complement each other.

18.3 Conclusion

The proposed method for rapid and non-contact, quality control of chemical composition of raw materials in the manufacturing of ceramics gives various options. Firstly we aim to improve product quality, but saving energy and having an environmental impact can also be achieved. The latter follows from the fact that maintaining the right balance between clay and coal slurries minimizes the need to adjust the temperature in the furnace by adding fuel. It could also encourage the use of waste materials as fuel. The option to automate the monitoring of mixing the two components would be very useful in this regard. Materials are now observed in bulk form and information on their homogeneity can be obtained. Similar methods could be developed for other materials, including solids and liquids. This technology and its wide spectrum of uses provides a method for protection and optimization of production facilities not only for ceramics, but for wide range of other industries, some of which are essential for the economic and social state of any given country. Those can be accomplished through monitoring expressly whether incoming plant materials are not subject to malicious action. Such an action is likely to be executed by adding a component that will reflect negatively on the technology cycle and will change the finished product.

References

1. Andrés A, Diaz MC, Coz A, Abellán MJ, Javier RV (2009) Physico-chemical characterisation of bricks all through the manufacture process in relation to efflorescence salts. J Eur Ceram Soc 29:1869–1877
2. Ctvrtnickova T, Cabalin L, Laserna J, Kanicky V, Nicolas G (2009) Laser ablation of powdered samples and analysis by means of laser-induced breakdown spectroscopy. Appl Surf Sci 255:5329–5333
3. Alia JM, Edwards HGM, Garcia-Navarro FJ, Parras-Armenteros J, Sanchez-Jimenez CJ (1999) Application of FT-Raman spectroscopy to quality control in brick clays firing process. Talanta 50:291–298
4. Belozerova OY (2009) Investigation of soil mineral component in the Baikal Region by X-ray electron probe microanalysis. Spectrochim Acta B 64:1248–1252
5. Ivanov O (2006) Sensor applications of field-matter interactions. In: Grimes CA, Dickey EC, Pishko MV (eds) Encyclopedia of sensors, vol 9. American Scientific Publishers, Stevenson Ranch, pp 165–197
6. Ivanov O, Vaseashta A, Stoichev L (2008) Rapid, contactless, and non-destructive testing of chemical composition of samples. In: Vaseashta A, Mihailescu I (eds) Proceedings of the NATO advanced study institute on functionalized nanoscale materials, devices and systems for chem-bio sensors, photonics, and energy Generation and storage, Springer, Sinaia, pp 331–334

Chapter 19
Nanoplatforms for Detection, Remediation and Protection Against Chem-Bio Warfare

Nanoplatforms Against Chem-Bio Warfare

E.B. Denkbaş, C. Bayram, D. Kavaz, T. Çirak, and M. Demirbilek

Abstract Chemical and biological substances have been used as warfare agents by terrorists by varying degree of sophistication. It is critical that these agents be detected in real-time with high level of sensitively, specificity, and accuracy. Many different types of techniques and systems have been developed to detect these agents. But there are some limitations in these conventional techniques and systems. Limitations include the collection, handling and sampling procedures, detection limits, sample transfer, expensive equipment, personnel training, and detection materials. Due to the unique properties such as quantum effect, very high surface/volume ratio, enhanced surface reactivity, conductivity, electrical and magnetic properties of the nanomaterials offer great opportunity to develop very fast, sensitive, accurate and cost effective detection techniques and systems to detect chemical and biological (chem.-bio) warfare agents. Furthermore, surface modification of the materials is very easy and effective way to get functional or smart surfaces to be used as nano-biosensor platform. In that respect many different types of nanomaterials have been developed and used for the detection, remediation and protection, such as gold and silver nanoparticles, quantum dots, Nano chips and arrays, fluorescent polymeric and magnetic nanoparticles, fiber optic and cantilever based nanobiosensors, nanofibrillar nanostructures etc. This study summarizes preparation and characterization of nanotechnology based approaches for the detection of and remediation and protection against chem.-bio warfare agents.

Keywords Chem-bio warfare • Nanotechnological approaches • Nanomaterials

E.B. Denkbaş (✉) • C. Bayram • D. Kavaz • T. Çirak • M. Demirbilek
Nanotechnology and Nanomedicine Division, Hacettepe University, 06800, Beytepe
Ankara, Turkey
e-mail: denkbas@hacettepe.edu.tr

A. Vaseashta et al. (eds.), *Technological Innovations in Sensing and Detection of Chemical, Biological, Radiological, Nuclear Threats and Ecological Terrorism*,
NATO Science for Peace and Security Series A: Chemistry and Biology,
DOI 10.1007/978-94-007-2488-4_19, © Springer Science+Business Media B.V. 2012

19.1 Introduction – Nanoparticles, Nanotubes, Nanowires, Nanofibres

19.1.1 Nanoparticles

Nanoparticles can be defined as the particles having different shape/geometry and base materials (i.e., metals, ceramics, polymers etc.) with the size range in submicron and mostly < 200 nm. Nanoparticles have been used in many different types of applications including electronics, textile, and coating applications. Due to their unique size and ease of functionalization, they have gained attention for their use in diagnosis and/or therapy for applications in nano-medicine, especially in the last decades. Different polymeric [1] and metal nanoparticles [2–4], liposomes [5–7], micelles [8, 9], quantum dots [10–13], dendrimers [14–17], nanocapsules, cell ghosts, lipoproteins and many different nanoassemblies are the frontiers of these applications [18]. A schematic representation of these nanoassemblies is given in Fig. 19.1.

The synthesis and fabrication procedures of nanoparticles are directly related to the nature of base materials of targeted nanoparticles, using approaches that are either bottoms-up or top-down [2]. Bottoms-up approaches are summarized as below.

- Homogeneous nucleation from liquid or vapor, or by heterogeneous nucleation on substrates,
- Phase segregation through annealing appropriately designed solid materials at elevated temperatures,
- Confining chemical reactions, nucleation and growth processes in a small space such as micelles;

While, some of the top-down approaches for the nanoparticle production, include;

- Milling or attrition
- Repeated quenching
- Lithography.

Various applications of different nanomaterials in biosensoric devices are used for the detection of pathogenic microorganisms that have importance to food and environmental safety, biosecurity, and biowarfare. Magnetic polymer nanostructures are a new class of multifunctional nanomaterials that have received considerable attention for bioseparation [19], tumor hyperthermia [20] magnetic resonance imaging diagnostic contrast agents [21], magnetically guided site- specific drug delivery agents [22], immunological assays etc. [23]. Magnetic particles (MPs) are becoming increasingly popular for biosensors based on antibody recognition that have a wide range of monitoring applications in clinical, environmental, homeland security, and food security. Using a magnetic nanoparticle not only for labeling and separation of an analyte, but also for direct quantification, provides an easy and simple

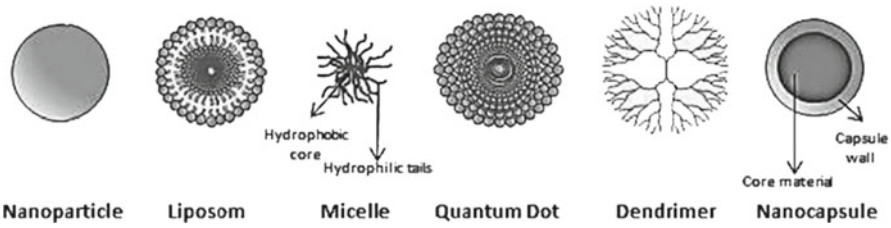

Fig. 19.1 Schematic representations for different types of nanoassemblies

way of detection [24]. These magnetic nanoparticles easily show response to external magnetic fields and are easily and readily removed from solutions.

Figure 19.2a, b show AFM images of magnetic Fe_3O_4 (a) and magnetic Fe_3O_4 encapsulated chitosan nanoparticles (b). Highly sensitive detection of *E. coli* was achieved by using magnetic Fe_3O_4 loaded chitosan nanoparticles that were synthesized by co-precipitation method and are mostly core-shell structures with a range of approximately 180–220 nm in diameter and a saturation magnetization of 24.8 emu/g.

Streptavidin was used as a model antibody which covalently bonded onto the magnetic Fe_3O_4 loaded chitosan nanoparticles via carbodiimide activation. The binding efficiency of Avidin was 88%. These nanoparticles were used for the detection of bacterial cells from complex matrices. The capture efficiency of *E. coli* from a complex medium was 56%. Based on these results these nanoparticles can be used for rapid, label-free, sensitive and selective detection of *E. coli*.

19.2 Nanotubes

19.2.1 Carbon Nanotubes

Carbon nanotubes have stimulated extensive research into the properties of nanometer-scale cylindrical carbon networks after their discovery by Iijima in 1991 [25]. The researchers have fabricated several forms of the carbon nanotubes (CNTs) documented in the form of books and reviews in [26–29]. Carbon can exist in three allotropic forms in the solid phase such as graphite, diamond, and fullerene as seen in Fig. 19.2. Graphite is made by layered planar sheets of sp^2 hybridized carbon atoms bonded together in a hexagonal network. The different geometry of the chemical bonds makes graphite soft, slippery, opaque, and electrically conductive. Single Walled Nanotubes (SWNT) can be considered as long wrapped graphite sheets. Nanotubes generally have a length to diameter ratio of about 1,000 so they can be considered as nearly one-dimensional structures. The lengths of single-walled carbon nanotubes (SWCNTs) changes from several 100 nm to several micrometers and diameters of 0.4–2 nm and the diameter of coaxial multiple-walled (MWCNTs)

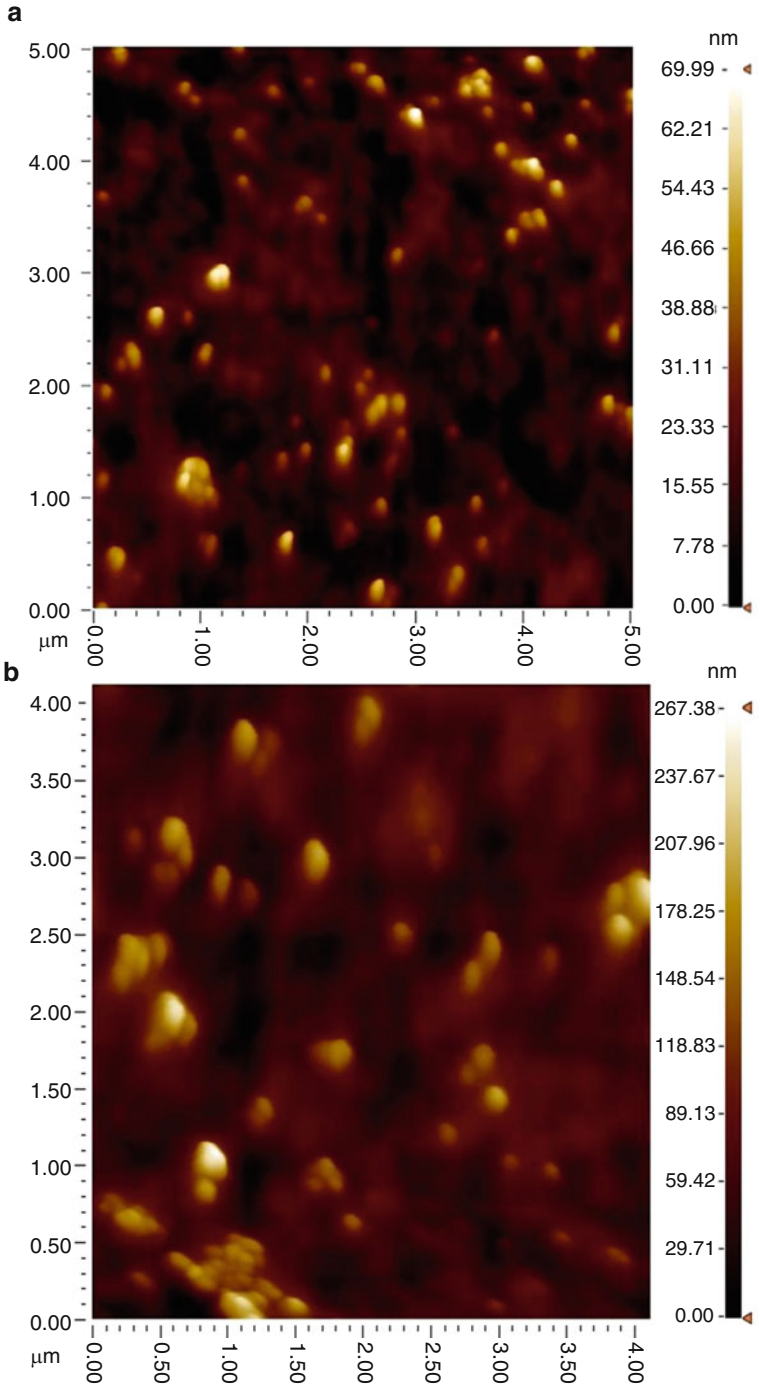

Fig. 19.2 (**a**) Magnetic. Fe_3O_4 chitosan nanoparticles, (**b**). Magnetic Fe_3O_4 encapsulated chitosan nanoparticles

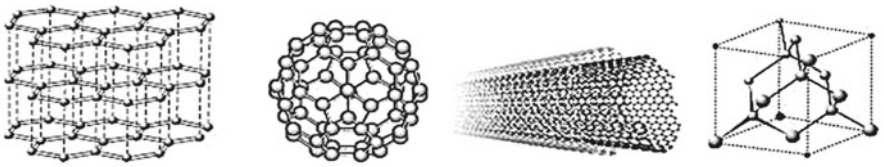

Fig. 19.3 Allotropic forms of carbon

carbon nanotubes changes between 2 and 100 nm [29]. Their remarkable material properties, such as strength, rigidity, durability, chemical vigor, thermal conductivity, and (perhaps most importantly) electrical conductivity, make them very versatile [30] (Fig. 19.3).

The potential applications of CNTs include energy storage (i.e., hydrogen storage, lithium intercalation and electrochemical supercapacitors), molecular electronics (i.e., FETs), nanoprobes/sensors, composite materials, templates and biomedical applications. For biomedical applications, one of the concerns is due to lack of solubility in aqueous medium, which can be overcome by chemical modification and functionalization. Additionally, recent studies have shown that biological and bioactive molecules such as amino acids, proteins, carbohydrates and nucleic acids can be conjugated with CNTs [31–35].

These modifications can be categorized into three main approaches; covalent attachment (chemical bond formation), noncovalent attachment (physical adsorption) and a hybrid attachment where a small molecule, called as anchor, is first noncovalently adsorbed to the CNT followed by a chemical reaction between the anchor and the biomolecules of interest [29].

19.2.2 Titania Nanotubes

High sensitivity, selectivity, the ability to operate in turbid solutions, amenability for rapid analysis and miniaturization are some of the advantages of electrochemical biosensors [36]. Modern electrochemical techniques are limited by very low detection limits (typically 10^{-9} M) and electro activity of the enzyme or protein while immobilizing onto electrode surface. Furthermore, unfavorable orientation or nonspecific adsorption of biomolecules generates serious reduction in catalytic activity [37]. The regular structure and high reactive surface of inorganic nanostructured materials show much promise for use in protein binding and thermal stability. TiO_2 is a widely used inorganic material for coatings, medical devices in the forms of tubular, particle or fibers. This material has also shown its utility in numerous applications such as gas sensing, solar cells and biosensing [38].

Since the nanostructured TiO2 has magnificent physical and chemical properties, the preparation of oriented, highly ordered nanotubular TiO2 by anodization of

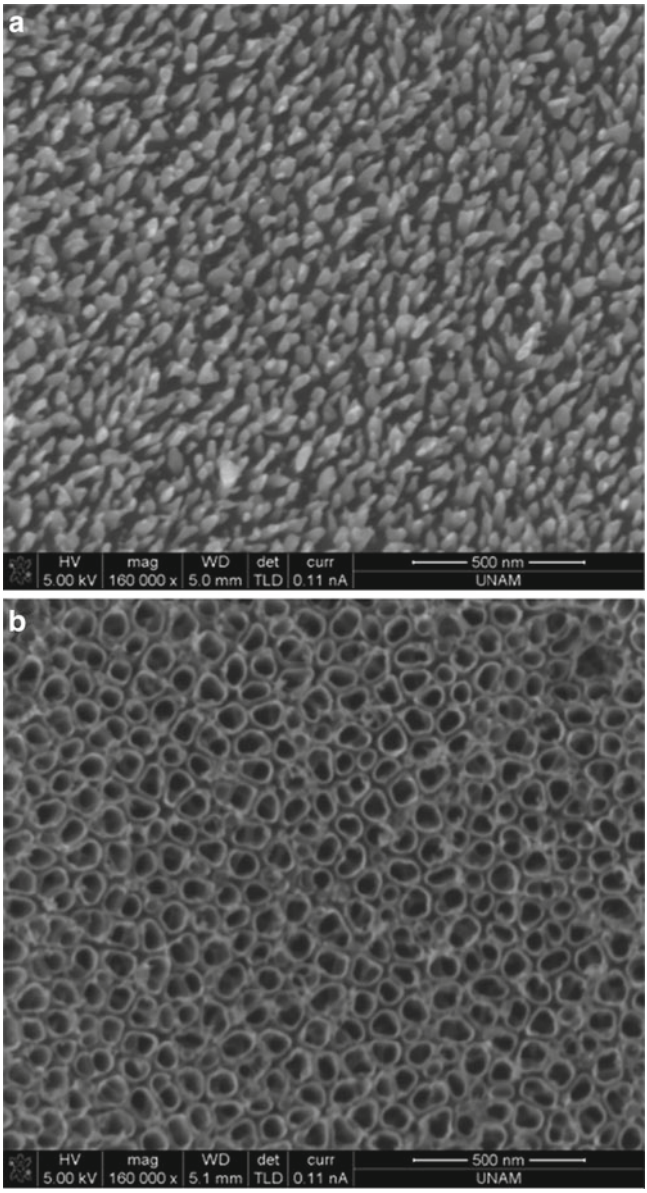

Fig. 19.4 Two types of Titania layer production. (**a**) Nanoridges and (**b**) nanotubes

titanium is an area receiving much attention in recent years. Titania nanotube layers can be easily produced by process called anodization. Nanotubular titania layers grow in acidic electrolytes under specific electrochemical conditions. TiO_2 nanotubes with large surface areas and good uniformity and conformability over large areas fabricated by the anodic oxidation of Ti substrates show much promise for the

immobilization of biomolecules in electrochemical biosensor design [39]. Besides nanotubes, TiO_2 layers can be produced as nanoridges by altering the anodization parameters. The ability of generating different forms of titania layers give flexibility towards design of electrode.

Surface-enhanced Raman spectroscopy (SERS) is a useful analytical tool that can provide signals with high information content (characterization of compounds due to the structural information) concerning a biological sample. This information is commonly used for detection of (bio) molecules. The SERS technique may provide up to 10^{14}-fold enhancement in Raman signal intensity, and this is sufficient to detect pico- to femtomolar amounts of biomolecules. Rough surface of conductive material is required for observation of the SERS signals. A biosensor design which combines highly rough TiO_2 nanotube layered and SERS tool would have an impact in detecting biomolecules from water sources (Fig. 19.4).

19.3 Nanowires

The nanowires are metallic, magnetic or semiconductive nanostructures with dimensions of a few nanometers. At this size due to importance of the quantum mechanical effects, nanowires can be called as quantum wires or nanorods. Silicon is the most widely used base materials for the production of nanowires, but silicon is not unique. Depending on the application; gold, silver, copper or manganese can be used to get incredible selectivity and specificity with diameters down to 12 in the form of metallic or multi-layered structures. Furthermore, nanowires can be made from other various starting materials such as manganese oxide, magnesium oxide, nickel, cadmium selenide, germanium, titanium dioxide, alumina, bismuth, indium phosphide, palladium, gallium nitride, zinc oxide, and silicon carbide. The nanowires can be produced by suspension or deposition techniques. In the suspension technique; a suspended nanowire is created in a vacuum chamber, made by chemically etching a bigger wire, by blasting a larger wire with high energy particles or by pushing a nanoprobe's tip into the soft surface of a partly melted metal and pulling it back to get a nanowire. In the case of deposition technique; metal nanowires can be produced by electrodeposition onto the cleaved edge of an molecular beam epitaxy, MBE-grown semiconductor heterostructure. The metal preferentially deposits onto the edge of one specific semiconductor layer, yielding a nanowire of a few nanometers in thickness [40].

The nanowires have unique electrical properties due to their super small size. The main problem with the electrical properties of the nanowire is form the edge effect, which comes from the atoms that are on the nanowire surface that are not completely bonded to adjacent atoms (like those within the nanowire interior). The anbonded atoms cause defects within the nanowire which affects its electrical conductivity. This effect increases by decreasing the size of the nanowire due to the higher amount of atoms on the surface than interior part in this size. Nanowires can be used in many different types of applications such as optical, magnetic, sensing, solar cell and/or electronic applications.

19.4 Nanofibers

Nanofibers are fibers having less than 100 nm in diameter that can be characterized by their flexibility and aspect ratio of 1,000:1. Their high specific surface area, flexibility and superior directional strength makes fibers very attractive materials in many different types of applications within the textile industry, aerospace industry, biomedical applications and so on. Polymeric nanofibers can be processed by a number of techniques such as drawing, template synthesis, phase separation, self-assembly and electrospinning [41–44].

In the drawing process to produce nanofibers; a micropipette with a few micrometers in diameter was dipped into the droplet near the contact line using a micromanipulator. The micropipette was then withdrawn from the liquid and moved at a speed of approximately 1×10^{-4} m/s, resulting in a nanofiber being pulled. The pulled fiber was deposited on the surface by touching it with the end of the micropipette. The drawing of nanofibers was repeated several times on every droplet. The drawing process can be considered as dry spinning at a molecular level [45].

A particular template or mold is used to produce required material or structure in the template synthesis. In the case of nanofiber creation by template synthesis; the template refers to a metal oxide membrane with through thickness pores of nanoscale diameter. The application of water pressure on one side and restrain from the porous membrane causes extrusion of the polymer which, upon coming into contact with a solidifying solution, gives rise to nanofibers whose diameters are determined by the pores [46].

In the drawing process, only viscoelastic materials that can withstand applied stresses can actually be used, which limits the application of this method. On the other hand, the template synthesis method does not result in the production of continuous fibers. Therefore, phase separation, self-assembly and electrospinning are the most important methods that can be used for the production of nanofibers. Each of these methods has its own advantages and limitations [47].

In general, the technique the self-assembly technique involves the spontaneous organization of individual components into an ordered and stable structure with preprogrammed non-covalent bonds. While self-assembly process is responsible for producing several essential biological components (nucleic acid synthesis, protein synthesis, and energy transduction), it is a rather complex laboratory procedure that is limited to only a select few polymer configurations (di-block copolymers, triblock copolymers, triblocks from peptide-amphiphile, and dendrimers) [44].

The most common of these configurations for the production of nanofibers are the peptide-amphiphiles (PA). Other self-assembly methods include divalent ion induced self-assembly (addition of Ca^{2+} ions to cause gelation of the solution) and drying on surfaces (simply allowing the pH 8 water solution to dry on a surface) [48, 49].

Phase separation is a thermodynamic separation of a polymer solution into polymer-rich and polymer-poor/solvent-rich components. Briefly, a polymer is dissolved in a solution and the phase separation is induced, either thermally (most common

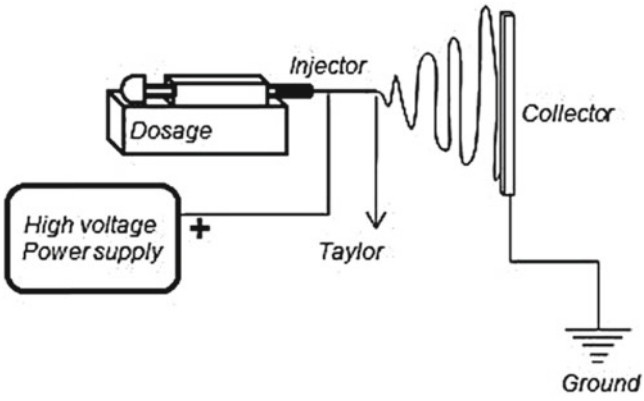

Fig. 19.5 Schematic representation of electrospinning technique for nanofiber production

method) or through the addition of a nonsolvent to the polymer solution to create a gel. Afterwards the gel is cooled to the temperature below the glass transition value of the polymer and freeze dried under vacuum to produce scaffold with nanofibrous structure [41, 44].

Porous nature of the scaffolds can be controlled by addition of any porogen such as sugar, inorganic salt or paraffin spheres. Porogen concentration, size and geometry can be used as the effective parameters over the pore size and nature. Actually phase separation is a simple technique, because it does not need very sophisticated equipment and phase separation and can be used to produce nanoporous foams in batch to batch consistency, but it is a time-consuming process and is limited only a few polymers.

The most popular and effective nanofiber production technique is *electrostatic spinning* or briefly *electrospinning* technique [50]. It was first used by Formhals in 1934 and it was patented by him shortly thereafter. The study consisted of an experimental setup for the production of polymer filaments by using electrostatic force [51]. In this technique; the nanofibers can be created through an electrically charged polymer solution or melt. Here a low current and high potential (i.e., in kV range) DC power supply is used and the polymer drop was drawn into the fiber form due to this high voltage application. A schematic representation of the electrospinning technique is given in Fig. 19.5. As seen from the figure polymeric nanofibers are formed from the solution/melt of the polymer stock between two electrodes (i.e., spinneret and collector as the anode and cathode) bearing electrical charges of opposite polarity. During the process charged polymer solution/melt is drawn out of a metal hole (i.e., from the end of a needle) and is converted into the jet form towards the collector.

Electrospun nanofibers are accumulated over the collector and have randomized structures. An example of scanning electron microscope (SEM) micrograph of a polymeric nanoscaffold is given in Fig. 19.6.

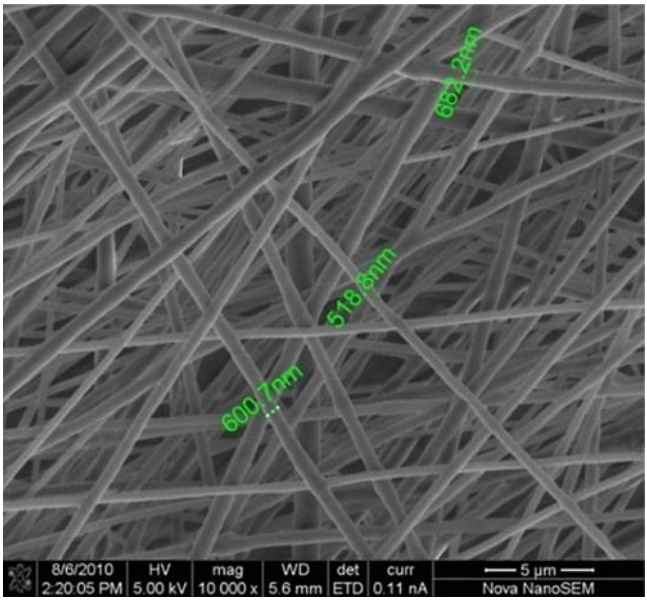

Fig. 19.6 Polymeric nanoscaffold prepared by electrospinning technique

The most effective parameters over the nature of nanofibers in the electrospinning technique can be categorized into the three main topics as follow:

- Polymer solution/melt characteristics (i.e., viscosity/molecular weight, elasticity, surface tension of the polymer solution)
- System parameters (i.e., spinneret characteristics, electric potential at the capillary tip, gap between the spinneret and collector etc.)
- Process conditions (i.e., polymer solution/melt temperature, medium humidity, air velocity in the electrospinning chamber etc.) [52].

Up to date many different types of applications have been investigated for electrospinning technique [50]. Some of them include;

- *cosmetic applications* (i.e., skin cleaning and healing)
- *medical applications* (i.e., drug delivery systems, wound dressing, tissue engineering, artificial blood vessel and/or nerve guide),
- *military clothes* (i.e., protective clothes against to chemical or biological hazardous materials),
- *sensor applications* (i.e., thermal sensor, piezoelectric sensor, biochemical sensor),
- *filtration processes* (i.e., liquid or gas filtration, molecular filtration) and other industrial applications.

19.5 Cantilever Based Nanobiosensors

Biosensors are defined as analytical devices, which are able to detect the existence, amount and activity of biological molecules due to conversion of physical and chemical changes coming from the interactions between analytes and their recognition elements into signals by using transducers. Nanobiosensor systems consist of molecular recognition elements, reporter elements and microfluidics. Whether it is micro- or nanoplatform biosensors, molecular recognition mechanisms are similar in principle and based on binding of targets (analyte molecules) with specific probes. However, related to advances in the miniaturization technologies, demand for portable analytical biosensing devices are increased dramatically. As the sensor size decreases, required sample volume and analysis time decreases [53].

The importance of more advanced biosensor systems arise from their rapid response capabilities in lower concentrations, for potential use in defense against chemical and biological threats especially in pathogen detection or applications such as early diagnosis of cancer like diseases. There is a significant demand of portable devices in field studies, which are capable of performing analyzes precisely, accurately and rapidly, as field laboratory type instruments [7, 54]. Nanotechnology based single cell detection methods investigate how the cells are responding to environmental conditions, and how they are interacting with neighbor cells [53, 55]. Nanobiosensors must consist of proper components to achieve successful applications. Micro- or nanofluidics (channels, pumps, mixers, valves) are crucial components, which control nanoliter amounts of fluids in microscale volumes. It is important to design suitable conditions to biological elements. The other important factor for a sensor system is its operating mechanism. Nanobiosensor mechanisms are divided into labeled (gold nanoparticles, quantum dots, fluorescence bindings, magnetic beads) and label-free (cantilever-based sensors, nanowires, surface plasmon resonance sensors, nanopores, and surface enhanced Raman scattering) methods [56, 57].

References

1. Rozenberg BA, Tenne R (2008) Polymer-assisted fabrication of nanoparticles and nanocomposites. Prog Polym Sci 33:40–112
2. Guozhong C (2004) Nanostructure & nanomaterials synthesis properties & applications. Imperial College Press, London, p 51
3. Schon G, Simon U (1995) A fascinating new field in colloid science – small ligand-stabilized metal-clusters and possible application in microelectronics. 1. State-Of-The-Art. Colloid Polym Sci 273:101
4. Schmid G (ed) (1994) Clusters and colloids. VCH, New York
5. Gregoriadis G, Ryman BE (1971) Liposomes as carriers of enzymes or drugs – new approach to treatment of storage diseases. Biochem 124:58
6. Gabizon A (2001) Pegylated liposomal doxorubicin: metamorphosis of an old drug into a new form of chemotherapy. Cancer Invest 19:424–436

7. Jain RK (2001) Delivery of molecular medicine to solid tumors: lessons from in vivo imaging of gene expression and function. Control Release 74:7–25
8. Kataoka K, Harada A, Nagasaki Y (2001) Block copolymer micelles for drug delivery: design, characterization and biological significance. Adv Drug Del Rev 47:113–131
9. Chang SF, Chang HY, Tong YC, Chen SH, Hsaio FC, Lu SC, Liaw J (2004) Nonionic polymeric micelles for oral gene delivery in vivo. Hum Gene Ther 15:481–493
10. Chan WCW, Nie S (1998) Quantum dot bioconjugates for ultrasensitive nonisotopic detection. Science 281:2016–2018
11. Dubertret B, Skourides P, Norris DJ, Noireaux V, Brivanlou AH, Libchaber A (2002) In vivo imaging of quantum dots encapsulated in phospholipid micelles. Science 298:1759–1762
12. Gao X, Cui Y, Levenson R, Chung LW, Nie S (2004) In vivo cancer targeting and imaging with semiconductor quantum dots. Nat Biotechnol 22:969–976
13. Liu S, Lee CM, Wang S, Lu DR (2006) A new bioimaging carrier for fluorescent quantum dots: Phospholipid nanoemulsion mimicking natural lipoprotein core. Drug Deliv 13:159–164
14. Stirib SE, Frey H, Haag R (2002) Dendritic polymers in biomedical applications: From potential to clinical use in diagnostics and therapy. Angew Chem Int Ed 41:1329–1334
15. Aulent F, Hayes W, Rannard S (2003) Dendrimers: a new class of nanoscopic containers and delivery devices. Eur Polym J 39:1741–1771
16. Boas U, Heegaard PMH (2004) Dendrimers in drug research. Chem Soc Rev 33:43–63
17. Duncan R, Izzo L (2005) Dendrimer biocompatibility and toxicity. Adv Drug Deliv Rev 57:2215–2237
18. Torchilin VP (2006) Nanocarriers for drug delivery: needs and requirements. In: Torchilin VP (ed) Nanoparticulates as drug carriers, Imperial College Press, London
19. Gu HW, Xu KM, Xu CJ, Xu B (2006) Biofunctional magnetic nanoparticles for protein separation and pathogen detection. Chem Commun 12:941–949
20. Ciofani G, Riggio C, Raffa V, Menciassi A, Cuschieri A (2009) A bi-modal approach against cancer: Magnetic alginate nanoparticles for combined chemotherapy and hyperthermia. Med Hypotheses 73:80–82
21. Jing XH, Yang L, Duan XJ, Xie B, Chen W, Li Z, Tan HB (2008) In vivo MR imaging tracking of magnetic iron oxide nanoparticle labeled, engineered, autologous bone marrow mesenchymal stem cells following intra-articular injection. Joint Bone Spine 75:432–438
22. Guo SJ, Li D, Zhang LX, Li J, Wang EK (2009) Monodisperse mesoporous superparamagnetic single-crystal magnetite nanoparticles for drug delivery. Biomaterials 30:1881–1889
23. Xu CJ, Sun SH (2007) Monodisperse magnetic nanoparticles for biomedical applications. Polym Int 56:821–826
24. Li GY, Zhou ZD, Li YJ, Huang KL, Zhong M (2010) Surface functionalization of chitosan-coated magnetic nanoparticles for covalent immobilization of yeast alcohol dehydrogenase from Saccharomyces cerevisiae. J Magn Magn Mater 322:3862–3868
25. Iijima S (1991) Helical microtubules of graphitic carbon. Nature 354:56
26. Gogotsi Y (2006) Carbon nanomaterials. In: Gogotsi Y, Presser V (eds). CRC Press, Taylor and Francis Group, Florida
27. O'Connell MJ (2006) Carbon nanotubes: properties and applications. In: O'Connel MJ (ed), CRC Press, Taylor & Francis Group, Florida
28. Endo M, Iijima S, Dresselhause M (eds) (1996) Carbon nanotubes, A Pergamon Title, New York
29. Yang W, Thordarson P, Gooding JJ, Ringer SP, Braet F (2007) Carbon nanotubes for biological and biomedical applications. Nanotechnol 18:41
30. Williams L, Adams W (2007) Nanotechnology demystified. McGraw Hill Co., New York
31. Chen X, Lee GS, Zettl A, Bertozzi CR (2004) Biomimetic engineering of carbon nanotubes by using cell surface mucin mimics. Angew Chem Int Edn 43:6111–6116
32. Thordarson P, Le Droumaguet B, Velonia K (2006) Well-defined protein-polymer conjugates-synthesis and potential applications. Appl Microbiol Biotechnol 73:243–254
33. Wei W, Sethuraman A, Jin C, Monteiro-Riviere NA, Narayan RJ (2007) Biological properties of carbon nanotubes. J Nanosci Nanotechnol 7:1284–1297

34. Wang ZL (1998) Structural analysis of self-assembling nanocrystal superlattices. Adv Mater 10:13
35. Cui DX (2007) Advances and prospects on biomolecules functionalized carbon nanotubes. J Nanosci Nanotechnol 7:1298–1314
36. Torun O, Dudak FC, Bas D, Tamer U, Boyaci IH (2009) Thermodynamic analysis of the interaction between 3-aminophenylboronic acid and monosaccharides for development of biosensor. Sens Act B Chem 140:597–602
37. Zhang WJ, Li GX (2004) Third-generation biosensors based on the direct electron transfer of proteins. Anal Sci 20:603–610
38. Mor GK, Varghese OK, Paulose M, Shankar K, Grimes CA (2006) A review on highly ordered, vertically oriented TiO_2 nanotube arrays: fabrication, material properties, and solar energy applications. Sol Energ Mater Sol C 90:2011–2075
39. Liu SQ, Chen AC (2005) Coadsorption of horseradish peroxidase with thionine on TiO_2: nanotubes for biosensing. Langmuir 21:8409–8413
40. Kelsall RW, Hamley IW, Geoghegan M (2005) Nanoscale science and technology. Wiley, Hoboken/London
41. Smith LA, Ma PX (2004) Nano-fibrous scaffolds for tissue engineering. Colloids Surfaces B 39:125–131
42. Ramakrishna S, Fujihara K, Teo W-E, Lim T-C, Ma Z (2005) An Introduction to electrospinning and nanofibers. World Scientific Publishing Co. Pte. Ltd, Singapore
43. Ma Z, Kotaki M, Inai R, Ramakrishna S (2005) Potential of nanofiber matrix as tissue-engineering scaffolds. Tissue Eng 11:101–109
44. Barnes CP, Sell SA, Boland ED, Simpson DG, Bowlin GL (2007) Nanofiber technology: designing the next generation of tissue engineering scaffolds. Adv Drug Deliver Rev 59:1413–1433
45. Ondarcuhu T, Joachim C (1998) Drawing a single nanofibre over hundreds of microns. Europhys Lett 42:215–220
46. Feng L, Li SH, Li HJ, Zhai J, Song YL, Jiang L, Zhu DB (2002) Super-hydrophobic surface of aligned polyacrylonitrile nanofibers. Angew Chem Int Ed 41:1221–1223
47. Ashammakhi N, Ndreu A, Yang Y, Ylikauppila H, Nikkola L (2007) Nanofiber-based scaffolds for tissue engineering. Eur J Plast Surg. doi:10.1007/s00238-008-0217-3
48. Hartgerink JD, Benias E, Stupp SI (2001) Self-assembly and mineralization of peptide-amphiphile nanofibers. Science 294:1684–1688
49. Zhang S (2001) Fabrication of novel biomaterials through molecular self-assembly. Nat Biotechnol 21:1171–1178
50. Huanga ZM, Zhang YZ, Kotaki M, Ramakrishna S (2003) A review on polymer nanofibers by electrospinning and their applications in nanocomposites. Compos Sci Technol 63:2223–2253
51. Formhals A (1934) US Patent 1,975,504
52. Doshi J, Reneker DH (1995) Electrospinning process and applications of electrospun fibers. J Electrostat 35:151–160
53. Kim J, Junkin M, Kim DH, Kwon S, Shin YS, Wong PK, Gale BK (2009) Applications, techniques, and microfluidic interfacing for nanoscale biosensing. Microfluidics Nanofluidics 7:149–167
54. Urban GA (2009) Micro- and nanobiosensors-state of the art and trends. Meas Sci Technol 20:012001
55. Vo-Dinh T (2008) Nanosensing at the single cell level. Spectrochim Acta b 63:95–103
56. Choi JW, Oh BK, Kim YK, Min HJ (2007) Nanotechnology in biodevices. J Microbiol Biotechnol 17:5–14
57. Jain KK (2005) Nanotechnology in clinical laboratory diagnostics. Clin Chim Acta 358:37–54

Part IV
Processing/Fabrication

Chapter 20
ZnO Thin Films Deposited on Textile Material Substrates for Biomedical Applications

ZnO Thin Films Deposited on Textiles

L. Duta, A.C. Popescu, G. Dorcioman, I.N. Mihailescu, G.E. Stan, I. Zgura, I. Enculescu, and I. Dumitrescu

Abstract We report on the coating with ZnO adherent thin films of cotton woven fabrics by Pulsed laser deposition technique in order to obtain innovative textile materials, presenting protective effects against UV radiations and antifungal action.

Keywords ZnO thin films • Pulsed laser deposition • Antifungal action

20.1 Introduction

Fabrics combined with metal or oxide nanostructures may acquire properties that increase the wearer's degree of comfort over time. One of the materials that increase the efficiency of fabrics in creating comfort is zinc oxide (ZnO). ZnO is a semiconductor compound from the II–VI family that is nontoxic, biocompatible, and chemically stable under exposure to high temperature with a direct band gap (3.37 e-V at RT) in the UV range [1]. A pulsed laser deposition (PLD) technique was applied to obtain high-quality ZnO films [2–7].

The morphology and structure of ZnO depositions confer them a hydrophobic or hydrophilic behavior. When water comes in contact with the deposition, oxygen molecules are captured, thus minimizing the contact between water droplets and particles [8]. The hydrophobic behavior is associated with the high surface roughness. The purpose of this study was to cover fabrics with metal oxides thin films

L. Duta (✉) • A.C. Popescu • G. Dorcioman • I.N. Mihailescu
National Institute for Lasers, Magurele, Romania
e-mail: liviu.duta@inflpr.ro

G.E. Stan • I. Zgura • I. Enculescu
National Institute of Materials Physics, Magurele, Romania

I. Dumitrescu
National Institute for Textile and Leather, Bucharest, Romania

A. Vaseashta et al. (eds.), *Technological Innovations in Sensing and Detection of Chemical, Biological, Radiological, Nuclear Threats and Ecological Terrorism*, NATO Science for Peace and Security Series A: Chemistry and Biology,
DOI 10.1007/978-94-007-2488-4_20, © Springer Science+Business Media B.V. 2012

(TFs) by PLD, in order to promote their UV protective, antifungal and super hydrophobic behavior.

20.2 Materials and Methods

The PLD experiments were conducted inside a stainless steel deposition chamber. For the multi-pulse ablation of ZnO targets, we used a UV KrF* Excimer laser source ($\lambda = 248$ nm, $\tau_{FWHM} \approx 25$ ns, $\upsilon = 5$ Hz). The incident laser fluence was set at 3.3 J/cm^2.

We manufactured targets in the form of 2 cm diameter and 0.5 cm thick ZnO pellets, from commercially available powders that were pressed in a mould and sintered. The used substrates were plane fabric samples containing 56/44% cotton/polyester. For the deposition of one TF structure, we applied 10,000 subsequent laser pulses. The polyester side of the fabric was deposited with TF, while the cotton side, designed to enter in prolonged contact with the human skin, remained uncoated. For physical-chemical characterizations, we used Si(100) wafers, and for contact angle (CA) measurements, microscope slides.

The substrates were placed parallel to the target, at 4 cm separation distance. All depositions were carried out at room temperature. The ZnO TF coatings were deposited in high vacuum ($2*10^{-4}$ Pa). The identification of crystalline phases was carried out on a thick micronic ZnO film deposited on Si(100) by grazing the incidence X-ray diffraction (GIXRD). We used a Bruker D8 Advance diffractometer, in parallel beam setting, with monochromatised Cu $K_{\alpha 1}$ radiation ($\lambda = 1.5406$ Å). The incidence angle was set at 1°, and the scattered intensity was scanned in the range 20–60° (2θ), with a step size of 0.04°, and 30 s per step. The investigation of reflectivity properties on (200–3,300) nm domain were performed using a UV–Vis-NIR (Lambda 950, Perkin-Elmer) spectrometer. Air was considered as a reference.

The hydrophilic/hydrophobic features of the fabrics were investigated by static/dynamic CA studies. The measurements were made using the Drop Shape Analysis System, DSA100 model. The angle between the baseline of the drop and the tangent at the three-phase-line (solid/liquid/vapor) was measured. CAs were estimated by fitting a polynomial equation of second degree to the shape of the sessile drop and then calculating the slope of the tangent to the drop at the liquid-solid-vapor interface line. Aspergillus Niger (AN) fungi were used for mycological testing. The freshly prepared innoculus was mixed with the culture media (Czapek-Dox with 20% glucose) at 45°C. Further on, the mix was poured in Petri plates and left to solidify for 20 min. The textile samples were placed in the plates with the deposited side in contact with the medium. The samples incubation lasted up to 28 days and observations were performed after 3, 14, and 28 days, respectively.

20.3 Results and Discussion

As visible from SEM, the films were smooth copying the fibers morphology. A characteristic feature was the appearance of very fine cracks in the films extending along fibers. Their advent was a consequence of the tensions in the films developing during the bending of the textile fibers.

A GIXRD analyses evidenced that the PLD film consisted of a pure ZnO monophasic hexagonal wurtzite-type structure identical to the raw powder material. From reflection spectra, we observed that for control fabrics, the reflectivity was high and relatively constant over all investigated spectral domains, while for coated fabrics, it decreased to 40% for VIZ-NIR and 50–60% in the UV domain. We can assume that the reflectivity drop was due to the more intense absorption by the deposited ZnO TF.

For the CA studies, during the deposition process, a mask was interposed in order to functionalize only a precise region of the fabrics. Two water droplets (~2 μl each) were poured on the sample: one on the uncoated area (Fig. 20.1a), the other one on the deposited region (Fig. 20.1b). In the first case, the water droplet was instantaneously absorbed into the fabric's depth, while for the TF coating, it remained on the material's surface, in minimal contact till evaporation. The CA in case of the water droplet poured onto the TF was of 156.6°. Such high values of the CA are specific to a super hydrophobic behavior [9].

After 3 days on the control fabric, fungal activity was observed (Fig. 20.2a). This activity was enhanced after 14 and 28 days, AN proliferating on the entire surface of the fabrics (Fig. 20.2c, e). In case of the coated fabrics, fungal activity was completely stopped after 3 days (Fig. 20.2b). After 28 days, no traces of AN were remnant on the textiles, demonstrating the strong antimycotic effect of the TF structure (Fig. 20.2f).

20.4 Conclusions

ZnO TFs were pulsed laser deposited onto textile materials, in order to obtain antifungal and UV protective cloths for biomedical applications. SEM investigations evidenced smooth films with fine cracks covering entirely the textile fibers. The GIXRD investigations showed that the ZnO TF consisted of the hexagonal wurtzite-type phase only.

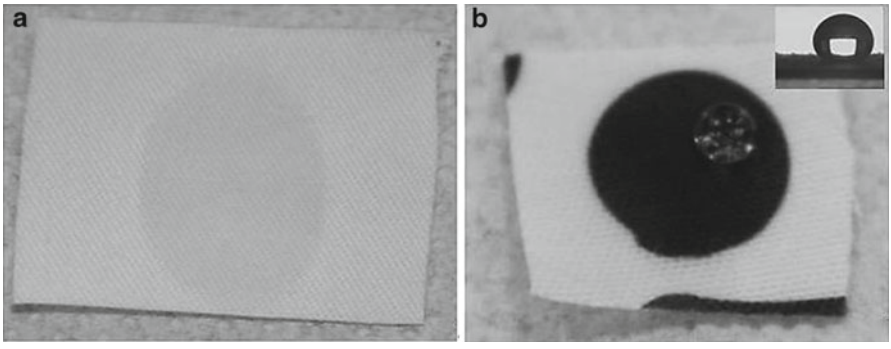

Fig. 20.1 Fabrics on which two water droplets were poured: on non-deposited region (**a**), the water droplet was completely absorbed while on deposited region (**b**), it was repelled. Shown in the inset is the image of static water droplet on the deposited fabric

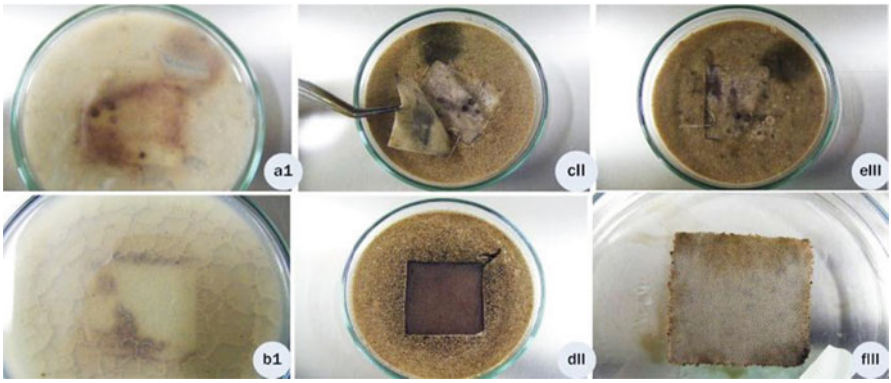

Fig. 20.2 Proliferation of AN fungi inoculated on control (**a**, **c**, **e**) and deposited fabrics (**b**, **d**, **f**), after 3 (I), 14 (II) and 28 (III) days

The optical measurements showed a decrease of reflectivity by a PLD coating suggesting the use of ZnO TF as anti protective layers. CA and wettability tests evidenced a super hydrophobic behavior for the ZnO depositions. Biological investigations presented inhibition of fungal development on the deposited fabrics, proving their antimycotic effect. All results support the conclusion that fabrics with TF coatings show improved UV protective, super hydrophobic, and antifungal performances.

References

1. Chen YF, Bagnall DM, Koh HJ, Park KT, Hiraga KJ, Zhu ZQ, Yao TF (1998) Plasma assisted molecular beam epitaxy of ZnO on c -plane sapphire- Growth and characterization. J Appl Phys 84(7):3912
2. Sasaki A, Hara W, Matsuda A, Tateda N, Saito K, Yoshimoto M (2005) Buffer-enhanced room-temperature growth and characterization of epitaxial ZnO thin films. Appl Phys Lett 86:231911
3. Jin BJ, Im S, Lee SY (2000) Violet and UV luminescence emitted from ZnO thin films grown on sapphire by pulsed laser deposition. Thin Solid Films 366(1–2):107
4. Fan XM, Lian JS, Guo ZX, Lu HJ (2005) Microstructure and photoluminescence properties of ZnO thin films grown by PLD on Si(111) substrates. Appl Surf Sci 239:176
5. Fan XM, Lian JS, Guo ZX, Lu HJ (2005) ZnO thin film formation on Si(111) by laser ablation of Zn target in oxygen atmosphere. J Cryst Growth 279:447
6. Ristoscu C, Mihailescu IN, Caiteanu D, Mihailescu CN, Mazingue TH, Escoubas L, Perrone A, Du H (2008) Nanostructured thin optical sensors for trace gas detection. In: Vaseashta A, Mihailescu IN (eds) Functionalized nanoscale materials, devices, & systems. Springer Science, Dordrecht, The Netherlands, pp 27–50
7. Socol G, Axente E, Ristoscu C, Sima F, Popescu A, Stefan N, Escoubas L, Ferreira J, Bakalova S, Szekeres A, Mihailescu IN (2007) Enhanced gas sensing of Au nanocluster –doped or –coated zinc oxide thin films. J Appl Phys 102:083103
8. Kuan CY, Hon MH, Chou JM, Leu IC (2009) Wetting characteristics on micro/nanostructured zinc oxide coatings. J Electrochem Soc 156(2):J32–J36
9. Wang S, Jiang L (2007) Definition of superhydrophobic states. Adv Mater 19:3423–3424

Chapter 21
Synthesis of Multifunctional Acrylic Copolymers for Chemical-Biosensors

Synthesis of Multifunctional Acrylic Copolymers

O. Slisenko, A. Tolstov, and R. Makuska

Abstract Functional acrylic copolymers of linear molecular architecture and different molecular weights based on $–SO_3H$ and –OH groups containing monomers were successfully synthesized via AGET ATRP in mixed solvents medium and characterized by NMR, SEC. The polymers could find different applications as stimuli-responsive modifiers to prepare high sensitive sensor surfaces.

Keywords ATRP • Acrylates • Polyelectrolytes • Sensing

21.1 Introduction

Nowadays, a controlled/living radical polymerization approach for the synthesis of polymers having well-defined structure, molecular weight and polydispersity [1] shows promise for preparation of advanced materials. These polymers could be widely used as sensors [2], efficient organics adsorbing, and/or ion-exchange materials for decontamination of environment [3].

One of the major applications of anionic-type polyelectrolytes is the preparation of sensor surfaces. Any action on the polymer-coated surface, like solvent replacement, change in a pH, temperature or other parameters of media induces changes in surface properties of modified substrate. Schematically, this process could be presented as follows (see Fig. 21.1).

O. Slisenko • A. Tolstov (✉)
Institute of Macromolecular Chemistry of the NAS of Ukraine, Kharkivske shose 48, 02160 Kyiv, Ukraine
e-mail: tolstov.aleksandr@rambler.ru

R. Makuska
Vilnius University, Naugarduko 24, Vilnius, Lithuania

A. Vaseashta et al. (eds.), *Technological Innovations in Sensing and Detection of Chemical, Biological, Radiological, Nuclear Threats and Ecological Terrorism*, NATO Science for Peace and Security Series A: Chemistry and Biology,
DOI 10.1007/978-94-007-2488-4_21, © Springer Science+Business Media B.V. 2012

Fig. 21.1 Molecular response of sensor polymer coatings under external influence

The aim of this work was to synthesize functional anionic polyelectrolytes having well-defined structure based on 2-acrylamido-2-methyl-1-propanesulfonic acid and 2-hydroxyethyl acrylate, which could be applied as efficient modifiers to prepare polymer-based sensor coatings.

21.2 Experimental

21.2.1 Materials

2-Acrylamido-2-methyl-1-propanesulfonic acid (AMPS; M_1), 2-hydroxyethyl acrylate (HEA; M_2), NaOH, $CuCl_2$ (or $CuBr_2$), 1,1,4,7,10,10-hexamethyltriethylenetetramine (HMTETA; L), ethyl 2-bromoisobutyrate (EBB; I), L-ascorbic acid (LAA; R) were analytical grade. Methanol, pyridine (Py) and distilled water were used optionally as solvents. HEA was additionally purified according to [4].

21.2.2 Synthesis of Copolymers

The synthesis of linear poly(AMPS-*co*-HEA) copolymers was carried out via a typical AGET ATRP procedure [5]. Before polymerization, the AMPS monomer was changed in sodium salt form to prevent Cu-catalyst decomposition. The reagents ratio and conditions of the process were summarized in Table 21.1. The resulting copolymer solutions were intensively dialyzed for 48 h against distilled water followed by passing methanol solution through silica gel column. The purified polymers were dried on air at ambient temperature and further in a high vacuum to a constant weight. The scheme of the synthesis of poly(AMPS-*co*-HEA) polyelectrolytes is presented in Fig. 21.2.

21.2.3 Characterization

A ^{1}H-NMR was measured on a Bruker AC-250 instrument at room temperature with D_2O as a solvent. The SEC curves were obtained using SEC instrument

Table 21.1 Samples composition and synthesis conditions

Sample	$[M_1/M_2]:[I]:[Cu^{2+}]:$ [L]:[R] ratio, mol	Medium (v/v)	Conditions (hours/°C)
PolyAMPS	200/0:1:2[a]:2:1	H_2O	10/25
PolyHEA	0/200:1:2[a]:2:1	$Py/H_2O = 1/1$	0.5/25[b]
Copolymer-1	180/20:1:2[c]:2:1	$Py/H_2O = 1/1$	10/25
Copolymer-2	140/60:1:2[c]:2:1	$Py/H_2O = 1/1$	10/25
Copolymer-2a	700/300:1:5[a]:5:2,5	$Py/H_2O = 1/1$	10/25
Copolymer-3	100/100:1:2[c]:2:1	$Py/H_2O = 1/1$	10/25

[a]$CuCl_2$
[b]Crosslinking
[c]$CuBr_2$

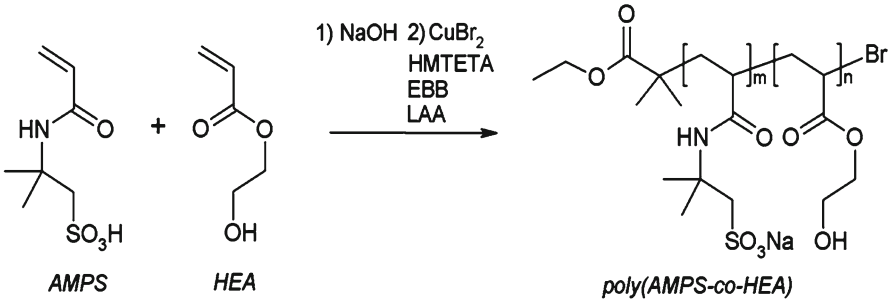

Fig. 21.2 Synthetic route of poly(AMPS-co-HEA) copolymers preparation

equipped with two columns with PL gel MIXED-B LS, PL-ELS-1000 detector. A 0.1 M NaCl solution was employed as eluant at a flow rate of 0.5 mL/min and the injection volume of the sample solution of 0.1 mL. The values of M_n, M_w and polydispersity, PD, were estimated.

21.3 Results and Discussion

Copolymers composition calculated from ^{1}H-NMR data was summarized in Table 21.2. It was found that a deviation of the composition of synthesized copolymers, as well as molecular weights, from the initial (or theoretical) values is applicable and could be due to some undesired processes realized during polymerization process. According to the literature data for polymers of similar chemical structure, the polydispersity values for AMPS/HEA-based polymers are narrow and depend on the components ratio in the initial reactive composition.

Table 21.2 Characteristics of synthesized homo- and copolymers

Sample	$[M_1]:[M_2]$, mol		$M_{n,theor} \times 10^{-3}$	$M_{n,SEC} \times 10^{-3}$	$M_{w,SEC} \times 10^{-3}$	PD
	Initial	Obtained				
PolyAMPS	200:0	200:0	46.1	297.3	715.1	2.41
PolyHEA	0:200	0:200	23.2	–	–	–
Copolymer-1	180:20	162:38	43.8	59.6	133.7	2.24
Copolymer-2	140:60	130:70	39.2	48.4	128.5	2.65
Copolymer-2a	700:300	681:319	196.0	57.2	177.2	3.10
Copolymer-3	100:100	100:100	34.6	104.4	196.2	1.88

Thus, the polydispersity of synthesized polymers have appropriate value for preparation of efficient sensor polymer coatings on different substrates. To prove this conclusion, corresponding studies are planned.

21.4 Conclusions

Based on the results the follow conclusions are drawn. Functional acrylic copolymer anionic-type polyelectrolytes have been successfully synthesized and characterized. M_n and M_w values of the copolymers are varied in the range of ~0.48–1.05 × 10^5 and 1.29–1.96 × 10^5. The polydispersity values of poly(AMPS-*co*-HEA) for such molecular weights are appropriate for preparation of efficient sensor, stimuli-responsive polymer coatings.

References

1. Braunecker WA, Matyjaszewski K (2007) Controlled/living radical polymerization: features, developments, and perspectives. Prog Polym Sci 32(1):93–146
2. Kurata K, Dobashi A (2004) Novel temperature- and pH-responsive linear polymers and cross-linked hydrogels comprised of acidic L-α-amino acid derivatives. J Macromol Sci A 41(2): 143–164
3. Cavus S, Gurdag G (2008) Competitive heavy metal removal by poly(2-acrylamido-2-methyl-1-propane sulfonic acid-co-itaconic acid). Polym Adv Technol 19(9):1209–1217
4. Coca S, Jasieczek CB, Beers KL, Matyjaszewski K (1998) Polymerization of acrylates by atom transfer radical polymerization. Homopolymerization of 2-hydroxyethyl acrylate. J Polym Sci A 36(9):1417–1424
5. Zhao K, Cheng Z, Zhang Z, Zhu J, Zhu X (2009) Synthesis of fluorescent poly(methyl methacrylate) via AGET ATRP. Polym Bull 63(3):355–364

Chapter 22
Synthesis of Hollow Silica Microspheres with High-Developed Surface Area

Synthesis of Hollow Silica Microspheres

I. Bei, A. Tolstov, and A. Ishchenko

Abstract Hollow silica microspheres (HSM), as efficient drug delivery carriers, were successfully prepared via a facile water-in-oil emulsion method using water glass precursor. The kinetics of drug release in aqueous medium was simulated using water-soluble erythrosine. Hollow silica microspheres show intensive release of active component at the beginning stages of introduction into aqueous (organism-imitating) conditions. Release rate of the model compound decreased and desorption time increased in the follow range: hollow silica microspheres > porous silica microparticles > silica nanoparticles.

Keywords Silica microspheres • Carriers • Absorbents • Controlled release

22.1 Introduction

The highly intensive search of new materials for drug delivery is a priority area in medicine and chemical science for the last decade [1]. Some known carriers do not provide an appropriate release rate when introduced into the inward parts of human body. Thus, the search and development of high-performance nontoxic and biocompatible carriers for efficient drug delivery and release procedures is a very important goal for modern material, medical and pharmaceutical sciences.

In this work, the hollow silica microspheres, HSM, were successfully synthesized and analyzed for efficient drug release using water-soluble model compounds.

I. Bei (✉) • A. Tolstov • A. Ishchenko
Institute of Macromolecular Chemistry of the NAS of Ukraine, Kharkivske shose 48, 02160 Kyiv, Ukraine
e-mail: irynabei@meta.ua

A. Vaseashta et al. (eds.), *Technological Innovations in Sensing and Detection of Chemical, Biological, Radiological, Nuclear Threats and Ecological Terrorism*, NATO Science for Peace and Security Series A: Chemistry and Biology,
DOI 10.1007/978-94-007-2488-4_22, © Springer Science+Business Media B.V. 2012

22.2 Experimental

22.2.1 Reagents

Water glass ($Na_2O{\cdot}xSiO_2{\cdot}yH_2O$, $Na_2O/SiO_2 = 3.0$, density 1.40 g/mL), hexane, distilled water, $NaHCO_3$, *i*-$C_9H_{19}C_6H_4O(C_2H_4O)_nH$ and N,N-di-(2-hydroxyethyl)-cocamide (both are non-ionic surfactants) were analytical grade and used as received. A water-soluble erythrosine was used as a model compound. For reference samples two types of silica, namely highly porous silica microparticles and silica nanoparticles (AEROSIL A-175) were used.

22.2.2 Preparation of Hollow Silica Microspheres

Preparation of HSM was carried out using a slightly modified water-in-oil emulsion technique [2] using hexane as organic (oil) phase and non-ionic surfactants of other chemical structure. Raw microspheres were washed by hexane and water for several times to remove all reagents.

22.2.3 Loading and Release of Erythrosine

Erythrosine, which was used as a model, has been loaded into HSM by immersing of the sample in 1 mg/mL water solution for 96 h. After that, the solution was decanted from the silica sample and kinetics of the model release in aqueous medium was studied. A release rate (mg/h) of erythrosine during desorption process and desorption time were determined and discussed. The same procedures were performed with other types of the silica samples.

22.2.4 Characterization

FTIR studies of the samples were carried out by a Bruker Tensor™ 37 FTIR analyzer. SEM characterization was performed by a JEOL JSM 6060 microscope at an operating voltage of 30 kV. The kinetics of erythrosine release was studied by a spectrophotometer SP-46. The erythrosine content was determined at $\lambda_{abs} = 540$ nm.

22.3 Results and Discussion

In Fig. 22.1, it can be seen that the size of prepared HSM is in the range of 100–350 nm, but actually, a sphere size of main fraction (>90%) is at about 250 nm. The wall thickness of prepared spheres is about 35 nm and varied unsubstantially.

Figure 22.2 shows FTIR curves of HSM, model compound and HSM/model before desorption process. Due to a relatively low concentration of erythrosine, corresponding bands of the model are unresolved at presented scale. This fact did not make it possible to determine the physical bonding of model compounds with silanol groups of HSM surface. However, it was clearly found that a strong high frequency shift of ν_{OH} complex band centered at 3,291–3,394 cm^{-1} occurred due to adecreasing H-bonded hydroxyls content as a result of adsorption of the model molecules onto silica surface and their interaction with one.

Erythrosine release kinetics studies are presented in Table 22.1. It was found that the particle size did not play a significant role in the release process, whereas porosity and, especially, structure features of the particles are very important parameters. The hollow structure of silica microspheres provides an erythrosine release rate ten times higher than that of the other types of silica samples. Moreover, desorption

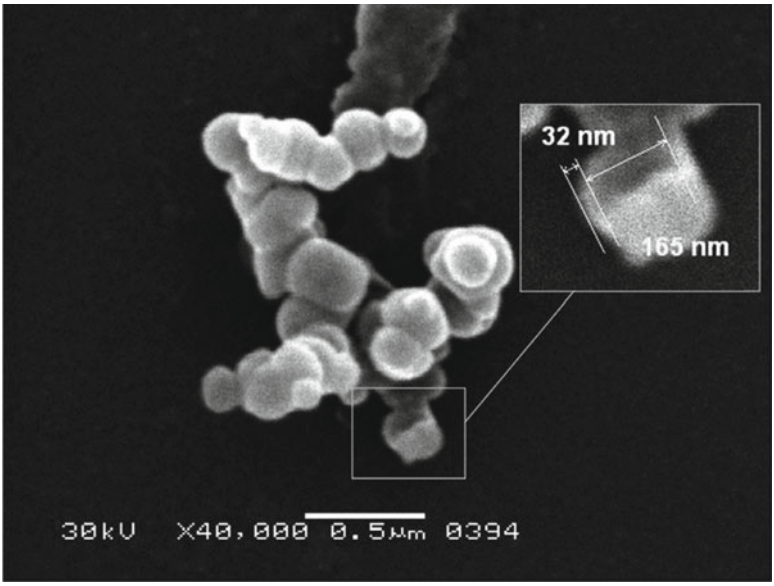

Fig. 22.1 SEM image of prepared hollow silica microspheres. Inset image is an enlarged photograph of a single sphere

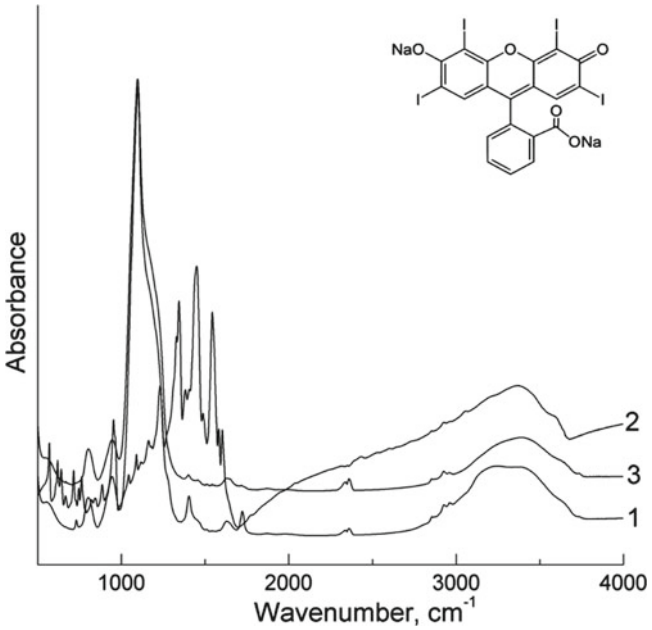

Fig. 22.2 FTIR curves of (*1*) HSM, (*2*) erythrosine, and (*3*) HSM/erythrosine system. The inset image presents the structure of erythrosine

Table 22.1 Erythrosine release kinetics studies data

Sample	Averaged SiO_2 particles size, μm	Release rate, mg/g· hour (for first 10 h)	Desorption time, hours (desorption >90%)
Eryth-SiO_2-spheres	0.25	0.204	33.6
Eryth-Silica gel	30	0.018	36.3
Eryth-AEROSIL	0.012	0.019	39.0

time of erythrosine for HSM sample is shorter than that for silica samples. These features of behavior should also provide fast delivery of corresponding active agents, like antibiotics, for efficient action of the drugs on pathogens.

22.4 Conclusions

The results suggested that it is possible to prepare hollow silica microspheres carriers for efficient release of drug simulated compound. The release kinetics studies have shown that these microspheres are much more efficient than other silica

samples (micrometer sized silica gel, silica nanoparticles). Prepared hollow silica particles could be widely applied as non-toxic and biocompatible drug delivery carriers for internal uses.

References

1. Wang S (2009) Ordered mesoporous materials for drug delivery. Micropor Mesopor Mater 117(1):1–9
2. Fujiwara M, Shiokawa K, Tanaka Y, Nakahara Y (2004) Preparation and formation mechanism of silica microcapsules (hollow sphere) by water/oil/water interfacial reaction. Chem Mater 16(25):5420–5426

Chapter 23
Inorganic Nanoparticle as a Carrier for Hepatitis B Viral Capsids

Inorganic Nanoparticle as a Viral Capsid Carrier

Yu. Dekhtyar, M. Romanova, A. Kachanovska, D. Skrastiņa, R. Reinhofa, P. Pumpens, and A. Patmalnieks

Abstract Virus like particles (VLP) are used to transport immune response-modulating agents to target cells to treat them. In order to deliver a high concentration of VLP to the cell, a number of VLP can be attached to a nanoparticle to be used as a nanolorry. In this study, SiO_2 nanoparticles were attached to Hepatitis B VLP. Spectrophotometry measurements, electron, and fluorescent microscopy evidence showed that the SiO_2 – Hepatitis B VLP complexes were formed.

Keywords Virus like particles • Silica nanoparticles • Nanolorry • Immunomodulation

23.1 Introduction

Virus like particles (VLP) can be used as immune response-modulating agents that stimulate immune system to respond effectively to a viral infection. VLP are injected into the blood vessels to be delivered to specific cells, thus causing treatment effects. Treatment efficiency is higher when the concentration of VLP near the target cells is high as well. However, the latter can lead to toxic effects.

Yu. Dekhtyar • D. Skrastiņa • R. Reinhofa • P. Pumpens
Biomedical Research and Study Centre, Riga, Latvia

M. Romanova (✉) • A. Kachanovska
Institute of Biological Engineering and Nanotechnology, Riga Technical University, Kalku Str. 1, Riga, Latvia
e-mail: marina.romanova@inbox.lv

A. Patmalnieks
University of Latvia, Riga, Latvia

A. Vaseashta et al. (eds.), *Technological Innovations in Sensing and Detection of Chemical, Biological, Radiological, Nuclear Threats and Ecological Terrorism*, NATO Science for Peace and Security Series A: Chemistry and Biology,
DOI 10.1007/978-94-007-2488-4_23, © Springer Science+Business Media B.V. 2012

To avoid this, the high concentration of VLP has to be supplied only in a vicinity of the target cells. To reach this, a number of VLP could be attached to a nanoparticle that will act as the nanolorry to deliver VLP. Thus, the overall concentration of VLP in the human organism will be decreased in spite of the high concentration near the cell. Taking into account that the electrical charge is localized at the surface of VLP [1], the latter could be attached to the nanoparticle due to the Coulomb interaction, if the surface of a nanoparticle has an opposite charge. The nanoparticle must be harmless in respect to the human organism. Both conditions are satisfied by SiO_2 nanoparticles [2, 3]. The aim of the study is to verify a capability of SiO_2 nanoparticles to attach VLP, hepatitis B viral capsids being in use as a model.

23.2 Materials

VLP (hepatitis B viral capsids) were provided by the Latvian Biomedical Research and Study Centre. Certified SiO_2 nanoparticles were bought from the Sigma-Aldrich. Size of the nanoparticles was equal to 10–20 nm.

23.3 Methods

To study the capability of SiO_2 nanoparticles to attach VLP, the optical absorbance spectra of VLP, SiO_2 nanoparticles and VLP+SiO_2 mixture in buffered solutions were recorded and compared. Alterations of optical absorbance spectra of VLP+SiO_2 mixture and their time dependent behaviour in comparison with the spectra of VLP and/or SiO_2 were expected because of the attachment of VLP to silica nanoparticles.

The Thermo Spectronic Helios Gamma spectrophotometer was in use to record absorbance at wavelengths 200–1,090 nm. VLP were contained in buffered solution prepared from 20 mM Tris-HCl pH 7.8, 5 mM EDTA, 150 mM NaCl, and 1 l distilled water. NaCl concentration was equal to the concentration in the physiological solution. 1 mg of SiO_2 nanoparticles was mixed with 1 ml of the buffer solution. The concentration of VLP was 12 μl in 1 ml of the solution that corresponded to optical absorbance value 1 (±5%) at wavelength 260 nm. The value 12 μl resulted from the calibration procedure to reach the Beer-Lambert condition. Transmission electron microscopy (TEM) and fluorescence microscopy (FM) were employed to observe VLP. JEOL JEM-1200EX microscope was in use for TEM, and Leica DMI 3000 B microscope for FM. To record the fluorescence, VLP were marked with green FITC agent that forms covalent bonds with VLP amino acids. Fluorescence was excited at 490 nm and detected at 515 nm.

23.4 Results and Discussion

Figure 23.1 provides the optical absorbance spectra of the SiO_2 and VLP+SiO_2 solutions. The absorbance decreased during 24 h and precipitations were observed at the bottom of the test-tube. Precipitation could obviously result due to the gravitation forces. The absorbance of the VLP solution did not change during 24 h and no precipitations were formed. It was assumed that SiO_2 nanoparticles remained motionless during the absorbance measurement because measurement time was much shorter (~1 min) than the time interval needed to observe the instability of the spectra (24 h).

The absorbances of the VLP and SiO_2 solutions relaxed in time were superposed at 260 nm and compared with the one observed from the experiment (Fig. 23.2). The superposed graph (the dashed line) differs from the one from the experiment (the solid line).

This gives evidence that VLP and SiO_2 nanoparticles form complexes. TEM showed that VLP and SiO_2 nanoparticles attached to each other (Fig. 23.3).

Fluorescence microscopy gave more evidence on the VLP+SiO_2 coupling (Fig. 23.4). The VLP solution without the nanoparticles had homogeneous fluorescence. When SiO_2 nanoparticles were added to the VLP solution, fluorescence existed only in the areas where SiO_2 nanoparticles were present.

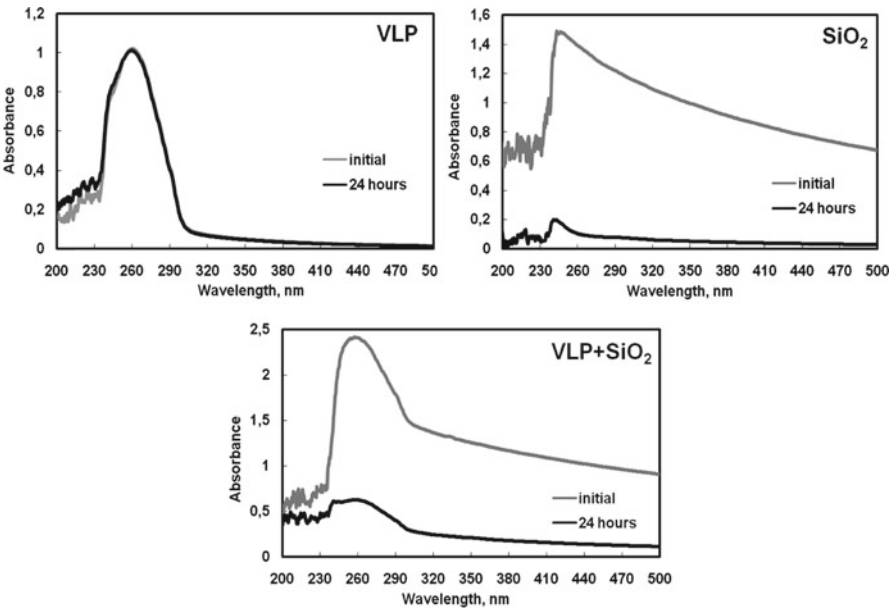

Fig. 23.1 The alteration of optical absorbance of the VLP, SiO_2 and VLP+SiO_2 solutions influenced by time

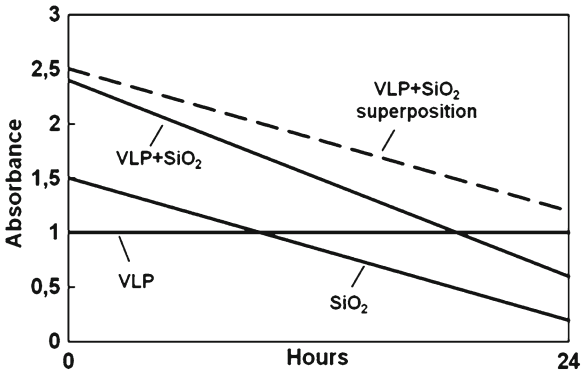

Fig. 23.2 Changes in the optical absorbance (at 260 nm) in solutions during 24 h

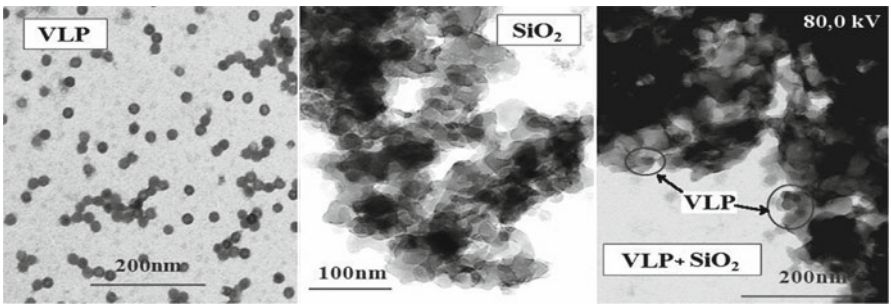

Fig. 23.3 TEM micrographs of the VLP, SiO_2, VLP+SiO_2 solutions

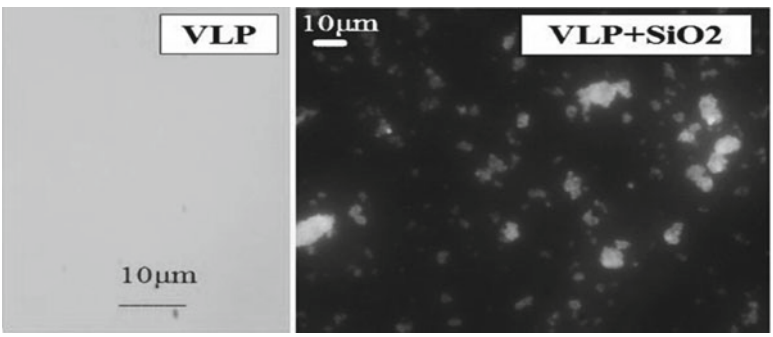

Fig. 23.4 FM micrographs of VLP and VLP+SiO_2 solutions

23.5 Conclusions

Spectrophotometry and fluorescence microscopy showed that the hepatitis B VLP+SiO_2 complexes were achieved in buffered solution. The hepatitis B VLP+SiO_2 complexes perhaps could be in use to transport VLP to the cells.

References

1. Virus Particle Explorer. Human Hepatitis B Viral Capsid. http://viperdb.scripps.edu/info_page.php?VDB=1qgt
2. He-sheng C, Zhen-ya S, Li-hui X (2004) Properties of nano SiO_2 modified PVF adhesive. J Wuhan Univ Technol Mater Sci Ed 19:73–75
3. Sealy C (2006) Silica key to drug delivery. Nano Today 1:19

Chapter 24
Glycerine Treatment of Poly-Perfluorosulphonic Acid Membrane Modified by Sulfonamide Groups

Glycerine Treatment of PFSA-NH Membrane

A. Andronie, I. Stamatin, S. Iordache, Ana Cucu, S. Stamatin, and S. Antohe

Abstract Poly-perfluorosulfonic acid (PFSA) membranes modified by sulfonamide groups are obtained by ammonia treatment followed by a glycerine treatment. Fourier transform infrared spectroscopy (FT-IR) was used for identifying the specific functional groups. Thermal properties, such as glass transition and degradation, are studied by Differential Scanning Calorimetry (DSC) and by Thermo Gravimetric Analysis (TGA). The in-plane four-electrode technique was used for obtaining proton conductivity values as function of temperature.

Keywords PFSA membrane • Proton conductivity • Fuel cell

24.1 Introduction

Proton exchange membrane fuel cells research focused on developing new proton conducting polymer membranes operating at high temperatures, of up to 200°C, and less expensive catalysts for replacing Pt and Ru – based catalysts and bipolar plates [1]. Among proton exchange membranes, PFSA membranes are the most commonly used [1]. A major disadvantage of PFSA membranes is the low ionic conductivity at a low relative humidity and/or at high operating temperatures, because of the chemical degradation processes [2–4]. In this paper, physical properties of perfluorosulfonated

A. Andronie (✉) • I. Stamatin • S. Iordache • A. Cucu • S. Stamatin
Physics Department, 3Nano-SAE Research Centre, University of Bucharest, Magurele, Bucharest, Romania
e-mail: andronie@3nanosae.org

S. Antohe
Physics Department, University of Bucharest, Bucharest, Romania

A. Vaseashta et al. (eds.), *Technological Innovations in Sensing and Detection of Chemical, Biological, Radiological, Nuclear Threats and Ecological Terrorism*, NATO Science for Peace and Security Series A: Chemistry and Biology,
DOI 10.1007/978-94-007-2488-4_24, © Springer Science+Business Media B.V. 2012

modified/cross linked by amide groups are studied as a potential mechanical and chemical stable proton exchange membrane for fuel cell applications.

24.2 Experimental

A Fumapem-1050 PFSA membrane was treated as follows: immersed in a solution of 500 mg potassium hydroxide in 50 ml of 28% aqueous ammonia at 10°C for 3 h, heated at 200°C for 30 min, then the procedure was repeated, treated in 10% solution of potassium hydroxide for 2 h at 80°C, acid exchange treatment in 10% hydrochloric acid solution, soaked in glycerine for 48 h. Samples were indexed as follows: F1050 – the initial PFSA membrane, F1050-NH-Gy – the modified membrane.

The membrane water uptake (WU) was determined as follows: samples were soaked in water for 24 h and weighed immediately after blotting the free surface water; then, the wet membranes were dried for 12 h at 80°C: $WU(\%) = (M_{wet} - M_{dry})/M_{dry} * 100$.

The ion exchange capacity (IEC) was determined as follows: acidic form membranes were converted to salt form by immersion in 1M NaCl solutions for 24 h; the exchanged H+ ions in solutions were titrated with 0.05 M NaOH solutions: IEC(meq/g) = ml NaOH x molarity NaOH/dry membrane weight. The FT-IR spectra were obtained in transmission in the interval 4,000–400 cm^{-1} with a FT-IR Jasco Spectrometer, 4 cm^{-1} resolution.

Thermal analyses were performed by means of DSC (Mettler Toledo) and TGA (Mettler Toledo) in air at a heating rate of 10°C/min in range 25–470°C. The conductivity was measured via four-point BekkTech conductivity test cell (BT-512 Membrane Conductivity Test System, Bekktech LLC, USA) in the temperature interval 30–95°C.

24.3 Results

Conformational differences between F1050 and F1050-NH-Gy have a strong influence on WU and on IEC (Table 24.1). This difference can be justified by the cross linking of the membrane, an effect that limits the hydration level and affects also IEC values.

FT-IR spectra (Fig. 24.1) show specific peaks of the perfluorosulfonated membrane backbone, similar to other reported results [5]. In the F1050-NH-Gy spectrum, the 2,300 cm^{-1} peak shows an increase in cross-linking degree, due to carboxyl groups.

Table 24.1 PFSA membrane characteristics

Sample code	Water uptake (%)	IEC (meq/g)
F1050	28.50%	1.018
F1050-NH-GY	17.02%	0.625

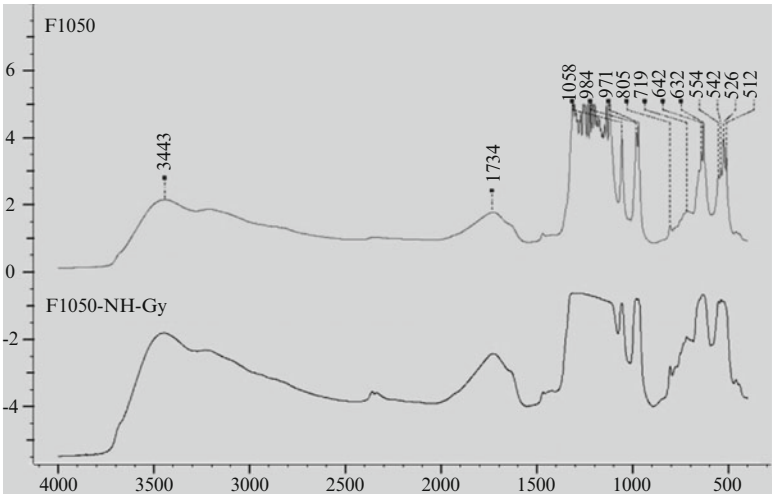

Fig. 24.1 FT-IR spectra of F1050 and F1050-NH-Gy membranes

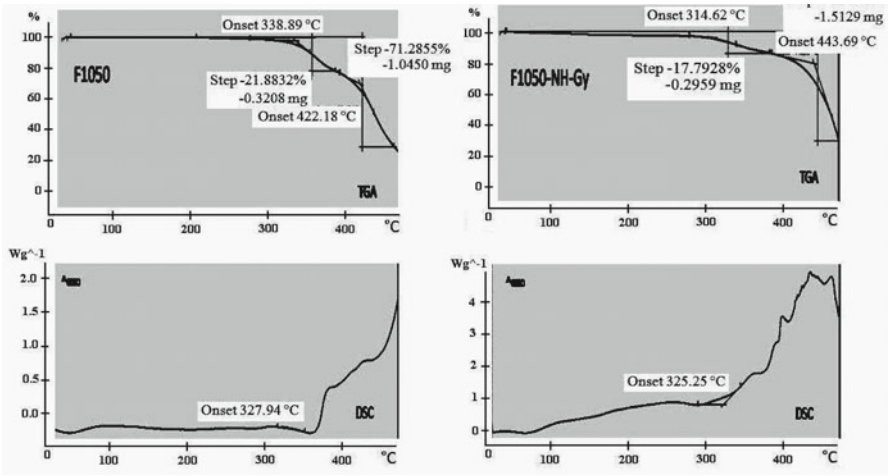

Fig. 24.2 Thermal behaviour of F1050 and F1050-NH3 – TGA and DSC (^exo)

DSC and TGA curves (Fig. 24.2) reveal specific thermal behavior features. Although the onset temperature is lower for the modified membrane, the mass loss associated to this process is lower.

Ionic conductivity measured at a fixed relative humidity (70%) has a specific dependence on the temperature, whereas three distinct regions appear in the conductivity vs. temperature logarithmic representation (Fig. 24.3).

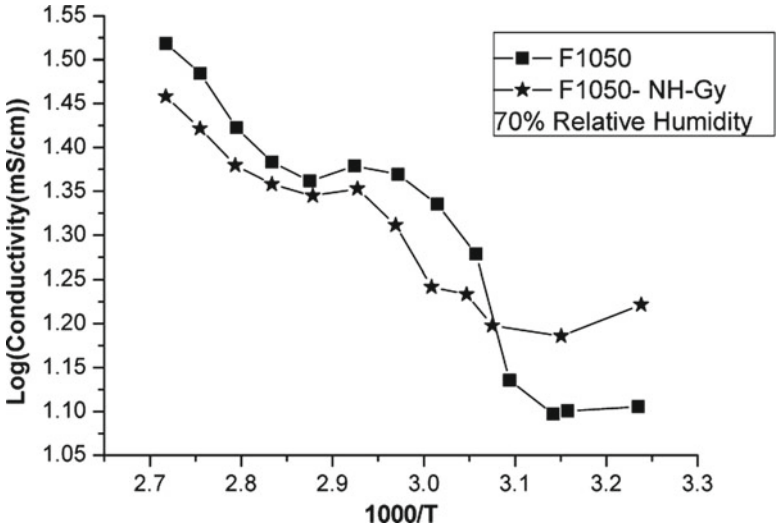

Fig. 24.3 Logarithmic representation of the conductivity vs. temperature at a relative humidity of 70% for F1050 and F1050-NH-Gy membranes

24.4 Conclusions

F-1050 PFSA membrane was modified by sulfonamide groups via ammonia treatment followed by a glycerine treatment. DSC and TGA analyses prove that the modified membrane has a thermally stable structure. The F1050-NH-Gy membrane shows a higher conductivity than F1050 at low temperatures, without a notable influence at temperatures above 55°C. Therefore, studies are planned in order to analyze the possibility of direct methanol fuel cell application.

Acknowledgements The authors acknowledge research support provided under Grant PNII No. 11-024/2007, 22-136/2008, 72-177/2008.

References

1. Ho WS, Sirkar KK (1992) Membrane handbook. Van Nostrand Reinhold, New York
2. Yeo SC, Eisenberg A (2003) Physical properties and supermolecular structure of perfluorinated ion-containing (Nafion) polymers. J Appl Polym Sci 21(4):875–898
3. Wakizoe M, Velev OA, Srinivasan S (1995) Analysis of proton exchange membrane fuel cell performance with alternate membranes. Electrochim Acta 40(3):335–344
4. Gebel G (2000) Structural evolution of water swollen perfluorosulfonated ionomers from dry membrane to solution. Polymer 41(15):5829–5838
5. Liang Z, Chen W, Liu J, Wang S, Zhou Z, Li W, Sun G, Xin Q (2004) FT-IR study of the microstructure of Nafion® membrane. J Membr Sci 233(1–2):39–44

Chapter 25
Pulsed Laser Processing of Functionalized Polysaccharides for Controlled Release Drug Delivery Systems

Functionalized Polysaccharides Processed for Drug Delivery

R. Cristescu, C. Popescu, A.C. Popescu, G. Socol, I. Mihailescu, G. Caraene, R. Albulescu, T. Buruiana, and D. Chrisey

Abstract We report on the deposition of triacetate-pullulan polysaccharide thin films on drug pellets (diclofenac sodium) by matrix assisted pulsed laser evaporation method. The radiation generated by a pulsed excimer KrF* laser source ($\lambda = 248$ nm, $\tau = 20$ ns) operated at 2 Hz repetition rate was used for ice targets evaporation. The timed – controlled drug delivery was proved by spectroscopic *in vitro* studies and *in vivo* anti-inflammatory investigations on rabbits. We showed that the coating of drug pellets with triacetate-pullulan thin films resulted in the delayed delivery of the drug for up to 30 min.

Keywords Controlled drug release • Triacetate • MAPLE

R. Cristescu (✉) • C. Popescu • A.C. Popescu • G. Socol • I. Mihailescu
Plasma and Radiations Physics, National Institute for Lasers, 409 Atomistilor, Bucharest-Magurele, Romania
e-mail: rodica.cristescu@inflpr.ro

G. Caraene • R. Albulescu
Institute for Chemical-Pharmaceutical, Bucharest, Romania

T. Buruiana
Petru Poni Institute of Macromolecular Chemistry, Iasi, Romania

D. Chrisey
Department of Materials Science & Biomedical Engineering, School of Engineering, Rensselaer Polytechnic Institute, Troy, NY, USA

A. Vaseashta et al. (eds.), *Technological Innovations in Sensing and Detection of Chemical, Biological, Radiological, Nuclear Threats and Ecological Terrorism*, NATO Science for Peace and Security Series A: Chemistry and Biology,
DOI 10.1007/978-94-007-2488-4_25, © Springer Science+Business Media B.V. 2012

25.1 Introduction

Research in drug delivery and targeting systems has traditionally focused on maintaining the drug levels within a desired therapeutic range inside the affected regions, and to prevent side effects associated with over and under dosing [1–3]. However, to accomplish precise control of the drug, biodegradable coating multilayers are required and these prerequisites are generally incompatible with conventional wet chemical casting. We proposed the use of biopolymer (triacetate-pullulan) coating of active drug substance pellets (diclofenac sodium) to ensure the controlled drug delivery in the organism of test (rabbits) animals. To this purpose, we deposited triacetate-pullulan thin films onto the surface of active drug pellets by matrix-assisted pulsed laser evaporation (MAPLE) method using a KrF* excimer laser source ($\lambda = 248$ nm, $\tau = 20$ ns, $\nu = 2$ Hz). The novel part of our contribution consists in studying the biocompatibility and active substance release by dedicated *in-vitro* and *in-vivo* studies.

25.2 Experimental

25.2.1 Materials

We synthesized triacetate-pullulan, a derivative of pullulan (P-20 type), following a patented original method by the National Institute for Chemical-Pharmaceutical R&D, Bucharest, Romania [4]. Triacetate-pullulan with a substitution degree of about 2.9 was obtained by an esterification reaction of the hydroxyl groups with acetic anhydride in acetic acid medium and in the presence of sulphuric acid. This biopolymer is soluble in organic solvents as chloroform, methylene chloride, acetone, DMF and DMSO. In our study we used the chloroform (having a melting point of 209 K) as a solvent in MAPLE experiments because of its good absorptivity at the 248 nm (the KrF* laser wavelength) [5, 6]. As an active pharmaceutical agent, we selected the diclofenac sodium in tablets of 25 mg dose. This is a well-known non-steroidal anti-inflammatory drug.

25.2.2 Deposition Conditions

The colloidal solutions containing less than 2% triacetate-pullulan in chloroform were carefully mixed and then frozen at liquid nitrogen temperature. After freezing, the obtained ice targets were rapidly mounted inside the deposition chamber and rotated with 0.25 Hz to avoid overheating and possible piercing by multipulse laser evaporation. Prior to deposition, the chamber was evacuated down to a residual pressure of 13 Pa. Thin films of triacetate-pullulan were obtained with a KrF*

laser source generating pulses of 248 nm wavelength and 20 ns duration at a frequency repetition rate of 2 Hz. The laser radiation was focused by a fused silica lens placed outside the chamber. The incident angle of the laser beam was 45°. During deposition, the drug pellet substrate was kept at room temperature. The target–substrate distance was set at 4 cm. After preliminary tests and according to previous experience [7, 8] we used an incident laser fluence of 400 mJ/cm^2. The irradiation spot area was 11.5 mm^2. The number of pulses applied for the deposition of one film was 15,000.

For *in vitro* tests, few trials have been performed in view of establishing the dispersion/solubilization conditions of the active substance. The diclofenac sodium was solved in different dispersion/solubilization environments: (i) Physiologic serum (pH = 5.5), (ii) Basic physiologic serum with NaOH, (pH = 8.5 corresponding to small intestine), and (iii) Acidic physiologic serum with HCl, (pH = 3 corresponding to stomach). The used concentration was 25 mg active substance in 10 ml dispersion/solubilization environment. To measure *in vitro* time-release profiles from uncoated and coated (with MAPLE-deposited thin films) drug pellets we followed a specific protocol: two sets of uncoated and coated pellets were immersed in 50 ml basic physiologic serum (pH = 8.5) placed in two Erlenmeyer recipients. All experiments were performed at 37°C while recipients were stirred at every 30 min. UV/VIS spectra of the active substance in solution were recorded with a Secomam – Dathelie UV/VIS spectrophotometer taking the dispersion/solubilization environment as reference. In case of *in vivo* tests the pellets were administered (12 mg/kg) to two sets of *Chinchilla* rabbits. After 30 min, both rabbits' ears were moistened for 35 times with an inflammatory solution: pyridine (10 ml), distilled water (2.5 ml), volatile Oleum Sinapis and ethylic ether. The ear thickness was monitored every 30 min.

25.3 Results and Discussion

25.3.1 In Vitro Tests

The dispersion/solubilization conditions and corresponding response times of gastroresistant coating were given in Table 25.1. Following these data, the basic physiologic serum with NaOH, pH = 8.5 was further used due to the resonable response time of 30 min only. The diclofenac sodium concentration in the dispersion/solubilization environment was 0.05 mg/ml.

To monitor *in vitro* time release profile of the active drug the UV/VIS spectra were recorded (Fig. 25.1).

The spectrum in Fig. 25.1 exhibits two absorption maxima at 214 and 277 nm. *In vitro* time release profiles of the active drug were next obtained at these two characteristic wavelengths. The absorbance results at 214 and 277 nm for 3 h and 30 min recording time were represented in Figs. 25.2 and 25.3.

Table 25.1 Dispersion/solubilization conditions and response times

#	Dispersion/solubilization environment @ 37°C (25 Mg/10 Ml)	Dispersion/solubilization response time of gastroresistant coating (H)
1	Physiologic serum, pH = 5.5	6 – too slow
2	Basic physiologic serum with NaOH, pH = 8.5	0.5 – optimal conditions
3	Acidic physiologic serum with HCl, pH = 3	No solubility

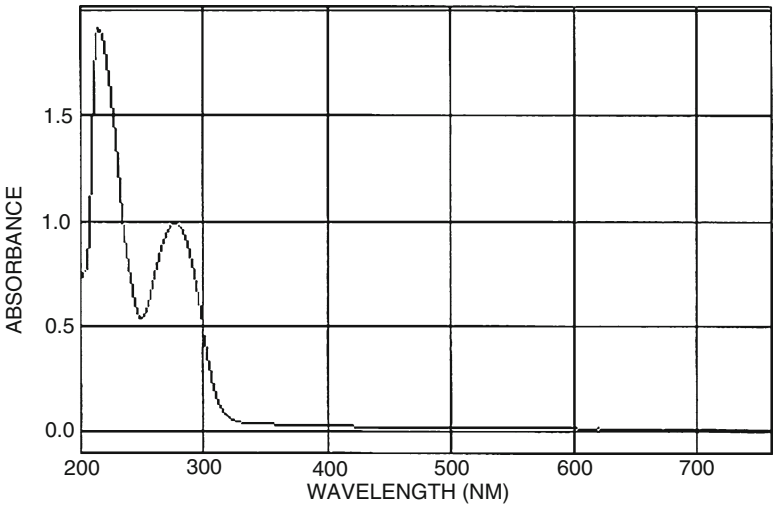

Fig. 25.1 Absorbance spectra of diclofenac sodium in physiologic serum w/NaOH

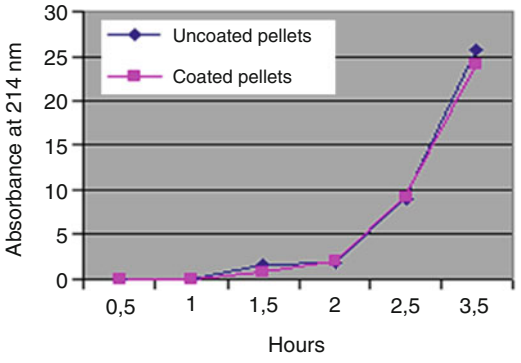

Fig. 25.2 Time release profile of uncoated and coated pellets at 214 nm

From Figs. 25.2 and 25.3, a retard of about 1 h was visible in case of both uncoated and coated pellets. In Fig. 25.2, a larger active substance delivery was noticed after 1.5 h for the uncoated pellets indicative for the existence of a controlled release effect. After 2 h, the delivery got again similar for the two pellets.

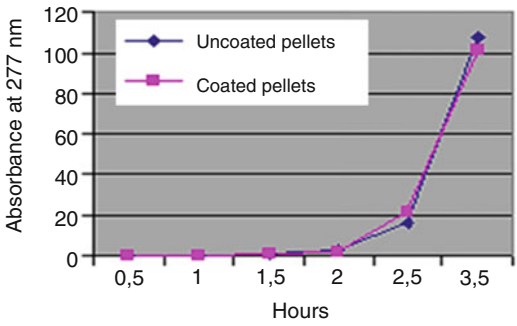

Fig. 25.3 Time release profile of uncoated and coated pellets at 277 nm

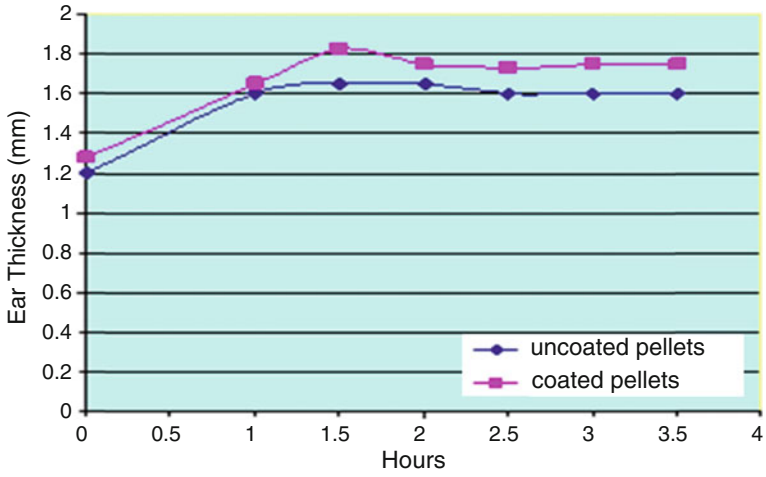

Fig. 25.4 Ear oedema thickness versus drug release time

25.3.2 In Vitro Tests

Ear oedema presence, consistence and vascular patterns were monitored after the inflammatory solution application. The total observation time was 3 h and 30 min. Initially the ear aspect was rather similar in both cases. Then the vascular pattern was accentuating reaching a maximum after 1–1.5 h from induced inflammation (1.5–2 h after drug administration).

From Fig. 25.4, it is observed that the coating of pellets does not impede enteric active drug dispersion and absorption. Nevertheless for coated pellets a slight (30 min.) retardation of inflammatory effect was noticed. Indeed, in the

case of uncoated pellets the maximum effect was reached after 30 min to the difference of coated pellets when the maximum effect was reached after 1 h from the inflammation installation. Results indicated that the triacetate-pullulan thin films coating induced a retard dispersion/absorption effect of the active drug action at the enteric level.

25.4 Conclusion

We showed that MAPLE can provide an improved approach to growing high quality triacetate-pullulan thin films with close resemblance to the starting composition and accurate thickness highly required in controlled release drug delivery systems. *In vitro* tests revealed that MAPLE-deposited thin films allowed proper dispersion/solubilization of active diclofenac sodium. Our spectroscopy studies performed at the diclofenac sodium absorption peak maxima at 214 and 277 nm evidenced a noticeable time release difference between uncoated and coated drug pellets. The coating with triacetate-pullulan thin films induced a retard effect (up to 30 min) of the drug release. This data were congruent with the results of the *in vivo* anti-inflammatory tests on rabbits after the dosage of the uncoated and coated drug pellets.

Acknowledgements C.P, G.S. and I.N.M, acknowledge with thanks the financial support of this research by CNCSIS under the IDEI contract 511/16.01.2009.

References

1. Saltzman WM (2001) Drug delivery: engineering principles for drug therapy. Oxford University Press, New York
2. Langer R (2001) Perspectives: drug, delivery – drugs on target. Science 293:58–59
3. Gao Z, Schulze Nahrup J, Mark JE, Sakr A (2003) Poly(dimethylsiloxane) coatings for controlled drug release. I. Preparation and characterization of pharmaceutically acceptable materials. J Appl Polym Sci 90(3):658–666
4. Moscovici M, Ionescu C, Oniscu C, Fotea O, Protopopescu P, Hanganu LD (1996) Improved exopolysaccharide production in fed-batch fermentation of Aureobasidium pullulans, with increased impeller speed. Biotechnol Lett 18(7):787
5. Chrisey DB, Pique A, McGill RA, Horwitz JS, Ringeisen BR, Bubb DM, Wu PK (2003) Laser deposition of polymer and biomaterial films. Chem Rev 103(2):553–576
6. Cristescu R, Mihailescu IN, Jelinek M, Chrisey DB (2006) Functionalized thin films and structures obtained by novel laser processing issues. In: Kassing R, Petrov P, Kulisch W, Popov C (eds) Functionalized properties of nanostructured materials, NATO science series II: mathematics, physics and chemistry. Springer, Dordrecht, pp 211–226. ISBN 1-4020-4595-6
7. Cristescu R, Stamatin I, Mihaiescu DE, Ghica C, Albulescu M, Mihailescu IN, Chrisey DB (2004) Pulsed laser deposition of biocompatible polymers: a comparative study in case of pullulan. Thin Solid Films 453–454 C:262–268
8. Cristescu R, Dorcioman G, Ristoscu C, Axente E, Grigorescu S, Moldovan A, Mihailescu IN, Kocourek T, Jelinek M, Albulescu M, Buruiana T, Mihaiescu D, Stamatin I, Chrisey DB (2006) Matrix assisted pulsed laser evaporation processing of triacetate-pullulan polysaccharide thin films for drug delivery systems. Appl Surf Sci 252(13):4647–4651

Chapter 26
Exploring the Mechanism of Biomolecule Immobilization on Plasma-Treated Polymer Substrates

Biomolecule Immobilization on Plasma-Treated Polymer

E.H. Lock, S.H. North, J. Wojciechowski, C.R. Taitt, and S.G. Walton

Abstract An electron beam-generated plasma source developed at NRL was used to modify polystyrene microtitre plates. A combination of complementary surface analytical and biochemical techniques was applied to evaluate the relationship between the biotic and abiotic layers, with particular emphasis on the efficiency of the preparation of polymer surfaces and its effectiveness for bioimmobilization. We conclude that the development of novel interface materials with superior transducing capabilities is dependent on the deeper understanding of the complex physicochemical, nanoscale interactions between the substrate surface and the biological components attached to it.

Keywords Polystyrene • Silanization • Characterization • Functionalization

26.1 Introduction

Microtitre plates are widely used in clinical diagnostics, biotech and pharmaceutical research and development. They are manufactured using a variety of polymeric materials, but polystyrene is most commonly employed because it readily adsorbs proteins, has excellent optical as well as mechanical properties, and is cost-effective.

E.H. Lock (✉) • S.G. Walton
Plasma Physics Division, U.S. Naval Research Laboratory, 4555 Overlook Ave. SW, Washington, DC, USA
e-mail: evgeniya.lock@nrl.navy.mil

S.H. North • J. Wojciechowski • C.R. Taitt
Center for Bio/Molecular Science & Engineering, U.S. Naval Research Laboratory, Washington, DC, USA

A. Vaseashta et al. (eds.), *Technological Innovations in Sensing and Detection of Chemical, Biological, Radiological, Nuclear Threats and Ecological Terrorism*, NATO Science for Peace and Security Series A: Chemistry and Biology,
DOI 10.1007/978-94-007-2488-4_26, © Springer Science+Business Media B.V. 2012

Typically, biomolecules are non-covalently immobilized through physisorption to the polymer substrate. However, this type of biomolecule attachment is often unstable and may cause protein denaturation, desorption and/or loss of biomolecule activity [1]. Thus, covalent biomolecule immobilization schemes are often preferred because they provide more stable attachment and functional display of the biomolecule of interest [2].

Plasmas are widely used as a preparation step of polymer substrates prior to bioimmobilization as signified by numerous review articles on this subject [3, 4]. Plasmas are effective in polymer surface functionalization, thin film deposition, and grafting of different functionalities onto the polymer surface. However, even though plasmas can produce the desired chemical modifications, in most cases, they also cause morphological modifications. The latter has been shown to affect the activity of the immobilized biomolecules [2], which is dependent on biomolecules presentation and orientation [5]. Therefore, we sought to develop a method that allows for precise control over polymer surface characteristics and thus allowing for better control over the biomolecule attachment. We use a combination of dry and wet chemistry to enhance selectivity in biomolecule immobilization. As a first step we use an electron beam-generated plasma characterized by its ability to introduce chemical modification without surface roughening [6] to activate the polymer surfaces. After microtitre plates functionalization, they were silanized and then cross-linkers were used to immobilize biomolecules of interest. We explored a broad range of experimental parameters to determine the optimal conditions for successful attachment of the biological recognition elements on a transducing polystyrene substrate surface.

26.2 Materials and Methods

26.2.1 Materials

26.2.1.1 Preparation of Fluorescently Labeled IgG

Rabbit IgG was conjugated with Cy3 mono-reactive dye following manufacturer's instructions. The labeled IgG was purified from unincorporated dye by gel filtration on BioGel P-10.

26.2.1.2 Surface Characterization

Contact angle measurements were performed with an automated goniometer (AST Products, Inc.) and surface energy estimations were performed as previously described [7]. *Surface elemental and chemical state analyses* were performed on K-Alpha X-ray photoelectron spectroscopy as discussed previously [8]. To produce

Table 26.1 Summary of experimental conditions

Exp. #	Pressure (mTorr)	Time (min)	Duty Factor (%)
1	60	0.5	10
2	90	2	10
3	95	2	10
4	90	1	10
5	90	5	10
6	90	2	20

consistent fits of minor C 1s components, their widths were constrained to the FMHW of the first peak (285 eV) and their positions were assigned as follows C-CO_2 285.7 eV, C-O 286.6 ± 0.2 eV, C=O 287.6 ± 0.2 eV, O-C=O 289 ± 0.2 eV, π-π* 291.7 ± 0.2 eV. A linear combination of Shirley and linear functions with consistent parameters was used to model the background. *The polymer surface morphology* was examined using an atomic force microscope (Nanoscope III, Veeco Metrology, Santa Barbara, CA) operated in tapping mode. Surface images were obtained from 5×5 μm^2 scans at resolution of 256×256 pixels and scan rate of 1 Hz. For a quantitative evaluation of the topography changes the root-mean square (RMS) roughness was calculated as previously shown [8].

26.2.1.3 Plasma Treatment of Microtitre Plates

The experimental apparatus has been discussed previously [9]. The microtitre plates were placed on a 10.2 cm diameter stage located at 2.5 cm from the nominal edge of the electron beam. The stage was held at ground potential and room temperature. The total gas flow rate was held constant at 50 sccm. The experimental conditions are summarized in Table 26.1.

26.2.1.4 Microtitre Plate Silanization and Immobilization of IgG

Plasma-treated or untreated NUNC Microfluor I microtitre plates (Thermo Fisher Scientific) were treated for 30 min with 2% (3-mercaptopropyl)triethoxysilane (MPTES) in acidic methanol (pH 4). Plates were treated for 30 min with 1 mM 4-maleimidobutyric acid N-hydroxysuccinimide ester (GMBS, Amersham-Pharmacia). Cy3-labeled antibody (1, 3, or 10 μg/mL in PBS) was added into each microwell and incubated for 2 h at room temperature with gentle agitation; each concentration was patterned in quadruplicate. The plate was read on a Tecan Safire microplate reader.

26.3 Results and Discussion

26.3.1 Effects of Process Parameters on Reactive Species Generation

It is important to note that plasma production by electron beams differs from conventional discharges. When high electron energy beam is injected in the background gas approximately half of its energy goes into gas ionization and dissociation and only a small fraction into gas excitation. Because there is no electric field to heat the secondary electrons (those produced during electron-impact ionization), they quickly cool to produce a large population of low energy electrons. These electrons determine the plasma density, electron temperature, and thus plasma potential. The latter is particularly important to the polymer modification process, since it will determine the kinetic energy of the ions as they impact the polymer surface.

We have already shown that the electron temperature in argon is about 1 eV [10, 11] and is largely independent of process parameters. As shown in Fig. 26.1a, the ions bombarding the surface have energies in the range of about 3 eV. In conventional discharges, ion energies could be greater by an order of magnitude or more. Energies of a few eV are comparable to the bond strengths in polystyrene; C–C (π-bond) energies are 2.6 eV, while C–C and C–H are higher (~4 eV). Thus, the mechanism of hydrogen abstraction might differ from the well-accepted physical sputtering mechanism in conventional discharge processing.

Metastables and photons are important species to consider in polymer processing. Metastables carry approximately 11 eV of energy, which is substantial and can cause hydrogen abstraction, radical formation, local heating and thus chain scission and/or crosslinking. Photons are important because they can penetrate deep into the polymer structure and cause crosslinking and further surface rearrangement as well. In conventional discharges, metastables and photons are often the dominant species. However, their influence in this work is limited because their production rates are low in electron beam-plasmas. Based on theoretical predictions, in argon the amount of metastables is an order of magnitude lower than the amount of ions produced [6].

A summary of experimental conditions is shown in Table 26.1. The influence of process parameters, e.g. duty factor, treatment time, and pressure, on the generation of species and the flux on the surface of polystyrene has been explored [12]. Variations in the duty factor and treatment time are directly correlated with the flux of species. Increasing the duty factor increases the time the beam is on, i.e. the time between beam pulses is reduced, while increasing the treatment time simply increases the total plasma exposure time. However, changing the operating pressure affects both the electron beam intensity [12] and plasma density [10] in this system. Figure 26.1b shows the increase in beam current density with increasing argon pressure. While ion and electron production is increased, their destruction via ambipolar diffusion to the walls is decreased ($D_a \sim 1/p$), which leads to enhanced ion flux bombarding the polymer surface. Thus, changing the pressure significantly influences polymer processing.

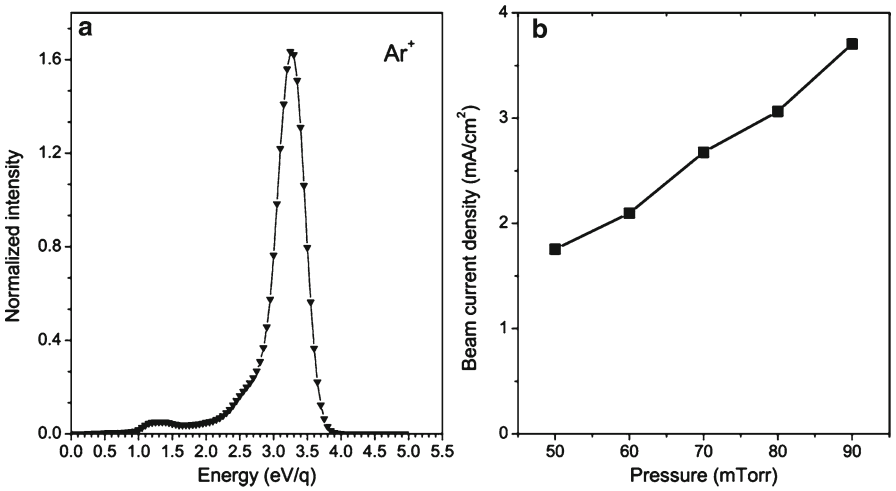

Fig. 26.1 Ion energy distribution at a pressure 50 mTorr (**a**) and beam current density as a function of pressure (**b**)

26.3.2 Polymer Surface Characterization

As variation in pressure has the greatest influence on the production of plasma species – charged particles, metastables and photons, it is expected to produce the most pronounced difference in oxygen incorporation. The highest degree of oxygen incorporation was observed at a pressure of 90 mTorr (exp #2, Tables 26.1 and 26.2) (O/C = 0.3) resulting in the highest polar component of the surface energy as well. The most likely mechanism of polystyrene modification in argon is the formation of carbon-centered polymer free radicals (P•), which preferentially crosslink. However, chain scission and formation of polyenes are also possible [13]. Higher pressures (exp # 3, Table 26.1) did not improve the surface chemical composition. In fact, the O/C ratio, C–O group concentration and γ^p decreased. This might be due to an excessive ion flux, which may cause an increase in etching and favor chain scission over crosslinking as the dominant mechanism. The surface roughness decreased at all pressures, which might be caused by ablation of low molecular weight fragments residing on the polymer surface.

Variations in both treatment time and duty factor at a fixed pressure led to similar conclusions. Increase in treatment time from 1 to 2 min (exp # 4 and 2, Tables 26.1 and 26.2) resulted in higher O/C ratios, increased amount of oxygen functionalities (C–O, C=O, COO groups) and improved polar component of the surface energy with no change in surface roughness. However, when the polystyrene substrate was treated for 5 min (exp # 5, Tables 26.1 and 26.2) the O/C ratio decreased and surface roughness increased. These results suggested that prolonged plasma exposure increases etching, increases surface roughness and promotes chain scission and not crosslinking. Increase in duty factor (exp #2 and #6) did not increase

Table 26.2 Summary of polymer surface characterization and bioimmobilization results

Exp. #	O/C	C–C(H)[a], C–CO_2[a]	C–O[a]	C=O[a]	COO[a]	π–π*[a]	γ_p[b]	γ_d[b]	γ_{tot}[b]	RMS[c]	Bio efficacy
Ref	0.03	92.61	1.58	0	0	5.81	0	40	40	19	–
1	0.27	89.84	5.12	2.94	1.08	1.01	24	32	56	11	–
2	0.30	86.07	8.24	4.04	1.65	0	26	38	64	12	+
3	0.20	73.03	5.56	3.24	1.05	0	10	43	53	12	–
4	0.22	77.74	3.14	0.33	0	0.9	20	36	56	11	–
5	0.23	87.53	7.8	2.85	1.02	0.8	19	39	58	16	–
6	0.14	81.32	6.17	1.56	0	0	13	40	53	ND	–

[a]Concentration of functional groups was measured in at. %

[b]Surface energy was measured in mJ/m^2

[c]RMS roughness was measured in nanometers (nm)

[d]ND means not determined

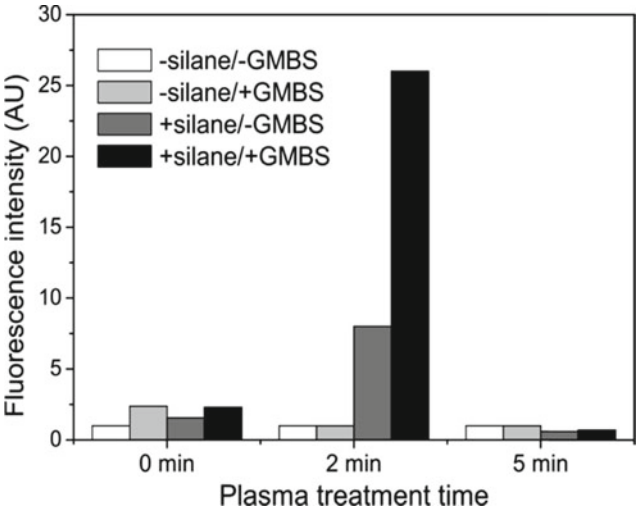

Fig. 26.2 Biomolecule immobilization efficacy as a function of plasma treatment time

the oxygen incorporation. In fact, it resulted in decrease of O/C ratio as well as a decrease of the polar component of the surface energy by a factor of two. Although the reasons are not clear, it appears that reducing the time between pulses does not promote the incorporation of OH-groups.

26.3.3 Biomolecule Immobilization

Covalent bioimmobilization was observed only at a pressure of 90 mTorr, treatment time of 2 min and 10% duty factor (exp. #2 Table 26.2, Fig. 26.2). At this condition the increase in fluorescent signal, signifying specific biomolecule attachment, was 26-fold above the background levels. These results are in direct correlation to the presence of oxygen functional groups on the polystyrene surface. That is, when the oxygen functionalities concentration on the polymer surface was optimized, it allowed for efficient silanization and thus *specific* biomolecule immobilization occurs.

26.4 Conclusions

The relationship between the plasma generated reactive species and photons, the chemical and morphological characteristics of the plasma treated surface and the following bio-immobilization were explored. High flux of low energy ions, low

amount of metastables and photons are needed for successful hydroxylation of the polystyrene surface without increase in surface roughness. Covalent bio-immobilization was achieved at narrowly defined conditions characterized by the highest oxygen functionalities concentration and by the highest surface energy.

Acknowledgements J. W. is recipient of an American Society of Engineering Education postdoctoral fellowship. This work is funded by Joint Science & Technology Office for Chemical & Biological Defense/Defense Threat Reduction Agency and the Office of Naval Research. The views expressed here are those of the authors and do not represent the opinions of the U.S. Navy, the U.S. Department of Defense, or the U.S. government.

References

1. Rebeski DE, Winger EM, Shin YK, Lelenta M, Robinson MM, Varecka R, Crowther JR (1999) Identification of unacceptable background caused by non-specific protein adsorption to the plastic surface of 96-well immunoassay plates using a standardized enzyme-linked immunosorbent assay procedure. J Immunol Methods 226:85
2. Goddard JM, Hotchkiss JH (2007) Polymer surface modification for the attachment of bioactive compounds. Prog Polym Sci 32:698
3. Desmet T, Morent R, Geyter ND, Leys C, Schacht E, Dubruel P (2009) Nonthermal plasma technology as a versatile strategy for polymeric biomaterials surface modification: a review. Biomacromolecules 10:2351
4. Siow KS, Britcher L, Kumar S, Griesser HJ (2006) Plasma methods for the generation of chemically reactive surfaces for biomedical immobilization and cell colonization – a review. Plasma Process Polym 3:392
5. Kulagina NV, Shaffer KM, Ligler FS, Taitt CR (2007) Antimicrobial peptides as new recognition molecules for screening challenging species. Sens Actuators B 121:150
6. Lock EH, Walton SG, Fernsler RF (2009) Physico-chemical modifications of polystyrene and poly(propylene) surfaces by electron beam-generated plasmas produced in argon. Plasma Process Polym 6:234
7. Owens DK, Wendt RC (1969) Estimation of the surface free energy of polymers. J Appl Polym Sci 13:1741
8. Lock EH, Petrovykh DY, Mack P, Carney T, White RG, Walton SG, Fernsler RF (2010) Surface composition, chemistry and structure of polystyrene modified by electron-beam-generated plasma. Langmuir 26:8857
9. Leonhardt D, Muratore C, Walton SG (2005) Applications of electron-beam generated plasmas to material processing. IEEE Trans Plasma Sci 33:783
10. Lock EH, Fernsler RF, Walton SG (2008) Experimental and theoretical evaluations of electron temperature in continous electron beam generated plasmas. Plasma Sources Sci Technol 17:025009
11. Walton SG, Leonhardt D, Fernsler RF (2005) Time-resolved diagnostics in a pulsed, electron beam-generated plasmas. IEEE Trans Plasma Sci 33:838
12. Walton SG, Lock EH, Ni A, Baraket M, Fernsler RF, Pappas DD (2010) Study of plasma-polyethylene interactions using electron beam-generated plasmas produced in Ar/SF_6 mixtures. J Appl Polym Sci 117:3515
13. Knobloch G (1990) Einfluss von verarbeitungsbedingungen und additiven auf die abbaureaktionen von SIS-blockcopolymeren. Angew Makromol Chem 176–177:333

Chapter 27
Synthesis of New Carbon Compounds: N-doped Fullerene $(C_{50}N_{10})O_3H_{10}$ and "Pyridine" Nanocarbon

Synthesis of New Carbon Compounds

O. Kharlamov, G. Kharlamova, N. Kirillova, O. Khyzhun, and V. Trachevskii

Abstract Fullerene N-doped fullerene $(C_{50}N_{10})O_3H_{10}$ has been synthesized at thermal transformation of pyridine molecules. The synthesis was carried out at special reaction conditions, which are optimum for polycondensation of pyridine molecules. O and H atoms bind to nitrogen atoms and they are positioned exohedrally with respect to the pyridine net, $(C_{50}N_{10})$. Nitrogen atoms in $(C_{50}N_{10})O_3H_{10}$ molecule reside in a hypercoordinated state: there are four bonds with carbon atoms belonging to the pyridine net and one bond is realized either with surface oxygen atoms (participating in 3 N–O–H bonds) or hydrogen (participating in 7 N–H bonds). N-doped nanocarbon (or "pyridine" nanocarbon) has also been synthesized with content of nitrogen not less than 10%wt. containing pyridine (not graphene) fragments. Methods of FTIR, XPS, X-ray diffraction patterns, NMR ^{13}C and ^{1}H, mass-spectroscopy were used.

Keywords N-doped fullerene • Hyper-coordinated nitrogen • Pyridine • Nanocarbon • Polycondensation

O. Kharlamov (✉) • N. Kirillova • O. Khyzhun
Frantsevich Institute for Problems of Materials Science of NAS, Krzhyzhanovsky St. 3, 03142 Kiev, Ukraine
e-mail: akharlamov@ukr.net

G. Kharlamova
Kiev National Taras Shevchenko University, Kiev, Ukraine

V. Trachevskii
Institute of Metal Physics of NAS, Vernadskyi Bulvar 36, 03142 Kiev, Ukraine

A. Vaseashta et al. (eds.), *Technological Innovations in Sensing and Detection of Chemical, Biological, Radiological, Nuclear Threats and Ecological Terrorism*, NATO Science for Peace and Security Series A: Chemistry and Biology,
DOI 10.1007/978-94-007-2488-4_27, © Springer Science+Business Media B.V. 2012

27.1 Introduction

Carbon nanomaterials are the most effective detectors in the change of properties of separate molecules both in live organisms and gas phases. Chemical nanosensors based on carbon nanotubes allow the determination of mutations in DNA, the degree of ionization of molecules, and traces of explosive substances. Carbon nanotubes used as coating materials have unique sensing characteristics according to the synthesis method used.

Since inventing fullerenes and single-walled carbon nanotubes (SWCNT), much research has examined mechanisms for constructing these types of molecules. At issue is how to resolve the selective synthesis of graphene isomers (chair and zigzag) of carbon nanotubes. The hypothesis prevails that spherical molecules and carbon nanostructures with different morphology (multi-walled carbon nanotubes, onions, toroids, nanofibers) are formed from carbon atoms, which are generated at superhigh temperatures (>3500°C) of graphite evaporation (or another carbon material) and at catalytic destruction of organic molecules. The growth of nanotubes during pyrolysis process is carried out in accordance with the vapor-liquid-solid (VLS) mechanism [1, 2] on the surface of a catalytic active particle that is subsequently a component of SWCNT and other carbon nanostructures. The possibility of formation of fullerene molecules as well as of fullerenes hydrides at the usual process of pyrolysis of hydrocarbons in accordance with the VLS mechanism was excluded completely. However, experimental results by Kharlamov et al. [3, 4] have demonstrated that it is possible to develop a new route of transformation of organic molecules at which a direct thermal polycondensation and polymerization of benzene molecules [5, 6] in fullerenes and their hydrides can be quite real (Fig. 27.1) and technological. Note that direct synthesis of fullerenes from benzene is carried out in flame jet at benzene combustion at deficit of oxygen and at low pressure [7, 8].

Pyridine, C_5H_5N, is a heterocyclic analogue of benzene, C_6H_6, with high basity. Therefore, it is suggested that thermal polycondensation of pyridine molecules can realize with the formation of a nitrogen-containing fullerene-like molecule. In this work, we report results of a new route of thermal transformation of pyridine molecules.

27.2 Experimental Procedure

These studies were carried out using modified (concerning input of initial reagents and concentration of reaction products) equipment usually used for synthesis of carbon nanostructures. Studies of thermal transformation of pyridine are made in reaction conditions providing realization of basically reactions of polycondensation and polymerization. Pyrolysis results in the destruction of precursor molecules, and subsequent polycondensation and polymerization result in the formation of aromatic polymer molecules present on its surface. Kharlamov et al. have established

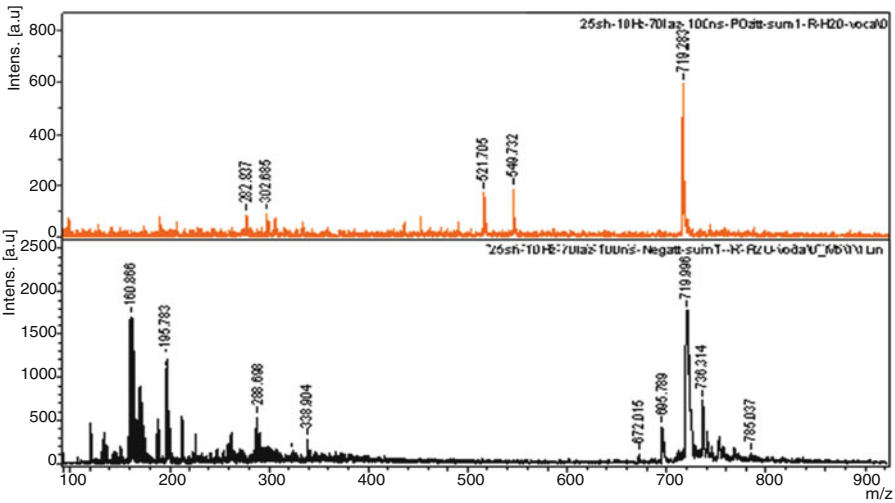

Fig. 27.1 Mass-spectra of positive and negative ions of toluene extract from products of direct transformation benzene molecules

that among dissolved pyrolysis products, there are transparent threadlike carbon crystals [9] in addition to fullerenes and fullerenes hydrides [3, 4]. Therefore, this study focuses on solid and solving products of pyridine thermal transformation.

The XPS valence-band and core-level spectra of the product synthesized were measured using the UHV-Analysis-System assembled by SPECS Surface Nano Analysis Company (Germany). The system is equipped with a PHOIBOS 150 hemispherical analyzer. A base pressure of a sublimation ion-pumped chamber of the system was less than 5×10^{-10} mbar during the present experiments. The Mg Kα radiation ($E = 1253.6$ eV) was used as a source of XPS spectra excitation. The XPS spectra were measured at the constant pass energy of 25 eV. The energy scale of the spectrometer was calibrated by setting the measured Au $4f_{7/2}$ and Cu $2p_{3/2}$ binding energies to 84.00 ± 0.05 eV and 932.66 ± 0.05 eV, respectively, with regard to E_F. Figure 27.1 shows a survey of the XPS spectra of the products studied. For this sample, all the spectral features are attributed to the constituent element core-levels or Auger lines.

NMR ^{1}H and ^{13}C studies were carried out using a universal AVANCE 400 spectrometer (Bruker, Germany). Extracts of reactionary mixtures and solutions of individual compounds in D_2O, C_2H_50H and $(CH_3)_6N_3PO_2H_2$ (hexamethylthreeamides of phosphorous acid) were placed in glass ampoules with 5 mm diameter; solids specimens were placed in rotors made from ZrO_2 with 4 mm diameter (rotation speed at magic angle was 12 kHz). When determining chemical shifts (δ, m.d.) in the NMR spectra, signals of tetramethylsilane and adamantane (CPMLS) were used.

The FTIR spectra in a reflectance mode were recorded in the range from 4,000 to 400 cm^{-1} with a spectral resolution of 8 cm^{-1} using a Nexus Nicolet FTIR spectrometer

(Thermo Scientific) equipped with a Smart Collector reflectance accessory. Samples under investigation were powdered with KBr in 1:10 ratio.

27.3 Studies of Products of Thermal Transformation of Pyridine

A study of the thermal conversion of pyridine is also important with respect to the possibility of the synthesis of N-doped carbon as nanotubes and nanofibers, nanospheres and nanographite with high nitrogen content. It is assumed that the introduction of nitrogen atoms (as well as boron and oxygen atoms) into graphene layers can lead to significant modification of electro-physical and acidic-basic properties of nanomaterials and, as a consequence, to significant changes of their catalytic and absorption characteristics. Non-aromatic nitrogen-containing organic substances (in particular, acetonitrile, ethyl and diethylamines) as well as melamine and ammonia are used usually as precursors in the pyrolysis processes for obtaining N-doped nanocarbon. However, carbon nanotubes derived by pyrolysis (900°C) of acetonitrile, contain less than 3 wt.% of nitrogen [10] (less than 10% of nitrogen contained in acetonitrile passes to carbon nanotubes). When using a mixture of ammonia as a nitrogenized reagent with ethylene, the nitrogen content in synthesizing nanocarbon increases up to 7 wt.% [11].

27.3.1 Synthesis of "Pyridine" Nanocarbon

Pyridine having undergone thermal polycondensation transforms into a product consisting of a solid phase as well as a liquid phase on the surface of the solid phase. From this product, substance (A) solved mainly in alcohol (water, toluene) are extracted consequentially. Precipitate B after treatment of the product with different chemical solvents is a nanocarbon as evidenced from data of chemical and XRD analyses [12] and electron microscopy. In accordance with the chemical analysis, nanocarbon derived at different conditions contains nitrogen (up to 15 wt.%), oxygen (up to 7 wt.%), and hydrogen (up to 0.8 wt.%) atoms. It is worth mentioning that nanocarbon deriving at a usual process of pyridine pyrolysis contains up to 4 wt.% of nitrogen.

From XPS (Fig. 27.2), it is seen that this sample of nanocarbon comprises also nitrogen and oxygen. The binding energy of C1s is 285, 0 eV and N1s is 399,8 eV. However, the spectrum of O1s has two different intensity maximums: 530,1 eV and 532,0 eV.

From comparison of FTIR spectra of samples of N-doped nanocarbon with different nitrogen content it is obvious that these spectra resemble each other except of the absorption band at 1,680 cm^{-1}. Absorption bands at 1,428 cm^{-1} and (1,558–1,570) cm^{-1} can be attributed to vibrations of carbon skeleton with conjugated bonds.

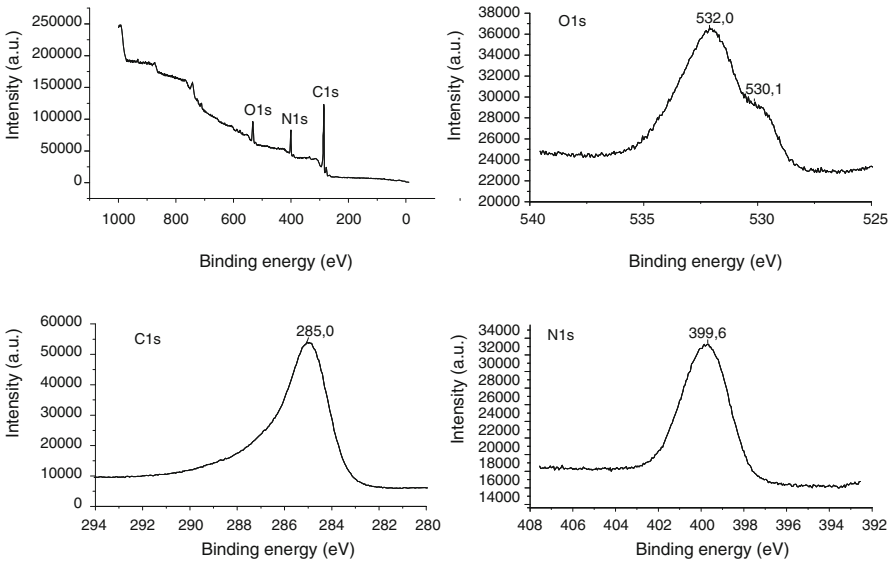

Fig. 27.2 XPS survey and core level N1s, O 1s, and C 1s spectra of nanocarbon

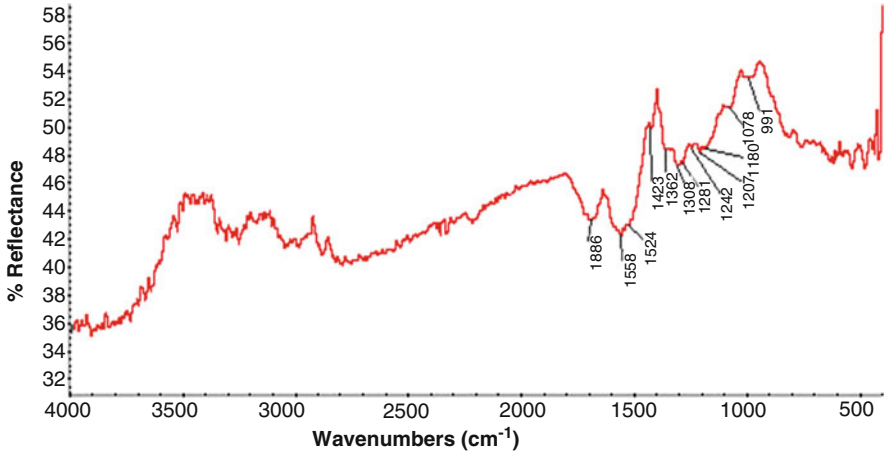

Fig. 27.3 FTIR spectrum of "pyridine" nanocarbon

Bands which are characteristic of valence C–H bonds are absent (Fig. 27.3). The band at 1,686 cm^{-1} (as well as the band at 1,524 cm^{-1}) is most likely responsible for the presence of amide groups, NH–C (O): the tendency of increasing the intensity of this band with increasing contents of nitrogen and oxygen in the sample has been detected. Additionally, the absorption bands at 1,361, 1,308 and 1,281 cm^{-1} can be attributed to strain (N-H) and (C-N) vibrations. It is worth mentioning that in

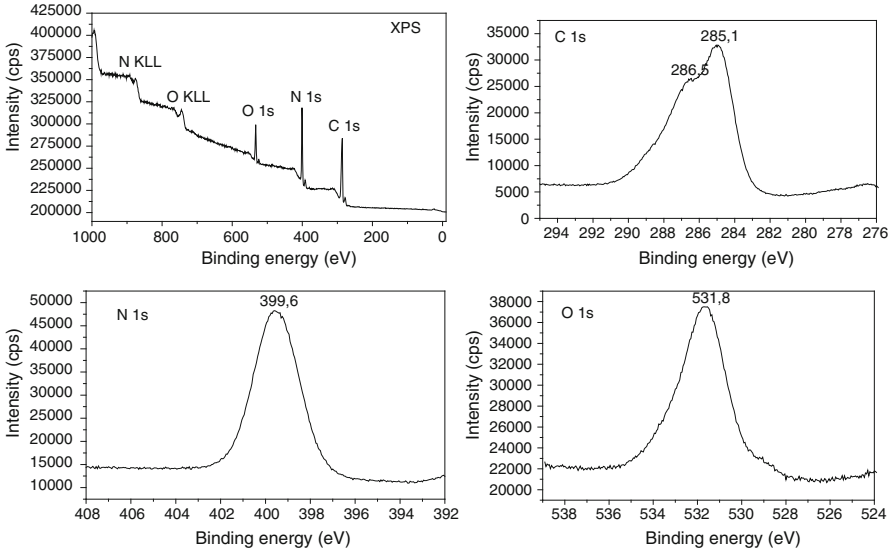

Fig. 27.4 XPS survey and core level N1s, O 1s, and C 1s spectra of $C_{6.01}N_{1.22}O_{0.344}H_{1.2}$

paircyanogen $(CN)_x$ and many other substances containing C═N bonds, the absorption occurs at 1,570 cm^{-1}, i.e. like the band for conjugated bonds C═C. Consequently, N-doped nanocarbon derived from pyridine and containing pyridine nets (not grapheme ones) is "pyridine carbon".

27.3.2 Synthesis of N-doped Fullerene $(C_{50}N_{10})O_3H_{10}$

The substance A is precipitated from alcohol (or water) solution either as transparent bright-red crystals or as a nanopowder (at quick alcohol evaporation). The degree of substance crystallinity depends on solvent and intensity of its precipitation [4].

After several subsequent recrystallization events, the substance A in accordance with the chemical analysis contains nitrogen (17.1 wt.%), oxygen (5.5 wt.%), hydrogen (1.2 wt.%) and carbon (72.2 wt.%) and its formula can be written as $C_{6.01}N_{1.22}O_{0.344}H_{1.2}$.

Figure 27.4 shows the survey XPS spectrum of the product under study. For this sample, all the spectral features are attributed to the constituent element core-levels or Auger lines. It is obvious that the substance A contains carbon, nitrogen and oxygen atoms. XPS N 1s and O 1s core-level spectra have their maxima at binding energies 399.6 eV and 531.8 eV, respectively. It can be suggested that the molecule of the substance under study contains two energy-different types of carbon. The value 285.1 eV is characteristic of C 1s binding energy of all carbon modifications.

The presence of a shoulder on the C 1s core-level spectrum with its binding energy at 286.5 eV indicates the existence in the molecule under study of carbon atoms binding with a more electronegative atom, i.e. with nitrogen. Therefore, the molecule of the substance under consideration with respect to the electronic structure of carbon is heteroatomic.

An alcohol solution of $C_{6.01}N_{1.22}O_{0.344}H_{1.2}$ was studied using chromatographic and mass-spectrometry methods. The mass-spectrum demonstrates the presence of four lines with the following mass values: 802.6, 413.0, 364.8, and 339.9. The main, most intensive peak corresponds to a molecular mass 802.6. Therefore, the molecular formula of the main substance, in accordance with its content, can be written as $(C_{50}N_{10})O_3H_{10}$ with a molecular weight of 798 (the small difference in four units can be explained by the presence of higher isotopes of some elements).

In the Raman spectrum of $(C_{50}N_{10})O_3H_{10}$ [4], the presence of absorption lines indicate the existence of conjugated –C═C– bonds as well as bonds in the OH and NH groups in the molecule. Two intensive lines at 1,375 and 1,500 cm^{-1} correspond, respectively, to sp^3- and sp^2-hybridized states of carbon atoms. The line corresponding to the sp^2-hybridized carbon atom is shifted significantly (by about 90 cm^{-1}) towards lower values of frequency. Probably, the shift is accompanied with the presence of nitrogen atoms in the system of the conjugated bonds.

The FTIR spectrum of $(C_{50}N_{10})O_3H_{10}$ [4] reveals absorption bands at 1,656, 1,556 and 1,387 cm^{-1} which are characteristic of a carbon skeleton with the conjugated bonds and that of amide NH-C(O) groups. Nevertheless, despite the FTIR spectrum of N-doped nanocarbon, the FTIR spectrum of $(C_{50}N_{10})O_3H_{10}$ indicates the presence of bands at 3,182 and 3,300 cm^{-1}, that can be originated from O-H and N-H groups respectively. Furthermore, the spectrum contains the absorption band at 2,218 cm^{-1}, which usually is characteristic of nitrile –CN group conjugated with olefin or benzene. Since the bands that are characteristic of C–H bonds are absent in the FTIR spectrum, we suggest that carbon atoms in the molecule under consideration participate in bonds with carbon and nitrogen atoms.

The NMR ^{13}C spectrum of $(C_{50}N_{10})O_3H_{10}$ solution in $(CH_3)_6N_3PO_2H_2$ is presented in Fig. 27.5. The spectrum reveals two signals δ at 116.4 ppm and 105.1 ppm corresponding to two states of sp^2-hybridized carbon atoms. The NMR ^{13}C spectrum of a water solution of $(C_{50}N_{10})O_3H_{10}$ also contains two signals (Fig. 27.5). However, the δ values of these signals (110 and 105 ppm.) differ slightly from those observed in the spectrum of $(C_{50}N_{10})O_3H_{10}$ solution in $(CH_3)_6N_3PO_2H_2$ that is likely explained by differences of molecular interactions in these systems.

In the NMR ^1H spectrum (Fig. 27.6) there are signals which characterize the H-O and H-N bonds: the most intensive signal with δ at 8.05 ppm. reveals the presence of 3 H–O bonds, while the signals with δ at 8.66, 8.39, 8.02, 7.67 and 7.46 ppm. reveals the existence of 7 H-N bonds. The observing differences in δ values indicate that in $(C_{50}N_{10})O_3H_{10}$ molecule nonequivalent H-N bonds exist.

Thus, according to data of XPS (Fig. 27.4) and NMR (Fig. 27.5), spectra carbon atoms in pyridine net $(C_{50}N_{10})$ of synthesized molecule $((C_{50}N_{10})O_3H_{10})$ are in two different valent states: namely (C_2)–**C**–C and (C_2)–**C**–N. The polycondensation of pyridine molecules is formed by the transition of the polymeric aromatic structure

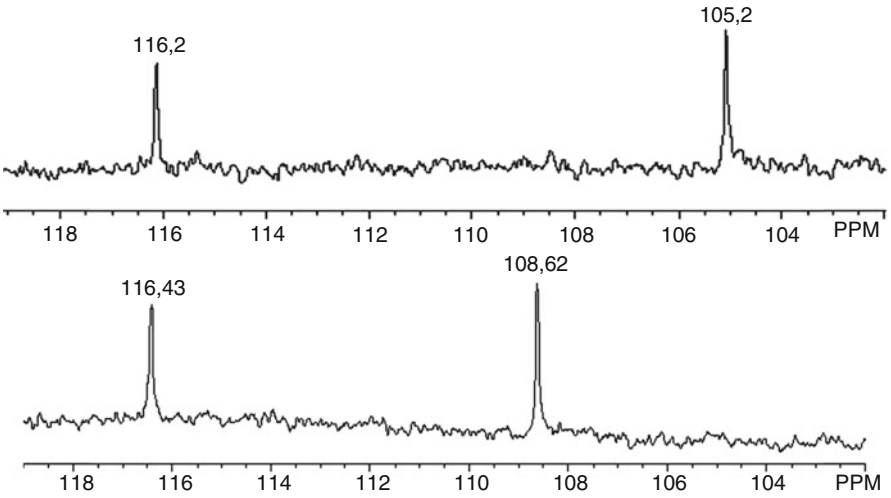

Fig. 27.5 NMR ^{13}C spectrum of the solution of $(C_{50}N_{10})O_4H_{10}$ in $((CH_3)_6N_3PO_2H_2)$ (*up*) and H_2O (*down*)

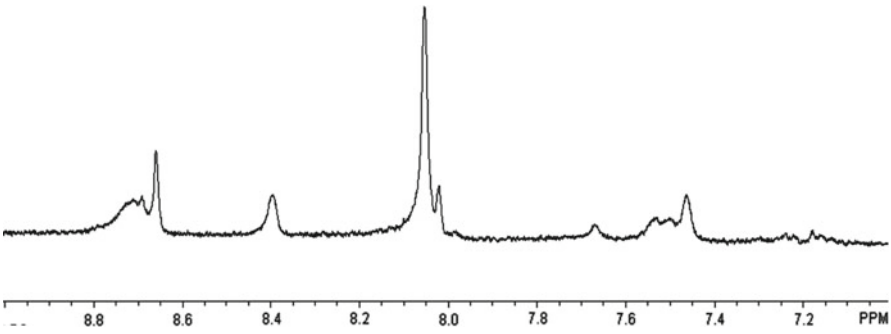

Fig. 27.6 NMR ^{1}H spectrum of the solution of $(C_{50}N_{10})O_3H_{10}$ in $((CH_3)_6N_3PO_2H_2)$

$(C_{50}N_{10})$ with a number of conjugated –C═C– and –N═C– bonds in which nitrogen and carbon atoms can be in the excited state. Further interaction between nitrogen atoms with unshared electronic pair and a nearby (in this plane transition structure) carbon atom in the neighboring pyridine ring results to forming of a new covalent N–C bond and the appearance of curved (or closed) net $(C_{50}N_{10})$. The fifth electron of the nitrogen atom in this net (N-doped fullerene) can participate in forming of exohedral bonds with atoms of hydrogen and oxygen. Therefore, the nitrogen atom in molecule $(C_{50}N_{10})O_3H_{10}$ is in the hypercoordinated state having four bonds with carbon atoms in $(C_{50}N_{10})$, one bond is realized with surface oxygen atoms (3 N–O–H bonds), and hydrogen atoms (7 N–H bonds). Due to these polar exohedral bonds, the substance dissolves in water and alcohol.

27.4 Conclusions

We propose a new route of pyrolysis process – the direct transformation molecules of benzene and pyridine to fullerene C60 (and fullerenes hydrides) and closed fullerene-like $(C_{50}N_{10})O_3H_{10}$ molecule (N-doped fullerene) respectively. These new substances that were synthesized show promise as good optical sensors.

Acknowledgements The authors are grateful to colleagues from the Center of collective use MALDI (Institute of surface chemistry, Kiev, Ukraine) for mass-spectroscopic study.

References

1. Oberlin A, Endo M, Koyama T (1976) High resolution electron microscopy of graphitizable carbon fiber prepared by benzene decomposition. J Cryst Growth 32:335–349
2. Tibbetts GG (1985) Lengths of carbon fibers grown from iron catalyst particles in natural gas. J Cryst Growth 73:431–438
3. Kharlamov AI, Kirillova NV (2009) Fullerenes and hydrides of fullerenes as products transformation (polycondensation) of molecules of aromatic hydrocarbons. Report of academia of science of Ukraine, vol 5. pp 110–118 (Russian)
4. Kharlamov A, Kharlamova G, Khyzhun O, Kirillova N (2011) New substances: red carbon suboxide (C>5,4), red N-doped fullerene (C50N10O3H10) and "red carbon". In: Zaginaichenko S, Schur D, Skorokhod V, Veziroglu A, İbrahimoğlu B (eds) Carbon nanomaterials in clean – energy hydrogen systems. Springer, Dordrecht, The Netherlands, pp 257–268
5. Kharlamov AI, Ushkalov LN, Kirillova NV, Fomenko VV, Gubareny NI, Skripnichenko AV (2006) Synthesis of onion nanostructures of carbon at pyrolysys of aromatic hydrocarbons. Report of academia of science of Ukraine, vol 3. pp 97–103 (Russian)
6. Kharlamov A, Kirillova N, Fomenko V (2008) Persistent organic pollutants at nanotechnology and their impact on people health. In: Mehmetli E, Koumanova B (eds) The fate of persistent organic pollutants in the environment. Springer, Dordrecht, The Netherlands, pp 425–441
7. Goel A, Hebgen P, Vander Sande J, Howard J (2002) Combustion synthesis of fullerene nanostructures. Carbon 40:177–182
8. Hebgen P, Goel A, Howard JB, Rainey LC, Vander Sande JB (2000) Nanostructures in a low pressure benzene/oxygen diffusion flame. Proc Combust Inst 28:1397–1404
9. Kharlamova G, Kirillova G, Kharlamov N, Skripnichenko A (2008) Novel transparent molecular crystals of carbon. In: Vaseashta A, Mihailescu I (eds) Functionalized nanoscale materials, devices, and systems. Springer, Dordrecht, The Netherlands, pp 373–379
10. Khavrus VO, Ibrahim EMM, Leonhardt A, Hampel S, Taschner C (2008) Simultaneous synthesis and separation of single- and multi-walled CNX nanotubes. In: International symposium on carbon for catalysis, Fritz Haber Institute of the Max Planck Soceity, Fritz Haber Institute of the Max Planck Soceity, Berlin, Germany 9–12 Nov 2008, p 17
11. Ismagilov ZR (2008) Design of nitrogen doped carbon materials for preparation of advanced catalysts. In: International symposium on carbon for catalysis, Fritz Haber Institute of the Max Planck Soceity, Berlin, Germany, 9–12 Nov 2008, p 7
12. Kharlamov AI, Kirillova NV (2011) New substance: molecular crystals of fullerene-like N-containing molecule of carbon - $(C_{50}N_{10})O_3H_{10}$. Report of academia of science of Ukraine, vol 6. pp 156–163 (Russian)

Chapter 28
Controlled Structure-Dependent Synthesis of Polymer/Nanosilver Composites for Highly Efficient Antibacterial Coatings

Controlled Synthesis of Polymer Composites

A. Tolstov, V. Matyushov, and D. Klimchuk

Abstract Silver containing polymer composites were successfully synthesized via *in-situ* reduction approach. Different functional polymers with hydroxyl, amide and amine functionalities have been used as matrices. An influence of polymer structure and functionality on a size and shape of silver nanoparticles was established via FTIR/TEM complex analysis. The materials based on these composites could be effectively applied as advanced antibacterials.

Keywords Nanocomposite • Controlled synthesis • Antibacterial materials

28.1 Introduction

The development of new efficient antimicrobial agents is important to combat newly appearing highly resistant microorganisms, which has potential to be weaponized by terrorists. Nobel metal nanoparticles, especially silver nanoparticles, due to low price and high activity, are attracting attention as highly efficient antibacterial and antiviral drugs and materials [1]. In this work, we synthesized silver containing polymer nanocomposites based on polymer matrices of different chemical structure via in-situ reduction approach. The size and shape of silver nanoparticles, and chemical structure and functionality of the polymer component was studied in this

A. Tolstov (✉) • V. Matyushov
Institute of Macromolecular Chemistry of the NAS of Ukraine,
Kharkivske shose 48, 02160 Kyiv, Ukraine
e-mail: tolstov.aleksandr@rambler.ru

D. Klimchuk
N.G. Kholodny Institute of Botany of the NAS of Ukraine,
Tereshchenkivska street 2, 01601 Kyiv, Ukraine

A. Vaseashta et al. (eds.), *Technological Innovations in Sensing and Detection of Chemical, Biological, Radiological, Nuclear Threats and Ecological Terrorism*,
NATO Science for Peace and Security Series A: Chemistry and Biology,
DOI 10.1007/978-94-007-2488-4_28, © Springer Science+Business Media B.V. 2012

investigation. The results show that it is possible to use developed materials as efficient antimicrobial coatings for multiple applications.

28.2 Experimental

28.2.1 Materials

As a source of Silver- silver nitrate (Aldrich) was used. Poly(vinyl alcohol) (PVA), ($M_w = 1.3 - 2.1 \times 10^4$; CCE GmbH), polyacrylamide (PAAm), ($M_w = 1.0 \times 10^4$; Aldrich) and especially developed poly(ether-urethane) (PEU), and epoxy amine resin (EAR), based on commercially available low-molecular or oligomer precursors have been used. Solvents used in this work, viz. water, 1,4-dioxane, methanol as received, were used.

28.2.2 Preparation of Polymer/Silver Nanocomposites

Preparation of the polymer/silver composites was carried out via in-situ reduction of silver salt in a polymer solution followed by casting of prepared solutions. The silver nitrate dissolved in corresponding polymer solution (polymer content varied from 20 to 50 wt.%). The Silver content was 5 wt.% for all prepared compositions. In situ reduction was primary induced by short time lightening followed by continuation of the reduction in dark. Prepared polymer films were treated at 80°C for 1 h. for solvents removing and finishing the reduction process.

28.2.3 Characterization

FTIR analysis of the composites was carried out using a Bruker Tensor™ 37 FTIR analyzer in the spectral region of 4,000–600 cm^{-1}. TEM characterization was performed by a JEOL JSM 6060 LA microscope at an accelerating voltage up to 120 kV.

28.3 Results and Discussion

The mechanism of controlling reduction of silver ions to silver nanoparticles in the polymer matrix can be explained from FTIR data (Fig. 28.1) [2]. The shift of characteristic bands of OH stretching vibration centered at 3,421 cm^{-1} (pure PVA) to 3,253 cm^{-1} (PVA/Ag) is due to coordination of Ag^+ and, latter, Ag nanoparticles by

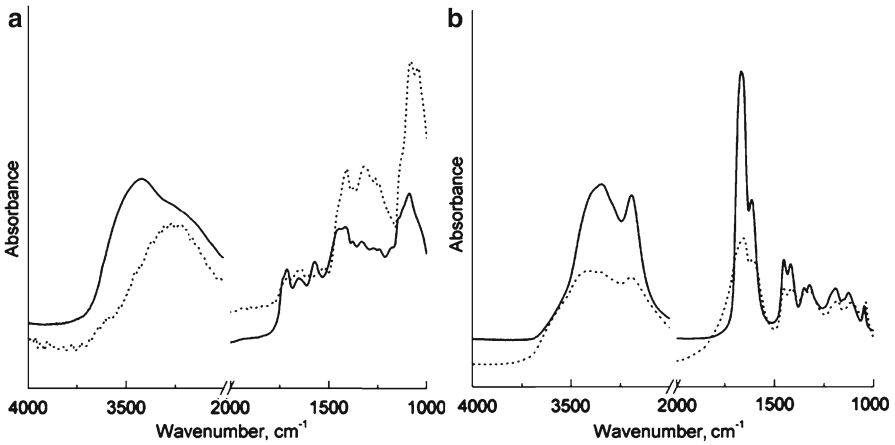

Fig. 28.1 FTIR curves of (**a**) poly(vinyl alcohol) and (**b**) polyacrylamide based composites: (*straight line*) – pure polymer; (*dot line*) – composite with 5 wt.% of silver

Table 28.1 Characteristics of polymer/silver nanoparticles composites

Sample	Coordination/stabilization	Particles shape	Particles size, nm
PVA/Ag	–(H)O···Ag··· O(H)–	Spheres	~15
PAAm/Ag	–C=O···Ag···O=C–	Triangular prisms; rods	~25; 120×235
EAR/Ag	–R···Ag···R–, (R = NR_3 and/or OH)	Rods	12×180
PEU/Ag	–$(R)_2$N··Ag··N$(R)_2$–	Spheres	~4

hydroxyls of the polymer. The shift of C-O stretching vibration band from 1,088 to 1,064 cm^{-1} also justifies our conclusion above. Figure 28.1b shows the coordination behavior of silver ions/particles by PAAm functional groups. NH of amide groups do not create any coordination bond with silver species (the position of NH band at 3,347 and 3,193 cm^{-1} and C–N band at 1,412 cm^{-1} did not change), whereas C=O of amide bonds with silver species results in a shift of ν_{CO} bands from 1,670 to 1,656 cm^{-1}. The data summarized in Table 28.1 show the coordination mechanism of silver ions/particles with corresponding functional groups of the polymer matrices for all prepared composites. Early experiments show that coordination interactions between metal ions and polymers provide the control of the silver nanoparticles formation process.

From Fig. 28.2, it is clearly seen that it is possible to prepare polymer nanocomposites with different shapes and sizes of silver nanoparticles, when polymer matrices of different functionality were used. As found from literature [3], the antibacterial activity of silver nanoparticles drastically depends on shape and size of the particles. Most efficient antibacterial activity is observed for triangular shaped particles, even though their size is relatively large.

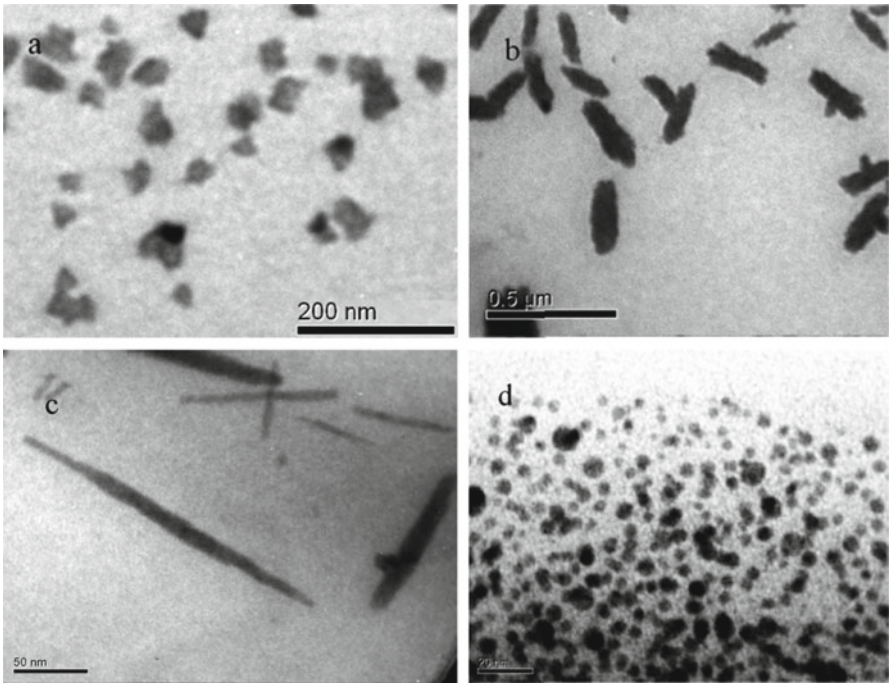

Fig. 28.2 Shapes of silver nanoparticles in the composites based on: (**a**, **b**) polyacrylamide; (**c**) epoxy amine resin and (**d**) polyurethane

28.4 Conclusions

Silver nanoparticles containing polymer composites have successfully been synthesized via an *in-situ* reduction approach. Changing functionality of polymers and, respectively, strength of coordination bonding between silver ions/particles and functional groups of polymer matrices provide a formation of polymer composites with defined shapes and sizes of silver nanoparticles. It supports a possibility for controlling or improving the antibacterial activity of synthesized materials.

References

1. Rai M, Yadav A, Gade A (2009) Silver nanoparticles as a new generation of antimicrobials. Biotechnol Adv 27(1):76–83
2. Silverstein RM, Webster FX, Kiemle D (2005) Spectrometric identification of organic compounds. Academic, New York
3. Pal S, Tak YK, Song JM (2007) Does the antibacterial activity of silver nanoparticles depend on the shape of the nanoparticle? A study of the gram-negative bacterium *Escherichia coli*. Appl Environ Microbiol 73(6):1712–1720

Part V
Water

Chapter 29
Recent Advances in Point-of-Access Water Quality Monitoring

Water Quality

O. Korostynska, K. Arshak, V. Velusamy, A. Arshak, and Ashok Vaseashta

Abstract Clean water is one of our most valuable natural resources. In addition to providing safe drinking water it assures functional ecosystems that support fisheries and recreation. Human population growth and its associated increased demands on water pose risks to maintaining acceptable water quality. It is vital to assess source waters and the aquatic systems that receive inputs from industrial waste and sewage treatment plants, storm water systems, and runoff from urban and agricultural lands. Rapid and confident assessments of aquatic resources form the basis for sound environmental management. Current methods engaged in tracing the presence of various bacteria in water employ bulky laboratory equipment and are time consuming. Thus, real-time water quality monitoring is essential for National and International Health and Safety. Environmental water monitoring includes measurements of physical characteristics (e.g. pH, temperature, conductivity), chemical parameters (e.g. oxygen, alkalinity, nitrogen and phosphorus compounds), and abundance of certain biological taxa. Monitoring could also include assays of biological activity such as alkaline phosphatase, tests for toxins such as microcystins and direct measurements of pollutants such as heavy metals or hydrocarbons. Real time detection can significantly reduce the level of damage and also the cost to remedy the problem. This paper presents overview of state-of-the-art methods and devices used for point-of-access water quality monitoring and suggest further developments in this area.

O. Korostynska
Dublin Institute of Technology, Dublin, Ireland

K. Arshak (✉) • V. Velusamy • A. Arshak
University of Limerick, Limerick, Ireland
e-mail: khalil.arshak@ul.ie

A. Vaseashta
Institute for Advanced Sciences Convergence, NUARI, Herndon, VA, USA

A. Vaseashta et al. (eds.), *Technological Innovations in Sensing and Detection of Chemical, Biological, Radiological, Nuclear Threats and Ecological Terrorism*, NATO Science for Peace and Security Series A: Chemistry and Biology,
DOI 10.1007/978-94-007-2488-4_29, © Springer Science+Business Media B.V. 2012

Keywords Water quality monitoring • Sensor arrays • Real-time detection

29.1 Introduction

Water is not a commercial product, but a heritage which must be protected, defended and treated as such. The water industry is one of the major sectors in the EU. Strong scientific base is needed for training, new knowledge and innovation to support the sector. In May 2007, the European Parliament proposed increasing from 33 to 61 the toxic products covered by European legislation on water quality. Forty five of these were classified as priority substances and should no longer be used by 2015.

Current measurements of nutrients, such as phosphorous, ammonia and volatile fatty acids in water are mostly based on off-line monitoring and imply low frequency data sampling and delay between sampling and availability of the results. According to the World Health Organisation (WHO), waterborne diseases are the world's leading cause of death [1]. To ensure a life-cycle approach to water treatment, the EU's WFD requires member states to establish monitoring programmes to assess the status of surface and groundwater. Real-time monitoring of wastewater quality remains an unresolved problem to the wastewater treatment industry. Thus, new standards and improved comparability and reliability of existing techniques are imperative [2].

Environmental water monitoring includes measurements of physical characteristics (e.g. pH, temperature, conductivity), chemical parameters (e.g. oxygen, alkalinity, nitrogen and phosphorus compounds), and abundance of certain biological taxa. Monitoring could also include assays of biological activity such as alkaline phosphatase, tests for toxins and direct measurements of pollutants such as heavy metals or hydrocarbons. Real time detection can significantly reduce the level of damage and the cost to remedy the problem.

Traditionally, the quality of treated wastewater is defined by the measurement of global parameters such as Biological Oxygen Demand (BOD), Chemical Oxygen Demand (COD), Total Organic Carbon (TOC), and Total Suspended Solids (TSS) [3]. Table 29.1 above summarizes normal methods of analysis of some water quality parameters.

When ammonia is present in levels above 0.1 mg/l N, sewage pollution or industrial contamination may be indicated. The vast majority of water supplies are treated with chlorine, a powerful oxidizing agent and an extremely efficient disinfectant requiring continuous monitoring. The treatment works for a public water supply characterized by a geographically distributed system that may be prone to leaks. Phosphorus is widely used as an agricultural fertilizer and within domestic detergents.

Table 29.2 above lists current techniques in monitoring wastewater quality and their limitations. Examples of molecular methods used to identify specific microorganisms and to assess microbial community diversity using DNA sequences [4] are

Table 29.1 Normal methods of analysis of some water quality parameters

Water quality parameter	Normal method(s) of analysis
Acidity	Titration with Sodium Hydroxide
Aluminium	Colorimetry; Atomic Absorption Spectrometry
Antimony	Atomic Absorption Spectrometry
Ammonia	Colorimetric (Manual; Nessler's Reagent; Automated; Berthelot Reaction)
Chlorine	Colorimetric
Phosphates	Manual or Automated Colorimetry

Table 29.2 Status of current techniques in monitoring wastewater quality and their limitations

Parameter	Technique	Limitations [2]
BOD	Non-specific sensor array (electronic nose)	Relationship is source/site specific and time dependent, further development needed
BOD, COD	Oxidation by hydrogen peroxide with UV light	Limited range and long (~55 min) measurement times, range and correlation are source dependent
OD, COD, TOC, TSS, Nitrates and anionic surfactants	UV spectral measurements and multivariate calibration	Sample handling is problematic, acquisition of reference spectra and calibration necessary for samples of different origin
BOD, nitrates, (TOC and COD)	Optical scattering (fluorescence)	Still in infancy, research needed, fluorescence affected by pH and temperature, correlation with BOD is plant sensitive.
BOD	UV adsorption (280 nm)	Poor sensitivity, uses only one wavelength, interferences from particles and toxic metals
COD, TOC	UV adsorption	Immerged sensor (fouling), influence of suspended particulate material
RQ value	Off-gas analysis (CO_2 and O_2)	Does not distinguish C-oxidation from N-removal, only big changes in nitrification activity can be monitored
COD, NH_4, NO_3	Artificial neural network + multi sensor (pH, temp, conductivity, redox potential DO, turbidity)	Approximate estimation, training needed, problems in case of sudden changes in wastewater composition, reliable for a short period only

listed in Table 29.3. These methods are applicable for detecting and identifying microorganisms (e.g. fecal indicators, pathogens) and examining community composition using microbial community DNA [5, 6].

Consequently, alternative cost-effective point-of-source solutions are necessary to assure the safety of water consumption, in particular for real-time wastewater quality monitoring.

Table 29.3 Status of current genomic tools that can be used to assess water quality

Tool	Description	Current status
Direct hybridization	Detection of genes, gene expression	Requires sequence knowledge and DNA to label for probe
PCR, RT-PCR	Rapid, sensitive detection of specific taxa, genes, or gene expression (RT-PCR)	In wide use, requires DNA sequence information
RAPD, RFLP, AFLP, AP-PCR, DGGE, T-RFLP, RFLP, ARDA	PCR-based, provides "fingerprint" of microbial community or the genome of microbial strains. Useful for description of community composition and source tracking	Widely used
Q-PCR, real-time PCR	Rapid, sensitive, quantitative detection of target	Use increasing rapidly, requires sequence knowledge
Fluorescent in situ hybridization (FISH)	Allows detection, visualization of individual cells	Widely used, requires actively growing cells. Can be combined with activity assays

29.2 Conventional and Analytical Techniques

Water quality assessments are based on the analysis of the physical, chemical and bacteriological parameters and require customized apparatus and trained staff. Such analytical procedures differ in duration. For example, conventional and standard bacterial detection methods such as culture and colony counting methods, immunology-based methods and polymerase chain reaction based methods, may take up to several hours or even a few days to yield an answer. Recently many researchers are focusing towards the progress of rapid methods and lead to the design and construction of high-selectivity biosensors enabling the presence of chemical and biological water pollutants to be detected rapidly. Felfoldi et al. [7] studied the occurrence of Pseudomonas *aeruginosa* and *Legionella* species with taxon-specific PCRs in samples taken at ten points of a municipal drinking water supply system in 3 months. Sequence analysis confirmed the positivity of samples and revealed a diverse community of legionellae. The results showed that chlorination was an important and effective disinfection method against pathogenic bacteria in drinking water, but pathogenic bacteria could reoccur in the system farther away from the chlorination point. No strong correlation was found between the presence of the investigated potentially pathogenic bacteria and the measured abiotic and biotic parameters within the investigated range. It was hypothesized that instead of physicochemical parameters, the main factors influencing the presence of pathogens in the drinking water were rather the composition of the microbial community, the biotic interactions between individual non-pathogenic and pathogenic microorganisms (competition or

promotion of growth) and the structure of biofilm grown on the inner surface of the supply system.

Lee et al. [8] developed a DNA microarray with 21 oligonucleotide probes to detect most of the common waterborne protozoan pathogens. The DNA microarray accurately identified 3 test protozoa strains based on the small subunit (SSU) rRNA gene sequence. The detection limit was approximately 1×10^3 target genes, or 50 *Cryptosporidium* parvum oocysts, per assay. The detection method developed by Kim et al. [9] to test for the presence of *E. coli O157:H7* was a multiple use technique which has very low susceptibility to background contaminants. It can be constructed mostly from off the shelf components minimizing costs. The sensor targets a DNA sequence specific to *E. coli O157:H7*. This process amplifies by approx. 10^9 the target DNA present in the sample. The amplified sample is deposited onto a microarray containing the exact opposite DNA sequence. If the target DNA is present in the sample the two sequences bond together.

Sungkanak et al. [10] demonstrated the first cantilever based *cholerae* sensor. Commercial gold-coated AFM microcantilevers are immobilized with monoclonal antibody (anti-V. *cholerae O1*) by self-assembled monolayer method. *V. cholerae O1* detection experiment was conducted in concentrations ranging from 1×10^3 to 1×10^7 CFU/ml. the reported that the microcantilever-based sensor has a detection limit of ~1×10^3 CFU/ml and a mass sensitivity, $\Delta m/\Delta F$, of ~146.5 pg/Hz, which was at least two orders of magnitude lower than other reported techniques.

29.3 Onsite Monitoring Stations

The monitoring demands are not being met due to the infrastructure and maintenance costs of conventional sensing models. Advanced autonomous platforms capable of performing complex analytical measurements at remote locations still require individual power, wireless communication, processor and electronic transducer units, along with regular maintenance visits. Hence the cost base for these systems is prohibitively high, and the spatial density and frequency of measurements are insufficient to meet requirements. Fay et al. developed a wireless aquatic navigator for detection and analysis water quality using a cost effective approach [11]. The paper demonstrated a low cost mobile sensing/communications platform together with very low cost stand-alone ‘satellite’ indicator stations that have an integrated colorimetric sensing material. The mobile platform was equipped with a wireless video camera that is used to interrogate each station to harvest information about the water quality. VanderNoot et al. [12] presented a unattended water sensor which employed microfluidic chip-based gel electrophoresis for monitoring proteinaceous analytes in a small integrated sensor platform. The instrument collects samples directly from a domestic water flow. The unattended water sensor prototype was configured to detect protein biotoxins such as ricin as a first step toward a total bioanalysis capability based on protein profiling.

29.4 Polymer Nanocomposite Sensors

Conducting polymer nanocomposite (CPC) materials are of special interest to the gas sensor industry where arrays of polymer composites may be used to detect gases and odours. These composite gas sensors operate at room temperature, which provides an advantage over thick film metal oxide gas sensors. Arshak et al. [13] reported the use of an array of conducting polymer nanocomposite sensors containing both carbon black and polyaniline to detect and identify the food and waterborne bacterial pathogens such as *Salmonella* spp., *Bacillus cereus* and *Vibrio parahaemolyticus* through production of an individual response pattern for each bacterium. Four sensor materials were used to analyse the bacteria vapors. The first material consisted of 20% wt. short chain polyaniline (emeraldine salt) grafted to lignin (PgL). The next three materials contained polyethylene adipate (PEA) and hypermer PS3 surfactant with 10%, 15% and 20% w/w of polyaniline loaded carbon black (PAN\CB), respectively. Figure 29.1 shows the responses obtained for the PgL sensor when exposed to the vapors given off each bacterium.It has been reported that the PgL sensor produced the highest response when exposed to vapours given off *Salmonella* with a 70% drop in baseline voltage. However, it did not return back to its original baseline voltage afterwards. The sensor's responses to *B. cereus* and *Vibrio* were similar showing that this sensor could not be used on its own as a means to differentiate between these three bacteria. The sensor with 10 w/w% PAN\CB produced the highest response to each bacterium. This was followed by the sensor with 15% PAN\CB while the lowest response was obtained from the sensor with 20% PAN\CB. Their results showed that sensors with lower volume fraction of conducting particles have higher sensitivity. Later the same group [14] studied the responses of polymer nanocomposite sensors to detect the presence of *Ralstonia pickettii*. M9 minimal growth medium was used to grow the bacteria and three different concentrations were prepared by taking samples after 2 , 4 and 6 h of growth. The sensor responses to *Ralstonia pickettii*is shown in Fig. 29.2. The sensors showed large sensitivity to each concentration of bacteria and produced a decrease in response over the growth cycle of the bacteria. These sensors demonstrated the

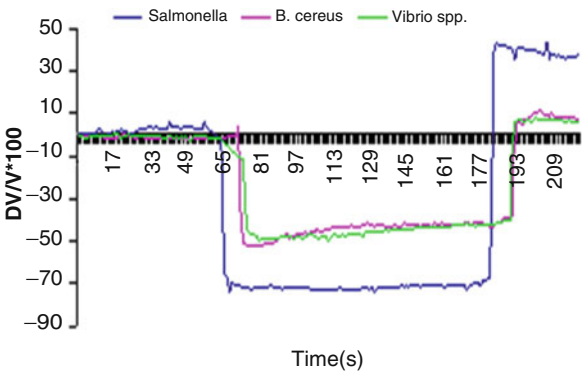

Fig. 29.1 The responses obtained for the PgL sensor when exposed to the vapours given off each bacterium [13]

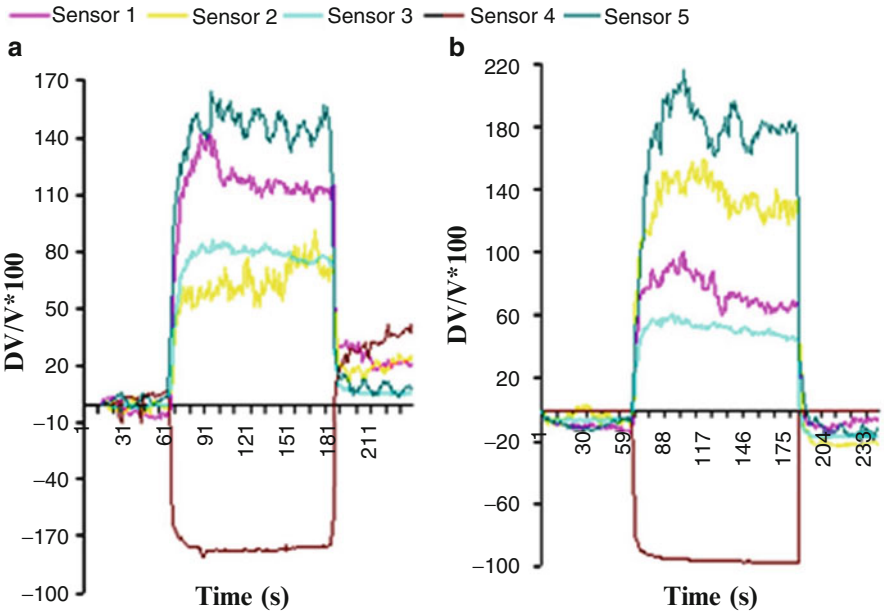

Fig. 29.2 (**a**) Sensor responses to M9 control. (**b**) Sensor responses to bacteria growing for 2 h in the M9 growth medium [14]

ability to detect early stage actively growing cells in real time, which is of large benefit to high purity water applications. The paper demonstrated that these kinds of sensors can be used to detect both lag phase and late exponential and stationary phase growing cells in a minimal nutrient environment.

29.5 Conclusion

Time is a vital factor in water quality monitoring, as there is the potential risk that pathogens will be transmitted in the aquatic environment, which is also open to bioterrorist attacks. The research at the intersection between nanotechnology, biotechnology and information technology is enabling the development of effective solutions to highly complex problems that were previously irresolvable. Biosensors combine the sensitivity and selectivity of classic analytical methods with a wide spectrum of advanced technological designs. The integration of biosensor technologies for water quality analysis with informatics systems for rapid, reliable and cost effective detection of contaminants is dependent on optimising sensor response and selectivity. To apply biosensor systems for water quality and site monitoring it is necessary to consider factors such as low detection limits, the toxicity of the compound, routes of migration and the concentration at which a compound becomes a significant threat to environment and health.

References

1. WHO (2005) Burden of disease and cost-effectiveness estimates http://www.who.int
2. Bourgeois W, Burgess J, Stuetz R (2001) On-line monitoring of wastewater quality: a review. J Chem Technol Biotechnol 76(4):337–348
3. Thomas O (1997) Wastewater quality monitoring. Trends Anal Chem 16(7):419–424
4. Devereux R (2006) Development and applications of microbial ecogenomic indicators for monitoring water quality: report of a workshop assessing the state of the science, research needs, and future directions. Environ Monit Assess 116:459–479
5. Campbell GA, Mutharasan R (2006) Detection of Bacillus anthracis spores and a model protein using PEMC sensors in a flow cell at 1 mL/min. Biosensors Bioelectron 22(1):78–85
6. Arora K, Chand S, Malhotra BD (2006) Recent developments in bio-molecular electronics techniques for food pathogens. Anal Chim Acta 568 (1–2):259–274
7. Felfoldi T, Tarnoczai T, Homonnay ZG (2010) Presence of potential bacterial pathogens in a municipal drinking water supply system. Acta Microbiol Immunol Hung 57(3):165–179
8. Lee DY, Seto P, Korczak R (2010) DNA microarray-based detection and identification of waterborne protozoan pathogens. J Microbiol Methods 80(2):129–133
9. Kim H, Kane MD, Kim S, Dominguez W, Applegate BM, Savikhin S (2007) A molecular beacon DNA microarray system for rapid detection of E. coli O157: H7 that eliminates the risk of a false negative signal. Biosensors Bioelectron 22(6):1041–1047
10. Sungkanak U, Sappat A, Wisitsoraat A, Promptmas C, Tuantranont A (2010) Ultrasensitive detection of Vibrio cholerae O1 using microcantilever-based biosensor with dynamic force microscopy. Biosensors Bioelectron 26(2):784–789
11. Fay C, Lau KT, Beirne S, Conaire CO, McGuinness K, Corcoran B, O'Connor NE, Diamond D, McGovern S, Coleman G, Shepherd R, Alici G, Spinks G, Wallace G (2010) Wireless aquatic navigator for detection and analysis (WANDA). Sens Actuat B Chem 150(1):425–435
12. VanderNoot VA, Renzi RF, Mosier BP, de Vreugde JLV, Shokair I, Haroldsen BL (2010) Development of an integrated microfluidic instrument for unattended water-monitoring applications. Electrophoresis 31(15):2632–2640
13. Arshak K, Adley CC, Moore E, Cunniffe C, Campion M, Harris J (2007) Characterisation of polymer nanocomposite sensors for quantification of bacterial cultures. Sens Actuat B 126:226–231
14. Arshak K, Adley CC, Moore EG, Cunniffe C, Campion M, Menvielle I (2007) Detection of Raistonia Pickettii bacteria in M9 medium using polymer nanocomposite sensors in IEEE sensors applications symposium. IEEE Computer Society, San Diego

Chapter 30
Fe-Oxides in Water Remediation Technologies

Fe-Oxides in Water Remediation

M. Vaclavikova, K. Stefusova, and G.P. Gallios

Abstract Water is essential for life, a strategic resource for every country and population. Its availability and sanitary safety is highly connected with the health and economic status of a population. The burden of disease due to polluted water is a major public health problem throughout the world. Many pollutants in water streams have been identified as toxic and harmful to the environment and human health, and among them arsenic, mercury and cadmium are considered those with the highest priority. Iron is the fourth most abundant element in the Earth's crust, and reactions involving iron play a major role in the environmental cycling of a range of important contaminants. Our earlier research has shown that Fe oxides/oxyhydroxides are particularly effective adsorbents of a range of contaminants (toxic metals), due to their high (reactive) specific surface area. It has been proven that Fe is particularly effective in As removal as a chemical bond is created on Fe surface and As is stabilised and can be safely deposited. Removal of contaminants from waste streams through precipitation with (hydrous) ferric oxides is an established methodology in a number of industrial processes (high density sludge systems for arsenic control in effluents from the mining industry, and in the treatment of textile dye effluent).

Keywords Iron oxides • Water remediation • Toxic metals • Arsenic

M. Vaclavikova (✉) • K. Stefusova
Institute of Geotechnics, Slovak Academy of Sciences, Watsonova 45,
Košice, SK-040 01, Slovakia
e-mail: vaclavik@saske.sk

G.P. Gallios
Lab of General & Inorganic Chemical Technology, School of Chemistry,
Aristotle University, Thessaloniki, Greece

A. Vaseashta et al. (eds.), *Technological Innovations in Sensing and Detection of Chemical, Biological, Radiological, Nuclear Threats and Ecological Terrorism*,
NATO Science for Peace and Security Series A: Chemistry and Biology,
DOI 10.1007/978-94-007-2488-4_30, © Springer Science+Business Media B.V. 2012

30.1 Introduction

In most developed nations, we take access to safe water for granted along with accessible water supplies. However, still today nearly one billion people (about 1/8) lack access to clean water [1]. Water contamination provides a significant threat to human health and the environment, and has been caused by a number of natural and anthropogenic inefficiencies, such as, spillage of pesticides and herbicides, industrial discharges from metal finishing, wood preserving operations and textile production and discharges from service industries involving fuels, solvent use, cleaning and paint removal. Over time, these toxic compounds can be carried downstream to contaminate groundwater or other receiving streams, poisoning sensitive ecosystems and contaminating drinking water resources. Many pollutants such as heavy metals, radionuclides and other substances in water streams have been identified as highly toxic and harmful to the environment and human health. Heavy metals are non-biodegradable species and thus the special attention should be given to the development of techniques for their removal and/or immobilisation. In the aqueous environment they occur in dissociated forms (cations i.e. Cd^{2+}, Pb^{2+}, Cu^{2+}, Zn^{2+}; anions/oxyanions i.e. $HAsO_4^{2-}$, CrO_4^{2-}, $HSeO_4^{-}$, $HSeO_3^{-}$, $HMoO_4^{-}$). Various treatment processes have been proposed for the removal of toxic substances from aqueous solutions including oxidation/reduction, coagulation/precipitation, reverse osmosis, adsorption and ion exchange. These methods are quite efficient for cations removal; however, their applicability for anions removal is quite limited. As cation removal is explored quite well, the proposed study deals with design of nanoscale materials suitable for removal of toxic metal anions/oxyanions i.e. chromates, arsenates, molybdenates etc. from waters.

Arsenic is considered as a high priority pollutant and carcinogen as well. In natural waters it occurs in the form of oxyanions as arsenites (As^{III}) and arsenates (As^{V}). Redox potential (Eh) and pH are the most important factors controlling As speciation. The arsenic distribution in aqueous system calculated and designed using Geochemist workbench 6.0 is given in Fig. 30.1.

It is obvious from the thermodynamic diagram (Fig. 30.1) that under oxidizing conditions arsenate species (H_3AsO_4, $H_2AsO_4^{-}$, $HAsO_4^{2-}$ a AsO_4^{3-}) predominate, while under reducing conditions arsenite species (H_3AsO_3 a $H_2AsO_3^{-}$) are predominant. Under oxidizing conditions, $H_2AsO_4^{-}$ is dominant at low pH (less than about pH 6.9), whilst at higher pH, $HAsO_4^{2-}$ becomes dominant ($H_3AsO_4^{0}$ and AsO_4^{2-} may be present in extremely acidic and alkaline conditions, respectively). Under reducing conditions at pH less than about 9.2, the uncharged arsenite species $H_3AsO_3^{0}$ will predominate [2, 3]. As the presence of arsenic species in drinking water, even in low concentrations, is a threat to human health, the World Health Organization (WHO) recommended the new maximum contaminant level (MCL) of arsenic in drinking water to 10 $\mu g.L^{-1}$ from an earlier value of 50 $\mu g.L^{-1}$ [4]. This greatly reduced limit was recently accepted by authorities of European Union (EU) as well as by United States Environmental Protection Agency (US-EPA) [5, 6].

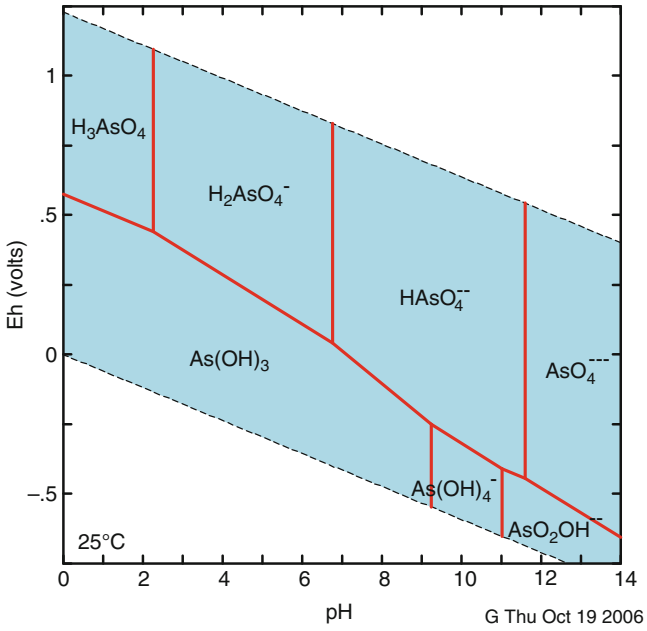

Fig. 30.1 Arsenic distribution in aqueous system

In the environment, iron plays an important role in contaminant mobility, sorption and breakdown due to its role as an electron donor (i.e. during the oxidation of Fe^{2+} to Fe^{3+}), and in its various forms, as a precipitant/sorbent substrate. Freshly precipitated, amorphous Fe oxyhydroxides (hydrous ferric oxides or HFO) are known to be particularly effective adsorbents of a range of contaminants, due to their high (reactive) specific surface area [7]. Removal of contaminants from waste streams through precipitation with (hydrous) ferric oxides is an established methodology in a number of industrial processes (high density sludge systems for arsenic control in effluents from the mining industry, and in the treatment of textile dye effluent). Iron based oxides are known to be good sorbents for oxyanion removal. Sorbed contaminants can either be surface adsorbed, co-precipitated or incorporated into the (Fe) oxide structure. Our earlier research has shown that Fe-oxide/oxyhydroxide based nanomaterials have high affinity towards arsenic and chromium oxyanions. However, the use of free nanoparticles is problematic due to their difficult manipulation and/or non-controllable behavior, as well as potential health and environmental effects. Thus, the incorporation of iron nanoparticles into a well organized zeolite matrix is an effective technique for the secure deposition of nanoparticles, while retaining the sorption affinity of both iron and zeolite sites towards toxic species in both anionic as well as cationic forms from aqueous media. This contribution presents the development, characterization and testing of Fe-zeolite composite sorbents towards arsenic oxyanions from aqueous media.

30.2 Experimental

Analytical grade chemicals were used in all experiments. Arsenic model solutions were prepared by dissolving $AsHNa_2O_4 \cdot 7H_2O$ in deionized water; $NaNO_3$ was used as electrolyte (0.01 and 0.1 M). The pH of the solutions was adjusted with suitable concentrations of analytical grade NaOH and HNO_3.

Natural zeolite (clinoptinolite type) from Nizny Hrabovec (Slovakia) was used for the preparation of the Fe-zeolite composite. Zeolite was added in a reaction vessel together with salts of Fe(III) and Fe(II) and a suitable quantity of alkaline solution was added. The suspension was stirred and magnetic zeolite was produced. The new sorbent was washed and dried. Its surface area and pore volume were determined using low temperature nitrogen adsorption and its point of zero charge was calculated from zeta potential measurements (ZetaPlus, Brookhaven Instruments).

30.2.1 Sorption Study

The sorption properties of modified zeolite were tested under both static (batch) as well as dynamic (column) conditions. The effect of pH, ionic strength, initial arsenic concentration, sorbent concentration, temperature, contact time of sorbent and arsenic solution were studied. The batch type experiments were performed in a rotary shaker set at 30 rpm and equilibrium time 24 h. The column experiments were performed using laboratory column as shown at Fig. 30.2. The arsenic quantity

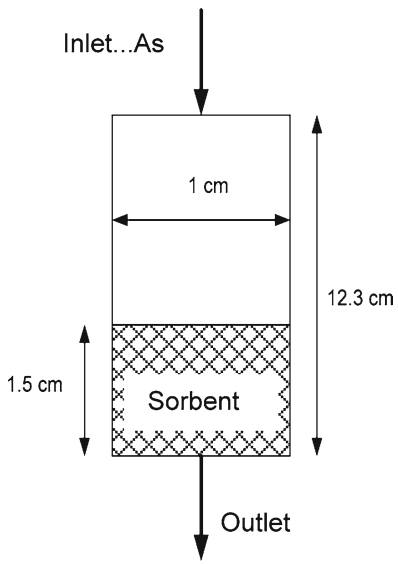

Fig. 30.2 Scheme of column experiment

in solutions was determined by AAS and UV-Vis spectrophotometry before and after the sorption experiments.

30.3 Results and Discussion

Zeolites (natural or synthetic) are very well known for their effectiveness in removing metal cations from water streams. They have been studied also for the removal of radioactive materials (i.e. thorium and uranium) and found to be quite effective. However, their affinity to metal anions is very limited. In our previous studies, iron oxides have been used effectively to remove arsenic from water streams. Their effectiveness increases with a decrease of the particle size. Nanosize materials are found to be very effective on the removal of As from water [3]. However, the subsequent solid/liquid (S/L) separation is more difficult as the particle size decreases. Magnetic iron oxides have the advantage of easy S/L separation but due to their small particle size are not suitable as fillers in sorption columns as the pressure drop increases dramatically. Moreover, there is an increasing number of reports on toxicity of manufactured nanoparticles for microbes, plants and mammals and the impact of free nanoparticles release to the environment, which create a lot of concerns and restrictions of the use of free nanoparticles. The magnetic zeolite produced here has shown good magnetic properties and also size suitable for sorption columns. The added value of this material is that the iron particles are safely incorporated into porous zeolite matrix while retaining the bulk of their particle reactivity. It is well known that the pH of solution plays an important role in sorption experiments in aqueous systems. It determines the aquatic chemistry of the system and also the charge density of the solid surface. It is related to the sorption mechanisms and reflects the nature of the physicochemical interactions of the species in solution and the active sites on the sorbent. For this reason, the pH is one of the first parameters that are examined in sorption studies.

The effect of initial arsenic concentration (20–200 mg/L) was studied with 2 g/L sorbent concentration, ambient temperature and pH values 3.5, 5.0 and 7.0. The results are given in Fig. 30.3. Sorption isotherms were fitted using the Freundlich model. The maximum sorption capacity was around 33 and 19 mg As(V)/g for pH values 3.5 and 7.0 respectively. The coefficient of determination (R^2) was over 0.95 and shows a good agreement of the model to the experimental data. As expected, the sorption capacity was much higher at acidic pH (3.5) than at neutral (pH 7.0). However, the results at pH 7.0 are also considered promising, as it is the usual pH of drinking water treatment. A techno-economical study that will take into account the actual quantities of water to be treated, the additional treatment needed for the removal of other contaminants and the cost of the total process will be needed in order to define if it is more cost effective to use As removal at pH 3.5, where the sorption efficiency is greater but the additional steps of pH adjustment before and after treatment are needed or remove it at pH 7.0 with less efficiency but no extra steps. In order to get additional information about the sorption process, the

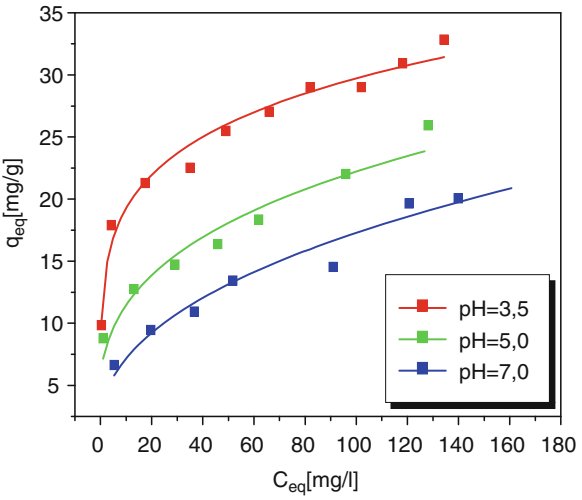

Fig. 30.3 Arsenic removal: initial concentration and pH dependence

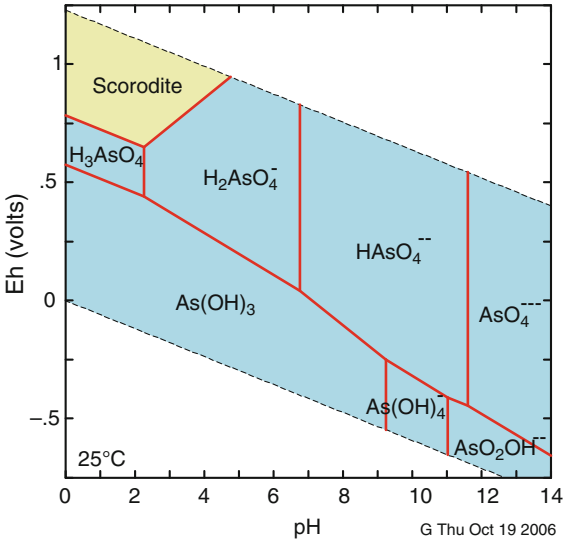

Fig. 30.4 Arsenic distribution in aqueous system in the presence of magnetite

experimental study has been supported by thermodynamic calculations using the Geochemist Workbench 6.0 sw. Figure 30.4 presents the effect of redox potential on the speciation of arsenic in the presence of iron (100 mg/L).

It is obvious that at acidic pH and oxidizing conditions, arsenic reacts with iron to form the mineral scorodite. Magnetite has both iron(II) and iron(III) on its surface and can locally create a redox system with arsenic. It is not possible to measure the redox potentials at the surface of small particles at the moment, so, the behavior

was simulated in the software by assuming a certain amount of iron in solution (100 mg/L in this case). However, the iron in magnetite is fixed on the surface and it is available to more alkaline pH values and it is expected to form chemical bonds with arsenic at higher pH values as well. This has also been confirmed by Deliyanni et al. [8]. The greater efficiency of magnetic zeolite at pH 3.5 than pH 5.0 and pH 7.0, coincides very well with the predictions of the thermodynamic diagram.

The zeta potential of zeolite and magnetic zeolite was measured as a function of pH (pH values 3.0–9.5) [9]. Zeolite was negatively charged at the whole pH range studied showing a smooth increase of negative charge from −5 mV at pH 3.0 to around −30 mV at pH 9.5. A point of zero charge (PZC) was not observed in this pH range. Given that arsenic is also negatively charged at this pH range (see Fig. 30.1) the electrostatic forces are repulsive. The only way for arsenic to be sorbed on zeolite is through specific sorption usually by creation of chemical bonds. The low sorption efficiency of zeolite for arsenic shows that special sorption forces do not exist in any significant degree. The shape of the zeta potential curve of magnetic zeolite has been totally different. A PZC was observed at pH around 5.0. Its surface was positively charged at pH values smaller than 5.0 with around +17 mV at pH 3.0 (around +15 mV at pH 3.5). At pH values greater than 5.0 its surface was negatively charged. The charged decreased sharply (increased negative charge) from pH 5.0 to pH 9.5 where it was around −30 mV (it was −25 mV at pH 7.0). This coincides pretty well with our sorption experiments. At pH 3.5 magnetic zeolite has a positive surface charge and the arsenic form that predominates is the negatively charged $H_2AsO_4^-$; the electrostatic forces are attractive and help the chemical affinity forces (formation of scorodite as shown in Fig. 30.4) and sorption affinity is high. At pH 5.0 the surface of magnetic zeolite is neutral so, only chemical sorption is present and the material has still quite good efficiency. At pH 7.0, the negative $HAsO_4^{2-}$ predominates and the electrostatic forces with the negatively charged magnetic zeolite forces are repulsive. The efficiency of the material is mainly due to the higher attraction created by the chemical forces, but their effect is reduced by the opposite electrostatic forces and lower efficiency is observed. This is also proven by the shift of the PZC and the reverse of the charge from positive to negative when the zeta potential is studied in the presence of 100 mg/L arsenic in solution [9].

30.3.1 Column Experiments

Column experiments were performed using two different size fractions of magnetic zeolite (250–400 and 400–500 μm) and the results are shown in Fig. 30.5. It is shown that the performance of both materials is very similar. At the important part (before the breakthrough point), their performance is almost identical. If we consider that the bigger size (400–500 μm) has a smaller pressure drop, this size fraction would be more economical to be used as a filler in sorption columns.

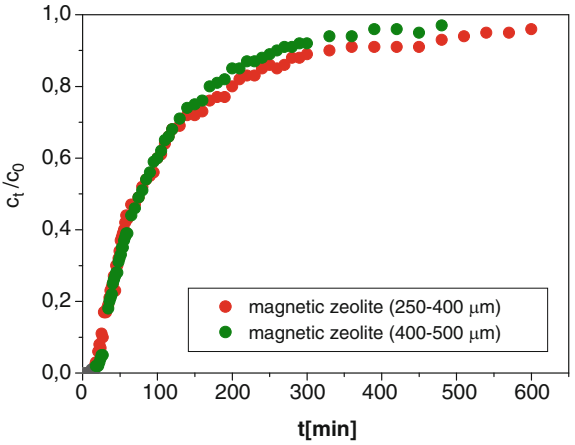

Fig. 30.5 Removal of arsenic using column (initial $c_{As} = 100$ mg/L)

30.4 Conclusions

Magnetic zeolite is an efficient sorbent for the removal of arsenic from water streams. The best efficiency is observed at acidic pH values (pH 3.5) but its efficiency was significantly good also at pH 7.0 which is very close to the pH of natural waters. Iron oxides incorporated within a zeolite structure of particle size 400–500 μm can be used as fillers in sorption columns and have good performance in removing arsenic from water. Sorption of arsenic on magnetic zeolite is of chemical nature (creation of scorodite mineral on the surface); at pH values smaller than 5.0 (which is the PZC) the electrostatic forces are attractive and favour arsenic removal while at pH values greater than 5.0 the repulsive electrostatic forces decrease the overall efficiency of the sorbent.

Acknowledgement This research has been supported by Slovak Research and Development Agency within the project No APVV-0252-10.

References

1. water.org™ (2011) Nearly one billion lack access to safe water. http://.water.org/ (site accessed on 01/03/2011)
2. Smedley PL, Kinniburgh DG (2002) A review of the source, behaviour and distribution of arsenic in natural waters. Appl Geochem 17(5):517–568
3. Vaclavikova M, Gallios GP, Hredzak S, Jakabsky S (2008) Clean Techn Environ Policy 10(1):89–95
4. WHO (2004) Guidelines for drinking water quality. 3rd ed. vol 1, Recommendations. WHO Geneva, Switzerland
5. European Commission Directive 98/83/EC (1998), related with drinking water quality intended for human consumption. Brussels, Belgium
6. US-EPA (2002) Office of Ground Water and Drinking Water. Implementation guidance for the arsenic rule. EPA report-816-D-02-005, Cincinnati
7. Cundy A, Hopkinson L, Whitby R (2008) Sci Total Environ 400:42–51
8. Deliyanni EA, Bakoyannakis DN, Zouboulis AI, Matis KA (2003) Chemosphere 50(1):155–163
9. Stefusova K (2009) Iron based sorbents for the removal of toxic species from waters. PhD thesis, Technical University Košice. 115 p

Chapter 31
Electrochemical Oxidation of Synthetic Dyes in Simulated Wastewaters

Electrochemical Oxidation of Dyes in Wastewaters

G. Gallios, X. Violintzis, I. Voinovskii, and A. Voulgaropoulos

Abstract An electrochemical oxidation method for the degradation of synthetic reactive azodyes found in textile wastewaters is discussed. Four commercial synthetic dyes (black, blue, red and yellow) commonly used in dying operations were studied in single, binary and ternary mixtures. Low (100 mg/L) and high (500, 1,000 and 2,000 mg/L) initial dye concentrations were studied. The effect of various sodium chloride concentrations (as supporting electrolyte) on the effectiveness of electrochemical oxidation was examined. The effect of current intensity (1.5, 2.5 and 3.0 A) and pH (vales 3, 5, 7 and 10) was studied as well. The kinetics of the electrochemical oxidation for each dye were studied and compared. The conditions for effective dye degradation even from 2,000 mg/L initial concentration were established. The method was proved very effective even with binary and ternary mixtures of basic synthetic dyes. The Chemical Oxygen Demand (COD) and the Total Organic Carbon (TOC) were reduced by 60% and 25% respectively, meaning that the treated solutions were friendlier to the environment.

Keywords Synthetic dyes • Oxidation • Electrochemical • Removal • Wastewater

G. Gallios (✉) • I. Voinovskii
Department of Chemical Technology and Industrial Chemistry, School of Chemistry, Aristotle University of Thessaloniki, Thessaloniki 54124, Greece
e-mail: gallios@chem.auth.gr

X. Violintzis • A. Voulgaropoulos
Department of Physical, Analytical & Environmental Chemistry, School of Chemistry, Aristotle University of Thessaloniki, Thessaloniki, Greece

A. Vaseashta et al. (eds.), *Technological Innovations in Sensing and Detection of Chemical, Biological, Radiological, Nuclear Threats and Ecological Terrorism*, NATO Science for Peace and Security Series A: Chemistry and Biology,
DOI 10.1007/978-94-007-2488-4_31, © Springer Science+Business Media B.V. 2012

31.1 Introduction

Textile industries produce large quantities of wastewater from the dyeing and finishing processes that cause severe pollution problem. Textile wastewater is strongly colored and has high values of pH, temperature and COD, while it shows low biodegradability. The release of colored effluents into the environment is undesirable because of their color, and because many dyes from wastewater and their breakdown products exhibit toxic, even mutagenic or carcinogenic properties, affecting the aquatic ecological system [1–5].

Today nearly one million metric tones of dyes is annually produced in the world; azo dyes ($R_1-N=N-R_2$) represent about 70% on weight basis of this amount. Recent estimates indicate that 12% of the synthetic dyes used yearly are lost to wastewater streams. Approximately 20% of these enter the environment through effluents from wastewater treatment plants [6].

Increased color intensity is the most serious problem from textile industry wastewater. Additionally, azodyes can produce hazardous aromatic amines and highly toxic by-products that occur from metabolic processes in plants and animals after disposal in lakes, rivers, or seas. The low biodegradability of the synthetic azodyes is due to the lack of natural biodegradation paths, and to stereochemical interferences concerning the accession of the reductant or oxidant molecule to the azo-group [1].

Textile industry wastewaters are treated by conventional methods such as adsorption, chemical oxidation or reduction, and biological degradation. Adsorption shifts the pollution problem into solid waste disposal, while chemical treatment produces final wastewaters contaminated with significant amounts of chemical reagents. Biological treatment, the most commonly used procedure, causes sludge formation and cannot degrade the pollutants completely given that huge polyaromatic organic molecules are hard to biodegrade because of stereochemical interferences [2, 3].

Because textile wastewater composition varies widely, traditional treatment methods are becoming less effective; however, newly developed electrochemical treatment of textile wastewaters is proving very effective because of its versatility, energy efficiency, automation, and cost effectiveness. Electrochemical treatment methods remove color with little or no consumption of chemicals; and degradation of recalcitrant pollutants can be achieved [7, 8]. This study demonstrates the effectiveness of electrochemical degradation of four synthetic reactive azodyes widely used in the textile industry at both low and high initial dye concentrations.

31.2 Materials and Methods

Four (4) commercial synthetic reactive dyes (Kahafix Reactive Black XL, CI Direct Red 239, CI Reactive Blue CI 19 and CI Reactive Yellow 176) were used for creating the simulated solutions. Kahafix Reactive Black XL is a mixture of 75% Reactive Black 5% and 25% Reactive Orange, and is widely used for cotton dyeing. The other colors used were single colors. The electrochemical cell used in the

experiments was constructed from Plexiglas, with a working volume of 500 mL and electrode placements at 1 cm distance. One anode placed between two cathodes in the center of the cell was used as electrodes. The anode was made of niobe/synthetic diamond doped with boron (Nd/D) and the cathodes from stainless steel (SS). Initial solutions were prepared by dissolving appropriate amounts of the respective dye in deionized water. The examined concentrations were 100, 500, 1,000, 2,000 mg/L. Sodium chloride (NaCl) was used as supporting electrolyte.

All experiments were carried out at room temperature. For each experiment a model dye solution was prepared of a certain concentration. The pH was adjusted to the desirable value (3–10 ± 0.2) by the addition of NaOH or HNO_3 solutions. A certain volume of the dye solution (500 mL) was transferred to the electrochemical cell, a small amount of supporting electrolyte (4–20 mL NaCl 1 mol/L) was added and potential was applied with a galvanostat. The current intensity was kept constant (at 1.6, 2.5 A or 3 A) during the experiment. An air pump supplied air at the base of the cell. Samples of 10 mL were taken at various time intervals. The concentration of the dye was determined by measuring the absorbance peaks, at wavelengths corresponding to each azodyes using a Hitachi 2000 UV-Vis spectrophotometer. COD was measured with cuvette test LCK 114 and LCK 314 and TOC using a Shimanzu TOC-V CSH, Total Organic Carbon Analyzer.

31.3 Results and Discussion

31.3.1 Kinetics of Dye Degradation

The physical methods used to remove azodyes from the wastewaters of textile industries, such as sorption procedures and membrane ultrafiltration, produce azodye concentrates that are disposed off as toxic wastes. The best solution is to degrade them to smaller biodegradable compounds before disposal. Our previous work showed that electrochemical oxidation is effective in degrading synthetic dyes from low initial dye concentrations (5–100 mg/L). This work examined higher initial dye concentrations (500, 1,000 and 2,000 mg/L) that are not usually found in textile wastewaters (due to the dilution from washing operations), but are produced from other treatment methods. For example, concentrates of reactive dyes produced by flotation of synthetic dye solutions were degraded effectively by power ultrasounds [9].

The kinetics of the commercial black dye degradation is given in Fig. 31.1a, b. This dye is a mixture with black and orange components both were measured at the respective wavelengths (602 nm for black and 489 nm for orange). The treatment conditions were current intensity 2.5 A, pH 10.0 and 12 mL of 1M NaCl added as electrolyte. A fast decoloration was observed for all the examined solutions. The time needed for the degradation of the dye increased proportionally with the initial dye concentration. Almost complete decoloration was achieved for all concentrations in about 30 min, showing the effectiveness of the method. This is considered a great achievement since

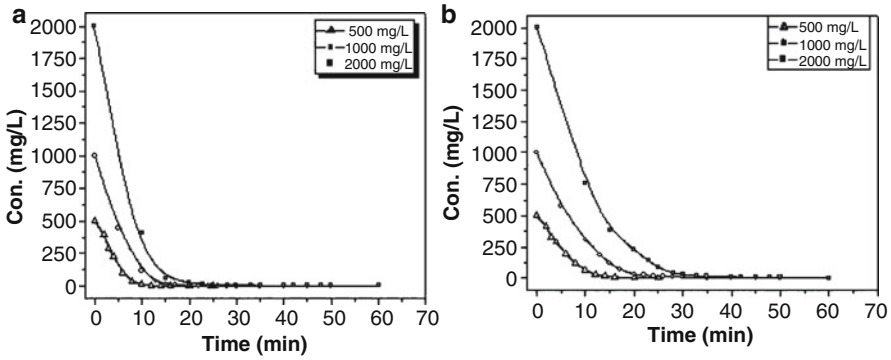

Fig. 31.1 (**a**) Black dye degradation (measured at 602 nm) as a function of time. (**b**) Orange dye degradation (measured at 489 nm) as a function of time

Table 31.1 Half-lives for various initial dye concentrations

Initial dye conc. (mg/L)	500	1,000X	2,000
$t_{1/2\ (Reactive\ Black)}$ (min)	3.5	4.6	5.2
$t_{1/2\ (Reactive\ Orange)}$ (min)	4.9	6.5	7.2

other advanced oxidation methods need more than 60 min to achieve similar results with lower initial dye concentrations. Very little published work demonstrates high concentrations reduced to less than the current limit (of 1 mg/L) for pure dyes in such a short amount of time. With 500 mg/L initial concentration, the black component was completely removed in 10 min (Fig. 31.1a) while 15 min were needed for the orange color component (Fig. 31.1b). For initial concentrations 1,000 mg/L and 2,000 mg/L, more time was needed for complete decoloration (20 min for black and 30 min for orange component). However, both were completely decolorized at the end of the respective time treatments. As expected, higher initial dye concentrations needed more time for complete decoloration. However, after 30 min treatments, complete decoloration of all dye solutions was obtained (even that of 2,000 mg/L initial dye concentration). Final concentrations were below the limit and no further treatment was needed for color removal. The results showed that the black color component had faster kinetics than the orange component at all studied concentrations.

The corresponding half-lives of black and orange components are given in Table 31.1. The optimized oxidation conditions used here of 7.2 min are enough to reduce dye concentration to half even from 2,000 mg/L.

Real textile wastewaters contain other components that may adsorb at different wavelengths. Sometimes when a dye is oxidized, components that adsorb at different wavelengths may be formed. To examine this effect, the full visible spectra of the studied dyes were recorded at different treatment times with results given in Fig. 31.2. The initial values were clipped at three units of Absorbance (meaning that the original absorbance was more). The initial dye has a high absorbance at the whole range of the visible spectra (400–700 nm).

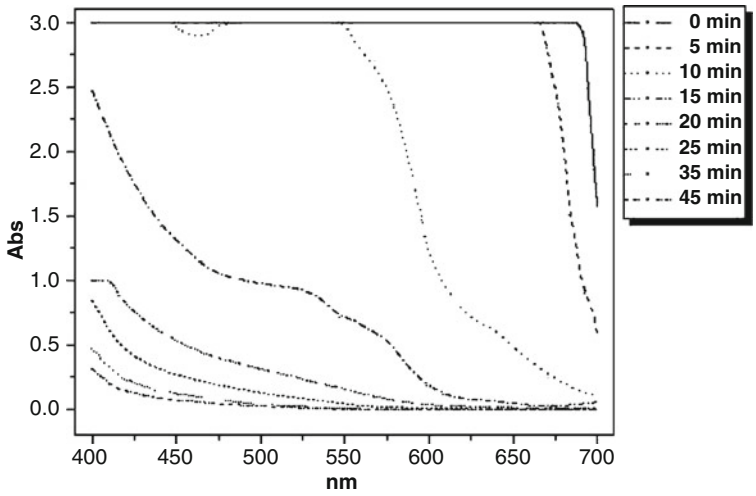

Fig. 31.2 The UV-Vis spectra of the black azodye during the electrochemical treatment. Initial dye conc. 1,000 mg/L, current intensity 2.5 A, 16 mL NaCl 1M and pH 10.0

With a 5 min treatment, the black component was reduced by 50% (Table 31.1, 1,000 mg/L) but the absorbance is still very high. After 10 min of treatment, a visible effect in the black region is observed. At 20 min, the absorbance is decreased significantly at the whole visible range. After 30–35 min treatment, the decoloration is almost complete. A very small absorbance is observed after 45 min of treatment. Under these conditions, the rate of dye degradation is controlled by mass transfer limitations. The dye molecules diffuse to the electrodes' surfaces, react there, and the reaction products diffuse from the electrodes' surface to the bulk of the solution. As the concentration increases, the reaction rate becomes diffusion controlled, since the rate of the electron transfer is much faster than the diffusion rate, rendering the degradation rate proportional to the bulk concentration of the dye [8].

31.3.2 Effect of Electrolyte Concentration

In electrochemical processes, the type and concentration of the supporting electrolyte is very important. Typical textile wastewaters contain significant quantities of NaCl for improving the dye efficiency, thus our study used NaCl as the supporting electrolyte. The results are presented in Fig. 31.3a (black) and 31.3b (orange). Clearly, NaCl significantly affects the kinetics of dye decoloration. With increased quantities of NaCl (4, 8 and 12 mL), the decoloration rate increases significantly. However, further addition of an electrolyte (12, 16 and 20 mL) had minimal effect on the decoloration rate.

The drastic effect of chlorides on the dye's degradation rate can be explained, if the electrolysis of NaCl is considered. The electrolysis of NaCl results in some very

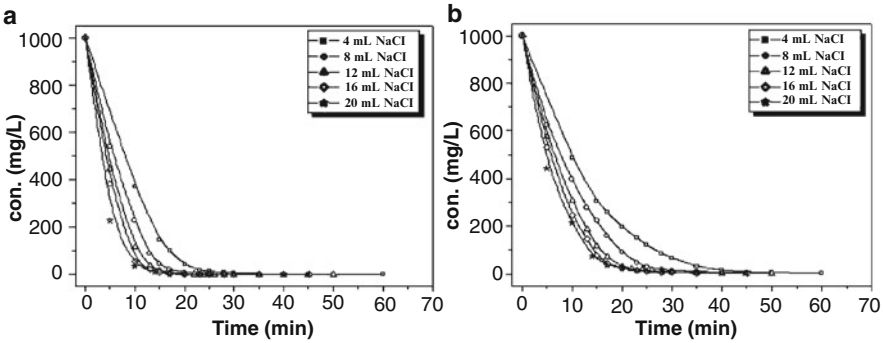

Fig. 31.3 (**a**) Effect of 1M NaCl quantity on black dye component removal (measured at 602 nm). Dye conc. 1,000 mg/L, current intensity 2.5 A and pH 10.0. (**b**) Effect of 1M NaCl quantity on orange dye component removal (measured at 489 nm). Dye conc. 1,000 mg/L, current intensity 2.5 A and pH 10.0

strong oxidants, such as free chlorine (Cl_2), at the anode, with subsequent formation of hypochlorite anions (ClO^-). The whole decoloration proceeds via direct oxidation reactions on the electrodes, enhanced by indirect oxidation reactions by the produced oxidants. Stronger oxidants achieve better enhancement. Consequently, dye molecules can effectively be degradated in aquatic media containing chloride anions (Cl^-) [2]. Concentrations of chloride ions above certain value cannot improve the decoloration rate. So, the best results are taken by the addition of 12 mL of 1M NaCl, which achieves a satisfactory degradation process with minimum production of environmentally unfriendly chemical compounds. Note that chloride ions are present in significant quantities in textile industry wastewater and adequate decoloration should occur with no further addition of electrolyte.

31.3.3 Effect of pH

In all wastewater treatment operations, the pH of solution is an important parameter to be tested. However, as total concentrations increase, the effect of pH becomes less important. We studied the effect of pH on dye decoloration under optimized oxidation conditions for 1,000 mg/L initial dye concentration. The results are shown in Fig. 31.4a for black and 31.4b for orange dye component. Four different pH values (3, 5, 7 and 10) common to pH values of wastewaters were used. A small effect of pH is observed on dye decoloration and is the same for both black and orange components. At acidic pH values, the degradation process is initially faster, achieving a higher degree of decoloration than at higher pH values. However, after 20 min for black and 25 min for orange, the final decoloration is similar at all pH values studied. Acidic-neutral pH is the optimal range for the production of some very important oxidants, such as (Cl_2) and (ClO^-) anions, which enhance the decoloration process.

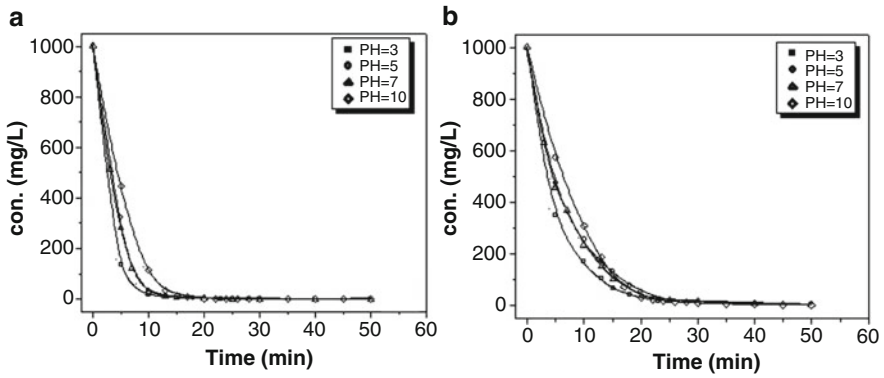

Fig. 31.4 Effect of pH on (**a**) black dye component removal (at 602 nm). Dye conc. 1,000 mg/L, I = 2.5 A and 12 mL NaCl 1M. (**b**) orange dye component removal (at 489 nm). Dye conc. 1,000 mg/L, I = 2.5 A and 12 mL NaCl 1M

In alkaline pH, the formation of the above-mentioned important agents is restrained. However, our results show that the pH does not play an important role for the complete treatment at 30 min.

31.3.4 Effect of Current Intensity

The amount and the type of the supporting electrolyte are strictly coupled with the applied voltage for the same current intensity. A high concentration of electrolyte needs low voltage to attain the current intensity, while a low concentration requires higher voltage for the same result. In any case, the lowest possible potential value should be applied to achieve a satisfactory level of decoloration. Higher values lead to energy loss, high temperatures and faster electrode damage. As the voltage varies during the process, the current intensity was chosen as the parameter to keep constant through the experiments. The current intensity directly affects the flow of electrons, and consequently the whole oxidation process. However, once enough electrons are present for all redox processes, further increases should not affect the whole process. In previous work with smaller current intensities (0.5–1.5 A), the increase of current intensity increased the kinetics of the process. We chose 2.5 A as a value for effective and fast treatment of dye solutions with initial concentrations up to 2,000 mg/L. However, to test if a further increase in current intensity would affect the kinetics, 3.0 A was also tested and the results were compared with those for 2.5 A current intensity. The results are presented in Fig. 31.5a for the black and 31.5b for the orange component of the dye. A small difference is observed at the initial decoloration steps but the final result is the same for both current intensities; thus 2.5 A was chosen for our work.

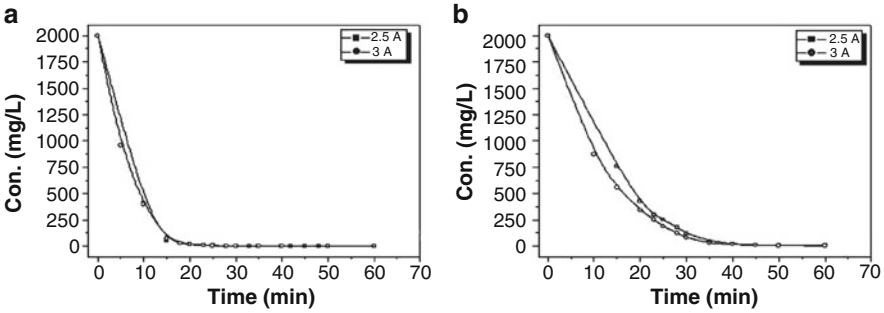

Fig. 31.5 Effect of applied current intensity on (**a**) black dye component removal (at 602 nm). Dye conc. 2,000 mg/L, 12 mL NaCl 1M and pH 10.0. (**b**) on orange dye component removal (at 489 nm). Dye conc. 2,000 mg/L, 8 mL NaCl 1M and pH 10.0

31.3.5 Decoloration of Artificial Mixtures

The real wastewaters of textile dying operations contain mixtures of dyes and many other components. Basic dyes such as blue, red, yellow, and black are usually found with varying concentrations. Therefore, a good treatment method to be applied in existing installations should be able to effectively treat various mixtures of dyes. For this reason, we studied the electrochemical oxidation of basic synthetic reactive dyes of Blue (CI 19), Red (CI 239) and Yellow (CI 176) in single, binary and ternary mixture solutions. The results are presented in Fig. 31.6a for single solutions and in Fig. 31.6b for mixtures of the basic dyes. The applied current intensity was 1.6 A and 4 mL of NaCl 1M was added as an electrolyte. Results showed that in single solutions, the blue color is degraded faster than the other two (Fig. 31.6a), and red is degraded faster than yellow. At around 30 min, all colors are degraded satisfactory. With single solutions, it is easy to determine the final concentration of each color; but with mixtures of colors, it is much more difficult. The American Dye Manufacturers Institute recommends the ADMI units method that determines all visible wavelengths, so even colors produced from treatment are accounted for. The limit for safe discharge is 300 ADMI units. The ADMI units' method was used for presenting the results from electrochemical oxidation of binary and ternary mixtures shown in Fig. 31.6b. The horizontal line represents the discharge limit of 300 ADMI units. Results showed that the yellow and blue mixture is degraded in 12 min which is much faster than the degradation of the yellow and red mixture of approximately 30 min. The ternary mixture containing contains all three colors degraded slowly but completely after 55 min of treatment (Fig. 31.6b). The decoloration curves show some hysteresis at the beginning which might be due to the partial reactions taking place between the intermediate products from the oxidation of dyes.

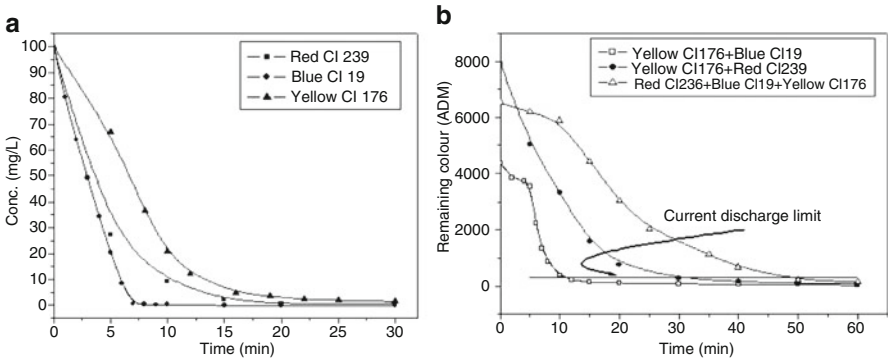

Fig. 31.6 (**a**) Decoloration of (**a**) individual dyes – Initial conc. 100 mg/L, I = 1.6 A, 4 mL NaCl 1M and pH 10.0. (**b**) mixtures of dyes. Initial conc. 100 mg/L, I = 1.6 A, 4 mL NaCl 1M and pH 10.0

Comparing the yellow-blue and yellow-red mixtures (Fig. 31.6b) with the yellow degradation curve (Fig. 31.6a); it seems that the presence of the blue color causes the yellow to degrade faster. This might be due to interactions between partial oxidation products of the basic dyes, but further study with analysis of intermediate products is needed. The final conclusion is that electrochemical oxidation is effective in treating mixtures of basic dyes to values below the discharge limit of 300 ADMI units.

31.3.6 Total Organic Carbon (TOC) and Chemical Oxygen Demand (COD)

A significant decrease of COD (63% from 1,000 mg/L, 55% from 2,000 mg/L) and TOC (22% for 1,000 mg/L and 28% for 2,000 mg/L) values is observed after the electrochemical oxidation. This shows that around 25% of organic carbon has been oxidised to harmless inorganic compounds and the final wastewater is friendlier to environment. As the colour completely disappeared, the recalcitrant non-biodegradable polyaromatic compounds were broken into smaller more biodegradable compounds which could be easily eliminated by existing biological treatment methods. Similar TOC reduction was observed for the other colours. Figure 31.6a results show that the blue colour degrades most quickly meaning that the break of the azo bonds is fast, but as the TOC decrease is only 6%, the oxidation does not proceed to carbon mineralization. The yellow colour degrades most slowly, but carbon mineralization is obtained by 21%, indicating that the final products from yellow colour are friendlier to the environment than ones coming from the blue colour.

31.4 Conclusions

Electrochemical oxidation is an effective method for decoloration of commonly used commercial synthetic reactive azodyes from solutions of single dyes and binary and ternary mixtures of blue, red and yellow dyes. It effectively treats high initial concentrations of a commonly used commercial black dye. Chloride anions play a very important role in decreasing the decoloration time. Since this electrolyte exists in the textile wastewater as a remaining dye-bath additive, experiments with real samples should run without further addition of any chemical reagent. The process is effective in a wide range of pH between 3.0 and 10.0 when high initial concentrations of dyes and appropriate current intensity are used. This wide optimal pH range renders the method rather versatile. The final treated wastewaters are friendlier for the environment as the TOC is reduced by 25% and the COD by 60%.

Acknowledgements The dye and relevant information on their use were supplied by KYKE Hellas.

References

1. Sakalis A, Mpoulmpasakos K, Nickel U, Fytianos K, Voulgaropoulos A (2005) Evaluation of a novel electrochemical pilot plant process for azodyes removal from textile wastewater. Chem Eng J 3:63–70
2. Sakalis A, Nickel U, Fytianos K, Voulgaropoulos A (2006) A comparative study of platinised titanium and niobe/synthetic diamond as anodes in the electrochemical treatment of textile wastewater. Chem Eng J 119:127–133
3. Gallios G, Voinovschi I, Voulgaropoulos A (2010) Effect of electrolytes on the electrochemical oxidation of synthetic dyes. In: Vaclavikova M et al (eds) Water treatment technologies for the removal of high-toxicity pollutants. Springer, Dordrecht, pp 169–176
4. Santos AB, Cervantes FJ, Lier JB (2007) Review paper on current technologies for decolourisation of textile wastewaters: perspectives for anaerobic biotechnology. Bioresour Technol 98:2369–2385
5. Hao OJ, Kim H, Chiang PH, Nickel U (2000) Decolorization of wastewater. Crit Rev Environ Sci Technol 30:449–505
6. Wijetunga S, Wenquan R, Li X, Chen J (2006) Decolourization of textile wastewater containing acid dyes in UASB reactors system under mixed anaerobic granular sludge. Electron J Environ Agric Food Chem 3(1):1224–1234
7. Mohan N, Balasubramanian N, Basha CA (2007) Electrochemical oxidation of textile wastewater and its reuse. J Hazard Mater 147:644–651
8. Fern.andes A, Morao O, Magrinho M, Lopes A, Goncalves I (2004) Electrochemical degradation of C. I. Acid Orange 7. Dye Pigment 61:287–296
9. Dafnopatidou EK, Gallios GP, Tsatsaroni EG, Lazaridis NK (2007) Reactive dyestuffs removal from aqueous solutions by flotation, possibility of water reuse and dyestuff degradation. Ind Eng Chem Res 46:2125–2132

Chapter 32
Electrochemical Methods for Cleansing of H_2S and SO_2 in Industrial and Natural Contaminated Waters

Elcox Method

Konstantin Petrov

Abstract Hydrogen sulfide and sulfur dioxide are hazardous to the environment pollutants. They are contained in industrial and utility waste gases and waters as well as in some natural lakes and Seas. The present paper is a review of our studies on the electrochemical oxidation-reduction processes for SO_2 and H_2S cleansing by their oxidation with oxygen contained in the air. An innovative Carbon-Teflon structure of the electrodes (membranes) allows for the simultaneous electro-catalytic reactions of SO_2, H_2S and oxygen, proceeding on dispersed micro-galvanic elements, based on their chemical affinity without external power application. The physical model of electrochemical reactions in Carbon-Teflon electrodes is presented. The electrochemical nature of the processes is revealed using the additive principle. The results are used for development of processes for purification of SO_2 and H_2S from industrial gasses and waters. The major relations describing the processes, namely the impacts of sulfur dioxide and sulfuric acid concentrations have been studied. The revealed simplified expressions facilitate the performance estimation of an innovative process for SO_2 cleansing in waste gases, labeled ELCOX.

Keywords Hydrogen sulfide • Sulfur dioxide • Electrochemical processes

32.1 Introduction

Many electrochemical systems feature one or more oxidation-reduction couples. When in disequilibrium, two opposing processes of reduction and oxidation occur onto one and the same surface [1–3]. These two processes take part in a

K. Petrov (✉)
Institute of Electrochemistry and Energy System,
Bulgarian Academy of Science, Sofia, Bulgaria
e-mail: kpetrov@bas.bg

A. Vaseashta et al. (eds.), *Technological Innovations in Sensing and Detection of Chemical, Biological, Radiological, Nuclear Threats and Ecological Terrorism*,
NATO Science for Peace and Security Series A: Chemistry and Biology,
DOI 10.1007/978-94-007-2488-4_32, © Springer Science+Business Media B.V. 2012

commensurable manner and with equal rate, preserving the parity between the lost by oxidation and gained by reduction electrons per unit of time. The electrochemical mechanism assumes that the individual processes of oxidation and reduction obey their inherent potential-current relationships accountable for the process rate. The joint process kinetics is determined by the kinetics of the partial oxidation and reduction processes that not necessarily occur on the same point on the surface. The independent but commensurable occurrence of these processes allows for the apportioned process consideration taking into account the partial anodic and cathodic processes. The common current density (the process rate) is obtained as the sum of the current densities i_1 (ε) and i_2 (ε) reflecting the individual processes for the corresponding equal potentials. This concept has been proposed by Wagner and Traud [4] who introduced the additivity principle applied to the partial polarization curves when particular system contains two, or more, redox couples.

It is well known that the oxidation-reduction processes [5–9], more particularly the metals' oxidation (corrosion), may proceed only when ε_{red} is more negative than ε_{ox}. If the metal is spatially separated from the oxidant, a galvanic element of the following type may be expressed as: Me | Mez+ | | ox, red | Me', where Me is the due for oxidation active metal; "ox" and "red" designate the oxidized and reduced form of the oxidant; Me' is the hypothetic inert metal that is not being oxidized by the given oxidant, but onto which the kinetics of the process ox → red is the same to that onto the active metal Me. On this account the metal surface is considered as a system of anodes (basic metal) and microscopic cathodes. The electrode surface not necessarily includes only two types of anodes and cathodes. The simultaneous existence of several admixtures results to developing of a system with multiple electrode elements, characterized by several types of cathodes and anodes with differing potentials and polarization characteristics. The founder of the theory of the local elements existence is A. de la Reeve [10].

32.2 Formulation of the Problem and the Present Study Basic Concept

Hydrogen sulfide and sulfur dioxide are harmful to the environment pollutants and their cleansing is still a challenge to the contemporary science and technology. At present SO_2 and H_2S oxidation by the oxygen takes place at elevated temperatures and is incomplete [11]. The present paper subject is to develop methods for electrochemical oxidation-reduction processes of SO_2 and H_2S oxidation by the contained in the air oxygen at room temperatures. Our innovative idea is the SO_2 and H_2S oxidation to proceed electrochemically according to the theory of the conjugated oxidation-reduction reactions. Our aim is to demonstrate the feasibility of SO_2 and H_2S oxidation at room temperature onto scattered micro-galvanic catalysts. Our belief is these elements' origination is facilitated by the specific Carbon-Teflon structure of the gas diffusion electrodes, GDEs. These GDEs are similar to the developed at the IEES [12] oxygen electrodes. The fundamental construction

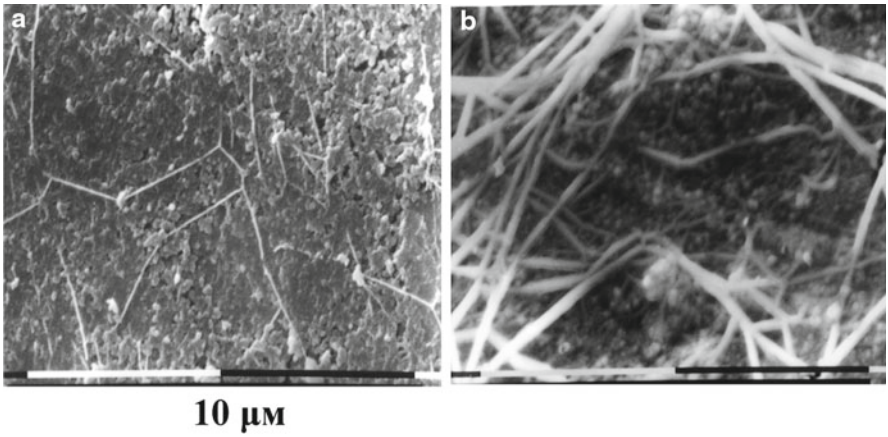

Fig. 32.1 Scanning electron microscope images of a GDE's surface (**a**) Gas diffusion membrane, GDM; (**b**) GDM + catalyst

element of a GDE is the material containing teflonized acetylene blacks (XC-30) developed by Iliev, Kaisheva et al. [13]. Utilizing XC-30 as a mixture with the relevant catalyst, the active GDE layer creates a system of pores that are: (i) dry (for gas transport); (ii) wetted (for electrolyte transport); and (iii) partially wetted, thus creating a tri-phase boundary where the electrochemical reactions occur. To clarify our concept we present a physical model of the Carbon-Teflon structure shaping up the GDEs' active layer. Figure 32.1 illustrates registered by scanning electron microscope images of a GDE's surface. It should be emphasized that the incorporated in the electrode teflonized blacks considerably hinder the microscopic methods accuracy. Nonetheless it can easily be seen that the teflonized blacks, Fig. 32.1a, create a grid-like structure built up of threads, fibers and chains of teflonized blacks that are obtained after electrode preparation at to = 320°C and P = 300 bar.

The catalyst is deposited on these fibers, Fig. 32.1b, and follows the padding structure. The image illustrates a catalyst that has been electrochemically deposited since in such cases all fibers are best visible. Figure 32.2 depicts schematically a structure of this type where several internal pores of a GDE are present. The same Fig. 32.2 illustrates two fibers, chains of teflonized blacks with deposited catalytic particles (the yellow points). The chains are surrounded by electrolyte. The sulfur dioxide and oxygen arriving through the dry pores (Teflon) reach the electrolyte where they are dissolved and react onto the neighboring catalytic particles according to the designated reactions. The electronic transfer is implemented through the charcoal (red lines) while the ionic transfer is realized through the sulfuric acid (violet arrows).

In this manner galvanic couples are created where with no external current flow the process of the sulfur dioxide oxidation takes place setting up a mixed potential.

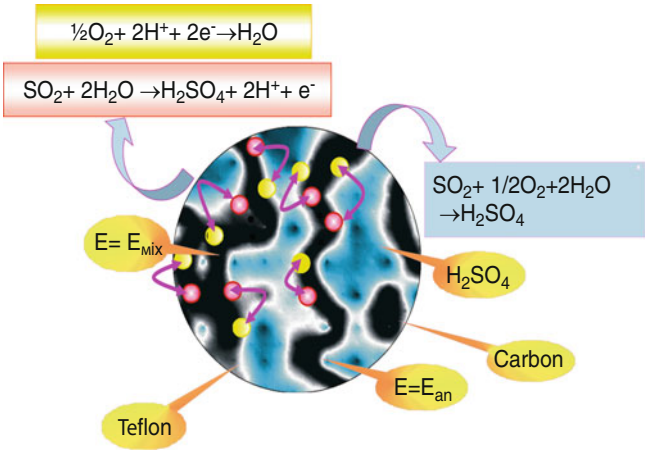

Fig. 32.2 Diagram of the internal pores of charcoal-Teflon structured GDE

32.3 Investigations on the Reactions' Electro-Catalytic Mechanism

All studies of the simultaneous SO_2 or H_2S oxidation and O_2 reduction reactions have been conducted on gas diffusion electrodes, GDEs. First, however, the most suitable for the purpose catalysts had to be determined as well as the electrodes structure and composition optimized. No passable theory exists backing up the relation of the electrodes' electrochemical characteristics to the techniques of their preparation, namely the quantity and type of catalyst used, the electrodes' components, their ratio, etc. Therefore the GDEs' optimization is experimentally performed. Each parameter is varied with all others constant. The procedure, described previously [14], asks for setting up of numerous experiments and relies heavily on the researcher skills. To be more precise it should be noted that the originally developed at IEES hydrophobic blacks were teflonized to full hydrophobicity, i.e. they were not wettable and were electrochemically neutral. Similar materials had been utilized for the GDEs' gas conducting layer. In some cases of GDEs active layer optimization, etc., we have used lower Teflon content to allow for wetting of the materials, hence to provide for electrochemical reactions to proceed. On this account we designate these materials as teflonized charcoals (blacks) to distinguish them from the hydrophobized blacks.

32.4 Hydrogen Sulfide Oxidation with Concurrent Oxygen Reduction

The experimental GDEs have geometric area S equal to 200 cm^2. The experimental reaction cell was of the illustrated in Fig. 32.3 particular design, where: 1 – GDE; 2 – Reaction space; 3 – Line for waste solution; 4 – Argon gas cylinder; 5 – Line

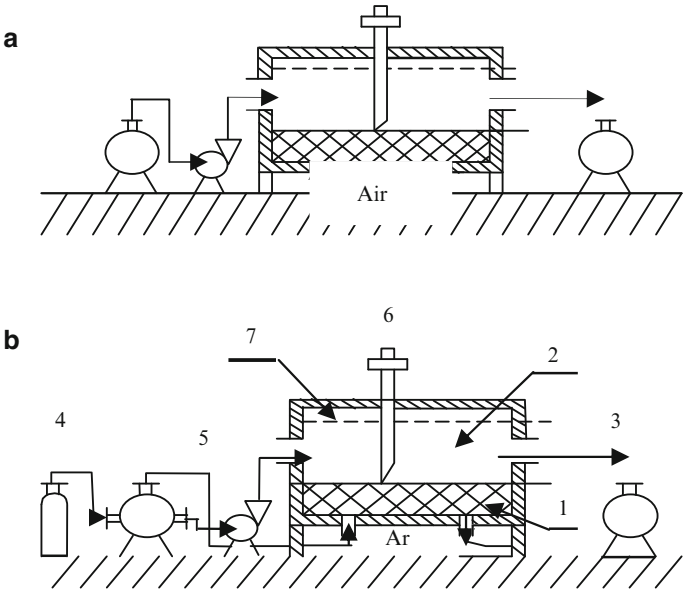

Fig. 32.3 (**a, b**) Schematic diagram of a reaction cell: *1* – GDE; *2* – Reaction space; *3* – Line for waste solution; *4* – Argon gas cylinder; *5* – Line feeding operational solution; *6* – Reference electrode; *7* – Counter electrode

feeding operational solution; 6 – Reference electrode (Hg/HgO); 7 – Counter electrode.

Functionally the GDE is a wall of the cell shaping the reaction space (2) where the electrolyte containing 10% Na_2S (15 $gS^{2-}{\cdot}L^{-1}$) and 1% NaOH (0.25 N NaOH) enters into the cell. The GDE active layer faces the electrolyte while its arresting layer contacts the air. The electrolyte circulates between the two reservoirs assisted by a peristaltic pump. Samples for analysis are taken at every other hour. The electrodes' potential is measured by a mercury-mercury oxide reference electrode (Hg/HgO) and all potentials are referenced to it. The catalysts' complex is cobalt(II) phthalocyanine [$CoPc(SO_3H)_2$] and nickel hydroxide $Ni(OH)_2$ deposited onto the GDE active layer by means of appropriate solutions (ethyldiamin hydrochloride and nickel nitrate), followed by heating to 100°C. The common sulfide oxidation reaction rate was measured by administering of 10% Na_2S (15 $gS^{2-}{\cdot}L^{-1}$) and 1% NaOH (0.25 N NaOH) solution through the reaction space. Under these conditions the sulfide ion is oxidized by the oxygen entering via the GDE arresting layer. The reaction takes place with no external current flow. The reaction rate (V) is determined as gram equivalents of transformed sulfide per unit area, at equal for all electrodes solution flow rates and room temperature. The quantity of the converted to sulfur sulfide is analytically determined [15]. The reaction rate transforms again into current following the Faraday equation:

$$V = \Delta NS^{2-}/\Delta t = I_F/nF \qquad I_F = V.nF = \Delta NS^{2-}.nF/\Delta t \qquad (32.1)$$

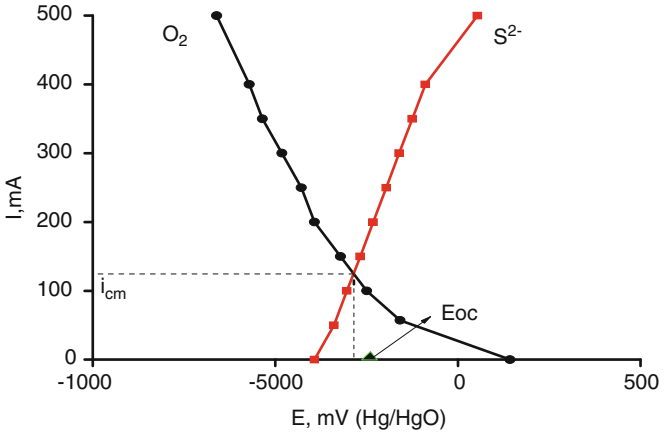

Fig. 32.4 Partial polarization curves: Cathodic plot (■) – 15 gS^{-2} L^{-1} and 0.25 N NaOH + Ar; Anodic plot (●) – 0.25 N NaOH + O_2 (B – x); E_{oc} (▲) – 15 $gS^{-2}{\cdot}L^{-1}$ and 0.25 N NaOH + O_2 (B – x). t^o = 20°C; Non-modified GDE; Flow rate – v_r = 24.15 cm^3 per minute; S_{GDE} = 200 cm^2

where: V (M/s) is the reaction rate; n is the number of the exchanged electrons; F is the Faraday constant; ΔN^{S2} are the oxidized per time unit Δt gram-equivalents.

The partial polarization curves of GDEs with, or without, a catalyst were measured employing the same cell. The partial curves of the sulfide ion oxidation onto the respective electrode were measured by isolating the cell from the oxygen contained in the air, Fig. 32.4b. The GDE arresting layer is shut for air penetration and in concert with the electrolyte is argon blown. The electrolyte content remains the same, namely 10% Na_2S (15 $gS^{-2}{\cdot}L^{-1}$) and 1% NaOH (0.25 N NaOH).

The oxygen partial curves were measured by transporting oxygen (air) through the GDE but with no sulfide ion in the electrolyte, i.e. the electrolyte content was only 1% NaOH (0.25 N NaOH). The calculated values for the mixed potential E_{mix} were compared to the experimentally determined open circuit potentials (with no external current flow) while the cell was open for oxygen penetration and sulfide ions were present in the electrolyte (15 $gS^{-2}{\cdot}L^{-1}$ and 0.25 N NaOH), i.e. with both redox couples present.

The measured relationship reaction rate versus solution flow rate (within the range of 14–53 cm^3 per minute) disclosed an optimum solution flow rate of 24 cm^3 per minute. It was this flow rate used for the measurements of the partial polarization curves of the sulfide ion oxidation and oxygen reduction. Figure 32.4 illustrates these relationships for non-catalyzed GDE.

The crossover point determines both the mixed current and potential. The point designated (▲) illustrates the open circuit potential. Figure 32.5 depicts the partial curves for a catalyzed GDE. Both the steepest anodic plot slope and shifted in cathodic direction mixed potential, compared to the non-catalyzed GDE, stand for a hindered oxygen reaction. The higher mixed currents magnitudes (higher process rate) point out to an increased electrode catalytic activity. Table 32.1 summarizes

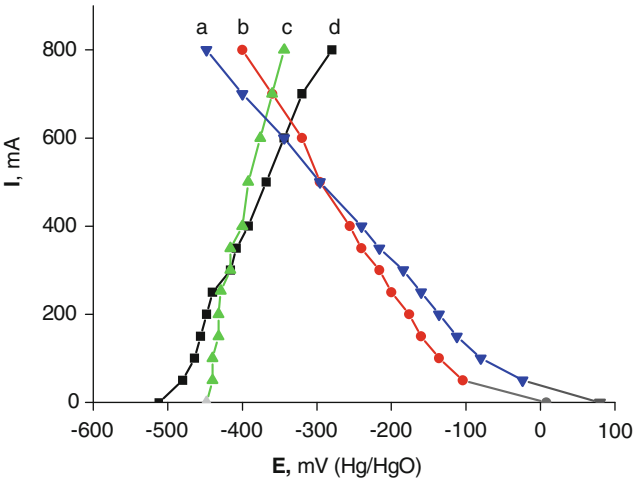

Fig. 32.5 Partial polarization curves: Cathodic plots (15 $gS^{-2} \cdot L^{-1}$ and 0.25 N NaOH + Ar), (**a**), (▼) – $Ni(OH)_2$ and (**b**), (●) – $[CoPc(SO_3H)_2]$; Anodic plots (0.25 N NaOH + O_2, Air) (B-x), (**c**), (▲) – $Ni(OH)_2$ and (**d**), (■) – $[CoPc(SO_3H)_2]$; Flow rate – $v_r = 24.15$ cm^3 per minute; $S_{GDE} = 200$ cm^2; $t^o = 25°C$

Table 32.1 Electrochemical and chemical parameter determinations for the three catalysts studied

Catalyst	E_{mix} [mV]	E_{oc}[mV]	I_{mix} [mA]	I_F[mA]
GDE	−295	−297	125	124
GDE/$CoPc(SO_3H)_2$	−348	−320	615	556
GDE/$Ni(OH)_2$	−385	−408	645	908

the values for the calculated from the electrochemical partial curves mixed currents and potentials, as well as the values of the measured open circuit potentials. Presented also are the magnitudes of the analytically measured reaction rates converted into currents obeying the Faraday equation. The good agreement of these magnitudes for the non-catalyzed GDEs substantiates the electrochemical nature of the process.

A GDE with a cobalt(II) phthalocyanine $[CoPc(SO_3H)_2]$ shows $I_{mix} > I_F$ and more negative E_{mix} values, compared to E_{oc}, which is a deviation from the additivity principle. This probably is due to reaction products adsorption as already explained theoretically. The observed with the nickel hydroxide $Ni(OH)_2$ catalytic activity is higher than anticipated. This presumes that two simultaneous reactions take place – oxidation on the GDE and homogeneous sulfide oxidation in the solution [16]:

$$S^{2-} + HO_2^- + H_2O \rightarrow S^0 + 3OH^- \tag{32.2}$$

The peroxide ions presence in the reaction solution has been spectrally confirmed [17]. The results presented evidence that the sulfide ion oxidation process proceeds predominantly in accord with the predicted electrochemical mechanism.

32.5 Studies of the Sulfur Dioxide Oxidation and Oxygen Reduction Electrochemical Nature

To clarify this issue, the measured at different potentials magnitudes of current flow were compared to the respective values calculated by the Faraday law from the experimentally determined quantity of sulfur dioxide at the very same potentials [18]. The experiment has been carried out with a GDE of 200 cm^2 area, catalyzed solely with Noirt–NK. The large operational area results to an increased sulfur dioxide "consumption" by the GDE. This provides for more accurate determination of the SO_2 concentration differences. A concentration of $C_{SO2} = 1\%$ by volume has been selected since this value represents a good agreement with the SO_2 content in the industrial waste gases. Figure 32.6 illustrates an experimental (i_F) and calculated (i_{cal}) i/E relations.

The current intensity corresponding to the transformed (oxidized) in the GDE total quantity of sulfur dioxide has been determined applying two different techniques:

(a) From the sulfur dioxide concentration changes in the gas mixture at the gas chamber inlet and outlet, maintaining constant gas mixture flow rate of 50 L/h, where the current corresponding to the sulfur dioxide concentration alteration is calculated applying the Faraday law:

$$I = \frac{\Delta N so_2 F}{\Delta t}, \tag{32.3}$$

where ΔN is the oxidized during the experiment (Δt, sec.) quantity of sulfur dioxide (gram-equivalent).

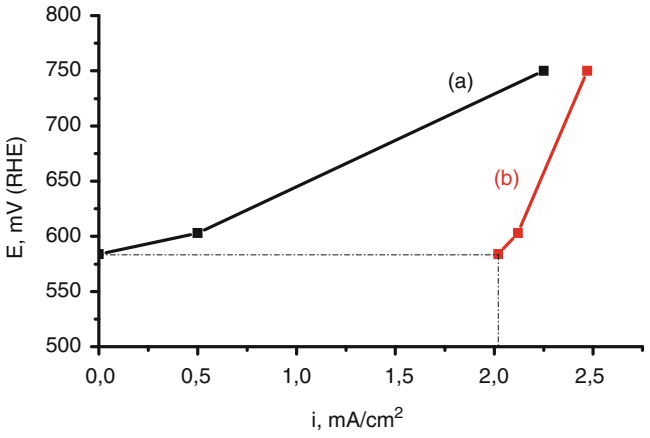

Fig. 32.6 Polarization relations: (**a**) Experimental and (**b**) Calculated; GDE area = 200 cm^2; 1.0% by volume SO_2 + Air; $t^o = 20°C$; 4.5 N H_2SO_4

The calculated current intensity is recalculated and presented as current density related to the GDE area of 200 cm^2. These measurements are taken repeatedly during the experiment and show constant values within the error limits of the iodometric titration, for our case defined as some 2%.

(b) From the sulfuric acid changes in the electrolyte at the initial and final experimental points, maintaining a constant volume of V = 400 mL. This particular change is converted to current intensity according yet again to Eq. 32.3. There is a satisfactory agreement of the two measurements' data.

The illustrated in Fig. 32.4 two plots comparison reveals considerable differences since fairly large sulfur dioxide quantities are additionally oxidized not under the Faraday current flow impact. This is particularly noticeable at the point designated $i_F = 0$, i.e. when there is no external current flow through the electrode. In this case the sulfur dioxide oxidation rate, expressed as current density, is comparatively high, $i_{cal} = 2$ mA·cm^{-2} or $I_{cal} = 412$ mA. Imposing low overvoltages does not considerably increase the oxidized sulfur dioxide quantity. In cases when the process proceeds at higher electrode polarizations (over 100 mV) the sulfur dioxide is oxidized mostly by the flowing through the electrode current.

This, naturally, raises some queries related to the oxidation mechanism with no external current flow. In this case the sulfur dioxide oxidation reaction could take place chemically in a gas phase [11]:

$$SO_2^g + \frac{1}{2}O_2^g \rightarrow SO_3^g \tag{32.4}$$

$$SO_3^g + H_2O \rightarrow H_2SO_4 \tag{32.5}$$

or electrochemically onto short circuited micro-galvanic elements dispersed in the GDE catalytic layer. The presumptive reactions are:

$$1/2O_2 + 2H^+ + 2e^- = H_2O \text{ (cathode)} \tag{32.6}$$

$$SO_2 + 2H_2O = H_2SO_4 + 2H^+ + 2e^- \text{ (anode)} \tag{32.7}$$

$$\text{total}: \quad SO_2 + 1/2O_2 + H_2O \rightarrow H_2SO_4 \tag{32.8}$$

Supporting the electrochemical nature of the oxidation process is the experimentally established fact that the SO_2 oxidation to SO_3 in gas phase at room temperature proceeds infinitely slow.

This assumption for electrochemical mechanism may be tested by the anodic and cathodic partial curves measurements taken at similar to the illustrated in Fig. 32.6 conditions (since the electrode area is S = 10 cm^2, the flow rate is correspondingly reduced to 2.5 L/h). In our case these are the cathodic (reagent-Air) and anodic (reagent-Ar + SO_2) curves shown in Fig. 32.7. The symbol Δ denotes the magnitude of E_{OC} at external current $i_F = 0$ for a gas mixture of Air + 1% vol. SO_2. From the partial curves crossover point we may judge for the mixed (short circuited) current density $i_{MIX} = 2$ mA·cm^{-2}, which accurately coincides with the calculated from the

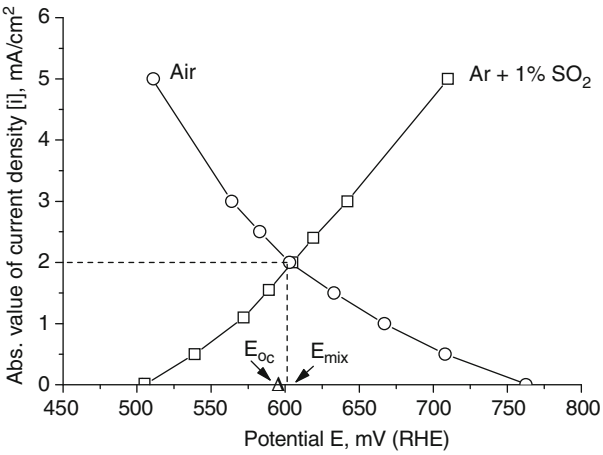

Fig. 32.7 Partial polarization relations: (**a**) Cathodic, Air; (**b**) Anodic, 1.0% vol. SO_2 + Ar; t^o = 20°C; 4.5 N H_2SO_4

sulfur dioxide quantity value at zero external current flow illustrated in Fig. 32.6. Good agreement is exhibited also for the E_{OB} potentials coincidence in the case of $i_F = 0$ for the gas mixture

(Air + 1% SO_2) in Figs. 32.6 and 32.7, and E_{CM} corresponding to the cross-over point of the anodic and cathodic potential curves in Fig. 32.7, i.e. $E_{OC} = E_{MIX} = 590 - 600$ mV.

The equivalence of the values for the mixed current and the calculated by Eq. 32.3 current as well as the equivalence of the mixed potential E_{MIX} and the open circuited potential E_{OC} confirm the electrochemical nature of the sulfur dioxide oxidation by the contained in the air oxygen when no external current flow is registered through the electrode.

Another interesting fact should also be mentioned here. Figure 32.6 demonstrates that when external anodic current is imposed, up to certain values, simultaneous sulfur dioxide oxidation processes within the electrode take place due both to the imposed current and to the micro-galvanic elements' current. This indicates that within one and the same physical object (electrode) with imposed anodic current two concurrent anodic and cathodic processes occur simultaneously.

This effect occurrence and the mechanism of the processes onto the micro-galvanic elements of electrodes with charcoal-Teflon composition may be explained by the specific structure created within these electrodes. We shall make an effort to clarify this by presenting in Fig. 32.8 the physical model of a charcoal-Teflon structured electrode. The internal, operational, GDE surface is highly developed. The roughness factor is close to f.r. = 500 [19]. The active layer is partially hydrophobized, in other words some pores are dry and some are wet. It is even possible that part of a single pore may be wetted, while the other part is dry, etc [20].

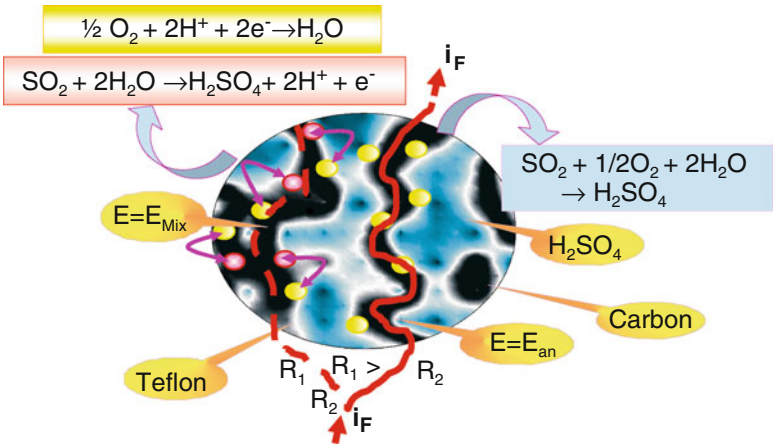

Fig. 32.8 Schematic diagram of the internal pores of a charcoal-Teflon structured electrode

In this manner galvanic couples or elements are shaped. With no external current applied the process of sulfur dioxide oxidation proceeds onto these micro-galvanic elements resulting to establishment of mixed potential. When imposing low external current ($i = 0.5 - 2.0$ mA·cm^{-2}, Fig. 32.6) it does not flow through each of the fibers due to the highly developed surface area including huge number of fibers. For some reason certain paths are more resistive than others and the electronic current does not flow there. The reason may be due to the high Teflon content since no matter how experienced the experimenter is, the nonuniform Teflon distribution is quite unavoidable. In such cases the paths with no current flow exhibit no external (in our case anodic) current and consequently potential. These routes are isolated while mixed potential still exists there as well as micro-galvanic elements where sulfur dioxide is oxidized. The physical model displayed reveals that the charcoal-Teflon structured GDEs do not represent a unified physical object but consist of multiple micro-electrodes. This explains the simultaneous occurrence of oxidation and reduction processes onto one and the same electrode when external (in this case anodic) current is imposed.

The analytical calculations of such systems are quite complex. This is the reason we expressed the major relations describing the processes taking place experimentally. These are namely the impacts due to the sulfur dioxide concentration in gas mixtures (concentrations under 1% by volume sulfur dioxide have been studied, corresponding to the industrial waste gases concentrations) and the sulfuric acid concentration. The C_{SO2} and C_{H2SO4} influence has been investigated by measuring the short circuit current densities derived from the crossover point of the anodic (with a reagent of Ar^+ varying SO_2 concentrations) and cathodic (with Air as a reagent) curves. The C_{H2SO4} influence at constant $C_{SO2} < 1.0\%$ vol. within the range of 1–10 H_2SO_4 is negligible. The short circuit current density versus sulfur dioxide content in the gas mixture is presented in Fig. 32.9. Within the concentrations range of

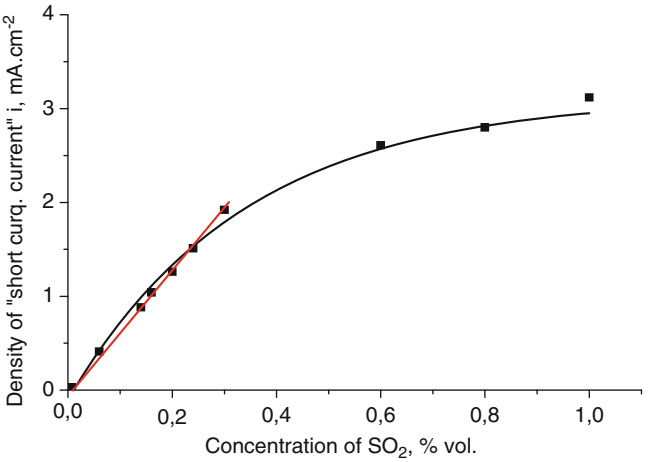

Fig. 32.9 Relation determining oxidation rate (i_{mix}) versus sulfur dioxide concentration; Noirt–NK + 10% CoPc; $C_{H2SO4} = 4.5$ N; $t^o = 20°C$; $S_{GDE} = 10$ cm^2

0.03–0.3% vol. SO_2 a linear region is observed (shown in red), which allows for exploiting the following expression:

$$v = \frac{i_{sc}}{F} = \frac{\Delta N_{SO2}}{\Delta t} = kC_{SO2} \tag{32.9}$$

where, v is the SO_2 oxidation rate represented as a number of gram-equivalents oxidized for a given period of time Δt.

The SO_2 concentrations range under 0.3% by volume is very interesting from the practical point of view when cleansing of waste gases is the main concern. All existing techniques for "hot" SO_2 oxidation do not perform well within this range of concentrations. Based on the results described above an innovative technique for SO_2 cleansing in waste gases has been developed and labeled ELCOX [21]. The revealed simplified expressions facilitate the performance estimation of functioning according to the already described principle ELCOX equipment for waste gases cleansing within the operational concentrations range from 0.03% to 0.3% (300–3,000 ppm) sulfur dioxide in air [22].

32.6 Conclusions

An original investigation on simultaneous electrochemical reactions of oxidation of H_2S and SO_2 by oxygen has been conducted. The additivity principle has been employed. The electrochemical nature of processes has been revealed. It has been proven that reactions proceed on spread micro-galvanic elements. An original Carbon-Teflon structure of the electrodes has been achieved by use of teflonized blacks.

The mechanism of simultaneous anodic and cathodic reactions taking place in the same electrode with or without external current has been explained. A physical model of the system has been presented. It has been shown that Carbon-Teflon structure of GDE creates a discrete (disordered) system. There are parts with different charge and potentials. The electrode is not unified physical object but a sum of micro-electrodes.

References

1. Scorchelletti VV (1969) Theoretical electrochemistry. Himija, Leningrad
2. Vetter K (1961) Electrochemishe kinetik. Springer, Berlin
3. Antropov LI (1965) Theoretical electrochemistry. Visshaja Shkola, Moscow
4. Wagner C, Traud W (1938) Additive hypothesis for oxidation-reduction reactions. Z Electrochem 44:391
5. Evans JR (1962) Corrosion and metals protection. Mashgiz, Moscow
6. Archer MD, Ferreira MIS, Albery WJ, Hilman AR (1980) Photogalvanic cells. Part XII. The dark electrochemistry of the iron-thionine system at platinum. J Electroanal Chem 111:295
7. Herbelin JM, Andersen TN, Eyring H (1970) Kinetic parameters by the method of mixed potentials. Electrochem Acta 15:1455
8. Svetlicic V, Ztic V, Clavilier J, Chevalet J (1985) Supramolecular phenomena in organic redox films at electrodes. Part I. The methylene blue/leucomethylene blue redox couple at the platinum electrode. J Electroanal Chem 195:307
9. Spiro M, Griffin PW (1969) Proof of an electron-transfer mechanism by which metals can catalyse oxidation-reduction reactions. J Chem Soc D: Chem Commun 262
10. De la Rive A (1938) Electrochemical theory of corrosion. ONTI, Moscow
11. Boreskov GK (1954) Catalysis in sulphuric acid production. Goshimisdat, Moscow
12. Iliev I, Kaisheva A, Gamburtsev S (1975) Carbon oxygen (air) gas-diffusion electrodes of hydrophobic type. Dept Chem Bulg Acad Sci 8:367
13. Iliev I, Gamburtsev S, Kaisheva A, Mrha J (1979) Influence of mass transport on the performance of carbon oxygen (air) gas-diffusion electrodes in alkaline solution. J Appl Electrochem 5:291
14. Petrov K, Nikolov I, Vitanov T (1984) Gas diffusion electrodes for oxidation of sulphur dioxide. Int J Hydrogen Energy 8(11):901
15. Kivalo P (1955) Complexometric determination of sulfide. Anal Chem 27:1809
16. Spiro M (1986) Polyelectrodes: evidence for and against the wagner and traud additivity hypothesis. Chem Soc Rev 15:141
17. Andreev A, Khristov P, Losev A (1996) Electrocatalityc oxidation of hydrogen sulfide. Appl Catal B Environ 1:105
18. Nikolov I, Petrov K, Vitanov T (1996) Low temperature electrochemical oxidation of sulfur dioxide. J Appl Electrochem 26:703
19. Mrha J, Iliev I, Gamburtsev S, Kaisheva A, Musilova M (1976/1977) On the effect of various active carbon catalysts on the behaviour of carbon gas-diffusion air electrodes: 2. Acid solutions. J Power Sources 1:47
20. Bagotzky VS, Tarasevich MR, Radyushkina KA, Levina OA, Andruseva SI (1977/1978) Electrocatalysis of the oxygen reduction process on metal chelates in acid electrolyte. J Power Sources 2:233
21. Vitanov T, Budevski E, Nikolov I, Petrov K, Naidenov V, Christov Ch (1990) Electrocatalytic oxidation of sulphur dioxide (the ELCOX process). Int Chem Eng Symp Ser, Leeds, England, 116:251
22. Budevski E, Donchev T, Naydenov V, Nikolov I, Petrov K, Hristov H (1988) Verfahren und Vorrichtung zur elektrochemischen, katalytischen Oxidation von Schwefeldioxid zu Schwefejsaure, Europaische Patentschrift. Patent EUR 0302224B1

Part VI
Information Security

Chapter 33
Co-operative Generation of Entangled Photons and Its Application in Quantum Cryptography

Co-operative Generation of Entangled Photons

Nicolae A. Enaki, M. Turcan, and Ashok Vaseashta

Abstract This study examines the coherence properties among the Stokes and anti- Stokes fields and their applications in Communications. We investigate a novel two-photon entangled sources approach which takes into account the coherence and collective phenomena between the fields. The quantum propriety of realistic sources of powerful coherent bi-boson radiation (coherent entanglement of Stokes and anti-Stokes photons) is analyzed. Finally, we examine experimental applications of coherence between the Stokes and anti-Stokes photons obtained in super-radiance and resulting lasing effects in quantum communications and cryptography.

Keywords Collective phenomena • Correlation • Photonics losses • Two-photon lasing

33.1 Introduction

Cryptography in the digital world can be used to protect identities and data from unauthorized access or modification. Cryptography is essential for modern e-commerce and standard transactions; however, the Internet is inherently insecure. Data is the cornerstone of Information Technology and is vulnerable at every stage of its life cycle; conversion, storage, processing, transmission, retrieval, etc.

N.A. Enaki (✉) • M. Turcan
Institute of Applied Physics, Academy of Sciences of Moldova, Chisinau, MD, Republic of Moldova
e-mail: enaki_nicolae@yahoo.com

A. Vaseashta
Institute for Advanced Sciences Convergence, NUARI, 13873 Park Center Rd., Suite 500, Herndon, VA, USA

A. Vaseashta et al. (eds.), *Technological Innovations in Sensing and Detection of Chemical, Biological, Radiological, Nuclear Threats and Ecological Terrorism*, NATO Science for Peace and Security Series A: Chemistry and Biology,
DOI 10.1007/978-94-007-2488-4_33, © Springer Science+Business Media B.V. 2012

The property of entanglement between the emitted photons in the processes of light generation is an enabling technology of quantum computing, and information security [1]. Research connected with the manipulation of quantum fluctuations of the generated light and its application in transmission and detection of information with a high degree of security play an important role in modern defense arsenals. Some interesting behavior of Stokes [2] and anti-Stokes generated modes in the Raman processes [3] can be observed for the small number of the pumped photon in nonlinear media. The cooperative coherent establishments between these two modes can be used for transmitting and processing of information with higher cryptographic levels [4]. This article proposes a new type of two photon comunication through the bi-boson field which can be regarded as a two coherent field generated in the lasing process [5–7] of Stokes and anti-Stokes modes in nonlinear mediums. Such quantum correlations can be obtained in the processes of Raman scattering [3]. New coherent states are obtained between Stokes and anti-Stokes fields belonging to SU(2) algebra that could be used in quantum communication. The cooperative nonlinear scattering processes between two resonator modes stimulated by the excited atomic beam has been studied [6].

We demonstrate that these collective scattering phenomena between the Stokes and Anti-Stokes cavity modes take place due to information transfer between the photons of two fields. Study of the quantum fluctuations of the number of photon using the Stokes and Anti-Stokes fields are proposed for communication with a higher degree of information security. The new peculiarities of the second order correlation functions between these fields are considered as potential algorithms in cryptography and are expressed through the lasing parameters of the source. In the second section, a review of information transmission through entangled photons obtained in parametric down conversion [4, 8] is provided. In this section, we propose a new method of information transmission involving the two-field coherent states.

The main difference between the Ekert model [9] and new possibilities which include the second order coherent effects is given. We consider that such coherence between the photon of two fields can be conserved in the process of propagation of the Stokes and anti-Stokes photon through different fibers over long distances. The information encapsulated into coherent bi-boson light can be destroyed in the dispersive medium and restored over a certain distance. In both methods of transmission of the Stokes and anti-Stokes photons, the nature of the quantum communication between two points A (Alice) and B (Bob) does not allow eavesdropper, E (Eve), to decrypt the transferred information.

33.2 Descriptions of Quantum Cryptography, History and New Architecture

Confidential communication needs encryption in order to ensure that no unauthorized party could misuse the content. Quantum cryptography provides long-term security and thus conforms to the requirements of a number of recent legal

regulations for protecting information. Quantum cryptographic technologies provide information-theoretically secure keys for encryption. The basic approach includes sending streams of specially prepared particles of light (photons), their measurement by the legitimate parties and the subsequent post-processing of the measurement data. The output is the cryptographic key consisting of identical random bit strings. A potential eavesdropper cannot gain any information on this key irrespectively of his resources. This property which has no classical counterpart is due to the fundamental laws of quantum physics which ensure that any measurement leaves indelible traces behind. These traces manifest themselves in an error-rate that can be identified by the legitimate users. There exists a quantitative relationship between the error-rate and rate of key generation. In case the error is below a certain upper bound, and therefore the eavesdropper's invention was sufficiently weak, the process of generating the cryptographic key is still possible with the same security standard but at a accordingly reduced rate. The latter gets equal to zero if the error-rate exceeds the bound. Below we shall discuss the cryptographic model on the basis of two entanglement photons obtained in parametrical down conversion and our model based on the two-field coherence effect between the Stokes and anti-Stokes fields. These models are described in the Sects. 33.2.1 and 33.2.2.

33.2.1 Protocol with Entanglement Effect Between Photons

This QKD system was developed by an Austrian-Swedish consortium consisting of the University of Vienna, the Austrian Research Centers GmbH and the Royal Institute of Technology from Kista. The principal idea of this setup is to use the unique quantum mechanical property of "entanglement" in order to transfer the correlated measurements into a secret key [1]. A passive system performing measurements was implemented, where all photons find their way towards their detectors without the need to control any of their properties actively. As a result, correlated measurements are generated at Alice and Bob without any input for choice of basis or bit value for individual q-bits. For long-distance fiber-communication systems it is essential to have a high flux of photon pairs that we realized using spontaneous parametric down conversion (SPDC) in the orthogonally oriented two crystal geometry (see Fig. 33.1). Our compact source (40×40 cm) is pumped by a 532-nm-laser and its polarization is rotated to 45° for equal crystal excitation. The two nonlinear periodically-poled KTiOPO4 (ppKTP) crystals are quasi-phase matched for all three wavelengths.

The transmission of information through entangled photons is based on Ekert's protocol [9]. This protocol is encoded by its physical nature, and the system based on the entanglement effect between the photons consists as follows: Alice receives one of the photons of the pair and Bob the second. Alice and Bob have the same detection basis and for every particle pair, each chooses an axis independently, and measures the polarization along the axis. After that a series of photons pair are transmitted, they announce what axis of polarizer were chosen in the process of

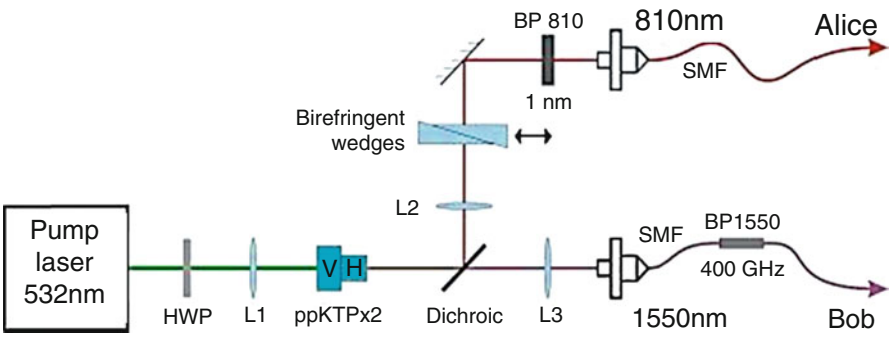

Fig. 33.1 Schematic of the source of entangled photons. Within the nonlinear ppKTP crystals, single pump photons are converted to two photons at 810 and 1,550 nm. If two indistinguishable conversion processes are possible within the V- and H-oriented crystals, polarization entanglement is generated

measurement and analyze in which cases they obtained the particles simultaneously. This process establishes the channel. This system is encoded automatically. A detailed description can be found in the literature [9].

The pulses formed from pairs of entangled photons can be applied in quantum communication and cryptography as investigated in quantum optics. It was demonstrated that in the process of transmission of correlated two photons which were obtained with parameter down-conversion effect through two optical fibers, the correlation between the photons pairs is conserved at a very big distance (30 km) [9], for more than 6 km in free-space [1]. Recent revolutionary progress was achieved by introducing the idea of a decoy state, and by transforming the concept into systematical and rigorous theory and scheme. Using a decoy state, much higher key generation rates and longer distances are possible, in the same level compared with the case of using true single photon sources which was successfully demonstrated by Lo's group from Canada for 15 km, and later for 60 km. Recent research by Pan Jianwei has extended the distance to 200 km. Alternatively, it is possible to have cryptographic channels that cannot be eavesdropped (Eve), because the nature of the communication through pairs of photons does not allow this.

The below listed Fig. 33.3 describes the process of transmission at a distance of 13 km. The generator of pairs of photons is by a nonlinear MgO:LiNbO3 crystal without an inversion center. The flux of entangled photons was separated into two directions, as shown in Fig. 33.2. Each pair was separated so as "one idler photon" goes to right and "one signal photon" goes to left (de facto, the same photon goes to left and to right). The flux was expanded using a optic telescope. The signal was compressed with telescopes of the same type at the detectors, Alice and Bob situated in USTC (University of Science and Technology of China, see Fig. 33.3) and the place Taouhua. The protocols Alic and Bob coincided indicating high efficiency in the information transmission process.

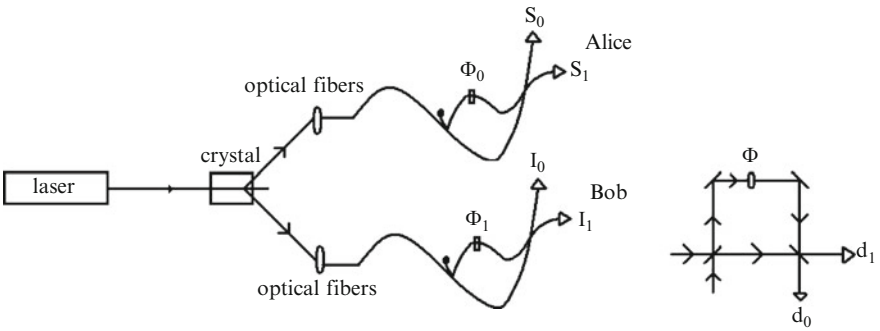

Fig. 33.2 The scheme of E91 protocol

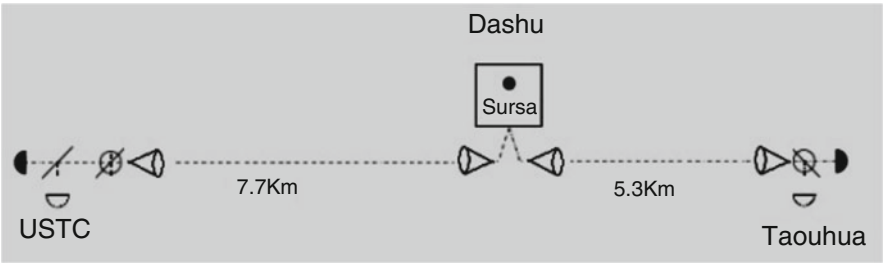

Fig. 33.3 The experimental realization of E91 protocol in China

33.2.2 New Architecture Using the Coherence Between Stokes and Anti-Stokes Fields

We propose a novel architecture for quantum communication. The amplitude of a simple block of coherent Stokes and anti-Stokes photons obtained after two-photon interaction in scattering lasing effects can be described by the square value of electrical vector $\Pi(t) = \varepsilon^2 \sum_k \hat{b}^+_{k0-k} \hat{a}^+_k Exp[\omega_0 t - (k_a - k_s)z + \varphi_0]$. $\Pi(t) = E^+_A E_S$, representing these amplitudes through $E^+_A = \sum_k \hat{b}^+_k \exp[i(\omega_A t - k_z z)] g_{k,a}$ and $E^-_S = \sum_k \hat{a}_k \exp[-i(\omega_S t - k_S z)] g_{k,S}$, where $\hat{b}^+_k$ and $\hat{a}^+_k$ are creation photon operators in the anti-Stokes and Stokes fields respectively, $\hat{b}_k$ and $\hat{a}_k$ are annihilation photon operators in these fields.

In the quasi-classical limits the amplitude $\Pi_0(t) = \varepsilon^2 \sum_k \left\langle b^+_k b_k \right\rangle$, has the same proprieties as amplitude of coherent laser field. In this approximation, a nice idea is to use the modulation of this square amplitude for transmission of information. At first glance, it is observed that this method does not have a substantial differences in comparison with classical methods of information processing, but if we send this information in dispersive media, which separates anti-Stokes and Stokes photons from coherent entanglement fields, the information is drastically destroyed, because

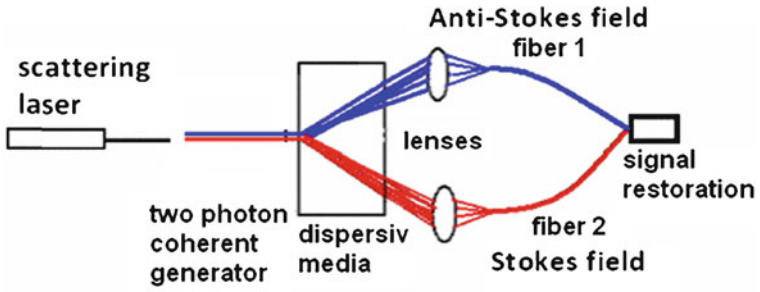

Fig. 33.4 Mixing of the anti-Stokes and Stokes photons into different optical fibers

$\left\langle b_{k0+k}^{+} \right\rangle$ and $\left\langle b_{k}^{+} \right\rangle$ take zero values. The possibility of restoration of information on the square amplitudes $\Pi_0(t)$, is interesting problem of many particle coherent states, formed from blocks of Stokes and anti-Stokes photons [2].

These studies are necessary because in a bi-boson lasing effect, the photon statistics depend on the statistics of the ignition field. Of course, the start up from vacuum fluctuations preserves the entanglement character of the generated Stokes and anti-Stokes coherence state. This effect is very interesting in quantum communication.

We propose an interesting effect that takes into account the classical method of registration of information. As Π(t) plays the role of electromagnetic field intensity strength for the two- fields Stokes and anti-Stokes, at the detector can be considered as a classical field described by $\Pi(t) = \Pi_0(t)\cos[\tilde{\omega}t - (k_a - k_s)z + \varphi_0]$, where Π_0 is the envelope of cooperative two-photon interaction in scattering processes. A large number of modes in the coherent states give as the possibilities of the increase the security of information storages in bimodal field.

In this approximation, the classical information may be introduced in the amplitude $\Pi_0(t)$. At the first glance one observes that such registration of information may have nothing to do with the traditional method. If the bi-boson pulses pass through a dispersive medium, the anti-Stokes and Stokes photons from the field change their directions. Focusing the anti-Stokes and Stokes photons into different optical fibers we are totally dropping the coherence among the photons. However, after a certain time interval, anti-Stokes and Stokes photons from the field are mixed again, and we shall show that the coherence is restored (see Fig. 33.4).

The coherent state obtained in two-photon coherent emission $|\Psi\rangle = \exp\left[\Pi^{+} - \Pi^{-}\right]|0\rangle$, takes into account not only entanglement between the pair photons but the coherence between the fields too, and can be used in mixed processing problems in which the quantum entanglement between the Stokes and anti-Stokes photons is used simultaneously with classical coherence [10] between the fields. Of course the probability of experimental realization of logic gates for quantum circuits in this case increase. In the next section we demonstrate that such coherent states between Stokes and anti-Stokes fields can be realized in cooperative scattering effects [8].

33.3 Cooperative Generation of the Coherences States Between Stokes and Anti-Stokes Fields

We consider a stream of atoms [11–17] with two levels traveling through the cavity as is shown in Fig. 33.5. The total Hamiltonian which describes the interaction of the atoms with Stokes and anti-Stokes fields of the cavity can be represented through the atomic and field operators

$$H_T = \sum_{j=1}^{N} \hbar\omega_0 R_{zj} + \hbar\omega_a a^+ a + \hbar\omega_b b^+ b + i\sum_{j=1}^{N} G(k_a, k_b)\left\{\left\langle R_j^-(t)J^+ - J^- R_j^+(t)\right\rangle\right\} \quad (33.1)$$

where the last term represent the interaction Hamiltonian, here R_{zj} is the population inversion of atom j; $\hat{R}_j^+$ and $\hat{R}_j^-$ represent the operators which describe the transitions from $|g\rangle$ - ground state to $|e\rangle$ - excited state and from $|e\rangle$ - excited state to $|g\rangle$ - ground state, respectively (see Fig. 33.6). The operator $a^+(a)$ is the creation (annihilation) of Stokes photons and $b^+(b)$ is the creation (annihilation) of anti-Stokes field operators. The interaction constant $G(k_a, k_b)$ describes the effective nonlinear coupling of atom j with cavity modes k_a and k_b with the energies $\hbar\omega_a$ and $\hbar\omega_b$.

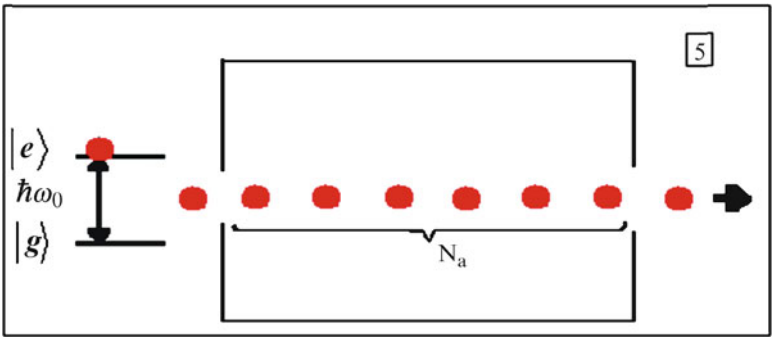

Fig. 33.5 The atomic pump of scattering process with transformation of n-Stokes photons in anti-Stokes field

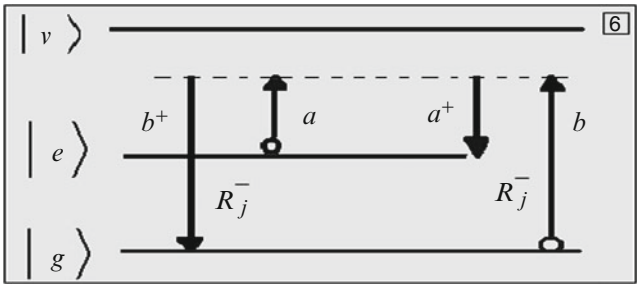

Fig. 33.6 This scheme shows the collective excitation of atom with absorption of Stokes photon and generation of anti-Stokes quantum and vice versa

In order to describe the scattering processes, let us introduce the collective operators for Stokes and anti-Stokes modes, $J^+ = ab^+$ and $J^- = ba^+$. The operator $J^+ = ab^+$ describes the simultaneously process of creation of anti-Stokes and annihilation of Stokes photons. The inverse process is described by operator: $J^- = ba^+$. As the full number of photons in the cavity [5], in the small time moment the interaction is conserved [7], we shall introduce the operator of photons inversion between the Stokes and anti-Stokes photons: $J_z = (b^+b - a^+a)/2$ and energy difference: $\hbar\tilde{\omega} = \hbar\omega_b - \hbar\omega_a$.

Taking into account, that the lifetime of atoms in the cavity are shorter than the time of scattering processes and considering that the atomic system is prepared in excited state, let us eliminate the atomic operators $\hat{R}_j^+$ and $\hat{R}_j^-$ from Heisenberg equation of arbitrary field operator $\hat{O}(t)$. After consecutive elimination of free parts of these operators the master equation for Stokes and anti-stokes field can be represented in the fourth order on the interaction constant $G(k_a, k_b)$

$$\begin{aligned}\frac{d}{dt}\langle O(t)\rangle = {} & i\chi\gamma_\perp\left\langle[\hat{J}_z(t),\hat{O}(t)]\right\rangle + \tilde{\alpha}_1\left\{\left\langle 2\hat{J}^-(t)\hat{O}(t)\hat{J}^+(t) - \hat{J}^-(t)\hat{J}^+(t)\hat{O}(t) - \hat{O}(t)\hat{J}^-(t)\hat{J}^+(t)\right\rangle\right\} \\ & -\tilde{\alpha}_2\left\{\frac{1-\chi^2}{(1+\chi^2)^2}\left[\left\langle\hat{J}^-(t)\hat{J}^+(t)\hat{J}^-(t)[\hat{O}(t),\hat{J}^+(t)]\right\rangle + \left\langle[\hat{J}^-(t),\hat{O}(t)]\hat{J}^+(t)\hat{J}^-(t)\hat{J}^+(t)\right\rangle\right]\right. \\ & +\frac{1}{1+\chi^2}\left[\left\langle\hat{J}^-(t)\hat{J}^-(t)[\hat{O}(t),\hat{J}^+(t)]\hat{J}^+(t)\right\rangle + \left\langle\hat{J}^-(t)[\hat{J}^-(t),\hat{O}(t)]\hat{J}^+(t)\hat{J}^+(t)\right\rangle\right] \\ & \left.+i\frac{2\chi}{(1+\chi^2)^2}\left[\left\langle\hat{J}^-(t)\hat{J}^+(t)\hat{J}^-(t)[\hat{O}(t),\hat{J}^+(t)]\right\rangle - \left\langle[\hat{J}^-(t),\hat{O}(t)]\hat{J}^+(t)\hat{J}^-(t)\hat{J}^+(t)\right\rangle\right]\right\} \end{aligned} \tag{33.2}$$

Here the new constants are represented through interaction parameter, $G^2(k_a k_b)$, detuning, $\tilde{\omega} - \omega_0$, number of atoms, N, and atomic losses [9], γ: $\tilde{\alpha}_1 = \alpha_1\tau_\perp$; $\alpha_1 = NG^2(k_a k_b)/\hbar^2$ and $\tau_\perp = \gamma_\perp^{-1}/(\chi^2+1)$, where $\chi = (\tilde{\omega} - \omega_0)\gamma_\perp^{-1}$, $\gamma \approx \gamma_\perp \approx \gamma_{II}$, respectively, $\tilde{\alpha}_2 = \alpha_2\gamma_{II}^{-1}(\gamma_\perp^{-1})^2$ and respectively $\alpha_2 = 2G^4(k_a, k_b)N/\hbar^4$. The first term in Eq. 33.3 describes the rate of collective transformation of anti-Stokes photons into Stokes photons.

The constant α_1, represents the transformation rate of this processes. The terms proportional to the constant α_2, represents the attenuation processes of generation which together with first term in Eq. 33.4 have the tendency to stabilization of scattering process. Passing from atomic operator $\hat{O}(t)$ to density matrix $Sp\{\rho(t), O(0)\} = Sp\{\rho(0), O(t)\}$ in Eq. 33.3, one can obtain the following master equation

$$\begin{aligned}\frac{d\rho(t)}{dt} = {} & -i\chi\gamma_\perp[\hat{J}_z,\rho(t)] + \tilde{\alpha}_1\left\{2\hat{J}^+\rho(t)\hat{J}^- - \rho(t)\hat{J}^-\hat{J}^+ - \hat{J}^-\hat{J}^+\rho(t)\right\} \\ & -\tilde{\alpha}_2\left\{\frac{1-\chi^2}{(1+\chi^2)^2}\left[\hat{J}^+\rho(t)\hat{J}^-\hat{J}^+\hat{J}^- - \rho(t)\hat{J}^-\hat{J}^+\hat{J}^-\hat{J}^+ + \hat{J}^+\hat{J}^-\hat{J}^+\rho(t)\hat{J}^- - \hat{J}^-\hat{J}^+\hat{J}^-\hat{J}^+\rho(t)\right]\right. \\ & +\frac{1}{1+\chi^2}\left[\hat{J}^+\hat{J}^+\rho(t)\hat{J}^-\hat{J}^- - \hat{J}^+\rho(t)\hat{J}^-\hat{J}^-\hat{J}^+ + \hat{J}^+\hat{J}^+\rho(t)\hat{J}^-\hat{J}^- - \hat{J}^-\hat{J}^+\hat{J}^+\rho(t)\hat{J}^-\right] \\ & \left.+i\frac{2\chi}{(1+\chi^2)^2}\left[\hat{J}^+\rho(t)\hat{J}^-\hat{J}^+\hat{J}^- - \rho(t)\hat{J}^-\hat{J}^+\hat{J}^-\hat{J}^+ - \hat{J}^+\hat{J}^-\hat{J}^+\rho(t)\hat{J}^- + \hat{J}^-\hat{J}^+\hat{J}^-\hat{J}^+\rho(t)\right]\right\}. \end{aligned} \tag{33.3}$$

This equation describes the collective transformation of Stokes photons in anti-Stokes fields and is similar to super-radiant master equations studied traditionally in this study [11, 18, 19]. As we neglect the losses from the cavity the steady state solution of this equation are applicable for the time intervals $\gamma^{-1} < t < k^{-1}$. The numerical and analytical studies of the kinetics of this process are given in the next section. Following is the solution of the master Eq. 33.3. In according with the mathematical approach we can expand density matrix on the coherent states like this is proposed in the papers [11, 18, 19]. As follows from Q- and P-diagonal representation [3] of density matrix [12], in the case when the right hand side of master equation has biquadrate form relatively the operators J^+ and J^- the solution of master equation it is represented through diagonal bra-ket operators of SU (2) algebra

$$\rho(t) = \sum_{m=-j}^{+j} C_m(t) \left| m, j \right\rangle \left\langle m, j \right|. \tag{33.4}$$

Here the Hilbert's vector $\left| m, j \right\rangle$ belongs to angular momentum vector sets. Introducing the representation (33.4) in Eq. 33.3 it is easy to obtain the following system of equations for the coefficient $C_m(t)$.

The coefficients $\{C_m\}$describe the probability of simultaneously existence of (2j + 1) Dicke states in the scattering process. The initial condition for the system of Eq. 33.5 is $C_{-j} = 1, \quad C_{-j+1} = C_{-j+2} = ... = C_j = 0$.

$$\begin{aligned}
\frac{dC_m(t)}{dt} &= \tilde{\alpha}_1 \left\{ C_{m-1}(t)[(j-m+1)(j+m)] - C_m(t)[(j-m)(j+m+1)] \right\} \\
&-2\tilde{\alpha}_2 \left\{ \frac{1-\chi^2}{(1+\chi^2)^2} [C_{m-1}(t)[(j-m+1)(j+m)]^2 - C_m(t)[(j-m)(j+m+1)]^2 \right. \\
&+ \frac{1}{1+\chi^2} [C_{m-2}(t)[(j-m+2)(j+m-1)][(j-m+1)(j+m) \\
&\left. - C_{m-1}(t)[(j-m+1)(j+m)][(j-m)(j+m+1)]] \right\}; \quad -j \le m \le j;
\end{aligned} \tag{33.5}$$

Following, we demonstrate the steady state solution from the system of Eq. 33.5. In according with this system of equation we obtain the following recursion algebraic equation between the coefficients. In according with this, the following recursion algebraic equation between the coefficients C_m, C_{m-1} and C_{m-2} is established:

$$\begin{aligned}
C_m &= C_{m-1} \frac{[(j-m+1)(j+m)]\{\beta_1 - \beta_2[(j-m+1)(j+m)] + \beta_3[(j-m)(j+m+1)]\}}{\beta_1[(j-m)(j+m+1)] - \beta_2[(j-m)(j+m+1)]^2} \\
&- C_{m-2} \frac{\beta_3[(j-m+2)(j+m-1)][(j-m+1)(j+m)]}{\beta_1[(j-m)(j+m+1)] - \beta_2[(j-m)(j+m+1)]^2};
\end{aligned} \tag{33.6}$$

where $\beta_1 = \tilde{\alpha}_1; \beta_2 = \tilde{\alpha}_2 \frac{1-\chi^2}{(1+\chi^2)^2}$ and $\beta_3 = \tilde{\alpha}_2 \frac{1}{1+\chi^2}$.

The distribution function is described by these coefficients. This steady state solution describes the stabilization process in the resonator. As a function of time,

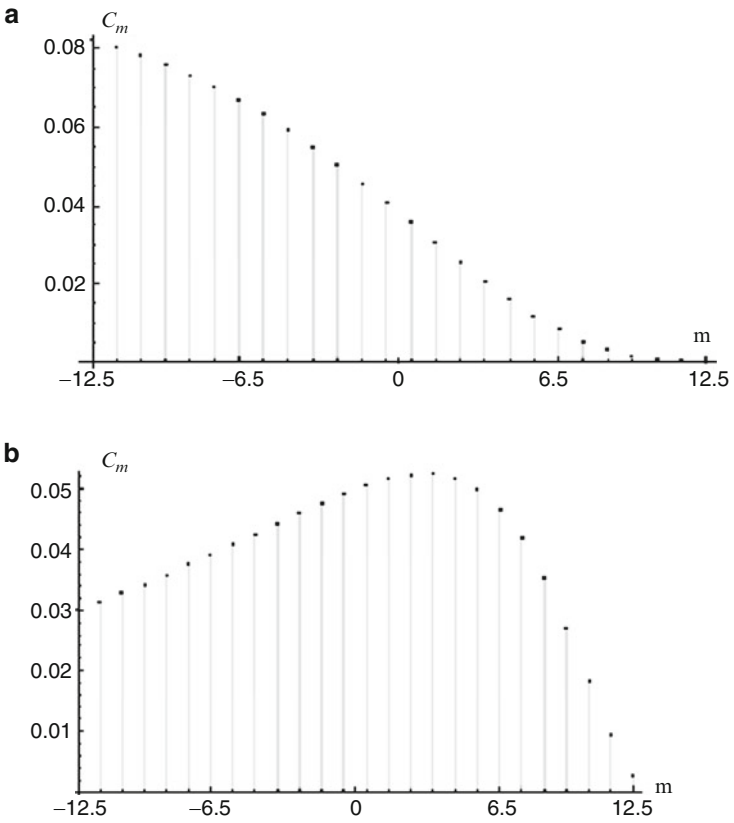

Fig. 33.7 (**a**, **b**) The distribution of the energies between Stokes and anti-Stokes photons in the time moments, $t = 0.4 / \alpha_1$, The dependence P_m as function label "m" is shifted by number j = 12 – 6.5

the correlation function achieved its maximum value corresponding to a steady state stabilization of scattering processes in the resonator [5–7]. As a result, the transformation of 2j + 1 = 26 Stokes photons into 26 anti-Stokes photons take places in a very interesting way. For example, the distribution of probabilities C_m as function of the label number "m" at earlier stage of radiation, $t = 0.1 / \tilde{\alpha}_1$, is described in Fig. 33.7a while in Fig. 33.7b this distribution is plotted at later time moments $t = 0.4 / \tilde{\alpha}_1$. This distribution can be regarded as the probabilistic repartitions between Stokes and anti-Stokes photons: (0,25); (1,24); (2,23); (3,22); (4,21); … (21,4); (22,3); (23,2); (24,1); (25,0), which are described by simultaneous existence of such repartitions with the probabilities: $C_{12}(t)$, $C_{11}(t)$, … $C_0(t)$ … C_{-12}. In the brackets, the first number (n, m) represents the Stokes photons and the second number – the anti-Stokes photons. The sum of these probabilities is equal to unity: $\sum_{m=-j}^{+j} C_m(t) = 1$. In Fig. 33.7 we have plotted the distributions of the energies.

This effects have many analogies with anti-bunging behavior of Stokes and anti-Stokes fields, described by J^+ and J^- operators of SU (2) group. The intensity of such field is described by second order correlation function $< J^+(t)J^-(t-\tau) >$ which is proportional to $\cos[(\omega_a - \omega_s)t + \phi]$ as in traditional coherence effect with single mode laser field.

33.4 Conclusions

Recent advances in quantum communication by using quantum optical proprieties of light are reviewed. The quantum communication protocols are carefully discussed. On the basis of these protocols, much research investigates the development and implementation of quantum optics devices. We proposed a new method of quantum communication, which takes in to account the coherence between the entangled photon fields and the application of this effect in cryptography and quantum communication. Considering coherent and corpuscular properties of light, consisted of photon fields, the new scheme for quantum communication has been offered for the quantum communications. At present, the most accessible two and even multi photon entangled states are produced by optical parametric down conversion. Such sources are probabilistic and post-selection is needed in some cases.

It is demonstrated that this non-stationary collective effect has many analogies with super radiance in atomic subsystems in free space. The dynamical transformation of Stokes photons in anti-Stokes photons and vice versa as function of the preparation of atomic inversion is investigated. The unique features of the field consisted from both Stokes and anti-Stokes photons are studied by solving numerically the master equation.

References

1. Aspelmeyer M, Böhm HR, Gyatso T, Jennewein T, Kaltenbaek R, Lindenthal M, Molina-Terriza G, Poppe A, Resch K, Taraba M, Ursin R, Walther P, Zeilinger A (2003) Long-distance free-space distribution of quantum entanglement. Science 301:621; Zeilinger A et al (1997) Experimental quantum teleportation. Nature 390:575–579
2. Agarwal GS, Puri RR (1991) Quantum theory of Stokes-anti- Stokes scattering in a degenerate system in a cavity and vacuum-field Raman splitting. Phys Rev A 43:3949
3. Balko B, Kay IW (1993) Critique of the Bonifacio-Lugiato superfluorescence model. Phys Rev B 48(14):10011–10021
4. Lee SKY, Law CK (2007) Collective photon-atom states by Raman coupling inside a cavity: a dynamic field-mode approach. Phys Rev A 76:033809
5. Bonifacio R, Lugiato LA (1975) Cooperative radiation processes in two-level systems: super fluorescence. Phys Rev A 11(5):1507
6. Enaki N, Turcan M, Vaseashta A (2008) Two photon multi mode laser model based on experimental observations. J Optoelectron Adv Mater 10(11):3016
7. Enaki N, Turcan M (2009) The kinetic of the two-photon lasing with one and two quanta cavity losses. Proc SPIE 7297:72970W.1–72970W.5

8. Enaki N, Eremeev V (2005) Two-photon lasing stimulated by collective modes. Opt Commun 247:381–392
9. Brown KR, Dani KM, Stamper-Kurn DM, Whaley KB (2003) Deterministic optical Fock-state generation. Phys Rev A 67:043818
10. Ekert AK (1991) Quantum cryptography based on Bell's theorem laser. Phys Rev Lett 67:661; Ekert AK, Palma GM (1994) Quantum cryptography with interferometric quantum entanglement. J Mod Opt 41:2413
11. Guzman R, Retamal JC, Solano E, Zagury N (2006) Field squeeze operators in optical cavities with atomic ensembles. Phys Rev Lett 96:010502
12. Jonathan S, Haruka T, Thompson JK, Vuletic V (2007) Interfacing collective atomic excitations and single photons. Phys Rev Lett 98:183601
13. Drummond PD, Gardiner CW (1980) Generalized P-representations in quantum optics. J Phys A 13:2353–2368; Gardiner CW (1996) Quantum noise. Springer, New York
14. Miller R, Northup TE, Birnbaum KM, Boca A, Boozer AD, Kimble HJ (2005) Trapped atoms in cavity QED: coupling quantized light and matter. J Phys B At Mol Opt Phys 38:S551
15. Parkins AS, Solano E, Cirac JI (2006) Unconditional two-mode squeezing of separated atomic ensembles. Phys Rev Lett 96:053602
16. Pfister O, Brown WJ, Stenner MD, Gauther DJ (1999) Two-photon stimulated emission in laser-driven alkali-metal atoms using an orthogonal pump-probe geometry. Phys Rev A 60:R4249–R4252
17. Wang ZC, Haken H (1984) Theory of two-photon lasers I: semi-classical theory. Z Phys B-Cond Matter 55:361–370; ibid. Quantum theory of the two-photon laser. (1988) ibid. 71:253–259
18. Dicke RH (1954) Coherence in spontaneous radiation processes. Phys Rev 93(1)
19. Gauthier D, Wu Q, Morin SE, Mossberg TW (1992) Realization of a continuous-wave, two-photon-optical laser. Phys Rev Lett 68:464; Gauthier DJ (2003) Progress in optics, vol 45. Chapter X, Elsevier, Amsterdam

Chapter 34
Lithographic Limit and Problems of Two-Photon Holograms in Quantum Optics: Application in Secured Communications

Quantum Communication and Holography

Nicolae A. Enaki

Abstract The application of coherence proprieties of bimodal field in quantum lithography and quantum holography is proposed. The coherence effect between the photons from Stokes and anti-Stokes waves generated in Raman lasing emission is established. The application of Stokes and anti-Stokes bimodal coherent field in lithography and holography are given in according with the definition of amplitude and phase of such entangled states of light. The optical scheme of holographic representation of object in bimodal representation is proposed.

Keywords γ- and x-ray radiation • Extended nuclei system • Two-photon sources • Cooperative emission

34.1 Introduction

The creation of entangled photons in two- and multi-quanta processes opens new possibilities in quantum lithography and quantum holography. For example in the paper of Teich et al. [1] it is proposed to make use of quantum entanglement for extracting holographic information about a remote 3-D object in a confined space which light enters, but from which it cannot escape. Light scattered from the object is detected in this confined space entirely without the benefit of spatial resolution. Quantum holography offers this possibility by virtue of the fourth-order quantum coherence inherent in entangled beams. This new concept is based on the application of second ordered

N.A. Enaki (✉)
Institute of Applied Physics, Academy of Sciences of Moldova, Academiei Str. 5, Chisinau, MD, Republic of Moldova
e-mail: enache@asm.md

A. Vaseashta et al. (eds.), *Technological Innovations in Sensing and Detection of Chemical, Biological, Radiological, Nuclear Threats and Ecological Terrorism*, NATO Science for Peace and Security Series A: Chemistry and Biology,
DOI 10.1007/978-94-007-2488-4_34, © Springer Science+Business Media B.V. 2012

coherence function, proposed first by Glauber and Sudarshan [2, 3], which has subsequently been intensively developed in the last few years. The possibility by virtue of the fourth-order quantum coherence of entangled beams was studied by Belinskii and Klyshko [4] which proposed a two-photon analog of classical holography.

This article is describe applications of coherent emission of two subgroups of photons, the sum (or difference) energies of which can be regarded as a constant so that coherence appear between the blocs of product of two electromagnetic field strength. It was shown recently that spatial-multimode broadband squeezed light can generate coherent states of bimodal electromagnetic field, as observed in photon counting experiment, the statistics of which are regular not only in time, but also in the plane of observation. The application of second order space-time coherence of light formed from entangled photons in holography and lithography follows from the definition of the quantum states of such bimodal fields.

In the second part of this article, a definition of bimodal coherent states is given in analogy with single photon coherent states. The definition of phase and amplitude of this bimodal field is provided. Taking into account the coherent states of Stokes and anti-Stokes modes the lithographic limit for this bimodal field is defined.

In the third part of this article, an application of product strength amplitudes and phases in holographic registration is proposed. The superposition of two vectors of bimodal field obtained in two-photon or Raman laser effect is proposed for contraction of holographic image of the object. For observation of this hologram, the two-photon detection scheme is proposed.

34.2 Coherent Proprieties of Two Photon Fields and Their Application in Lithography

Let us consider two nonlinear processes of light generation in lasers and collective decay phenomena. In the second order of interaction of light with matter these processes strongly connect two waves in output detection region and give us the possibility to study the coherent effects between these fields. One of these effects is connected with lithographic optical limits in measurements [5]. Taking into account a concept of the dropped lithographic limit $\Delta \geq \lambda / 2$ in two quanta coherent processes, Boto et al. [6] have observed a new lithographic limits in parametrical down-conversion effect. This process generates two waves with frequencies ω_s -signal and ω_i -idler. The lithographic limit for these two waves is smaller than traditional limit $\Delta \geq \lambda / 4$. Following this concept, we introduced a similar coherence between the photons in Raman lasing processes. In this case one photon in from driving field is absorbed (Stokes photon a_s), and the other photon is generated as (anti-Stokes $b_a{}^+$). Taking into account product of Sakes and anti-Stokes amplitudes $P^-(t,z)$, one can construct a common phase interference figures between two space points z and $z+\Delta$. These interfere figures are similar with coherence coincidences observed in double slits experiment with single amplitude coherent field $G_2(\Delta) = \langle P^-(z) P^+(z+\Delta) \rangle$.

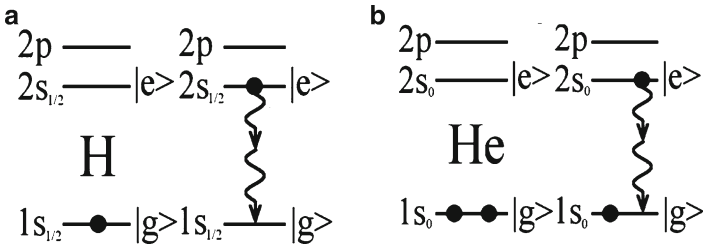

Fig. 34.1 The two-photon spontaneous emission in (**a**) Hydrogen-like (**b**) and Helium-like atoms

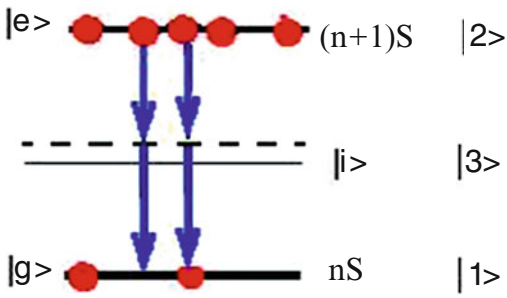

Fig. 34.2 Two-photon cooperative decay stimulated by discrete mode structure of micro-cavity (*chain line*) observed in experiment [10]

(A) Let us first describe the nonlinear effects in which coherence between two photons is possible. The experiments for determination of two-photon decay time for metastable states for hydrogen-like or helium-like atoms (see Fig. 34.1) relatively to dipole-forbidden transitions $2^2S_{1/2} \to 1^2S_{1/2}$ and $2^1S_0 \to 1^1S_0$ was studied in the experiments [7, 8].

The two-photon co-operative phenomena can appear in similar experiments if at the distance less than the mean value of radiation wavelength $\lambda_m = 2\mathrm{hc}/(\mathrm{E_{2S}} - \mathrm{E_{1S}}) = 2400\,[\mathrm{A}^0]/Z^2$ certain number of inverted atoms $N \cup 10-100$ is situated. In this case, the transition probability is found in the second order of perturbation theory $M(k_1,k_2)\delta(\hbar\omega_{k_1} + \hbar\omega_{k_2} - (\mathrm{E_{2s}} - E_{1s}))$ of the living time of metastable state 2S. The cooperative decay time, $\tau_r = \tau_0/N$, delay time of superradiant pulse $t_0 = (\tau_0/N)\ lnN$ decreases in accordance with the superradiance law. Here $\tau_0 = 0.121Z^{-6}$ s is the two-photon decay time for hydrogen- or helium-like atoms, Z is the order number of the element. In extended systems of atomic radiators the super-fluorescence is observed in the case when the mean distance between the atoms is of the order of the radiation wavelength [9]. These experiments give the hope that in gamma diapason, when the mean distance between the inverted nuclei is comparable with the radiation wavelength, the super-radiance can be observed as well. An interesting effect of two photon cooperative emission is possible in micro-cavities $\lambda_m = 2\mathrm{hc}$. In this case the mode structure of the cavity stimulate the two-photon decay effect in comparison with cascade effect [9, 10] (see Fig. 34.2).

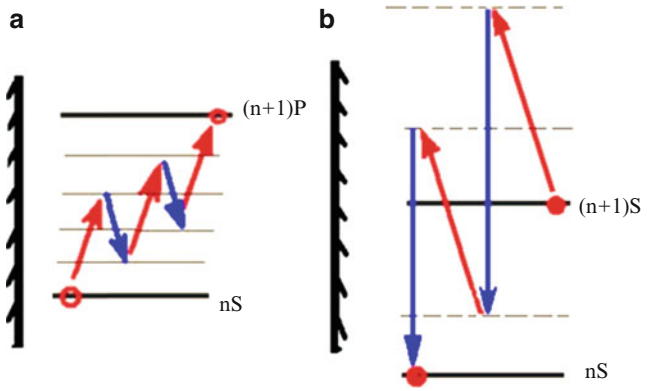

Fig. 34.3 Sources of entangled photons in multi-photon processes. (**a**) Scattering diagram for two-photon laser beam amplification in laser-driven two level-atoms; (**b**) Hyper Raman four-photon process with emission of two big energy entangled photons and absorption of two photons with smaller energy

The property of entanglement between the photons emitted in the two photon lasers and parametrical dawn conversion has a great impact in application in quantum information. The possibility of induced two-photon generation per atomic transition was suggested by Sorokin, Braslau, and Prohorov [11]. The scattering effects in two-photon amplifier attenuate the possibility to realize two-photon lasing.

The first experiments demonstrated that two-photon amplification and lasing in the presence of external sources are possible [12] (see Fig. 34.3). These ideas open new concept about the coherence. By introducing the amplitude of two boson field crated in two-photon lasers we can observe that the generation amplitude is described by the field product

$$P^{(+)}\left(t,z\right)=E_b^{(+)}(z,t)E_a^{(+)}(z,t)=G(k_b,k_a)ab\exp[i\omega_0 t-i(k_a+k_b)z]; \quad (34.1)$$

where $\omega_0=\omega_b+\omega_a=\omega_{21}$ is the total frequency of generated photons. In this case we can introduce the following operators of bi-boson field,

$$I^+=b^+a^+;\ I^-=ab;\ I_z=(a^+a+b^+b)/2 \quad (34.2)$$

In with coherent state of single photon lasers we can introduce the following coherent state for these bi-boson fields

$$\left|\mu\right\rangle=\exp\{\mu I^+\}\left|j,j.\right\rangle\{1-|\mu|^2\}^j \quad (34.3)$$

which belong to $SU(1,1)$ symmetry represented in the Fig. 34.3a, b. Here μ is the coherent displacement of bi-boson oscillator. In accordance with this concept, the function $P^{(+)}\left(t,z\right)$ has the same behavior as the electrical component of single photon laser. For example, the mean value of this function on the coherent

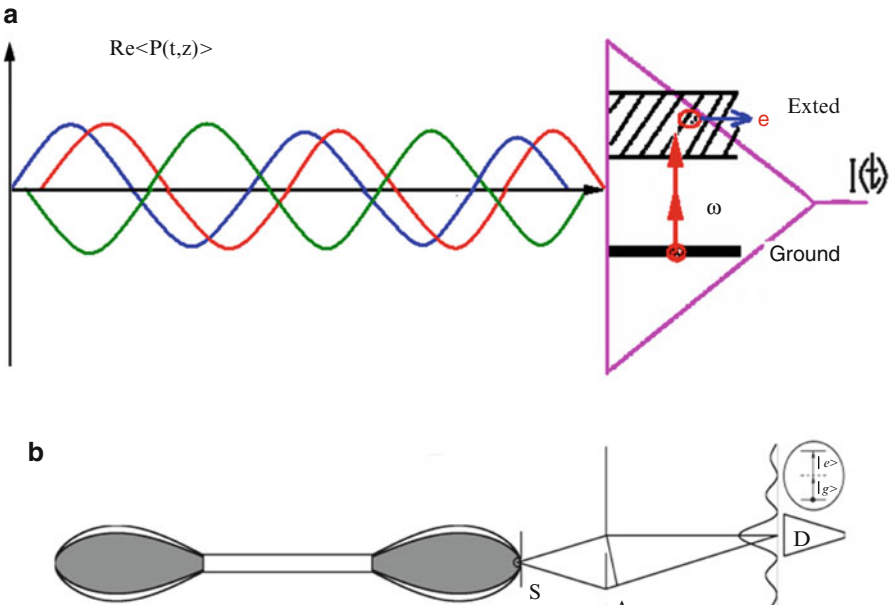

Fig. 34.4 (**a**) The proprieties of two-ray coherence have similar behavior as a coherent strength of single photon laser field. (**b**) Two slits experiments with interference between pairs of modes which form the strengths product of EMF. The interference picture can be observed in photon excitation of the detector

state (34.3) can be represented through the harmonically functions with phase and amplitude

$$\left\langle P^{(+)}\left(t,z\right)\right\rangle = P_0 \exp[i\omega_0 t - i(k_a + k_b)z + \varphi] \tag{34.4}$$

where $P_0 = G(k_b,k_a)\left|\left\langle \hat{a}\hat{b}\right\rangle\right|$ is the amplitude and $\varphi = Arg\left\langle \hat{a}\hat{b}\right\rangle$ is the phase of electrical field strengths of two fields a and b. In Fig. 34.4a it is represented time or z- dependence of such functions. The lithographic limit follows from the difference between the maximum and minimum of two slits experiment represented in Fig. 34.4b. According with expression (34.4) and the distinguish distance Δ between the slits follows that the second order correlation function $G_2\left(\Delta\right) = \left\langle P^{-}(z)P^{+}\left(z+\Delta\right)\right\rangle$ pass from maximal to minimal values for the value of $\Delta(k_1 + k_2)\sin\theta = \pi$. From this expression follows that lithographic limit is realized for $\sin\theta \to 1$. Or the distance between two stresses on the (x,y) plan must be,

$$\Delta \to \lambda_a\lambda_b / [2(\lambda_a + \lambda_b)] \tag{34.5}$$

In the case when the wavelengths of the fields "a" and "a" coincide we $\lambda = \lambda_a = \lambda_b$ obtain the lithographic limit [11].

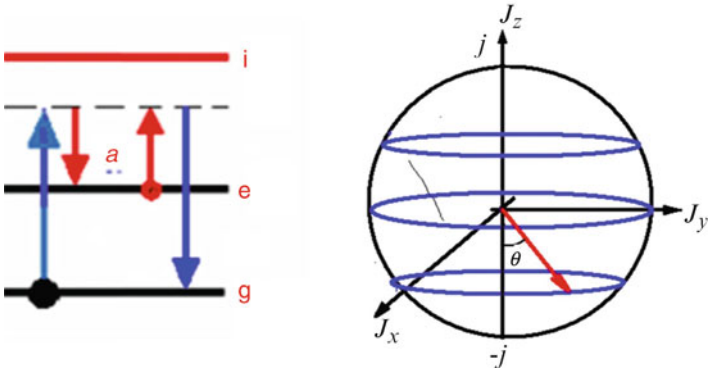

Fig. 34.5 Scattering-generation diagram with generation of Stokes (or Anti-Stokes) photons (*left*) and the representation of the symmetry of such generation in phase space of bimodal field (*right*)

(B) Let us propose the coherent phenomena which can appear between two fields in Raman processes. If we study generation of Stokes light under the non-coherent pumping with anti-Stokes field we can introduced the following representation of bi-boson field

$$\Pi^{-}(t,z) = E_s^{(+)}(z,t)E_a^{-}(z,t) = G(k_s,k_a)\hat{a}_s\hat{b}_a^{+}\exp[i\omega_0 t - i(k_a - k_s)z] \quad (34.6)$$

where $E_s^{(+)}(z,t)$ $E_a^{-}(z,t)$ $E_s^{(+)}(z,t)$ and $E_a^{-}(z,t)$ are positive and negative defined strength of Stokes and anti-Stokes field (see Fig. 34.5), $\hat{a}_s^{+}$, $\hat{b}_a^{+}$ and $\hat{a}_s$, $\hat{b}_a$ are the annihilation and creation operators of electromagnetic field at Stokes, ω_s, and anti-Stokes, ω_a, frequencies respectively; $\omega_a - \omega_s = \omega_0$ is the fixed frequency of bi-boson field accordingly with the transition diagram represented in Fig. 34.5a.

According with this definition, one can introduce the new bi-boson operators $J^{-} = b^{+}a$; $J^{+} = a^{+}b$; $J_z = (a^{+}a - b^{+}b)/2$ which for constant number of photons in resonator it is possible for conservation of Kasimir vector, $J^2 = J^2{}_z + J_x^2 + J_y^2$ represented in Fig. 34.5b (here $J_x = (J^{+} + J^{-})/2$, $J_y = (J^{+} - J^{-})/2i$).

If we consider that at initial time the number of anti-Stokes photons is N = 2j, one describes the two photon scattering lasing processes by coherent state for this bi-boson field belonging to SU(2) algebra

$$|\alpha\rangle = \exp\{\alpha J^{+}\}|-j,j\rangle\{1+|\alpha|^2\}^{-j}, \quad (34.7)$$

where $\alpha = \tan(\theta/2)$ is the amplitude of this bi-boson field obtained in the Raman lasing processes. Taking into account the coherent state (34.7) one can find the mean value of strength product

$$\langle\Pi(t,z)\rangle = [\langle\Pi^{-}(t,z)\rangle + \langle\Pi^{+}(t,z)\rangle]/2$$
$$\langle\Pi(t,z)\rangle = \Pi_0\cos[\omega_0 t - (k_a - k_s)z + \varphi], \quad (34.8)$$

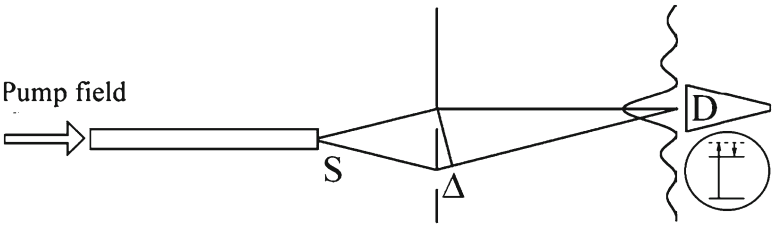

Fig. 34.6 The pump of bimodal field in the Raman scattering effect in pencil shape cavity according with the scheme represented in Fig. 34.5

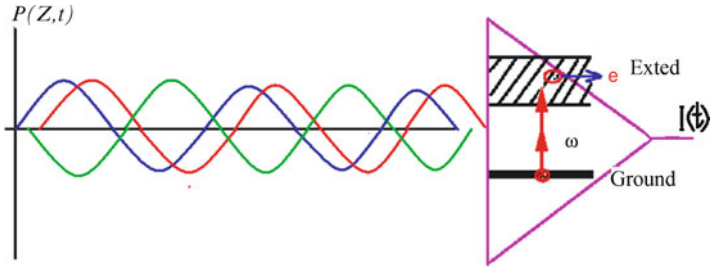

Fig. 34.7 The time dependence of mean value of vector <P (z,t)> and method of detection

where $\Pi_0 = G(k_s, k_a)\left|\left\langle \hat{a}_s \hat{b}_a^{+} \right\rangle\right|$ and $\varphi = \arg\left\langle \hat{a}_s \hat{b}_a^{+} \right\rangle$ are the amplitude and phase of bimodal field formed from Stokes and anti-Stokes photons. The minimal distance between maximal and minimal values of amplitude of correlation function $G_2(\Delta) = \left\langle \Pi^{-}(z)\Pi^{+}(z+\Delta) \right\rangle$ in the two slits experiments observed with two photon detectors corresponds to lithographic limit of this conjugate entangled bimodal field (see Fig. 34.6).

This distance is inversely proportional with wave vectors difference $\Delta \geq \pi / (k_a - k_s)$ and of course is manifested in the second order coherence between Stokes and anti-Stokes field. We emphasize here that Stokes and anti-Stokes field can be incoherent field in its boson representation. Of course, these two field representation must be regarded as a bi-boson coherent state of light formed from the action of the operator product of Stokes and anti-Stokes fields $a_s b_a^{+}$ on the vacuum of electromagnetic field respectively. If the frequency of anti-Stokes field is larger than the Stokes frequency, we can approximate this limit with the expression $\Delta \geq \lambda_a / 2$, λ_a and λ_a are the anti-Stokes and Stokes wave length respectively. This coherent phenomenon between Stokes and anti-Stokes fields can be used in Holography and other coherent processes with phase memory (see Fig. 34.7).

The minimal distance between maximal values of amplitude of the above correlation corresponds to lithographic limits of this conjugate entangled bimodal field,

$\Pi^{-}(z)$. This distance is inversely proportional with wave vectors difference $\Delta \geq \pi / (k_a - k_s)$ and of course is manifested in the second order coherence between the Stokes and anti-Stokes field. We emphasize here that the Stokes and anti-Stokes field can be an incoherent field in its boson representation. Of course these two field representation must be regarded as a bi-boson coherent state of light formed from the action of operator product of Stokes and anti-Stokes fields $a_s b_a^{+}$ on the vacuum of e.m. field respectively: $|\mu>= \exp[\mu a_s b_a^{+} - \mu a_s^{+} b_a]|0>$, where μ is the amplitude of this bi-boson field obtained in the Raman lasing processes, $|0>$ is the vacuum state of this bi-boson field. If the frequency of anti-Stokes field is larger than the Stokes frequency we can approximate this limit with expression $\Delta \geq \lambda_a / 2$, λ_a and λ_a are the anti-Stokes and Stokes wave length respectively. This coherent phenomenon between Stokes and anti-Stokes fields can be used in Holography and other coherent processes with phase memory.

34.3 Holographic Proprieties of Bi-Boson Coherent Field

In this section we discuss how a hologram can be constructed using the recording phase information of bimodal field on a medium sensitive to this phase, using two separate beams of bimodal field (one is the "usual" beam associated with the image to be recorded and the other is a known as the reference beam). By exploiting the interference pattern between these bi-boson fields described in the last section in principle, this is possible. For example the Stokes and anti-Stokes fields can be regarded as a field with electromagnetic strength product (34. 6), so that the common phases $\phi = \omega_0 t - k_0 z$ of this two fields amplitude a_s and b_a^{+} has similar behavior as the phase of single mode coherent field, here $\omega_0 = \omega_a - \omega_s$ and $k_0 = k_a - k_s$ are the frequencies and wave vectors difference between the Stokes and anti-Stokes fields respectively. The coherent propriety of this product of electric field components is proposed to apply in possibilities to construct the time space holograms of real objects, taking in to account the conservation of phase of amplitude product in the propagating and interference processes. The quantum phase between the radiators can be used in holography too.

At present, there are several experiments that manifest holographic principles of processing of quantum information. One of them is the model of Teich [1], which describes correlation between the entangled photons obtained in parametrical down-conversion. In the Fig. 34.8 the principle of such holography is given. Here S is a source of entangled-photon pairs. C is a (remote) single photon-sensitive integrating sphere that comprises the wall of the chamber concealing the hidden object (bust of Plato). D is a (local) 2-D single-photon-sensitive scanning or array detector. In addition, *h1* and *h2* represent the optical systems that deliver the entangled photons from S to C and D, respectively. The quantity *p2(x*2) is the marginal coincidence rate, which is the hologram of the concealed object. Thin and thick lines represent optical and electrical signals, respectively. The hologram in parametrical down conversion

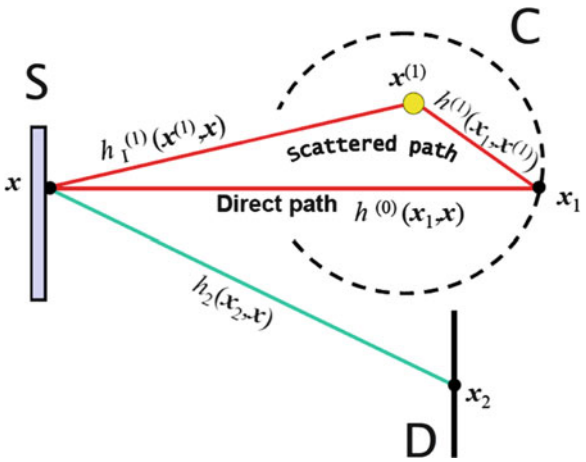

Fig. 34.8 The hologram principle of registration of information with entangled photons proposed in paper [1]

is realized in terms of the correlations between the entangled photon in the single pair. The coherence between the pairs is not takes in to account.

Following the idea of second order coherence proposed in papers [6, 9], we propose the new type of hologram registration in bimodal photon field based on the coherent proprieties (34.5) and (34.8). As is well known that the holographic code in single photon coherent effects is based on mixing of the original wave (hereafter called the object wave) I_0 with a known reference wave I_r and subsequently recording their interference pattern in the z = 0 plane. The intensity of the sum of the two waves is added photographically.

Recorded and a transparency of complex amplitude transmittance T, proportional to the intensity, is proposed in the literature (see for example [13, 14]). Following this idea, we can construct such a hologram using the vector (34.1) for two-photon coherence or vector (34.6) for scattering bimodal field. According to its classical definition, one can represent the original bimodal field through $P_O(z,t) = (P_O^+(z,t) + P_O^-(z,t))/\sqrt{2}$ and known reference bimodal wave through,

$$P_r(z,t+\tau) = (P_r^+(z,t+\tau) + P_r^-(z,t+\tau))/\sqrt{2}$$

In this case the sum of interference pattern is represented in Fig. 34.9 and has many analogies with classical holograms. The transmittance is given by interference between the original and reference bimodal wave in the point in point z = 0.

$$T = <: (P_O(z,t) + P_r(z,t+\tau))^2 :> = < P_O^-(0,t)P_O^+(0,t) > + < P_r^-(0,t+\tau)P_r^+(0,t+\tau) > + < P_O^-(0,t)P_r^+(0,t+\tau) > + < P_r^-(0,t+\tau)P_O^+(0,t) >. \quad (34.9)$$

This transmittals can be detected by two photon detectors on the plane (x,y) and the interpretation of imagine can be expressed in classical terms

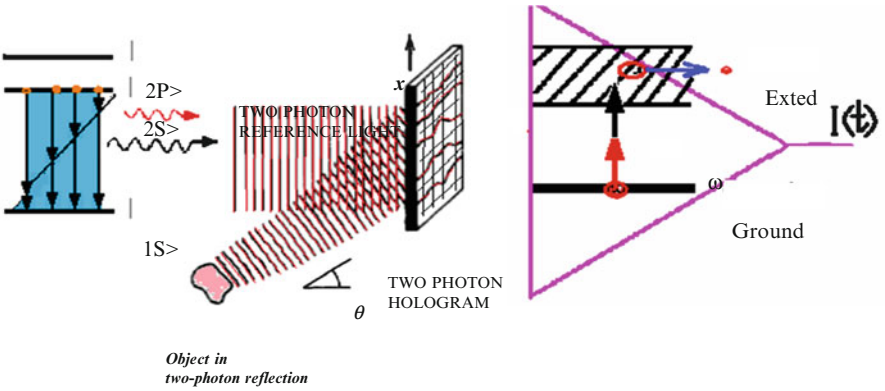

Fig. 34.9 Two-photon coherent light and principle of hologram registration taking into account the phase and amplitude of bimodal field

$$T = G_{O2} + G_{r2} + 2\sqrt{G_{r_2}G_{O2}}\cos[\arg(P_O^+(0,t)) - \arg(P_r^+(r,t+\tau))] \quad (34.10)$$

Here $G_{O2} =< P_O^-(0,t)P_O^+(0,t) >$ is the intensity of detected bi-photons. From the original bimodal field; $G_{r_2} =< P_r^-(0,t+\tau)P_r^+(0,t+\tau) >$ is the intensity of detected bi-photons from reference bimodal wave from the object. The phase dependence of the imaginary component can be described by argument of complex number

$$< P_O^-(0,t)P_r^+(0,t+\tau) > \quad \text{or} \quad \arg(P_O^+(0,t)) - \arg(P_r^+(r,t+\tau)).$$

The same behavior has the bimodal field formed from the Stokes and anti-Stokes photons. In this case, in expressions (34.9) and (34.10) the field $P^+(0,t)$ must be substituted with $\Pi^+(0,t)$. The propriety of last bimodal field is described by the expressions (34.6–34.8). The detection scheme on the plan z = 0 is represented in Fig. 34.6.

34.4 Conclusion

We propose new possibilities in decreasing of lithographic limit using coherent bimodal electromagnetic field formed from the Stokes and anti-Stokes waves. If initially the field is prepared in the Stokes state with photon number $N = 2j$ and atoms in excited state, the lithographic limit is described by the expression $\Delta \geq \lambda_a\lambda_a / (2(\lambda_s - \lambda_a))$. In the case, when wave-length of generated anti-Stokes field fall in the x-ray spectral region, the lithographic limit can achieved in the Nano-scale diapason. This is an important limit for modern Nano-electronics and bio-physics. The application of coherent effect of bimodal field in holography opens the new perspectives in transmission of information not only through entangled state of photons but through the second order coherence. Much of current literature

addresses holographic principles of processing quantum information [15, 16]. All of these methods manifest new perspectives in the coding and decoding of information.

References

1. Teich C et al (2001) Role of entanglement in two-photon imaging. Phys Rev Lett 87:123602
2. Glauber RJ (1963) Coherent and incoherent states of the radiation field. Phys Rev 131:2766
3. Sudarshan ECG (1963) Equivalence of semiclassical and quantum mechanical descriptions of statistical light beams. Phys Rev Lett 10:277
4. Belinskiĭ V, Klyshko DN (1993) The interference of light and the Bell's theorem. Usp Fiz Nauk 163(8):1
5. Pfister O, Brown WJ, Stenner MD, Gauthier DJ (2001) Polarization instabilities in a two-photon laser. Phys Rev Lett 86:4512
6. Boto AN et al (2000) Quantum interferometric optical lithography: exploiting entanglement to beat the diffraction limit. Phys Rev Lett 85:2733
7. Marrus R, Schmieder RW (1972) Forbidden decays of hydrogenlike and helium-like argon. Phys Rev A 5:1160
8. Van Dyck RS, Johnson CE, Shugart HA (1970) Radiative lifetime of the metastable 21S0 state of helium. Phys Rev Lett 25:1403
9. Enaki NA (1988) Superradiance in two-photon spontaneous emission. Sov Phys JETP 67:2033
10. Enaki NA, Macovei MA (1999) Two-photon cooperative decay in a cavity in the presence of a thermalized electromagnetic field. JETP 88:633 [(1999) Zh Eksp Teor Fiz 115:1153]
11. Sorokin PP, Braslau N (1964) Some theoretical aspects of a proposed double quantum stimulated emission device. IBM J Res Dev 8:177; Prokhorov AM (1965) Science 10:828
12. Nikolaus B, Zhang D, Toschek P (1981) Two-photon laser. Phys Rev Lett 47:171
13. Brune M et al (1987) Realization of a two-photon maser oscillator. Phys Rev Lett 59:1899
14. Saleh BEA, Teich MC (1991) Fundamentals of photonics. Wiley, New York, p 947. ISBN 0-471-83965-5
15. Polzik S et al (2008) Quantum memory for images: a quantum hologram. Phys Rev A 77:020302(R)
16. Bjork G et al (2002) Two-photon imaging and quantum holography. arXiv:quant-ph (Quantum-Physics)/0211120v1 19 Nov 2002

Chapter 35
Using Informatics-, Bioinformatics- and Genomics-Based Approaches for the Molecular Surveillance and Detection of Biothreat Agents

Biological Agent and Naturally-occurring Pathogen Surveillance

Donald Seto

Abstract The convergence and wealth of informatics, bioinformatics and genomics methods and associated resources allow a comprehensive and rapid approach for the surveillance and detection of bacterial and viral organisms. Coupled with the continuing race for the fastest, most cost-efficient and highest-quality DNA sequencing technology, that is, "next generation sequencing", the detection of biological threat agents by 'cheaper and faster' means is possible. With the application of improved bioinformatic tools for the understanding of these genomes and for parsing unique pathogen genome signatures, along with 'state-of-the-art' informatics which include faster computational methods, equipment and databases, it is feasible to apply new algorithms to biothreat agent detection. Two such methods are high-throughput DNA sequencing-based and resequencing microarray-based identification. These are illustrated and validated by two examples involving human adenoviruses, both from real-world test beds.

Keywords Bioinformatics • Genomics • Adenoviruses • Threats

35.1 Introduction

Biological pathogens, including "biological threat" (biothreat) agents, pose unique problems in that they will amplify, i.e., grow and reinfect, in a susceptible population and perpetuate their biological effects if unchecked. In other words, by definition, biological agents are living organisms that reproduce and sustain an epidemic

D. Seto (✉)
Department of Bioinformatics and Computational Biology, George Mason University, 10900 University Boulevard, MSN5B3 Manassas, VA, USA
e-mail: dseto@gmu.edu

A. Vaseashta et al. (eds.), *Technological Innovations in Sensing and Detection of Chemical, Biological, Radiological, Nuclear Threats and Ecological Terrorism*, NATO Science for Peace and Security Series A: Chemistry and Biology,
DOI 10.1007/978-94-007-2488-4_35, © Springer Science+Business Media B.V. 2012

until either a biological or a man-made barrier (or intervention) is reached. Therefore, applying a defined and validated protocol for recognizing and identifying the correct organism is the first step in the interruption of the cycle.

Biotechnology and technology have provided solutions to problems recently, particularly in the context of recombinant DNA technology and the resources available through the world-wide web and computational power. In addition, biotechnology and technology have also generated additional, new and unanticipated problems for society- as the proverbial 'double-edged sword'. While a goal is and should always be the alleviation of human pain and suffering, with the improvement of living conditions, there are those who pursue a counter goal- one that produces bio-threat agents for example. While this may seem to be a major and unproductive problem, that is, one that may divert resources from the "more noble" goals, it may also be approached as a re-phrasing of another long-standing biological problem, one that must be solved to ensure human health and safety. This related problem is that of detecting, identifying and characterizing naturally occurring pathogens, particularly in the food chain.

Both aspects of this same problem may be reflected upon and solved given the context of the many advances and available resources in technology, e.g., computational power, database development, information technology and internet-based networking, and in bioinformatics, e.g., genomic data and computational tools for data mining. Described in this presentation is the recent convergence of informatics-, bioinformatics- and genomics- based approaches for the molecular surveillance and detection of biothreat agents, whether they are "nature-made", i.e., naturally occurring, or "man-made", i.e., laboratory-conceived. These resources include protocols, data, databases and accessibility.

35.2 The Problem

Biological pathogens interact with humans and the human population as viruses, bacteria and eukaryotic organisms (e.g., fungi). These pathogens represent a very diverse range of organisms with no seemingly common attributes, other than affecting their hosts. Again, the organisms may be the result of naturally occurring events, i.e., evolution, or man-made events. The problem, therefore, is how are they recognized and identified.

As naturally occurring pathogens, these organisms may arise as "common" occurrences causing 'expected' illnesses, such as influenza on a healthy population, or "special cases" occurrences, such as secondary opportunistic pathogens on an immune suppressed or deficient population, causing coinfections (multiple simultaneous infections of pathogens) and often 'unanticipated' but more severe illnesses. Another related but less common problem is that the human populations, both healthy and immune suppressed, may be subjected to "unanticipated" illnesses through consuming contaminated or infected foods, such as meats and vegetables. These agricultural products may become (accidental or introduced) carriers for

pathogens that affect only the human 'end-users'. The pathogens may include variants of bacteria normally found associated with humans commensally, such as *Escherichia coli* as strain O157:H7 and other *E. coli* strains [1] or those synthesized potentially.

For all intents and purposes, "The Problem" comprises detection, identification and characterization of these pathogens, the topic of this discussion. These are the first steps in the containment of pathogens and in the treatment of the health problems caused by these organisms. Of course, once identified, the overall problem is only partially solved but it is a necessary first step. Both human pathogens and non-human pathogens, e.g., those acting against flora and fauna, e.g., agriculturally important produces, may be approached using the same paradigm: exploitation and application of the genome sequence data. Logically and practically, the detection, identification and characterization of naturally occurring and synthetic "man-made" biological pathogens call for the same protocols, tools and approaches. These are enhanced and improved by current advances in informatics, bioinformatics and genomics.

35.3 Historical Perspectives

The association of disease with microorganisms, specifically bacteria (and including eukaryotic, such as fungi), has not changed since Robert Koch's postulates (1890) were established detailing the etiology of anthrax and tuberculosis. These postulates include isolating the microorganism in all organisms suffering from the disease, growing the putative pathogen in culture and demonstrating that subsequent reinfection with this passaged organism causes the identical symptoms and disease in virgin and susceptible hosts (http://en.wikipedia.org/wiki/Koch%27s_postulates). Current accepted and standardized clinical laboratory protocols and practices call for identifying bacterial pathogens using laboratory assays that include physical cell staining (e.g., Gram stain), biochemical methods for proteins and other metabolites, and immunochemical assays, including antibody reagents. In addition, recent updates from technological advances are now being used, e.g., genomics-based approach, including the sequencing of certain defined genes and DNA sequences (especially including rRNA) [2].

Viruses are treated in a similar manner, albeit with the caveat that they must be grown in particular and specific hosts as they are not independently replicating life forms. Previously, the lack of success in growing viral pathogens was a barrier to the identification and association of a particular virus with a disease; this is partially overcome by random primer-based DNA sequencing (metagenomics and database mining). Past and current methods of characterizing viral pathogen include electron microscopic examination of shape and size, biochemical assays of proteins, immunochemical assays of proteins, including antibody reagents, and reinfection of virgin and susceptible hosts. As with the bacterial pathogens, identification of viral pathogens also now includes the acquisition and analysis of partial or full genomic sequence data [3, 4].

35.4 A Solution

In the past, the available laboratory tools limited microbial pathogen surveillance and identification. Prior to DNA sequencing, the highest resolution techniques provided only protein and peptide-level structures as targets for analysis and assays. As indicated earlier, many of the established and currently used protocols call for examination of the shape and size of the pathogen along with the examinations of expressed proteins through biochemical and immunochemical assays. Proteins are unique and therefore define a particular organism (pathogen). However, they are "interpretations" of the genome with their own physical properties. Secondary and tertiary structures of proteins, for example, form epitopes as three-dimensional structures for antibody recognition, an immunochemical assay. Using this as the primary method for the identification of an organism may lead to the misidentification of a pathogen, as using epitopes may be switched and not reflective of the complete primary genome sequence data and the pathogen itself [3].

The advent of DNA sequencing [5], and its refinement, including more efficient and cost-effective high throughput methods ("Next Generation" sequencing technology), allows the examination of a pathogen at the highest level of resolution. The DNA sequence, i.e., the particular nucleotide composition and their order, is absolutely unique to a particular pathogen. Minute changes, as in naturally occurring mutations as well as man-made modifications, in the genome sequence may be monitored by genome and DNA sequence analysis, along with other genomics-based methods that will not be discussed due to time limitations, e.g., polymerase chain reaction-based methods, genotyping, etc. Methods for taking advantage of the genomics and bioinformatics approach allow for rapid and exact identification of microbial pathogens, including viral, bacterial and eukaryotic. The methods to be discussed include Sanger-based DNA and genome sequencing and microarray-based organism identification and DNA sequencing (as "resequencing"). To simplify the discussion, these are illustrated and validated by two examples involving human adenoviruses, both from real-world test beds. The first example is whole genome sequence determination and analysis, as discussed earlier in the context of identifying a reemergent human adenovirus pathogen [3].

As noted, three potential solutions to pathogen detection and surveillance are presented: whole genome sequencing, microarray-based pathogen detection and microarray-based genome resequencing. The whole genome sequencing and microarray-based genome resequencing will be explored in the context of adenoviruses, a human pathogen. Adenoviruses are viruses that affected all vertebrates and have been studied extensively in the context as a human infectious disease agent. It is an important model organism in biology and is shown recently to be a model organism for understanding and applying pathogen detection methods. The biological, pathogenic and clinical implications of adenoviruses will not be discussed due to the immensity of the subject; the audience is directed to one of many excellent reviews [6]. Suffice it to say, strains of human adenoviruses can cause highly contagious respiratory and ocular human diseases, among other diseases, with high infection rates, high morbidity and rare but observed mortality. These are of particular importance in dense populations, which includes basic military training cohorts- the site of a real world test-bed validation of a microarray-based surveillance tool [7].

Additionally, novel virus strains and types arise as emergent and reemergent pathogens, as exemplified by the human adenoviruses [3, 8]. The focus of my research is primarily in these adenoviruses, with emphasis on the molecular evolution mechanisms by which novel types arise, and by using the genomics and bioinformatics approach [9]. As part of this work, a microarray-based assay tool has been developed and validated to monitor genome changes in adenovirus pathogens; this has been applied to a real world test-bed and was shown to be useful in monitoring and characterizing adenoviral pathogens [10].

35.4.1 Convergence of Informatics-, Bioinformatics- and Genomics-Based Approaches for the Molecular Surveillance and Detection

The non-availability of tools limits and restricts possibilities and research! Informatics has allowed world-wide networking opportunities and open computational and data resources to be made available via the world-wide web (internet), including databases such as GenBank as well as computational tools (as bioinformatics) and resources for genome and sequence data mining and analysis (e.g., genomics: http://www.binf.gmu.edu/wiki/index.php/Main_Page and http://molbiol-tools.ca/), allow researchers and clinicians to utilize and exploit genome and DNA sequence data fully. These valuable resources, e.g., internet, allow bioinformatics, e.g., computational analysis of genomes and databases, to be widely available and therefore useful, particularly given the continuing acquisition and accumulation of genomics data (e.g., genome sequences, genome pathogen signatures). Microarray-based approaches and tools allow the application of informatics, bioinformatics and genomics to the detection, identification and characterization of human and non-human pathogens, as demonstrated with human adenovirus.

35.4.2 Genome Sequencing and Bioinformatics

There are currently over 70 human and simian adenovirus genomes archived in GenBank, with the number of newly sequenced adenoviral genomes rising as tremendously as a tsunami. This is reflective of the genomes of other organisms, including pathogens. Data mining and analysis of these genomes are providing insights into viral (both non-pathogenic and pathogenic) emergence, reemergence and evolution [3, 4, 8]. Bioinformatics tools and protocols have been developed to take advantage of the rapid increase in data [9]. Comparative genomics of human adenovirus types, strains and substrains have revealed underlying genome stability amongst types [11–13] with genome drift, e.g., base substitutions and insertion/deletions (indels), observed as would be expected for a double-stranded DNA virus, as well as recombination events that cause antigen shifts and changes in epitopes that are recognized by the host immune response system [8].

Genome sequence analysis of a query, and potential biothreat, agent can reveal changes, e.g., insertions, into the genome. As an example and as an in silico exercise, the insertion of an antibiotic resistance gene (ampicillin resistance) into a human

adenovirus genome is immediately detected using a rapid sequence comparison and alignment tool called BLAST. There are multiple versions of this tool, one of which is freely accessible on the internet from the NIH webserver (http://blast.ncbi.nlm.nih.gov/Blast.cgi). BLAST allows for the 1:1 comparisons and alignments of nucleotide sequences and provides alignments and scores of homologs, similar and divergent sequences. When subjected to this analysis, the in silico insertion of a 1,000 base gene into a 35,000 base adenovirus genome results in an unambiguous determination of an altered query genome. This is presented as a table, with quantitative alignment scores.

Following this BLAST analysis with the application of a dot-blot genome sequence comparison tool, PipMaker [14], an immediate visualization of the insert within the adenovirus genome is available. PipMaker is also freely accessible on the internet (http://pipmaker.bx.psu.edu/pipmaker/). This method of comparative genomic analysis may be used also to determine the naturally occurring mutations within circulating viral pathogens, for example in natural variations of human adenovirus strains as demonstrated in comparisons of two strains [13], in which genome changes, including insertions and deletions are detected and visualized.

As an aside, genomics and bioinformatics tools and techniques have revealed origins of some human pathogens. For example, an important and predominant acute respiratory disease viral agent currently circulating as a public health problem in the U.S. military training cohorts is human adenovirus "HAdV-E4". This particular type has been shown to have a zoonotic origin, that is, it "jumped" from the chimpanzee to the human [15]. This was shown using bioinformatics tools, including comparative gene and protein sequence analysis and phylogenetic analysis, all of which relied on the existing informatics resources, including GenBank, an open access genome and genes database, as well as the recently available bioinformatics and genomics resources.

35.4.3 Microarray-Based Pathogen Detection

GenBank whole genome sequence data and whole genome sequencing, along with bioinformatic analysis, of pathogens provide researchers with access to the DNA sequences of organisms. In comparisons with non-pathogen counterparts, "genome sequence signatures" may be revealed, allowing the detection of pathogens. "Genome sequence signatures" are defined as unique DNA sequences, however long, that are found in one genome and not in another. A "pathogen genome sequence signature" is one that is found in a pathogen uniquely and may be used to identify the particular pathogen.

DNA and genome sequencing allow the exploitation of these pathogen genome signature sequences, once identified and characterized. One application is the microarray-based assay that incorporates multiple DNA sequence probes, that define multiple pathogens, onto a single physical entity [16]. These microarray-based methods call for the identification, synthesis and attachment, of specific DNA probes corresponding to unique signatures from multiple potential pathogens, to a physical substrate (chip) to allow the interrogation of a query biological sample. If present in the biological sample, a pathogen will give positive signals in multiple, redundant and confirming locations within this "chip" [16].

35.5 Microarray-Based Pathogen Resequencing Chip

An enhancement and a variation of the microarray probe technique are demonstrated by the microarray-based DNA resequencing chip. In this approach, the pathogen genome signature sequences are assembled onto a microarray chip as multiple permutations of the sequence. As this microarray chip interrogates the genome DNA, which is isolated from the biological query sample, one of the unique microarray-embedded permutations of a particular pathogen sequence (there are multiple pathogens that may be assembled onto a chip) will hybridize and therefore provide the exact DNA sequence information for that portion of the genome. By incorporating and interrogating a contiguous series of such probes, either a limited or full genome sequence for the query pathogen will be revealed, depending on the extent of the sequence data embedded onto the microarray chip. As demonstrated for human adenovirus respiratory pathogens, specifically ones that are in circulation and are of interest to the U.S. military and as a demonstration of a real world test-bed, this approach was applied successfully and the microarray-based resequencing detection method was validated [10]. As an aside, this approach also allowed first observation of and the confirmation of adenovirus coinfections, a situation in which two or more adenoviruses may infect a host [17]. This may provoke an increased morbidity and perhaps increased mortality due to the multiple viruses. Interestingly, the coinfection of two adenoviruses does not necessarily lead to a recombination event [12] that may produce an emergent [8] or reemergent pathogen [3], although it provides an opportunity for recombination events to occur.

35.6 Conclusions

Innovations and advances in informatics, bioinformatics and genomics are allowing tremendous possibilities and potentials in pathogen detection and surveillance. This confluence allows for a solution to the problem of determining if a biological agent or pathogen is present in an environment, regardless of whether the pathogen is naturally occurring or man-made. Realizing this as a single problem has made the approach and solution cost-effective, that is, the resources developed have multiple applications.

As discussed here, the circulation and recurring epidemics of human adenovirus pathogens, for example, the ones causing acute respiratory disease, allow for the development and validation of “advanced molecular diagnostic” tools, specifically microarray-based assays that can survey and identify multiple diverse viral and bacterial (and eukaryotic) pathogens based on their genome and DNA sequences. The requirements are genome sequences and bioinformatics tools that allow the identification and selection of particular and specific probes. Again, as shown, these probes may allow the simultaneous partial or full determination of the query genome sequence. This has been tested in a small military test-bed both as a broad population-based screening tool and as a single genome sequence determination tool. The recent availability and convergence of informatics, bioinformatics and genomics tools allow previously unimaginable queries into human pathogens and epidemics.

References

1. Karch H, Tarr P, Bielaszewska M (2005) Enterohaemorrhagic Escherichia coli in human medicine. Int J Med Microbiol 295:405–418
2. Falkow S (1988) Molecular Koch's postulates applied to microbial pathogenicity. Rev Infect Dis 10(Suppl 2):S274–S276
3. Walsh MP, Seto J, Jones MS, Chodosh J, Xu W, Seto D (2010) Computational analysis identifies human adenovirus type 55 as a re-emergent acute respiratory disease pathogen. J Clin Microbiol 48:991–993
4. Torres S, Chodosh J, Seto D, Jones MS (2010) The revolution in viral genomics as exemplified by the bioinformatic analysis of human adenoviruses. Viruses 2:1367–1381
5. Sanger F, Nicklen S, Coulson AR (1977) DNA sequencing with chain-terminating inhibitors. Proc Natl Acad Sci USA 74:5463–5467
6. Wadell G (1984) Molecular epidemiology of human adenoviruses. Curr Top Microbiol Immunol 110:191–220
7. Binn LN, Sanchez JL, Gaydos JC (2007) Emergence of adenovirus type 14 in US military recruits–a new challenge. J Infect Dis 10:1436–1437
8. Walsh MP, Chintakuntlawar A, Robinson CM, Madisch I, Harrach B, Hudson NR, Torres S, Schnurr D, Heim A, Chodosh J, Seto D, Jones MS (2009) Evidence of molecular evolution driven by recombination events influencing tropism in a novel human adenovirus that causes epidemic keratoconjunctivitis. PLoS One 4:e5635
9. Seto J, Walsh MP, Mahadevan P, Zhang Q, Seto D (2010) Applying genomic and bioinformatic resources to human adenovirus genomes for use in vaccine development and for applications in vector development for gene delivery. Viruses 2:1–26
10. Lin B, Wang Z, Vora GJ, Thornton JA, Schnur JM, Thach DC, Blaney KM, Ligler AG, Malanoski AP, Santiago J, Walter EA, Agan BK, Metzgar D, Seto D, Daum LT, Kruzelock R, Rowley RK, Hanson EH, Tibbetts C, Stenger DA (2006) Broad-spectrum respiratory tract pathogen identification using resequencing DNA microarrays. Genome Res 16:527–555
11. Mahadevan P, Seto J, Tibbetts C, Seto D (2010) Natural variants of human adenovirus type 3 provide evidence for relative genome stability across time and geographic space. Virology 397:113–118
12. Seto J, Walsh MP, Metzgar D, Seto D (2010) Computational analysis of adenovirus serotype 5 (HAdV-C5) from an HAdV coinfection shows genome stability after 45 years of circulation. Virology 404:180–186
13. Purkayastha A, Su J, McGraw J, Ditty SE, Carlisle S, Hadfield TL, Seto J, Russell KL, Tibbetts C, Seto D (2005) Genomic and bioinformatics analyses of HAdV-4vac and HAdV-7vac, two human adenovirus (HAdV) strains that constituted original prophylaxis against HAdV-related acute respiratory disease, a reemerging epidemic disease. J Clin Microbiol 43:3083–3094
14. Schwartz S, Zhang Z, Frazer KA, Smit A, Riemer C, Bouck J, Gibbs R, Hardison R, Miller W (2000) PipMaker–a web server for aligning two genomic DNA sequences. Genome Res 10:577–586
15. Purkayastha A, Ditty SE, Su J, McGraw J, Hadfield TL, Tibbetts C, Seto D (2005) Genomic and bioinformatics analysis of HAdV-4, a human adenovirus causing acute respiratory disease: implications for gene therapy and vaccine vector development. J Virol 79:2559–2572
16. Wang D, Coscoy L, Zylberberg M, Avila PC, Boushey HA, Ganem D, DeRisi JL (2002) Microarray-based detection and genotyping of viral pathogens. Proc Natl Acad Sci USA 99:15687–15692
17. Vora GJ, Lin B, Gratwick K, Meador C, Hansen C, Tibbetts C, Stenger DA, Irvine M, Seto D, Purkayastha A, Freed N, Gibson ML, Russell KL, Metzgar D (2006) Co-infections of adenovirus species in previously vaccinated patients. Emerg Infect Dis 12:921–930

Chapter 36
Quantum Cryptography for Information-Theoretic Security

Quantum Cryptography

Barry Sanders

Abstract This article explains quantum computing and its potential for rendering current encrypted communication via public channels insecure. A review of quantum key distribution is given as a way to ensure secure public-channel communication regardless of the computational power of an adversary, that may possesses a quantum computer. Finally, state-of-the-art quantum key distribution is discussed with an insight into its future.

Keywords Quantum computing • Quantum key distribution • Quantum cryptography • Quantum communication • Information security

36.1 Introduction

For business and pleasure, we need to send secrets through public channels, whether by telephone, fax, telex or the internet. Let us consider the following example. Suppose you wish to make a payment via a web page using your credit card, but you want to ensure that your credit card details are safe from eavesdropping criminals.

This criminal eavesdropper, whom we call "Eve", could be powerful beyond your dreams, for example using devices and mathematics we do not yet imagine. Is our communication protected against such powerful adversaries? Here is one

B. Sanders (✉)
Institute for Quantum Information Science, University of Calgary,
2500 University Drive N.W., Calgary, AB, Canada
e-mail: sandersb@ucalgary.ca

A. Vaseashta et al. (eds.), *Technological Innovations in Sensing and Detection of Chemical, Biological, Radiological, Nuclear Threats and Ecological Terrorism*,
NATO Science for Peace and Security Series A: Chemistry and Biology,
DOI 10.1007/978-94-007-2488-4_36, © Springer Science+Business Media B.V. 2012

way that our communication is kept safe nowadays. Alice, who works for the company waiting for your payment, generates a pair of numbers expressed as strings of binary digits, or "bits". She sends you one string, which is called the public key, and she keeps the other string for herself, which is called the private key.

The message you plan to send, such as your credit card number, can also be expressed as a binary string. To send the message securely, you compute some function of both your message and Alice's public key, and then you send her the calculated result. This function is considered to be hard-to-crack – without knowing the private key, inverting the function to reveal the message is believed to be beyond the capability of the eavesdropper's computers within a reasonable timeframe.

When Alice receives the result of your computation, she uses her private key to decode the message from your result. Because Alice holds the corresponding private key, inverting the function to find the message, i.e. decoding, is easy for her. On the other hand, Eve knows the public key and the result but is unable to decode the message without having access to the private key.

We are prepared to take the risk that Eve could crack the code when making financial transactions, but what about more important information? Could a national secret be transmitted safely via a public channel in this way? There are three reasons not to do so. One reason is that some secrets have to be secrets for a long time, maybe forever. For many years, the power of computers has improved exponentially so Eve could record the message and wait for a more powerful computer to be created that would make cracking the code easy. Another risk is that Eve is so smart she devises a way to invert the function in a way that we have not figured out yet: the difficulty of breaking these codes is not proven but rather just assumed, albeit with strong evidence supporting this assumption.

The third reason to be wary with computationally-secure cryptography is the threat posed by a quantum computer: a scalable quantum computer, meaning a computer that can run quantum algorithms and can be made larger at a cost that grows only as a polynomial function of the computer's size, renders these coding functions easy-to-crack. Thus, computationally-secure cryptography can be regarded as secure against a non-quantum computer, subject to the provisos above, but insecure against a computer that exploits the full potential of quantum mechanics.

The quantum computer could make today's methods of cryptography instantly unsafe and thereby threatens public-key cryptography. On the other hand, a technique known as quantum key distribution also uses quantum technology but for the purpose of creating a shared key that is intended to be unbreakable no matter what kind of computer Eve possesses or what algorithms she knows. In other words quantum cryptography, which uses quantum key distribution, is information-theoretically secure – it cannot be broken by computational attacks – in contrast to today's bounded-computational security where Eve is believed to have limited computational capability.

36.2 The Quantum Computing Threat

36.2.1 What Is a Quantum Computer?

Let us consider what defines a quantum computer [1] Defining the quantum computer is, in fact, rather subtle [2]. As we believe that quantum mechanics underpins all of science, then all computers are quantum, in the same sense that everything around us is quantum. Yet we are safe in regarding most things in the world as non-quantum so a better criterion is needed.

We know that the Heisenberg uncertainty principle [3] and entanglement [4], which are two of the distinguishing features of quantum mechanics, are negligible in our macroscopic world. Therefore, we could think of a quantum computer as a computing machine that exhibits quantum properties whereas existing computers do not. The problem with this definition is that modern computers use transistors, and transistors operate on quantum principles.

Perhaps the best definition of a quantum computer is as a computing machine that is described by quantum mechanics and can perform computations that a device built entirely out of non-quantum components could not do. This definition gets around the problem of a modern computer using a transistor: although we use transistors that operate on quantum principles, we could equally well build the computer out of billiard balls and achieve the same computational power, albeit more bulky, fragile and expensive. More technically, a quantum computer is a computing machine that can run any quantum algorithm.

36.2.2 What Will the Quantum Computer Look Like?

In the early days of computers, logical elements were built from different media: vacuum tubes, germanium or silicon. Similarly, various quantum computer media are available, and we are figuring out which one is the best.

One type of quantum computer technology uses light [5]. Light is quite versatile. Its degrees of freedom include polarization of the field, path of the beam, time of the pulse and more. One polarization state can be the logical zero state and the other polarization state the logical one, or a beam can take two possible paths labeled zero and one. Alternatively the pulse can be created early to make a zero or late to make a one. In this way, the state of the light field can encode a bit, and a quantum field can encode a superposition of zeros and ones, hence encode quantum information.

The electromagnetic field can be processed with passive optical elements, linear and parametric amplifiers, nonlinear phase modulations and photon counting with feedback to enable universal transformations of the field state. In this way, a quantum computer can be realized with light by exploiting one or more of light's degrees of freedom.

Electronic states of atoms provide another promising quantum information medium. A lower energy state can be a zero and an upper energy state a one, with other energy levels available for helping to prepare, control and read the state. The atoms can be neutral or ionized, with each case offering its own advantages and disadvantages. The electronic state can even be coupled with the nuclear state to take advantage of the long nuclear lifetimes for storage and memory [6].

Each approach and each medium has advantages and disadvantages. One medium may be better at storage, another better at effecting quantum gates and another better at readout. At this stage of research, we do not know which media will be winners and which will be losers. More investigation is required.

36.2.3 Hybridizing the Technology

We will probably find it easier not to overcome the disadvantages of one medium but, rather, combine several media to take advantage of the positives and avoid the negatives. To make such a hybrid device we need to transfer quantum information between media at opportune times. As mentioned above, coupling the electronic and nuclear degrees of freedom enables the quantum computer to exploit the advantages of both degrees of freedom. We can generalize this idea of combining the advantages of various media.

For example we could couple electronic and light degrees of freedom, which presents the advantage that light is the favored medium for communicating long distances and electrons are natural quantum information media in solid-state systems so may work well with existing computer chips. Another exciting possibility is using superconducting junctions in conjunction with microwave fields and using molecules to couple microwave and optical fields together to deliver scalable quantum information processing [7].

36.2.4 Scaling Up

The goal of scalability is to make a quantum computer work on a small scale – dozens of qubits and dozens of gate operations – and then to increase the size and number of operations efficiently. By ‘efficiently’ the increasing size and complexity should come at a cost that is no worse than a polynomial function of the size of the problem to be solved. This mathematical characterization of ‘efficiency’ is germane to the computer science notions of efficient *vs* hard problems.

Although quantum computer technology is improving steadily, we are still wrestling with getting small systems to work. Fortunately we do not have to make quantum computers as big as today’s computers to make quantum computers outperform today’s computers. For example, it might take the storage capacity of thousands of laptops in a network to break existing encryption algorithms in a few years, whereas

storage capacity of only a 100 quantum kilobytes would break existing encryption algorithm in less than a second.

In a similar vein, a laptop computer operates at gigahertz speeds that completes billions of operations per second, but the quantum computer could operate as fast and complete the calculation in a few thousand cycles, namely in a millionth of a second. The important message is that, for certain problems, a quantum computer is so powerful that even a small prototype is more threatening to information security than combining thousands of the most powerful computers in existence today, if we continue to use the same means for encryption.

36.3 Quantum Cryptography to the Rescue

The quantum computer dashes our hope of information security using existing encryption schemes, but two alternatives restore this hope: new encryption schemes or using quantum cryptography [8]. Here we consider the second possibility, especially as the technology is viable now whereas quantum computing is still a futuristic technology.

36.3.1 Encryption Mechanism

Existing public-key encryption works by having sender Alice transmit to receiver Bob a public key and keeping her own private key. The goal of quantum key distribution is to have Alice and Bob generate an identical key: at the end of the generation process, Alice and Bob would each hold identical strings of bits using a public channel in such a way that omnipotent Eve is denied enough knowledge of this key so that she is incapable of learning anything about the messages encoded by this key using a 'one-time pad'. Secret keys used with one-time pads are information-theoretically secure.

Sounds impossible? The uncertainty principle [3] traps Eve: if she wants to learn the shared random keys, her observation disturbs the system, and Alice and Bob can learn of her intrusion before they make the mistake of using the key to construct messages. Alice and Bob discuss publicly the noise in their keys and use a technique known as 'privacy amplification' to circumvent Eve from using a little knowledge to crack the codes.

There are four important catches though. One is that Alice and Bob need to authenticate the channel in advance; otherwise Eve could impersonate them. So far the only information-theoretically secure way to authenticate is to use a private channel. As information-theoretically secure authentication through a public channel has not been achieved, quantum key distribution is actually a key amplification scheme whereby the initial authentication key is amplified, but here we use the standard terminology of "distribution" rather than amplification and bear in mind the authentication problem.

The second catch is that Eve could just disrupt the communication by a denial-of-service attack whereby Alice and Bob do not have a working communication channel: Alice and Bob do not reveal their secrets but unfortunately also fail to communicate secrets with each other. Thus, security is maintained at the expense of not communicating at all.

The third catch is that current quantum key distribution technology is limited to distances of hundreds of kilometers. In principle, efficient quantum communication over any length scale is possible using quantum repeaters, but quantum repeaters are almost as hard to build as quantum computers.

The fourth catch is that equipment does not work perfectly, and Eve may know weaknesses that Alice and Bob do not. She thereby exploits a hidden weakness to learn the key without Alice and Bob realizing that weakness is exploited. Recently, though, entanglement-based quantum key distribution has been shown to offer another stunning advantage. Alice and Bob can check quantum correlations between their received quantum signals and thereby rule out attacks based on imperfect devices [9]. This kind of "device-independent security" is not possible in non-quantum cryptography.

36.3.2 State of the Art

Quantum key distribution works and is even available as a commercial technology, but its performance is not yet competitive with other key distribution technologies. This statement needs some qualification, though.

If existing key distribution is regarded as insecure, for any of the reasons given in Sect. 36.1, then even a poorly-performing but secure quantum key distribution system is infinitely better than a better-performing but insecure key distribution based on today's computationally-secure protocols. However, quantum key distribution needs to reach comparable levels of performance to existing schemes, i.e. achieve high levels of key generation rates, if quantum key distribution is to be regarded as viable in the sense that it can step in and replace existing key distributions with a small price to pay in terms of secure-bit distribution rates.

Due to loss, the key generation rate is sensitive to distance. Let us consider a 10-km distance, commensurate with urban-scale security. A rate of two million pulses of light generated per second is reasonable. For security, the average energy per pulse corresponds to one photon per five pulses. Yes, this means that most pulses are effectively empty (no energy), but which ones are empty is random.

Avalanche photodiodes are typically used as detectors, although better detectors are on the horizon. These photodiodes operate with a quantum efficiency of 0.1, a dark-count probability of 0.00001 and a gate time of 2 ns. The gate time is not reducible without causing deleterious after-pulses. With this technology, and after

sifting, error correction, privacy amplification and authentication of the raw key, the resultant key rate is around 10 kHz.

This rate of 10 kHz is significantly slower than existing key distribution rates but can be dramatically improved by new detector technology and eventually faster software and integrating the processors on a single chip. New protocols and faster encoding on the pulses will also help to enhance performance.

36.3.3 Symmetric Encryption

For quantum key distribution to deliver information-theoretic security that is impervious to non-quantum computational attacks, the key should be employed in a Vernam cipher, or one-time pad. In practice, the Vernam cipher is off-putting because the length of the shared key needs to be as long as the message.

In practice, the key is used much more efficiently when employed in a symmetric encryption scheme such as the Advanced Encryption Standard, or AES, based on a substitution permutation network. As this method of encryption can be broken, the key is changed frequently; this is known as refreshing the key. Quantum key distribution can be used to generate the key for AES. Then the key rate is important because the length of the key per refresh and the rate of refreshing determines the level of communication security attained.

36.3.4 Long Distance

Because of losses of light during transmission, the secure key rate falls precipitously with increasing distance. Rather than send through optical fiber or free space over the earth, an alternative method is to use satellites to communicate. The great advantage of satellites is their long reach, on a planetary scale, without too much intervening air, which induces losses and scattering of the light. The effective distances, taking into account air density, is much shorter for satellite communication than for over-earth communication although the actual distances can be much larger.

Another strategy to beat the distance limit is to plug in quantum repeaters [10] along the path. Quantum repeaters are much harder to make than existing repeaters used in communication networks. The quantum repeater exploits entanglement-swapping processing of the resultant quantum states to deliver a fixed key rate at a cost that is only a polynomial function of overall distance, hence “efficient” in computer-science parlance. Much effort is now directed to quantum memories [11], which will store and release quantum states on demand, and are required for managing a quantum communication network with quantum repeaters.

36.4 Conclusions

Quantum cryptography is a rapidly developing technology that aims to deliver information-theoretically secure communication. In other words, quantum cryptography's goal is to circumvent the weakness of today's methods: an adversary with a sufficiently strong computer, obtained by recording and breaking the code in the future or by possessing a computer more powerful than envisaged or by building a quantum computer, could break the code. Quantum cryptography would eliminate the computational bound assumption built into today's belief in security.

Development of a quantum computer is slow but steady. Challenges exist in each of the candidate media for realizing quantum computation, but clever ways are being found to surmount the challenges such as hybridizing the media. Hybridization enables quantum information to be prepared or processed or read in various media depending on their strengths and transferred to another medium that is more suitable for one of the tasks. The outlook for quantum computing would be described as optimistic, but patience is required.

Quantum cryptography is a prudent tool to protect against quantum computing. Although the quantum computer will take a long time to build, quantum cryptography also requires a long time to bring its performance up to today's standards for non-quantum key distribution, including high key rates, developing an appropriate authentication protocol, and breaking the current distance barrier. Therefore, quantum cryptography needs to be studied and developed as a long-term strategic effort to protect communication against future communication-security threats.

Acknowledgements BCS has benefitted enormously from valuable discussions with W. Tittel and pedagogical feedback from L. Moore. This work is supported by Alberta's Informatics Circle of Research Excellence (*i*CORE), Canada's Natural Science and Engineering Research Council (NSERC), General Dynamics Canada, Canada's Networks of Centers of Excellence for the Mathematics of Information Technology and Complex Systems (MITACS), the Pacific Institute for Mathematical Sciences (PIMS), and the United States Army Research Office (ARO). BCS is a Fellow of the Canadian Institute for Advanced Research (CIFAR).

References

1. Knill E (2010) Physics: quantum computing. Nature 463:441–443
2. Bartlett SD, Sanders BC (2003) Requirement for quantum computation. J Mod Opt 50(15–17):2331–2340
3. Heisenberg W (1927) Über den anschaulichen Inhalt der quantentheoretischen Kinematik und Mechanik. Zeitschrift für Phys 43:172–198. English translation; Wheeler JA, Zurek H (1983) Quantum theory and measurement. Princeton University Press, Princeton, pp 62–84
4. Schrödinger E (1935) Discussion of probability relations between separated systems. Proc Camb Philos Soc 31:555–563; (1936) 32:446–451
5. O'Brien JL (2007) Optical quantum computing. Science 318(5856):1567–1570
6. Childress L, Gurudev Dutt MV, Taylor JM, Zibrov AS, Jelezko F, Wrachtrup J, Hemmer PR, Lukin MD (2006) Coherent dynamics of coupled electron and nuclear spin qubits in diamond. Science 314(5797):281–285

7. André A, DeMille D, Doyle JM, Lukin MD, Maxwell SE, Rabl P, Schoelkopf RJ, Zoller P (2006) A coherent all-electrical interface between polar molecules and mesoscopic superconducting resonators. Nat Phys 2:636–642
8. Gisin N, Ribordy G, Tittel W, Zbinden H (2002) Quantum cryptography. Rev Mod Phys 74(1):145–195. doi:dx.doi.org
9. Acin A, Brunner N, Gisin N, Massar S, Pironio S, Scarani V (2007) Device-independent security of quantum cryptography against collective attacks. Phys Rev Lett 98:230501–230505
10. Briegel HJ, Dür W, Cirac JI, Zoller P (1998) Quantum repeaters: the role of imperfect local operations in quantum communication. Phys Rev Lett 81:5932–5935
11. Lvovsky AI, Sanders BC, Tittel W (2009) Quantum optical memory. Nat Photonics 3(12): 706–714

Part VII
Radiation Detection

Chapter 37
Co-operative Gamma Ray Generation Stimulated by X-Ray Pulse

Co-operative Gamma Ray Generation

Nicolae A. Enaki, M. Turcan, N. Ciobanu, T. Rosca, and Ashok Vaseashta

Abstract The second-order coherent function at two-photon cooperative emission is investigated. As was observed the co-operative generation of γ-ray light is possible if the duration of X-ray pulse is longer than the co-operative delay super-radiant time of gamma photons. In this case, the amplitude of the X-ray field is constant in the process of co-operative γ-photon emission and the quasi-energetic levels for the extended nuclei system are dressed. Achievement of viable two-photon sources of correlated photons in optical, X- and gamma-rays diapasons would have major impact applications in biological and medical diagnostics of bio-molecules, viruses etc.

Keywords γ- and x- ray radiation • Extended nuclei system • Two-photon sources • Cooperative emission

37.1 Introduction

The coherent generation of γ-rays in the excitation process of long-living isomeric states stimulated by X-ray photons, and the possibility of realizing the cooperative emission from long-living isomeric states in process of two-photon transitions are ones of the most interesting problems of quantum nucleonic. An important mechanism for coherent emission in the gamma spectrum region is the super-radiant

N.A. Enaki (✉) • M. Turcan • N. Ciobanu • T. Rosca
Institute of Applied Physics, Academy of Sciences of Moldova,
Chisinau, MD, Republic Of Moldova
e-mail: enache@asm.md

A. Vaseashta
Institute for Advanced Sciences Convergence, NUARI, 13873 Park
Center Rd., Suite 500, Herndon, VA, USA

A. Vaseashta et al. (eds.), *Technological Innovations in Sensing and Detection of Chemical, Biological, Radiological, Nuclear Threats and Ecological Terrorism*,
NATO Science for Peace and Security Series A: Chemistry and Biology,
DOI 10.1007/978-94-007-2488-4_37, © Springer Science+Business Media B.V. 2012

emission of photons [1–4]. The coherence of gamma emission from quantum states excited by the primary X-ray pulse depends strongly on the coherent property of the X-rays.

Recently, the Cooper pairing of Luttinger liquid with bosonic atoms has been predicted. In fact, the collective coupling between biphoton and nuclei is abruptly reduced upon entering regime III, indicating that the phase transition is most likely triggered by Copper paring with the 4-photon singlet rather than with a biphoton BEC [5, 6].

Here we analyse the second order coherent effects between the X-ray and γ-ray photons in order to understand the interaction with excited nuclei of the generation field. We investigated the feasibility of the two-photon super-radiant emission from extended excited nuclear systems to produce intense sources of correlated photons in X-ray and γ-ray regimes.

37.2 Two-Photon Cooperative Gamma Ray Generation

The resonant photo-excitation of 19 isomeric nuclei and the possibility of coherent γ-ray emission of the stored energy were examined in recent works [1, 2]. The phenomenon of new cooperative emission associated with the dipole-forbidden transitions of inverted radiators can be observed [5, 6] in the two-photon spontaneous emission. It has been shown [7] by the present authors that in the process of spontaneous emission, the radiators enter a regime of two-photon super-radiance, and the rate of bi-photon emission increases with the square of the radiator number. It has also been demonstrated that for hydrogen- or helium-like atoms, the dipole-forbidden transitions 2s-1s generate pairs of correlated photons (bi-photons) [7–9], as is illustrated in Fig. 37.1.

The two-photon decay time for metastable states of hydrogen- or helium-like atoms relative to dipole-forbidden transitions $2^2S_{1/2} \rightarrow 1^2S_{1/2}$ and $2^1S_0 \rightarrow 1^1S_0$ has been studied experimentally [9, 10]. The two-photon cooperative phenomena appear in similar experiments if a certain number of inverted atoms ($N \approx 10 \sim 100$) is clustered within a distance less than the mean radiation wavelength $\lambda_m = 2hc/(E_{2s} - E_{1s}) = 2{,}400/Z^2$ in the unit A°. In this case, the lifetime of the metastable state 2S decreases in accordance with the super-radiance law: $t_a = t_0 = (\tau_0/N)\ \ln N$. Here $\tau_0 = 0.121Z^{-6}$ s is the two-photon decay time of hydrogen- or helium-like atoms, Z is the atomic number. In extended systems of atomic radiators, super-fluorescence is observed when the mean distance between atoms is of the order of the radiation wavelength [11, 12]. These experiments suggest that the super-radiance may also be observed in gamma diapason when the mean distance between the inverted nuclei is comparable to the radiation wavelength.

As the lifetime of the metastable state 2s in hydrogen- and helium-like atoms is long for low Z, the cooperative emission can be stimulated by an external coherent or incoherent electromagnetic field [13, 14]. It is shown by Collins [1–3, 8] that in

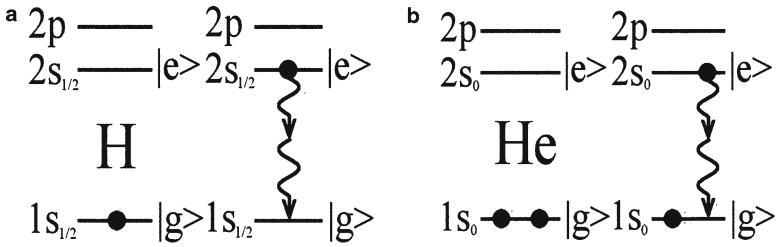

Fig. 37.1 The energetic schemes for the dipole forbidden transition in (**a**) hydrogen- and (**b**) helium-like atoms

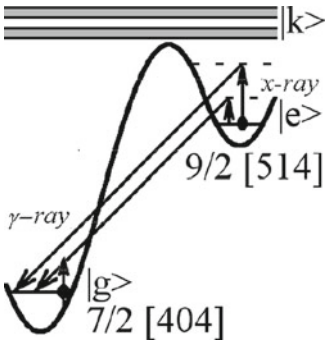

Fig. 37.2 The possible transition in Hf nucleus from isomer to the ground state

analogy to the formation of metastable helium, there is the excitation of protons in the interesting region of the periodic table near Hafnium and Tantalum. In the case of Hf, the ground state is persistent 7/2 [4] (Fig. 37.2) for protons with all lower levels filled.

Exciting one of the protons to the first open state 9/2 [14] and "flipping" it, one obtains an analogy of the metastable He atom. Since there are two unpaired particles contributing to the total J, such a combination is termed a 2-quasiparticle state of excitation. The resulting total angular momentum is $J = 7/2 + 9/2 = 8$ with $K = 8$. This is a state of very large total angular momentum for spontaneous radiation. A typical example is Hf, with $K = 8$ state that has a half-life of about 4 s – quite long for nuclear excited states. The excitation energy is equal to the energy required to break a pair, and is about 1 ~ 1.5 MeV. A long-living excited isomer makes a transition to its ground state under the action of photon, neutron, or alpha-particle pulses. In a similar situation, the stored energy of excited isomers can be transformed into γ-rays. It is known that the projection K of the total angular momentum on the symmetry axis of a deformed spheroidal nucleus is a constant of motion. In isomers, however, K is not conserved in general [3, 12, 15–17]. The excited isomer states are separated from the ground state by some potential barrier of a nucleus, depending on the γ-deformation parameter [16].

Nonlinear characteristic emissions of K-α, K-β and K-γ with a significant triplet splitting at room temperature are observed by Cheng et al. [5, 6] from the long-lived

nuclear state of ^{103m}Rh excited by bremsstrahlung irradiation. A pronounced phase-transition-like narrowing of the emission profiles occurs immediately after the sample is cooled down to 77 K. The room temperature profiles reappear again abruptly and almost reversibly as the temperature drifts freely back to approximately the ice point after the filling with liquid nitrogen is stopped. These emission properties at 300 K and at low temperature may indicate that the ^{103m}Rh nuclei are in collective states. Entering the strong-coupling regime, the loss of the energy and the momentum due to the biphoton emission via the Stokes process is immediately recovered by the anti-Stokes process, thereby conserving energy and momentum by exchanging the biphoton with the phonon. The small Stokes and anti-Stokes shifts of the biphoton lead to the observed AE peaking around EM/2; i.e., at 19.9 keV for ^{103m}Rh, 6.2 keV for 45mSc, and 15.4 keV for ^{93m}Nb. Analogous to the plasma mode screened by electrons, ^{103m}Rh is screened by the biphoton field at resonant nuclei forming a nuclear spin-density wave (NSDW), also called a nuclear exciton. Via the Anderson-Higgs mechanism the NSDW conspires with the longitudinal phonon to acquire an eV mass. The hard-core neutral quasiparticle carrying a spin current travels over the ^{103}Rh matrix like a quantum fluid. Due to the light eV mass, NSDWs exhibit a giant magneton on the order of meV/G. The strong end-to-end interaction between NSDWs forms 1D spin chains with a 2D antiferromagnetic ordering due to their bosonic exchange. The anisotropic emission of the NSDW texture depends on the macroscopic sample geometry, revealing that rotational symmetry is spontaneously broken. Beyond a critical density, massive quasiparticles undergo dynamic Bose-Einstein condensation (BEC).

37.3 Two-Photon Super-Radiance and Second Order Coherent Effects Between the X-Ray and γ-Ray Photons

In order to investigate the two-quantum transitions between the excited isomer state and ground state of nuclei, we will calculate the quantum transition probability of such processes as a function of the intensity, frequency, and the coherence properties of the applied external X-ray or γ-ray radiation. Such model corresponds to the two-photon super-radiance of excited radiators relative to dipole-forbidden transitions (Fig. 37.3).

The quantum properties of a system of radiators with dimensions smaller than the radiated wavelength were studied extensively in the literature [7]. It is, however, interesting to study the possibility of two-photon cooperative emission in the extended system of radiators since the inter-nuclear distance plays an important role in the gamma emission diapason.

We emphasise here that the problem of two-photon cooperative emission is more complicated than the one-photon super-radiance in extended system. In Dicke's super-radiance, the exchange integral between j-th and i-th nuclei is described by a simple function $\sin\left(k_0 r_{ji}\right)/ k_0 r_{ji}$ while in two-photon super-radiance, the exchange

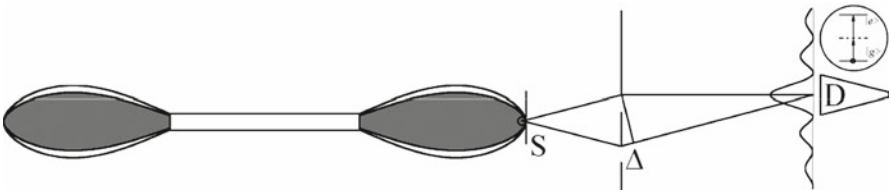

Fig. 37.3 Two-photon super-radiance of excited radiators relative to dipole-forbidden transitions

integral between two radiators is given by more complicated function $\sin\left(k_1 r_{ji}\right)/k_1 r_{ji} \cdot \sin\left(k_2 r_{ji}\right)/k_2 r_{ji}$ where k_0, k_1, k_2 and r_{ji} are the wave vectors of emitted waves and the distance between radiators, respectively. In the case of two-photon emission where the transition frequency of the two-level radiator is $\omega_{21} = 2ck_0$, we have the biphoton wave vectors connection $k_1 + k_2 = 2k_0$. The pure two-photon super-radiance is possible when the decay time τ_0 is larger than the flying time of the entangled photon pairs through the sample. In the case when the flying time L/c has the same value as the cooperative decay time τ_0/N the two-photon induced effect becomes comparable with the cooperative one and the behaviour of the inverted.

It is obvious that all these two-photon transitions take place virtually through the *K*-mixing states of nuclei. If the nuclear recoil is neglected, the scattering of the super-radiant pulse occurs with the absorption of non-coherent γ-photons from the external applied field. The study of such collective effects in scattering processes with the generation of γ-quanta of energy larger than the gap between the ground and isomer states is described below.

Let us investigate a system in which the transition from long-lived isomer state $|2\rangle$ to ground state $|1\rangle$ occurs via the mixing states of nuclei in the process of photon absorption from coherent X-ray or incoherent γ-ray pulses. We will consider that the external X-ray pulse is in resonance or off resonance with the short-living mixed state $|3\rangle$ (see Fig. 37.4a, b). It will be shown that in the resonance case the co-operative generation of γ-ray light is possible if the duration of X-ray pulse is longer than the co-operative delay super-radiant time of gamma photons. In this approximation one shall consider the amplitude of X-ray field constant in the process of the co-operative γ-photon emission. Here it is possible to find the dressed quasi-energetic levels for the extended nuclei system.

In the second case when the X-ray pulse is off resonance with the short-living mixed state 3 (Fig. 37.4b), the co-operative two-photon transition from the excited to ground isomer state is possible via the virtual mixed states of the nucleus and the super-radiant decay rate is proportional to the intensity of X-ray field. The two-photon transition takes place with the absorption of X-ray photons and the emission of γ-photons, or with the radiation of both X-ray and gamma photons, simultaneously. In other words, the two γ-pulses of the co-operative emission from the isomer state to the ground one of the nucleus in two-photon transitions are also possible. When the frequency of the X-ray pulse is near resonance with one of the mixing

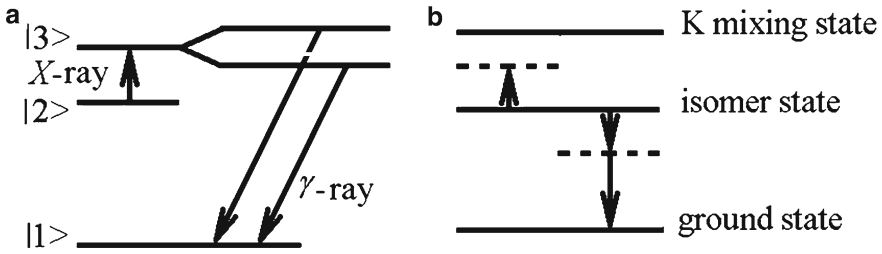

Fig. 37.4 Schemes for a three level nuclei in (**a**) resonance and (**b**) off resonance with external x-ray pulse

states, the two-photon co-operative emission of one X-ray photon absorption and one γ-photon emission dominates the transition with the simultaneous emission of one X-ray and one γ-ray photons.

In the following we investigate the coherent properties of the emitted field in these processes. For this purpose, we introduce two different second-order coherent functions. The first function is given by

$$G_1(z) = \left\langle \Pi^-(z)\Pi^-(z)\Pi^+\left(z+\Delta\right)\Pi^+\left(z+\Delta\right)\right\rangle$$

where $\Pi^+(z,t) = g_{k_0}^2 I^- \exp\{-2i(\omega_0 t + k_0 z)\}$ contains only positive-frequency Fourier components of the product of two components of the electromagnetic field strength of γ- rays, $I^- = \sum_k a_k a_{2k_0-k}$ and $I^+ = [I^-]^+$ satisfy the commutation relations for the SU(1,1) algebra [3], and $2\omega_0 = 2\pi(E_e - E_g)/h$.

For two-photon detectors, the coherent function can be regarded as a correlation between the bi-quanta of the product of the field strength intensity Π obtained from the double slit experiment at z and $z+\Delta$ at the detection point in the Young scheme 3. The second-order correlation is larger than the first-order correlation function in the two-photon super-radiant light obtained in the first type of the proposed emission. For instance, it is shown [7] that for the concentrated system of radiators, the two-photon absorption probability is proportional to the rate $G_1(z)$ at which the coherent radiation photon pairs are produced. The coherent propriety of such photons was already studied [18, 19] and biphoton coherent states were obtained from the vacuum state $|0\rangle$ of the electromagnetic field by using the displacement; $\exp\{\xi I^+ - \xi^* I^-\}|0\rangle$.

The excitation rate of two-photon detectors with such fields is more efficient than the excitation rate obtained from the usually coherent sources. Evidently, this type of coherence is less manifested in the one-photon measurements. The quantum interferometric lithography of such fields beats the usual diffraction limit. For example, the usual limit for a coherent field is $\Delta = \lambda/2$ while the diffraction limit for the two-photon coherent field is only half of that, namely, $\Delta = \lambda/4$ [20].

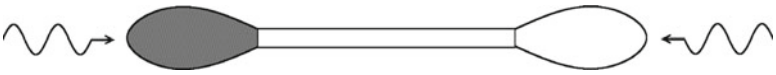

Fig. 37.5 Cooperative emission of entangled photon pairs propagating in opposite directions

Other model deals with the cooperative emission of entangled photon pairs, in which the entangled photons from a pair propagate in opposite directions (Fig. 37.5), which differ from γ pulses of the induced radiation.

It is well known that the Doppler shift to the frequencies of such biquantum emissions are equal in value but opposite in sign (for the case when $\hbar\omega_{k_1} = \hbar\omega_{k_2}$) [20]. As was shown by Rivlin in [20], when any nucleus of the system emits simultaneously two quanta in opposite directions, there is no recoil and the coherence in the induced radiation increases. In this case, the cooperative emission rate in the case of excited isomers nuclei is increasing substantially.

These schemes for the two-photon super-radiation in the γ diapason can be used for the short-lived inverted nuclei (isomers) relatively to the dipole-forbidden transitions. In many cases the excited isomers have a long living time, for example ^{178}Hf [3]. In order to obtain the super-radiance in the pencil shape system it is necessary to ignite such two-photon cooperative transition by two γ-ray non-coherent counter-propagating beams [21]. It is clear that the recoil in the cooperative radiation processes of two quanta with opposite directions of wave vectors and with the same energies equal to a half of the nuclear transition energy $E_0 = h\nu_0$ may be neglected too. On the other hands, this ignition drastically accelerates the two photon cooperative spontaneous emission and in this way the excited isomers can emit the stored energy in a shorter time. Taking into account the estimation obtained from cooperative radiance this lifetime is inversely proportional to the number of radiators in the system.

For two-photon cooperative emission of long-living nuclei excited on the isomer states, accompanied with the absorption of the X-ray photons from the external pump field and the radiation of the γ-ray photons, one can introduce a new second-order coherent function

$$G_2(z,\Delta) = \left\langle P^-(z)P^+(z+\Delta)\right\rangle,$$

where $P^+(z) = E_x^-(z)E_\gamma^+(z)$ and $P^-(z) = E_x^+(z)E_\gamma^-(z)$.

As $E_x^-(z)$, $E_\gamma^-(z)$ and $E_x^+(z)$, $E_\gamma^+(z)$ are the negative and positive frequency part of both the X-ray and γ-ray fields, the strength product of these two fields can have the fixed phase in the detection point $P^+(z) = P_0 \exp\{-i(\omega_\gamma - \omega_x)t - i(k_\gamma - k_x)z\}$. Taking into account the relations $\omega_\gamma - \omega_x = \omega_{21}$ and $k_\gamma - k_x = \omega_{21}/c$, one observes that the two-photon excitation of the detector with absorption of γ-ray and generation of

X-ray photons are proportional to $G_2(z)$. Thus, the correlation function of two coherent sources of such fields can be approximated as

$$G_2(z,\Delta) = G_2(z)\exp\{i(k_\gamma - k_x)\Delta\}$$

The minimal difference between the maximal and minimal two-photon detection rate correspond to $\Delta_{\min} = \pi/(k_\gamma - k_x)$ (or $\Delta_{\min} = (\lambda_x - \lambda_\gamma)/(2\lambda_\gamma\lambda_x)$). This new behaviour of $\Delta_{\min}$ which can be observed in the Stokes two-photon coherent excitation of detector nuclei is studied in the collective anti-Stokes emission of the γ-ray. The first order coherence is manifested when external X-ray source is coherent. In this case the second order coherent function can be factorized

$$G_2(z,\Delta) = \left\langle E_X^-(z)E_X^+(z+\Delta)\right\rangle\left\langle E_\gamma^-(z)E_\gamma^+(z+\Delta)\right\rangle,$$

and the coherence properties of γ-rays are traditional. The *K*-mixing states are situated very high in many nuclei so that it is impossible to depopulate the excited isomers with traditional X-ray sources. Instead, one uses the coherent γ-ray light to depopulate such isomer states [22, 23]. Thus, the first-order coherence function is zero, but the second-order coherent function between the excited and the emitted γ-field can be nonzero. Then the coherent two-photon Stokes excitation of the detector is possible.

37.4 Conclusions

In this paper, we have presented a model that describes the second order coherent effects between the X-ray and γ-ray photons in order to understand the interaction with excited nuclei of the generation field. As was observed in the resonance case, the co-operative generation of γ-ray light is possible if the duration of X-ray pulse is longer than the co-operative delay super-radiant time of gamma photons. In this approximation, one shall consider the amplitude of X-ray field constant in the process of the co-operative γ-photon emission; and it is possible to find the dressed quasi-energetic levels for the extended nuclei system. The possibility of the two-photon super-radiance with minimal recoil in the processes of opposite propagation of the photons from an entangled pair was investigated.

References

1. Collins CB et al (1988) Depopulation of the isomeric state 180Tam by the reaction 180Tam(γ,γ′)180Ta. Phys Rev C 37:2267
2. Carroll JJ et al (1991) Photoexcitation of nuclear isomers by (γ,γ') reactions. Phys Rev C 43:1238

3. Collins CB, Carroll JJ, Oganessian YuTs, Karamian SA (1997) Progress in the pumping of gamma-ray laser. Hyperfine Interact 107:141
4. Dicke RH (1954) Coherence in spontaneous radiation processes. Phys Rev 93:99
5. Cheng Y, Xia B. Phase transition of trapped nuclear exciton of long-lived Rhodium Mossbauer States. http://arxiv.org/abs/0706.2628; Gamma standing wave in the photonic crystal of resonant Rh nuclei. http://arxiv.org/abs/0711.2776; Rhodium Mossbauer superradiance of observable gravitational effect. http://arxiv.org/abs/ 0707.0960
6. Cheng Y, Xia B, Chen CP (2009) Cooling effect in emissions of 103mRh excited by bremsstrahlung. Phys Scr 79:055703, 8 pp
7. Enaki NA (1988) Superradiation from two-photon spontaneous decay. Sov Phys JETP 67:2033; Enaki NA, Macovei MA (1997) Cooperative emission in the process of cascade and dipole-forbidden transitions. Phys Rev A 56:3274
8. Lee YC, Lin DL (1969) Coherent enhancement of the natural Linewidth. Phys Rev 183:147; Coherent radiation from atoms in random motion. ibid 183:150; (1972) Renormalized frequency shift of coherent radiation. Phys Rev A 6:388
9. Marrus R, Schmieder RW (1972) Forbidden decays of hydrogenlike and heliumlike argon. Phys Rev A5:1160
10. Van Dyck RS, Johnson CE, Shugart HA (1970) Radiative lifetime of the metastable 21S0 state of helium. Phys Rev Lett 25:1403
11. Vrehen QHF, Hikspoors HMJ, Gibbs HM (1976) Quantum beats in superfluorescence in atomic cesium. Phys Rev Lett 38:764
12. Collins CB et al (1990) Resonant excitation of the reaction 180Tam(γ,γ')180Ta. Phys Rev C 42:1813
13. Enaki N, Macovei M (1999) Cooperative gamma-ray generation stimulated by X-ray pulse. In: Proceedings of the first international induced gamma emission workshop'97, August 16–20, Predeal, Romania, 603–614
14. Enaki NA, Mihalache D (1997) Two-photon cooperative emission in the presence of athermal electromagnetic field. Hyperfine Interact 107:333
15. Walker PM et al (1990) High-K barrier penetration in 174Hf: A challenge to K selection. Phys Rev Lett 65:416
16. Oganessian YuTs, Karamian SA (1997) K-mixing in nuclear reactions. Hyperfine Interact 107:43
17. Rekstad J, Tveter TS, Guttormsen M (1990) Chaos in nuclei and the K quantum number. Phys Rev Lett 65:2122
18. Caves CM, Schumaker BL (1985) New formalism for two-photon quantum optics. I. Quadrature phases and squeezed states. Phys Rev A 31:3068; Gery CC (1991) Correlated two-mode SU(1,1) coherent states: nonclassical properties. J Opt Soc Am B8:685
19. Perina J Jr, Saleh BEA, Teich MC (1998) Multiphoton absorption cross section and virtual-state spectroscopy for the entangled n-photon state. Phys Rev A57:3972
20. Boto AN et al (2000) Quantum interferometric optical lithography: exploiting entanglement to beat the diffraction limit. Phys Rev Lett 85:2733
21. Rivlin LA (1997) Gamma-ray lasing by free nuclei and bymatter-antimatter beams. In: Proceedings of the 1st international gamma-ray laser workshop, Predeal, Romania, Hyperfine Interact 107:57
22. Zadernovsky AA (1999) Two-quantum doppler-free induced gamma-emission. In: IGE '97 Proceedings of the first international induced gamma emission workshop, vol 42. Predeal, Romania
23. Karamian SA, Collins CB, Carroll JJ, Adam J (1999) In: IGE '97 Proceedings of the first international induced gamma emission workshop, vol 76. Predeal, Romania

Chapter 38
Separation of Uranium by an Extractant Encapsulated Magnetic Alginate Gels

Separation of U(Vi) by Mag-Alg Gels

Z. Portakal, C. Gok, and S. Aytas

Abstract The aim of this work is to prepare environmentally friendly and practically applicable alginate magnetic biopolymers encapsulated tri-n-butyl phosphate (TBP) for the removal uranium ions. Some important process parameters such as initial pH, initial U(VI) concentration, adsorbent dosage, time, temperature and sorption isotherms for uranium uptake were studied and the thermodynamic parameters for U(VI) were determined.

Keywords Adsorption • Extraction • Uranium • TBP • Magnetic alginate beads

38.1 Introduction

Alginate, a natural polysaccharide extracted from brown seaweeds, is a very promising biosorbent material due to several advantageous properties, viz. biodegradability, hydrophilic properties, natural origin, abundance and presence of binding sites due to its carboxylate functions. Alginate consists of linear copolymers composed of β-D-Mannuronate (M) and α-L-Guluronate (G), linked by β 1,4- and α 1,4-glycosidic bounds [1]. In the environmental field, alginate beads are widely used for the removal of heavy metals from wastewater [2]. On the other hand, alginate beads containing different components to enhance the adsorption capacity of the system are also widely investigated [3]. Recently the applications of microcapsules (MCs) enclosing extractants for the separation and recovery of metal ions attracted considerable interests. However, a limited amount of information is available concerning the uptake behavior of radioactive nuclides on these polymer

Z. Portakal (✉) • C. Gok • S. Aytas
Institute of Nuclear Sciences, Ege University, Bornova-Izmir, Turkey
e-mail: gizemsry@gmail.com

A. Vaseashta et al. (eds.), *Technological Innovations in Sensing and Detection of Chemical, Biological, Radiological, Nuclear Threats and Ecological Terrorism*, NATO Science for Peace and Security Series A: Chemistry and Biology,
DOI 10.1007/978-94-007-2488-4_38, © Springer Science+Business Media B.V. 2012

gels [4]. In environmental applications, the use of magnetic alginate beads remains rare [5, 6]. Nevertheless the incorporation of magnetic particles in a polymer matrix might provide several advantages such as the facility to remove beads from the effluent to reuse them after their regeneration [7, 8]. In this study, an organic extractant tri-*n*-butyl phosphate (TBP) and magnetic iron particles was encapsulated by calcium alginate to develop magnetic alginate beads to remove uranium from aqueous solutions at reasonable cost. The effect of some experimental parameters on removal of U(VI) ion was investigated and also sorption isotherms and thermodynamics parameters were discussed.

38.2 Experimental

38.2.1 Preparation of Magnetic Alginate Beads

Magnetic alginate beads encapsulated with TBP were prepared as follows. 1% of TBP was dispersed in 2% of viscous sodium alginate solution (w/v) and then, 1 g of Fe metal filings were added to this solution. Thereafter, this resultant solution was added dropwise to a 0.5 mol/L $CaCl_2$ solution using a needle with stirring at 4°C for 1 h. After 1 h aging, beads prepared were separated from the solution, washed with distilled water and finally dried at 55°C for 5 h. The average diameter of the dry beads was 1.42 ± 0.20 mm with the loss of volume 89% after drying.

38.2.2 Adsorption Experiments

The removal efficiency of the U(VI) ions from aqueous solutions using magnetic alginate beads encapsulated with TBP was studied in a batch mode by mixing 10 mL of aqueous solutions of $UO_2(NO_3)_2.6H_2O$ at different concentrations with 25 mg of dried beads. The pH value was adjusted to the desired pH with either nitric acid or sodium hydroxide solution. The beads were then easily removed from the solution by a magnet. The amounts of uranium in the solution were determined by PAR method with UV-VIS spectrophotometer at 510 nm. The adsorption capacity and the percent adsorption (%) were calculated using the following equations:

$$q = \frac{(C_i - C_e)V}{m} \text{ (mg/g)} \tag{38.1}$$

$$\text{Ads.}(\%) = \frac{(C_i - C_e)}{C_i} \text{x} 100 \tag{38.2}$$

Where C_i and C_e are the concentrations of the metal ion in initial and equilibrium solutions respectively. V is the volume of the solution (mL), m is the weight of the adsorbent (g).

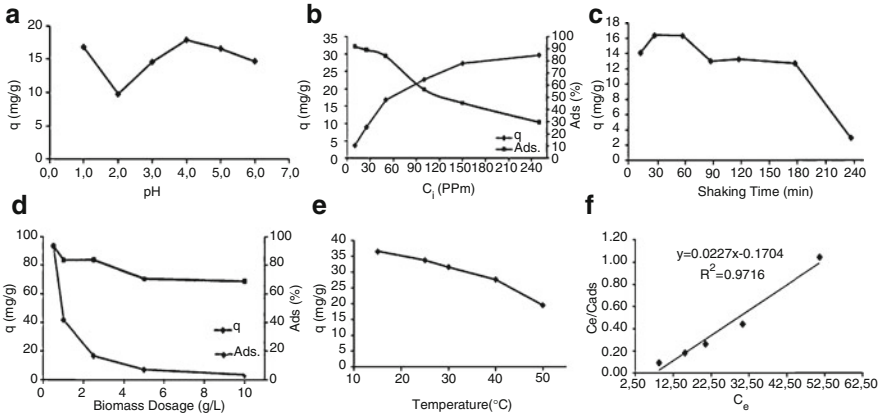

Fig. 38.1 Adsorption of uranium on biosorbent as a function of initial pH (**a**), initial uranium concentration (**b**), shaking time (**c**), biomass dosage (**d**), temperature (**e**), and Langmuir sorption isotherm (**f**)

38.3 Results and Discussion

The dependence of metal adsorption on pH is related to both the metal chemistry in the solution and ionization state of the functional groups of the biosorbent, which affects the availability of binding sites. The effect of the pH on the U(VI) adsorption by biosorbent was studied in the pH region between 1.0 and 6.0. As seen in Fig. 38.1a, the removal of uranium reached a maximum of 98% at pH 1 and 4, above pH 4; the sorption yield decreases with increasing pH. TBP extraction is considerably efficient at pH 1. Therefore pH 1 was considered as an optimum condition and was used for further studies. The optimized process parameters were as follows; 50 mg/L of initial U(VI) concentration, 30 min of shaking time, 1 g/L adsorbent dosage and 15°C of temperature shown in Fig. 38.1. The percent adsorption (%) for uranium were found as 91 ± 3 under the optimized experimental conditions.

The sorption data fit the Langmuir isotherms well (Table 38.1), but do not fit the Freundlich and Dubinin-Radushkhevic (D-R) (R^2: 0.5313) isotherm. The adsorption isotherms of UO_2^{2+} exhibit Langmuir behavior, which indicates a monolayer adsorption.

Various thermodynamic parameters, such as ΔH°, ΔS°, ΔG° were calculated from the experimental data. The thermodynamic of the U(VI) ion/adsorbent system indicate exothermic, spontaneous and reversible nature of the process. The numerical value of ΔG increase with an increase in temperature as shown in Table 38.2 indicating that the reaction is spontaneous and more favorable at lower temperature.

38.4 Conclusion

The experimental studies showed that potential biomaterial magnetic alginate biopolymer beads encapsulated with TBP could be used as an economic, efficient and natural biosorbent to remove uranium ions from dilute aqueous streams. The process

Table 38.1 Isotherm parameters of uranium ion adsorption on magnetic alginate beads encapsulated with TBP

Langmuir parameters			Freundlich parameters		
Q_0 (mg/g)	b (l/g)	R^2	K (mg/g)	n	R^2
44.05	0.13	0.9716	208.45	2.92	0.8783

Table 38.2 Thermodynamic parameters for the adsorption of uranium on magnetic alginate beads encapsulated with TBP

Thermodynamic parameters					
Variation of enthalpy (ΔH°)	−51.71 kJ/mol				
Variation of entropy (ΔS°)	−109.72 J/mol K				
Temperature	288 K	298 K	303 K	313 K	323 K
Gibbs free energy (ΔG°) in kJ/mol	−20.10	−19.00	−18.45	−17.36	−16.26

is competitive with conventional and existing technologies. The percent adsorptions for uranium ions were more than 90% under the optimized experimental conditions. From the thermodynamic study, the negative value of enthalpy change indicates that the interaction between uranium ions and beads is exothermic in nature.

References

1. Ibanez JP, Umetsu Y (2002) Potential of protonated alginate beads for heavy metals uptake. Hydrometallurgy 66:89–99
2. Pandey AK, Pandey SD, Misra V, Devib S (2003) Role of humic acid entrapped calcium alginate beads in removal of heavy metals. J Hazard Mater 98:177–181
3. Moreno-Garrido I, Campana O, Lubian LM, Blasco J (2005) Calcium alginate immobilized marine microalgae, experiments on growth and short-term heavy metal accumulation, Marine Pollution Bulletin 4th International Conference on Marine Pollution and Ecotoxicology, 51: 823–829
4. Wu Y, Mimura H, Niibori Y (2009) Selective uptake of plutonium (IV) on calcium alginate gel polymer and TBP microcapsule. J Radioanal Nucl Chem 281:513–520
5. Lim SF, Chen JP (2007) Synthesis of an innovative calcium-alginate magnetic sorbent for removal of multiple contaminants. Appl Surf Sci 253:5772–5775
6. Huidong L, Zhao L, Ting L, Xiao X, Zhihui P, Le D (2008) A novel technology for biosorption and recovery hexavalent chromium in wastewater by bio-functional magnetic beads. Bioresour Technol 1:6271–6279
7. Rocher V, Siaugue J-M, Cabuil V, Bée A (2008) Removal of organic dyes by magnetic alginate beads. Water Res 42:1290–1298
8. Ngomsik AF, Bee A, Siaugue JM, Talbot D, Cote VCG (2009) Co(II) removal by magnetic alginate beads containing Cyanex 272. J Hazard Mater 166(2–3):1043–1049

Chapter 39
PBS Nanodots for Ultraviolet Radiation Nanosensor

PBS Nanodots for UV Radiation Nanosensor

Yu. Dekhtyar, M. Romanova, A. Anischenko, A. Sudnikovich, N. Polyaka, R. Reisfeld, T. Saraidarov, and B. Polyakov

Abstract PbS nanodots embedded in a zirconium oxide nanofilm were explored as possible ultraviolet (UV) sensors for nanodosimetry purposes. The nanodots were excited by ultraviolet photons to get emission of weak electrons. The emitted charge correlated to UV exposure indicates that PbS nanodots have potential for use as UV sensors for nanodosimetry.

Keywords PbS nanodots • Ultraviolet radiation • Electron emission • Nanodosimetry

39.1 Introduction

Radiobiological effects of ultraviolet radiation (UV) depend on interaction of photons with biomacromolecules (BMM) and are induced by the absorbed dose. BMM are scaled to nanodimensions, therefore, it is necessary to have a UV nano volumetric sensor. Such approach is likely satisfied by a nanodot sensor and by detection of its emission of low energy photo excited electrons (~1 eV) that have mean free path on the order of several nanometers. It was reported that lead sulfide (PbS) nanodots inserted in a matrix using sol-gel method have interesting optical properties [1, 2].

Yu. Dekhtyar • M. Romanova (✉) • A. Anischenko • A. Sudnikovich • N. Polyaka
Institute of Biological Engineering and Nanotechnology, Riga Technical University, Kalku Str. 1, Riga, Latvia
e-mail: marina.romanova@inbox.lv

R. Reisfeld • T. Saraidarov
Hebrew University of Jerusalem, Jerusalem, Israel

B. Polyakov
Institute of Solid State Physics, University of Latvia, Riga, Latvia

A. Vaseashta et al. (eds.), *Technological Innovations in Sensing and Detection of Chemical, Biological, Radiological, Nuclear Threats and Ecological Terrorism*, NATO Science for Peace and Security Series A: Chemistry and Biology,
DOI 10.1007/978-94-007-2488-4_39, © Springer Science+Business Media B.V. 2012

Taking this into account, the target of the research was to examine photoemission properties of PbS nanodots influenced by UV radiation for possible application of the nanodots for ultraviolet radiation nanosensor.

39.2 Samples

PbS nanodots were embedded in ZrO_2 matrix. To prove that PbS not the matrix is responsible for dosimetric effect, samples with PVA (polyvinyl alcohol) matrix were studied as well. Both ZrO_2:PbS and PVA:PbS films were made using the sol-gel technology [3]. Samples with 10%, 20% and 50% concentration of PbS in ZrO_2 matrix and 20% PbS in PVA matrix were studied. The films were deposited on a glass substrate. Thickness of the films was in a range 0.1−1 μm. Typical size of the PbS nanodots was 2–4 nm in ZrO_2 matrix and 2–3 nm in PVA matrix. To verify size of nanodots, the atomic force microscope Solver P-47 PRO was employed.

39.3 Methods

The samples were irradiated with xenon-mercury UV lamp for 0–50 min. The photoemission spectra of irradiated and nonirradiated samples were recorded by a spectrometer, made locally. The photoelectron emission was excited by photons in energy range 4–6 eV, provided by a deuterium lamp (LOT-Oriel Europe). Emitted electrons were detected using secondary electron multiplier (VEU-6, Russia), in vacuum condition $\approx 10^5$ torr.

39.4 Results and Discussion

Derivatives of photoelectron emission (PE) current of nonirradiated ZrO_2:PbS and PVA:PbS films are shown in Fig. 39.1.

ZrO_2:50%PbS film has an emission interval 4.8–6 eV with a maximum at 5.5 eV. Interval width is 1.2 eV that exceeds several times the uncertainty 0.02 eV of the photon energy hν. Therefore, the interval can be associated with emission from localized states inside the energy gap. The monotonous rise of the derivative curve when UV photon energy exceeds 6 eV might belong to the edge region of the valence band.

Derivatives of PE current of ZrO_2 films with smaller PbS concentration (10% and 20%) have an inflection point at the same photon energy as the maximum detected for ZrO_2:50%PbS films (5.5 eV). The inflection point is followed by monotonous rise of the derivative curve when UV photon energy exceeds 5.7 eV. That is similar to the behavior of ZrO_2:50% PbS spectrum when UV photon energy exceeds 6 eV.

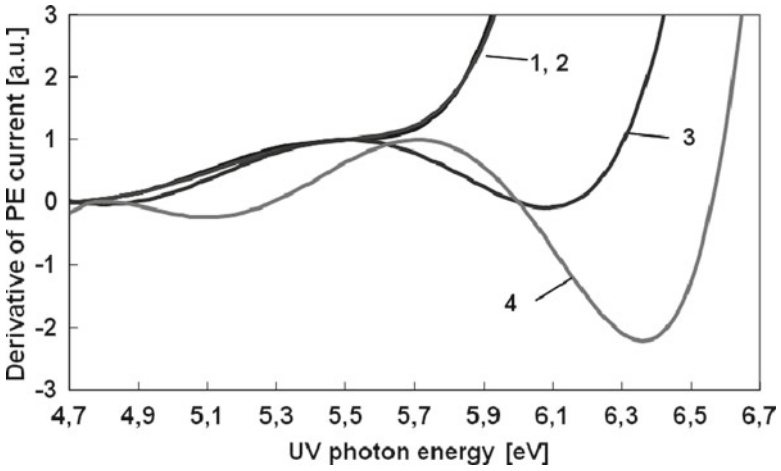

Fig. 39.1 Derivatives of PE current of nonirradiated ZrO_2:PbS films: *1*: ZrO_2:10%PbS; *2*: ZrO_2:20%PbS; *3*: ZrO_2:50%PbS; *4*: PVA:20%PbS

Considered features of the spectra allowed to suppose that localized states and the valence band are overlapped for ZrO_2:10%PbS and ZrO_2:20%PbS films, and concentration of localized states is not sufficient to provide a clear emission maximum.

The shape of PVA:20%PbS derivative of PE current (Fig. 39.1) is similar to ZrO_2:50% PbS derivative but the maximum is shifted to 5.7 eV and the derivative curve starts to rise when UV photon energy exceeds 6.35 eV.

However, the shape of PVA:20% PbS spectrum differs from that of ZrO_2:20% PbS spectrum. Taking into account the similarities in the spectra shape, it was possible to suppose that localized states were created by PbS nanodots but PVA matrix had strong influence on localized states. Figure 39.2 shows derivatives of PE current for 50 min UV irradiated films.

UV radiation influences band structure of the films in a way that makes it possible to evaluate UV radiation dose. Band structure of a solid can be described with the scheme shown in Fig. 39.3. The information about all the parameters from the scheme was derived from the spectra in Figs. 39.1 and 39.2. The band structure of ZrO_2:PbS and PVA:PbS films is shown in Fig. 39.4.

Analysis of the Fig. 39.4 shows:

- Density of localized states decreases under influence of UV radiation for both ZrO_2:PbS and PVA:PbS films. Tails appear at the edge of the valence band of nonirradiated ZrO_2:10%PbS and ZrO_2:20%PbS films. Localized states of ZrO_2:50% PbS film disappear completely after 50 min of UV irradiation. This can indicate that interaction between the localized states increases with increase of PbS nanodot concentration.
- The position E_1 of localized states has a trend to be closer to the edge of the valence band when concentration of PbS increases.

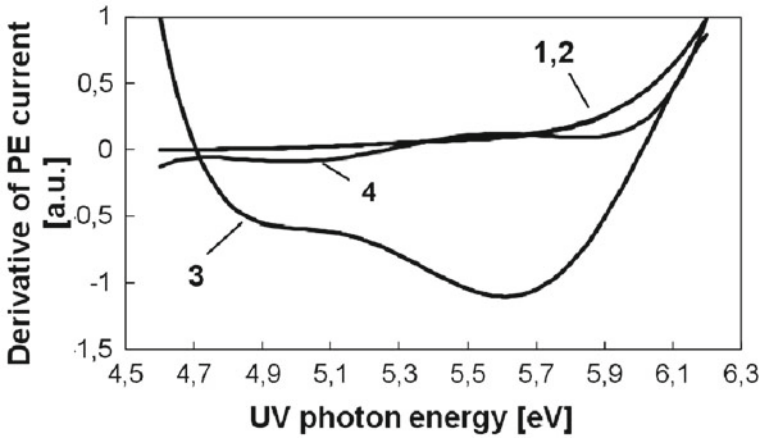

Fig. 39.2 Derivatives of PE current of UV irradiated films: *1*: ZrO_2:10%PbS; *2*: ZrO_2:20%PbS; *3*: ZrO_2:50%PbS; *4*: PVA: 20%PbS

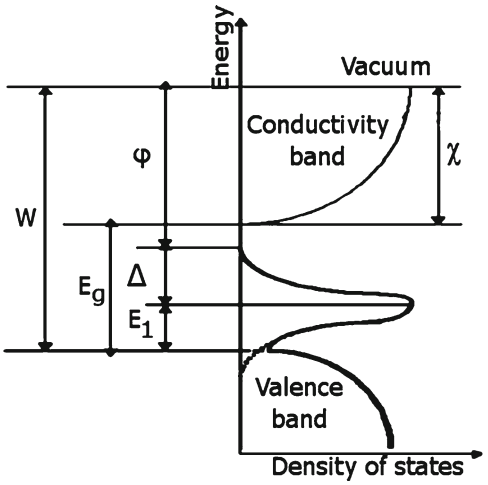

Fig. 39.3 Band structure of a solid: φ – electron work function; *Eg* – energy gap; *W* – electron work function from the valence band; Δ – half-width of the band of localized states; E_1 – distance between the valence band and the midpoint of the band of localized states; χ – electron affinity

- The electron affinity χ increases with increase in PbS concentration in ZrO_2 matrix. According to [4], increase in PbS concentration results in formation of larger PbS nanodots. Therefore, it is possible that larger nanodots are characterized with higher χ values.

The electron affinity of the irradiated ZrO_2:PbS films is smaller than of nonirradiated films. However, the difference Δχ between irradiated and nonirradiated films depends on PbS concentration. Δχ is smaller for films with higher PbS concentration. At the same time Δχ of PVA: 20% PbS films (0.75 eV) is significantly higher than of ZrO_2:20%PbS films (0.2 eV). It means that the matrix (environment) has strong influence on χ.

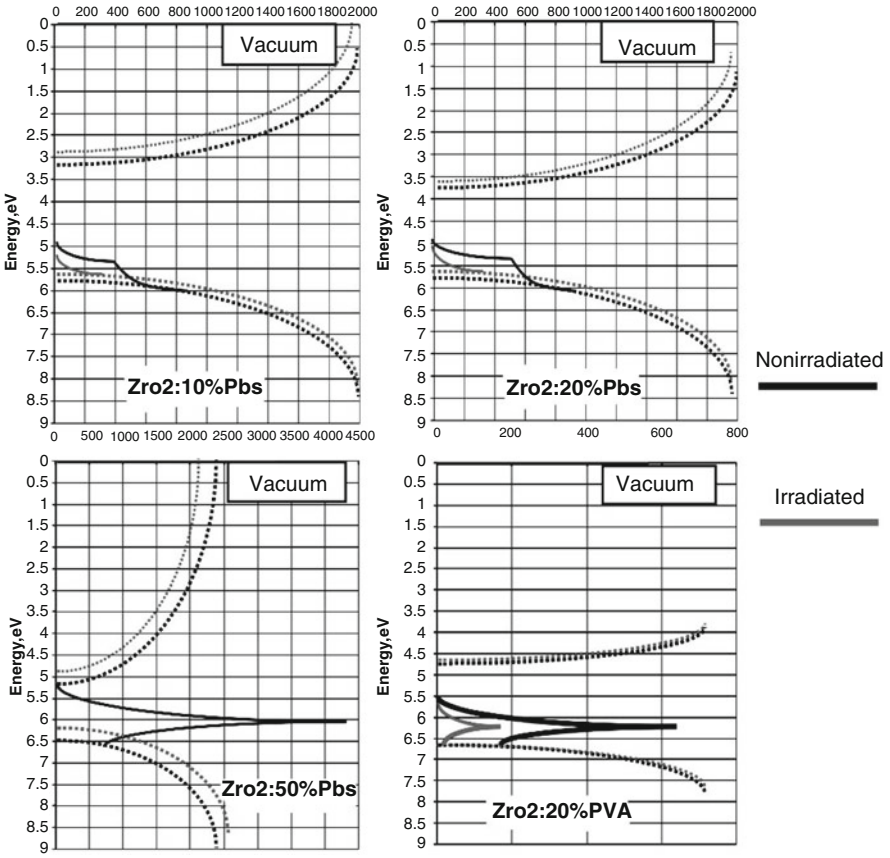

Fig. 39.4 Band structure of ZrO_2:PbS and PVA:PbS films

The semi-width Δ of band of localized states increases with increase in PbS concentration in ZrO_2:PbS films. It might mean that quantity of localized states increases with increase in PbS concentration that also might evidence that the detected emission was provided by localized states created by PbS nanodots.

Density of localized states of ZrO_2:PbS films can also be evaluated by calculating areas below the photoemission maximums at 5.5 eV shown in Figs. 39.1 and 39.2 (Fig. 39.5).

The area below the photoemission maximum decreases after irradiation. It means that UV radiation releases electrons from localized states. Films with 50% PbS have the largest value of area. It means that density of localized states increases with increase in PbS concentration. The area below the photoemission maximums decreases with increase in irradiation time.

Photoemission spectra of ZrO_2 and PVA matrixes were recorded as well. UV radiation did not change the spectra significantly. This gave more evidence that the emission maximums shown in Fig. 39.1 were provided by PbS nanodots.

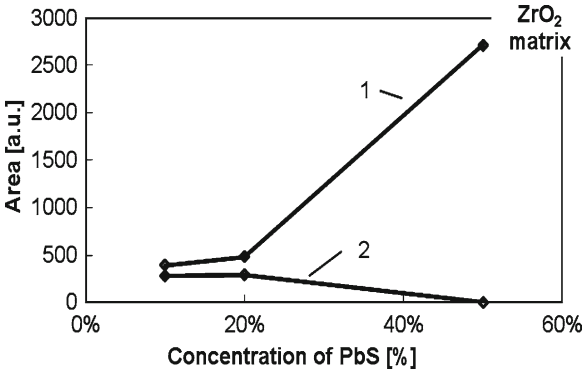

Fig. 39.5 Area below photoemission maximum (5.5 eV) of ZrO_2:PbS films as a function of PbS concentration: *1*: non-irradiated films; *2*: irradiated films (50 min)

39.5 Conclusions

Density of localized states of ZrO_2:PbS films increases with PbS concentration. UV radiation decreases quantity of localized states of ZrO_2:PbS and PVA:PbS films. The semi-width Δ of localized states band of ZrO_2:PbS films increases with PbS concentration that perhaps depends on increase of the nanodots size. Increase of Δ might evidence that localized states are created by PbS nanodots. The electron affinity χ of ZrO_2:PbS films decreases after UV irradiation. The electron affinity χ of ZrO_2:PbS films increases with increase of PbS concentration. However, higher concentrations of PbS nanodots lead to smaller difference $\Delta\chi$ between nonirradiated and irradiated ZrO_2:PbS films. The matrix of films influences χ value and density of localized states. Density of localized states is higher in ZrO_2 matrix than in PVA matrix.

References

1. Reisfeld R, Saraidarov T (2006) Innovative materials based on sol-gel technology. Opt Mater. Polish–French–Israeli symposium on spectroscopy of modern materials in physics 28(1–2): 64–70
2. Saraidarov T, Reisfeld R, Sashchiuk A, Lifshitz E (2005) NanoCrystallites of lead sulfide in hybrid films prepared by sol-gel process. J Sol-Gel Sci Technol 34:137–145
3. Sashchiuk A, Lifshitz E, Reisfeld R, Saraidarov T, Zelner M, Willenz A (2002) Optical and conductivity properties of PbS nanocrystals in amorphous zirconia sol-gel films. J Sol-Gel Sci Technol 24:31–38
4. Saraidarov T, Reisfeld R, Sashchiuk A, Lifshitz E (2003) Synthesis and characterization of lead sulfide nanoparticles in zirconia-silica-urethane thin films prepared by the sol-gel process. J Sol-Gel Sci Technol 26:533–540

Chapter 40
Overview of the Usage of Chemometric Methods for Remediation Techniques of Radionuclides

Chemometric Methods on the Remediation Techniques

C. Yilmaz and M.A.A. Aslani

Abstract The aim of this study is to investigate the treatment of chemometric tools on remediation techniques for removal of Cs-137, Sr-90 and Ra-226 from environmental samples. In this study; statistical data are collected from literature about applications of chemometric methods.

Keywords Chemometric tools • Environmental sciences • Radionuclides

40.1 Introduction

Environmental science can be described as an academic field which integrates physical and biological sciences to study and solve environmental problems. Environmental science provides an integrated interdisciplinary approach to the study of environmental systems [1]. The nineteenth century industrial revolution and subsequent technological advances have dramatically increased environmental pollution, described as anthropogenic activities – contamination of air, water, and soil. Likewise, radioactive pollutants, which are formed by nuclear tests, explosions, accidents, and leakages, are extremely dangerous in comparison to most pollutants. The radionuclides of greatest concern that contaminate the soil, water, and air by these kinds of activities are – Cesium, Strontium, and Radium. With long half-lives, their effects on the environment remain active for many years.

C. Yilmaz • M.A.A. Aslani (✉)
Institute of Nuclear Sciences, Ege University, Bornova-Izmir 35100, Turkey
e-mail: ceyhunyilmaz@gmail.com; mahmoud.aslani@ege.edu.tr

A. Vaseashta et al. (eds.), *Technological Innovations in Sensing and Detection of Chemical, Biological, Radiological, Nuclear Threats and Ecological Terrorism*, NATO Science for Peace and Security Series A: Chemistry and Biology,
DOI 10.1007/978-94-007-2488-4_40, © Springer Science+Business Media B.V. 2012

Environmental problems are increasingly complex and multilayered. Because modern analytical methods produce significant amounts of data; classical descriptive statistics are inefficient in handling multidimensional data sets. Necessity and the availability of applications software that can analyze multivariate data sets, have led to the use of chemometric methods for diverse and complicated problem solving [2].

40.2 Chemometrics

Chemometrics is best defined as the application of mathematical and statistical (both univariate and multivariate) methods to any kind of chemical data. Chemometrics is a powerful tool for comprehensive evaluation and interpretation; assessment of environmental data; and objective evaluation. Chemometrics have been applied in many areas of research such as food science technology, analytical chemistry, environmental and computer sciences. The first known techniques were cluster and factor analysis of multiple regressions. In recent years, however, cluster imaging, multiway partial least squares (PLS) regression and projection pursuit have been developed and increased in usage [2].

40.2.1 Opportunities and Challenges

There are many problems encountered while using classical statistical methods. These methods have failed in dealing with multivariate data sets. More complicated analytical questions need powerful statistical tools because

- the environmental data are multidimensional and highly variable due to geological & meteorological effects,
- the data contain uncertainties highly due to the analytical processes like sampling, sample conservation, calibration and measurement
- modern analytical methods like multi element ICP-OES and ICP-MS, and multi component methods like GCMS and LCMS produce huge amounts of data.

Also, the usage of univariate statistical methods in addition to the quantity of information arising from data evaluation and the interpretation has often resulted in the neglect of correlation between different pollutants and relationships among different sampling sites.

We propose a solution requiring the application of additional methods of analysis which can provide a relationship using established and modern methods of multivariate data analysis (chemometric methods) in dealing with more complicated analytical questions.

The main benefit of chemometric methods arises from the power to analyze complex sets of multidimensional data. These tools enable a deeper and more objective assessment and interpretation of data. Chemometric methods can identify

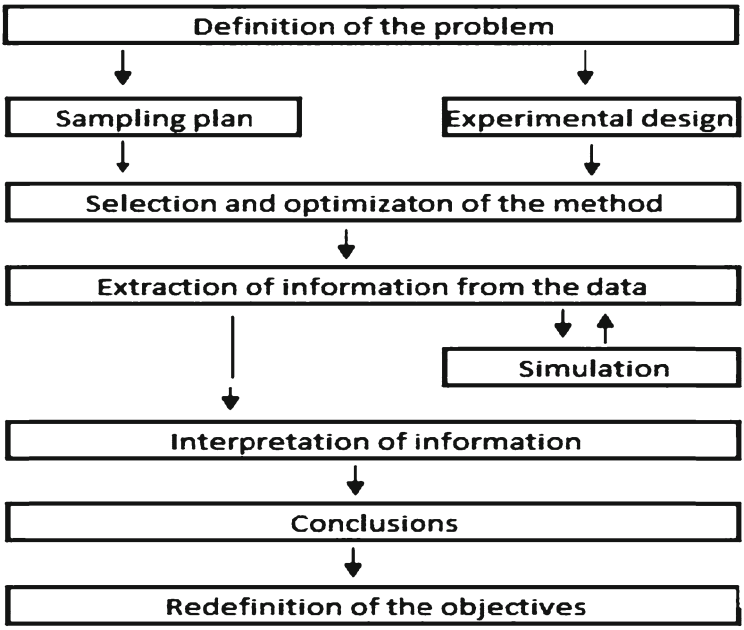

Fig. 40.1 A generic holistic strategy for a chemometric project [3]

multidimensional data sets structures, similarities, and the substantial influencing factors. A generic strategy for a chemometric project can be seen from Fig. 40.1. Chemometric methods are known to be effectual in these areas: to compress large data sets; to extract latent information; to eliminate redundancy and "noise"; to visualize multidimensional data sets; to hypothesize the information; and to detect pollution sources or correlate different environmental variables [2].

40.3 Applications

Chemometric tools have been applied to a variety of areas for more than 25 years. In 1979, the first known article involving a chemometric study was published in the area of "food science and technology" [4]. Since then, chemometric methods have been used in analytical chemistry, instrumentation, applied chemistry, computer sciences, and environmental sciences. Schuetzle et al. [5] used chemometrics to model waste-water treatment processes as the first chemometric study in "environmental sciences" [5]. Since 1979, of 5,081 articles about chemometric methods applied in more than 140 subject areas, 197 of them are in "environmental sciences" [4]. Also, chemometric studies increase yearly having an all-time high of 572 in 2009 [4]. The number of articles in environmental sciences from 1991 to May 2010 is shown in Fig. 40.2.

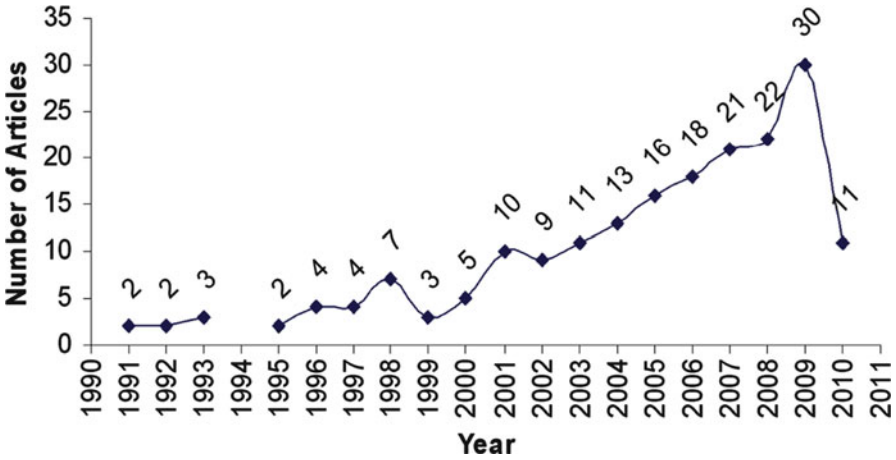

Fig. 40.2 Number of publications in environmental sciences by year (total of 197)

40.3.1 Applications on Radionuclides

Three important radionuclides used in this work are Cs-137, Sr-90, and Ra-226. Cs-137 is a fission product of uranium and plutonium which emits beta and gamma radiation with a half-life of ~30 years. Sr-90 is a radionuclide formed by nuclear fission and emits beta radiation with a half-life of ~29 years. Radium is a naturally-occurring radionuclide formed by the decay of uranium and thorium. The well-known isotope of radium is Ra-226 which emits alpha and gamma radiation and has a half-life of 1,600 years [6].

The literature shows that chemometrics is not used enough for remediation of radionuclides with only 3 results found for Ra-226, 2 for Sr-90 and 1 for Cs-137[4]. Only one study about these three radionuclides together is done by Tsikritzis [7] to investigate the distribution and origin of K-40, Ra-226, Ra-228 and Cs-137 in trees, mosses and lichens in the basin of the West Macedonia Lignite Centre. Application of chemometrics assists in understanding of the origin of the radionuclides [7].

40.4 Conclusion

Chemometric methods have been used for dealing with complex data sets in many areas for many years. Because radioactive pollutants are a heightened environmental concern, research on the origination and remediation of radioactive pollutants from the environment is very important. We conclude that chemometric tools are valuable in studying the distribution and remediation of radionuclides from environmental samples.

References

1. http://en.wikipedia.org/wiki/Environmental_science. 02 Feb 2010
2. Kowalik C, Einax JW (2006) Modern chemometric data analysis – methods for the objective evaluation of load in river systems. Acta Hydrochim Hydrobiol 34:425–436
3. Einax JW, Zwanziger HW, Geiß S (1997) Chemometrics in Environmental Analysis, VCH, Weinheim, p 384
4. http://pcs.isiknowledge.com. 31 May 2010
5. Schuetzle D, Koskinen JR, Horsfall FL (1982) Chemometric modeling of wastewater treatment processes. J Water Pollut Control Fed 54:457–465
6. http://www.epa.gov/radiation/radionuclides/. 25 Feb 2010
7. Tsikritzis LI (2005) Chemometrics of the distribution and origin of 226Ra, 228Ra, 40K and 137Cs in plants near the West Macedonia Lignite Center (Greece). J Radioanal Nucl Chem 264:651–656

Chapter 41
Characterization of Au Irradiated Glassy Polymeric Carbon at 2,000°C for Nuclear Applications

Characterization of GPC After Ion Irradiation

M. Abunaemeh, M. Seif, A. Batra, A. Elsamadicy, Y. Yang, L. Wang, C. Muntele, and D. Ila

Abstract The TRISO fuel has been used in some of the Generation IV nuclear reactor designs [1]. It consists of a fuel kernel of UO_x coated with several layers of materials with different functions. Pyrolytic carbon (PyC) is one of the materials in the layers. In this study we investigate the possibility of using Glassy Polymeric Carbon (GPC) as an alternative to PyC. In this work, we are comparing the changes in physical and microstructure properties of GPC after exposure to irradiation fluence of 5 MeV Au equivalent to a 1 displacement per atom (dpa) for GPC prepared at 2,000°C. The GPC material is manufactured and tested at the Center for Irradiation Materials (CIM) at Alabama A&M University using Transmission electron microscopy (TEM) and stopping range of ions in matter (SRIM) software.

M. Abunaemeh (✉) • D. Ila
Center for Irradiation of Materials, Alabama A&M University, Normal, AL, USA

Physics Department, Alabama A&M University, Normal, AL, USA
e-mail: malcom@cim.aamu.edu

M. Seif
Mechanical Engineering Department, Alabama A&M University, Normal, AL, USA

A. Batra
Physics Department, Alabama A&M University, Normal, AL, USA

A. Elsamadicy
Department of Physics, University of Alabama, Huntsville, AL, USA

Y. Yang
Engineering Physics Department, University of Wisconsin, Madison, WI, USA

L. Wang
Engineering Physics Department, University of Michigan, Ann Arbor, MI, USA

C. Muntele
Center for Irradiation of Materials, Alabama A&M University, Normal, AL, USA

A. Vaseashta et al. (eds.), *Technological Innovations in Sensing and Detection of Chemical, Biological, Radiological, Nuclear Threats and Ecological Terrorism*, NATO Science for Peace and Security Series A: Chemistry and Biology,
DOI 10.1007/978-94-007-2488-4_41, © Springer Science+Business Media B.V. 2012

Keywords Transmission electron spectroscopy • Glassy polymeric carbon

41.1 Introduction

Current high temperature gas cooled rectors are designed with the use of coated fuel particles that are dispersed in a graphite matrix to form fuel elements called Tristructural-isotropic (TRISO) [1, 2]. As seen in Fig. 41.1[3], TRISO consists of a microspherical kernel of uranium oxide (UO_x) coated with a layer of porous carbon buffer surrounding it to contain any particle dimensions changes or gas buildup. This layer is followed with an inner pyrolitic carbon (PyC) followed by a layer of silicon carbide (SiC) followed by an outer PyC layer.

The pebbles or the graphite blocks containing the TRISO fuel are directly immersed in the cooling fluid that extracts the heat outside of the reactor core while keeping the inside within the operational temperature limits [4, 5]. If the fissile fuel is in direct contact with the cooling fluid, there are great chances that radioactive fission fragments will be carried out of the reactor core and contaminate all other equipment [6]. Therefore, in order to minimize such leaks, TRISO is designed with PyC as the diffusion barrier material.

GPC is widely used for various applications from artificial heart valves to heat-exchangers and other high-tech products that are developed for the space and medical industries. This lightweight material can maintain dimensional and chemical stability in adverse environment and very high temperatures (up to 3,000°C).

The primary purpose of this study is to understand the changes in fundamental properties (chemical and mechanical stability) of GPC prepared at 2,000°C. The sample was bombarded with 5 MeV Au to an effect of 1 DPA. More generally, we are trying to understand the fundamental mechanisms of defect creation in sp^2-bonded carbons under particle radiation. The type and concentration of such defects have deep implications in the physical properties of carbon-based materials for various applications from carbon-based quantum electronics to structural components for aerospace applications. Here, in particular, the specific application is in

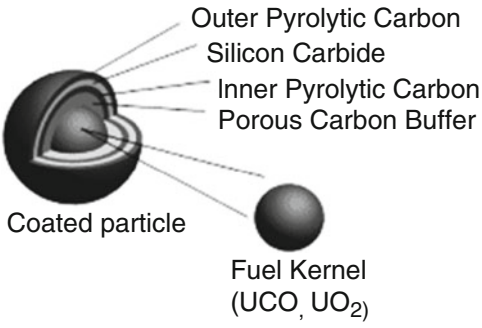

Fig. 41.1 TRISO fuel layers structure

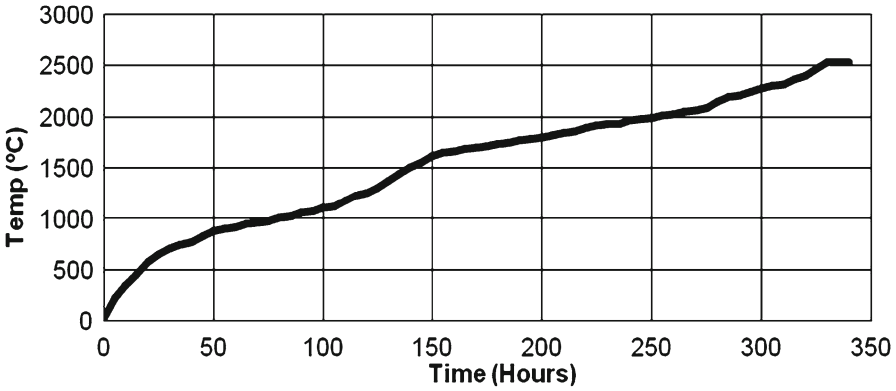

Fig. 41.2 Heating profile used for the GPC sample in graphite furnace

an extreme radiation environment, the core of nuclear reactor. This study will help to determine GPC eligibility for future irradiation testing for a specific application in an extreme radiation environment in the nuclear reactor. It will also help to determine if GPC will be a good choice as a diffusion barrier in the TRISO fuel that will be used in the next generation of nuclear reactors.

41.2 Experimental Details and Discussion

A procedure for making the GPC sample was developed at CIM. It starts by taking phenolic resin that is placed in a beaker and in a sonication bath for about 1–2 h. The resin is then taken out of the sonication bath and is poured carefully in the desired mold. The mixture is then heated slowly at a rate of 20°C/day for 6 days to lower the possibility of any bubble forming during the gelling stage. The hardened gel is removed from the mold and heated to 2,000°C slowly over the course of 5 days. At this stage they are a fully pyrolized GPC sample. The heating profile that was developed for GPC in our lab was followed during this process [7, 8]. This developed heating profile can be used to heat samples up to 2,500°C. The sample is then left to cool off in the furnace until it reaches room temperature. Figure 41.2 shows a plot of the heating profile that was followed to prepare the sample. The material undergoes modification of its molecular structure during different heat stages that are shown in Fig. 41.3.

TEM was used for characterizing the microstructures of the pre irradiated GPC sample prepared at 2,000°C as seen in Fig. 41.4. TEM was done at the Department of Nuclear Engineering & Radiological Sciences at the University of Michigan. This HRTEM shows the graphite-like layered structure. There is a noticeable alignment of layers associated with this temperature.

The GPC sample irradiation took place at the Center for Irradiation of Materials (CIM) with 5 MeV Au with a fluence of 1.3×10^{16} ions/cm^2 to an effect of 1 dpa.

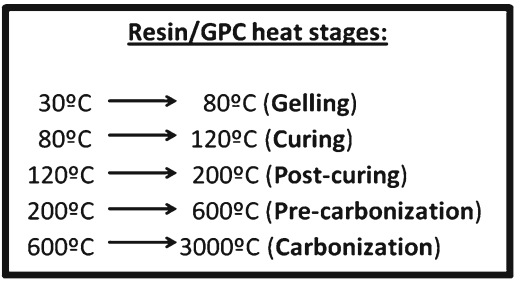

Fig. 41.3 Different resin/GPC heating stages

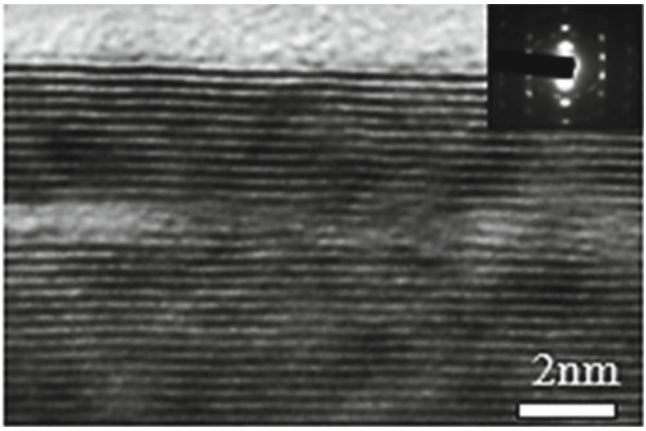

Fig. 41.4 TEM of pre-irradiated GPC sample prepared at 2,000°C [9]

Fig. 41.5 TEM of Au irradiated GPC

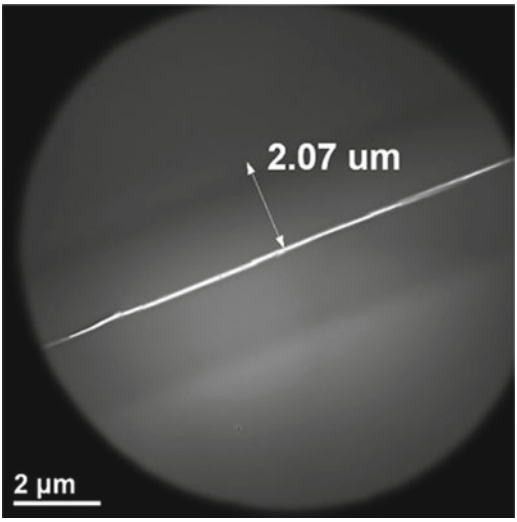

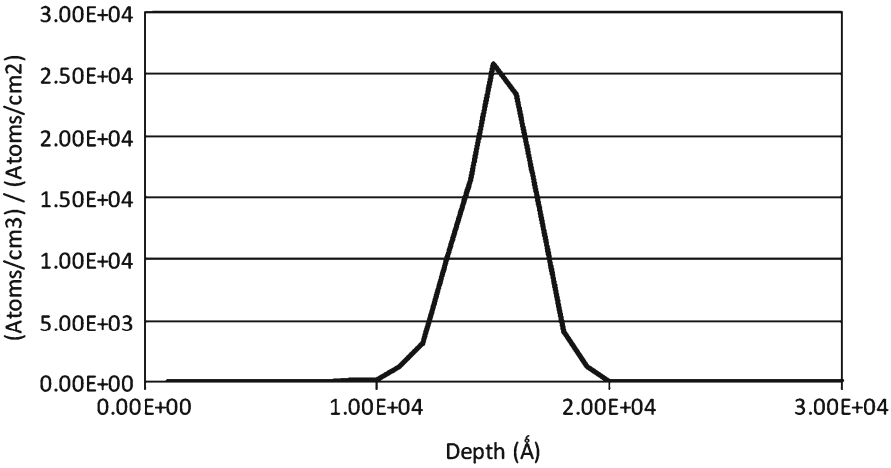

Fig. 41.6 SRIM Simulation of Au irradiated GPC

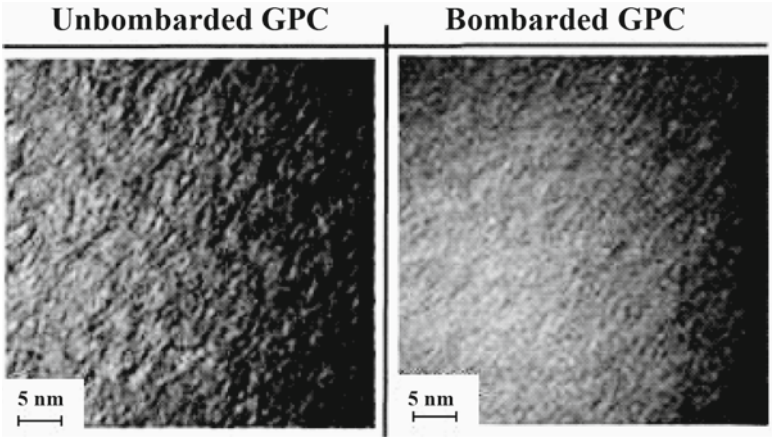

Fig. 41.7 A comparison of unbombarded and bombarded GPC

TEM on the post irradiated sample was done at the Engineering Physics Department at the University of Wisconsin. Figure 41.5 shows that the gold distribution was about 1.5 μm inside the GPC, matching the SRIM simulation as seen in Fig. 41.6. Figure 41.7 shows a comparison of the preiradiated and irradiated GPC at an effect of 1 DPA.

41.3 Conclusions

TEM showed the ordered, graphite-like, layered structure of GPC sample fabricated at 2,000°C. TEM also showed that Au penetrated 1.5 μm deep into the sample, which matched the SRIM simulation. An observation of the bombarded and unbombarded GPC that the samples prepared at 2,000°C were completely damaged. The next step is to implant Ag and other fission product elements to GPC prepared at 2,000°C and to compare the results of the diffusivity of these elements in GPC with PyC to determine if GPC was a better barrier for fission products than PyC for use in the TRISO fuel for the next generation of nuclear reactors.

Acknowledgments This research was supported and funded by the AAMRI Center for Irradiation of Material, NSF Alabama GRSP EPSCOR, and DoE NERI-C project number DE-FG07-07ID14894. Acknowledgment also goes for Dr. Edwards, the Dean of the school of Arts and Sciences at Alabama A&M University for the travel support.

References

1. Association of German Engineers (1990) AVR - Experimental high-temperature reactor: 21 years of successful operation for a future energy technology (pp. 9–23). Available from http://www.nea.fr/abs/html/nea-1739.html
2. Fukuda K, Ogawa T, Hayashi K, Shiozawa S, Tsuruta H, Tanaka I, Suzuki N, Yoshimuta S, Kaneko M (1991) Research and development of HTTR coated particle fuel. J Nucl Sci Technol 28:570
3. Next Generation Nuclear Plant (2009) Retrieved from www.nextgenerationnuclearplant.com/i/triso.gif
4. Olander D (2009) Nuclear fuels - Present and future. J Nucl Mater 389(1):1–22
5. McCullough CR (1947, September15) Summary report on design and development of high temperature gas-cooled power pile (DOE Contract No. W-35-058-ENG-71). Oak Ridge National Laboratory, Oak Ridge. doi: 10.2172/4359623
6. Petti DA, Buongiorno J, Maki JT, Hobbins RR, Miller GK (2003) Key differences in the fabrication, irradiation and high temperature accident testing of US and German TRISO-coated particle fuel, and their implications on fuel performance. Nucl Eng Des 222(2–3):281–297
7. Fisher J (1996) Active crucible bridgman system: crucible characterization, rf inductor design and model. Dissertation, Alabama A&M University
8. Maleki H, Holland LR, Jenkins GM, Zimmerman L, Porter W (1996) Maximum heating rates for producing undistorted glassy carbon were determined by wedge-shaped samples. J Mater Res 11(9):2368–2375
9. Abunaemeh M, Seif M, Yang Y, Wang L, Chen Y, Ojo I, Muntele C, ILA D (2010) Characterization of changes in properties and microstructure of glassy polymeric carbon following Au ion irradiation. Materials Research Society Proceeding, 1215. doi:10.1557/PROC-1215-V16-26

Chapter 42
Fiber Optic Interferometric Method for Registration of IR Radiation

Fiber Optic Interferometric Method

Ion Culeac, I. Nistor, M. Iovu, and A. Andriesh

Abstract A high sensitivity speckle based fiber-optic method for registration of low intensity IR radiation is described. The method is based on the effect of variation of the speckle pattern in the far-field of a multimode fiber. IR radiation that falls on a lateral surface of the fiber leads to variation of the speckle image. Computer processing of the speckle image provides information on the amplitude of perturbation that interacts with the fiber. An algorithm was developed for processing of the speckle image and determining of the intensity of IR radiation. The results of the computer simulation correlate well with the experimental ones.

Keywords Multimode fiber • Speckle pattern • Modal interference • CCD • IR

42.1 Introduction

When injecting a coherent light beam into a multimode optical fiber the light is guided in a determined number of propagation modes. Each of these modes has a specific propagation constant, spatial field distribution, and polarization. The number and the shape of confined modes are a function of the index of refraction, the diameter of the fiber core, and the wavelength of light. At the exit end of the fiber the propagation modes interfere in the far field producing a random interference image – the speckle pattern. This pattern is highly sensitive to external perturbations and carries information on the conditions of light propagation in the fibers. The changes in the speckle pattern produced by external perturbations may

I. Culeac (✉) • I. Nistor • M. Iovu • A. Andriesh
Institute of Applied Physics, Academy of Sciences of Moldova, Chisinau, Republic of Moldova
e-mail: ion.culeac@gmail.com

A. Vaseashta et al. (eds.), *Technological Innovations in Sensing and Detection of Chemical, Biological, Radiological, Nuclear Threats and Ecological Terrorism*, NATO Science for Peace and Security Series A: Chemistry and Biology,
DOI 10.1007/978-94-007-2488-4_42, © Springer Science+Business Media B.V. 2012

be determined by variation in the optical path length due to changes in the index of refraction, geometrical path, and the propagation constants of each fiber mode. This effect is laid dawn on the basis of a measurement technique that employs modal interference in an optical fiber [1]. Speckle-based methods are widely used for registration of physical parameters [2–4]. These methods have been extensively used for industrial applications in measurements of deformation and displacement, object shape, vibrations, etc. [5, 6]. Electronic speckle interferometry combined with PC processing technique offer powerful tools for registration of physical quantities and industrial control. In a previous paper [1] we have reported a fiber optic method for registration of low intensity infrared (IR) radiation based on the effect of interference of propagation modes in the far field of a multimode fiber. In this paper we present new results and details on the method.

42.2 Experimental Set-Up

The experimental set-up is represented in Fig. 42.1. It consists basically of a multimode optical fiber coupled to a coherent light source, a CCD detector, and a PC for processing of the speckle image. The probing light from the coherent light source is injected into the input face of the fiber and at the output end of the fiber in the far-field the modal distribution of the probing light intensity (the speckle image) is registered. When a physical perturbation hits the fiber, the speckle pattern changes. The CCD is used for registration of the variations of the speckle pattern of the multimode fiber for subsequent PC processing.

The probing light source was a HeNe Laser at 633 nm. A segment of multimode commercially available optical fiber with a parabolic index profile and the core/cladding diameter 50/125 μm was used as sensing element. A common electrical heater was used as IR radiation source. Variation of the intensity of IR radiation was performed by variation of the distance between electrical heater and optical fiber. The speckle pattern in the far field of the fiber was registered with a HDCS-1020 CMOS image sensor with the pixel size 7.4×7.4 μm and image array sizes VGA 640×480. The full frame video rate at 8-bit resolution was 30 fps.

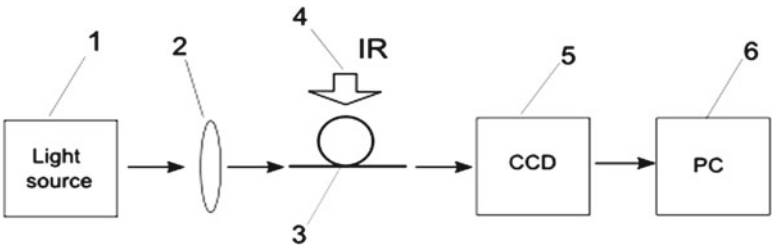

Fig. 42.1 Schematic representation of the method: *1* – a coherent light source; *2* – microscope objective; *3* – multimode optical fiber; *4* – IR radiation source; *5* – CCD detector; *6* – computer

42.3 Experimental Results

A typical speckle pattern of the fiber used for measurements is shown in Fig. 42.2a. Analyses of spatial distribution of light intensity in the speckle pattern *I(x,y)* in the far-field of the fiber provides information about the conditions of light propagation in the multimode fiber as well as on the perturbations that affect the optical fiber. The speckle image represents the result of destructive and constructive interference of propagating modes in the far field of the fiber (Fig. 42.2b). For a separate mode at the output end of fiber the magnitude of electric field $\vec{E}$ can be represented as:

$$\vec{E} = \vec{A}_0 \cos(\omega t + \varphi) \tag{42.1}$$

where $\vec{A}_0$ is the amplitude of electric field, ω is the frequency of electromagnetic wave, t is the time. The phase for a separate mode φ is determined by the geometrical path length L, the wavelength λ and the effective index of refraction n ($\varphi = 2\pi n \frac{L}{\lambda}$). The total amplitude of the electric field in any point of speckle pattern in the plane of CCD sensor can be represented as the sum of contributions of all N propagating modes of the fiber:

$$E = \sum_{k=1}^{N} |A_k| \exp(j\varphi_k) \tag{42.2}$$

where A_k is the amplitude of the *k-th* mode of the fiber, ϕ_k is the phase for the *k-th* mode at the output end of the fiber, N is the total number of modes propagating in the core of the fiber.

When two modes interfere in the point *P(x,y)* of the CCD plane the resulting intensity *I(x,y)* can be described by the relation:

$$I(x,y) = I_k(x,y) + I_{k+1}(x,y) + 2\sqrt{I_k I_{k+1}} \cos(\varphi_k - \varphi_{k+1}) \tag{42.3}$$

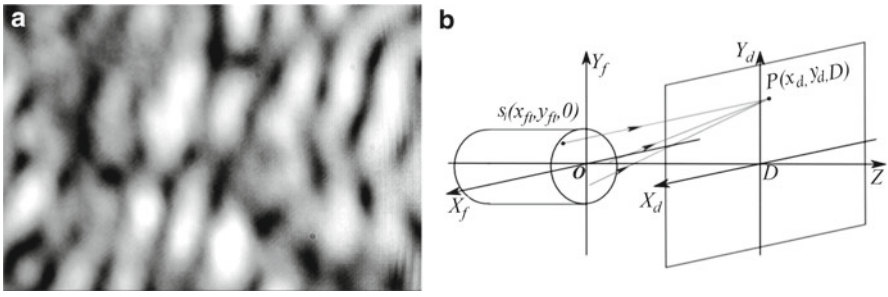

Fig. 42.2 Illustration of the far field speckle pattern of the fiber registered by CCD sensor: (**a**) A typical speckle pattern of the fiber; (**b**) Schematic representation of the interference of the modes in the far-field of the fiber

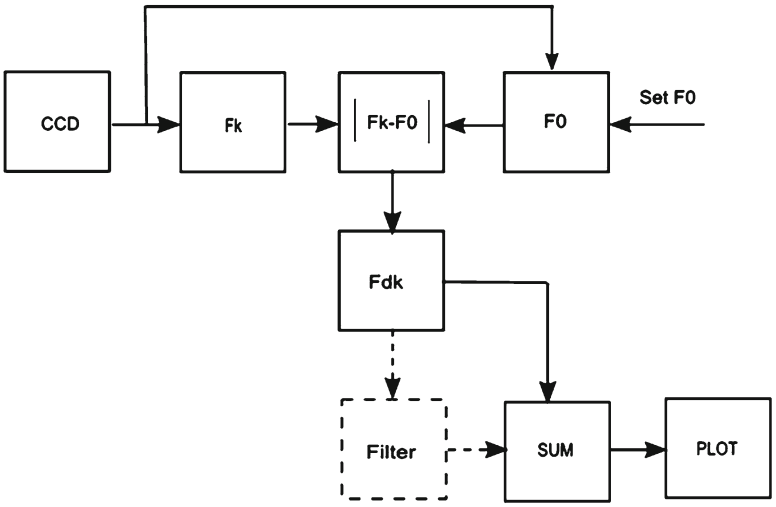

Fig. 42.3 Illustration of the speckle image processing algorithm

where $I_k(x,y)$ and $I_{k+1}(x,y)$ are the intensities of the *k-th* and *(k + 1)-th* modes in the point *P(x,y)* of the CCD plane X_dY_d, φ_k and φ_{k+1} are respectively the phase of the *k-th* and *(k + 1)-th* modes in the point *P(x,y)*. The structure of the speckle pattern depends on the coherence properties of the laser beam, refractive index profile, characteristics of the fiber and the external conditions at the core/cladding boundary.

The algorithm for processing of the speckle images registered by the CCD camera is based on comparison of speckle image taken at $t = 0$ and each one of the subsequent speckle images taken in the time moment t_k, where $k = 1,2,3,\ldots k_{max}$. A schematic illustration of the speckle processing algorithm is represented in the Fig. 42.3. The CCD camera takes an image of the speckle in the initial time t_0, and this image is stored in the buffer memory. The following speckle images are taken at the time t_k. Then the initial image I_0 is subtracted pixel-by-pixel from each of the current image I_k, and the current difference image I_k^d is obtained, where for a separate pixel belonging to I_k^d, the procedure obeys the relation:

$$I_k^d(x_i,y_j) = \left| I_k\left(x_i,y_j\right) - I_0\left(x_i,y_j\right) \right|,\ i = 1,2,3...,r_1,\ j = 1,2,3...,r_2, \tag{42.4}$$

where $i = 1,2,3\ldots,r_1$; $j = 1,2,3\ldots,r_2$; and r_1 and r_2 corresponds to the CCD's *X* and *Y* resolution respectively. The next processing step represents summation of all pixels' intensity from the image I_k^d and determination of the current sum S_k for the current moment t_k as follows:

$$S_k = \sum_{i=1}^{r_1}\sum_{j=1}^{r_2} I_k^d\left(x_i,y_j\right) \tag{42.5}$$

The resulting value of the sum S_k is plotted on the PC screen as the output signal of the CCD detector for a specific time moment t_k. The screenshot of the speckle

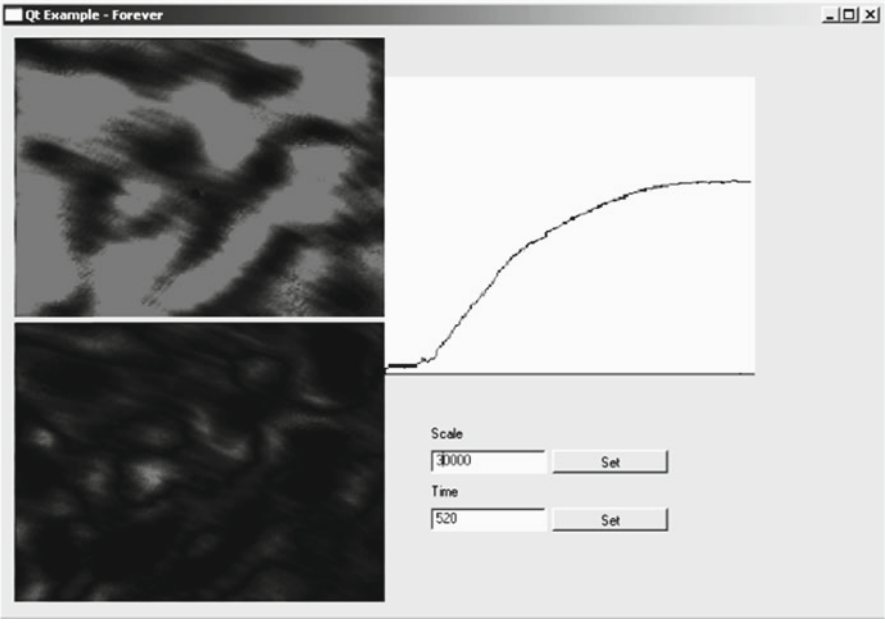

Fig. 42.4 The screenshot of the speckle image processing software

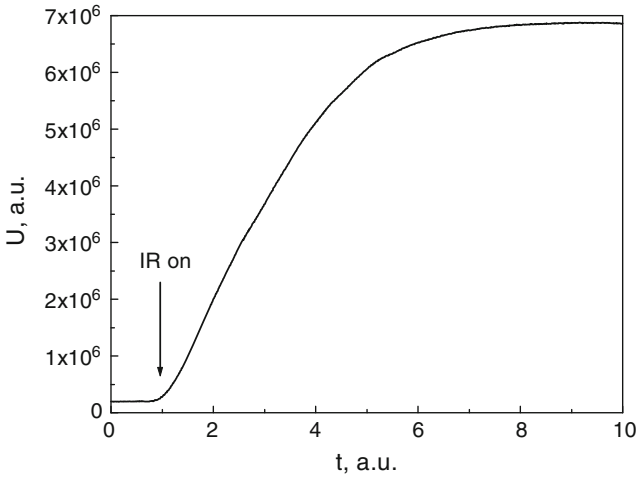

Fig. 42.5 Output signal characteristic after switching on the IR radiation $P_{IR} = 27$ μW. The light source is a HeNe laser at 633 nm

image processing software is represented in Fig. 42.4. The variation of the output signal after switching on the IR radiation is represented in Fig. 42.5.

Application of this algorithm offers the possibility to plot on the PC screen in the real-time scale the difference of the speckles images as the output signal of the

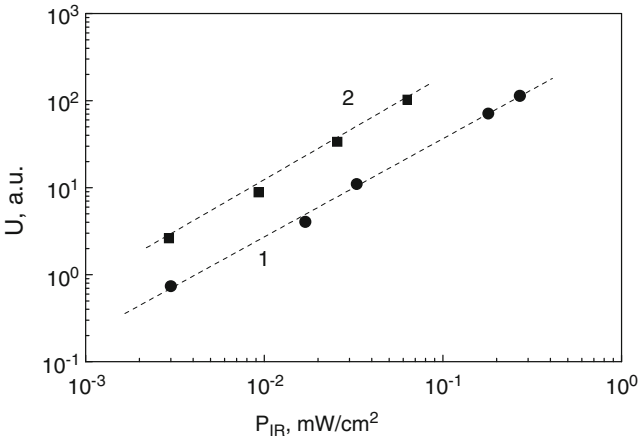

Fig. 42.6 The amplitude of the output signal vs. the intensity of infrared radiation. The light source is a HeNe laser at 633 nm. The temperature of the fiber: T, K = 290 (*1*); 278 (*2*)

method. The magnitude S_k correlates with the amplitude of the perturbation that hits the fiber and can be calibrated to represent exactly the amplitude of the perturbation that affects the fiber. Because we do not utilize too many routines for image processing, the rate of the procedure is sufficiently high.

On the other hand, because we do not take into account the coordinate of the pixels, this algorithm does not permit to eliminate the elements that are symmetric in the speckle images. Consequently, this reduces the sensitivity and dynamic range of the method. The dependence of the output signal vs. the amplitude of the perturbation keeps linear for a sufficient wide segment of the speckle spot. Consequently, the output signal plotted on the PC screen keeps linear for a sufficient large range of the intensity of IR radiation. The sensitivity of the speckle pattern to IR radiation strongly increases when cooling down the optical fiber (Fig. 42.6).

42.4 Computer Simulation

Consider interference of propagation modes in the far-field of the fiber. According to the Huygens' principle each of the point on the fiber end face $s(x_f, y_f)$ can be considered as a source of spherical waves (Fig. 42.3). These waves interfere constructively or destructively in the image plane of the CCD camera. The speckle pattern represents the contributions of propagating modes with a certain mutual phase difference. When external perturbation (heat, IR radiation, et.) hits the fiber the phase difference between modes will change.

The first speckle image I_0 is captured by CCD camera at initial time $t = 0$ when launching the procedure. Then at each subsequent time moment t_k ($k = 1,2,3\ldots k_{max}$) the CCD takes the current image I_k. The difference of the two speckle images is

calculated by subtracting pixel-by-pixel of two images and the value of the sum S_k is calculated with subsequent plotting on the PC monitor. The program for computer simulation of the modal interference in the far-field of the fiber has been developed on the basis of *C++* language and run on the GNU/*Linux* platform. The PC technical profile is characterized by *AMD Sempron Processor 3000+ 1.61 GHz, 1 GB RAM*. The basic parameters that have been set for numerical simulation were as follows: CCD resolution, the pixel area S_p, the distance between the end face of the fiber and CCD plane D, the diameter of the core of the fiber d_{core}, the total number of propagating modes N, and the wavelength of the probing light λ.

Computer simulation of the output signal variation vs. the time after switching on the perturbation IR radiation has been obtained. The simulation procedure has been carried out for two cases: *(a)* the ideal case without noise; *(b)* the case when the far-field speckle pattern is composed of "true" signal speckle pattern, accompanied by a speckle noise. For modeling of the speckle pattern in the far-field of the fiber several points have been chosen randomly on the end face of the fiber. The speckle pattern in the far-field was obtained by coherently adding up the spherical waves originating from the random points. As few as 14 randomly selected points are enough to produce a simulated speckle pattern that correlate quite well with the signal speckle. The distance between the CCD plane and the end face of the fiber was set at 3 cm. The characteristics of the CCD in the simulation procedure have been set of the same values as ones for the real CCD in the experiment (512×512 pixels).

The results of simulation of the speckle patterns and the corresponding output signal curves are represented in Figs. 42.7 and 42.8. The coordinates of the sources s_m on the fiber end face (x_{fm}, y_{fm}) have been generated arbitrarily to follow the relation:

$$x_{fm}^2 + y_{fm}^2 \le \rho^2, \quad m = 1,2,3,...N \tag{42.6}$$

where ρ represents half of the diameter of the core of the fiber. The intensity in the point with the coordinates (x_d, z_d, y_d) that lay in the plane of the CCD sensor $X_d Y_d$, is determined by the interference of the light waves (modes) generated by the all the sources s_m with the coordinates $(x_{fm}, y_{fm}, 0)$:

$$I\left(x_d, y_d\right) = \frac{\varepsilon_0 c}{T} \int_0^T E^2\left(x_d, y_d, t\right) dt, \tag{42.7}$$

$$E\left(x_d, y_d, t\right) = \sum_{m=1}^{N} E_m(x_d, y_d, t) = \sum_{m=1}^{N} E_{0m} \cos\left(2\pi \frac{d_m}{\lambda} - 2\pi \frac{t}{T} + 2\pi \frac{\varphi_m}{\lambda}\right), \tag{42.8}$$

where $T = \frac{c}{\lambda}$, and d_m is the distance between the source point $s_m(x_{fm}, y_{fm}, 0)$ and the element of the CCD matrix with the coordinates $P(x_d, z_d, D)$

$$d_m = \sqrt{\left(x_d - x_{fm}\right)^2 + \left(y_d - y_{fm}\right)^2 + D^2} \tag{42.9}$$

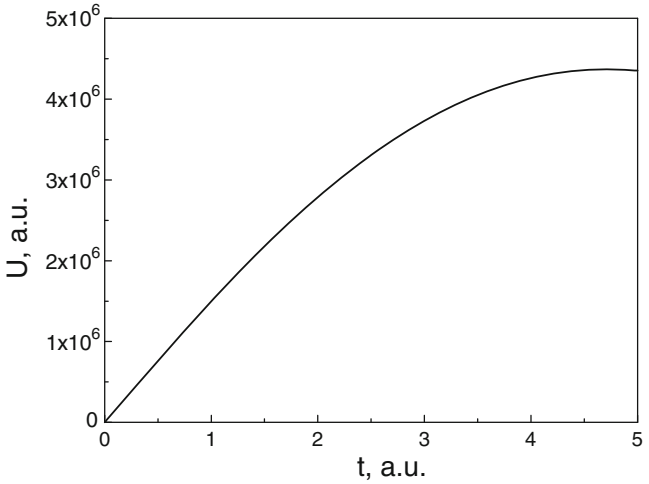

Fig. 42.7 Computer simulation of output signal for the case of no CCD noise

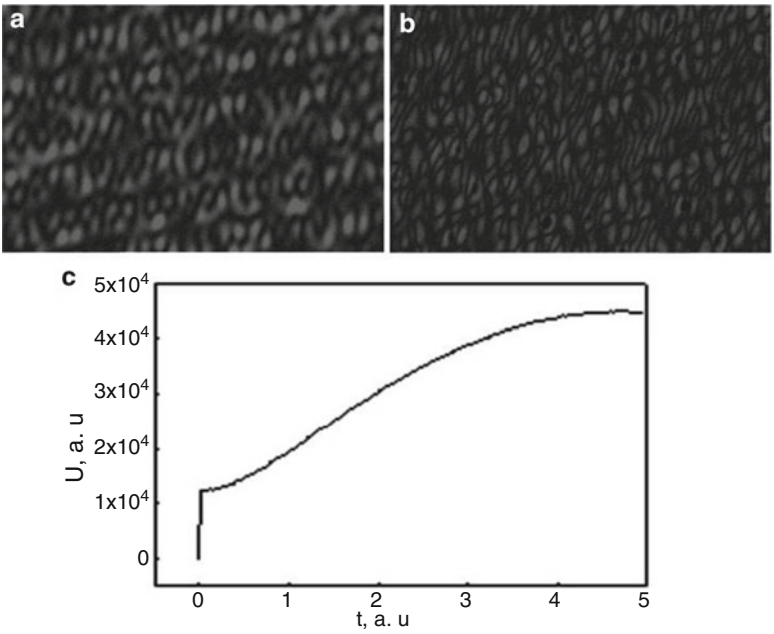

Fig. 42.8 Computer simulation of the speckle pattern in the far-field of the fiber and the plot of the corresponding output signal for the case of CCD noise: (**a**) the image of the simulated reference speckle pattern; (**b**) the image of the difference of the reference and the current speckle patterns; (**c**) the plot of the output signal

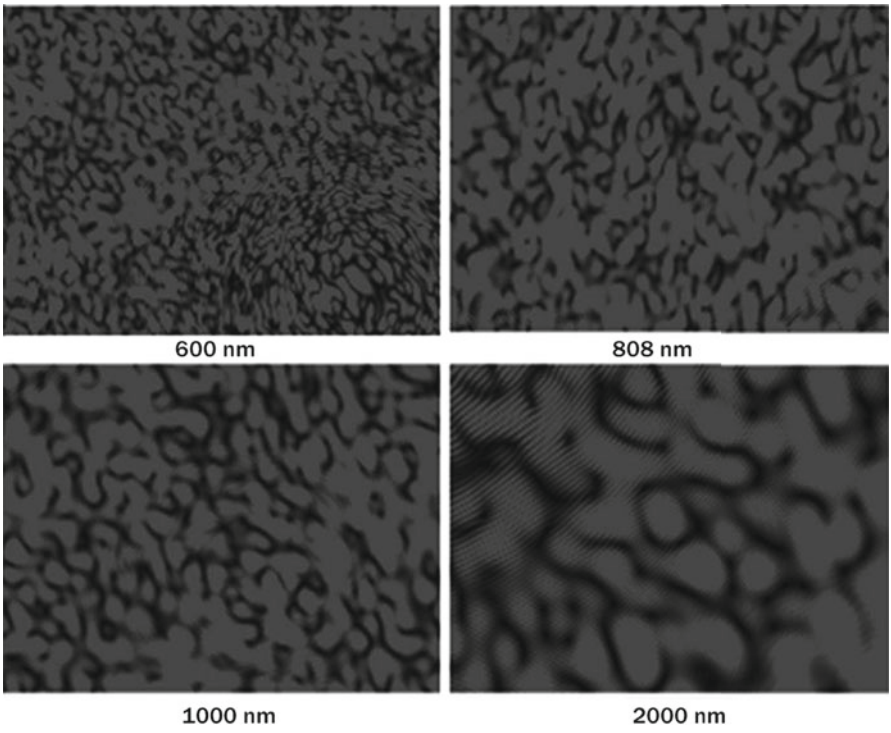

Fig. 42.9 Computer simulation of the speckle image at the output end of the step index fiber for different wavelengths, λ = 600, 808, 1,000 and 2,000 nm

As far as the index of refraction n varies very slowly across the fiber cross-section and the optical pathway varies differently for different modes We assumed that the phase of the mode φ_m linearly changes for a small variation of the parameter τ according to the relation:

$$\varphi_m(\tau) = \varphi_{0m} + \delta_m \tau \tag{42.10}$$

Where φ_{0m} has been generated arbitrarily for the domain *[0, λ]*. The linearity coefficient δ_m has been also generated arbitrarily, so that the phase variation $\Delta\varphi_m$ for each mode is different. The final intensity of the speckle image that contains a noise component the intensity of each pixel is represented as follows:

$$I\left(x_d, y_d\right)_{noise} = I\left(x_d, y_d\right) + n(x_d, y_d) \tag{42.11}$$

Where $n(x_d, y_d)$ represents the noise and $I\left(x_d, y_d\right)$ represents the true signal.

The results obtained from computer modeling agree quite well with the experimental result. Figures 42.5, 42.7, 42.8, and 42.9 demonstrate a good correlation of the results obtained in the simulation procedure and experimental results. Optimizing

the geometry of the fiber core/cladding structure, the glass composition, the core index profile and its temperature dependence one can obtain high sensitivity IR sensing device.

42.5 Summary

A high sensitivity speckle based fiber-optic method for registration of infrared radiation has been proposed. The method is based on the effect of variation of the speckle pattern in the far-field of the fiber under the action of IR radiation. The IR radiation that falls on the lateral surface of the fiber leads to variation of the phase difference between the propagating modes that gives rise to variation of the speckle pattern in the far-filed of the fiber. Computer processing of the speckle image provides information on the amplitude of IR radiation that hits the fiber. The algorithm has been developed for processing of the speckle image and determining the intensity of IR radiation. Both experimental results as well as computer simulation data are presented. The principle of the method can be applied for registration of IR radiation, temperature, vibrations, to name a few.

References

1. Culeac IP, Nistor IH, Iovu MS (2009) Fiber optic method for measuring the intensity of IR radiation. J Optoelectron Adv Mater 11(4):380–385
2. Balboa I, Ford HD, Tatam RP (2006) Low-coherence optical fibre speckle interferometry. Meas Sci Technol 17(4):605–616
3. Kaufmann GH, Galizzi GE (2002) Phase measurement in temporal speckle pattern interferometry: comparison between the phase-shifting and the Fourier transform methods. Appl Opt 41(34):7254–7263
4. Francis TS, Yu KP, Dazun Z, Ruffin PB (1995) Dynamic fiber specklegram sensing. Appl Opt 34(4):622–626
5. Jones R, Wykes C (1983) Holographic and speckle interferometry. Cambridge University Press, Cambridge
6. Wei An (2002) Industrial applications of speckle techniques. Doctoral thesis, Royal Institute of Technology, Stockholm

Chapter 43
Modern Methods of Real-Time Gamma Radiation Monitoring for General Personal Protection

Radiation Monitoring

O. Korostynska, K. Arshak, A. Arshak, and Ashok Vaseashta

Abstract Real-time radiation detectors become an essential part of emergency personnel who may have to respond to unknown accidents, incidents or terrorist attacks, which could involve radioactive material. More and more ordinary citizens are interested in personal radiation protection as well. Reasons include lost sources, nuclear industrial accidents, nuclear or radiological terrorism and the possibility of nuclear weapons being used in a war. People want to have the ability to measure it for themselves and they want to be notified when the radiation levels are increased. To meet this demand, considerable research into new sensors is underway, including efforts to enhance the sensor performance through both the material properties and manufacturing technologies. Deep understanding of physical properties of the materials under the influence of radiation exposure is vital for the effective design of dosimeter devices. Detection of radiation is based on the fact that both the electrical and the optical properties of the materials undergo changes upon the exposure to ionizing radiation. It is believed that radiation causes structural defects. The influence of radiation depends on both the dose and the parameters of the films including their thickness: the degradation is more severe for the higher dose and the thinner films. This paper presents overview of modern methods of real-time gamma radiation monitoring for personal protection of radiation workers and general public and suggests further developments in this area.

Keywords Gamma radiation monitoring • Real-time dosimetry • Personal protection

O. Korostynska (✉)
Dublin Institute of Technology, Dublin, Ireland
e-mail: olga.korostynska@dit.ie

K. Arshak • A. Arshak
University of Limerick, Limerick, Ireland

A. Vaseashta
Institute for Advanced Sciences Convergence, 13873 Park Center Rd. Ste 500, Herndon, VA, USA

A. Vaseashta et al. (eds.), *Technological Innovations in Sensing and Detection of Chemical, Biological, Radiological, Nuclear Threats and Ecological Terrorism*, NATO Science for Peace and Security Series A: Chemistry and Biology,
DOI 10.1007/978-94-007-2488-4_43, © Springer Science+Business Media B.V. 2012

43.1 Origin of Ionizing Radiation

Ionizing radiation is energy in the form of waves or particles that has enough force to remove electrons from atoms. One source of radiation is the nuclei of unstable atoms. As these radioactive atoms (also referred to as radionuclides or radioisotopes) seek to become more stable, their nuclei eject or emit particles and high-energy waves. This process is known as radioactive decay. Some radionuclides, such as radium, uranium, and thorium, have existed since the formation of the earth. The radioactive gas radon is one type of radioactive material produced as these naturally-occurring radioisotopes decay. Human activities, such as the splitting of atoms in a nuclear reactor, can also create radionuclides. Regardless of how they are created, all radionuclides release radiation. The major types of radiation emitted during radioactive decay are alpha particles, beta particles, and gamma rays.

43.2 Modern Applications of Radiation

Ionizing radiation is encountered under many circumstances in medicine, and specifically in oncology. It is used to identify and locate the cancer, to target it, and to treat it, with approximately 50% of cancer patients receiving radiation therapy for management of their disease. High energy photons (referred to as x-rays and gamma rays) are known to damage tissue. Although the exact details of tissue damage are still not fully understood, it is believed high energy photons induce ionization of important molecules within the cells, such as deoxyribonucleic acid. Ionization refers to removal of an electron from a molecule, making it unstable. These unstable molecules may react in a way that would prevent them from functioning properly, eventually leading to cell death. Cell damage from ionizing radiation may result in several different outcomes, and depending on the type of damage and the tissue irradiated, the biological effect can take anywhere between a few hours (acute) to many years (late) to manifest. Therefore, care should be taken to ensure that radiation exposure to the patient is kept to a minimum where it is unnecessary. Contrary, in treating cancer, large doses of radiation are used to destroy diseased tissue.

In industry, radiation is beneficial in quality control of materials, measuring the level of containers, or monitoring the thickness or consistency of paper, for example. Devices which monitor industrial processes consist of radiation sources and detectors. When the material between the radioactive source and the detector changes thickness or density, the level of radiation detected also changes. The process can be controlled by weakening or strengthening the signal from the detector. Industrial radiography is a method of non-destructive testing, used to check for flaws in metal structures and welding seals, among others. The principle is the same as in medical imaging: radiation passes through the object to be tested and exposes the X-ray film placed behind it. Dark patches in the developed film reveal flaws.

Radiography devices create radiation using either X-ray machines, or for thicker material, a gamma source or linear accelerator.

43.3 Need for Continuous Radiation Monitoring

Humans do not possess any sense organs that can detect ionizing radiation, therefore, they must relay entirely on instruments for detection and measurement of radiation [1]. A wide variety of instrument types are available. For example, the Geiger-Muller counter and scintillation counter measure particles; film badges, pocket dosimeters, and thermoluminescent dosimeters (TLD) measure accumulated doses; while ionization-chamber type instruments can measure both the dose and dose rate.

Radiation dosimeters are different, since they are designed for various applications, such as, for example, routine environmental monitoring, monitoring of occupational exposure, measuring contamination of surfaces, air, water and food [2]; measuring radon level, medical radiation measurements; and non-destructive inspection in the context of antiterrorism and homeland security [3]. The specific operating requirements vary according to the intended use of the radiation measuring instrument. Personal monitoring for external radiation is the continuous measurement of an individual' exposure dose by means of one or more of the above-stated instruments, which are carried by the individual at all times. The choice of personal dosimeter should be compatible with the type and energy of the radiation being measured.

The rise in worldwide terrorism led to a great deal of concern that some of the licensed widespread radioactive sources that are being used for peaceful purposes might be stolen or diverted to a terrorist group for use in "dirty bomb", which refers to a high-explosive bomb that is packed with highly radioactive material. Detonation of such bomb results in the dispersal of the packed radioactivity, and thus creation of an area of high-level contamination that could lead to radiation casualties as well as to a terrorized public [1]. Real-time radiation detectors become an essential part of emergency personnel who may have to respond to unknown accidents, incidents or terrorist attacks, which could involve radioactive material. More and more ordinary citizens are interested in personal radiation protection as well. Reasons include lost sources, nuclear industrial accidents, nuclear or radiological terrorism and the possibility of nuclear weapons being used in a war. People want to have the ability to measure it for themselves and they want to be notified when the radiation levels are increased.

To meet this demand, considerable research into new sensors is underway, including efforts to enhance the sensor performance through both the material properties and manufacturing technologies. Therefore, continuous radiation monitoring is an issue of paramount importance.

It is necessary to evaluate exposure dose to workers or general public according to the As Low As Reasonably Achievable (ALARA) principle. Adequate dosimetry

with proper statistical controls and documentation is the key factor of the quality control process, which is necessary to assure safe radiation usage. International Commission on Radiological Protection (ICRP) offers recommendations for the maximum permissible dose of gamma radiation to which people should be exposed, that is 1 mGy per year for general public and 20–50 mGy per year for radiation workers [4].

43.4 Impact of Radiation on Human Health

Radiation affects people by depositing energy in body tissue, which can cause cell damage or cell death. In some cases there may be no noticeable effect. In other cases, the cell may survive but become abnormal, either temporarily or permanently. Additionally, an abnormal cell may become malignant. Both large and small doses of radiation can cause cellular damage. The extent of the damage depends upon the total amount of energy absorbed, the time period and dose rate of the exposure, and the particular organs exposed. By damaging the genetic material (DNA) contained in the body's cells, radiation can cause cancer. Damage to genetic material in reproductive cells can cause genetic mutations that can be passed on to future generations. In rare occurrences where there is a large amount of radiation exposure, sickness or even death can occur in a limited amount of hours or days.

43.5 Interaction of Ionizing Radiation with Matter

The basic requirement of any instrument is that its detector interacts with the radiation in such a manner that the magnitude of the instrument's response is proportional to the radiation effect of radiation property being measured.

The interaction of ionizing radiation with matter results in a dose deposited within that matter, where dose is defined as the absorbed energy per mass (J/kg, or Gy) [5]. The ionizing radiation can be directly ionizing (charged particles) or indirectly ionizing (photons). The photons, as they pass through the medium, are attenuated by the medium and scatter from their original path. The processes of attenuation are due to coherent scattering, photoelectric effect, Compton effect, pair/triplet production, or photonuclear interactions.

Photoelectric effect is the predominant interaction for low-energy photons (below 100 keV). In a Compton interaction, the photon interacts with a valence shell electron, transferring part of photon's energy to an electron and the two then continue at a given angle from each other from the point of interaction, such that the momentum is conserved. In this interaction, the photon does not transfer all of its energy to the electron. The probability of this interaction occurring in a medium of given density is approximately independent of the atomic number (Z) of the medium, and is predominant for photon energies around 1 MeV. For high energy photons

(over 1.022 MeV) pair production can occur. In these interactions, as the photon interacts with the Coulomb field near the nucleus, the photon is absorbed giving rise to an electron and a positron.

The probability of pair production for a medium of given density is roughly proportional to Z of the medium. The electrons that result from these interactions of photons with the medium in turn travel through the medium themselves. The electron interacts with almost every atom in its path whose electric field is detectable. Most of these interactions transfer small fractions of the electron's energy, and thus the electron is often thought of as losing the energy gradually in a frictionlike process. Some of these energy losses result in a photon (Bremsstrahlung) being emitted when the electron changes direction due to an electric field from a nearby nucleus. The energy lost in this way does not contribute to the locally deposited dose. Electron interactions that do contribute to local dose will either excite the shell electrons of a nearby atom to a higher energy level, or ionize it. The rate of energy loss per distance decreases with increasing Z of the medium and increasing kinetic energy of the electron.

43.6 Recent Developments in Real-Time Radiation Dosimetry

Real-time low-power wireless neutron and gamma ray detector modules for personal dosimetry and remote monitoring were designed and tested in [6]. CdZnTe Frisch collar gamma-ray spectrometers have been used in this wireless package, and high resolution gamma-ray spectra have been sent through wireless communication to a central receiver where the pulse height spectral features were displayed. The battery life of such device can be extended, if instead of fixed interval reporting (every 10 s) an as-needed event detection scheme is employed, where data are transmitted only when a pre-determined number of data points is collected, after a specified time period has passed, or in the case of emergency if safe dose or dose rate are exceeded.

Dosimeters based on the Direct Ion Storage (DIS) technology were recently used as the first approved electronic personal dosimeter in Sweden at the County Councils in Östergötland and Kalmar, according to [7]. The DIS dosimeter is based on a small ion chamber mounted directly on a open floating gate non-volatile solid-state memory cell. Ionization in the airspace between the chamber wall and the gate, caused by electrons generated by photon interaction in the wall material, will alter the charge of the gate. At read out the conductivity over the transistor (proportional to the charge) is measured non-destructively. Two DIS elements measure the personal dose equivalent Hp(10) covering the dose ranges 1–4,500 μSv and up to 1 Sv respectively. The software determines which element to use for dose report. One MOSFET transistor is used for high doses up to 40 Sv, where the damage to the transistor itself is measured. Measurements of Hp(0.07) are provided by the third DIS element and a second MOSFET transistor behind a thin foil. The advantages of these dosimeters are longer issue periods and instant read outs, appreciated by both the service and the holders.

The radiation-sensing properties of numerous thin and thick films made from a wide range of metal oxides and their mixtures in various proportions were studied with cost-effective personal dosimetry application in mind [4]. In particular, the radiation nose concept was proposed [8], where films with different sensitivity to radiation and working dose range were combined into one sensors array system to offer better performance.

Similarly, small scale radiation detectors sensitive to alpha, beta, gamma, and neutron radiation using glass and quartz doped with ^{10}B nanoparticles utilizing CMOS fabrication techniques were recently developed [9]. They are based on the fact that radiation impinging the scintillation matrix produces varying optical pulses which are differentiated by on-chip pulse height spectroscopy. The quartz substrates are more transparent to the wavelength of the created optical pulses, resulting in higher count rates when compared to glass.

43.7 Conclusion

Radiation dosimeters have dose response characteristics with certain level of sensitivity and working dose range, conditioned by particular sensing material properties and the device structure including its thickness [10–13]. Therefore, a combination of a number of sensors with different response parameters into sensor arrays would enhance the overall performance of the radiation detection system, including broadening the measured dose range and lowering a minimum detectable dose. Availability of cost-effective real-time radiation monitors is necessary to guarantee safe usage of radiation all over the world.

References

1. Cember H, Johnson TE (2009) Introduction to health physics, 4th edn. McGraw Hill, New York
2. Desrosiers MF, Le FG (1993) Estimation of the absorbed dose in radiation-processed food – 3: the effect of time of evaluation on the accuracy of the estimate. Appl Radiat Isot 44:439–442
3. Arshak K, Korostynska O (2005) Thin and thick film real time gamma radiation detectors. IEEE Sens Spec Issue Sens Prev Terrorist Acts 5:574–580
4. Arshak K, Korostynska O (2006) Advanced materials and techniques for radiation dosimetry. Artech House, Boston
5. Arshak K, Korostynska O (2006) Thin and thick film gamma radiation sensors. In: Encyclopaedia of sensors, vol 10. American Scientific Publishers, New York, pp 291–350
6. McGregor DS, Bellinger SL, Bruno D, Cowley SA, Dunn WL, Elazegui M, Kargar A, McNeil WJ, Oyenan H, Patterson E, Shultis JK, Singh G, Solomon CJ, Unruh TC (2007) Wireless neutron and gamma ray detector modules for dosimetry and remote monitoring. In: Proceedings 2007 IEEE nuclear science symposium, Honolulu, Hawaii, pp 808–812
7. Gårdestig MR, Pettersson HBL (2009) Approved personal dosimetry for medical personnel using direct ion storage dosimeters. WC 2009, IFMBE Proc 25/III, 352–354

8. Arshak K, Korostynska O (2006) Gamma radiation nose system based on In_2O_3/SiO thick-film sensors. IEEE Sens 6:380–384
9. Waguespack R, Berry H, Pellegrin S, Wilson CG (2009) Glass and quartz microscintillators for CMOS compatible multispecies radiation detection. In: Proceedings 2009 IEEE 22nd international conference micro electro mechanical systems MEMS 2009, Sorrento, Italy, pp 833–836
10. Arshak K, Korostynska O (2004) Thick film oxide diode structures for personal dosimetry application. Sens Actuators A Phys 113:319–323
11. Arshak K, Korostynska O, Molloy J, Harris J (2004) MnO/TeO2 thin films as optical gamma radiation sensors. In: Proceedings IEEE sensors, Vienna, 2004, pp 1285–1288
12. Arshak K, Korostynska O (2004) Influence of gamma radiation on the electrical properties of MnO and MnO/TeO_2 thin films. Ann Phys 13:87–89
13. Arshak K, Korostynska O (2006) Gamma radiation sensors arrays based on metal oxide thick films. Sens Rev 26:70–75

Author Index

A. Vaseashta et al. (eds.), *Technological Innovations in Sensing and Detection of Chemical, Biological, Radiological, Nuclear Threats and Ecological Terrorism*, NATO Science for Peace and Security Series A: Chemistry and Biology, DOI 10.1007/978-94-007-2488-4, © Springer Science+Business Media B.V. 2012

Keyword Index

A. Vaseashta et al. (eds.), *Technological Innovations in Sensing and Detection of Chemical, Biological, Radiological, Nuclear Threats and Ecological Terrorism*, NATO Science for Peace and Security Series A: Chemistry and Biology, DOI 10.1007/978-94-007-2488-4, © Springer Science+Business Media B.V. 2012

ASI Group Photograph

NATO Advanced Study Institute on Technological Innovations in Detection and Sensing of Chemical, Biological, Radiological, Nuclear - Threats and Ecological Terrorism Chisinau, Moldova June 6-17, 2010

ASI Selected Photographs


DEMIEI DE ŞTIINȚE A MOLD


NATO
OTAN
and Security Programme

gical Innovations in Detection and Sensin
al Bi
Threa


VILA VERDE